WOMEN IN SCIENCE - TRANSLATIONAL MEDICINE 2021

EDITED BY: Victoria Bunik and Claudine Habak
PUBLISHED IN: Frontiers in Medicine

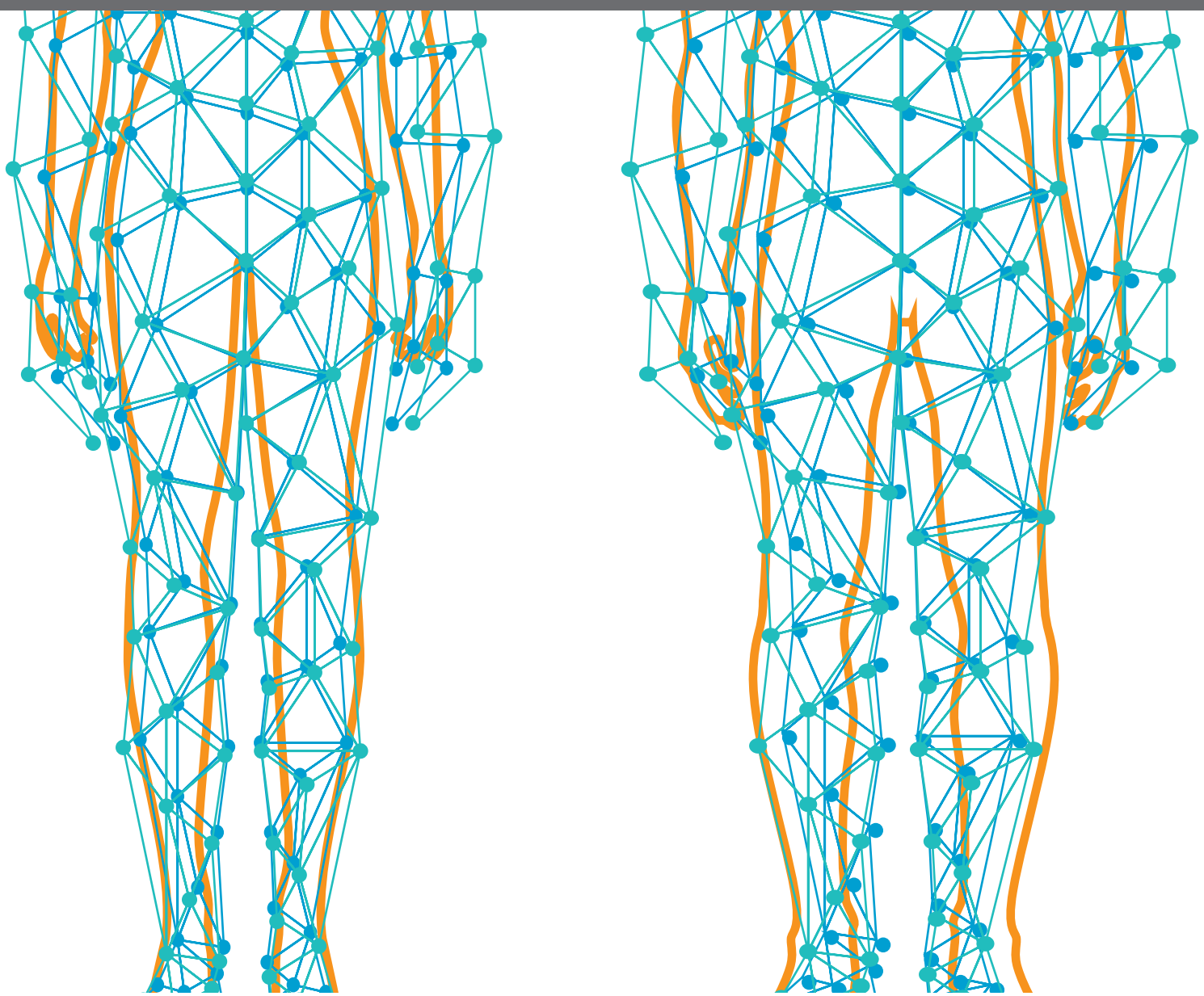

frontiers Research Topics

frontiers

ISSN 1664-8714
ISBN 978-2-83250-320-1
DOI 10.3389/978-2-83250-320-1

About Frontiers

Frontiers is more than just an open-access publisher of scholarly articles: it is a pioneering approach to the world of academia, radically improving the way scholarly research is managed. The grand vision of Frontiers is a world where all people have an equal opportunity to seek, share and generate knowledge. Frontiers provides immediate and permanent online open access to all its publications, but this alone is not enough to realize our grand goals.

Frontiers Journal Series

The Frontiers Journal Series is a multi-tier and interdisciplinary set of open-access, online journals, promising a paradigm shift from the current review, selection and dissemination processes in academic publishing. All Frontiers journals are driven by researchers for researchers; therefore, they constitute a service to the scholarly community. At the same time, the Frontiers Journal Series operates on a revolutionary invention, the tiered publishing system, initially addressing specific communities of scholars, and gradually climbing up to broader public understanding, thus serving the interests of the lay society, too.

Dedication to Quality

Each Frontiers article is a landmark of the highest quality, thanks to genuinely collaborative interactions between authors and review editors, who include some of the world's best academicians. Research must be certified by peers before entering a stream of knowledge that may eventually reach the public - and shape society; therefore, Frontiers only applies the most rigorous and unbiased reviews.
Frontiers revolutionizes research publishing by freely delivering the most outstanding research, evaluated with no bias from both the academic and social point of view. By applying the most advanced information technologies, Frontiers is catapulting scholarly publishing into a new generation.

What are Frontiers Research Topics?

Frontiers Research Topics are very popular trademarks of the Frontiers Journals Series: they are collections of at least ten articles, all centered on a particular subject. With their unique mix of varied contributions from Original Research to Review Articles, Frontiers Research Topics unify the most influential researchers, the latest key findings and historical advances in a hot research area! Find out more on how to host your own Frontiers Research Topic or contribute to one as an author by contacting the Frontiers Editorial Office: frontiersin.org/about/contact

WOMEN IN SCIENCE - TRANSLATIONAL MEDICINE 2021

Topic Editors:
Victoria Bunik, Lomonosov Moscow State University, Russia
Claudine Habak, Emirates College for Advanced Education, United Arab Emirates

Citation: Bunik, V., Habak, C., eds. (2022). Women in Science - Translational Medicine 2021. Lausanne: Frontiers Media SA. doi: 10.3389/978-2-83250-320-1

Table of Contents

frontiers | Frontiers in Medicine

TYPE Editorial
PUBLISHED 07 September 2022
DOI 10.3389/fmed.2022.1021894

OPEN ACCESS

EDITED AND REVIEWED BY
Matteo Becatti,
University of Firenze, Italy

*CORRESPONDENCE
Victoria I. Bunik
bunik@belozersky.msu.ru

SPECIALTY SECTION
This article was submitted to Translational Medicine, a section of the journal Frontiers in Medicine

RECEIVED 17 August 2022
ACCEPTED 24 August 2022
PUBLISHED 07 September 2022

CITATION
Bunik VI and Habak C (2022) Editorial: Women in science - translational medicine 2021. *Front. Med.* 9:1021894. doi: 10.3389/fmed.2022.1021894

Editorial: Women in science - translational medicine 2021

Victoria I. Bunik[1,2,3]* and Claudine Habak[4]

[1]Faculty of Bioengineering and Bioinformatics, Lomonosov Moscow State University, Moscow, Russia, [2]Department of Biokinetics, A. N. Belozersky Institute of Physico-Chemical Biology, Lomonosov Moscow State University, Moscow, Russia, [3]Department of Biochemistry, Sechenov University, Moscow, Russia, [4]Cognitive Neuroimaging Unit, Emirates College for Advanced Education, Abu Dhabi, United Arab Emirates

KEYWORDS

diagnostic markers, diabetes, exaggerated inflammation, gender diversity in research, NAD in demyelinating diseases, chronic fatigue, low back pain

Editorial on the Research Topic
Women in science - translational medicine 2021

Gender diversity in research, ranging from team composition to methods and questions, can benefit scientific innovation (1) and impact (2). While the representation of women in early-career research roles is relatively equal to that of men, there is an under-representation in later-stage career roles (3), in corresponding authorship (4), and in lead authorship positions [first and last (5, 6)]. Globally, the pandemic has specific pressure on women's work, likely due to differences in family responsibilities (9–11). In science, women's research output has been affected disproportionately (7, 8), with a larger decrease in the number of pre-prints compared to men (12), and in the number of new projects and authorship—the medical literature included (7). Other special issues have addressed factors underlying gender gaps in science [e.g., (13)]. Here, we take action, by promoting the equal participation of women and men in science through the Research Topic "*Women in Translational Medicine*." We create a space for translational studies by teams with female leaders, where the first and last authors are researchers identifying as female.

What comes across strongly in this collection, is the drive of female researchers to move translational medicine by reporting experimental data in unexplored and/or intricate fields (12 of the 13 papers consist of original research) and by highlighting novel approaches, such as a new paradigm in cancer diagnostics, presented by Glyn and Purcell in our only review of the series. The review exemplifies critical scientific discourse, providing a refreshing voice with strong and informative messaging: it demonstrates how whole-genome sequencing of microbiomes can discriminate between healthy and cancer subjects, even at early stages I and II. Advantages and limitations of this approach are compared to the diagnostic value of other types of DNA markers in cancer.

In the collection, over half the papers (7/13; including the review) are dedicated to diagnostic procedures for timely and effective intervention to treat complex pathologies and predict their course. One of the papers has acquired the highest number of views (>6,000 in 2 months post-publication) of all papers published in *Translational Medicine* over the past year. The work by González-Cebrián et al. offers a novel approach to diagnosing Chronic Fatigue Syndrome, which is a debilitating condition that can occur post-virally. The authors compared 15 female patients and 15 controls, and yet, reached significant discriminative power (healthy vs. patient), by analyzing 817 variables. As the microRNA profiles in the blood of patients are limited in diagnostic power, Raman micro-spectroscopy of blood extracellular vesicles along with other differences abundant in human patients are added to consideration. The authors stress that omics-based diagnostics should be enriched with statistical methods to reveal complex interactions among variables, which go beyond changes in individual markers. This approach is certainly key to personalized medicine.

The practical and financial costs of routinely measuring a wide array of data for single patients in clinical settings can be challenging, and several papers address the use of more feasible biomarkers. For example, biological markers of age correlate with the severity of chronic pulmonary obstructive disease (Campisi et al.), or can serve in organ transplantation (Pavanello et al.). These papers illustrate how determining biological age through cellular DNA methylation and telomere length can address various medical challenges. The use of another biomarker, a vitamin B3 derivative, NAD^+, is presented by Balashova et al. Unlike previous findings in other human and animal tissues, NAD^+ concentration in human blood does not decrease significantly with age. However, its decrease marks demyelinating neurological diseases and cardiopathologies, pointing to potential diagnostic applications of this test easily incorporated into routine blood analyses. Pia-Mara Wippert et al. show that readily available biomarkers, such as indicators of glucose metabolism in blood or the cortisol content in hair, complement psychometric tests in evaluating stress levels and long-term development of chronic low back pain. As the differential expression of symptoms may depend on individual levels of specific vitamins or other metabolic/hormonal indicators, devising and introducing biochemical tests in clinical practice improves the interpretation of symptoms and disease treatment.

Investigation of biochemical parameters is useful, yet often limited to smaller patient samples (e.g., dozens of patients in all the papers cited above), whereas questionnaires can readily be used in a wider segment (e.g., hundreds in Pia-Mara Wippert et al., and thousands in Hüfner et al.). In addition to the material and labor costs of biochemical tests, patient willingness is also a limiting factor: only one third of patients with chronic low back pain committed to an additional biochemical test battery even if it could assist in diagnosis (Wippert et al.). Fortunately, questionnaire scales can be highly informative: analyzing the response patterns of stress ratings, Hüfner et al. suggest that these profiles may be linked to published findings on neuroinflammation, levels of vitamin D, gut dysbiosis, and mitochondrial dysfunction. This link points to the importance of incorporating biochemical indicators with scales, to (1) increase diagnostic power, (2) refine scale interpretation by linking symptom profiles to specific underlying conditions, and (3) aid in the faster development of pointed scales for assessment of specific conditions.

In addition to the development of clinically accessible tests, the integration of biochemical parameters with diagnostic procedures is promoted through the understanding that similar symptoms may arise from different molecular mechanisms. This implies that personalized treatment should consider a panel of biochemical markers that could point to a specific underlying molecular origin. To support these approaches, infrastructure in translational medicine should be created, helping the research to address patient needs and new treatments. Matera-Witkiewicz et al. characterize Poland's biobanking network across research infrastructure, quality management, and private-public comparisons, to ascertain quality processes, materials, and data for research and preclinical work that could serve patients world-wide. The piece by Knoppers et al. investigates the rarely-addressed patient and caregiver voices in personalized medicine, exploring the relationship between research and specifically affected communities, such as patients with cystic fibrosis and their caregivers. Findings show that a lifelong progressive and terminal disease stimulates the relationship between the patients/caregivers and researchers, with patients/caregivers considering research intrinsic to their experience and seeking greater access to research results and advancements. Promoting such interactions would foster awareness that the joint effort greatly enriches translation of new therapies and personalized medicine. The communication between patients, caregivers, researchers, and clinicians in designing and implementing research would not only address patient needs, but also feed into advancement through diversity in research.

While there have been significant advances in the technologies and standards involved in storing and analyzing human samples, certain types of questions cannot be answered using human cells or organoids, but require animal experiments due to complex regulation of physiological functions by subordination and interaction of different cells/tissues in the organism. Translational medicine *via* animal models is presented in four of the 13 papers in this collection, which are dedicated to molecular mechanisms of pathologies and/or their therapies. Boyko et al. study a recently discovered *DHTKD1*-encoded enzyme whose expression is associated with obesity and diabetes, but the underlying mechanisms are unknown. They show that the enzyme impacts biological

function through protein glutarylation and that pyruvate dehydrogenase complex is among the glutarylated proteins. As the complex is essential for glucose oxidation, its *DHTKD1*-dependent glutarylation may explain *DHTKD1* involvement in diabetes. Yang et al. address molecular mechanisms of the osteogenesis stimulation by the widely used hypoglycemic drug metformin. This drug has potential therapeutic effects in both the diabetes-induced and postmenopausal osteoporosis. The researchers reveal molecular markers and pathways involved in the metformin-induced osteogenic differentiation, which may be useful for personalized medicine to control the different actions of metformin. Two papers of the collection deal with exaggerated systemic inflammation, which has drawn extensive attention during the recent pandemic. Müllebner et al. aim at dissecting specific pathways during the exaggerated systemic inflammation, leading to tissue damage in a model of peritonitis and its surgical treatment. The authors reveal a causal relationship between unfolded protein response and onset of systemic inflammation, which must be accounted for in therapeutic approaches to prevent liver damage. A "cytokine storm" is a key feature of the exaggerated inflammation observed in SARS-CoV-2 infection and sepsis. *In vitro* and *in vivo* models are used by Schapovalova et al. to demonstrate beneficial effects of a herbal treatment on the excessive pro-inflammatory responses associated with changed blood formula and "sickness behavior". Such herbal compositions are intensely studied within the PhytoAPP project supported by the European Union's Horizon 2020 research and innovation program, as they offer affordable solutions in communities that are in need of stronger healthcare systems.

Through this collection findings, insights, and future directions, we would like to highlight the importance of diversity in research across any dimension, including ethnicity, age, and health status. We offer our thanks to the participants, authors, reviewers, and editors involved in this collection to promote women in translational medicine. We look to the diversity of current and future work in contributing to the highest quality of research in health science and translation.

Author contributions

All authors listed have made a substantial, direct, and intellectual contribution to the work and approved it for publication.

Funding

VB acknowledges financial support by RFBR grant 20-54-7804.

Conflict of interest

The authors declare that the research was conducted in the absence of any commercial or financial relationships that could be construed as a potential conflict of interest.

Publisher's note

All claims expressed in this article are solely those of the authors and do not necessarily represent those of their affiliated organizations, or those of the publisher, the editors and the reviewers. Any product that may be evaluated in this article, or claim that may be made by its manufacturer, is not guaranteed or endorsed by the publisher.

References

1. Nielsen MW, Bloch CW, Schiebinger L. Making gender diversity work for scientific discovery and innovation. *Nat Hum Behav.* (2018) 2:726–34. doi: 10.1038/s41562-018-0433-1

2. AlShebli BK, Rahwan T, Woon WL. The preeminence of ethnic diversity in scientific collaboration. *Nat Commun.* (2018) 9:5163. doi: 10.1038/s41467-018-07634-8

3. James A, Chisnall R, Plank MJ. Gender and societies: a grassroots approach to women in science. *R Soc Open Sci.* (2019) 6:190633. doi: 10.1098/rsos.190633

4. The 2018. OECD International Survey of Scientific Authors [Internet]. (2020). (OECD Science, Technology and Industry Working Papers; vol. 2020/04). Report No.: 2020/04. Available online at: https://www.oecd-ilibrary.org/science-and-technology/the-2018-oecd-international-survey-of-scientific-authors_18d3bf19-en (accessed August 15, 2022).

5. West JD, Jacquet J, King MM, Correll SJ, Bergstrom CT. The role of gender in scholarly authorship. *PLoS ONE.* (2013) 8:e66212. doi: 10.1371/journal.pone.0066212

6. Ni C, Smith E, Yuan H, Larivière V, Sugimoto CR. The gendered nature of authorship. *Sci Adv.* (2021) 7:eabe4639. doi: 10.1126/sciadv.abe4639

7. Viglione G. Are women publishing less during the pandemic? here's what the data say. *Nature.* (2020) 581:365–6. doi: 10.1038/d41586-020-01294-9

8. Reese TA, Harris-Tryon TA, Gill JG, Banaszynski LA. Supporting women in academia during and after a global pandemic. *Sci Adv.* (2021). 7:eabg9310. doi: 10.1126/sciadv.abg9310

9. Sevilla A, Smith S. Baby steps: the gender division of childcare during the COVID-19 pandemic. *Oxford Rev Econ Policy.* (2020) 36:S169–86. doi: 10.1093/oxrep/graa027

10. Yavorsky JE, Qian Y, Sargent AC. The gendered pandemic: the implications of COVID-19 for work and family. *Sociology Compass.* (2021) 15:e12881. doi: 10.1111/soc4.12881

11. Petts RJ, Carlson DL, Pepin JR, A. gendered pandemic: Childcare, homeschooling, and parents' employment during COVID-19. *Gender Work Organization.* (2021) 28:515–34. doi: 10.1111/gwao.12614

12. King MM, Frederickson ME. The pandemic penalty: the gendered effects of COVID-19 on scientific productivity. *Socius.* (2021). doi: 10.1177/23780231211006977

13. Williams WM. Editorial: underrepresentation of women in science: international and cross-disciplinary evidence and debate. *Front Psychol.* (2018) 8:2352. doi: 10.3389/fpsyg.2017.02352

frontiers in Medicine

ORIGINAL RESEARCH
published: 23 July 2021
doi: 10.3389/fmed.2021.690312

DNA Methylation-Based Age Prediction and Telomere Length Reveal an Accelerated Aging in Induced Sputum Cells Compared to Blood Leukocytes: A Pilot Study in COPD Patients

Manuela Campisi[1], *Filippo Liviero*[1], *Piero Maestrelli*[1], *Gabriella Guarnieri*[2] *and Sofia Pavanello*[1]*

[1] Occupational Medicine, Department of Cardiac, Thoracic, and Vascular Sciences and Public Health, University Hospital of Padua, Padua, Italy, [2] Respiratory Pathophysiology Unit, Department of Cardiac, Thoracic, and Vascular Sciences and Public Health, University Hospital of Padua, Padua, Italy

OPEN ACCESS

Edited by:
Ulrich Martin,
Hannover Medical School, Germany

Reviewed by:
Hai Bac Tran,
University of Adelaide, Australia
Hanlin Zhang,
University of California, Berkeley, United States

***Correspondence:**
Sofia Pavanello
sofia.pavanello@unipd.it

Specialty section:
This article was submitted to Translational Medicine, a section of the journal Frontiers in Medicine

Received: 02 April 2021
Accepted: 08 June 2021
Published: 23 July 2021

Citation:
Campisi M, Liviero F, Maestrelli P, Guarnieri G and Pavanello S (2021) DNA Methylation-Based Age Prediction and Telomere Length Reveal an Accelerated Aging in Induced Sputum Cells Compared to Blood Leukocytes: A Pilot Study in COPD Patients. Front. Med. 8:690312. doi: 10.3389/fmed.2021.690312

Aging is the predominant risk factor for most degenerative diseases, including chronic obstructive pulmonary disease (COPD). This process is however very heterogeneous. Defining the biological aging of individual tissues may contribute to better assess this risky process. In this study, we examined the biological age of induced sputum (IS) cells, and peripheral blood leukocytes in the same subject, and compared these to assess whether biological aging of blood leukocytes mirrors that of IS cells. Biological aging was assessed in 18 COPD patients (72.4 ± 7.7 years; 50% males). We explored mitotic and non-mitotic aging pathways, using telomere length (TL) and DNA methylation-based age prediction (DNAmAge) and age acceleration (AgeAcc) (i.e., difference between DNAmAge and chronological age). Data on demographics, life style and occupational exposure, lung function, and clinical and blood parameters were collected. DNAmAge (67.4 ± 5.80 vs. 61.6 ± 5.40 years; $p = 0.0003$), AgeAcc (−4.5 ± 5.02 vs. −10.8 ± 3.50 years; $p = 0.0003$), and TL attrition (1.05 ± 0.35 vs. 1.48 ± 0.21 T/S; $p = 0.0341$) are higher in IS cells than in blood leukocytes in the same patients. Blood leukocytes DNAmAge ($r = 0.927245$; $p = 0.0026$) and AgeAcc ($r = 0.916445$; $p = 0.0037$), but not TL, highly correlate with that of IS cells. Multiple regression analysis shows that both blood leukocytes DNAmAge and AgeAcc decrease (i.e., younger) in patients with FEV_1% enhancement ($p = 0.0254$ and $p = 0.0296$) and combined inhaled corticosteroid (ICS) therapy ($p = 0.0494$ and $p = 0.0553$). In conclusion, new findings from our work reveal a differential aging in the context of COPD, by a direct quantitative comparison of cell aging in the airway with that in the more accessible peripheral blood leukocytes, providing additional knowledge which could offer a potential translation into the disease management.

Keywords: DNA methylation age, age acceleration, induced sputum, chronic obstructive pulmonary disease, lung aging, telomere length

INTRODUCTION

The aging of the population, also called the "gray" revolution, is undoubtedly an emerging social and public health problem. Aging is an individual and very complex process characterized by a progressive decline in the body's ability to respond to internal and/or external stressors (1). This deterioration is the primary risk factor for major human degenerative pathologies, including cancer and cardiovascular, neurodegenerative, and respiratory diseases (1). Chronic obstructive pulmonary disease (COPD) is one of the major causes of chronic morbidity (2) and the third leading cause of death worldwide[1] which is projected to rise (3) because of the aging population. Some individuals, however, have a physiological senescence that is faster than that of others (1). In fact, not all individuals grow older in the same way (4); consequently, chronological age may not be a reliable indicator of physiological decline (5).

Exploring the aging process, defining measurable estimates of "biological aging" (in contrast to chronological aging), has become a major initiative in medical research (6). Two "pillars of aging" have been proposed as the most promising early indicators for aging (6), i.e., telomere shortening and epigenetic alterations in DNA, which primary cause damage to cellular functions. Telomeres act as a mitotic clock that, by reducing itself at each cell division, leads to cellular senescence (replicative senescence) or cell death. A powerful emerging marker of non-mitotic cellular aging is the epigenetic age often defined as DNA methylation age (DNAmAge) (7, 8). DNAmAge in human (9–11) is assessed from methylation at a species-specific subset of cytosine–guanine dyads (CpG), and it is strongly correlated with chronological age (9–13). Development of epigenetic predictors has addressed to an "epigenetic clock" theory of aging, according to which the difference between DNAmAge and chronological age is defined as "age acceleration" (AgeAcc) (14), which is indicative of altered biological functions (8) and elevated risk for morbidity and mortality (15).

COPD shows striking lung aging-associated features including the reduction of function, pulmonary inflammation (2), and progressive airway obstruction (16, 17). Understanding of age-related pathomechanisms associated with COPD is decisive to also uncovering novel strategies for disease treatment. Smoking is the primary cause for COPD worldwide (18), and in developing countries, COPD also arises as a result of exposure to household air pollution (18, 19). The mechanisms linking tobacco smoke and other air pollutants with COPD have not yet been fully elucidated. One main working hypothesis is that air pollutants, especially the particulate matter (PM) of aerodynamic diameter of 2.5 μm or less, can deeply penetrate into the lung, deposit in the alveolar area, and locally trigger oxidative stress and inflammatory response (20). The pulmonary local oxidative–inflammatory reaction damages lung tissue, leading to structural pathological changes such as lung parenchyma destruction (emphysema), fibrosis of peripheral airways, and an increase in mucus-producing cells, with a consequent airflow limitation, which are all signs of an accelerated aging of the lung (20). This local oxidative–inflammatory reaction leads to a subsequent systemic inflammation (21). Several blood inflammatory markers, including C-reactive protein (CRP) (22), interleukin (IL)-6 (23), and blood leukocytes, are all found altered in COPD patients (24). Altered inflammatory responses and induced oxidative stress are two key mechanisms accelerating biological aging detected by early signs of cellular aging, including alterations in telomere length (TL) (25) and DNA methylation (26). Shorter TL in blood leukocytes has been described from patients with COPD (27) and in a meta-analysis of 14 studies (28). One recent study from two independent longitudinal large cohort studies relates DNAmAge in blood leukocytes to COPD incidence (29). However, no epigenetic age estimation was performed in the target organ of the disease, i.e., the lung.

While lung tissue is not routinely accessible, sputum induction represents a validated noninvasive method of lower respiratory tract sampling for analysis of cell components in the airways lumen and fluid-phase constituents (30). It has been successfully applied for assessing disease severity and progression in COPD, producing reliable results comparable to biopsy and bronchoalveolar lavage (31).

This study has two main objectives:

i) To determine the biological age of the induced sputum (IS) cells and peripheral blood leukocytes, by measuring the mitotic age (TL) and non-mitotic epigenetic age (DNAmAge).
ii) To compare blood leukocytes and IS cells in order to assess the reliability of blood leukocytes as an accurate indicator of lower respiratory tract biological age.

To these aims, COPD patients were examined as a positive paradigm of lung aging, taking into consideration their demographic data, life style and occupational exposure, lung function, and clinical and blood parameters.

MATERIALS AND METHODS

Study Design

The present study includes $n = 18$ moderate patients with COPD, diagnosed according to GOLD guidelines (32), enrolled at the ambulatory of Respiratory Physiopathology Ward – Occupational Medicine, Department of Cardio-Vascular-Thoracic Science and Public Health, University of Padova. The local Ethics Committee - University of Padova approved the study protocols (3843/AO/16 and 3054/AO/14). The recruiting of COPD patients was carried out between September 2018 and September 2019. The inclusion criteria for the study participation were post-bronchodilator forced expiratory volume in a 1-s (FEV_1)/forced vital capacity (FVC) ratio of <70% on spirometry and no acute exacerbation for at least 6 weeks. All patients were informed of the purpose of the study by trained interviewers and asked to sign an informed consent form. The study was

Abbreviations: AgeAcc, age acceleration; COPD, chronic obstructive pulmonary disease; CRP, C-reactive protein; DNAmAge, DNA methylation age; FEV_1, forced expiratory volume in one second; TL, telomere length.

[1]Available online at: https://www.who.int/news-room/fact-sheets/detail/chronic-obstructive-pulmonary-disease-(copd) (accessed June 01, 2021).

conducted in accordance with the Declaration of Helsinki. Participants were interviewed with structured questionnaires to collect information regarding demographic data (age, gender), age of parents at birth and educational level (years), smoking history and pack-years, alcohol intake in the last 12 months and habitual alcohol consumption measured as unit of drink/day (1 unit = 10–12 g alcohol intake), environmental exposure (diet, indoor, home, traffic, outdoor), physical activity (IPAQ score), clinical determinants (e.g., leukocytes, blood red cells, hemoglobin, glycemia, CRP), medical history, and therapy. Therapy information included inhalation device types available, such as metered-dose inhalers (MDIs), dry-powder inhalers (DPIs), and soft mist inhalers (SMIs). Specifically, therapy has been prescribed according to the GOLD guidelines (32), in which from 2011 the assessment approach acknowledges the limitations of FEV_1 in making treatment decisions for individualized patient care and highlights the importance of patient symptoms and exacerbation risk in guiding therapies in COPD, the "ABCD" assessment tool. All patients underwent a physical examination, and lung function was assessed by spirometry recording forced expiratory volume in 1 s (FEV_1), FVC, vital capacity (VC), total lung capacity (TLC), residual volume (RV), and FEV_1/VC ratio also defined as Tiffeneau index. For each patient, blood samples were collected in vacutainer K3EDTA tubes and PAXgene tubes, for basic biochemistry, TL determination, and DNAmAge assessment. A plasma sample was also collected and stored in a freezer at −80°C for further investigations. During medical examination, the procedure of sputum induction was carried out for each patient to collect a sample of airways cells on which to analyze TL and DNAmAge.

IS Procedure and Spirometry

All lung function measurements were measured using a spirometer (MasterScreen PFT, PRO, Viasys Sanità, Firenze, Italy) according to the guidelines/recommendations of the American Thoracic Society/European Respiratory Society (ATS/ERS) (33). FEV_1 was used as the primary variable of lung function which was measured both before and 10 min after the use of the post-bronchodilator. FEV_1 was expressed as liters and as a percentage of the predicted normal value (FEV_1%) according to reference values based on age, height, weight, sex, and race for each subject using the European Community for Steel and Coal as reference values (34). These values obtained are in turn used as reference standards/assessments for consecutive spirometries performed during the IS standard procedure (35). Nebulized sterile saline solutions (hypertonic at 3 and 4%) were consecutively administered using a nebulizer [UltraNeb, DeVilbiss, Desio (MB), Italy] with an output flow of ∼1 ml•min in four sequential 5-min inhalation periods. Since saline inhalation may cause bronchoconstriction, after each inhalation period FEV_1 was measured for the detection and monitoring of lung function during the process, stopping the procedure when FEV_1 decreased over 20% compared with that of post-salbutamol baseline. During the procedure, the patient was asked to cough and expectorate. Once collected, IS was processed according to a standard technique (35). The weight of the selected sputum plugs was recorded and the sample was diluted with a volume of phosphate-buffered solution (PBS) and 0.1% dithiothreitol (DTT) equal to 4:1 of selected plugs. After filtration with a nylon mesh (52–56 μm), the sample was centrifuged (3,000 rpm for 3 min) to separate cells and supernatant. The cell pellet was resuspended in 1 ml of PBS. The cells were stained for viability assessment using an equal volume (10 μl) of both sample and Trypan Blue. The cell concentration was adjusted to obtain a final concentration of ∼300,000 cells/ml. The cells were cytocentrifuged (Cytospin, Shandon Scientific, Milano, Italy) at 450 rpm for 6 min, onto glass slides treated with aptex (3-aminopropyltriethoxysilane) according to a standard method (36) and stained with Diff-Quik (Dade Behring, Milano, Italy). The differential cell count in IS was measured counting 400 nucleated cells per each of two slides stained reporting the percentage of eosinophils, neutrophils, macrophages, lymphocytes, and bronchial epithelial cells. The IS sample is considered acceptable and adequate if the percentage of squamous cells is <20% of the total cells, warranting the reproducibility of cell counts.

DNA Extraction From Blood Samples

DNA was extracted from whole blood using the QIAamp DNA Mini Kit (Qiagen, Milano, Italy) on a QIAcube System (Qiagen, Milano, Italy) for automated high-throughput DNA purification, according to a customized protocol as previously described (13). In particular, 400 μl of whole blood from each sample was processed for DNA extraction. DNA was quantified and checked for quality using QIAxpert Quantification System (Qiagen, Milano, Italy).

DNA Extraction From IS Samples

Once the IS sample was collected to analyze the differential cell count, a second aliquot of the same sample was processed as indicated in the protocol reported in IS procedure and spirometry up to the centrifugation step (3,000 rpm for 3 min) to separate cells and supernatant. The cell pellet was then resuspended in 180 μl of PBS. DNA extraction was performed on the automated QIAcube System (Qiagen, Milano, Italy) using QIAamp DNA Mini Kit (Qiagen, Milano, Italy) according to a customized protocol developed for highly viscous samples. After extraction, DNA was quantified and checked for quality using the QIAxpert Quantification System (Qiagen, Milano, Italy).

TL Analysis

TL was measured after DNA extraction from both whole blood and IS samples, by using quantitative real-time PCR as previously described (37, 38). This assay measures relative TL in genomic DNA by determining the ratio of telomere repeat copy number (T) to a single nuclear copy gene (S) in experimental samples relative to the T/S ratio of a reference pooled sample. The single-copy gene used was human (beta) globin (hbg). The PCR runs were conducted in triplicate on a StepOnePlus Real-Time PCR System (Applied Biosystems, Milano, Italy), and the average of the three T/S ratio measurements was used in the statistical analyses. Details of TL analysis are reported in the **Supplementary Materials**.

DNAmAge and AgeAcc Analyses

DNAmAge was determined by analyzing the methylation levels from selected markers using the bisulfite conversion and Pyrosequencing® methodology as previously reported (12, 13). This method is based on determination of the methylation level of a set of five markers (ELOVL2, C1orf132, KLF14, TRIM59, and FHL2) in genomic DNA, as described by Zbieć-Piekarska et al. (11) with some modifications based on the fact that the method was almost completely automated using the PyroMark Q48 Autoprep (Qiagen, Milano, Italy) (12, 13). AgeAcc was calculated as the difference between the detected DNAmAge of IS cells and blood leukocytes and the chronological age of patients. Details of DNAmAge analysis are reported in the **Supplementary Materials**.

Statistical Analysis

Statistical analyses were performed with StastDirects software. Data are expressed as mean ± SD or number and percentage. The diversity among the two groups of patients split per therapy (dual therapy and triple therapy with combined inhaled corticosteroid (ICS) assumption) was appraised with the Mann–Whitney *U*-test and chi-square test, respectively. Levels of TL, DNAmAge, and AgeAcc in IS cells, and blood leukocytes, of the same patient, were compared by the (two-tailed) paired *T*-test. Comparison between all samples in the two groups was also made using the Mann–Whitney *U*-test. Simple linear regression was evaluated in order to provide a measure of the strength of dependence between two variables. Correlations between age, leukocytes, differential cell count, and cigarette smoking (pack years) (independent variables) on blood leukocytes DNAmAge, AgeAcc, and TL measures (dependent variables) were evaluated by simple linear regression models. Lastly, age and differential cell counts of IS, including % macrophages, % neutrophils, and % eosinophils (independent variables), were related by simple linear regression to DNAmAge, AgeAcc, and TL, respectively. The influence of age, gender (female), ICS therapy, leukocytes (10^3/ml) (model a), and neutrophils (10^3/ml) (model b) and FEV_1% as indicator of lung function on blood leukocytes TL, DNAmAge, and AgeAcc was appraised by multiple linear regression analyses. Lastly, the influence of age, gender (female), ICS therapy, type of inhalers, neutrophil percentage (%), and FEV_1% on IS cell TL, DNAmAge, and AgeAcc was appraised by multiple linear regression analyses. Results were considered significant when a *p*-value of <0.05 was obtained.

Sample Size Estimation

Sample size estimation for a paired *T*-test was applied to calculate the sample size. The calculation was computed through a STATA command by specifying a mean difference = 0.43, 5.8, and 6.0, and standard deviation of differences 0.14, 0.40, and 1.52, respectively, for IS cells vs. blood leukocytes TL, DNAmAge, and AgeAcc, respectively. The group size to obtain statistical significance with α (two-tailed) = 0.05 and β = 0.20 was estimated to be $n = 4$, $n = 2$, and $n = 3$ subjects for TL, DNAmAge, and AgeAcc, respectively.

RESULTS

Characteristics of the Study Population

The characteristics of the study subjects are reported in **Tables 1**, **2**. Interval variables (mean ± SD) of all COPD patients ($n = 18$) with a long-acting β2 agonist/long-acting muscarinic antagonist (LABA/LAMA) ($n = 9$) and with combined ICS therapy and LABA/LAMA administration ($n = 9$), also defined as dual and triple therapy, respectively, are shown in **Table 1**. The comparison of two groups (Mann–Whitney *U*-test) indicates that patients in LABA/LAMA therapy present higher values of FEV_1 ($p = 0.0003$), FEV_1% ($p < 0.0001$), FVC ($p = 0.0003$), VC ($p = 0.0003$), and TLC ($p = 0.0008$) and also a lower systolic pressure ($p = 0.036$), than those with ICS therapy and LABA/LAMA. No difference in the other parameters is observed. In particular, functional data of COPD patients including FEV_1% are categorized according to inhalation therapy, dual therapy, or triple therapy. Furthermore, in our study population, the majority of patients in dual therapy used single or combinations of DPI inhalers ($n = 6$); only few cases used MDI ($n = 1$) and SMI inhalers ($n = 2$), alone. COPD patients in triple therapy used predominantly single or combinations of DPI inhalers ($n = 6$), $n = 1$ MDI with DPI devices, $n = 1$ SMI with DPI devices, and $n = 1$ combined SMI and MDI devices. Furthermore, patients in triple therapy, which are those with more symptoms and more exacerbations, presented also lower functional average values including FEV_1%, compared to patients in dual therapy. **Table 2** shows the number and percentage of categorical variables in the same groups. All characteristics are equally distributed among the two groups with dual and triple therapy, including in particular smoking history, the main risk factor for COPD insurgence (chi-square test p = not significant).

Biological Age of the IS Cells and Blood Leukocytes Determined by DNAmAge, AgeAcc, and TL

Figure 1A (**Supplementary Table 2**) shows that IS cell DNAmAge is older (mean 6.3 ± 2.08 years) than blood leukocyte DNAmAge in the same patient ($n = 7$, paired *t*-test mean 67.4 ± 5.80 years vs. mean 61.6 ± 5.40 years; $p = 0.0003$). IS cell AgeAcc (**Figure 1B**; **Supplementary Table 2**) is also extremely enhanced compared to that of blood leukocytes in the same patient ($n = 7$, paired *t*-test mean −4.5 ± 5.02 years vs. mean −10.8 ± 3.50 years; $p = 0.0003$) and in all patients ($n = 16$, Mann–Whitney *U*-test: mean −4.5 ± 5.02 years vs. mean −10.3 ± 3.63 years; $p = 0.0156$). Likewise, **Figure 2** (**Supplementary Table 3**) reports that IS cell TL mean is shorter than that of blood leukocytes in the same patient ($n = 8$, paired *t*-test: mean 1.05 ± 0.35 T/S vs. mean 1.48 ± 0.21 T/S; $p = 0.0341$) and in all patients ($n = 18$, Mann–Whitney *U*-test: mean 1.05 ± 0.35 T/S vs. mean 1.47 ± 0.26 T/S; $p = 0.0133$). The discordance, between number of samples displayed in **Figure 1** (**Supplementary Table 2**) and **Figure 2** (**Supplementary Table 3**), has to be ascribed to the insufficient amount of DNA available to perform the analysis of DNAmAge for three samples that was instead enough to analyze TL in all blood and IS samples.

TABLE 1 | Interval variables in COPD patients with long-acting β2 agonist (LABA)/long-acting muscarinic antagonist (LAMA) and inhaled corticosteroid (ICS)/LABA/LAMA treatments (mean ± SD) and *p*-values of the Mann–Whitney test comparing the two groups.

Variables	All patients *n* = 18	Laba/Lama *n* = 9	ICS/Laba/Lama *n* = 9	*p*-value
Age (years)	72.4 ± 7.7	71.1 ± 9.0	73.7 ± 6.4	0.502
Education (years)	9.9 ± 4.4	9.2 ± 4.5	10.7 ± 4.4	0.504
Body mass index (kg/m^2)	27.62 ± 4.5	27.1 ± 5.1	28.0 ± 4.0	0.561
Systolic pressure (mm Hg)	133.6 ± 12.5	128.3 ± 12.7	138.9 ± 10.2	**0.036**
Diastolic pressure (mm Hg)	81.4 ± 6.6	78.9 ± 6.9	83.9 ± 5.5	0.154
Mother age (years)	30.5 ± 5.9	29.4 ± 7.5	31.4 ± 4.6	0.319
Father age (years)	35.3 ± 6.8	32.8 ± 6.3	37.5 ± 6.8	0.236
Pack years [(cigarettes/20) × years]	33.4 ± 17.6	33.5 ± 15.5	33.3 ± 20.4	0.983
Drinking (age at start, years)	14.6 ± 10.4	15.3 ± 10.5	14.1 ± 11.0	0.910
Alcohol (daily intake last year)	0.6 ± 0.6	0.9 ± 0.7	0.3 ± 0.4	0.123
Sport (IPAQ score)	191.7 ± 376.8	363 ± 483.4	20 ± 42.4	0.077
Leukocytes (10^3/ml)	6.5 ± 1.9	5.9 ± 1.5	7.0 ± 2.3	0.385
Blood red cells (10^3/ml)	4.6 ± 0.4	4.6 ± 0.5	4.6 ± 0.4	0.983
Hemoglobin (g/dl)	13.2 ± 1.8	13.7 ± 2.1	13.7 ± 1.4	0.373
Platelet count (10^3/ml)	231.9 ± 49.5	231.2 ± 40.2	232.5 ± 59.9	0.843
Neutrophils (10^3/ml)	3.99 ± 1.4	3.4 ± 0.9	4.5 ± 1.6	0.094
Lymphocytes (10^3/ml)	1.6 ± 0.6	1.5 ± 0.5	1.6 ± 0.7	0.981
Monocytes (10^3/ml)	0.6 ± 0.2	0.5 ± 0.1	0.6 ± 0.2	0.351
Eosinophils (10^3/ml)	0.2 ± 0.3	0.3 ± 0.4	0.1 ± 0.1	0.979
Basophils (10^3/ml)	0.04 ± 0.04	0.03 ± 0.02	0.05 ± 0.05	0.493
Glycemia (mg/dl)	97.5 ± 35.9	110.3 ± 32.6	80.9 ± 35.3	0.238
C-reactive protein (mg/ml)	3.2 ± 3.2	2.7 ± 1.9	3.7±4.4	0.983
FEV_1 l/s	1.5 ± 0.6	1.9 ± 0.5	0.99 ± 0.3	**0.0003**
FEV_1%	63.1 ± 16.6	77.1 ± 9.1	49.1 ± 7.9	**<0.0001**
FVC l/s	2.4 ± 0.9	3.2 ± 0.8	1.7 ± 0.4	**0.0003**
VC	2.5 ± 0.9	3.2 ± 0.8	1.7 ± 0.4	**0.0003**
TLC	4.9 ± 1.3	5.8 ± 1.3	3.96 ± 0.5	**0.0008**
RV	2.4 ±0.6	2.6 ± 0.7	2.2 ± 0.4	0.474
FEV_1/VC%	58.6 ± 7	60.1 ± 8.0	57.0 ± 6.8	0.489

Bold character is displayed only for significant values.

TABLE 2 | Distribution of categorical variables in COPD patients with *p*-values of the chi-square test comparing the two groups.

Variables	Classes	All patients N (%)	Laba/Lama N (%)	ICS/Laba/Lama N (%)	*p*-value
Sex [@]	Males	9 (50)	6 (67)	3 (33)	0.202
Smoking	Nonsmokers	1 (5)	0 (0)	1 (11)	0.500
	Ex-smokers	15 (83)	8 (89)	7 (78)	0.603
	Smokers	2 (11)	1 (11)	1 (11)	0.999
Drink [@]	Drinkers	13 (72)	7 (78)	6 (67)	0.750
Binge	None	0 (0)	0 (0)	0 (0)	NA
Charlson index	≤1	1 (5)	1 (11)	0 (0)	0.500
	≥ 2 ≤ 4	10 (55)	4 (44)	6 (67)	0.395
	≥5	7 (39)	4 (44)	3 (33)	0.667

Simple linear regression analyses show that blood leukocytes DNAmAge and AgeAcc were highly associated with chronological age ($p < 0.0001$ and $p = 0.0326$ in **Figures 3A,B**), but not the IS cell DNAmAge and AgeAcc ($p = 0.1104$ and $p = 0.3717$, in **Supplementary Figures 1A,B**) as well as IS cell and blood leukocyte TL ($p = 0.460$ and $p = 0.2705$, in **Supplementary Figures 1C,D**). Furthermore, blood leukocyte DNAmAge, AgeAcc, and TL measures were

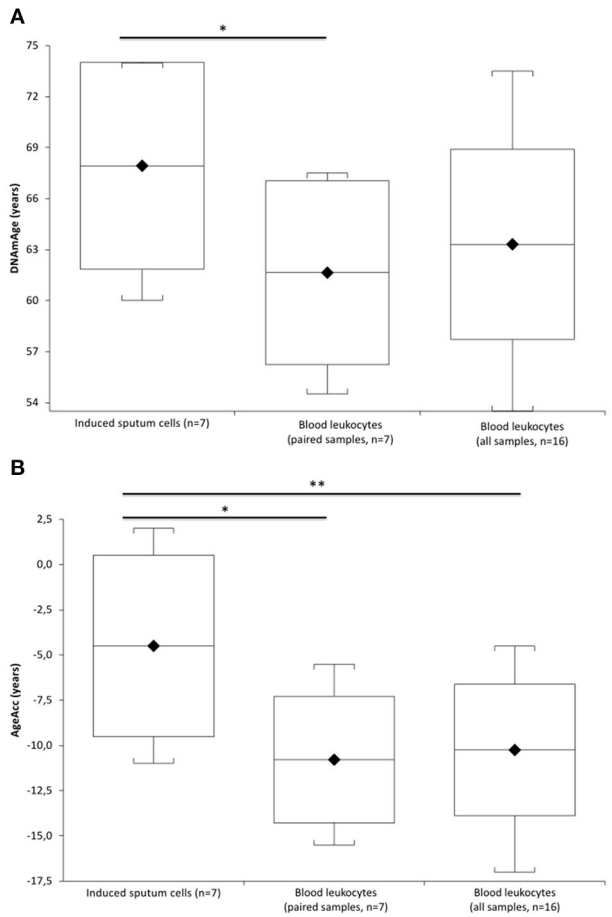

FIGURE 1 | DNAmAge and AgeAcc of the induced sputum cells and blood leukocytes in COPD patients. In **(A)**, box plots show levels of DNAmAge in induced sputum cells ($n = 7$) and in paired blood leukocytes of the same COPD patient ($n = 7$), and in blood leukocyte samples of all COPD patients ($n = 16$). In box plots, the boundary of the box closest to the x-axis indicates the 25th percentile, the line within the box marks the mean, and the boundary of the box farthest from the x-axis indicates the 75th percentile. Whiskers (error bars) above and below the box indicate the 95 and 5th percentiles. The horizontal bar with asterisk indicates the significant comparison between induced sputum cells ($n = 7$) and paired blood leukocytes DNAmAge of the same patient ($n = 7$) (*Paired *t*-test: mean 67.4 ± 5.80 years vs. mean 61.6 ± 5.40 years; $p = 0.0003$). In contrast, the comparison between the DNAmAge of the induced sputum cells ($n = 7$) and all blood leukocytes ($n = 16$) is not significant (Mann–Whitney *U*-test: mean 67.4 ± 5.80 years vs. mean 63.3 ± 5.60 years; $p = 0.1589$). In **(B)**, box plots show levels of AgeAcc in induced sputum cells ($n = 7$) and in paired blood leukocytes of the same COPD patient ($n = 7$), and in blood leukocytes samples of all COPD patients ($n = 16$). In box plots, the boundary of the box closest to the x-axis indicates the 25th percentile, the line within the box marks the mean, and the boundary of the box farthest from the x-axis indicates the 75th percentile. Whiskers (error bars) above and below the box indicate the 95th and 5th percentiles. The horizontal bar with an asterisk indicates the significant comparison between induced sputum cells ($n = 7$) and paired blood leukocytes AgeAcc of the same patient (*Paired *t*-test ($n = 7$): mean −4.5 ± 5.02 years vs. mean −10.8 ± 3.50 years; $p = 0.0003$]. The upper longer horizontal bar with two asterisks indicates the significant comparison between AgeAcc of the induced sputum cells ($n = 7$) and blood leukocytes in all patients ($n = 16$) (**Mann–Whitney *U*-test: mean −4.5 ± 5.02 years vs. mean −10.3 ± 3.63 years; $p = 0.0156$].

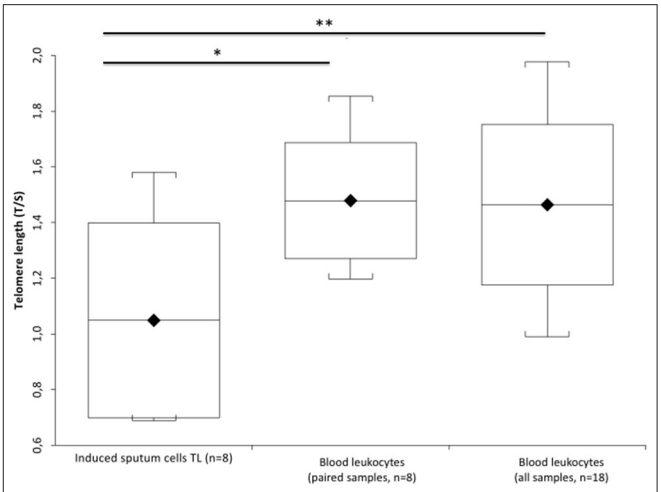

FIGURE 2 | TL of the induced sputum cells and blood leukocytes in COPD patients. Box plots show levels of TL in induced sputum cells ($n = 8$) and in paired blood leukocytes of the same patient ($n = 8$), and blood leukocyte samples of all patients ($n = 18$). In box plots, the boundary of the box closest to the x-axis indicates the 25th percentile, the line within the box marks the mean, and the boundary of the box farthest from the x-axis indicates the 75th percentile. Whiskers (error bars) above and below the box indicate the 95 and 5th percentiles. The horizontal bar with one asterisk indicates the significant comparison between induced sputum cells ($n = 8$) and paired blood leukocyte TL of the same patient ($n = 8$) (*Paired *t*-test: mean 1.05 ± 0.35 T/S vs. mean 1.48 ± 0.21 T/S; $p = 0.0341$). The upper longer horizontal bar with two asterisks indicates the significant comparison between TL of the induced sputum cells ($n = 8$) and blood leukocytes in all patients ($n = 18$) (**MannWhitney *U*-test: mean 1.05 ± 0.35 T/S vs. mean 1.47 ± 0.26 T/S; $p = 0.0133$).

not correlated with leukocytes and different blood cell counts (**Supplementary Table 4**) and to cigarette smoking (pack years) (**Supplementary Table 5**). On the other hand, differential cell counts of IS (**Supplementary Table 6**), in particular macrophage % negatively ($p = 0.033$) and neutrophil % positively ($p = 0.011$), but not eosinophil % ($p = 0.1239$), are related to DNAmAge, while IS cell AgeAcc and TL are not related to cell counts. Furthermore, as expected, neutrophils represent the higher cell type of IS (neutrophils: 68.06 ± 27.03 %, macrophages: 25.19 ± 16.81 % and eosinophils: 6.75 ± 15.70 %). We want also point out that no active smokers were in the IS samples.

Correlation Between Blood Leukocytes and IS Cells Biological Age

Simple linear regression analyses show that blood leukocyte DNAmAge (**Figure 4A**, $p = 0.0026$) and AgeAcc (**Figure 4B**, $p = 0.0037$), but not TL (**Supplementary Figure 2**, $p = 0.4165$), highly correlate with those of the IS cells.

Determinants of Blood Leukocytes and IS Cells DNAmAge, AgeAcc, and TL

Multiple regression analyses of the influence of age, gender, ICS therapy, leukocytes (model a in **Table 3**)/neutrophils (10^3/ml)

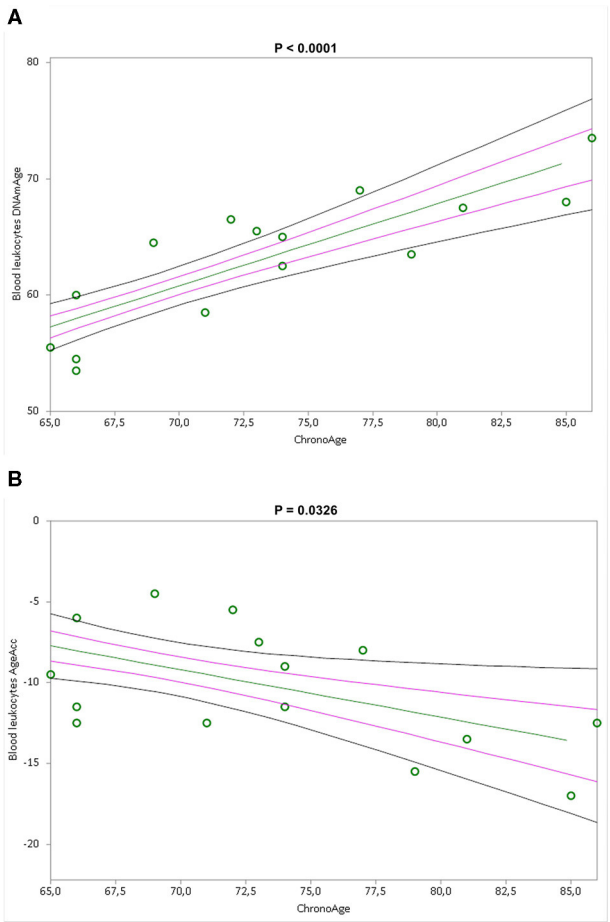

FIGURE 3 | Correlation curves between blood leukocytes DNAmAge **(A)** or AgeAcc **(B)** and chronological age of $n = 16$ COPD patients. In **(A)**, a simple linear regression plot shows the correlation between blood leukocyte DNAmAge and chronological age [correlation coefficient (r) = 0.836142; two-sided $p < 0.0001$], while in **(B)**, simple linear regression linear regression plot showing the correlation between blood leukocyte AgeAcc and chronological age [correlation coefficient (r) = −0.53542; two-sided $p = 0.0326$]. Mean, standard error (SE), and 95% coefficient intervals (CI) are represented as green, pink, and black lines, respectively.

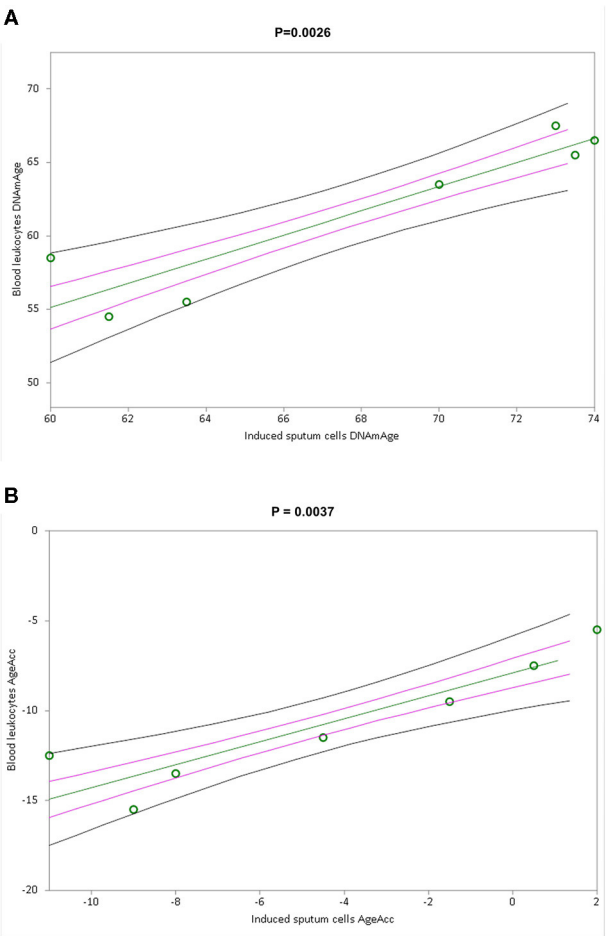

FIGURE 4 | Correlation curves between blood leukocytes and induced sputum cells DNAmAge **(A)** or AgeAcc **(B)** of $n = 7$ COPD patients. In **(A)**, a simple linear regression plot shows the correlation between blood leukocytes and induced sputum cell DNAmAge [correlation coefficient (r) = 0.927245; two-sided $p = 0.0026$], whereas in **(B)**, a simple linear regression plot shows the correlation between blood leukocytes and induced sputum cells AgeAcc [correlation coefficient (r) = 0.916445; two-sided $p = 0.0037$]. Mean, standard error (SE), and 95% coefficient intervals (CI) are represented as green, pink, and black lines, respectively.

(model b in **Supplementary Table 7**), and FEV_1% on rising blood leukocyte TL, DNAmAge, and AgeAcc show that the main determinants are therapy without ICS ($p = 0.0393$ and $p = 0.0538$/$p = 0.0285$ and $p = 0.0507$) and decline in FEV_1% ($p = 0.0158$ and $p = 0.0533$/$p = 0.0154$ and $p = 0.0595$) both when leukocytes and neutrophils (10^3/ml) were considered. Considering blood leukocyte DNAmAge (model a in **Table 3** and model b in **Supplementary Table 7**), age is confirmed as a determinant ($p < 0.0001$). None of the considered variables (age, gender, ICS therapy, leukocytes/neutrophils (10^3/μl), and FEV_1%) influence blood leukocyte TL (**Table 3** and **Supplementary Table 7**).

Multiple linear regression analyses show that IS cell DNAmAge, AgeAcc, and TL are not related to any of the variables considered including age, gender, ICS therapy, neutrophil %, and FEV_1% (**Supplementary Table 8**).

In a multiple linear regression analysis (**Supplementary Table 9**), in which also the type of inhalers was considered as independent variable, determinants that increase blood leukocyte DNAmAge are confirmed to be therapy without ICS, decline in FEV_1%, and age ($p = 0.0502$, $p = 0.0242$, and $p = 0.0001$), but not the type of devices.

DISCUSSION

Aging is an individual and very complex process, and in the multifaceted framework of biological aging a variety of molecular, biochemical, and metabolic changes occur at the cellular level. In

TABLE 3 | Multiple regression analysis (model a) of the influence of age, gender, ICS therapy, leukocytes (10^3/ml), and FEV_1% on blood leukocytes TL, DNAmAge, and AgeAcc.

	Variables	*B*	*R*	*t*	*p*-value
TL					
	Age	b1 = −0.013682	$r = -0.387393$	$t = -1.455632$	$p = 0.1712$
	Gender (female)	b2 = −0.044425	$r = -0.083364$	$t = -0.28979$	$p = 0.7769$
	ICS therapy	b3 = 0.163057	$r = 0.186039$	$t = 0.655908$	$p = 0.5243$
	Leukocytes (10^3/μl)	b4 = −0.041512	$r = -0.3143$	$t = -1.146886$	$p = 0.2738$
	FEV_1%	b5 = −0.002728	$r = -0.097522$	$t = -0.339446$	$p = 0.7401$
DNAmAge					
	Age	b1 = 0.725707	$r = 0.907802$	$t = 6.844848$	$\mathbf{p < 0.0001}$
	Gender (female)	b2 = 1.99263	$r = 0.351855$	$t = 1.188675$	$p = 0.262$
	ICS therapy	b3 = −6.191555	$r = -0.599726$	$t = -2.370016$	$\mathbf{p = 0.0393}$
	Leukocytes (10^3/μl)	b4 = 0.138452	$r = 0.117325$	$t = 0.373595$	$p = 0.7165$
	FEV_1%	b5 = −0.224894	$r = -0.675968$	$t = -2.900673$	$\mathbf{p = 0.0158}$
AgeAcc*					
	Gender (female)	b1 = 3.520267	$r = 0.481361$	$t = 1.821398$	$p = 0.0958$
	ICS therapy	b2 = −6.789407	$r = -0.538208$	$t = -2.11795$	$\mathbf{p = 0.0538}$
	Leukocytes (10^3/μl)	b3 = 0.437876	$r = 0.291221$	$t = 1.009633$	$p = 0.3344$
	FEV_1%	b4 = −0.200247	$r = -0.537241$	$t = -2.112601$	$\mathbf{p = 0.0533}$

*The variable Age is not considered for AgeAcc because of its own definition.
Bold character is displayed only for significant values.

this study, we have determined the biological age of the IS cells and of peripheral blood leukocytes, by measuring the mitotic age (TL) and the non-mitotic epigenetic age (DNAmAge), in COPD patients as a positive paradigm of lung aging.

The main findings stemming from this work reveal that:

a) IS cells are biologically older than blood leukocytes as determined by DNAmAge, AgeAcc, and TL.
b) IS cell DNAmAge and AgeAcc, but not TL, highly correlate with those of blood leukocytes.

To the best of our knowledge, in this study for the first time, DNAmAge and AgeAcc are determined in IS cells and blood leukocytes in the same subject, showing that IS cells are in turn biologically older than blood leukocytes. Furthermore, the accelerated aging of the IS cells compared to that of blood leukocytes confirms that tissues and organs in our body may age at different rates within the same individuals, as we have already proved for donors' heart, where instead DNAmAge is consistently younger than that of blood leukocytes (13). DNA methylation is currently the most promising molecular marker for monitoring biological aging and predicting life expectancy (39). In humans, DNA methylation changes start early in life, as demonstrated by longitudinal studies of infants' blood (40, 41). Notably, these early epigenetic profiles continue to accumulate changes with the advancement of age as shown in twins that do not share the same habits and/or environments (42, 43), indicating aging-associated DNA methylation changes depending on environmental factors. The present study would suggest that airways cells are more exposed/receptive, than blood leukocytes, to track epigenetic changes. Studies have shown smoking-related methylation signatures in peripheral blood (44) and in IS (45, 46). In our study, the higher DNAmAge and AgeAcc of IS cells would suggest that age-related methylation genes would be the target of cigarette smoke injury.

Furthermore, increasing evidence suggests that there is acceleration in lung aging in COPD, with the accumulation of senescent cells in the lung (47). In particular, the chronic inflammation in COPD involves the recruitment of the major inflammatory cells including neutrophils, monocytes/macrophages, and eosinophils into the airways. These cells can be detected in induced sputum (48). The increased percentage of sputum neutrophils is a characteristic of COPD, and this neutrophilic inflammation is induced by cigarette smoke, bacteria, viruses, and oxidative stress resulting in the release of neutrophilic mediators (48). Comparing healthy subjects and COPD patients (matched for age, gender, and tobacco habits), Guiot et al. (49) found a quite different IS cellular profile. In COPD patients, the proportion of sputum neutrophils is generally higher than that of macrophages and linked to the disease severity. In healthy controls, the percentage of macrophages is instead higher than the percentage of neutrophils (49). Our study confirms these results on COPD patients by reporting an increased percentage of neutrophils compared to that of macrophages. Furthermore, while the differential cell count of IS affects biological age, that of blood does not. In particular, we observe an older DNAmAge in relation to an increase in neutrophils and to a decrease in macrophage percentage. This indicates that neutrophils in IS are biological older than macrophages and it may be ascribed to the timeline of leukocytes (neutrophils) bone marrow exit, extravasation, and tissue infiltration (48). It is possible that these innate immune cells present in the IS are activated and thus show accelerated aging. The younger DNAmAge of macrophages may be attributed to their renewal capacity in response to lung injury

(50). Therefore, we cannot exclude that the increased biological aging in IS cells compared to that in blood leukocytes is also attributed to the migration of neutrophils into the lung tissue, suggesting that it may be in the context of COPD.

In line with results on epigenetic age, we found that IS cells' TL is shorter than that of blood leukocytes. The TL attrition found in the specimens derived from the target organ of the disease agrees with previous studies that reported shorter TL in lung tissues of COPD patients, associated with inflammation indicators (51). The TL shortening observed in IS cells of COPD patients is coherent with the hypothesis that an elevated oxidative stress and increased release of pro-inflammatory cytokines, probably derived from the past smoking history, lead to TL attrition (51). Cigarette smoke carries an abundance of well-known genotoxins including polycyclic aromatic hydrocarbons (PAHs), transition metals, and N-nitrosamines that directly, as catalysts for ROS production, and indirectly, through their metabolism, are important sources for ROS generation (52) and trigger the activation of proinflammatory responses in cells of the airway mucosa (53). These and our results disagree, however, with that of Saferali et al. (54) which reported longer TL in the DNA from lung biopsies compared to TL from blood of cancer patients. Divergent results may be ascribed to the disease, i.e., cancer, considered in the study of Saferali, and to the different cell types present in the lung biopsies. In the whole, our results suggest that heterogeneous aging among different tissues in the same disease may be in consequence of several factors, including differential exposure to environmental factors, the consequent oxidative stress, and inflammatory responses with a different tempo-spatial recruitment and distribution of cells.

We found a close nexus between DNAmAge and AgeAcc of the IS cells and blood leukocytes, advising that blood leukocytes, mirroring the respiratory tract status, could be a surrogate tissue for lung aging studies. Two recent large longitudinal studies from SAPALDIA and ECRHS cohorts (55) and KORA and NAS cohorts (29) found an increased blood leukocyte AgeAcc, estimated using the Horvath method (9), in relation to decline in FEV_1, of COPD patients (29) and the general population (55). According to our results, these findings obtained in blood leukocytes would mirror what happens in the respiratory airways. Furthermore, our results could allow us to translate the investigation on biological aging aspects, linked to COPD, into the clinical practice through a simple blood sample. In a real clinical scenario, blood sample may be easily and quickly acquired when visiting COPD patients and sent to the laboratory for biological age analysis. However, some caution is mandatory since, according to our findings, the difference between DNAmAge in IS cells describing biological markers in lung as target tissue and blood leukocytes of COPD patients is almost 6 years. Further studies are therefore needed to optimize the use of blood as a surrogate indicator of IS cells' biological age in clinical practice.

While we confirmed that DNAmAge highly correlates with chronological age, we found that blood leukocyte AgeAcc significantly decreased with increased chronological age, indicating that the epigenetic clock in older patients reduces its speed of aging. Our results agree with the hypothesis that the ticking rate of the epigenetic clock slows down in later life, as proposed by Horvath (9).

Furthermore, we observed that blood leukocyte DNAmAge and AgeAcc significantly decrease (become younger) in COPD patients, with ICS therapy (triple therapy) and with enhancement in lung function (FEV_1%). This also would imply that patients in dual therapy without ICS, because of a few exacerbations in the previous year and/or symptoms (according to the ABCD tool of GOLD guidelines 2021), are those that become older faster. By exploring the effects of systemic corticosteroid exposure, Wan et al. (56) found site-specific differences in blood DNA methylation of COPD patients. ICS anti-inflammatory therapy reduces pro-inflammatory mediator secretion from COPD alveolar macrophages exposed to microbial or oxidative stress triggers (57, 58). Since the inflammation represents a key aspect of aging, the anti-inflammatory role of ICS, together with their ability to determine alterations in the methylation profile, could explain the rejuvenating effect we found in COPD patients with ICS assumption in triple therapy. Our results are in line with those obtained from Lee et al. (59), reporting that asthmatic children exposed to air pollution who received ICS medication had longer TL than non-ICS users. With our findings, we strengthen the current literature that focuses on the role of age and aging-associated signaling pathways as well as their impact on current treatment strategies in the pathogenesis of COPD (60). However, future studies are warranted to determine the possible rejuvenating effect of ICS therapy we detected using biological age indicators.

Furthermore, we discovered that the severity of the disease measured by FEV_1% is associated with the speeding up of blood leukocyte DNAmAge and AgeAcc. In line with our results, the longitudinal data from SAPALDIA and ECRHS cohorts (55) and KORA and NAS cohorts (29) report the association between blood AgeAcc [estimated using the Horvath method (9)] and lung function decline evaluated by FEV_1 (55). FEV_1% punctually expresses lung function as a percentage of the predicted normal value according to reference values based on age, height, weight, sex, and race for each subject using the European Community for Steel and Coal as reference values (34).

The current study presents weak points including the limited sample size of patients. However, the sample size estimation reveals that it is sufficient to obtain statistical significant results. The low yield of samples obtained from the IS technique is another weak point. The IS technique that allows collecting cells from airways, like biopsies and bronchoalveolar lavages, has, however, the advantages of being simple, well-tolerated, safe, reproducible, cost-effective, and noninvasive, making it one of the best alternatives of choice of airway sampling. From our clinical experience, it is a suitable procedure that could be applied in future studies and represents at the same time a strong point of this study. Previous work by Hosgood et al. (61), which measured TL and genetic variation in telomere maintenance genes in IS cells, even if not in the blood of the same subjects, confirms that this method was successful at collecting cells from the lung and bronchi. However, the IS technique must be performed under medical supervision and requires thorough instructions to patients from the specialized operator and the cooperation

of patients, taking into account their medical condition, as respiratory efforts are needed. The last aspect explains the low success rate in our study. However, samples analyzed are adequate from the statistical point of view. The lack of an age-matched control group represents another limitation. Therefore, future research on COPD is mandatory and our future efforts will be directed to increasing the number of patients, also including a control group.

The strength of our study is that it supports the use of a validated noninvasive method of airway sampling for the analysis of biological age indicators in IS for future studies on biological aging of the lung. Furthermore, we showed that TL and DNAmAge in blood leukocytes correlate with those of IS cells. Determining the two most prominent biomarkers of biological age, DNAmAge and TL, with an almost totally automated workflow, is also a strong point of our study. We applied the method proposed by Zbieć-Piekarska et al. (11) to assess DNAmAge, on data from five CpG sites using the locus-specific technology pyrosequencing with some modification as described by Pavanello et al. (12, 13), which makes the technical analysis achievable in few hours. By using this process, we can perform the analyses in a standardized way while also reducing errors (see **Supplementary Figure 3**). It is noteworthy that pyrosequencing has the potential for multiplexing, which can simplify the protocol and reduce the cost of technical analysis. Although a real consensus on how to best detect and describe cellular senescence still remains to be achieved, we demonstrate the applicability of the IS cell mitotic age (TL) and non-mitotic epigenetic age (DNAmAge) analysis in molecular biological age profiling of COPD and relate them to the main clinical characteristics of the COPD disease. We add further information to what already exists on the analysis of IS.

In conclusion, new findings stemming from our study are that we detect a differential aging in the context of COPD by a direct quantitative comparison of cell aging in the airways with that in the more accessible peripheral blood leukocytes, providing additional knowledge which could offer certain potential translation into the disease management.

DATA AVAILABILITY STATEMENT

The raw data supporting the conclusions of this article will be made available by the authors, without undue reservation.

ETHICS STATEMENT

The studies involving human participants were reviewed and approved by Ethics Committee of University-Hospital of Padova (code number 3843/AO/16 and 3054/AO/14). The patients/participants provided their written informed consent to participate in this study.

AUTHOR CONTRIBUTIONS

SP and MC: conceived and designed the study and administrative, technical, or material support (i.e., reporting or organizing data, constructing databases). GG, FL, and PM: patients' enrollment. GG, MC, and SP: provided the samples. MC and SP: performed the samples' analysis and wrote the paper. SP and MC: analyzed the data. All authors contributed to the article and approved the submitted version.

FUNDING

This study was supported by the BIRD175721 funding, provided by the University of Padova, Department of Cardio-Vascular-Thoracic Science and Public Health.

ACKNOWLEDGMENTS

The authors want to thank Dr. Chiara Ventavoli for her contribution in patients' recruitment and the technician Anna Bordin for her contribution in sample collection.

SUPPLEMENTARY MATERIAL

The Supplementary Material for this article can be found online at: https://www.frontiersin.org/articles/10.3389/fmed.2021.690312/full#supplementary-material

REFERENCES

1. López-Otín C, Blasco MA, Partridge L, Serrano M, Kroemer G. The hallmarks of aging. *Cell.* (2013) 153:1194–217. doi: 10.1016/j.cell.2013.05.039
2. Global Initiative for Chronic Obstructive Lung Disease (GOLD). *Global Strategy for the Diagnosis, Management, and Prevention of Chronic Obstructive Pulmonary Disease*. GOLD (2021). Available online at: www.goldcopd.org.
3. MacNee W, Rabinovich RA, Choudhury G. Ageing and the border between health and disease. *Eur Respir.* (2014) 44:1332–52. doi: 10.1183/09031936.00134014
4. Fulop T, Larbi A, Witkowski JM, McElhaney J, Loeb M, Mitnitski A, et al. Aging, frailty and age-related diseases. *Biogerontology.* (2010) 11:547–63. doi: 10.1007/s10522-010-9287-2
5. Levine ME. Modeling the rate of senescence: can estimated biological age predict mortality more accurately than chronological age? *J Gerontol A Biol Sci Med Sci.* (2013) 68:667–74. doi: 10.1093/gerona/gls233
6. Kennedy BK, Berger SL, Brunet A, Campisi J, Cuervo AM, Epel ES, et al. Geroscience: linking aging to chronic disease. *Cell.* (2014) 159:709–13. doi: 10.1016/j.cell.2014.10.039
7. Lowe D, Horvath S, Raj K. Epigenetic clock analyses of cellular senescence and ageing. *Oncotarget.* (2016) 7:8524–31. doi: 10.18632/oncotarget.7383
8. Horvath S, Raj K. DNA methylation-based biomarkers and the epigenetic clock theory of ageing. *Nat Rev Genet.* (2018) 19:371–84. doi: 10.1038/s41576-018-0004-3
9. Horvath S. DNA methylation age of human tissues and cell types. *Genome Biol.* (2013) 14:R115. doi: 10.1186/gb-2013-14-10-r115
10. Hannum G, Guinney J, Zhao L, Zhang L, Hughes G, Sadda S, et al. Genome-wide methylation profiles reveal quantitative views of human aging rates. *Mol Cell.* (2013) 49:359–67. doi: 10.1016/j.molcel.2012.10.016
11. Zbieć-Piekarska R, Spólnicka M, Kupie T, Parys-Proszek A, Makowska, Z., Pałeczka A, et al. Development of a forensically useful age prediction method

based on DNA methylation analysis. *Forensic Sci Int Genet.* (2015) 17:173–9. doi: 10.1016/j.fsigen.2015.05.001
12. Pavanello S, Campisi M, Tona F, Dal Lin C, Iliceto S. Exploring epigenetic age in response to intensive relaxing training: a pilot study to slow down biological age. *Int J Environ Res Public Health.* (2019) 16:3074. doi: 10.3390/ijerph16173074
13. Pavanello S, Campisi M, Fabozzo A, Cibin G, Tarzia V, Toscano G, et al. The biological age of the heart is consistently younger than chronological age. *Sci Rep.* (2020) 10:10752. doi: 10.1038/s41598-020-67622-1
14. Dhingra R, Nwanaji-Enwerem JC, Samet M, Ward-Caviness CK. DNA methylation age—environmental influences, health impacts, and its role in environmental epidemiology. *Curr Envir Health Rpt.* (2018) 5:317–27. doi: 10.1007/s40572-018-0203-2
15. Fransquet PD, Wrigglesworth J, Woods RL, Ernst ME, Ryan J. The epigenetic clock as a predictor of disease and mortality risk: a systematic review and meta-analysis. *Clin Epig.* (2019) 11:62. doi: 10.1186/s13148-019-0656-7
16. Yoon YS, Jin M, Sin DD. Accelerated lung aging and chronic obstructive pulmonary disease. *Expert Rev Respir Med.* (2019) 13:369–80. doi: 10.1080/17476348.2019.1580576
17. Mercado N, Ito K, Barnes PJ. Accelerated aging of the lung in COPD: new concepts. *Thorax.* (2015) 70:482–9. doi: 10.1136/thoraxjnl-2014-206084
18. Burney P, Jithoo A, Kato B, Janson C, Mannino D, Nizankowska-Mogilnicka E, et al. Chronic obstructive pulmonary disease mortality and prevalence: the associations with smoking and poverty–a BOLD analysis. *Thorax.* (2014) 69:465–73. doi: 10.1136/thoraxjnl-2013-204460
19. Gordon SB, Bruce NG, Grigg J, Hibberd PL, Kurmi OP, Lam KB, et al. Respiratory risks from household air pollution in low and middle income countries. *Lancet Respir Med.* (2014) 2:823–60. doi: 10.1016/S2213-2600(14)70168-7
20. MacNee W. Is chronic obstructive pulmonary disease an accelerated aging disease? *Ann Am Thorac Soc.* (2016) 5:S429–37. doi: 10.1513/AnnalsATS.201602-124AW
21. van Eeden SF, Sin DD. Oxidative stress in chronic obstructive pulmonary disease: a lung and systemic process. *Can Respir J.* (2013) 20:27–9. doi: 10.1155/2013/509130
22. Li Y, Rittenhouse-Olson K, Scheider WL, Mu L. Effect of particulate matter air pollution on C-reactive protein: a review of epidemiologic studies. *Rev Environ Health.* (2012) 27:133–49. doi: 10.1515/reveh-2012-0012
23. Kido T, Tamagawa E, Bai N, Suda K, Yang HH, Li Y, et al. Particulate matter induces translocation of IL-6 from the lung to the systemic circulation. *Am J Respir Cell Mol Biol.* (2011) 44:197–204. doi: 10.1165/rcmb.2009-0427OC
24. Eagan TML, Ueland T, Wagner PD, Hardie JA, Mollnes TE, Damås JK, et al. Systemic inflammatory markers in COPD: results from the Bergen COPD cohort study. *Eur Resp J.* (2010) 35:540–8. doi: 10.1183/09031936.00088209
25. Pavanello S, Stendardo M, Mastrangelo G, Bonci M, Bottazzi B, Campisi M, et al. Inflammatory long pentraxin 3 is associated with leukocyte telomere length in night-shift workers. *Front Immunol.* (2017) 8:516. doi: 10.3389/fimmu.2017.00516
26. Myte R, Sundkvist A, Van Guelpen B, Harlid S. Circulating levels of inflammatory markers and DNA methylation, an analysis of repeated samples from a population based cohort. *Epigenetics.* (2019) 14:649–59. doi: 10.1080/15592294.2019.1603962
27. Savale L, Chaouat A, Bastuji-Garin S, Marcos E, Boyer L, Maitre B, et al. Shortened telomeres in circulating leukocytes of patients with chronic obstructive pulmonary disease. *Am J Respir Crit Care Med.* (2009) 179:566–71. doi: 10.1164/rccm.200809-1398OC
28. Albrecht E, Sillanpää E, Karrasch S, Alves AC, Codd V, Hovatta I, et al. Telomere length in circulating leukocytes is associated with lung function and disease. *Eur Respir J.* (2014) 43:983–92. doi: 10.1183/09031936.00046213
29. Breen M, Nwanaji-Enwerem JC, Karrasch S, Flexeder C, Schulz H, Waldenberger M, et al. Accelerated epigenetic aging as a risk factor for chronic obstructive pulmonary disease and decreased lung function in two prospective cohort studies. *Aging.* (2020) 12:16539–54. doi: 10.18632/aging.103784
30. Weiszhar Z, Horvath I. Induced sputum analysis: step by step. *Breathe.* (2013) 9:300–6. doi: 10.1183/20734735.042912
31. Fireman E. Induced sputum and occupational diseases other than asthma. *Curr Opin Allergy Clin Immunol.* (2009) 9:93–6. doi: 10.1097/ACI.0b013e32832921e0
32. Singh D, Agusti A, Anzueto A, Barnes PJ, Bourbeau J, Celli BR, et al. Global strategy for the diagnosis, management, and prevention of chronic obstructive lung disease: the GOLD science committee report 2019. *Eur Respir J.* (2019) 53:1900164. doi: 10.1183/13993003.00164-2019
33. Miller MR, Hankinson J, Brusasco V, Burgos F, Casaburi R, Coates A, et al. Standardisation of spirometry. *Eur Respir J.* (2005) 26:319–38. doi: 10.1183/09031936.05.00034805
34. Sterk PJ, Fabbri LM, Quanjer PH, Cockcroft DW, O'Byrne PM, et al. Airway responsiveness. Standardized challenge testing with pharmacological, physical and sensitizing stimuli in adults. Report working party standardization of lung function tests, European community for steel and coal. Official statement of the European respiratory society. *Eur Respir J Suppl.* (1993) 16:53–83. doi: 10.1183/09041950.053s1693
35. Paggiaro PL, Chanez P, Holz O, Ind PW, Djukanović R, Maestrelli P, et al. Sputum induction. *Eur Respir J Suppl.* (2002) 37:3s–8s. doi: 10.1183/09031936.02.00000302
36. Pavord ID, Pizzichini MM, Pizzichini E, Hargreave FE. The use of induced sputum to investigate airway inflammation. *Thorax.* (1997) 52:498–501. doi: 10.1136/thx.52.6.498
37. Pavanello S, Angelici L, Hoxha M, Cantone L, Campisi M, Tirelli AS, et al. Sterol 27-hydroxylase polymorphism significantly associates with shorter telomere, higher cardiovascular and type-2 diabetes risk in obese subjects. *Front Endocrinol.* (2018) 9:309. doi: 10.3389/fendo.2018.00309
38. Pavanello S, Campisi M, Mastrangelo G, Hoxha M, Bollati V. The effects of everyday-life exposure to polycyclic aromatic hydrocarbons on biological age indicators. *Environ Health*. (2020) 19:128. doi: 10.1186/s12940-020-00669-9
39. Bell CG, Lowe R, Adams PD, Baccarelli AA, Beck S, Bell JT, et al. DNA methylation aging clocks: challenges and recommendations. *Genome Biol.* (2019) 20:249. doi: 10.1186/s13059-019-1824-y
40. Herbstman JB, Wang S, Perera FP, Lederman SA, Vishnevetsky J, Rundle AG, et al. Predictors and consequences of global DNA methylation in cord blood and at three years. *PLoS ONE.* (2013) 8:e72824. doi: 10.1371/journal.pone.0072824
41. Martino DJ, Tulic MK, Gordon L, Hodder M, Richman TR, Metcalfe J, et al. Evidence for age-related and individual-specific changes in DNA methylation profile of mononuclear cells during early immune development in humans. *Epigenetics.* (2011) 6:1085–94. doi: 10.4161/epi.6.9.16401
42. Fraga MF, Ballesta,r E., Paz MF, Ropero S, Setien F, Ballestar ML, et al. Epigenetic differences arise during the lifetime of monozygotic twins. *Proc Natl Acad Sci USA.* (2005) 102:10604–9. doi: 10.1073/pnas.0500398102
43. Tan Q, Heijmans BT, Hjelmborg JVB, Soerensen M, Christensen K, Christiansen L. Epigenetic drift in the aging genome: a ten-year follow-up in an elderly twin cohort. *Int J Epidemiol.* (2016) 45:1146–58. doi: 10.1093/ije/dyw132
44. Machin M, Amaral AF, Wielscher M, Rezwan FI, Imboden M, Jarvelin MR, et al. Systematic review of lung function and COPD with peripheral blood DNA methylation in population based studies. *BMC Pulm Med.* (2017) 17:54. doi: 10.1186/s12890-017-0397-3
45. Sood A, Petersen H, Blanchette CM, Meek P, Picchi MA, Belinsky SA, et al. Wood smoke exposure and gene promoter methylation are associated with increased risk for COPD in smokers. *Am J Respir Crit Care Med.* (2010) 182:1098–104. doi: 10.1164/rccm.201002-0222OC
46. Meek PM, Sood A, Petersen H, Belinsky SA, Tesfaigzi Y. Epigenetic change (GATA-4 gene methylation) is associated with health status in chronic obstructive pulmonary disease. *Biol Res Nurs.* (2015) 17:191–8. doi: 10.1177/1099800414538113
47. Barnes PJ. Targeting cellular senescence as a new approach to chronic obstructive pulmonary disease therapy. *Curr Opin Pharmacol.* (2021) 56:68–73. doi: 10.1016/j.coph.2020.11.004
48. Barnes PJ. Inflammatory endotypes in COPD. *Allergy*. (2019) 74:1249–56. doi: 10.1111/all.13760
49. Guiot J, Demarche S, Henket M, Paulus V, Graff S, Schleich F, et al. Methodology for sputum induction and laboratory processing. *J Vis Exp*. (2017) 130:56612. doi: 10.3791/56612
50. Morales-Nebreda L, Misharin AV, Perlman H, Budinger GR. The heterogeneity of lung macrophages in the susceptibility to disease. *Eur Respir Rev*. (2015) 24:505–9. doi: 10.1183/16000617.0031-2015

51. Amsellem V, Gary-Bobo G, Marcos E, Maitre B, Chaar V, Validire P, et al. Telomere dysfunction causes sustained inflammation in chronic obstructive pulmonary disease. *Am J Respir Crit Care Med.* (2011) 184:1358–66. doi: 10.1164/rccm.201105-0802OC
52. Øvrevik J. Oxidative potential versus biological effects: a review on the relevance of cell-free/abiotic assays as predictors of toxicity from airborne particulate matter. *Int J Mol Sci.* (2019) 20:4772. doi: 10.3390/ijms20194772
53. Øvrevik J, Refsnes M, Låg M, Holme JA, Schwarze PE. Activation of proinflammatory responses in cells of the airway mucosa by particulate matter: oxidant- and non-oxidant-mediated triggering mechanisms. *Biomolecules.* (2015) 5:1399–440. doi: 10.3390/biom5031399
54. Saferali A, Lee J, Sin DD, Rouhani FN, Brantly ML, Sandford AJ. Longer telomere length in COPD patients with alpha1-antitrypsin deficiency independent of lung function. *PLoS ONE.* (2014) 9:e95600. doi: 10.1371/journal.pone.0095600
55. Rezwan FI, Imboden M, Amaral AFS, Wielscher M, Jeong A, Triebner K, et al. Association of adult lung function with accelerated biological aging. *Aging.* (2020) 12:518–42. doi: 10.18632/aging.102639
56. Wan ES, Qiu W, Baccarelli A, Carey VJ, Bacherman H, Rennard SI, et al. Systemic steroid exposure is associated with differential methylation in chronic obstructive pulmonary disease. *Am J Respir Crit Care Med.* (2012) 186:1248–55. doi: 10.1164/rccm.201207-1280OC
57. Higham A, Booth G, Lea S, Southworth T, Plumb J, Singh D. The effects of corticosteroids on COPD lung macrophages: a pooled analysis. *Respir Res.* (2015) 16:98. doi: 10.1186/s12931-015-0260-0
58. Higham A, Karur P, Jackson N, Cunoosamy DM, Jansson P, Singh D. Differential anti-inflammatory effects of budesonide and a p38 MAPK inhibitor AZD7624 on COPD pulmonary cells. *Int J Chron Obstruct Pulmon Dis.* (2018) 13:1279–88. doi: 10.2147/COPD.S159936
59. Lee EY, Oh SS, White MJ, Eng CS, Elhawary JR, Borrell LN, et al. Ambient air pollution, asthma drug response, and telomere length in African American youth. *J Allergy Clin Immunol.* (2019) 144:839–45.e10. doi: 10.1016/j.jaci.2019.06.009
60. Easter M, Bollenbecker S, Barnes JW, Krick S. Targeting aging pathways in chronic obstructive pulmonary disease. *Int J Mol Sci.* (2020) 21:6924. doi: 10.3390/ijms21186924
61. Hosgood HD 3rd, Cawthon R, He X, Chanock S, Lan Q. *Lung Cancer.* (2009) 66:157–61. doi: 10.1016/j.lungcan.2009.02.005

Conflict of Interest: The authors declare that the research was conducted in the absence of any commercial or financial relationships that could be construed as a potential conflict of interest.

Publisher's Note: All claims expressed in this article are solely those of the authors and do not necessarily represent those of their affiliated organizations, or those of the publisher, the editors and the reviewers. Any product that may be evaluated in this article, or claim that may be made by its manufacturer, is not guaranteed or endorsed by the publisher.

frontiers in Medicine

ORIGINAL RESEARCH
published: 10 January 2022
doi: 10.3389/fmed.2021.780294

Quality Management in Polish Biobanking Network—Current Status Before the Implementation of Unified and Harmonized Integrated Quality Management System

Agnieszka Matera-Witkiewicz[1,2]*, *Magdalena Krupińska*[1,2], *Patrycja Sitek*[1,2], *Michał Laskowski*[1,2], *Karolina Zagórska*[1,2] and *Joanna Gleńska-Olender*[1,2]

[1] Screening Biological Activity Assays and Collection of Biological Material Laboratory, Faculty of Pharmacy, Wroclaw Medical University Biobank, Wroclaw Medical University, Wroclaw, Poland, [2] BBMRI.pl Consortium, Wroclaw, Poland

OPEN ACCESS

Edited by:
Victoria Bunik,
Lomonosov Moscow State University, Russia

Reviewed by:
Xiaojiong Jia,
Harvard Medical School, United States
Helmuth Haslacher,
Medical University of Vienna, Austria

***Correspondence:**
Agnieszka Matera-Witkiewicz
agnieszka.matera-witkiewicz@umw.edu.pl;
agnieszka.matera-witkiewicz@umed.wroc.pl

Specialty section:
This article was submitted to Translational Medicine, a section of the journal Frontiers in Medicine

Received: 20 September 2021
Accepted: 29 November 2021
Published: 10 January 2022

Citation:
Matera-Witkiewicz A, Krupińska M, Sitek P, Laskowski M, Zagórska K and Gleńska-Olender J (2022) Quality Management in Polish Biobanking Network—Current Status Before the Implementation of Unified and Harmonized Integrated Quality Management System. Front. Med. 8:780294. doi: 10.3389/fmed.2021.780294

In 2017, Polish Biobanking Network was established in Poland, within BBMRI.pl project titled "Organization of Polish Biobanking Network within the Biobanking and Biomolecular Resources Research Infrastructure BBMRI-ERIC" as a strategic scientific infrastructure concept. One of the key elements of the project was the verification of the current status of QMS in the Polish biobanking institutions and the implementation of common solutions. The main goal was to indicate the current QMS level and determine the starting points for QMS development for each biobank of the Polish Biobanking Network (PBN). Within 3 years, 35 audit visits were performed. The current status and the level of QMS implementation in each biobank were assessed. Five hundred and seventy recommendations were prepared. The data was analyzed using Fischer Exact test to determine whether or not a significant association was observed. Three areas of analysis were covered: (1) BBMRI.pl status, (2) QMS implementation level and (3) private/public party, respectively. The results were discussed within 15 areas. Concluding remarks showed that some differences were observed in the case of subgroups analysis. There is convergence in QMS within the biobanks where Tissue Banks are located. Moreover, some discrepancies between the QMS implementation level in BBMRI.pl Consortium biobanks and PBN biobanks are observed. Nevertheless, the consortium members are obliged to prepare other biobanks willing to enter the PBN as Members/Observers or which already are in the PBN, so that they can meet the requirements of the quality management system that will enable efficient management of biobanking processes in these units. That is why some actions within BBMRI.pl projects are organized to help the whole biobanking community in Poland implement the harmonized solution.

Keywords: quality management system-QMS, audits, biobanking, BBMRI.pl, BBMRI-ERIC, harmonization

INTRODUCTION

One of the main goals of biobanking is an increase in the efficiency and excellence of biomedical research, leading to the creation and development of new medical treatments (1). It can be done by facilitating access to quality-well-defined resources such as biological material (BM) samples with associated data. The pre-analytical handling procedures during collection, transport, qualification, processing and storage of BM may directly implicate the occurrence of the most common errors at the analytical level (2–4). Furthermore, it must be pointed out that even the best analytical tools cannot perform reliable, repeatable and suitable results when the samples and associated data quality are insufficient. Pre-analytical processes consist of a series of complex steps that must be performed and supervised using appropriate tools. That guarantees constant monitoring of the obtained effects and ensures their high quality (5). It also finds application in translational medicine, where the results of preclinical studies directly translate into patient therapy. These studies have to be of the highest quality and credibility as they determine the well-being of patients. The key to ensuring the quality of research is working on the highest quality of biological material and data—this is what biobanks are responsible for.

Quality aspects present an increasing trend in biobanking and biomedical issues. Each year, more quality-derived events are observed. Moreover, professional biobanking infrastructures such as BBMRI-ERIC, societies and organizations, including ISBER (6), ESBB and IARC (7), highly promote and constantly develop the areas of quality management within the biobanking community (8, 9).

The effectiveness and credibility of biobanks require the adoption and implementation of optimal standards of practice, including general principles and standard operating procedures (SOP) (10). Standardization is a key factor that regulates and harmonizes the processes within an organization. BBMRI-ERIC, as an observer liaison for the International Organization for Standardization (ISO), contributes to the biobank relevant international standard developments (ISO/TC276 biotechnology and ISO/TC212 clinical laboratory testing and *in vitro* diagnostic test systems) and in bidirectional information exchange by communicating expert knowledge of the ISO working group to the BBMRI-ERIC community. In 2018, the first dedicated standard for Biobanks was published as ISO 20387:2018: *Biotechnology-Biobanking-General requirements for biobanking* (11).

Also within BBMRI.pl project (12), *Quality Standards for Polish Biobanks* (QSPB) were established as common standards for Polish Biobanking Network (PBN) entities (13). Moreover, a unified QMS audit process was invented and consistently implemented.

The main purpose of the work was to check the current state of QMS and the processes taking place in biobanks that belong to PBN. Based on the previous work, where the general audit areas were established, 15 dedicated areas were defined and analyzed (14). As an outcome, the possibility of a detailed analysis of the QMS level implementation in the PBN biobanks was created. The results were compared within three statistical subgroups with regard to BBMRI.pl status (BBMRI.pl consortium member, PBN Member/Observer), the level of QMS implementation and the type of biobank (private/public sector). The results of the work determine further directions for quality management aspects development within BBMRI.pl. Moreover, it will be a significant input for the biobanking community from all organizations interested in the development of biobanking quality aspects, where the Polish Biobanking Network would be an excellent case study example. The systematic audit process within PBN, where the objective assessment was performed, becomes an effective and reliable tool to support biobanking activity and improvement.

MATERIALS AND METHODS

Audit Process

Audits have been carried out in accordance with the requirements of ISO 19011:2018 regarding PERC (*Planning, Execution, Reporting, Close out/down findings*). The objective evidence was collected using observations, documented information and interviews. The assumption of the audit was based on an accessible process called "*friendly audit*"; a similar formula is also presented in BBMRI.de audit system (15). Also the QM audit process is being noticed in other partner countries from BBMRI-ERIC such as Austria (16) and Finland. Audits were performed as on-site and remote meetings. In total, 35 audits were carried out in 2018–2020.

The main scope of the preliminary audit was to encourage biobanks to start cooperation within BBMRI.pl/PBN and to indicate the starting points where the QMS implementation can be focused and started. The auditors have based the audit process on general ISO standards (9000 series: 9001:2015, 9004:2018) where quality aspects for all organizations are collected. The audit begins with an opening meeting conducted by the lead auditor to introduce the audit team and discuss the audit objectives, scope, and program. During the audit, the auditors took audit samples. During the first visit, the auditors got acquainted with the processes taking place in Biobank, documentation of the type of procedures and instructions (if established and implemented in Biobank), records of processes (paper and/or electronic). During the first visit, the auditors familiarize themselves with: the basis of Biobank's operations (e.g., organizational structure of the unit, approval of the Bioethics Committee or other); with protocols/instructions for handling biological material stored in the biorepository (if established); with the way of marking the material (tube/container description, coding, etc.); with the method of recording Biobank resources (paper documentation and/or an Excel list and/or specialized computer software, etc.); with the method of assessing the quality of the

Abbreviations: QMS, Quality Management System; BM, Biological Material; BBMRI-ERIC, Biobanking and BioMolecuar Resources Research Infrastructure; IC, informed consent; QSPB, Quality Standards for Polish Biobanks; ISBER, International Society for Biological and Environmental Repositories; IARC, International Agency for Research on Cancer; ESBB, European, Middle Eastern & African Society for Biopreservation and Biobanking; GMP, Good Manufacturing Practice; PBN, Polish Biobanking Network; ISO TC, International Organization for Standardization Technical Committee; SOPs, Standard Operating Procedures.

tasks performed (if there are intra-laboratory controls or the center takes part in external laboratory controls); with auxiliary processes concerning, inter alia, the process of hiring and training employees, assigning them authorizations, cooperation with suppliers. After the audit, at the closing meeting, the lead auditor presented and discussed the results of the audit, and the recommendations issued. A summary of the Audit report was a list of observations and recommendations for individual areas of QMS covered by the audit. It was planned that the 1st audit report will not contain non-conformities. The implementation and assessment of the effectiveness of the actions taken should be subject to verification, e.g., during the management review. Verification of the reference to the recommendations is also a part of the next audit (audit input no. 2). The background and audit preparation was presented also in our previous paper (14).

Audited Areas

Cooperation in QM BBMRI-ERIC WGs, the Polish Committee for Standardization in TC 287 Biotechnology and ISO TC 276 WG2 and WG4 provides the best knowledge on standards dedicated to biobanking. The previously determined 13 areas (14) were modified as follows: (1) *Training* was added to *Human Resources Management*, (2) *Traceability of technical and technological processes*, *Controlled storage process* were combined within one area of *Traceability*, (3) *Strategic and operational objectives* were added to *Quality Management*, (4) *Quality control of deliveries* were changed to *Supplies, material management*, (5) *Monitoring of environmental conditions* and *Handling of hazardous* waste were combined in one area of *Environmental and staff hygiene*. Some other areas were also changed or added, which resulted in the establishment of 15 areas (similar to QSPB) (1) *Management of Biobanks*, (2) *Quality management*, (3) *Documentation and records*, (4) *Human Resources Management*, (5) *Ethical and Legal Aspects-ELSI*, (6) *Supplies, materials management*, (7) *Equipment*, (8) *Traceability*, (9) *Environmental and staff hygiene*, (10) *Biobanking processes and quality control*, (11) *Deviations, non-conforming product/data or service*, (12) *Audits*, (13) *Improvement*, (14) *Biobank cooperation in the scientific, research and development area* and (15) *Safety&Security*.

No non-conformities are revealed in the first audit report. Furthermore, the scope of needs and expectations of each biobank toward BBMRI.pl QMS team was estimated.

Data Analysis

The obtained data were subject to statistical and descriptive analysis, with division into three main categories: group 1—comparison of Members/Observers from PBN (35 units) and Consortium members (6 units); group 2—the division into public (36 units) and private biobanks (5 units). Public biobanks were operating at universities, research institutes and public hospitals. Private biobanks operated as part of private laboratories; group 3—biobanks with QMS implemented (11 units), biobanks without QMS (30 units), biobanks operating within tissue and cell banks- the entities specialized with the collection, processing, storage and production of human tissues and cells for therapeutic issues (6 units). Units with established and applied integrated QMS were considered as biobanks with QMS implemented, regardless of whether they are ISO 9001 certified or not. Within the groups, specific subgroups were analyzed.

Categorical data were described using the scores for meeting the requirements of the audit area and percentage using the same criteria as described in the previous paper (14). The associations between the fulfillment of the requirements of the audit area in different groups were tested using Fisher's exact test, where non-random associations between two categorical variables are checked. The statistical significance used in the analysis of contingency tables, also known as cross tabulation, was used. The significance level was set at 0.05. The significance values were as follows: ****/*** extremely significant (p-value 0.001–0.001), ** very significant (0.001–0.01), * significant (0.01–0.05), ns- not significant (>0.05). All statistical analyses and graphs were performed using GraphPad Prism 8.0.1. The results were presented in all figures.

RESULTS

In 2018–2020, 41 audits were performed. The current status and the level of QMS implementation in each biobank were assessed. **Figure 1** presents the results for all PBN biobanks. Within the *ELSI*, 76% of biobanks met the requirements. The majority of biobanks possess well-prepared donor's documentation regarding national and international projects. Nevertheless, the most frequently identified deficiencies within the *ELSI* included incorrect IC forms in terms of the donor's rights and freedoms (20%); lack of records regarding the processing of personal data in accordance with the GDPR (16.7%); lack of procedures for obtaining IC (10%). The results show that effective activity is needed in *Traceability* and *Management of Biobanks* (12% fulfillment). Less than half of the biobanks (24%) had implemented the QMS system as well as the procedures and guidelines for biobanking processes, however, sufficient knowledge was presented. Recommendations indicate the lack of ability to quickly identify a critical device involved in the technological process (33.3%) and the lack of records for consumables and reagents used in the process (16.6%).

Furthermore, the relationship between the level of QMS implementation and the biobank status in PBN (Member/Observer vs. Consortium member) was examined (**Figure 2**). The results presented clearly indicate that differences in the fulfillment of the requirements strictly depend on the significance level. It is worth emphasizing that ELSI aspects are the strongest area where the rules are strictly complied with. The areas where the relatively largest discrepancies were noticed between the analyzed subgroups were *Safety&Security* and *Scientific cooperation*.

However, in the areas of *Traceability* and *Biobanking processes and quality control,* no evidence of dependence between the type of biobank membership and the fulfillment of the requirements was observed. Here, being a Member/Observer or a consortium member did not affect the fulfillment of the requirements.

Further analysis focused on the relationship between the biobanks which are located together with Tissue Banks or

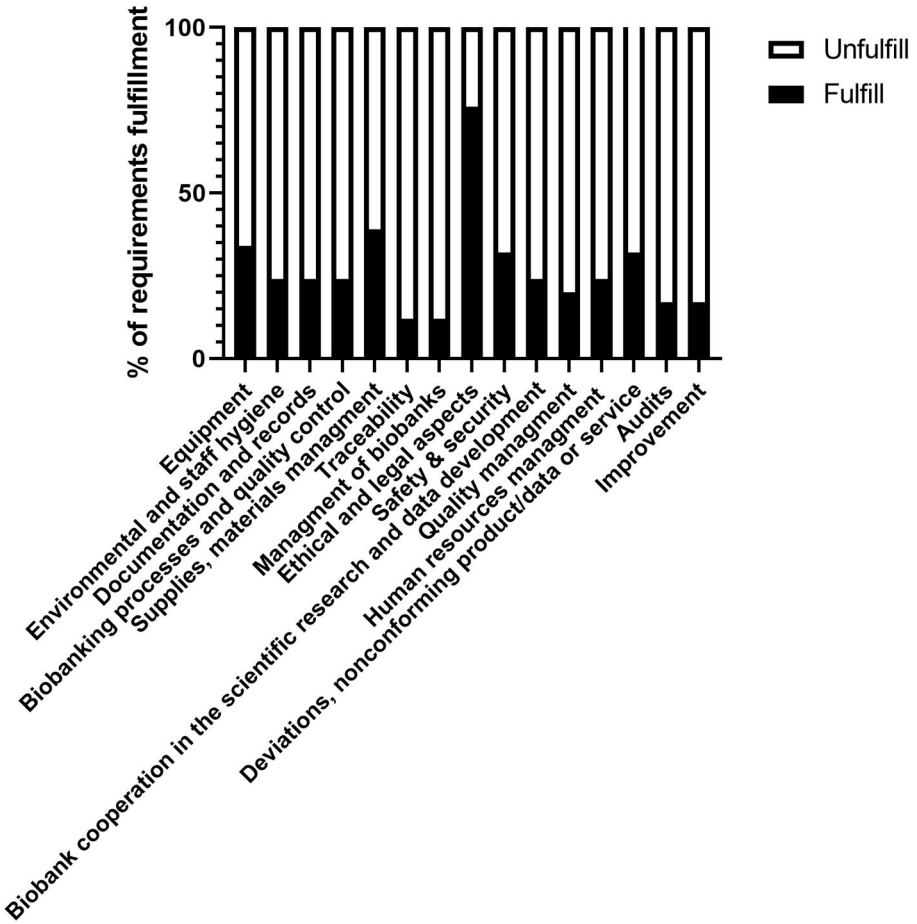

FIGURE 1 | Total number of requirements in the specific areas.

biobanks with different QMS systems (ISO 9001, ISO 17025) implemented vs. biobanks which did not implement any quality system so far (**Figure 3**). In the obtained results regarding *p*-value, the statement that extremely significance was estimated in all areas where the requirements comply with ISO 9001:2015 can be found. The strong importance of QMS implementation in all biobanks including Tissue Banks thus can be underlined. Only within the *ELSI*, no relevance was calculated. This might be due to the lack of any specific restrictions in the QMS. Moreover, the level of the fulfillment of the requirement is not determined by the implementation of different QMS, but it strongly depends on the method of obtaining biological material and related data. All statistically important results of the analysis indicate that the presence of the QMS system, compared to the absence of any system, has a great importance. Biobanks with Tissue Banks or any other quality management system, fulfill the requirements in high percentage level, which is as follows: *Equipment*-82%, *Environmental and staff Hygiene* 73%, *Documentation and records, Management of biobanks*, *Supplies and materials management, ELSI, Traceability, Safety&Security, Scientific Cooperation, Quality Management, Biobanking processes and quality control, Human Resources Management, Audits*, *Deviations, Incompatible product/data or service*, *Improvement*-respectively, 82% with the QMS system. It was also postulated that Biobanks with already implemented QMS systems are better prepared to meet the QSPB requirements. A set of SOPs already introduced in the parent organization helps Biobank to fulfill the QSPB documentation and create procedures which could be used as an integrated system. Also Biobank personnel is more aware when their work is already regulated by another quality system. Biobanks with an implemented quality system could also prepare biobank procedures based on the procedures existing in the other quality management system, which also facilitates compliance with the requirements.

The results show that there is a strong correlation between the implementation of the quality system, including the Tissue Banks requirement regarding GMP, and the lack of system implementation. Implementation of a quality system in the

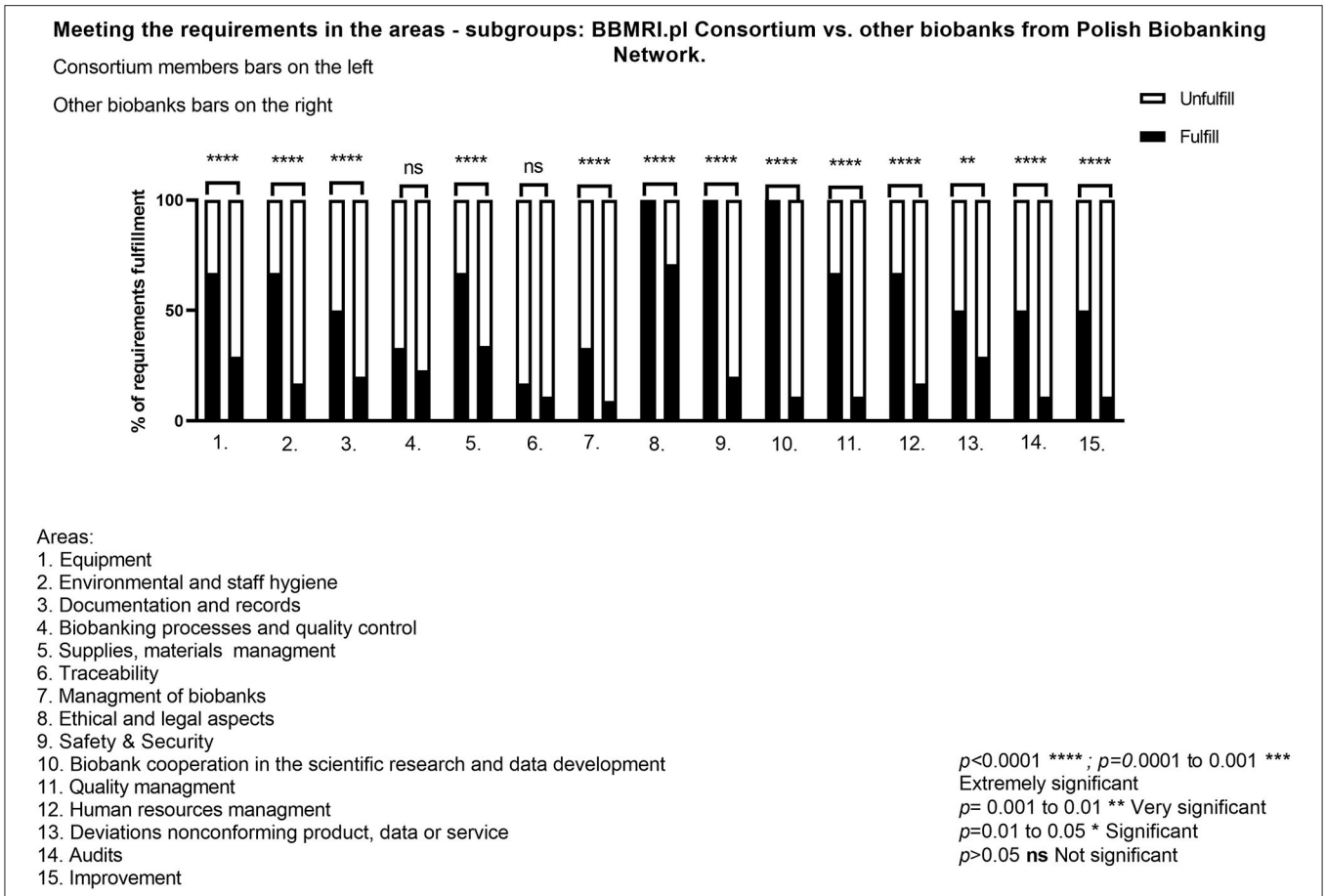

FIGURE 2 | Meeting the requirements in the areas—subgroups: BBMRI.pl Consortium vs. other biobanks from Polish Biobanking Network.

biobank's parent unit leads to better preparation of the entity to meet the requirements of the quality system in the specific areas of biobanking. During the audits, it was shown that biobanks which also functioned as Tissue and Cell Banks had a well-educated awareness of the need to develop and implement procedures describing the course of main and auxiliary processes. As a result, biobanks better understood the assumptions of the quality management system dedicated to biobanks and could more easily meet those assumptions. What is important in this context is the fact that a strong, well-developed quality system in Tissue and Cell Banks could be directly integrated with the arising quality system for biobanks. As a result, many procedures and forms could function simultaneously within two units. The most important aspect increasing the importance of the implementation of a properly prepared quality system in biobanks is the aspect of readiness for national and international cooperation within scientific projects, commercial use in the pharmaceutical industry and the development of personalized medicine, thanks to the awareness of the need for the implementation and maintaining of QMS system. Also, the implementation of the ISO 9001 or ISO 17025 system in the parent unit meant that the biobank staff was more aware of the processes taking place within the unit and the need to develop and use SOPs for well-maintained management of the biobank. It was also shown that the *p*-value factor is not significant for biobanks with QMS systems other than GMP as compared to biobanks with no QMS system implemented. It could be concluded that the reason for this is the fact that Tissue and Cell Banks, like Biobanks, collect human biological material and the way they function is similar despite differences in the final use of the target product.

Excluding Tissue Banks from the statement and comparing biobanks with any other QMS system vs. biobanks without QMS, there was no significant *p*-value (>0.05) in the field of *Traceability* and *ELSI* (**Figure 4**). In other areas, the *p*-value obtained was highly significant. This means that the implementation of the quality system in the organization is crucial for maintaining proper supervision over the areas as well as all system processes and ensuring the adequate quality level to meet the expectations of the customers.

The next analysis concerned the comparison of biobanks from the public and private sectors. It was shown that in three cases, there was no significant *p*-value (>0.05)—in the area of *Biobanking processes and quality control, Safety&Security, Scientific Cooperation.* The remaining comparison for the other twelve audited areas showed a high and extremely

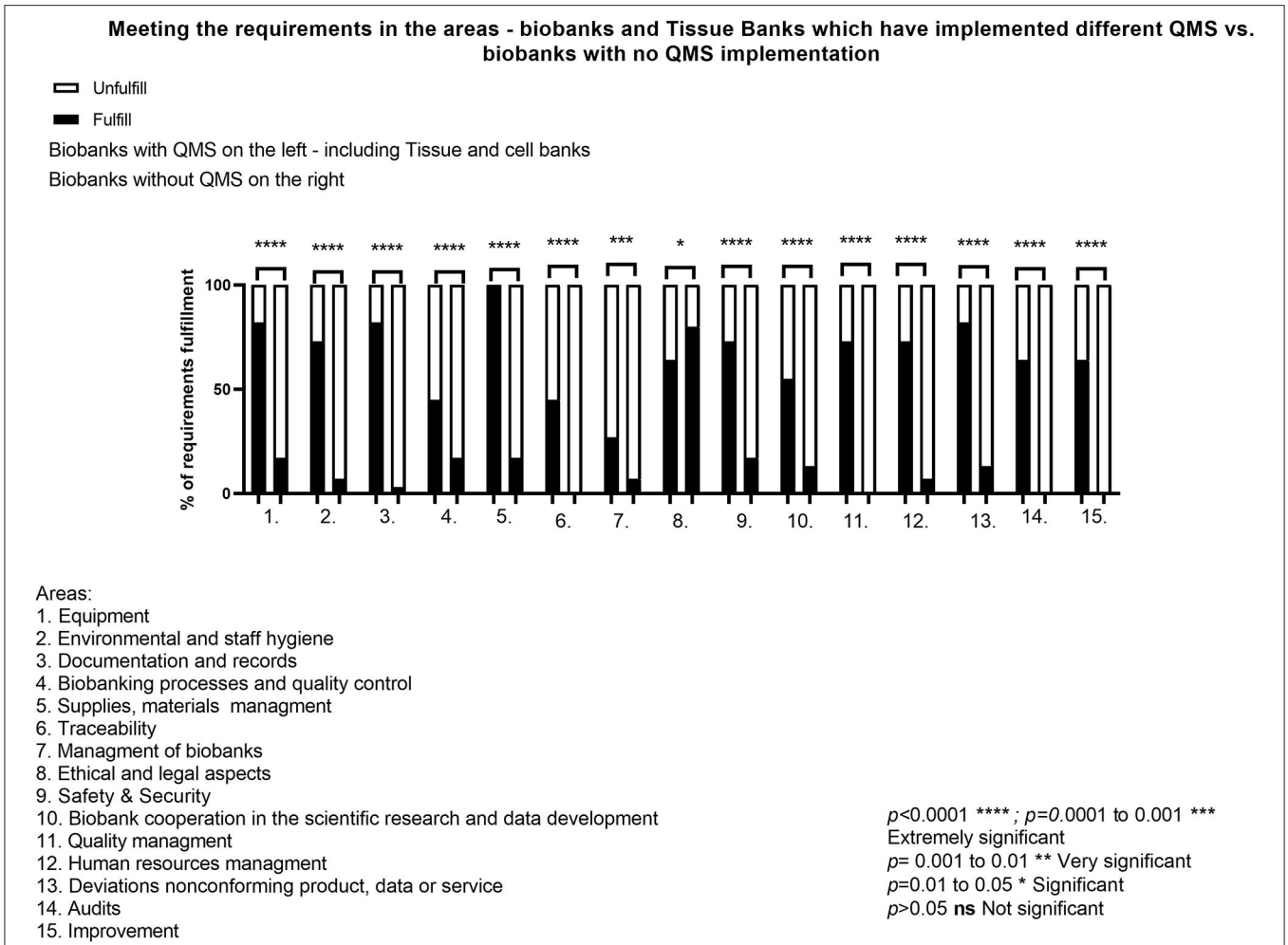

FIGURE 3 | Meeting the requirements in the areas—biobanks and Tissue Banks which have implemented different QMS vs. biobanks with no QMS implementation.

important statistical significance (*p*-value at rate 0.001–0.01 and <0.0001) (**Figure 5**). Almost 90% of the biobanks had developed rules for the collection and processing of BM. The information concerning the method of collection, securing and delivery was presented, but not always as documented information. The biobanks also had implemented the procedure for the supervision of non-conformities, which requires that all deviations from the adopted standards, e.g., technological processes, should be registered, analyzed and assessed in terms of potential risks.

For the ELSI area, public biobanks met the requirements to a higher extent than the private ones. The differences concerning the level of compliance with the requirements and implementation of the QMS system in public and private biobanks mainly depend on financial resources and the management of the units. Private entities usually have more resources to hire an adequate number of staff, as well as to prepare and implement certain procedures. Therefore, in private biobanks, a correlation was observed between the following areas: *Deviations/non-conforming product/data/service*, *Audits*, *Improvement*. When identified during an internal audit, a non-conformity is removed and a new, better solution is implemented. Also, it is important to "stay on the market" and ensure sustainability. The decisions are more efficient and much faster, especially when the implementation leads to potential scientific cooperation between the biobank and an external unit. No significant *p*-value in meeting the requirements related to *Biobanking processes and quality control*, *Safety&Security* and *Scientific cooperation* results mainly from the fact that in both public and private units these areas are usually at a similar level of development and their improvement does not depend on the status of the unit.

DISCUSSION

Comparison with the first summary of 2019 (14) showed a strong trend in ELSI aspects. There was a lower number of identified deficiencies. The verification of Bioethical Committee (BC) approval, donor Informed consent (IC) forms and donor information forms were performed. It was found that over 90%

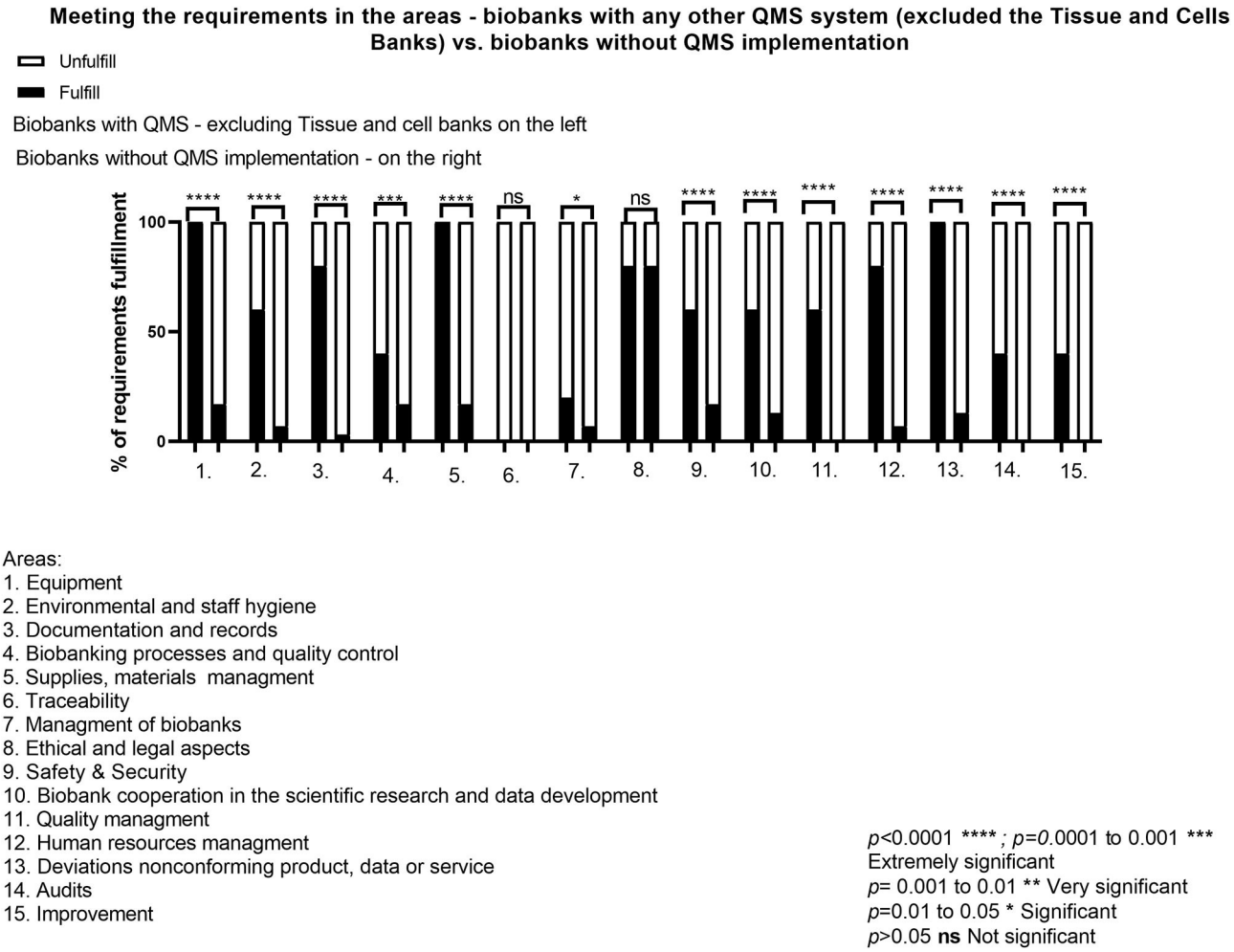

FIGURE 4 | Meeting the requirements in the areas—biobanks with any other QMS system (excluded the Tissue and Cells Banks) vs. biobanks without QMS implementation.

biobank units obtained BC positive opinions for the specific research projects and also IC was preceded before each study performance. Samples data are protected in a dedicated IT system with authorized persons access (password/login). The deficiencies that have been identified: (1) incorrect forms of IC regarding respect for the rights and freedom of a donor (2) lack of records regarding the processing of personal data in accordance with the GDPR, (3) lack of donor's IC, (4) lack of procedures for obtaining IC, (5) lack of procedure in regarding withdrawal of IC and the lack of proceeding in the event of the liquidation of the biobank.

The consciousness of relevance regarding the cooperation between the Data Protection Inspector in the organization, which can influence the improvement of the records which should be implemented on the IC in terms of processing personal data regarding GDPR.

It is worth to point out that on www.bbmri.pl "Code of Conduct on the processing of personal data for the purposes of scientific research by biobanks in Poland," developed by BBMRI.pl ELSI and IT group is available, where useful information are enclosed for ELSI area improvement.

Moreover, consortium members as model biobanks presented at least the level of 50% of the requirements implementation in most of the audited areas. In contrast, Ferdyn et al. indicated that the most developed areas were *Quality control, Environmental monitoring and hazardous waste handling*. During audits, a positive trend was observed that Biobanks present the highest activity in those three areas and developed other areas where biobanks are most active.

Furthermore, the results obtained in the group comparing the QMS level implementation in the biobanks from BBMRI.pl Consortium and biobanks from PBN indicate some significant differences between biobanks that belong to the BBMRI.pl consortium and other biobanks from the PBN. It is supposed that biobanks belonging to the BBMRI.pl consortium are characterized by a better prepared quality management system because they are located in the parent units that have implemented other quality systems, such as ISO 9001, ISO 17025

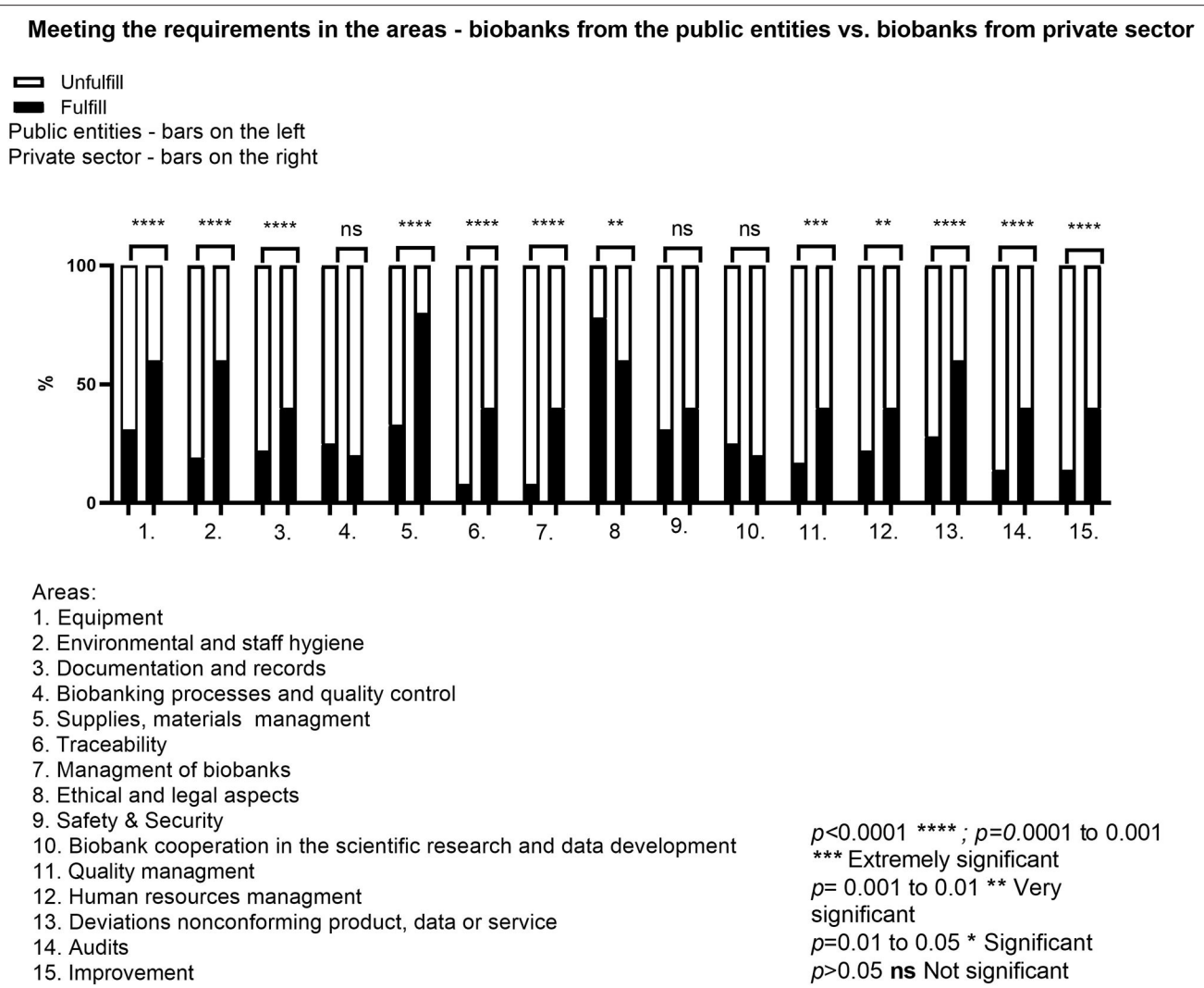

FIGURE 5 | Meeting the requirements in the areas—biobanks from the public entities vs. biobanks from private sector.

or GMP. Moreover, the consortium members are obliged to prepare other biobanks willing to enter the PBN as Members or Observers so that they meet the requirements of the quality management system to enable efficient management of biobanking processes in these units. It is possible to present the hypothesis that biobanks belonging to the BBMRI.pl consortium better meet the QSPB requirements and thus obtain better results during the audit for several important reasons: (1) they have a better developed infrastructure and more resources, (2) they have qualified personnel experienced in the development and implementation of quality systems (3) they have been selected for the consortium due to their high potential to create PBN and thus have an advantage at the start over biobanks outside the consortium.

Audits performed in 2018–2020 brought a lot of relevant information about the status of biobanks. Different levels of QMS implementation have been identified in PBN. The process supervision is highly variable between individual biobanks. Here lies a high potential for improvement and it is a challenge for BBMRI.pl QMS team. Nevertheless, the awareness of the biobank personnel and readiness to improve the QMS and other processes, allows the conclusion that quality assurance is an aspect on which the biobanks want to focus their efforts, using the tools developed as a part of the BBMRI.pl project.

The main goal was to indicate the direction of further harmonized and unified QMS development and improvement, as well as to determine the starting points for QMS development.

All actions prepared within the BBMRI.pl QM Task are carefully designed and planned for a dedicated biobanking unit to unify and implement common solutions in PBN, which are convergent with BBMRI-ERIC general outline. The activities performed were aimed at spreading the idea of biobanking with the assumption that high quality biobank services associated with PBN BBMRI.pl are guaranteed. They are to encourage M/O of

PBN to develop biobanking ideas and self-improvement, which will directly result in increased competitiveness, maintaining high position in the industry, reduced unit costs and, above all, improved quality of BM and associated data. It will also enhance the growth of the number and quality of scientific research and R&D carried out in cooperation with foreign scientific centers or enterprises.

The results of the work allow not only for current improvement but also indicate the direction of further activities of BBMRI.pl QM group, including the process of the cross-audit program in Poland. Thanks to the identification of the areas that require special attention, the training offer will be adapted in order to intensify work in these areas. Moreover, it helps to develop the audit's plans in order to increase their effectiveness, through more precise planning of the auditors' working time.

Today, biobanking units are no longer required to give access to BM only, but also to access high-quality material on which repeatable test results can be carried out. Therefore, the role and tasks of the Quality Management processes in biobanking units are subject to continuous development. Biobanks are responsible for building a quality model and creating a competitive, intuitive system that meets the requirements of a wide spectrum of stakeholders.

Our work clearly shows the improvement of the processes and of the quality system itself in biobanks. This is a positive factor for the further development of translational medicine, taking into account the special role of biobanks. Thanks to this, the activities of the biobanks associated in networks as well as the activities of organizations such as BBMRI.pl directly contribute to the improvement of the quality of preclinical research. This is beneficial both for research funding institutions, the healthcare system and, above all, for patients.

DATA AVAILABILITY STATEMENT

The raw data supporting the conclusions of this article will be made available by the authors, without undue reservation.

AUTHOR CONTRIBUTIONS

AM-W, JG-O, and PS: conceptualization. AM-W, PS, ML, MK, KZ, and JG-O: methodology, validation, investigation, and writing—original draft preparation. MK and AM-W: software. AM-W, PS, MK, and KZ: formal analysis. AM-W, PS, ML, KZ, and JG-O: resources and data curation. AM-W, PS, ML, and JG-O: writing—review and editing. AM-W, PS, and MK: visualization. AM-W: supervision, project administration, and funding acquisition. All authors have read and agreed to the published version of the manuscript.

FUNDING

The project was financed and supported by the Polish Ministry of Science and Higher Education (DIR/WK/2017/2018/01-1). Organization of Polish Biobanking Network within the Biobanking and Biomolecular Resources Research Infrastructure BBMRI-ERIC.

ACKNOWLEDGMENTS

The authors thank all biobanks that have contributed to this work by taking part in the audit process and all auditors for cooperation with QMS BBMRI.pl group during the audits.

REFERENCES

1. Calzolari A, Valerio A, Capone F, Napolitano M, Villa M, Pricci F, et al. The European Research Infrastrucutre of the ESFRI Roadmap in Biological and Medical Sciences: status and perspectives. *Ann Ist Super Sanità*. (2014) 50:178–85. doi: 10.4415/ANN_14_02_12
2. Vaught J, Abayomi A, Peakman T, Watson P, Matzke L, Moore H, et al. Critical issues in international biobanking. *Clin Chem*. (2014) 60:1368–74. doi: 10.1373/clinchem.2014.224469
3. Ellervik C, Vaught J. Preanalytical variables affecting the integrity of human biospecimens in biobanking. *Clin Chem*. (2015) 61:914–34. doi: 10.1373/clinchem.2014.228783
4. Lippi G, Betsou F, Cadamuro J, Cornes M, Fleischhacker M, Fruekilde P, et al. Preanalytical challenges – time for solutions. *Clin Chem Lab Med*. (2019) 57:974–81. doi: 10.1515/cclm-2018-1334
5. Betsou, F. Quality assurance and quality control in biobanking. *Biobank Hum Biospecimens*. (2017) 23–49. doi: 10.1007/978-3-319-55120-3_2
6. *ISBER Best Practices: Recommendations for Repositories*. 4th ed. Vancouver: ISBER (2018).
7. Mendy M, Caboux E, Lawlor RT, Wright J, Wild CP. *Common minimum technical standards and protocols for biobanks dedicated to cancer research – IARC technical publication no. 44*. Lyon: International Agency for Research on Cancer (2017).
8. Doucet M, Becker KF, Björkman J, Bonnet J, Clément B, Daidone MG, et al. Quality matters: 2016 annual conference of the national infrastructures for biobanking. *Biopreserv Biob*. (2017) 15:270–4.
9. Salman A, Baber R, Hannigan L, Habermann JK, Henderson MK, Mayrhofer MT, et al. Quality matters: a global discussion in Qatar. *Biopreserv Biob*. (2019) 17:487–90. doi: 10.1089/bio.2019.0073
10. Müller H, Dagher G, Loibner M, Stumptner C, Kungl P, Zatloukal K. Biobanks for life sciences and personalized medicine: importance of standardization, biosafety, biosecurity, and data management. *Curr Opin Biotechnol*. (2020) 65:45–51. doi: 10.1016/j.copbio.2019.12.004
11. ISO 20387:2018. *Biotechnology – Biobanking – General Requirements for Biobanking*. Available online at: https://www.iso.org/standard/67888.html (accessed December 13, 2021).
12. Witon M, Strapagiel D, Glenska-Olender J, Chróścicka A, Ferdyn K, Skokowski J, et al. Organization of BBMRI.pl: the polish biobanking network. *Biopreserv Biob*. (2017) 15:264–9. doi: 10.1089/bio.2016.0091
13. Ferdyn K, Glenska-Olender J, Zagórska K, Witoń M, Uhrynowska-Tyszkiewicz I, Matera-Witkiewicz A. *Standardy jakości dla biobanków polskich v. 1.00*. Wrocław: Wroclaw Medical University (2019) 195 s.
14. Ferdyn K, Glenska-Olender J, Witon M, Zagórska K, Kozera Ł, Chróścicka A, et al. Quality management system in the BBMRI.pl Consortium: status before the formation of the polish biobanking network. *Biopreserv Biobank*. (2019) 17:401–9. doi: 10.1089/bio.2018.0127

15. Klinger C, von Jagwitz-Biegnitz M, Hartung ML, Hummel M, Specht C. Evaluating the German biobank node as coordinating institution of the German biobank alliance: engaging with stakeholders via survey research. *Biopreserv Biobank*. (2020) 18:64–72. doi: 10.1089/bio.2019.0060
16. Haslacher H, Bayer M, Fiegl H, Gerner M, Hofer P, Korb M, et al. Quality management at the national biobanking level - establishing a culture of mutual trust and support: the BBMRI.at example. *Clin Chem Lab Med*. (2019) 57:301–5. doi: 10.1515/cclm-2019-0491

Conflict of Interest: The authors declare that the research was conducted in the absence of any commercial or financial relationships that could be construed as a potential conflict of interest.

Publisher's Note: All claims expressed in this article are solely those of the authors and do not necessarily represent those of their affiliated organizations, or those of the publisher, the editors and the reviewers. Any product that may be evaluated in this article, or claim that may be made by its manufacturer, is not guaranteed or endorsed by the publisher.

frontiers in Medicine

ORIGINAL RESEARCH
published: 14 March 2022
doi: 10.3389/fmed.2022.792881

Who Is at Risk of Poor Mental Health Following Coronavirus Disease-19 Outpatient Management?

Katharina Hüfner[1], Piotr Tymoszuk[2,3], Dietmar Ausserhofer[4], Sabina Sahanic[3], Alex Pizzini[3], Verena Rass[5], Matyas Galffy[1], Anna Böhm[3], Katharina Kurz[3], Thomas Sonnweber[3], Ivan Tancevski[3], Stefan Kiechl[5], Andreas Huber[6], Barbara Plagg[4], Christian J. Wiedermann[4], Rosa Bellmann-Weiler[3], Herbert Bachler[7], Günter Weiss[3], Giuliano Piccoliori[4], Raimund Helbok[5], Judith Loeffler-Ragg[3] and Barbara Sperner-Unterweger[1]*

[1] Department of Psychiatry, Psychotherapy, Psychosomatics and Medical Psychology, University Hospital for Psychiatry II, Medical University of Innsbruck, Innsbruck, Austria, [2] Data Analytics as a Service Tirol, Innsbruck, Austria, [3] Department of Internal Medicine II, Medical University of Innsbruck, Innsbruck, Austria, [4] Institute of General Practice and Public Health, Claudiana Bolzano, Bolzano, Italy, [5] Department of Neurology, Medical University of Innsbruck, Innsbruck, Austria, [6] Tyrolean Federal Institute for Integrated Care, Innsbruck, Austria, [7] Institute of General Medicine, Medical University of Innsbruck, Innsbruck, Austria

OPEN ACCESS

Edited by:
Victoria Bunik, Lomonosov Moscow State University, Russia

Reviewed by:
Rembert Koczulla, Andreas Rembert Koczulla, Germany
Jurjen Luykx, University Medical Center Utrecht, Netherlands

***Correspondence:**
Judith Loeffler-Ragg
judith.loeffler@i-med.ac.at

Specialty section:
This article was submitted to Translational Medicine, a section of the journal Frontiers in Medicine

Received: *11 October 2021*
Accepted: *11 February 2022*
Published: *14 March 2022*

Citation:
Hüfner K, Tymoszuk P, Ausserhofer D, Sahanic S, Pizzini A, Rass V, Galffy M, Böhm A, Kurz K, Sonnweber T, Tancevski I, Kiechl S, Huber A, Plagg B, Wiedermann CJ, Bellmann-Weiler R, Bachler H, Weiss G, Piccoliori G, Helbok R, Loeffler-Ragg J and Sperner-Unterweger B (2022) Who Is at Risk of Poor Mental Health Following Coronavirus Disease-19 Outpatient Management? Front. Med. 9:792881. doi: 10.3389/fmed.2022.792881

Background: Coronavirus Disease-19 (COVID-19) convalescents are at risk of developing a *de novo* mental health disorder or worsening of a pre-existing one. COVID-19 outpatients have been less well characterized than their hospitalized counterparts. The objectives of our study were to identify indicators for poor mental health following COVID-19 outpatient management and to identify high-risk individuals.

Methods: We conducted a binational online survey study with adult non-hospitalized COVID-19 convalescents (Austria/AT: n = 1,157, Italy/IT: n = 893). Primary endpoints were positive screening for depression and anxiety (Patient Health Questionnaire; PHQ-4) and self-perceived overall mental health (OMH) and quality of life (QoL) rated with 4 point Likert scales. Psychosocial stress was surveyed with a modified PHQ stress module. Associations of the mental health and QoL with socio-demographic, COVID-19 course, and recovery variables were assessed by multi-parameter Random Forest and Poisson modeling. Mental health risk subsets were defined by self-organizing maps (SOMs) and hierarchical clustering algorithms. The survey analyses are publicly available (https://im2-ibk.shinyapps.io/mental_health_dashboard/).

Results: Depression and/or anxiety before infection was reported by 4.6% (IT)/6% (AT) of participants. At a median of 79 days (AT)/96 days (IT) post-COVID-19 onset, 12.4% (AT)/19.3% (IT) of subjects were screened positive for anxiety and 17.3% (AT)/23.2% (IT) for depression. Over one-fifth of the respondents rated their OMH (AT: 21.8%, IT: 24.1%) or QoL (AT: 20.3%, IT: 25.9%) as fair or poor. Psychosocial stress, physical performance loss, high numbers of acute and sub-acute COVID-19 complaints, and the presence of acute and sub-acute neurocognitive symptoms (impaired concentration, confusion, and forgetfulness) were the strongest correlates of deteriorating mental health

and poor QoL. In clustering analysis, these variables defined subsets with a particularly high propensity of post-COVID-19 mental health impairment and decreased QoL. Pre-existing depression or anxiety (DA) was associated with an increased symptom burden during acute COVID-19 and recovery.

Conclusion: Our study revealed a bidirectional relationship between COVID-19 symptoms and mental health. We put forward specific acute symptoms of the disease as "red flags" of mental health deterioration, which should prompt general practitioners to identify non-hospitalized COVID-19 patients who may benefit from early psychological and psychiatric intervention.

Clinical Trial Registration: [ClinicalTrials.gov], identifier [NCT04661462].

Keywords: COVID-19, SARS-CoV-2, depression, anxiety, mental stress, neurocognitive, long COVID, machine learning

BACKGROUND

Prevalence of mental health disorders rose during the Coronavirus Disease-19 (COVID-19) pandemic in the general population from 4% in 2006 (1) to 20% for depression and from 5% in 2008 (2) to 19% for anxiety as of March 2020 (3). The mental health deterioration following COVID-19 was described primarily for hospitalized subjects (4). The frequency of depression or anxiety (DA) following inpatient COVID-19 treatment was estimated at approximately 25% at 5–12 months post-infection (5–7). A real-world analysis of 62,354 COVID-19 in- and outpatients at 14–90 days follow-up revealed the overall incidence of psychiatric conditions of 18.1% [95% CI: 17.6–18.6], out of which 5.8% [5.2–6.4] comprised *de novo* disorders (8). In the latter study, a pre-existing mental illness was put forward as a risk factor for severe acute respiratory syndrome coronavirus 2 (SARS-CoV-2) infection suggestive of a bi-directional relationship between psychiatric conditions and COVID-19 (8). A large, medical record-based comparison of long-term sequelae in COVID-19 and non-COVID-19 healthcare system users revealed an excess of sleep/wake- (relative risk: 14.5 [11.5–17.3]), anxiety/fear- (5.4 [3.4–7.3]), and trauma/stress-related disorders (8.9 [6.6–11.1]) in COVID-19 convalescents at 6 months after the disease onset (9). Post-acute sequelae, such as mental health symptoms, occurred in decreasing frequency in intensive care unit (ICU) patients, inpatients, and outpatients (9). However, a smaller study found that individuals treated as outpatients showed worse mental health outcomes than those treated as inpatients (10). Hence, the prevalence and especially risk factors of mental health conditions and diminished quality of life (QoL) in COVID-19 outpatients, which may be missed from large-scale medical record analyses, cross-sectional, or inpatient survivor studies, are still insufficiently characterized. Since mild ambulatory cases comprise the great majority of COVID-19 patients (11), mental health sequelae may pose a significant burden to the healthcare system. For this reason, the characteristic of risk factors and subsets of patients at particular risk of post-COVID-19 is of great importance.

Machine learning (ML) and clustering algorithms gain importance at risk profiling and patient classification in high dimensional data sets in multiple conditions, i.e., COVID-19 (7, 12–16). The Random Forest procedure employs ensembles of multiple regression or classifier tree models trained in random subsets of the data set to predict the outcome (17, 18). As such, this algorithm is resistant to over-fitting (17) and was shown to reliably deal with large, multi-parameter imbalanced medical data sets (18). It also provides variable importance measures, which allow drawing conclusions on mechanistic relationships between the outcome and specific explanatory factors (15–17, 19). Self-organizing maps (SOMs) are a class of artificial neural network algorithms that enable the reduction of dimensionality of multi-parameter data sets, classification, and clustering of observations with similar properties (20, 21).

The binational "Health after COVID-19 in Tyrol" study aimed at exploring the disease course as well as physical and mental recovery in two cohorts of non-hospitalized convalescents (12). Herein, using multi-parameter Random Forest modeling, we sought to assess the impact of demographics, socioeconomics, comorbidities, COVID-19 disease symptoms and course, and psychosocial stress on anxiety, depression, self-perceived overall mental health (OMH), and QoL. By clustering analysis with SOMs, we aimed to identify individuals at risk of worsening mental health and QoL, which may particularly benefit from early psychological and psychiatric support. Finally, we made the study results publicly available as an online dashboard[1] (22).

MATERIALS AND METHODS

Bioethics

The study was conducted in accordance with the Declaration of Helsinki and the European data policy. Each participant gave a digitally signed informed consent to participate. The study protocol was reviewed and approved by the institutional review boards of the Medical University of Innsbruck (AT, approval number: 1257/2020) and of the Autonomous Province of Bolzano – South Tyrol (IT: 0150701).

[1]https://im2-ibk.shinyapps.io/mental_health_dashboard/

Study Design and Approval

The multi-center online survey study "Health after COVID-19 in Tyrol" (ClinicalTrials.gov: NCT04661462) was conducted between the September 30, 2020 and July 11, 2021 in two cohorts independently recruited in Tyrol/Austria (AT) and South Tyrol/Italy (IT) (12). The study inclusion criteria were residency in the study regions, age of ≥16 (AT) or ≥18 years (IT), and a laboratory-confirmed SARS-CoV-2 infection (PCR or seropositivity). Respondents with a minimum observation time of <28 days between the infection diagnosis and survey completion or hospitalized because of COVID-19 were excluded from the analysis (**Figure 1**). The participants were invited by a public media call (AT and IT) or by their general practitioners (IT).

Measures, Definitions, and Data Transformation

The detailed description of the questionnaire variables is provided in **Supplementary Methods**, **Supplementary Table 1**, and by Sahanic et al. (12).

Symptoms were classified as acute complaints present during the first 2 weeks after clinical onset, sub-acute symptoms present at 2–4 weeks after clinical onset, and persistent symptoms present for ≥4 weeks (12, 15). Confusion, impaired concentration, and forgetfulness were subsumed under "neurocognitive symptoms."

Pre-existing health conditions, such as depression/anxiety and sleep disorders, were surveyed as single items each (question: "Previous illnesses (existing or previously experienced): (1) depression/anxiety, (2) insomnia," answers: present/absent) (12). Self-perceived OMH (question: "How do you currently estimate your mental health?") and QoL (question: "How do you estimate your current QoL?") were rated with a 4-point Likert scale ("excellent," "good," "fair," "poor," scored: 0, 1, 2, and 3). Anxiety and depression at the survey completion were investigated using the Patient Health Questionnaire (PHQ-4) questionnaire (anxiety: "Since the COVID 19 infection: (1) have you experienced nervousness, anxiety? (2) were you not able to stop or control worries?" depression: "Since the COVID 19 infection: (1) have you experienced little interest of satisfaction at your activities? (2) have you experienced prostration, melancholy, or hopelessness?" answers: "not at all," "at some days," "at more than half of the days," "almost every day," scored: 0, 1, 2, and 3) (12, 22, 23), with ≥3 points cutoffs for the clinical signs of depression (DPR) or anxiety (ANX). Psychosocial stress was measured with a modified 7 item PHQ stress module (questions: "How much have you felt affected since the COVID 19 infection by the following problems: (1) worries about your health? (2) Difficulties with the spouse/partner? (3) Burden of care for children parents or other relatives? (4) Stress at work or school/training? (5) Financial problems or worries? (6) Worries about your workplace? (7) Thoughts or dreams on COVID-19?"r answers: "no," "little," "some," "a lot," scored: 0, 1, 2, and 3) (22, 24), without items on weight, sexuality, and past traumatic/serious events; the item on worries/dreams was adapted to COVID-19. Substantial psychosocial stress was defined by a ≥7 points cutoff.

Statistical Analysis

Data were analyzed with R version 4.0.5 (25, 26). Statistical significance of variable median or distribution differences between groups were determined by the Mann–Whitney (effect size: r statistic), Kruskal–Wallis (effect size: η^2 statistic), or χ^2 test (effect size: Cramer's V), as appropriate. The correlation of numeric variables was investigated with Spearman ρ. Categorical variable co-occurrence was assessed by Cohen's κ and Z test. R packages, *DescTools*, *rstatix*, *R Companion*, and *vcd*, were employed in hypothesis testing and correlation analysis. Values of *p* were corrected for multiple comparisons with the Benjamini-Hochberg method (27).

Data pre-processing prior to Random Forest modeling and clustering included minimum/maximum normalization of numeric explanatory features (**Supplementary Table 1**) and mental health scores. Numeric variables were not stratified prior to modeling or clustering. Random Forest models for ANX, DPR, OMH, and QoL scoring were trained, optimized, calibrated, and cross-validated (10-fold) in the AT training cohort (packages *ranger, caret,* and *qgam*) (17, 28–30) and validated in the IT collective. To account for possible effects of diagnosis – survey time, a continuous observation time variable was included in the models (**Supplementary Table 1**). The importance of explanatory variables in Random Forest modeling was determined by the unbiased difference in mean squared error (ΔMSE) (19, 29). The set of common influential variables from mental health and QoL scoring was determined as a common part of the top 20 most influential factors for ANX, DPR, OMH, and QoL each. Modeling of the impact of the common influential variables on mental scoring was accomplished with uni- and multivariate, age- and sex-weighted Poisson regression (12). The effects of the survey duration and observation time on mental health and QoL scoring was investigated by GAM (generalized additive modeling, package mgcv, cubic spline transformation of the independent variable). Clusters of the training AT cohort individuals were defined with the self-organized map procedure (SOM, 13 × 13 unit hexagonal grid, Manhattan distance, package *Kohonen*) and subsequent hierarchical clustering (Ward D2 algorithm, Manhattan distance) (20, 21, 31). Assignment of the test IT cohort participants to the clusters was done with the k-nearest neighbor label propagation algorithm (12, 32). Details of statistical analysis are provided in **Supplementary Methods**.

RESULTS

Sociodemographic and Clinical Characteristics of the Study Cohorts

In total, 1,157 questionnaires in the AT and 893 in the IT cohort were analyzed (**Figure 1**). The observation time defined as the time period between the survey completion and the SARS-CoV-2 infection diagnosis was 79 (median, interquartile range [IQR]: 40–180) and 96 days (median, IQR: 60–140) in the AT and IT collective, respectively (**Table 1**). Detailed characteristics of the cohorts were reported by Sahanic et al. (12). In brief, study participants were predominantly working-age

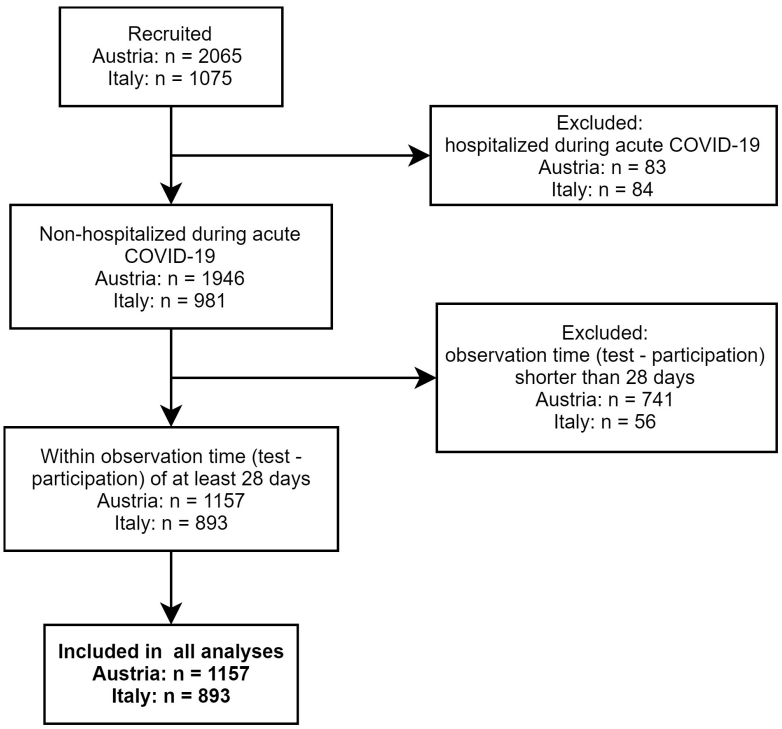

FIGURE 1 | Study inclusion flow diagram.

(31–65 years: AT: 71.9%, IT: 77.8%), women (AT: 65.1%, IT: 68.3%), and actively employed (>80%). Pre-existing co-morbidities were declared by 41.2% (IT) and 49.7% (AT) of participants. DA (AT: 6%, IT: 4.6%) and sleep disorders (AT: 4.6%, IT: 4%) before COVID-19 were reported by roughly 1 of 20 respondents (**Table 1**). Notably, the overlap between the pre-existing depression/anxiety and sleep problems was only minute (AT: Cohen's $\kappa = 0.21$ [95% CI: 0.1–0.31], IT: $\kappa = 0.17$ [0.048–0.3]). The collectives significantly differed in language, education, employment structure, completion time, and the time interval between the diagnosis and survey completion (**Table 1**).

The percentage of asymptomatic cases ranged between 8.3% (AT) and 12.3% (IT) (**Table 2**). Respondents declared a median of 13 complaints (out of 44 features queried, IQR: AT: 9–18, IT: 7–18) present in the first 2 weeks after clinical onset. Persistent symptoms lasting for ≥28 days (12, 15) were discerned in 47.6% (AT) and 49.3% (IT). Roughly half of the participants suffered from acute neurocognitive symptoms (AT: 48%, IT: 50.4%), such as memory or concentration deficits or confusion, in 18.2% (AT) and 22.6% (IT) at least one persistent neurocognitive symptom was present. Self-perceived complete convalescence was reported by 54% (AT) and 63% (IT) of the respondents. The median loss of physical performance following COVID-19 was 13% in the AT (IQR: 1–26%) and 11% in the IT collective (IQR: 0–25%) (**Table 2**).

At the time of study completion, i.e., approximately 12 weeks post-clinical COVID-19 onset, over one-fifth of the participants rated their OMH (AT: 21.8%, IT: 24.1%) or QoL (AT: 20.3%, IT: 25.9%) as fair or poor. At this time point, anxiety (ANX) was observed in 12.4% (AT) and 19.3% (IT), DPR in 17.3% (AT) and 23.2% (IT), and substantial psychosocial stress in 21.3% (AT) and 25.6% (IT) of the respondents [**Table 3** and (22)]. ANX, DPR, OMH, QoL, and stress score displayed non-normal distribution with a strong skewing toward low values (**Supplementary Figure 1**). Importantly, the investigated mental health and QoL rating variables were only weakly associated with the participant's observation time (R^2 <0.011, **Supplementary Figure 2**) and the total survey duration (R^2 <0.026, **Supplementary Figure 3**). ANX, DRP, OMH, and QoL scores were found moderately inter-correlated, with the strongest association between anxiety and depression scoring as well as OMH and QoL rating (**Supplementary Figure 4A**). The highest level of co-occurrence was found for clinical DPR and ANX (AT: Cohen's $\kappa = 0.46$, IT: $\kappa = 0.54$, **Supplementary Figure 4B**). Of note, a similar pattern of correlation and overlap between the investigated mental health and QoL variables was observed in the participant subsets with pre-existing DA (**Supplementary Figure 5**). The QoL rating as well as prevalence of ANX, DPR, and substantial stress were significantly higher in the IT than in the AT study collective, yet these differences were minor (Cramer's $V \leq 0.12$, $r \leq 0.14$) [**Table 3** and (22)].

Key Factors Impacting Mental Health and Quality of Life Outcomes in Coronavirus Disease-19 Convalescents

We sought to investigate how the broad set of 201 surveyed demographic, socioeconomic, medical history, COVID-19

TABLE 1 | Baseline characteristics of the study cohorts.

Variable	AT[1]	IT[1]	Test[2]	pFDR[3]	Effect size[4]
Survey completion	Fall 2020: 63% (734) winter/spring 2021: 37% (423) Complete: *n* = 1157	Fall 2020: 4.4% (39) winter/spring 2021: 96% (854) Complete: *n* = 893	χ^2	$p < 0.001$	$V = 0.6$
Time between survey and diagnosis	Median = 79 [IQR: 40 – 180] Range: 28 – 400 Complete: *n* = 1157	Median = 96 [IQR: 60 – 140] Range: 28 – 390 Complete: *n* = 893	Mann–Whitney	$p < 0.001$	$r = 0.12$
Sex	Female: 65% (753) Male: 35% (404) Complete: *n* = 1157	Female: 68% (610) Male: 32% (283) Complete: *n* = 893	χ^2	ns ($p = 0.19$)	$V = 0.034$
Age	Median = 43 [IQR: 31 – 53] Range: 16 – 94 Complete: *n* = 1156	Median = 45 [IQR: 35 – 55] Range: 18 – 95 Complete: *n* = 891	Mann–Whitney	$p = 0.0041$	$r = 0.069$
	Up to 30 years: 22% (259) 31 – 65 years: 72% (831) >65 years: 5.7% (66) Complete: *n* = 1156	Up to 30 years: 17% (148) 31 – 65 years: 78% (693) >65 years: 5.6% (50) Complete: *n* = 891	χ^2	$p = 0.0082$	$V = 0.073$
Education	Secondary: 44% (505) Apprenticeship: 14% (164) Elementary: 3.6% (41) Tertiary: 38% (444) Complete: *n* = 1154	Secondary: 64% (575) Apprenticeship: 0% (0) Elementary: 0.22% (2) Tertiary: 35% (315) Complete: *n* = 892	χ^2	$p < 0.001$	$V = 0.31$
Employment status	Employed: 81% (939) Unemployed: 9.4% (109) Leave: 1.9% (22) Retired: 7.5% (87) Complete: *n* = 1157	Employed: 82% (728) Unemployed: 8.5% (76) Leave: 1.8% (16) Retired: 8.2% (73) Complete: *n* = 893	χ^2	ns ($p = 0.88$)	$V = 0.02$
Smoking history	Never: 60% (690) Former: 31% (361) Active: 9.2% (106) Complete: *n* = 1157	Never: 66% (588) Former: 24% (215) Active: 10% (90) Complete: *n* = 893	χ^2	$p = 0.004$	$V = 0.079$
Number of co-morbidities	Absent: 50% (582) 1: 29% (332) 2: 12% (142) 3 and more: 8.7% (101) Complete: *n* = 1157	Absent: 59% (525) 1: 25% (219) 2: 11% (102) 3 and more: 5.3% (47) Complete: *n* = 893	χ^2	$p < 0.001$	$V = 0.095$
Daily medication	Absent: 59% (688) 1 – 4 drugs: 38% (440) 5 drugs and more: 2.5% (29) Complete: *n* = 1157	Absent: 73% (649) 1 – 4 drugs: 26% (231) 5 drugs and more: 1.5% (13) Complete: *n* = 893	χ^2	$p < 0.001$	$V = 0.14$

(Continued)

TABLE 1 | (Continued)

Variable	AT[1]	IT[1]	Test[2]	pFDR[3]	Effect size[4]
Depression/anxiety before COVID-19	DA-: 94% (1088) DA+: 6% (69) Complete: *n* = 1157	DA-: 95% (852) DA+: 4.6% (41) Complete: *n* = 893	χ^2	ns ($p = 0.27$)	$V = 0.03$
Sleep disorders before COVID-19	4.6% (53) Complete: *n* = 1157	4% (36) Complete: *n* = 893	χ^2	ns ($p = 0.66$)	$V = 0.013$
Bruxism	7.2% (83) Complete: *n* = 1157	5.3% (47) Complete: *n* = 893	χ^2	ns ($p = 0.14$)	$V = 0.039$
BMI before COVID-19	Normal: 56% (648) Overweigth: 28% (327) Obesity: 15% (175) Complete: *n* = 1150	Normal: 65% (570) Overweigth: 26% (231) Obesity: 9.1% (80) Complete: *n* = 881	χ^2	$p < 0.001$	$V = 0.1$
Hypertension	11% (130) Complete: *n* = 1157	9.4% (84) Complete: *n* = 893	χ^2	ns ($p = 0.27$)	$V = 0.03$
Cardiovascular disease	2.9% (34) Complete: *n* = 1157	2.9% (26) Complete: *n* = 893	χ^2	ns ($p = 1$)	$V = 8e-04$
Pulmonary disease	4.1% (48) Complete: *n* = 1157	2.6% (23) Complete: n = 893	χ^2	ns (p = 0.12)	V = 0.043
Hay fever/allergy	18% (208) Complete: n = 1157	11% (102) Complete: *n* = 893	χ^2	$p < 0.001$	$V = 0.091$
>2 respiratory infections per year	4.4% (51) Complete: *n* = 1157	2.9% (26) Complete: *n* = 893	χ^2	ns ($p = 0.14$)	$V = 0.039$
>2 bacterial infections per year	3.9% (45) Complete: *n* = 1157	1.3% (12) Complete: *n* = 893	χ^2	$p = 0.0021$	$V = 0.077$

[1] *For categorical variables: percentage of the complete answers (n individuals). AT: Austria/Tyrol cohort, IT: Italy/South Tyrol cohort.*
[2] *Statistical test used to compare differences in median values (numeric variables) or distribution (categorical variables) for the AT vs. IT comparison.*
[3] *Test values of p for the AT vs IT difference corrected for multiple comparisons with Benjamini-Hochberg (FDR) method, ns: not significant.*
[4] *Effect size of the AT vs. IT difference: Wilcoxon r for numeric variables or Cramer's V for categorical variables.*

TABLE 2 | Characteristics of the course of SARS-CoV2 infection and convalescence in the study cohorts.

Variable	AT[1]	IT[1]	Test[2]	pFDR[3]	Effect size[4]
SARS-CoV2 outbreak	Spring 2020: 27% (309) Summer/fall 2020: 68% (789) Winter/spring 2021: 5.1% (59) Complete: *n* = 1157	Spring 2020: 16% (144) Summer/fall 2020: 54% (484) Winter/spring 2021: 30% (265) Complete: *n* = 893	χ^2	$p < 0.001$	$V = 0.34$
Acute COVID-19 symptoms	92% (1060) Complete: *n* = 1156	88% (782) Complete: *n* = 892	χ^2	$p = 0.0067$	$V = 0.066$
Number of acute symptoms	Median = 13 [IQR: 9 – 18] Range: 0 – 42 Complete: *n* = 1156	Median = 13 [IQR: 7 – 18] Range: 0 – 39 Complete: *n* = 892	Mann–Whitney	ns ($p = 0.13$)	$r = 0.038$
Number of acute neurocognitive symptoms	Median = 1 [IQR: 0 – 2] Range: 0 – 3 Complete: *n* = 1157	Median = 0 [IQR: 0 – 2] Range: 0 – 3 Complete: *n* = 893	Mann–Whitney	ns ($p = 0.66$)	$r = 0.011$
	0: 50% (574) 1: 20% (236) 2: 17% (197) 3: 13% (150) Complete: *n* = 1157	0: 52% (464) 1: 14% (127) 2: 16% (146) 3: 17% (156) Complete: *n* = 893	χ^2	$p < 0.001$	$V = 0.095$
Persistent COVID-19 symptoms	48% (550) Complete: *n* = 1156	49% (440) Complete: *n* = 892	χ^2	ns ($p = 0.52$)	$V = 0.017$
Number of persistent symptoms	Median = 0 [IQR: 0 – 3] Range: 0 – 34 Complete: *n* = 1156	Median = 0 [IQR: 0 – 3] Range: 0 – 29 Complete: *n* = 892	Mann–Whitney	ns ($p = 0.56$)	$r = 0.015$
Number of persistent neurocognitive symptoms	Median = 0 [IQR: 0 – 0] Range: 0 – 3 Complete: *n* = 1157	Median = 0 [IQR: 0 – 0] Range: 0 – 3 Complete: *n* = 893	Mann–Whitney	$p = 0.0067$	$r = 0.065$
	0: 82% (946) 1: 7.3% (84) 2: 7.8% (90) 3: 3.2% (37) Complete: *n* = 1157	0: 77% (691) 1: 5.6% (50) 2: 9.6% (86) 3: 7.4% (66) Complete: *n* = 893	χ^2	$p < 0.001$	$V = 0.11$
Physical performance loss	Median = 13 [IQR: 1 – 26] Range: 0 – 100 Complete: *n* = 1151	Median = 11 [IQR: 0 – 25] Range: 0 – 100 Complete: *n* = 884	Mann–Whitney	ns ($p = 0.35$)	$r = 0.024$
Complete convalescence	54% (624) Complete: *n* = 1155	63% (563) Complete: *n* = 889	χ^2	$p < 0.001$	$V = 0.093$

[1] *Percentage of the complete answers (n individuals). AT: Austria/Tyrol cohort, IT: Italy/South Tyrol cohort.*
[2] *Statistical test used to compare differences in median values (numeric variables) or distribution (categorical variables) for the AT vs. IT comparison.*
[3] *Test value of p for the AT vs IT difference corrected for multiple comparisons with Benjamini-Hochberg (FDR) method, ns: not significant.*
[4] *Effect size of the AT vs. IT difference: Wilcoxon r for numeric variables or Cramer's V for categorical variables.*

TABLE 3 | Rating of the mental health following Coronavirus Disease-19 (COVID-19) in the study cohorts.

Variable	AT[1]	IT[1]	Test[2]	pFDR[3]	Effect size[4]
Overall mental health	Poor: 3.5% (40) Fair: 18% (212) Good: 49% (562) Excellent: 30% (343) Complete: *n* = 1157	Poor: 2.9% (26) Fair: 21% (189) Good: 48% (430) Excellent: 28% (248) Complete: *n* = 893	χ^2	ns ($p = 0.44$)	$V = 0.039$
Overall mental health score	Median = 1 [IQR: 0 – 1] Range: 0 – 3 Complete: *n* = 1157	Median = 1 [IQR: 0 – 1] Range: 0 – 3 Complete: *n* = 893	Mann–Whitney	ns ($p = 0.29$)	$r = 0.027$
Quality of life	Poor: 4.3% (50) Fair: 16% (185) Good: 51% (590) Excellent: 29% (332) Complete: *n* = 1157	Poor: 3.4% (30) Fair: 23% (201) Good: 54% (485) Excellent: 20% (177) Complete: *n* = 893	χ^2	$p < 0.001$	$V = 0.12$
Quality of life score	Median = 1 [IQR: 0 – 1] Range: 0 – 3 Complete: *n* = 1157	Median = 1 [IQR: 1 – 2] Range: 0 – 3 Complete: *n* = 893	Mann–Whitney	$p < 0.001$	$r = 0.1$
Depression Score	Median = 1 [IQR: 0 – 2] Range: 0 – 6 Complete: *n* = 1154	Median = 1 [IQR: 0 – 2] Range: 0 – 6 Complete: *n* = 892	Mann–Whitney	$p = 0.0082$	$r = 0.063$
Depression screening-positive	17% (200) Complete: *n* = 1154	23% (207) Complete: *n* = 892	χ^2	$p = 0.0028$	$V = 0.073$
Anxiety score	Median = 0 [IQR: 0 – 2] Range: 0 – 6 Complete: *n* = 1151	Median = 1 [IQR: 0 – 2] Range: 0 – 6 Complete: *n* = 893	Mann–Whitney	$p < 0.001$	$r = 0.14$
Anxiety screening-positive	12% (143) Complete: *n* = 1151	19% (172) Complete: *n* = 893	χ^2	$p < 0.001$	$V = 0.094$
Psychosocial stress score	Median = 4 [IQR: 2 – 6] Range: 0 – 19 Complete: *n* = 1153	Median = 4 [IQR: 2 – 7] Range: 0 – 19 Complete: *n* = 890	Mann–Whitney	ns ($p = 0.47$)	$r = 0.019$
Substantial psychosocial stress	21% (246) Complete: *n* = 1153	26% (228) Complete: *n* = 890	χ^2	$p = 0.045$	$V = 0.05$

[1]*Percentage of the complete answers (n individuals). AT: Austria/Tyrol cohort, IT: Italy/South Tyrol cohort.*
[2]*Statistical test used to compare differences in median values (numeric variables) or distribution (categorical variables) for the AT vs. IT comparison.*
[3]*Test value of p for the AT vs. IT difference corrected for multiple comparisons with Benjamini-Hochberg (FDR) method, ns: not significant.*
[4]*Effect size of the AT vs. IT difference: Wilcoxon r for numeric variables or Cramer's V for categorical variables.*

course, and recovery parameters (**Supplementary Table 1**) affects the minimum/maximum-normalized rating of anxiety, depression, self-perceived OMH, and QoL. To this end, Random Forest models were trained, optimized, and calibrated in the AT collective (17, 28–30). Such models demonstrated good performance with the training AT data (root mean squared error [RMSE]: 0.15–0.18) and moderate-to-good accuracy in the validation IT cohort (RMSE: 0.21–0.23). The amount of explained variance was roughly twice as large in the AT cohort (pseudo-R^2: 0.50–0.65) as in the validation IT data set (pseudo-R^2: 0.24–0.37) (**Figure 2A** and **Supplementary Figures 6–9**).

Psychosocial stress rating and percentage of physical performance following COVID-19 were found to affect the ANX, DPR, OMH, and QoL scoring to the greatest extent in the AT cohort. The set of the 20 most important factors for each investigated response also included the total number of acute, sub-acute, and persistent COVID-19 symptoms as well as the number of specific neurocognitive symptoms. DA before COVID-19 impacted substantially the ANX, DPR, and OMH rating, pre-existing sleep disorders were found to be an influential factor for the DPR and OMH scores (**Supplementary Figures 6–9**). A total of eight highly influential explanatory variables were shared by the ANX, DPR, OMH, and QoL rating and included psychosocial stress, physical performance loss, acute and sub-acute symptom burden, counts of acute and sub-acute neurocognitive symptoms, as well as concentration deficits during acute and sub-acute COVID-19 (**Figure 2B**). In multi-variate Poisson modeling, this influential parameter set was associated with 22–37% explained variability in the mental health and QoL scoring both in the AT and IT collective (**Supplementary Figure 10**). Psychosocial stress, acute concentration deficits, symptom burden, and physical performance impairment are the strongest single explanatory features both in univariate and multivariate Poisson modeling of the ANX, DPR, OMH, and QoL rating following COVID-19 (**Figures 3A–D**, **Supplementary Figure 10**, and **Supplementary Table 2**).

Of note, the performance of the Random Forest models of ANX, DPR, OMH, and QoL modeling developed in the entire AT

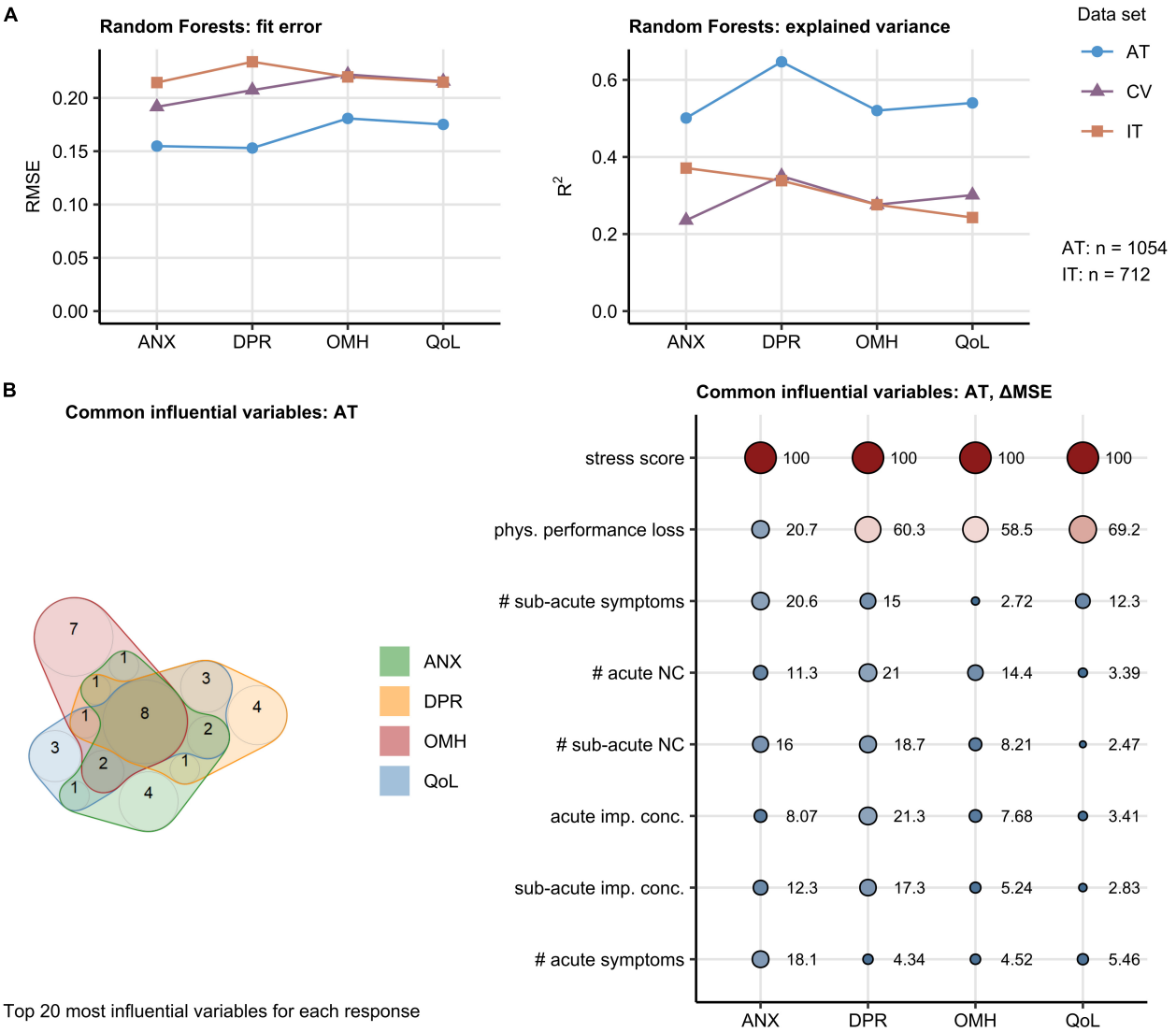

FIGURE 2 | Random Forest modeling of the mental health and quality of life scoring during Coronavirus Disease-19 (COVID-19) convalescence. The effects of 201 demographic, clinical, socioeconomic, and psychosocial factors (**Supplementary Table 1**) on the anxiety (ANX), depression (DPR), overall mental health (OMH), and quality of life (QoL) scoring were modeled with the Random Forest technique. Numeric variables were minimum/maximum normalized prior to modeling. The models were trained and calibrated in Austria (AT) cohort, 10-fold cross-validated (CV), and their predictions validated in Italy (IT) cohort. The top 20 most influential explanatory variables were identified in the AT cohort for each mental health and life quality score by unbiased ΔMSE statistic (**Supplementary Figures 6–9**). The numbers of complete observations are indicated in **(A)**. **(A)** Random Forest model performance measured by root mean squared error (RMSE) and the fraction of explained variance in mental health and quality of life scoring expressed as R^2. **(B)** Identification of common influential explanatory variables. Left: overlap in the top 20 most influential explanatory variables presented in a quasi-proportional Venn plot. Right: ΔMSE statistics for the most influential explanatory statistics shared by all responses, point size and color corresponds to the ΔMSE value. NC: neurocognitive symptoms, imp. conc.: impaired concentration, phys.: physical, #: number of.

cohort was similar in the subsets of participants with and without pre-existing DA (**Supplementary Figure 11**).

Acute and Sub-Acute Neurocognitive Symptoms and Polysymptomatic Coronavirus Disease-19 Define the Subjects at Risk of Poor Mental Health

Next, we explored whether the set of the eight most influential factors impacting the mental health and QoL in the AT or IT cohort (**Figure 2**) may be applied to identify convalescents at particular risk of mental health deterioration following COVID-19.

By an SOM and hierarchical clustering (20, 31), three participant subsets, termed "Low Risk" (LR), "Intermediate Risk" (IR), and "High Risk" (HR) Mental Health Risk Clusters, were defined in the training AT cohort and validated in the IT collective with high consistency (between-cluster to total variance ratio, AT: 0.90, IT: 0.90) (**Figure 4A** and **Supplementary Figure 12**). The primary hallmarks of the IR and HR subsets

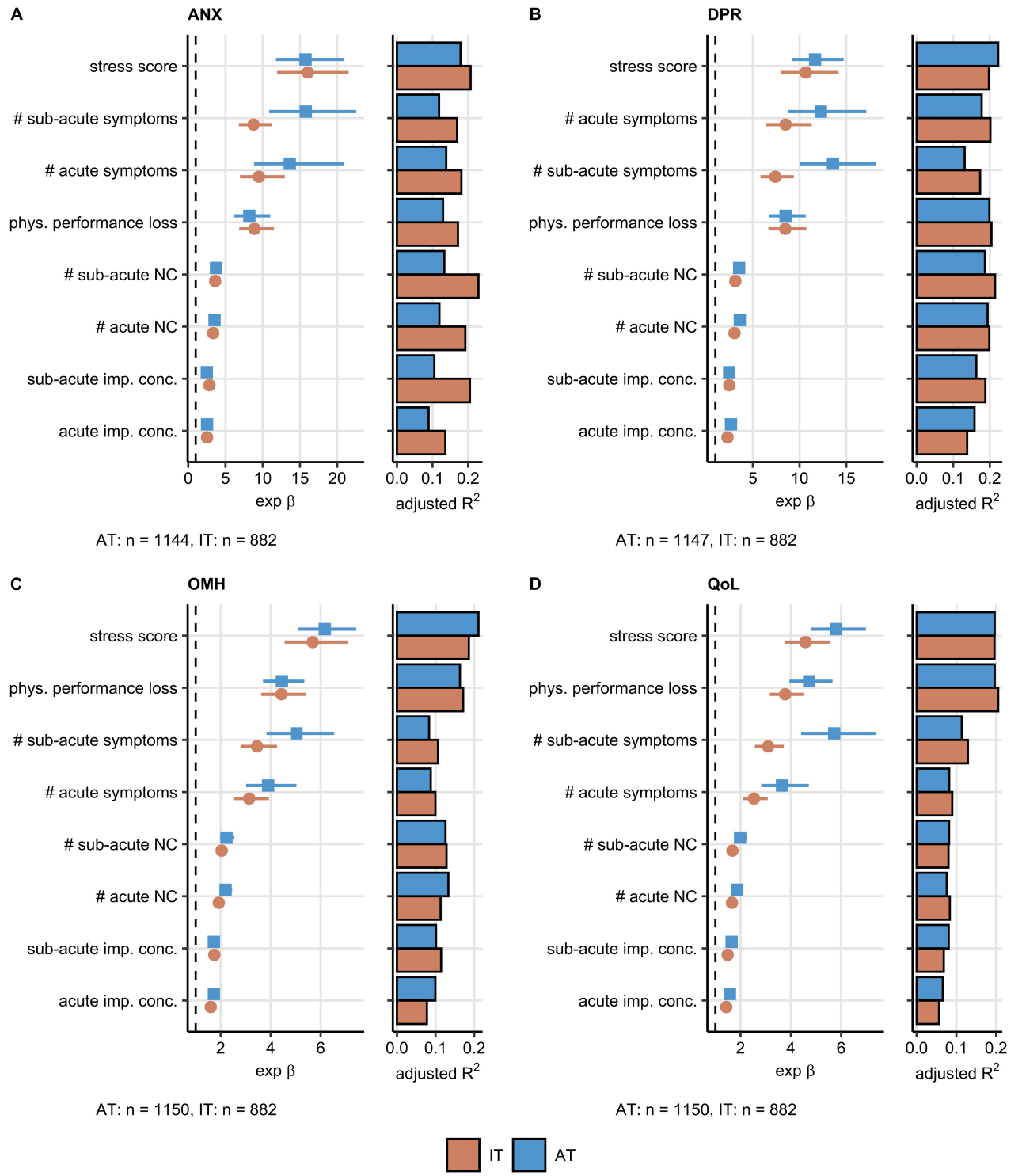

FIGURE 3 | Association of the most influential factors with the mental health readouts investigated by univariable modeling. Association of the most influential factors for the mental health and quality of life scoring (**Figure 2B**) with the anxiety (ANX) **(A)**, depression (DPR) **(B)**, overall mental health (OMH) **(C)**, and quality of life (QoL) **(D)** rating was investigated by univariable, age- and sex-weighted Poisson regression (**Supplementary Table 2**). Numeric variables were minimum/maximum normalized prior to modeling. Exponent β estimate values with 95% *Cis* presented as Forest plots. Explained variance fraction estimated by adjusted R^2 is presented in adjunct bar plots. The numbers of complete observations are shown under the plots. AT: Austria, IT: Italy. NC: neurocognitive symptoms, imp. conc.: impaired concentration, phys.: physical, #: number of.

were highly frequent acute neurocognitive symptoms and, in particular, impaired concentration as well as polysymptomatic acute COVID-19. The HR subset differed from the IR cluster by the presence of sub-acute neurocognitive complaints, i.e., confusion, memory, or concentration deficits beyond the first 2 weeks of the disease (**Figure 4B**).

Notably, the HR followed by the IR group demonstrated significantly worse ANX, DPR, OMH, and QoL rating as well as higher frequencies of clinically relevant anxiety (AT: 6.4% in LR, 25.4% in HR, IT: 8.6% in LR, 41.7% in HR) and depression (AT: 5.9% in LR, 36.6% in HR, IT: 10.7% in LR, 47.9% in HR) compared with the LR cluster [**Figure 5** and (22)]. In addition, the IR and HR clusters were characterized by lower frequency of self-reported complete convalescence, greater weight loss, higher levels of stress, higher symptom duration time, as well as higher frequency of acute and sub-acute fatigue, tiredness, and sleep problems as compared with the LR cluster in both AT and IT cohort (**Supplementary Figures 13**, **14** and **Supplementary Table 3**).

Depression or Anxiety Before Coronavirus Disease-19 Is Linked to a Higher Symptom Burden and Persistence

Finally, we sought to investigate differences in the pre-COVID-19 characteristics, disease course, and recovery between the participants with and without pre-existing DA.

In both study collectives, the DA-positive participants suffered from significantly more comorbidities, sleep disorders, and frequent respiratory infections before COVID-19 than the DA-negative respondents and, consequently, had a higher level of daily medication. Participants declaring anxiety/depression before the infection had a 20% higher median burden of overall acute COVID-19 symptoms and >30% more acute neurocognitive symptoms compared with the DA-free subset. The DA-positive participants were also more frequently affected by acute dizziness, acute, and sub-acute forgetfulness. DA before COVID-19 was also linked to a significantly worse self-perceived QoL, OMH, and a higher anxiety scoring (**Figure 6** and **Supplementary Table 3**).

DISCUSSION

In our binational survey, approximately 20% of non-hospitalized COVID-19 convalescents reported poor OMH, reduced QoL, or clinical DPR or ANX at about 3 months post-infection. High psychosocial stress and self-reported physical performance loss, high number of acute COVID-19 symptoms, incomplete symptom resolution within the first 2 weeks of the disease, as well as acute and sub-acute neurocognitive manifestations (impaired concentration, confusion, and forgetfulness) were identified as strong explanatory factors (**Figure 7**).

So far, mental health disorders following COVID-19 have been investigated primarily in hospitalized patients. Signs of at least one psychiatric sequelae (post-traumatic stress disorder [PTSD], depression, anxiety, insomnia, and obsessive-compulsive symptomatology) were discerned in 56% of inpatients at 1 month after discharge (10). Anxiety, depression, and sleep difficulties were present in approximately one-quarter of hospitalized COVID-19 individuals at the 5–12 months of follow-ups (5–7). In large-scale studies encompassing both in- and outpatients, COVID-19 was identified as an important risk factor for anxiety, stress-related, and depressive adjustment disorders (9) and mental health conditions were ascertained in nearly one-fifth of COVID-19 convalescents (8). Of note, this figure is comparable with the frequency of PHQ-4 positive anxiety (AT: 12.4%, IT: 19.3%) and depression screening (AT: 17.3, IT: 23.2%) in our study cohorts. The variability of the reported rates of depression or anxiety in COVID-19 convalescents could be explained both by the differences in assessment methods and by the differing regional containment policies reflected by the rising frequencies of mental conditions in the general population (3). This may explain the significantly higher prevalence of post-COVID-19 depression and anxiety in the IT than in the AT study cohort, despite the similar frequency of pre-existing depression or anxiety.

Our results underscore the negative impact of psychosocial stress, physical performance impairment during convalescence, acute and sub-acute neurocognitive symptoms, such as concentration and memory deficits on the mental health rating. This likely reflects a net influence of the disease itself and the pandemic management measures, such as restricted physical activity due to quarantine (33) or increased loneliness and boredom (34). Mental health status was also investigated during past outbreaks of infectious diseases, such as Ebola (35) or H1N1 influenza (36), however, it has never been evaluated as rigorously as during the SARS-CoV-2 pandemic (37). Compared to individuals who were hospitalized for seasonal influenza, COVID-19 inpatients show a higher burden of mental health problems (9), but nevertheless, it cannot unambiguously be concluded whether this is due to viral factors or associated psychosocial factors and pandemic management. Psychoneuroimmunological processes, such as low-grade inflammation and associated microglia changes, were suggested to contribute to mental health problems following COVID-19 (38, 39). Such neuropathological alterations may also provide an explanation as, why acute neurocognitive complaints posed a "red flag" of subsequent mental health deterioration in our study cohorts. Other factors, such as Vitamin D, mitochondrial dysfunction, or gut dysbiosis, might also link COVID-19 pathobiology and mental health (40). In Random Forest modeling of mental health scoring in our study collectives, impaired physical performance following COVID-19 was found to impact particularly depression, OMH, and QoL rating. A similar phenomenon was described by Evans et al. (7) in hospitalized COVID-19 patients, who linked physical impairment with poor mental health status, respiratory symptoms, fatigue, and protracted systemic inflammation. Of note, a reciprocal axis between physical performance and mental health, and especially depression, may exist since physical impairment is one of the diagnostic criteria of major depressive disorder (41).

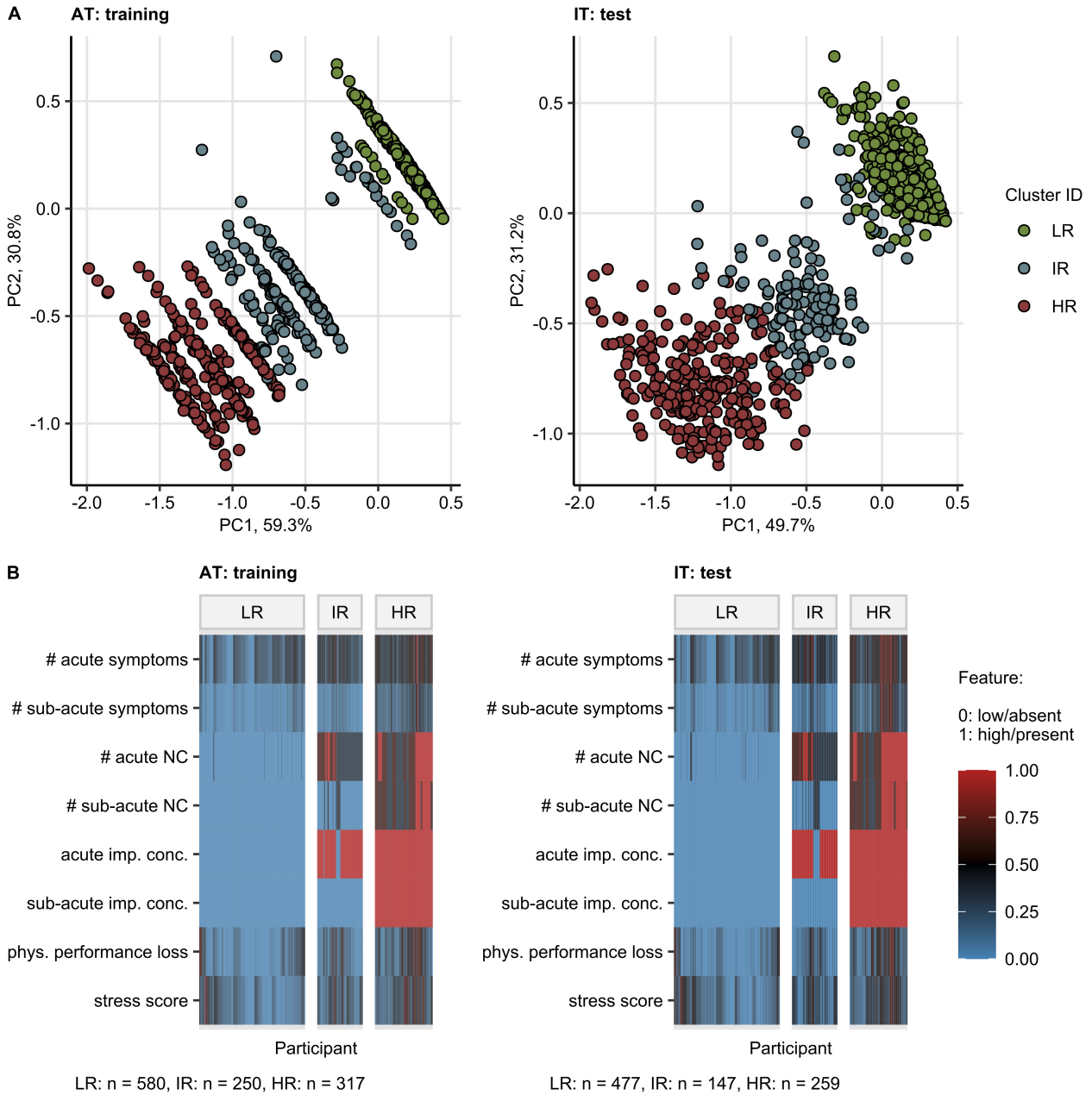

FIGURE 4 | Clustering of the study participants by the most influential factors affecting the mental health and quality of life scoring. Study participants were assigned to the Low Risk (LR), Intermediate Risk (IR), and High Risk (HR) subsets by clustering in respect to the most influential factors for the mental health and quality of life scoring (**Figure 2B**). Numeric variables were minimum/maximum normalized prior to modeling. The procedure in the training Austria (AT) cohort involved the self-organizing map (SOM, 13 13 hexagonal grid, Manhattan distance between participants) and the hierarchical clustering (Ward D2 method, Manhattan distance between the SOM nodes) algorithms. Assignment of Italy (IT) cohort participants to the clusters was accomplished by the k-nearest neighbors classification. The numbers of participants assigned to the clusters are presented in **(B)**. **(A)** Cluster assignment of the participants in the 3-dimensional principal component (PC) analysis score plot. The first two components are shown. Percentages of the data set variance associated with the particular PC are presented in the plot axes. **(B)** Heat map of the minimum/maximum-normalized clustering features. NC: neurocognitive symptoms, imp. conc.: impaired concentration, phys.: physical, #: number of.

The neurocognitive complaints during acute COVID-19 were found frequently accompanied by lower respiratory, cardiological, neurological symptoms, and sleep disorders (7, 9, 12, 15, 42–45). Such "multi-organ phenotype" of COVID-19 was found by us to be a correlate of protracted clinical recovery (12). Herein, the neurocognitive features together with the high symptom burden of acute COVID-19, fatigue, tiredness, and sleep problems hallmarked the IR and HR

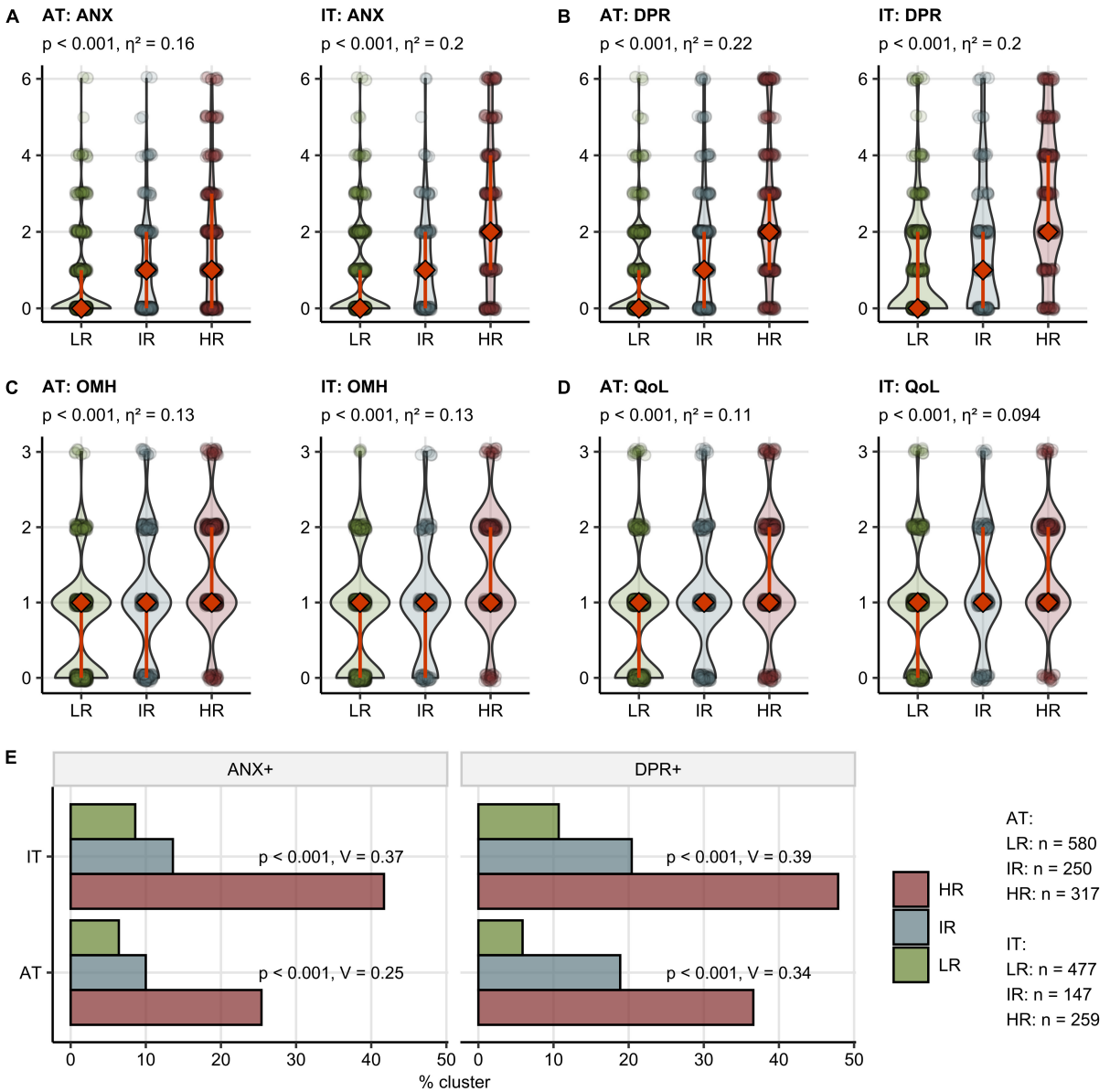

FIGURE 5 | Mental health and quality of life scoring, depression and anxiety prevalence in the mental health risk clusters. Study participants were assigned to the Low Risk (LR), Intermediate Risk (IR), and High Risk (HR) subsets as presented in **Figure 4**. The numbers of participants assigned to the clusters are presented in **(E)**. **(A–D)** Rating of anxiety (ANX) **(A)**, depression (DPR) **(B)**, overall mental health (OMH) **(C)**, and quality of life (QoL) **(D)** in the clusters presented as violin plots, diamonds with whiskers represent medians with IQRs. Statistical significance was assessed by the Kruskal–Wallis test. *P*-values corrected for multiple testing with the Benjamini-Hochberg method and η^2 effect size statistic values are shown in the plot captions. **(B)** Frequency of positive depression (DPR+) and anxiety (ANX+) screening in the clusters. Statistical significance was assessed by the Benjamini-Hochberg-corrected χ^2 test, the effect size was expressed as Cramer's V.

Mental Health Risk Clusters of the participants likely to develop a mental health condition in course of the recovery. Such "red flags" of deteriorating mental health present in the first 2 weeks of COVID-19 may be exploited for early diagnosis and psychological or psychiatric intervention.

Pre-existing depression or anxiety was reported by roughly 5% of the respondents and was linked to mental health deficits during recovery – a phenomenon known from non-COVID-19 medical conditions (46). The Random Forest models demonstrated a comparable performance in the DA-positive and -negative study participants. This suggests that the major factors determining the mental health rating following COVID-19 were likely common for individuals with and without pre-existing DA. Concomitantly, the subset with pre-existing DA was found to experience a significantly higher burden of acute symptoms as well as acute and sub-acute neurocognitive complaints. However, it needs to be clarified whether this is attributed to the observed higher level of additional co-morbidity, increased susceptibility

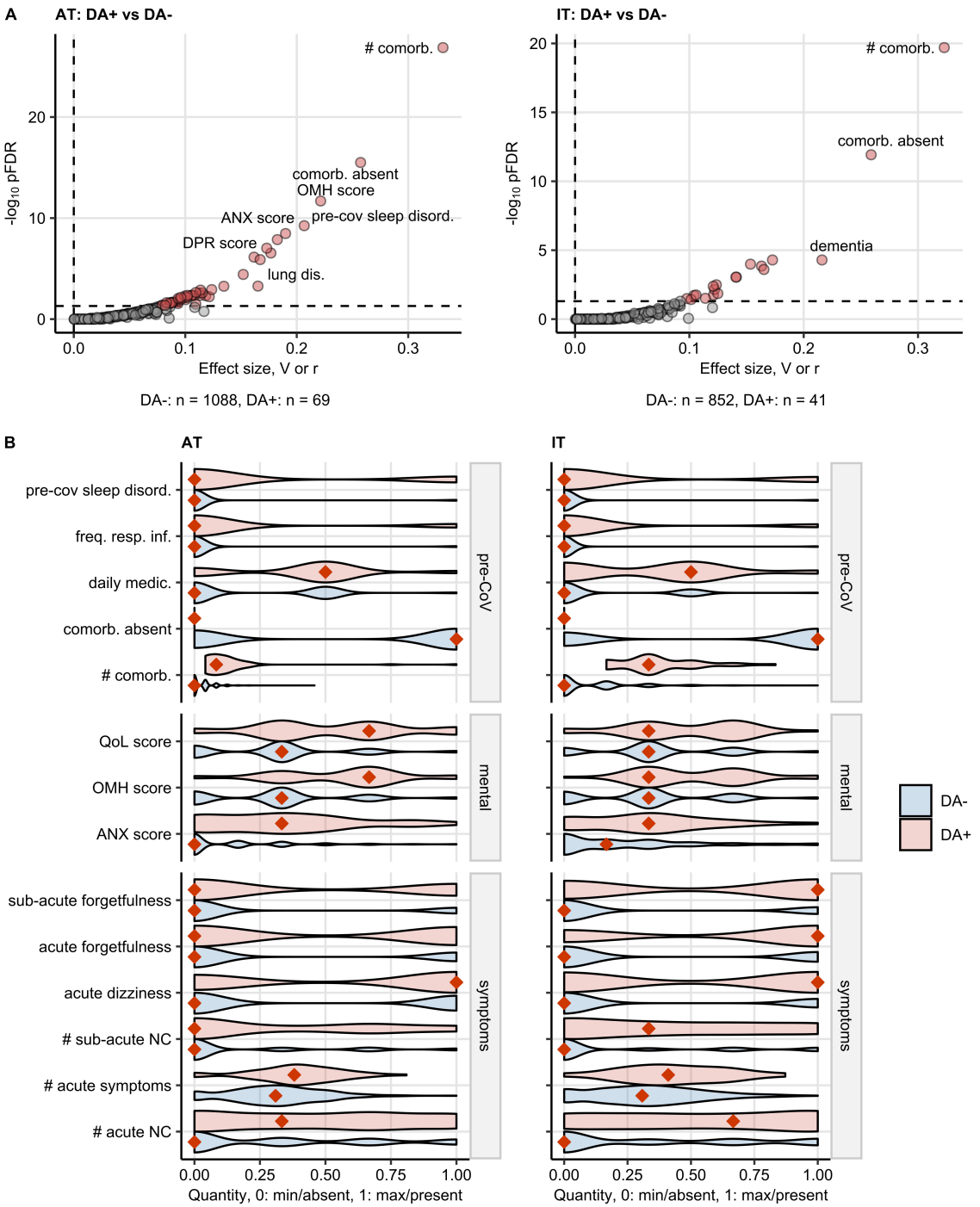

FIGURE 6 | Characteristic of baseline features, COVID-19 course, and recovery in participants with pre-existing depression or anxiety. Differences in baseline characteristic, COVID-19 course, recovery, mental health, and quality of life scoring between the participants with pre-existing depression or anxiety (DA+) and the subjects without depression/anxiety history (DA–) were assessed by the χ^2 or Mann–Whitney test in Austria (AT) and Italy (IT) cohort. The numeric variables were minimum/maximum normalized prior to modeling. The testing results were corrected from multiple testing with the Benjamini-Hochberg method (FDR: False Discovery Rate). The numbers of DA+ and DA– participants are shown in **(A)**. **(A)** Multiple testing-adjusted significance (pFDR) and effect size (categorical: Cramer's V for categorical factors, numeric features: Wilcoxon r) for the investigated variables. Variables significantly different between DA+ and DA – are highlighted in red. **(B)** Values of the features significantly different between DA+ and DA– participants in both AT and IT collectives presented in violin plots. The numeric features were minimum/maximum normalized. Orange diamonds represent mode (categorical variables) or median values (numeric variables). pre-CoV: before COVID-19, sleep disord.: sleep disorder, freq. resp. inf.: >2 respiratory infections per yes before COVID-19, daily medic.: number of drugs taken daily, comorb.: comorbidities, #: number of, QoL: quality of life, OMH: overall mental health, ANX: anxiety, NC: neurocognitive symptoms.

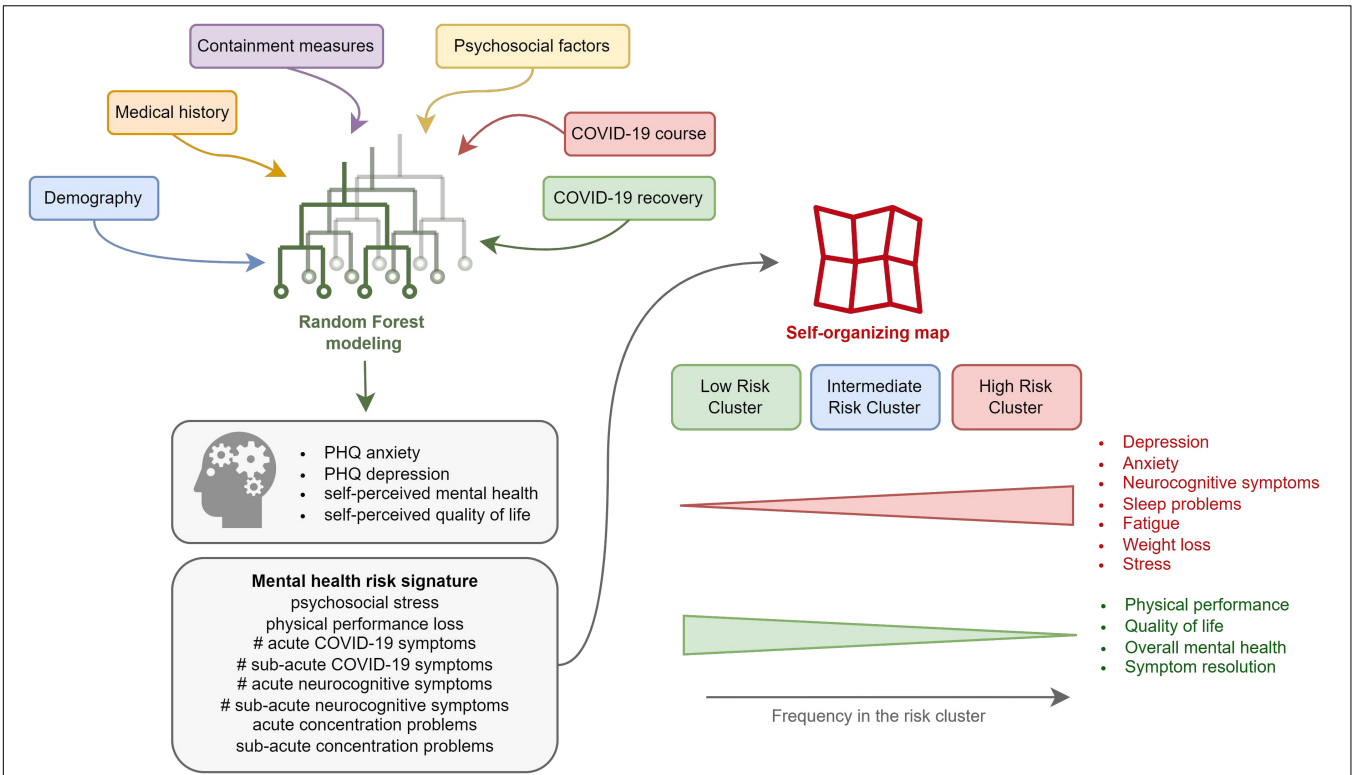

FIGURE 7 | Summary of the study results.

to respiratory infections, or different perception for symptoms in the DA subsets in our study. Conspicuously, psychiatric disorders before COVID-19 were described as age- and other comorbidity-independent risk factors for SARS-CoV-2 infection (8). This may indicate that alike chronic somatic diseases, pre-existing mental health conditions may predispose the patient to more severe and polysymptomatic COVID-19.

Several mechanisms might mediate the bidirectional associations of COVID-19, depression, anxiety, and psychosocial stress (47). Protracted systemic inflammation is an important pathogenetic factor in depressive-anxious disorders during COVID-19 convalescence (7, 10, 12, 48–50). Stress being the key co-variate of poor mental health in the study collectives was proposed to modulate anti-SARS-CoV-2 immunity culminating in more severe COVID-19 (51) and to perpetuate the systemic low-grade inflammation (46, 51). Other possible mechanisms include direct viral infection of the central nervous system, neuroinflammation, microvascular thrombosis, and neurodegeneration (52). The strong association of acute neurocognitive manifestations with poor mental health scoring in our study suggests that pathobiological processes triggered likely by the pathogen and anti-SARS-CoV-2 immunity early in the disease course may contribute to the mental health deterioration. Targeted investigations of COVID-19 recovery with mental health, biochemical, and immunological readouts are missing in our current survey study, and a case-control design is needed to shed more light on this phenomenon and to entangle the mechanistic interplay between acute COVID-19 pathobiology, recovery, and mental health status (53).

The prime strength of our study is the inclusion of two independently recruited cohorts differing in socioeconomic structure and national containment measures which allowed for identification and validation of common influencing factors. Furthermore, the study cohorts encompassed outpatients only insufficiently characterized so far. The most important study limitation is a possible participants' selection bias. The majority of respondents showed good mental health before COVID-19, and it is likely that predominantly individuals with severe or persistent COVID-19 symptoms and high health-awareness completed the survey (12). Modeling of the impact of the individual observation time and the total survey duration indicated that those two potential sources of bias had only a minor effect on the rating of mental health and QoL. Notably, the observation time variable was included in the multi-parameter models (22). Despite a broad set of independent study variables, the fraction of unexplained variability of the mental health and QoL scoring was substantial, especially in the validation Italian cohort. We could speculate that a higher explanatory power may be reached by the inclusion of additional explanatory variables concerning stringency of national containment measures, socioeconomic background (family status, income, and care duties), personal attitude to the pandemic management, or impact of the outbreak on one's lifestyle, which may drive the raising frequency of mental disorders in the non-infected population as well (3, 34).

This study underlines the importance of mental health in the follow-up care of COVID-19 individuals. Psychosocial stress, polysymptomatic disease, and neurocognitive complaints during acute COVID-19 are proposed as a risk signature of a subsequent mental disorder (**Figure 7**). They may prompt clinicians, i.e., general practitioners, to monitor outpatients with COVID-19 more closely for mental health deterioration and identify those who could benefit from early psychological and psychiatric intervention. Additionally, a pre-existing mental health condition may pose a risk factor of more severe COVID-19.

DATA AVAILABILITY STATEMENT

The raw data supporting the conclusions of this article will be made available by the authors, without undue reservation. Analysis of the psychosocial features is available as an online dashboard (https://im2-ibk.shinyapps.io/mental_health_dashboard). The complete R analysis pipeline is available at https://github.com/PiotrTymoszuk/mental-health-after-COVID-19.

ETHICS STATEMENT

The studies involving human participants were reviewed and approved by the Institutional Review Board of the Medical University of Innsbruck (approval number: 1257/2020) and the Institutional Review Board of the Autonomous Province of Bolzano – South Tyrol (approval number: 0150701). The patients/participants provided their digital written informed consent to participate in this study.

AUTHOR CONTRIBUTIONS

AH, AP, BS-U, CW, GP, GW, HB, JL-R, KH, MG, RB-W, RH, SK, SS, and VR designed the study. KH, DA, SS, AP, VR, MG, AB, KK, TS, IT, BP, CW, HB, and GP collected the data. KH, PT, and DA performed data analysis. PT, DA, KH, RH, BS-U, and JL-R interpreted the data. PT, DA, KH, BS-U, and JL-R wrote the manuscript. All authors critically reviewed the final version of the manuscript.

FUNDING

This study was funded by the Research Fund of the State of Tyrol, Austria (Project GZ 71934, JL-R).

ACKNOWLEDGMENTS

We acknowledge the commitment of the participants, healthcare administration, and general practitioners to the study and daily management of the COVID-19 pandemic. The manuscript is available as a preprint at medRxiv (54).

SUPPLEMENTARY MATERIAL

The Supplementary Material for this article can be found online at: https://www.frontiersin.org/articles/10.3389/fmed.2022.792881/full#supplementary-material

REFERENCES

1. Martin A, Rief W, Klaiberg A, Braehler E. Validity of the brief patient health questionnaire mood scale (PHQ-9) in the general population. *Gen Hosp Psychiatry.* (2006) 28:71–7. doi: 10.1016/j.genhosppsych.2005.07.003
2. Löwe B, Decker O, Müller S, Brähler E, Schellberg D, Herzog W, et al. Validation and standardization of the generalized anxiety disorder screener (GAD-7) in the general population. *Med Care.* (2008) 46:266–74. doi: 10.1097/MLR.0b013e318160d093
3. Pieh C, Budimir S, Probst T. The effect of age, gender, income, work, and physical activity on mental health during coronavirus disease (COVID-19) lockdown in Austria. *J Psychosom Res.* (2020) 136:110186. doi: 10.1016/j.jpsychores.2020.110186
4. Nasserie T, Hittle M, Goodman SN. Assessment of the frequency and variety of persistent symptoms among patients with COVID-19: a systematic review. *JAMA Netw Open.* (2021) 4:e2111417. doi: 10.1001/jamanetworkopen.2021.11417
5. Huang C, Huang L, Wang Y, Li X, Ren L, Gu X, et al. 6-month consequences of COVID-19 in patients discharged from hospital: a cohort study. *Lancet.* (2021) 397:220–32. doi: 10.1016/S0140-6736(20)32656-8
6. Huang L, Yao Q, Gu X, Wang Q, Ren L, Wang Y, et al. 1-year outcomes in hospital survivors with COVID-19: a longitudinal cohort study. *Lancet.* (2021) 398:747–58. doi: 10.1016/S0140-6736(21)01755-4
7. Evans RA, McAuley H, Harrison EM, Shikotra A, Singapuri A, Sereno M, et al. Physical, cognitive, and mental health impacts of COVID-19 after hospitalisation (PHOSP-COVID): a UK multicentre, prospective cohort study. *Lancet Respir Med.* (2021) 9:1275–87. doi: 10.1016/S2213-2600(21)00383-0/ATTACHMENT/A18E12DB-60DA-4539-9F71-2E180B86FFEA/MMC2.PDF
8. Taquet M, Luciano S, Geddes JR, Harrison PJ. Bidirectional associations between COVID-19 and psychiatric disorder: retrospective cohort studies of 62 354 COVID-19 cases in the USA. *Lancet Psychiatry.* (2021) 8:130–40. doi: 10.1016/S2215-0366(20)30462-4
9. Al-Aly Z, Xie Y, Bowe B. High-dimensional characterization of post-acute sequalae of COVID-19. *Nature.* (2021) 594:259–64. doi: 10.1038/s41586-021-03553-9
10. Mazza MG, De Lorenzo R, Conte C, Poletti S, Vai B, Bollettini I, et al. Anxiety and depression in COVID-19 survivors: role of inflammatory and clinical predictors. *Brain Behav Immun.* (2020) 89:594–600. doi: 10.1016/j.bbi.2020.07.037
11. Angulo FJ, Finelli L, Swerdlow DL. Estimation of US SARS-CoV-2 infections, symptomatic infections, hospitalizations, and deaths using seroprevalence surveys. *JAMA Netw Open.* (2021) 4:e2033706. doi: 10.1001/JAMANETWORKOPEN.2020.33706
12. Sahanic S, Tymoszuk P, Ausserhofer D, Rass V, Pizzini A, Nordmeyer G, et al. Phenotyping of acute and persistent COVID-19 features in the outpatient setting: exploratory analysis of an international cross-sectional online survey. *Clin Infect Dis.* (2021) ciab978. doi: 10.1093/CID/CIAB978
13. Demichev V, Tober-Lau P, Lemke O, Nazarenko T, Thibeault C, Whitwell H, et al. A time-resolved proteomic and prognostic map of COVID-19. *Cell Syst.* (2021) 12:780. doi: 10.1016/J.CELS.2021.05.005
14. Sudre CH, Lee KA, Lochlainn MN, Varsavsky T, Murray B, Graham MS, et al. Symptom clusters in COVID-19: a potential clinical prediction tool from the

COVID symptom study app. *Sci Adv.* (2021) 7:eabd4177. doi: 10.1126/sciadv.abd4177
15. Sudre CH, Murray B, Varsavsky T, Graham MS, Penfold RS, Bowyer RC, et al. Attributes and predictors of long COVID. *Nat Med.* (2021) 27:626–31. doi: 10.1038/s41591-021-01292-y
16. Heldt FS, Vizcaychipi MP, Peacock S, Cinelli M, McLachlan L, Andreotti F, et al. Early risk assessment for COVID-19 patients from emergency department data using machine learning. *Sci Rep.* (2021) 11:1–13. doi: 10.1038/s41598-021-83784-y
17. Breiman L. Random forests. *Mach Learn.* (2001) 45:5–32. doi: 10.1023/A:1010933404324
18. Khalilia M, Chakraborty S, Popescu M. Predicting disease risks from highly imbalanced data using random forest. *BMC Med Inform Decis Mak.* (2011) 11:51. doi: 10.1186/1472-6947-11-51/FIGURES/10
19. Nembrini S, König IR, Wright MN. The revival of the gini importance? *Bioinformatics.* (2018) 34:3711–8. doi: 10.1093/BIOINFORMATICS/BTY373
20. Kohonen T. *Self-Organizing Maps*. Berlin: Springer (1995). doi: 10.1007/978-3-642-97610-0
21. Wehrens R, Kruisselbrink J. Flexible self-organizing maps in kohonen 3.0. *J Stat Softw.* (2018) 87:1–18. doi: 10.18637/jss.v087.i07
22. Health after Covid-19 in Tyrol. *Mental Health After COVID-19 in Tyrol*. (2021). Available online at: https://im2-ibk.shinyapps.io/mental_health_dashboard/ (accessed September 9, 2021).
23. Löwe B, Wahl I, Rose M, Spitzer C, Glaesmer H, Wingenfeld K, et al. A 4-item measure of depression and anxiety: validation and standardization of the patient health questionnaire-4 (PHQ-4) in the general population. *J Affect Disord.* (2010) 122:86–95. doi: 10.1016/j.jad.2009.06.019
24. Gräfe K, Zipfel S, Herzog W, Löwe B. Screening psychischer störungen mit dem "gesundheitsfragebogen für patienten (PHQ-D)". Ergebnisse der deutschen validierungsstudie. *Diagnostica.* (2004) 50:171–81. doi: 10.1026/0012-1924.50.4.171
25. Wickham H, Averick M, Bryan J, Chang W, McGowan L, François R, et al. Welcome to the Tidyverse. *J Open Source Softw.* (2019) 4:1686. doi: 10.21105/joss.01686
26. Wickham H. *ggplot2: Elegant Graphics for Data Analysis*. 1st ed. New York, NY: Springer-Verlag (2016).
27. Benjamini Y, Hochberg Y. Controlling the false discovery rate: a practical and powerful approach to multiple testing. *J R Stat Soc Ser B.* (1995) 57:289–300. doi: 10.1111/j.2517-6161.1995.tb02031.x
28. Kuhn M. Building predictive models in R using the caret package. *J Stat Softw.* (2008) 28:1–26. doi: 10.18637/jss.v028.i05
29. Wright MN, Ziegler A. ranger: a fast implementation of random forests for high dimensional data in C++ and R. *J Stat Softw.* (2017) 77:1–17. doi: 10.18637/JSS.V077.I01
30. Fasiolo M, Wood SN, Zaffran M, Nedellec R, Goude Y. Fast Calibrated additive quantile regression. *J Am Stat Assoc.* (2020) 116:1402–12. doi: 10.1080/01621459.2020.1725521
31. Vesanto J, Alhoniemi E. Clustering of the self-organizing map. *IEEE Trans Neural Netw.* (2000) 11:586–600. doi: 10.1109/72.846731
32. Leng M, Wang J, Cheng J, Zhou H, Chen X. Adaptive semi-supervised clustering algorithm with label propagation. *J Softw Eng.* (2014) 8:14–22. doi: 10.3923/JSE.2014.14.22
33. Handschin C, Spiegelman BM. The role of exercise and PGC1α in inflammation and chronic disease. *Nature.* (2008) 454:463–9. doi: 10.1038/nature07206
34. Tutzer F, Frajo-Apor B, Pardeller S, Plattner B, Chernova A, Haring C, et al. Psychological distress, loneliness, and boredom among the general population of Tyrol, Austria during the COVID-19 pandemic. *Front Psychiatry.* (2021) 12:921. doi: 10.3389/FPSYT.2021.691896/BIBTEX
35. Reardon S. Ebola's mental-health wounds linger in Africa: health-care workers struggle to help people who have been traumatized by the epidemic. *Nature.* (2015) 519:13–4. doi: 10.1038/519013A
36. Chan SS, Lam LCW, Chiu HFK. The emergence of the novel H1N1 virus: implications for global mental health. *Int Psychogeriatr.* (2009) 21:987–9. doi: 10.1017/S1041610209990925
37. Maalouf FT, Mdawar B, Meho LI, Akl EA. Mental health research in response to the COVID-19, Ebola, and H1N1 outbreaks: a comparative bibliometric analysis. *J Psychiatr Res.* (2021) 132:198–206. doi: 10.1016/J.JPSYCHIRES.2020.10.018
38. Mondelli V, Pariante CM. What can neuroimmunology teach us about the symptoms of long-COVID? *Oxford Open Immunol.* (2021) 2:iqab004. doi: 10.1093/OXFIMM/IQAB004
39. Matschke J, Lütgehetmann M, Hagel C, Sperhake JP, Schröder AS, Edler C, et al. Neuropathology of patients with COVID-19 in Germany: a post-mortem case series. *Lancet Neurol.* (2020) 19:919–29. doi: 10.1016/S1474-4422(20)30308-2
40. Bókkon I, Kapócs G, Vucskits A, Erdöfi-Szabó A, Vagedes J, Scholkmann F, et al. COVID-19: the significance of platelets, mitochondria, vitamin D, serotonin and the gut microbiota. *Curr Med Chem.* (2021) 28:7634–57. doi: 10.2174/0929867328666210526100147
41. World Health Organization. *ICD-10: International Statistical Classification of Diseases and Related Health Problems: Tenth Revision*. (2004). Available online at: https://apps.who.int/iris/handle/10665/42980 (accessed February 1, 2022).
42. Blomberg B, Mohn KGI, Brokstad KA, Zhou F, Linchausen DW, Hansen BA, et al. Long COVID in a prospective cohort of home-isolated patients. *Nat Med.* (2021) 27:1607–13. doi: 10.1038/s41591-021-01433-3
43. Goërtz YMJ, Van Herck M, Delbressine JM, Vaes AW, Meys R, Machado FVC, et al. Persistent symptoms 3 months after a SARS-CoV-2 infection: the post-COVID-19 syndrome? *ERJ Open Res.* (2020) 6:00542–2020. doi: 10.1183/23120541.00542-2020
44. Atkinson SR, Hamesch K, Spivak I, Guldiken N, Cabezas J, Argemi J, et al. Serum transferrin is an independent predictor of mortality in severe alcoholic hepatitis. *Am J Gastroenterol.* (2020) 115:398–405. doi: 10.14309/ajg.0000000000000492
45. Davis HE, Assaf GS, McCorkell L, Wei H, Low RJ, Re'em Y, et al. Characterizing long COVID in an international cohort: 7 months of symptoms and their impact. *EClinicalMedicine.* (2021) 38:101019. doi: 10.1016/j.eclinm.2021.101019
46. Best C, Eckhardt-Henn A, Tschan R, Dieterich M. Psychiatric morbidity and comorbidity in different vestibular vertigo syndromes: results of a prospective longitudinal study over one year. *J Neurol.* (2009) 256:58–65. doi: 10.1007/s00415-009-0038-8
47. Postolache TT, Benros ME, Brenner LA. Targetable biological mechanisms implicated in emergent psychiatric conditions associated with SARS-CoV-2 infection. *JAMA Psychiatry.* (2021) 78:353–4. doi: 10.1001/jamapsychiatry.2020.2795
48. Jia Q, Shi S, Yuan G, Shi J, Shi S, Hu Y. Analysis of knowledge bases and research hotspots of coronavirus from the perspective of mapping knowledge domain. *Medicine (Baltimore).* (2020) 99:e20378. doi: 10.1097/MD.0000000000020378
49. Parker C, Shalev D, Hsu I, Shenoy A, Cheung S, Nash S, et al. Depression, anxiety, and acute stress disorder among patients hospitalized with coronavirus disease 2019: a prospective Cohort study. *Psychosomatics.* (2020) 62:211–219. doi: 10.1016/j.psym.2020.10.001
50. Mazza MG, Palladini M, De Lorenzo R, Magnaghi C, Poletti S, Furlan R, et al. Persistent psychopathology and neurocognitive impairment in COVID-19 survivors: effect of inflammatory biomarkers at three-month follow-up. *Brain Behav Immun.* (2021) 94:138–47. doi: 10.1016/j.bbi.2021.02.021
51. Peters EMJ, Schedlowski M, Watzl C, Gimsa U. Can stress interact with SARS-CoV-2? A narrative review with a focus on stress-reducing interventions that may improve defence against COVID-19. *Psychother Psychosom Med Psychol.* (2021) 71:61–71. doi: 10.1055/a-1322-3205
52. Nalbandian A, Sehgal K, Gupta A, Madhavan MV, McGroder C, Stevens JS, et al. Post-acute COVID-19 syndrome. *Nat Med.* (2021) 27:601–15. doi: 10.1038/s41591-021-01283-z
53. Amin-Chowdhury Z, Ladhani SN. Causation or confounding: why controls are critical for characterizing long COVID. *Nat Med.* (2021) 27:1129–30. doi: 10.1038/s41591-021-01402-w
54. Hüfner K, Tymoszuk P, Ausserhofer D, Sahanic S, Pizzini A, Rass V, et al. Who is at risk of poor mental health following COVID-19 outpatient

management? *medRxiv* [Preprint]. (2021). doi: 10.1101/2021.09.22.21263949

Conflict of Interest: PT owns Data Analytics as a Service Tirol and has received an honorarium from the 'Health after COVID-19 in Tyrol' study team from the Medical University of Innsbruck and Claudiana Bolzano for the study data management, curation and analysis, and minor manuscript work.

The remaining authors declare that the research was conducted in the absence of any commercial or financial relationships that could be construed as a potential conflict of interest.

Publisher's Note: All claims expressed in this article are solely those of the authors and do not necessarily represent those of their affiliated organizations, or those of the publisher, the editors and the reviewers. Any product that may be evaluated in this article, or claim that may be made by its manufacturer, is not guaranteed or endorsed by the publisher.

frontiers in Medicine

ORIGINAL RESEARCH
published: 16 March 2022
doi: 10.3389/fmed.2022.785285

Tissue Damage, Not Infection, Triggers Hepatic Unfolded Protein Response in an Experimental Rat Peritonitis Model

*Andrea Müllebner[1,2], Anna Herminghaus[3], Ingrid Miller[2], Martina Kames[2], Andreia Luís[1], Olaf Picker[3], Inge Bauer[3], Andrey V. Kozlov[1] and Johanna Catharina Duvigneau[2]**

[1] Ludwig Boltzmann Institute for Traumatology, The Research Center in Cooperation With AUVA, Vienna, Austria, [2] Department of Biomedical Sciences, Institute for Medical Biochemistry, University of Veterinary Medicine Vienna, Vienna, Austria, [3] Department of Anesthesiology, University Hospital Düsseldorf, Düsseldorf, Germany

OPEN ACCESS

Edited by:
Claudine Habak,
Emirates College for Advanced Education, United Arab Emirates

Reviewed by:
Rodrigo Tinoco Figueiredo,
Federal University of Rio de Janeiro, Brazil
Ekaterina Kolesanova,
Russian Academy of Medical Sciences (RAMS), Russia

***Correspondence:**
Johanna Catharina Duvigneau
Catharina.Duvigneau@vetmeduni.ac.at

Specialty section:
This article was submitted to Translational Medicine, a section of the journal Frontiers in Medicine

Received: 29 September 2021
Accepted: 10 February 2022
Published: 16 March 2022

Citation:
Müllebner A, Herminghaus A, Miller I, Kames M, Luís A, Picker O, Bauer I, Kozlov AV and Duvigneau JC (2022) Tissue Damage, Not Infection, Triggers Hepatic Unfolded Protein Response in an Experimental Rat Peritonitis Model. Front. Med. 9:785285. doi: 10.3389/fmed.2022.785285

Background: Abdominal surgery is an efficient treatment of intra-abdominal sepsis. Surgical trauma and peritoneal infection lead to the activation of multiple pathological pathways. The liver is particularly susceptible to injury under septic conditions. Liver function is impaired when pathological conditions induce endoplasmic reticulum (ER) stress. ER stress triggers the unfolded protein response (UPR), aiming at restoring ER homeostasis, or inducing cell death. In order to translate basic knowledge on ER function into the clinical setting, we aimed at dissecting the effect of surgery and peritoneal infection on the progression of ER stress/UPR and inflammatory markers in the liver in a clinically relevant experimental animal model.

Methods: Wistar rats underwent laparotomy followed by colon ascendens stent peritonitis (CASP) or surgery (sham) only. Liver damage (aspartate aminotransferase (AST), alanine aminotransferase (ALT) and De Ritis values), inflammatory and UPR markers were assessed in livers at 24, 48, 72, and 96 h postsurgery. Levels of inflammatory (IL-6, TNF-α, iNOS, and HO-1), UPR (XBP1, GRP78, CHOP), and apoptosis (BAX/Bcl-XL) mRNA were determined by qPCR. Splicing of XBP1 (XBP1s) was analyzed by gel electrophoresis, p-eIF2α and GRP78 protein levels using the western blots.

Results: Aspartate aminotransferase levels were elevated 24 h after surgery and thereafter declined with different kinetics in sham and CASP groups. Compared with sham De Ritis ratios were significantly higher in the CASP group, at 48 and 96 h. CASP induced an inflammatory response after 48 h, evidenced by elevated levels of IL-6, TNF-α, iNOS, and HO-1. In contrast, UPR markers XBP1s, p-eIF2α, GRP78, XBP1, and CHOP did not increase in response to infection but paralleled the kinetics of AST and De Ritis ratios. We found that inflammatory markers were predominantly associated with CASP, while UPR markers were associated with surgery. However, in the CASP group, we found a stronger correlation between XBP1s, XBP1 and GRP78 with damage markers, suggesting a synergistic influence of inflammation on UPR in our model.

Conclusion: Our results indicate that independent mechanisms induce ER stress/UPR and the inflammatory response in the liver. While peritoneal infection predominantly triggers inflammatory responses, the conditions associated with organ damage are predominant triggers of the hepatic UPR.

Keywords: sepsis, systemic inflammatory response syndrome (SIRS), ER stress, surgical trauma, colon ascendens stent peritonitis (CASP), unfolded protein response

INTRODUCTION

Abdominal surgery is the most efficient treatment of intra-abdominal sepsis. However, surgical trauma and peritoneal infection lead to the activation of multiple stress and inflammatory pathways. An exaggerated response can cause systemic inflammatory response syndrome (SIRS). Despite worldwide efforts to improve treatment and clinical outcomes, the mortality rate of sepsis, septic shock, and the consecutive multiorgan dysfunction syndrome (MODS) in humans remains very high (1). Notably, sepsis-associated liver failure and dysfunction are associated with a poor prognosis (2).

The liver plays a particular role in SIRS, as it mounts the acute phase response and represents the source but also a target organ of inflammatory mediators. The liver is a major regulator of immune and inflammatory responses at the systemic level (3). In response to infection and inflammation, the liver adapts its metabolism and switches protein synthesis toward the acute phase reactants (4). For these tasks, the hepatocytes critically depend on the functional endoplasmic reticulum (ER). However, SIRS is associated with profound derangements of the hepatic metabolism and the capacity to produce proteins. Recently, these derangements have been attributed to a dysfunctional ER of hepatocytes, a condition termed ER stress. ER stress is meanwhile considered an early sign of hepatocyte dysfunction preceding liver dysfunction caused by sepsis and SIRS (5, 6).

Endoplasmic reticulum stress elicits the unfolded protein response (UPR), an adaptive response that aims at restoring cellular protein homeostasis (7). Three ER stress sentinels drive UPR in a concurrent manner. Activation of inositol-requiring protein 1-2 (IRE1α) leads to alternative splicing of X-Box binding protein 1 (XBP1) mRNA, an early indicator for ER stress. Proteolytic cleavage of activating transcription factor 6 (ATF6) releases its cytosolic portion. The spliced isoform of XBP1 (XBP1s) and the cleaved ATF6 are potent transcription factors that promote an increase in protein-folding capacity of the ER by enhancing the expression of ER chaperones, such as the glucose-regulated protein 78 kDa (GRP78), and ER-associated protein degradation (8, 9). Activation of the protein kinase R-like ER kinase (PERK) causes translational attenuation by directly phosphorylating the α-subunit of the eukaryotic translation initiation factor 2 (eIF2α) (10). Prolonged activation of PERK commits the cell to UPR-induced apoptosis that can be initiated by increased CCAAT/enhancer-binding protein homologous protein (CHOP) expression. CHOP favors a proapoptotic phenotype by downregulating antiapoptotic mitochondrial proteins of the B-cell lymphoma family such as B-cell lymphoma-extra large (Bcl-XL) causing increased levels of proapoptotic proteins, such as Bcl2-associated X protein (BAX) (11). Thus, UPR can initiate apoptosis in a mitochondria-dependent manner, if ER stress remains unresolved (12).

In the last decade, ER stress and UPR have been explored as biomarkers and therapeutic targets in many diseases (13). Activation of ER stress and UPR have been associated with the induction of liver failure in several critical care disease models, e.g., endotoxemia (14), traumatic/hemorrhagic shock (THS) (15, 16), and sepsis (17–19). Besides trauma and burns, intra-abdominal infections are a common cause of sepsis, which therefore represent an important clinical problem in abdominal surgery (20). For translation into clinical practice, the impact of diverse factors, such as inflammation or tissue damage on ER stress activation in the peritonitis needs further characterization using appropriate biomedical research models.

The colon ascendens stent peritonitis (CASP) model closely mimics the clinical progression of sepsis after intra-abdominal surgery. This experimental peritonitis model is of high-clinical relevance since it allows controlling the severity of sepsis (21). It consists of two independent insults, first tissue damage because of the surgery and second infection because of the bacterial leakage from the gut (22). However, the impact of surgery on the markers for the hepatic stress response has not been addressed so far.

We applied a self-resolving model of CASP, with moderate peritonitis induction, in order to minimize secondary, inflammation-induced tissue injury and damage, which is a frequent septic complication. We assumed this model would be particularly suitable to dissect the effect of surgery and peritonitis-induced inflammation on the progression of UPR and inflammation markers in the liver. The clarification of a causal association between UPR signaling and onset of SIRS is of

Abbreviations: ATF4, activating transcription factor 4; ATF6, activating transcription factor 6; BAX, Bcl2 associated X protein; Bcl, B-cell lymphoma; Bcl-XL, Bcl-extra large; BRL3A, buffalo rat liver 3A cell line; CASP, colon ascendens stent peritonitis; CHOP, CCAAT/enhancer-binding protein homologous protein; Cyclo, cyclophilin A; eIF2α, α-subunit of the eukaryotic translation initiation factor 2; ER, endoplasmic reticulum; GRP78, glucose regulated protein 78 kDa; HO-1, heme oxygenase 1; HPRT, hypoxanthine-guanine phosphoribosyltransferase; iNOS, inducible NO synthase; IL-6, interleukin 6; IRE1α, inositol-requiring enzyme-1; LPS, lipopolysaccharide; MODS, multi-organ dysfunction syndrome; NF-κB, Nuclear factor kappa B; PERK, protein kinase R-like endoplasmic reticulum kinase; p-eIF2α, phosphorylated α-subunit of the eukaryotic translation initiation factor 2; SIRS, systemic inflammatory response syndrome; TNF-α, tumor necrosis factor α; THS, traumatic/hemorrhagic shock; TRAF2, tumor necrosis factor α receptor-associated factor 2; UPR, unfolded protein response; XBP1, X-Box binding protein 1; XBP1s, spliced isoform of XBP1.

translational significance, as it implies new medical approaches for preventing liver dysfunction in the clinical situation.

MATERIALS AND METHODS

Animals

In accordance with the ethical guiding principles for animal experiments (23), we aimed at obtaining maximal information from previous animal experiments. We used residual tissue samples of animals investigated in a previous study (24). From animals that did not undergo surgery (untreated control) no more tissue material was available, when we started this study. Because of the limited amount of tissue, we included 8 animals per group, although the previous study comprised 12 animals per group. Animals are described in detail in Herminghaus et al. (24). In brief, liver tissues of 64 adult male Wistar rats (374 ± 23 g body weight) were investigated in this study. Animals were randomly assigned to 8 groups: groups 1–4, sham-operated animals (laparotomy only, 24, 48, 72, and 96 h after surgery) and groups 5–8, CASP with a 14-G stent, 24, 48, 72, and 96 h after surgery (**Figure 1A**).

Colon Ascendens Stent Peritonitis/Sham Surgery

Polymicrobial abdominal infection was induced by leakage of feces into the abdominal cavity *via* a stent implanted in the colonic wall (CASP) as previously described (24). This previous study was approved by the local Animal Care and Use Committee (Landesamt für Natur, Umwelt und Verbraucherschutz, Recklinghausen, Germany), and all the experiments were performed in accordance with the NIH guidelines for animal care. In brief, the volatile anesthetic sevoflurane (3.0 Vol%, FiO_2 0.5) was used to induce and maintain anesthesia. Buprenorphine was applied at 0.05 mg/kg subcutaneously for analgesia. Animals were laparotomized and a 14-G stent penetrating the colonic wall (ca. 0.5 cm distal to the cecum) was fixed. Sham animals underwent anesthesia and laparotomy as stated earlier, but the stent was fixed outside on the wall of the gut without piercing it. After surgery, animals received analgesia (buprenorphine 0.05 mg/kg in 0.6 ml NaCl subcutaneously every 12 h), but no antibiotics and no additional fluid therapy were applied. The overall survival rate in the sham and CASP group were 100 and 94%, respectively. Animals were euthanized by intraperitoneal injection of pentobarbital (120 mg/kg) 24, 48, 72, or 96 h after sham/CASP surgery. Blood was obtained by cardiac puncture. Livers were collected, aliquots were shock frozen in liquid nitrogen, and stored at −80°C until further processing. The experimental scheme is shown in **Figure 1B**.

Plasma Analyses

Plasma levels of alanine aminotransferase (ALT) and aspartate aminotransferase (AST) of all animals included in this study ($n = 8$ per group) and also from untreated control animals ($n = 9$) were taken from a data set determined in a previous study (24) published under Creative Commons-by 4.0 license (25). In brief, plasma was obtained by centrifugation (4°C, 4000 × *g*, 10 min) from blood collected in EDTA tubes and stored at −80°C until further processing. ALT and AST activities were measured in the Central Institute of Clinical Chemistry and Laboratory Medicine of the University Hospital Duesseldorf, Germany (24).

Gene Expression Analyses

Liver tissue (25–50 mg) was homogenized in 1 ml of TriReagent® (Molecular Research Center Inc., Cincinnati, OH, USA). Total RNA was extracted according to the manufacturer's protocol. Extracted RNA was quantified and purity was checked with an Eppendorf BioPhotometer plus UV/VIS (Eppendorf, Wesseling-Berzdorf, Germany) using absorption at 260 nm and the 260/280 nm ratio, respectively. Reverse transcription of 1 µg of total RNA to cDNA was performed using Superscript™ II reverse transcriptase (200 U/reaction; Invitrogen; Carlsbad, CA, USA) and anchored oligo dT primers (3.5 µmol/l final concentration). Equal aliquots of each cDNA were pooled to generate an internal standard used as a reference for the quantification of qPCR.

Quantitative PCR was performed in reactions of 12 µl containing SYBR® green I (0.5×, Sigma Aldrich, Vienna, Austria), iTaq™ DNA polymerase™ (25 U/L; Bio Rad, Hercules, CA, USA), oligonucleotide primers (250 nmol/l each, Invitrogen; Carlsbad, California, USA), dNTP [200 µmol/l each], and $MgCl_2$ (1.5-3 mmol/l). All the reactions were performed in duplicates on a CFX96™ real-time cycler (Bio-Rad, Hercules, California, USA). Details on primer pairs are shown in **Supplementary Table S1**. Randomly assigned no-reverse transcriptase controls corresponding to ∼15% of all the samples investigated, a no-template control, and the internal standard was included in each measurement. ΔCq of no-reverse transcriptase controls to the respective sample was >7 for all the cases, while no-template control never yielded signals.

Data were analyzed using the CFX Manager (version 2.0, Bio-Rad, Hercules, CA, USA) in the linear regression mode. Target gene expression was calculated relative to the internal standard (ΔCq) and normalized by mean ΔCq values of two internal reference genes (hypoxanthine-guanine phosphoribosyltransferase, HPRT, and cyclophilin A, Cyclo), yielding ΔΔCq values, as previously described (26). The ΔΔCq values obtained from the technical replicates were averaged and used for statistical analyses. For visualization, data are presented as fold changes ($2^{-\Delta\Delta Cq}$ values) relative to the mean of the 96 h sham group. The 96 h time point was used as a reference point, owing to the lack of untreated control animals. Our previous study revealed (24) that not only CASP but also the surgical procedure itself transiently affected liver damage markers (AST and ALT) and the mitochondrial function of the liver. However, ALT and AST data obtained from the 96 h sham animals were nearly identical to those of the untreated control animals (**Figures 1C–E**). Therefore, we assume the values of the 96 h sham animals correspond to physiological levels. This is in line with previously published results (19).

Western Blot Analyses

Liver tissues were homogenized 1:10 (w/v) in RIPA lysis buffer (25 mmol/l Tris–HCl (pH 8.0), 0.5% Nonidet P-40,

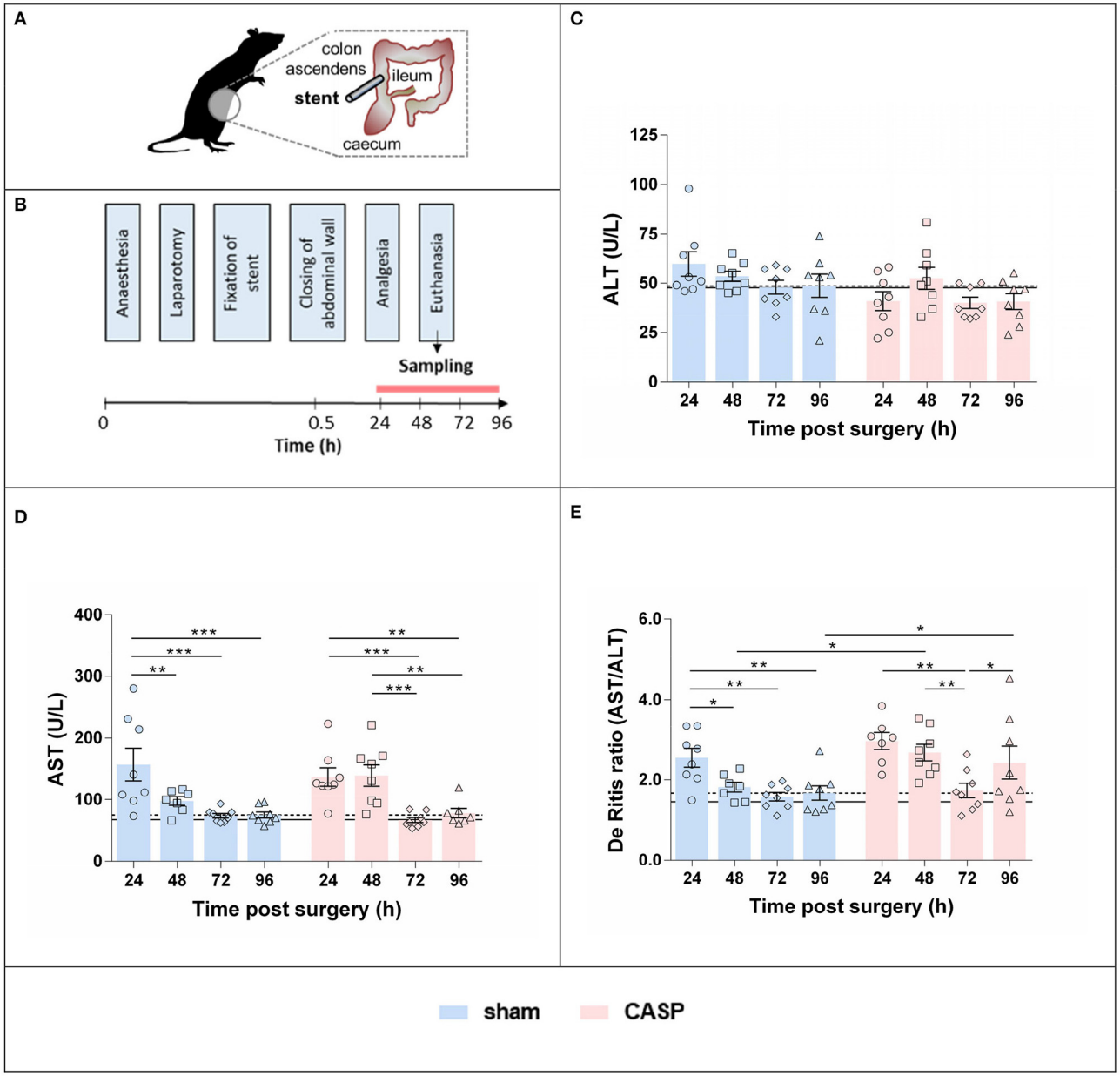

FIGURE 1 | Surgery and peritonitis induce liver damage in a self-resolving model. **(A)** Experimental model for the induction of experimental peritonitis using CASP surgery. **(B)** Plasma and liver samples were collected at consecutive time points after sham and CASP surgery. Plasma levels of **(C)** ALT and **(D)** AST were obtained from a data set determined for a previous study (24) published under Creative Commons-by 4.0 license (25). **(E)** De Ritis ratio was calculated from those data. Data are shown as mean ± SEM per group, with $n = 8$ for all the groups, except for **(D,E)** sham 48 h ($n = 7$), **(D)** CASP 24 h ($n = 7$), and **(D)** CASP 96 h ($n = 7$). The dashed line indicates the mean value of the sham group at 96 h. The solid line indicates the mean value of untreated control animals ($n = 9$). Statistical differences were calculated using two-way ANOVA followed by uncorrected Fisher's LSD test and are indicated by $^{*}p < 0.05$, $^{**}p < 0.01$, $^{***}p < 0.001$.

150 mmol/l NaCl, 0.25% sodium deoxycholate, 0.05% sodium dodecyl sulfate (SDS), 1 mmol/l EDTA, and 0.5 mmol/l DTT) freshly supplemented with protease and phosphatase inhibitor cocktails (Roche, Mannheim, Germany). After centrifugation (12,000×*g*) at 4°C for 10 min, protein concentration in the supernatant was determined using the Bradford method. Western blotting was performed essentially as previously described (15), on specimens of three randomly selected animals per group. Samples (20 µg protein per lane, reduced in Laemmli sample buffer) were separated by sodium dodecyl sulfate-polyacrylamide gel electrophoresis over a separation distance of 7 cm followed by semidry blotting onto nitrocellulose (Hybond ECL; GE Healthcare Life Sciences, Munich, Germany). Blots were first stained with the fluorescent dye ruthenium (II)

tris-(bathophenanthroline disulfonate) and overall protein pattern captured on a Typhoon RGB imager (GE Healthcare Life Sciences, Munich, Germany). Immunostaining was performed with specific antibodies against GRP78 (ALX-210-137, Enzo Life Sciences, 1:5,000) or p-eIF2α (No. 9721, Cell Signaling, 1:1000) followed by cross-adsorbed anti-rabbit-HRPO (No. A16104, Life Technologies). Reactive bands were detected by enhanced chemiluminescence (Clarity™ Western ECL Blotting reagent, Bio-Rad) on a Vilber Fusion FX system (Vilber-Lourmat, Eberhardzell, Germany). The overall protein-staining pattern was used as a loading control and for normalization.

Data Analyses and Statistics

Data were calculated and visualized using GraphPad Prism v6.01 (GraphPad Software Incorporation, La Jolla, California, USA). Outliers were detected by the ROUTs test (Q = 1%) (27) and excluded from analyses. Data were analyzed by two-way ANOVA followed by uncorrected Fisher's LSD test unless otherwise stated. Correlations were calculated using Pearson's correlation coefficient. Differences were considered significant when the p-value was <0.05.

RESULTS

Liver Damage Markers Are Increased 24–48 h After Surgery

The values for the plasma levels of liver damage markers, activities of ALT (**Figure 1C**) and AST (**Figure 1D**) of untreated control animals ($n = 9$), sham and CASP animals enrolled in this study ($n = 8$ per group), were taken from a previously determined data set (see Materials and Methods, Animals and Plasma Analyses). In the acute phase (24-48 h), AST was elevated two-fold compared to the postacute phase (72–96 h) in both sham and CASP groups. We did not observe any significant difference in AST and ALT levels between sham and CASP groups at any time point (24). In contrast, the De Ritis ratio (AST/ALT) was significantly higher in CASP groups compared to shams at 48 and 96 h (**Figure 1E**). The 96 h sham group displayed values for ALT and AST, and also the De Ritis ratio, that did not differ significantly from the non-operated control animals (ALT: $p = 0.9$; AST: $p = 0.3$; De Ritis: $p = 0.4$; two-sided, heteroscedastic Student's t-test), indicating resolution of liver injury.

Abdominal Infection Triggered Stress and Inflammatory Response in the Liver 48 h After CASP

To assess the inflammatory response in the liver, we analyzed gene expression levels of key inflammatory markers. The mRNA levels of stress responsive enzyme heme oxygenase 1 (HO-1; **Figure 2A**) were moderately, albeit, significantly increased in CASP compared to sham-operated animals at 48, 72, and 96 h. The mRNA levels of the proinflammatory cytokines tumor necrosis factor α (TNF-α; **Figure 2B**) and interleukin 6 (IL-6; **Figure 2C**), and inducible NO synthase (iNOS; **Figure 2D**), an enzyme required for bactericidal activity, were significantly higher in CASP compared with sham animals at 48 h after surgery. In addition, iNOS was significantly higher in CASP animals at 96 h (**Figure 2D**). These data show that our experimental CASP model causes abdominal infection, which is capable to trigger an inflammatory response in the liver.

XBP1 Splicing and eIF2α Phosphorylation Are Triggered by Surgical Stress

We studied the activation of canonical UPR signaling in response to CASP and sham operation by quantifying XBP1s and detecting p-eIF2α. XBP1s levels were the highest at 24 h after surgery and declined until 72 h after surgery. Subsequently XBP1s increased again. Changes reached significance between 48 and 72 h in the sham group and 24, and 72 h and 96 h in CASP animals (**Figures 3A,B**). The p-eIF2α continuously increased throughout the observation period in sham and CASP-operated animals (**Figures 3C,D**). Within the sham group, we found significantly higher levels of p-eIF2α at 72 h and 96 h compared with the 24 h time point. The CASP group displayed similar kinetics with significantly higher levels at 96 h compared with the values determined at 24 and 48 h. Although the CASP group displayed higher levels of XBP1s and p-eIF2α at the late time point (96 h), the differences between the sham and CASP group failed to be significant. This suggests that ER stress sentinels, IRE1α and PERK, were activated by surgery-associated stress rather than by moderate peritoneal infection.

Unfolded Protein Response Is Transient and Peaks at 24 h After Surgery

We next examined gene expression of UPR target genes, XBP1 and GRP78. Protein expression of GRP78 was additionally determined. The highest levels of XBP1 (**Figure 4A**) and GRP78 mRNA (**Figure 4B**) were found in sham and CASP groups at 24 h after surgery; however, no differences between the sham and CASP groups were found. In addition, we observed a close correlation of GRP78 mRNA levels with the marker for organ damage De Ritis ratio (**Figure 4C**) with a correlation coefficient (r) of 0.494 ($p < 0.01$) for the sham group and 0.518 ($p < 0.01$) for the CASP group, respectively. Although differences were not significant there was a trend toward lower GRP78 protein levels in the sham group at 96 h compared with the levels at 24 h, while we observed a slight increase at 96 h for the CASP group (**Figure 4D**; **Supplementary Figure S1**).

Unfolded Protein Response Triggered a Proapoptotic Shift in the Liver 48 h After Surgery

Since we found that p-eIF2α levels continued to increase after surgery, which is a sign for sustained activation of the PERK axis of the UPR, we next analyzed markers indicative of apoptosis activation. In both groups, we found the highest levels of CHOP, a downstream target of PERK activation, at 48 h after surgery. Thereafter, CHOP gene expression levels declined (**Figure 5A**). In addition, markers of the mitochondria-triggered apoptotic pathway, involving BAX and Bcl-XL, displayed a transient proapoptotic shift in both groups (**Figure 5B**). Compared with all the other time points, the ratio of the proapoptotic BAX to

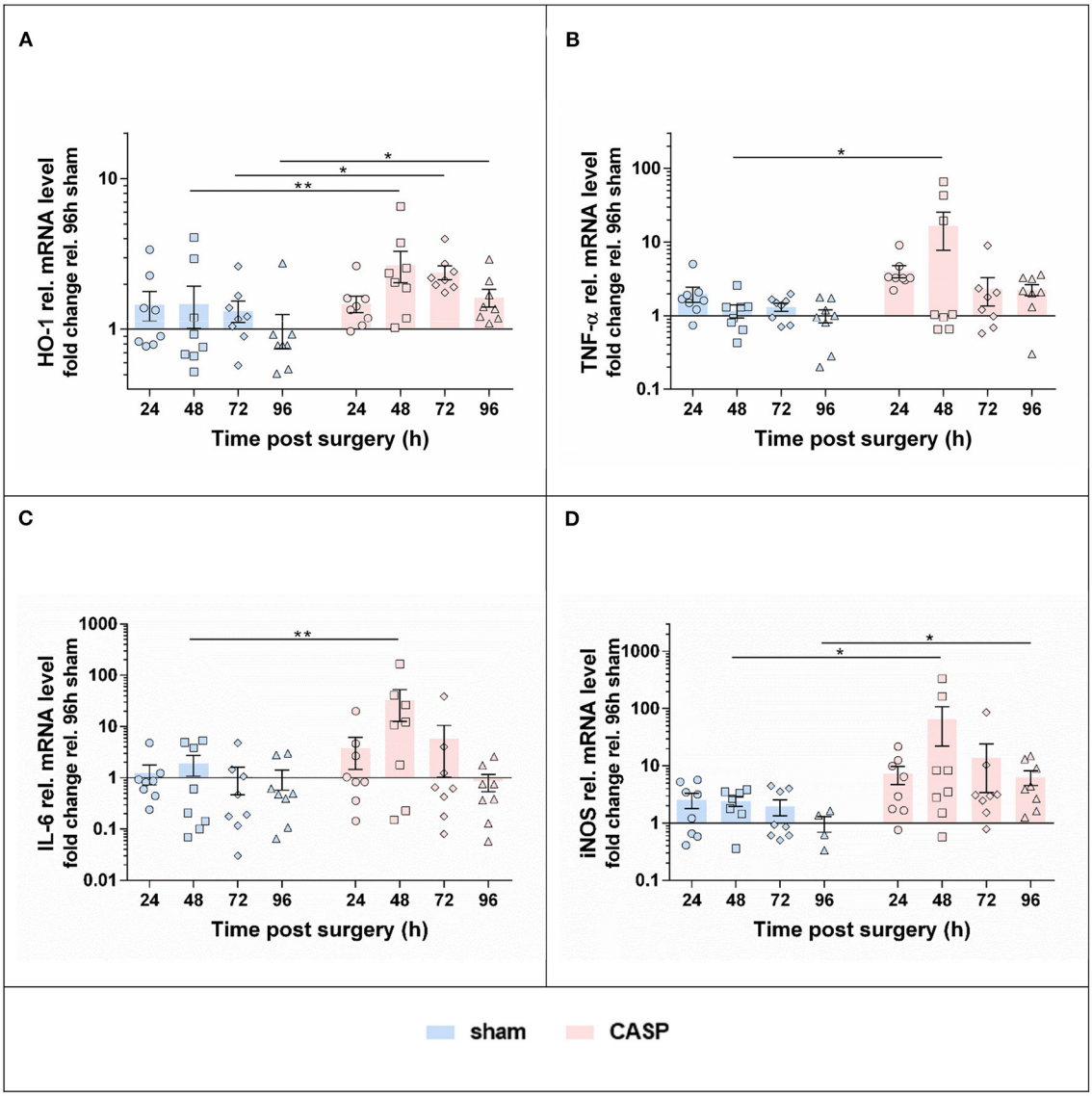

FIGURE 2 | Hepatic inflammatory response induced by abdominal infection peaks at 48 h. Gene expression levels of **(A)** HO-1, **(B)** TNF-α, **(C)** IL-6, and **(D)** iNOS were determined using qPCR in liver samples of rats that underwent sham or CASP surgery. Data are shown as mean ±SEM, with $n = 8$ for all the groups, except for **(D)** sham 48 h ($n = 7$) and **(D)** sham 96 h ($n = 4$). Statistical differences were calculated using two-way ANOVA followed by uncorrected Fisher's LSD test and are indicated by $^{*}p < 0.05$; $^{**}p < 0.01$.

the antiapoptotic Bcl-XL mRNA was significantly increased at 48 h after surgery in both, CASP and sham animals. However, no differences were found between the sham and CASP groups.

Unfolded Protein Response Activation Is Associated With the Surgical Stress

Considering that the degree of tissue damage caused by the surgical procedures was similar in all the experimental animals, the elicited effects are supposed to be influenced mainly by the time passed after surgery. In contrast, effects elicited by the peritoneal infection should distinguish sham animals from the CASP animals. In order to test the hypothesis that tissue damage, not peritoneal infection acts as a direct trigger for the hepatic UPR, we analyzed our data for both main effects, "time after surgery" and "peritoneal infection" and in addition for a potential interaction of both the conditions. We observed that inflammatory markers (TNF-α, IL-6, iNOS, and HO-1) were exclusively associated with the peritoneal infection, while UPR markers (XBPs, p-eIF2α, XBP1, GRP78, and CHOP) exclusively associated surgical stress (**Table 1**). There was no remarkable interaction between peritoneal infection and surgery for most markers. However, the interaction found for GRP78 mRNA in our study indicates that infectious stress in the peritoneum is capable of modulating the altitude of

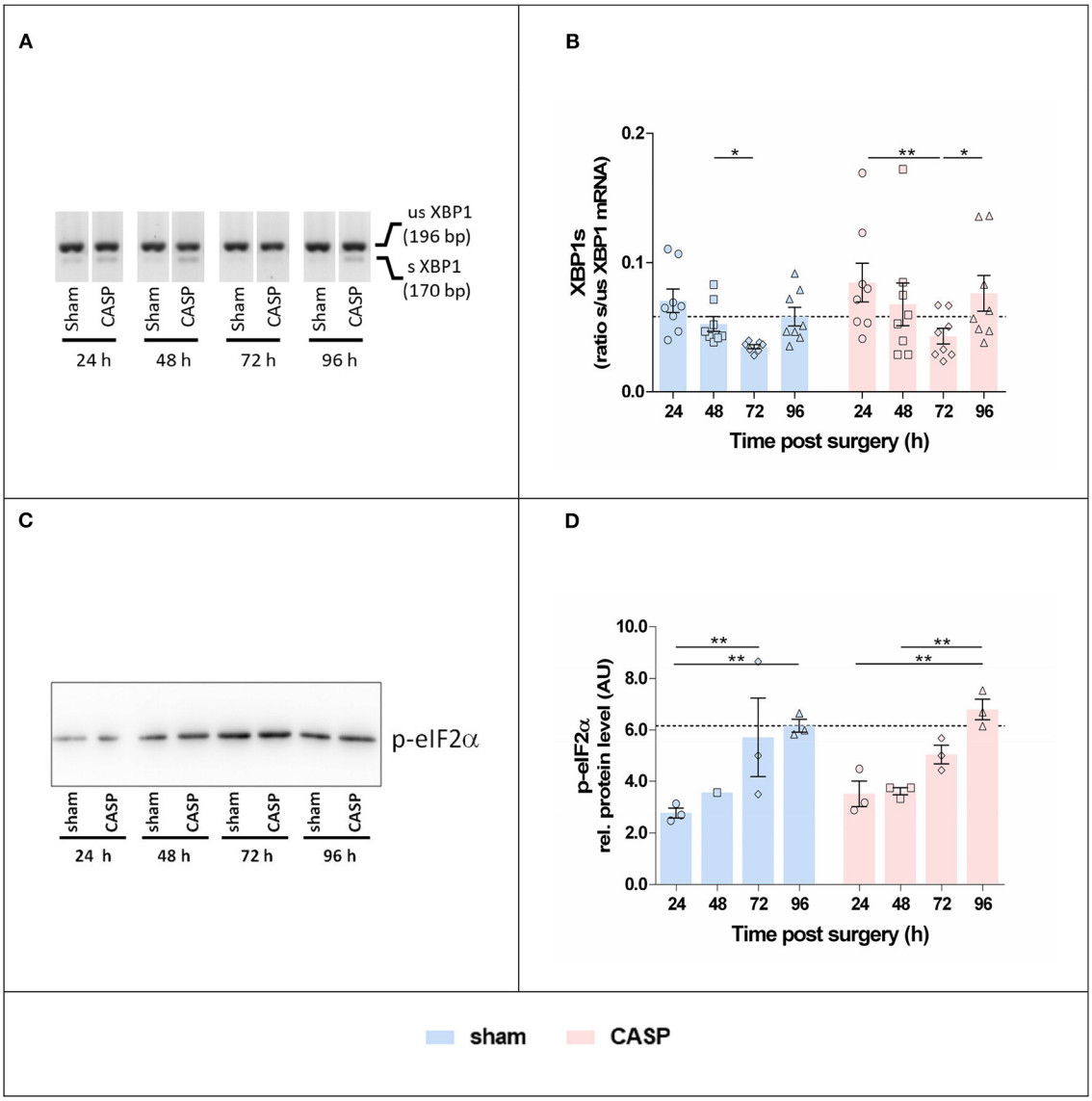

FIGURE 3 | Surgery induces hepatic XBP1 splicing and eIF2α phosphorylation. **(A)** Representative agarose gel electrophoresis of XBP1 PCR products showing the occurrence of the splice variant in the liver. **(B)** XBP1s indicated as the ratio of spliced (s) to unspliced (us) XBP1 mRNA determined by densitometric analyses. Data are given as mean ± SEM ($n = 8$ per group). **(C)** Liver homogenates were analyzed by SDS-PAGE and immunostaining for p-eIF2α. An exemplary blot is shown (the entire blot is shown in **Supplementary Figure S1A**). **(D)** Band intensities were normalized to the total protein of the respective gel lanes. Values are given as mean AU (arbitrary units) ± SEM ($n = 3$ per group, except for sham 48 h $n = 1$). The dashed line indicates the mean value of the sham group at 96 h. Statistical differences were calculated using two-way ANOVA followed by uncorrected Fisher's LSD test and are indicated by $^{*}p < 0.05$, $^{**}p < 0.01$.

hepatic GRP78 gene expression that was triggered by the surgical stress.

Activation of UPR Is Directly Correlated With the Level of Liver Damage During Abdominal Infection

We next analyzed the correlations among organ damage, UPR, or inflammation markers within sham and CASP animals using Pearson correlation (**Figure 6**). We found that UPR target genes GRP78 and XBP1 correlated significantly with liver damage markers De Ritis ratio (GRP78: sham $r = 0.49$, $p < 0.01$ and CASP $r = 0.52$, $p < 0.01$; XBP1: sham $r = 0.50$, $p < 0.01$ and CASP $r = 0.48$, $p < 0.01$) and AST (GRP78: sham $r = 0.52$, $p < 0.01$ and CASP $r = 0.59$, $p < 0.01$; XBP1: CASP $r = 0.60$, $p < 0.01$) in animals of both groups (**Figure 6**). Interestingly, these correlations were stronger among each other in animals of the CASP group. In addition, a strong positive correlation of XBP1s with liver damage markers (De Ritis ratio: $r = 0.56$, $p < 0.01$; AST: $r = 0.53$, $p < 0.01$) and with GRP78 ($r = 0.91$, $p < 0.01$) protein expression was found

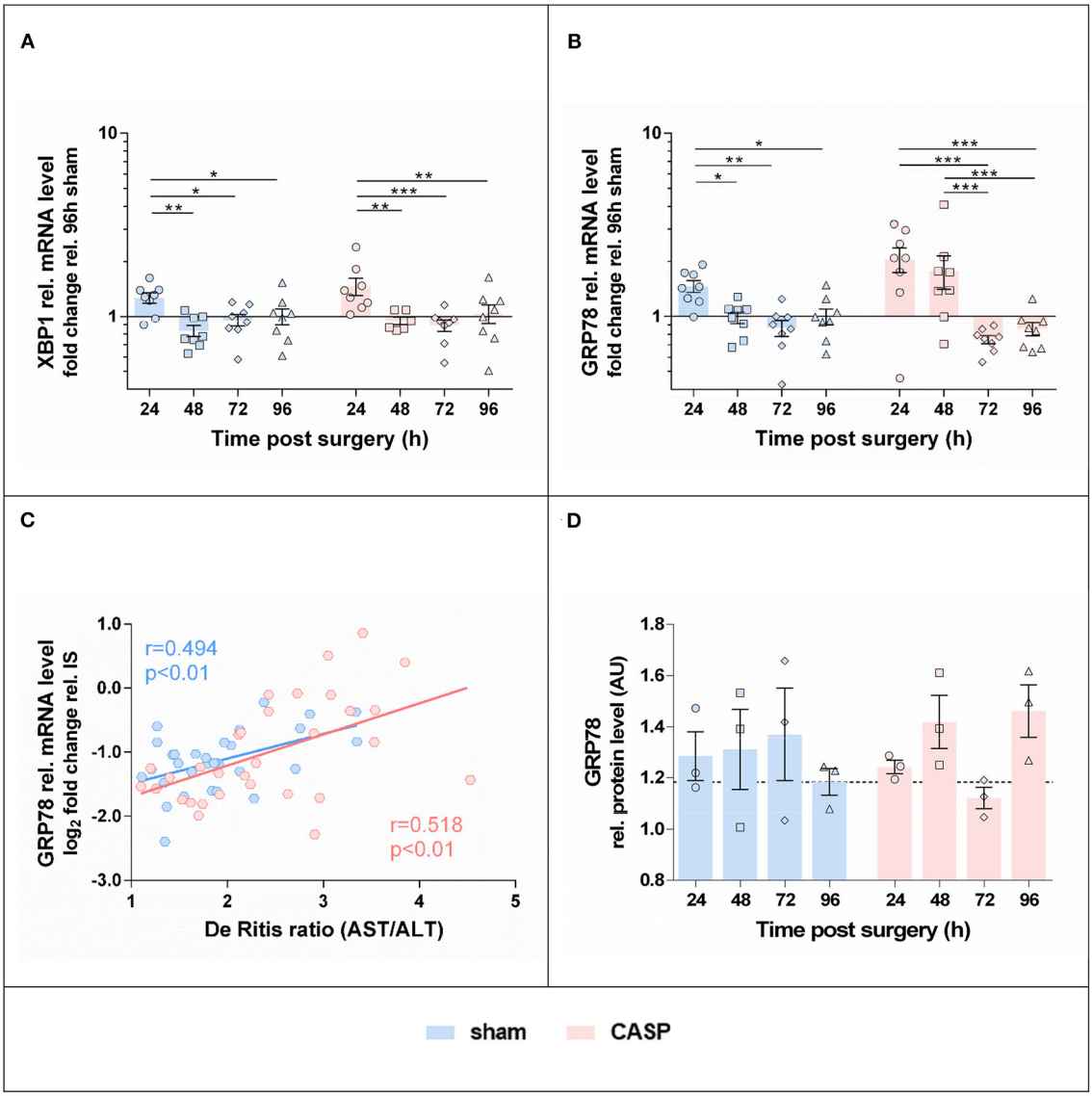

FIGURE 4 | Gene expression of UPR markers in the liver is highest at 24 h after surgery. Gene expression levels of **(A)** XBP1 and **(B)** GRP78 in the liver of sham and CASP operated rats were determined by means of qPCR. Data are shown as mean ± SEM ($n = 8$ per group). **(C)** Pearson correlation between GRP78 mRNA level and De Ritis ratio of sham ($n = 31$) and CASP ($n = 31$) operated animals. **(D)** GRP78 protein abundance in liver homogenates of single animals was analyzed by SDS-PAGE and immunostained for GRP78 (blot is shown in **Supplementary Figure S1B**). Band intensities of specific staining were normalized to the total protein of the respective gel lanes. Values are given as mean AU (arbitrary units) ± SEM ($n = 3$ per group). The dashed line indicates the mean value of the sham group at 96 h. Statistical differences were calculated using two-way ANOVA followed by uncorrected Fisher's LSD test and are indicated by $^*p < 0.05$; $^{**}p < 0.01$, and $^{***}p < 0.005$.

in CASP animals. Moreover, only in the CASP animals, the gene expression of the inflammatory marker TNF-α correlated with XBP1 mRNA ($r = 0.5$, $p < 0.01$). In sham animals, we found inverse correlations of CHOP and BAX/Bcl-XL with XBP1 mRNA (CHOP: $r = -0.42$, $p < 0.05$; BAX/Bcl-XL: $r = -0.54$, $p < 0.01$), which were not present in CASP animals. In contrast, no correlations between liver damage and markers of the inflammatory response were found. Taken together, our data suggest that not peritoneal infection, but organ damage triggers hepatic UPR.

Infectious Stimulants Are Weak, but Organ Damage-Triggering Factors Are Strong Inducers of UPR in the Liver

Since an upregulated hepatic UPR has been shown in several inflammatory animal models, including our own (15, 28), the question arises, which condition acts as a predominant trigger; the inflammation-inducing stimuli, or the tissue damage, which is accompanying severe inflammatory processes. To address this question more profoundly, we determined clustering of representative markers by reanalyzing data sets from

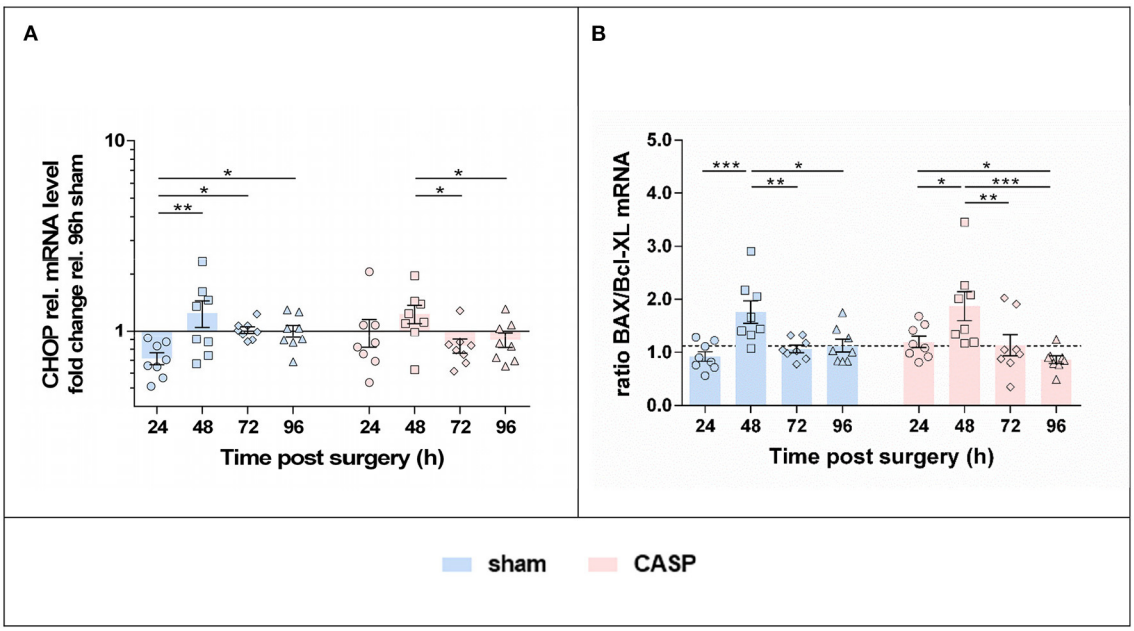

FIGURE 5 | UPR triggers a pro-apoptotic shift with maximum at 48 h after surgery. Gene expression levels of **(A)** CHOP, **(B)** BAX and Bcl-XL mRNA were determined by means of qPCR in liver samples after sham and CASP surgery. Data from BAX and Bcl-XL expression are presented as a ratio. The dashed line indicates the mean value of the sham group at 96 h. All data are shown as mean ± SEM ($n = 8$ per group). Statistical difference was calculated using two-way ANOVA followed by uncorrected Fisher's LSD test and is indicated by $^{*}p < 0.05$, $^{**}p < 0.01$, and $^{***}p < 0.005$.

two different acute experimental models, a THS model and an endotoxic shock model (*i.v.* application of LPS), which were part of studies previously published (15, 28). While the THS model induces initially acute tissue damage, *via* ischemia/reperfusion injury, intravenous LPS application leads acutely to a fulminant inflammatory response. Thus, analyzing a very early time point (2 h) in both models, we expected to see the predominantly triggered responses, without superimposing secondary effects. The applied analytical approach, of ranking the normalized effects of investigated markers (refer to Methods to **Supplementary Figure S2** in **Supplementary Material**), allows a direct comparison of marker clustering in both models. We found significant differences between the THS (2 h after trauma and hemorrhage) and the endotoxic shock group (LPS, 2 h). The LPS group showed higher cumulative ranks of inflammatory markers (iNOS, TNF-α) with lower ALT ranks, and lower ranks for UPR (CHOP, XBP1, XBP1s, and GRP78) compared with the THS animals. In contrast, the THS group showed higher ranks of ER-stress markers (CHOP, XBP1, and XBP1s) and higher ALT ranks, while an association with the inflammatory markers was nearly absent (**Supplementary Figure S2**). Of note: HO-1 levels were significantly increased compared with controls in both models, supporting the observation of HO-1 as an exquisite marker of the general hepatic cell stress.

In addition, our experiments performed with an immortalized liver cell line (BRL3A) described in the **Supplementary Material** (Methods to **Supplementary Figure S3**), support the finding of the weak capacity of inflammatory mediators to directly induce hepatic UPR. Although the BRL3A cells are capable of exquisitely responding to ER stress inducers, such as tunicamycin and thapsigargin (**Supplementary Figure S3A**), incubation with inflammatory mediators raised the expression of IL-6, without clearly affecting the UPR response markers, GRP78 and CHOP (**Supplementary Figure S3B**).

These additional data support the assumption that not infectious stimuli, but the conditions associated with organ damage are the predominant triggers of the hepatic UPR seen in our CASP model.

DISCUSSION

Animal Model

Abdominal infections are an important clinical problem. In Germany, abdominal infections cause 28.7% of all sepsis cases (29). Primary peritonitis caused by diverticulitis or Morbus Crohn, or secondary peritonitis through anastomotic failure after surgical procedures is a frequent problem in the clinical setting.

The CASP model is a well-established and clinically relevant animal model of polymicrobial sepsis. The stent used in CASP leads to continuous leakage of feces into the abdomen, and therefore, closely mimics the clinical course of diffuse peritonitis in patients with steadily increasing systemic infection and inflammation (22). The severity of sepsis and resulting mortality can be controlled in CASP models, as it is directly depending on the size of the stent (21). Mortality occurs already at early time points in the experimental models of severe sepsis, such as CASP with large stent, or cecal ligation and puncture models (22). In the model of moderate

TABLE 1 | Main effects of peritoneal infection and surgical stress on inflammatory markers, unfolded protein response, and interaction of both the conditions determined by two-way ANOVA.

Variable		Main effect (*p*-value)		Interaction (*p*-value)
		Peritoneal infection	Surgery	
AST	Activity	0.638	**<0.0001**	0.133
ALT	Activity	**0.008**	0.157	0.289
De Ritis ratio	(AST/ALT)	**0.002**	**0.0002**	0.396
TNF-α	mRNA	**0.002**	0.132	0.516
IL-6	mRNA	**0.035**	0.112	0.233
iNOS	mRNA	**0.0004**	0.4690	0.872
HO-1	mRNA	**0.000**	0.141	0.314
p-eIF2α	Protein	0.733	**0.0008**	0.697
XBP1s	mRNA	0.074	**0.007**	0.975
GRP78	mRNA	0.202	**<0.0001**	**0.044**
XBP1	mRNA	0.404	**<0.0001**	0.625
GRP78	Protein	0,765	0.680	0.134
CHOP	mRNA	0.897	**0.006**	0.118
BAX/Bcl-XL	mRNA	0.995	**<0.0001**	0.164

Significant effects ($p < 0.05$) are indicated by bold values.

peritonitis, which was applied in this study, the survival rate was more than 90% until 96 h after surgery (24). Therefore, this model is characterized as non-lethal but self-resolving peritonitis. Using this model, we previously demonstrated that CASP transiently compromised liver mitochondria early (24–48 h) after surgery (24). The transient nature of CASP-induced effects on functional parameters of the liver confirms the moderate and self-resolving character of the present peritonitis model.

Organ/Cell Damage

The levels of the liver damage markers AST, as published previously (24), and the De Ritis ratio were only moderately elevated. AST and De Ritis ratio were significantly higher at the early time point (24 h) in response to the surgical stress. Thereafter, these values declined successively supporting the self-resolving character of the CASP model. Abdominal infection only slightly modulated AST values, which resulted in moderately, albeit significantly higher De Ritis ratios in the CASP groups at 48 and 96 h after surgery. Thus, the surgical procedure exerted an acute, but transient stress that was associated with a moderate liver-damaging potential. Moderate peritonitis contributed little to liver damage, which occurred predominantly in response to surgery. We assume that this reaction was the consequence of tissue damage related to the surgery. The increased expression of ER stress response genes in the blood cells of patients 1 day after cardiac surgery with cardiopulmonary bypass supports our assumption (30).

Hepatic Inflammatory Response

In contrast to organ damage markers, expression of markers of inflammation in liver tissues showed a strong response to and a clear association with the abdominal infection. In CASP compared with the sham animals, gene expression of proinflammatory markers was maximally and significantly increased at 48 h. Thereafter, gene expression levels declined with HO-1 and iNOS still being significantly higher in the sham group up to the latest time point investigated (96 h). We attribute this late effect to the continuously increasing systemic response to infection and inflammation induced by CASP, as shown before (22). These data show that surgery contributes little if anything to the inflammatory response in the liver, which is essentially triggered by the abdominal infection. Of note, we have determined the inflammatory markers at gene expression levels, which reflect a quick response to infection. Thus, it can be assumed that in the present model, abdominal infection induced by CASP takes about 2 days (48 h) to reach the maximum. This is also the time point, at which high-mortality rates can be observed in severe sepsis models and septic patients (21, 31, 32). We assumed that UPR would follow the same kinetics if triggered by infectious stimuli.

Hepatic Unfolded Protein Response

Contrary to this assumption, the kinetics of expression of ER stress and UPR-related markers were different from those of the proinflammatory markers. The changes observed for the UPR-related markers were moderate, but most strikingly, markers associated with IRE1α activation were maximal at 24 h after surgery. Furthermore, we could not determine a significant effect of CASP on the UPR-related markers investigated.

Unfolded protein response activation in consequence of tissue damage (33), particularly because of hypoxia or ischemia/reperfusion (15, 16), has been demonstrated in the last couple of years. Thus, we assume that hepatic ER stress and UPR are a consequence of circulating damage-associated signals (possibly danger-associated molecular patterns) rather than inflammatory mediators.

This association was addressed more profoundly by reanalyzing data sets from two different acute models, a THS model and an endotoxic shock model (*i.v.* application of lipopolysaccharide (LPS)), which were part of studies previously published (15, 28). Both experimental models are associated with a substantial loss of animals (up to 50%) and are, in contrast to the CASP model, characterized by a nearly immediate response of the liver (15, 28). Therefore, we considered a very early time point (2 h) most suitable to dissect the direct impact of induced tissue damage vs. induced inflammation on the manifestation of the hepatic ER stress response.

The infectious stimulus, LPS, triggered predominantly an increased inflammatory response that was initially not associated with substantial organ damage (28) and only a weakly upregulated hepatic UPR at this time point. In contrast, THS, which triggered significant organ damage (15), was associated with a strongly upregulated hepatic UPR, while an inflammatory response was absent at this early time point. Of importance, in the THS model XBP1 and XBP1s nearly instantly followed organ damage as indicated by the increased levels of ALT (15). These data indicate that conditions associated with organ damage rather than infectious stimuli operate as direct triggers of the hepatic

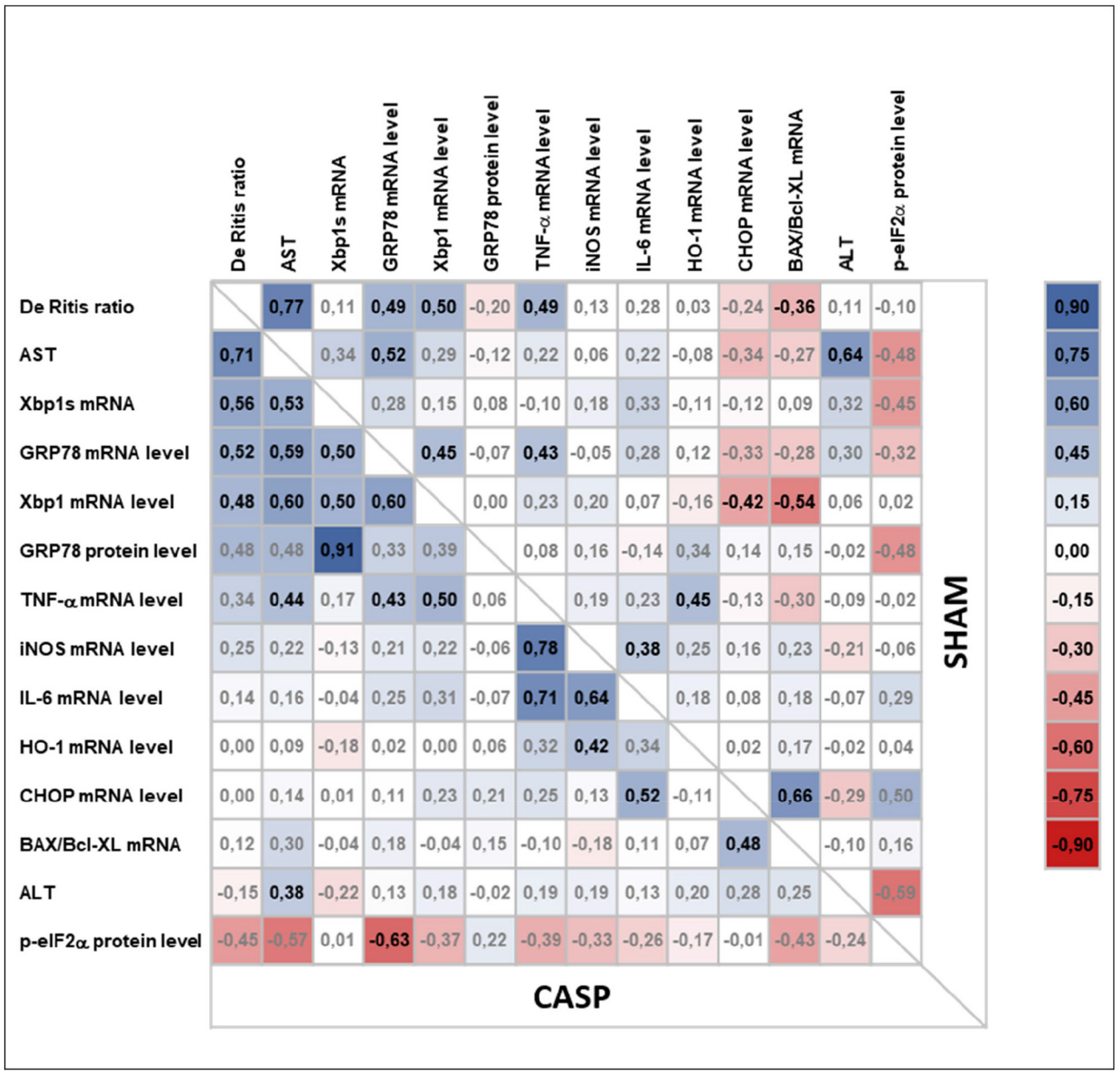

FIGURE 6 | Pearson correlation analysis of liver damage markers, UPR, and inflammatory response in animals subjected to surgery (sham) or CASP. Markers for organ damage (plasma ALT and AST and De Ritis ratio) and levels of hepatic markers for UPR (XBP1s mRNA, XBP1 mRNA, GRP78 mRNA/protein, p-eIF2α protein, CHOP mRNA), inflammatory response (IL-6 mRNA, TNF-α mRNA, iNOS mRNA), general stress response (HO-1 mRNA), as well as BAX/Bcl-XL mRNA ratio as a marker for a proapoptotic phenotype were correlated with each other in both, CASP and sham animals, using Pearson correlation ($n = 4$–8 for all mRNA data, $n = 1$–3 for all the protein data). In the upper right and the lower left part correlation coefficients (r) calculated from sham and CASP animals, respectively, are shown. A correlation plot was prepared using Microsoft Excel 2016. Positive correlations are highlighted in blue, negative correlations in red. Significant correlations are indicated by bold letters.

UPR. This assumption is further supported by our additional experiments using cultured immortalized liver cells, in which we show that inflammatory mediators were capable to induce an inflammatory response, but not a substantial ER stress response.

We found that UPR, which was triggered primarily by tissue damage, is associated with IRE1α and PERK activation. IRE1α activation, through the expression of XBP1s, has been extensively associated with cell survival (34). In the CASP model, IRE1α was temporarily activated early (24 h) after surgery, while the PERK-eIF2α-p-eIF2α pathway was activated throughout the entire observation period. Phosphorylation of eIF2α inhibits translation initiation resulting in a reduction of protein load in the ER, except for transcripts related to ER stress resolution (35). Persistent PERK-ATF4-CHOP signaling can commit the cell to

apoptosis (36). Indeed, CHOP levels peaked 48 h after surgery and resulted in transiently higher BAX/Bcl-XL ratios indicating a proapoptotic switch at the consecutive time point (48 h) in the present model. In addition, eIF2α phosphorylation and CHOP activation are associated with metabolic dysregulation during hepatic ER stress (37).

Although individual UPR-related targets increased only moderately in this model, the entity of upregulated UPR-related markers following tissue trauma because of the surgery likely reflects an early effort to rescue tissue function upon danger signaling, as was previously suggested (38).

In addition, both the XBP1 and the downstream target GRP78 correlated significantly with AST and De Ritis ratio in the present CASP model. Although a correlation does not imply a causal relationship, it is noteworthy that organ damage markers did not correlate with inflammatory markers, but with ER stress markers. Pharmacological induction of ER stress has been shown to result in increased mortality after trauma (33). In contrast, inhibition of ER stress has been shown to protect livers against ischemia/reperfusion injury in a model of hepatectomy (39). This indicates that possibly danger-associated molecular patterns, released in substantial amounts during trauma or surgery, but also secondary to substantial systemic inflammatory conditions are triggers of liver cell death employing mechanisms that involve ER stress pathways.

Interaction of Hepatic UPR With CASP-Induced Inflammatory Response Pathways

Even though abdominal infection had no significant effect on the expression of UPR markers, we found a stronger association between XBP1s and GRP78 with liver damage markers in rats that underwent CASP. Furthermore, CASP altered the kinetics of GRP78 gene expression following surgical trauma toward a later decline, suggesting cooperation between inflammatory and ER stress pathways. To the best of our knowledge, no experiments could show a direct induction of UPR by inflammatory mediators, such as cytokines. However, the secondary organ damage, which is typically accompanying inflammatory conditions, could well explain the increased ER stress response seen in SIRS. Vice versa, ER stress is capable to trigger inflammatory pathways acting as synergizing components in several pathologies (40). Both UPR branches, IRE1α and PERK can directly activate nuclear factor kappa B (NF-κB) (41, 42) leading to the production of inflammatory cytokines. ER stress activating IRE1α is further linked to TNF-α-mediated cell death through the adaptor protein tumor necrosis factor α receptor-associated factor 2 (TRAF2) and NF-κB (43). Therefore, cell death signals synergize in response to inflammation triggered by TNF-α, which also employs NF-κB. TNF-α levels in the plasma of CASP animals were elevated 96 h after surgery in the present model (24). The increased De Ritis ratio in the CASP group at this time point possibly reflects a converged synergism of cell death pathways. Although the low mortality of this CASP model indicates that the elicited inflammatory response may be self-resolving, it was sufficient to transiently affect mitochondrial function in the liver (24). Interestingly, mitochondrial damage driven by caspase 2 has been described as a mechanism underlying hepatocyte death upon ER stress that operated *via* NLRP3 inflammasome activation (44, 45).

Given the good outcome of our experimental rats, which were young and showed no clinical signs when enrolled in the study, we assume that the damage triggered hepatic UPR was well balanced and exerted a beneficial role in the present CASP model. However, since ER stress is a critical inflammation triggering factor, the role of surgery modulating UPR warrants closer consideration in patients suffering from comorbidities, i.e., metabolic diseases (46). Based on our results, we suggest therapeutic approaches, which target the ER to maintain liver function in conditions associated with inflammatory processes, such as sepsis. Of note, certain anesthetics or antibiotics have been shown to modulate ER stress induction in the liver (47–50). Thus, the choice of an appropriate anesthetic protocol during surgery followed by a suitable antibiotic therapy might help to shape UPR and limit consecutive liver damage.

Limitations

This study was focused on the progression of ER stress/UPR markers exclusively in the liver as a remote target organ in the peritonitis and abdominal surgery, because of its central role for the system. However, we did not analyze the local effects of peritonitis. Several studies have already highlighted the relevance of intestinal ER stress in peritonitis that is tightly linked to deranged intestinal tissue homeostasis and immunity (51, 52), and particularly the impairment of the intestinal barrier function (53). Further studies will be necessary to clarify the source or the nature of the compounds that trigger the ER stress/UPR and inflammatory response in the liver.

CONCLUSION

Using a clinically relevant experimental sepsis model, we found that surgical trauma activates hepatic UPR, presumably because of tissue injury. UPR activation occurred early and preceded the inflammatory response in the liver. This indicates that hepatic UPR and the inflammatory response are triggered by different mechanisms. Our data further suggest that secondary tissue injury, as it occurs in septic complications, may influence the severity of ER stress and UPR-mediated liver cell dysfunction. Thus, the hepatic ER appears to be an important target for shaping UPR in order to prevent liver dysfunction in abdominal surgery and severe SIRS.

DATA AVAILABILITY STATEMENT

The original contributions presented in the study are included in the article/**Supplementary Material**, further inquiries can be directed to the corresponding author.

ETHICS STATEMENT

The animal study was reviewed and approved by Landesamt für Natur, Umwelt und Verbraucherschutz, Recklinghausen, Germany (experiments were performed in accordance with the NIH Guidelines for Animal Care).

AUTHOR CONTRIBUTIONS

AM wrote the first draft of the manuscript, performed the statistical analysis and the graphical data presentation. AH and OP performed and supervised animal experiments. IM performed and interpreted WB analysis. AM and MK performed and interpreted PCR analysis. AL provided critical feedback and revised the manuscript. JD, IB, and AK designed and supervised the study. JD and AK provided critical feedback and wrote the final version of the manuscript. All authors gave intellectual input and approved the final version of the manuscript.

FUNDING

AM was supported by the Austrian Research Promotion Agency with a Ph.D. Grant: Industrienahe Dissertation (849090). MK was supported by an Internship for female students from the Austrian Research Promotion Agency (FFG). AL received funding from the European Union's Horizon 2020 Research and Innovation Program under the Marie Skłodowska-Curie Grant Agreement No. 675448.

ACKNOWLEDGMENTS

We thank H. P. Satzer, J. Paier-Pourani, and I. Kehrer for contributing the data of the cultured hepatocyte cells (BRL3A) treated with ER stressors, tunicamycin and thapsigargin, and inflammatory mediators, generated from white blood cells, which were included in the **Supplemental Material**.

SUPPLEMENTARY MATERIAL

The Supplementary Material for this article can be found online at: https://www.frontiersin.org/articles/10.3389/fmed.2022.785285/full#supplementary-material

REFERENCES

1. Hatfield KM, Dantes RB, Baggs J, Sapiano MRP, Fiore AE, Jernigan JA, Epstein L. Assessing variability in hospital-level mortality among US medicare beneficiaries with hospitalizations for severe sepsis and septic shock. *Crit Care Med.* (2018) 46:1753–60. doi: 10.1097/CCM.0000000000003324
2. Yan J, Li S, Li S. The role of the liver in sepsis. *Int Rev Immunol.* (2014) 33:498–510. doi: 10.3109/08830185.2014.889129
3. Strnad P, Tacke F, Koch A, Trautwein C. Liver-guardian, modifier and target of sepsis. *Nat Rev Gastroenterol Hepatol.* (2017) 14:55–66. doi: 10.1038/nrgastro.2016.168
4. Moshage H. Cytokines and the hepatic acute phase response. *J Pathol.* (1997) 181:257–66. doi: 10.1002/(SICI)1096-9896(199703)181:3<257::AID-PATH756>3.0.CO;2-U
5. Khan MM, Yang WL, Wang P. Endoplasmic reticulum stress in sepsis. *Shock.* (2015) 44:294–304. doi: 10.1097/SHK.0000000000000425
6. Thiessen SE, Van den Berghe G, Vanhorebeek I. Mitochondrial and endoplasmic reticulum dysfunction and related defense mechanisms in critical illness-induced multiple organ failure. *Biochim Biophys Acta Mol Basis Dis.* (2017) 1863:2534–45. doi: 10.1016/j.bbadis.2017.02.015
7. Hetz C, Zhang K, Kaufman RJ. Mechanisms, regulation and functions of the unfolded protein response. *Nat Rev Mol Cell Biol.* (2020) 21:421–38. doi: 10.1038/s41580-020-0250-z
8. Yamamoto K, Sato T, Matsui T, Sato M, Okada T, Yoshida H, et al. Transcriptional induction of mammalian ER quality control proteins is mediated by single or combined action of ATF6alpha and XBP1. *Dev Cell.* (2007) 13:365–76. doi: 10.1016/j.devcel.2007.07.018
9. Lee A-H, Iwakoshi NN, Glimcher LH. XBP-1 regulates a subset of endoplasmic reticulum resident chaperone genes in the unfolded protein response. *Mol Cell Biol.* (2003) 23:7448–59. doi: 10.1128/mcb.23.21.7448-7459.2003
10. Ron D. Translational control in the endoplasmic reticulum stress response. *J Clin Invest.* (2002) 110:1383–8. doi: 10.1172/JCI16784
11. Hu H, Tian M, Ding C, Yu S. The C/EBP homologous protein (CHOP) transcription factor functions in endoplasmic reticulum stress-induced apoptosis and microbial infection. *Front Immunol.* (2019) 10:1–13. doi: 10.3389/fimmu.2018.03083
12. Kaufman RJ. Orchestrating the unfolded protein response in health and disease. *J Clin Invest.* (2002) 110:1389–98. doi: 10.1172/JCI0216886
13. Almanza A, Carlesso A, Chintha C, Creedican S, Doultsinos D, Leuzzi B, et al. Endoplasmic reticulum stress signalling—from basic mechanisms to clinical applications. *FEBS J.* (2019) 286:241–78. doi: 10.1111/febs.14608
14. Kozlov A V, Duvigneau JC, Miller I, Nürnberger S, Gesslbauer B, Kungl A, et al. Endotoxin causes functional endoplasmic reticulum failure, possibly mediated by mitochondria. *Biochim Biophys Acta Mol Basis Dis.* (2009) 1792:521–30. doi: 10.1016/j.bbadis.2009.03.004
15. Duvigneau JC, Kozlov A V, Zifko C, Postl A, Hartl RT, Miller I, et al. Reperfusion does not induce oxidative stress but sustained endoplasmic reticulum stress in livers of rats subjected to traumatic-hemorrhagic shock. *Shock.* (2010) 33:289–98. doi: 10.1097/SHK.0b013e3181aef322
16. Jian B, Hsieh CH, Chen J, Choudhry M, Bland K, Chaudry I, et al. Activation of endoplasmic reticulum stress response following trauma-hemorrhage. *Biochim Biophys Acta Mol Basis Dis.* (2008) 1782:621–6. doi: 10.1016/j.bbadis.2008.08.007
17. Kleber A, Kubulus D, Rössler D, Wolf B, Volk T, Speer T, et al. Melatonin modifies cellular stress in the liver of septic mice by reducing reactive oxygen species and increasing the unfolded protein response. *Exp Mol Pathol.* (2014) 97:565–71. doi: 10.1016/j.yexmp.2014.10.009
18. Qian W-J, Cheng Q-H. Endoplasmic reticulum stress-mediated apoptosis signal pathway is involved in sepsis-induced liver injury. *Int J Clin Exp Pathol.* (2017) 10:9990−7.
19. Thiessen SE, Derese I, Derde S, Dufour T, Pauwels L, Bekhuis Y, et al. The role of autophagy in critical illness-induced liver damage. *Sci Rep.* (2017) 7:1–12. doi: 10.1038/s41598-017-14405-w
20. Hecker A, Reichert M, Reuß CJ, Schmoch T, Riedel JG, Schneck E, et al. Intra-abdominal sepsis: new definitions and current clinical standards. *Langenbeck's Arch Surg.* (2019) 404:257–71. doi: 10.1007/s00423-019-01752-7
21. Lustig MK, Bac VH, Pavlovic D, Maier S, Gründling M, Grisk O, et al. Colon ascendens stent peritonitis—a model of sepsis adopted to the rat:

physiological, microcirculatory and laboratory changes. *Shock.* (2007) 28:59–64. doi: 10.1097/SHK.0b013e31802e454f
22. Maier S, Traeger T, Entleutner M, Westerholt A, Kleist B, Hüser N, et al. Cecal ligation and puncture versus colon ascendens stent peritonitis: two distinct animal models for polymicrobial sepsis. *Shock.* (2004) 21:505–11. doi: 10.1097/01.shk.0000126906.52367.dd
23. Russel WMS, Burch RL. *The Principles of Humane Experimental Technique.* (1959) Available at: https://caat.jhsph.edu/principles/the-principles-of-humane-experimental-technique (accessed September 23, 2021)
24. Herminghaus A, Papenbrock H, Eberhardt R, Vollmer C, Truse R, Schulz J, et al. Time-related changes in hepatic and colonic mitochondrial oxygen consumption after abdominal infection in rats. *Intensive care Med Exp.* (2019) 7:4. doi: 10.1186/s40635-018-0219-9
25. Cerative Commons Corporation, Creative Commons Licence. (1996) Available online at: https://creativecommons.org/licenses/by/4.0/ (accessed September 23, 2021)
26. Müllebner A, Moldzio R, Redl H, Kozlov AV, Duvigneau JC. Heme degradation by heme oxygenase protects mitochondria but induces ER stress via formed bilirubin. *Biomolecules.* (2015) 5:679–701. doi: 10.3390/biom5020679
27. Motulsky HJ, Brown RE. Detecting outliers when fitting data with nonlinear regression - A new method based on robust nonlinear regression and the false discovery rate. *BMC Bioinformatics.* (2006) 7:1–20. doi: 10.1186/1471-2105-7-123
28. Nürnberger S, Miller I, Catharina Duvigneau J, Kavanagh ET, Gupta S, Hartl RT, et al. Impairment of endoplasmic reticulum in liver as an early consequence of the systemic inflammatory response in rats. *Am J Physiol Gastrointest Liver Physiol.* (2012) 303:1373–83. doi: 10.1152/ajpgi.00056.2012
29. SepNet Critical Care Trials Group. Incidence of severe sepsis and septic shock in German intensive care units: the prospective, multicentre INSEP study. *Intensive Care Med.* (2016) 42:1980–1989. doi: 10.1007/s00134-016-4504-3
30. Clavier T, Demailly Z, Semaille X, Thill C, Selim J, Veber B, et al. Weak response to endoplasmic reticulum stress is associated with postoperative organ failure in patients undergoing cardiac surgery with cardiopulmonary bypass. *Front Med.* (2020) 7:613518. doi: 10.3389/fmed.2020.613518
31. Mishra SK, Choudhury S. Experimental protocol for cecal ligation and puncture model of polymicrobial sepsis and assessment of vascular functions in mice. *Methods Mol Biol.* (2018) 1717:161–87. doi: 10.1007/978-1-4939-7526-6_14
32. Davies R, O'Dea K, Gordon A. Immune therapy in sepsis: are we ready to try again? *J Intensive Care Soc.* (2018) 19:326–44. doi: 10.1177/1751143718765407
33. Abdullahi A, Barayan D, Vinaik R, Diao L, Yu N, Jeschke MG. Activation of ER stress signalling increases mortality after a major trauma. *J Cell Mol Med.* (2020) 24:9764–73. doi: 10.1111/jcmm.15548
34. Lin JH Li H, Yasumura D, Cohen HR, Zhang C, Panning B, Shokat KM, et al. IRE1 signaling affects cell fate during the unfolded protein response. *Science.* (2007) 318:944–9. doi: 10.1126/science.1146361
35. Szegezdi E, Logue SE, Gorman AM, Samali A. Mediators of endoplasmic reticulum stress-induced apoptosis. *EMBO Rep.* (2006) 7:880–5. doi: 10.1038/sj.embor.7400779
36. McCullough KD, Martindale JL, Klotz L-O, Aw T-Y, Holbrook NJ. Gadd153 sensitizes cells to endoplasmic reticulum stress by down-regulating Bcl2 and perturbing the cellular redox state. *Mol Cell Biol.* (2001) 21:1249–59. doi: 10.1128/mcb.21.4.1249-1259.2001
37. Chikka MR, McCabe DD, Tyra HM, Rutkowski DT. C/EBP homologous protein (CHOP) contributes to suppression of metabolic genes during endoplasmic reticulum stress in the liver. *J Biol Chem.* (2013) 288:4405–15. doi: 10.1074/jbc.M112.432344
38. Soares MP, Gozzelino R, Weis S. Tissue damage control in disease tolerance. *Trends Immunol.* (2014) 35:483–94. doi: 10.1016/j.it.2014.08.001
39. Ben Mosbah I, Alfany-Fernández I, Martel C, Zaouali MA, Bintanel-Morcillo M, Rimola A, et al. Endoplasmic reticulum stress inhibition protects steatotic and non-steatotic livers in partial hepatectomy under ischemia-reperfusion. *Cell Death Dis.* (2010) 1:1–12. doi: 10.1038/cddis.2010.29
40. Zhang K, Kaufman RJ. From endoplasmic-reticulum stress to the inflammatory response. *Nature.* (2008) 454:455–62. doi: 10.1038/nature07203
41. Kaneko M, Niinuma Y, Nomura Y. Activation signal of nuclear factor-kappa B in response to endoplasmic reticulum stress is transduced via IRE1 and tumor necrosis factor receptor-associated factor 2. *Biol Pharm Bull.* (2003) 26:931–5. doi: 10.1248/bpb.26.931
42. Deng J, Lu PD, Zhang Y, Scheuner D, Kaufman RJ, Sonenberg N, et al. Translational repression mediates activation of nuclear factor kappa B by phosphorylated translation initiation factor 2. *Mol Cell Biol.* (2004) 24:10161–8. doi: 10.1128/MCB.24.23.10161-10168.2004
43. Schmitz ML, Shaban MS, Albert BV, Gökçen A, Kracht M. The crosstalk of endoplasmic reticulum (ER) stress pathways with NF-κB: complex mechanisms relevant for cancer, inflammation and infection. *Biomedicines.* (2018) 6:1–18. doi: 10.3390/biomedicines6020058
44. Lebeaupin C, Proics E, de Bieville CHD, Rousseau D, Bonnafous S, Patouraux S, et al. ER stress induces NLRP3 inflammasome activation and hepatocyte death. *Cell Death Dis.* (2015) 6:e1879. doi: 10.1038/cddis.2015.248
45. Bronner DN, Abuaita BH, Chen X, Fitzgerald KA, Nuñez G, He Y, et al. Endoplasmic reticulum stress activates the inflammasome via NLRP3- and caspase-2-driven mitochondrial damage. *Immunity.* (2015) 43:451–62. doi: 10.1016/j.immuni.2015.08.008
46. Hotamisligil GS. Endoplasmic reticulum stress and the inflammatory basis of metabolic disease. *Cell.* (2010) 140:900–17. doi: 10.1016/j.cell.2010.02.034
47. Liu D, Jin X, Zhang C, Shang Y. Sevoflurane relieves hepatic ischemia-reperfusion injury by inhibiting the expression of Grp78. *Biosci Rep.* (2018) 38:1–10. doi: 10.1042/BSR20180549
48. Seo EH, Piao L, Park HJ, Lee JY, Sa M, Oh CS, et al. Impact of general anaesthesia on endoplasmic reticulum stress: propofol vs. isoflurane. *Int J Med Sci.* (2019) 16:1287–94. doi: 10.7150/ijms.36265
49. Bellizzi Y, Anselmi Relats JM, Cornier PG, Delpiccolo CML, Mata EG, Cayrol F, et al. Contribution of endoplasmic reticulum stress, MAPK and PI3K/Akt pathways to the apoptotic death induced by a penicillin derivative in melanoma cells. *Apoptosis.* (2021) 2021:1–15. doi: 10.1007/s10495-021-01697-7
50. Burban A, Sharanek A, Guguen-Guillouzo C, Guillouzo A. Endoplasmic reticulum stress precedes oxidative stress in antibiotic-induced cholestasis and cytotoxicity in human hepatocytes. *Free Radic Biol Med.* (2018) 115:166–78. doi: 10.1016/j.freeradbiomed.2017.11.017
51. Eugene SP, Reddy VS, Trinath J. Endoplasmic reticulum stress and intestinal inflammation: a perilous union. *Front Immunol.* (2020) 11:1–10. doi: 10.3389/fimmu.2020.543022
52. Coleman OI, Haller D, ER. Stress and the UPR in Shaping Intestinal Tissue Homeostasis and Immunity. *Front Immunol.* (2019) 10:1–13. doi: 10.3389/fimmu.2019.02825
53. Sun S, Duan Z, Wang X, Chu C, Yang C, Chen F, et al. Neutrophil extracellular traps impair intestinal barrier functions in sepsis by regulating TLR9-mediated endoplasmic reticulum stress pathway. *Cell Death Dis.* (2021) 12:1–12. doi: 10.1038/s41419-021-03896-1

Conflict of Interest: The authors declare that the research was conducted in the absence of any commercial or financial relationships that could be construed as a potential conflict of interest.

Publisher's Note: All claims expressed in this article are solely those of the authors and do not necessarily represent those of their affiliated organizations, or those of the publisher, the editors and the reviewers. Any product that may be evaluated in this article, or claim that may be made by its manufacturer, is not guaranteed or endorsed by the publisher.

frontiers in Pharmacology

ORIGINAL RESEARCH
published: 21 March 2022
doi: 10.3389/fphar.2022.829830

Metformin Promotes Differentiation and Attenuates H_2O_2-Induced Oxidative Damage of Osteoblasts *via* the PI3K/AKT/Nrf2/HO-1 Pathway

Keda Yang, Fangming Cao, Shui Qiu, Wen Jiang, Lin Tao and Yue Zhu**

Department of Orthopedics, First Hospital of China Medical University, Shenyang, China

At present, the drug treatment of osteoporosis is mostly focused on inhibiting osteoclastogenesis, which has relatively poor effects. Metformin is a drug that can potentially promote osteogenic differentiation and improve bone mass in postmenopausal women. We aimed to detect the molecular mechanism underlying the osteogenic effect of metformin. Our study indicated that metformin obviously increased the Alkaline phosphatase activity and expression of osteogenic marker genes at the mRNA and protein levels. The PI3K/AKT signaling pathway was revealed to play an essential role in the metformin-induced osteogenic process, as shown by RNA sequencing. We added LY294002 to inhibit the PI3K/AKT pathway, and the results indicated that the osteogenic effect of metformin was also blocked. Additionally, the sequencing data also indicated oxidation-reduction reaction was involved in the osteogenic process of osteoblasts. We used H_2O_2 to mimic the oxidative damage of osteoblasts, but metformin could attenuate it. Antioxidative Nrf2/HO-1 pathway, regarded as the downstream of PI3K/AKT pathway, was modulated by metformin in the protective process. We also revealed that metformin could improve bone mass and oxidative level of OVX mice. In conclusion, our study revealed that metformin promoted osteogenic differentiation and H_2O_2-induced oxidative damage of osteoblasts *via* the PI3K/AKT/Nrf2/HO-1 pathway.

Keywords: metformin, osteogenic differentiation, RNA sequencing, oxidative damage, PI3K/AKT/Nrf2/HO-1

OPEN ACCESS

Edited by:
Andreas Nüssler,
University of Tübingen, Germany

Reviewed by:
Shyamsundar Pal China,
University of California, San Diego, United States
Sabrina Ehnert,
University of Tübingen, Germany

****Correspondence:***
Lin Tao
taolindr@163.com
Yue Zhu
zhuyuedr@163.com

Specialty section:
This article was submitted to Translational Pharmacology, a section of the journal Frontiers in Pharmacology

Received: *20 January 2022*
Accepted: *02 March 2022*
Published: *21 March 2022*

Citation:
Yang K, Cao F, Qiu S, Jiang W, Tao L and Zhu Y (2022) Metformin Promotes Differentiation and Attenuates H_2O_2-Induced Oxidative Damage of Osteoblasts via the PI3K/AKT/Nrf2/HO-1 Pathway. Front. Pharmacol. 13:829830. doi: 10.3389/fphar.2022.829830

INTRODUCTION

Osteoporosis is characterized by a decrease in the amount of bone tissue per unit volume and mainly occurs in postmenopausal women and diabetes patients (Chapurlat et al., 2020; Zhou et al., 2020). Estrogen deficiency and glucose overload reduce the inhibition of osteoclast differentiation and enhances bone resorption, leading to the loss of bone mass (Ponte et al., 2020; Cho et al., 2021; Sha et al., 2021). The current strategy for osteoporosis treatment is mainly to inhibit osteoclasts with drugs such as bisphosphonates, estrogen receptor modulators and calcitonin (Ukon et al., 2019; Hsiao et al., 2020; Toriumi et al., 2020). However, these drugs are limited because they only prevent further loss of bone mass, and do not restore it. To improve this condition, researchers can increase the activity of osteoblasts in patients, which will be an effective means of treatment. Weakened differentiation and declined activity of osteoblasts aggravate the deterioration of osteoporosis (Xu et al., 2020; Yang et al., 2020). Therefore, enhancing differentiation and increasing activity is essential in improving the treatment of osteoporosis.

The acceleration of the aging population has resulted in a gradual increase in the incidence of osteoporotic fractures. Estrogen deficiency and impaired glucose tolerance are important factors that accelerate aging (He et al., 2020; Kashima et al., 2021). And the decline in body function related to aging is caused by oxidative damage with the accumulation of reactive oxygen species (ROS) (Buccellato et al., 2021). Recent studies have determined that metformin shows anti-aging effects and resistance to diseases caused by aging, which indicates the potential application of metformin in osteoporosis (Martel et al., 2021; Sharma et al., 2021). Metformin is a hypoglycemic drug that has been verified to improve bone mass loss in diabetes-induced osteoporosis by decreasing the blood glucose level (Tseng, 2021). And metformin also shows potential therapeutic effects in postmenopausal osteoporosis (Yang et al., 2021). However, the direct effect of metformin on bone metabolism is unclear. The molecular mechanism of metformin on osteogenic differentiation and prevention of oxidative damage remain to be determined.

A new generation of high-throughput transcriptome sequencing methods have been used in basic research, clinical diagnostics and drug development (Koborova et al., 2009; Wang et al., 2013). RNA sequencing technology has become an important method in transcriptomic research. The principle is to sequence genomic cDNA, calculate the expression of different mRNAs by counting the number of related small cDNA fragments and analyze the expression level of the transcript (Niemi et al., 2015). This technology can elucidate gene function and structure at the overall level and reveal specific biological processes and molecular mechanisms in the occurrence of diseases (Cui et al., 2020; Wang Y et al., 2021). In previous studies, RNA sequencing has been widely used to determine the targets and pathways of drugs in disease research (Chen et al., 2021; Zhou et al., 2021). Therefore, we aimed to detect the molecular mechanism of metformin in osteogenic differentiation by using RNA sequencing.

MATERIALS AND METHODS

Reagents, Cell Culture and Osteogenic Differentiation

The reagents and chemicals used in this study are listed below. MC3T3-E1 cells were purchased from the Chinese Academy of Sciences Cell Bank. Metformin was purchased from Meilunbio (Dalian, China). Antibodies against Runx2 (1:1000; cat. no. ab236639), Collagen I (1:2500; cat. no. ab260043) Osteocalcin (OCN) (1:100; cat. no. ab93876), Nrf2 (1:1000, cat. no. ab92946) and HO-1 (1:5000; cat. no. ab68477) were obtained from Abcam (Cambridge, MA). β-actin antibodies (1:2000; cat. no. 66009-1-Ig) and a peroxidase-conjugated anti-rat secondary antibody (1:2000; cat. nos. SA00001-15) were purchased from Protein Tech Group, Inc. (Chicago, IL, United States). antibodies against PI3K (1:1,000; cat. no. 4257), phosphorylated (p-)PI3K (1:1,000; cat. no. 4228), AKT (1:1,000; cat. no. 4691) and p-AKT (1:1,000; cat. no. 4060) were purchased from Cell Signaling Technology, Inc. The PI3K/AKT signaling inhibitor LY294002 and AKT inhibitor MK2206 was purchased from Beyotime (Shanghai, China).

MC3T3-E1 cells were cultured in α-MEM (HyClone, Logan, UT, United States). The media were supplemented with 10% fetal bovine serum, 100 U/ml streptomycin sulfate, and 100 mg/ml penicillin. Osteogenic induction medium was prepared according to the following criterion: 100 mM β-glycerophosphate, 50 mg/L ascorbic acid and 10 nM dexamethasone. The parameters of the humidified incubator for MC3T3-E1 cell culture were set to 5% CO_2 and 37°C. Detection of ALP activity and mRNA and protein expression levels was performed after 7 days of osteogenic induction of MC3T3-E1 cells.

Cell Counting Kit-8 Assay

Cell Counting Kit-8 (CCK-8) (Dojindo Molecular Technologies, Inc. Japan) was used to detect cell viability after treatment with different concentrations of metformin. The reagent is an indicator of redox reactions. In the presence of the electron carrier 1-methoxy PMS, dehydrogenase in living cells can catalyze the tetrazolium salt WST-8 to generate formazan dyes, and the amount of formazan dye produced has a linear relationship with the number of living cells.

Alkaline Phosphatase Activity Detection

ALP is secreted by osteoblasts. ALP activity can directly reflect the differentiation level of osteoblasts. MC3T3-E1 cells were induced in osteogenic medium for 1 week. Then the ALP level was detected by ALP Analysis kits (Nanjing Jiancheng, China) according to the manufacturer's instructions.

Alizarin Red S Staining

Calcium salt variation is an indicator of osteoblast proliferation and differentiation. Alizarin Red S can form a complex with calcium salt in a chelating manner to identify the calcium salt component of tissue cells and produce orange-red deposits. MC3T3-E1 cells were cultured in 6-well plates and treated with induced medium for 28 days before Alizarin red S staining. The cells were first washed twice with PBS, fixed with 95% ethanol for 10 min, and washed with distilled water 3 times. Then 0.1% Alizarin Red-Tris-Hcl (pH 8.3) was added at 37°C for 30 min.

Reverse Transcription PCR (RT-qPCR) Assay

A miRNeasy RNA mini kit (Qiagen, MD, United States) was used to extract total RNA. Then, GoScript™ reverse transcription mix and oligo (dT) (Promega, Wi, United States) were used to synthesize cDNA. qPCR was performed using GoTaq® qPCR master mix (Promega, Wi, United States). The data were collected using a Roche Light Cycler® 480 II system (Roche, Basel, Switzerland). The conditions of PCR cycles were as follows: 2 min at 90°C, 15 s at 95°C and 60 s at 60°C for 45 cycles. *β*-actin was used as a standardized control. And the sequences of primers were listed in **Supplementary Table S1**. Gene expression was calculated by the $2^{-\Delta\Delta Ct}$ method.

Western Blotting

Protein was extracted after 7 days of treatment, and then frozen in a refrigerator at −80°C for later use.

Then, proteins were resolved by SDS-PAGE and transferred to polyvinylidene difluoride (PVDF) membranes. The membranes with proteins of various molecular weights were immersed in blocking buffer for 1.5 h. After the membranes were washed with 1% TBST, they were incubated with a primary antibody at 4°C overnight and a secondary antibody at 4°C the next day. After the membranes were thoroughly washed, the protein bands were coated with luminescent solution and visualized using a chemiluminescence (ECL) system (UVP Inc., CA, United States). The protein level was normalized to that of β-actin (molecular weight of 43 kDa). Finally, ImageJ software was used to calculate the optical density and relative protein expression levels.

RNA Sequencing Analysis

MC3T3-E1 cells were induced in osteogenic medium and metformin for 3 days. RNA sequencing analysis was performed by Novogene Institute (Tianjin, China). Differential expression analysis of two groups (three biological replicates per condition) was performed using the DESeq2 R package (1.20.0). Gene Ontology (GO) enrichment analysis of differentially expressed genes was implemented by the cluster Profiler R package, in which gene length bias was corrected. GO terms with corrected p values less than 0.05 were considered significantly enriched by differentially expressed genes. The KEGG pathway database was used in the cluster Profiler R package for the statistical enrichment of marker genes.

Gene Ontology Enrichment

GO enrichment analysis of marker genes was performed with DAVID Bioinformatics Resources 6.8. The gene length bias was corrected, and the GO terms with corrected p values less than 0.05 were considered significantly enriched for the marker genes. The biological domains examined in the GO database included three categories: molecular function, cellular component and biological process.

KEGG Pathway

The KEGG pathway database (KOBAS 3.0) was used for the statistical enrichment of marker genes. The database can help elucidate the high-level functions and utilities of cells, organisms and ecosystems and includes molecular-level information (especially large-scale molecular genome sequencing datasets) and information from other high-throughput experimental technologies.

Animal Experiments

Eight-week-old female mice were obtained from the Department of Laboratory Animal Science of China Medical University. The feeding environmental conditions were 20–26°C with constant temperature, 40–70% relative humidity, ≤14 mg/m3 ammonia concentration, ≤60 dB (A) noise and a 12 h/12 h alternating light and dark cycle. All animals were fed in this environment for 2 weeks before the experiments. Mice were randomly divided into three groups (n = 7 each group): a sham group, a bilateral ovariectomy (OVX) group and a OVX group with intragastric metformin (OVX + Met). We performed bilateral ovariectomy on mice under 1.4–1.5% isoflurane inhalation anesthesia with oxygen. The dosage of metformin for the OVX + Met mice was 100 mg/kg/day, which was dissolved in 0.9% normal saline. The mice in the other groups were fed only with equal amount of saline. After 8 weeks of treatment, all mice were sacrificed, and the bilateral femur and tibias were harvested for imaging and protein extraction. All animal experiments were approved by the Animal Ethics Committee of the First Affiliated Hospital of China Medical University and were performed according to the laboratory and animal welfare guidelines.

Microcomputed Tomography

Collected femurs were fixed with 4% formaldehyde solution for imaging by microcomputed tomography (μCT, Skyscan1276, Bruker, Germany). When X-rays pass through the sample, each part of the sample has different absorption rates for X-rays. The X-rays penetrate the sample and are finally imaged on the detector. Micro-CT uses tapered X-ray beams to image samples at different angles above 360°. The cone beam method can obtain isotropic volumetric images, improve spatial resolution, and increase ray utilization. X-ray images at each angle were reconstructed into a 3-dimensional image analyzed by the CT-analyser software CTAn 1.19.11.1 (Bruker Corporation). The parameters of the scan were as follows: X-ray voltage 50 kV, X-ray current 200 uA, Filter 0.5 mm aluminum, Image pixel size 8.9um, Camera resolution setting High (4,000 pixel field width), Tomographic rotation (180°/360°), Rotation step (0.3–0.5°), Frame averaging 1, Scan duration 20–50 min.

Biochemistry Assays

Mice-specific total antioxidant activities (T-AOC) was purchased from Nanjing Jiancheng Bioengineering Institute, Nanjing, China (A015-2-1) and superoxide dismutase (SOD) kits was purchased from Beyotime (S0101) to measure the serum T-AOC and SOD activity in mice. All experiments were performed according to the manufacturer's instructions.

Statistical Analysis

The experimental data were means ± standard deviation (SD) by using GraphPad Prism 8 (San Diego, CA, United States) and SPSS 22.0 (Chicago, IL, United States). Student's t-tests and one-way ANOVA were used for statistical analysis of three replicate experiments by SPSS. $p < 0.05$ was considered statistically significant.

RESULTS

Metformin Promotes Osteogenic Differentiation of MC3T3-E1 Cells

We first performed CCK-8 cell viability assays to detect MC3T3-E1 cell viability after treatment with different concentrations of metformin, and the results indicated that metformin had no inhibitory effect on osteoblast proliferation (**Figure 1A**). To determine whether metformin promoted osteogenic differentiation and the optimal concentration, we detected ALP activity with ALP Analysis kits. As shown in **Figure 1B**, metformin at 0.2 mM maximized osteogenic differentiation,

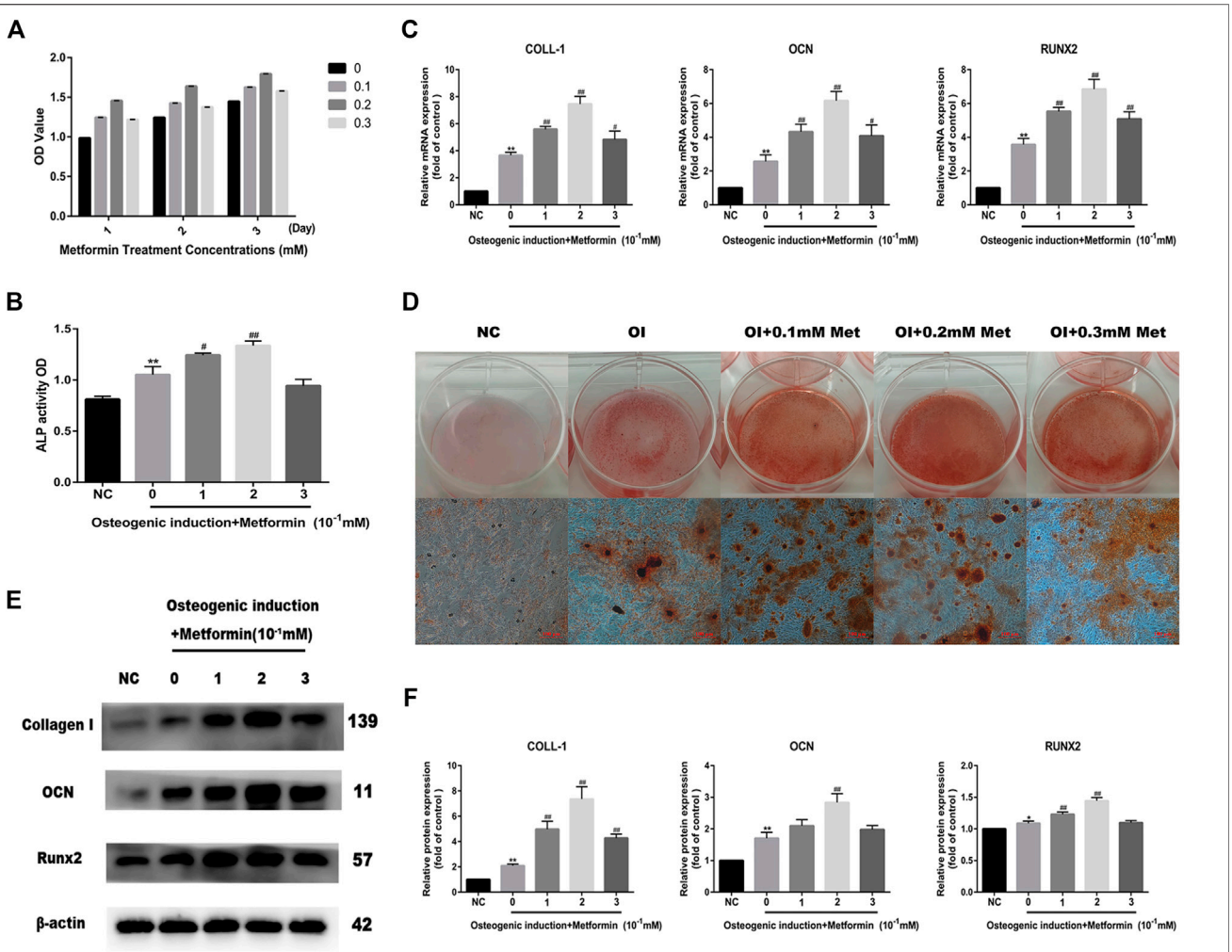

FIGURE 1 | Metformin promotes osteogenic differentiation of MC3T3-E1 cells. **(A)** Cell viability after treatment with different concentrations of metformin (0.1, 0.2 and 0.3 mM). **(B)** ALP activity was detected to explicit the osteogenic effect of metformin. **(C)** The mRNA level of COLL-1, OCN and Runx2 after osteogenic induction and treatment with metformin. **(D)** The mineralization of osteoblast demonstrated by Alizarin red S staining was most obvious after treatment with 0.2 mM metformin. **(E)** The protein level of Collagen I, OCN and Runx2 under different concentrations of metformin. **(F)** Relative protein expression level of the proteins in **(E)** compared with control group. Experiments were implemented in triplicate. Data are means ± SD, $^{*}p < 0.05$, $^{**}p < 0.01$ compared with control cells and $^{\#}p < 0.05$, $^{\#\#}p < 0.01$ compared with osteogenic induction alone analyzed by using ANOVA.

which was also verified by the mRNA expression of osteogenic genes including Runx2, OCN and COLL-1 (**Figure 1C**). Additionally, we performed Alizarin Red S staining and western blotting to evaluate the effect of metformin treatment on the differentiation of osteoblasts (**Figures 1D,E**). The protein levels of Collagen I, Runx2 and OCN increased most obviously with 0.2 mM metformin treatment (**Figure 1F**).

RNA-Sequencing Reveals That PI3K/AKT Signaling Pathway is involved in Metformin-Induced Osteogenic Differentiation

Based on the data mentioned above, we attempted to elucidate the mechanism by which metformin promoted osteoblast differentiation. We performed RNA sequencing to compare the differential expression of genes between osteogenic induction with and without 0.2 mM metformin treatment. Compared with osteogenic medium alone, a total of 1946 up-regulated and 1544 down-regulated genes were obtained when treating with metformin after quality control and differential analysis (**Figure 2A**). We performed KEGG pathway analysis of these up-regulated genes and the results showed that they were enriched in PI3K/AKT signaling pathway (**Figure 2B**). These genes included PI3K upstream regulators ITGA, ITGB and SYK; the AKT upstream regulators HSP90B1 and PPP2R5D; and the downstream regulators of the PI3K/AKT pathway GYS, PCK2 and CCND1 (**Figure 2C**). We firstly detected the effect of metformin on the PI3K/AKT pathway by western blotting. And the results indicated the expression of p-PI3K and

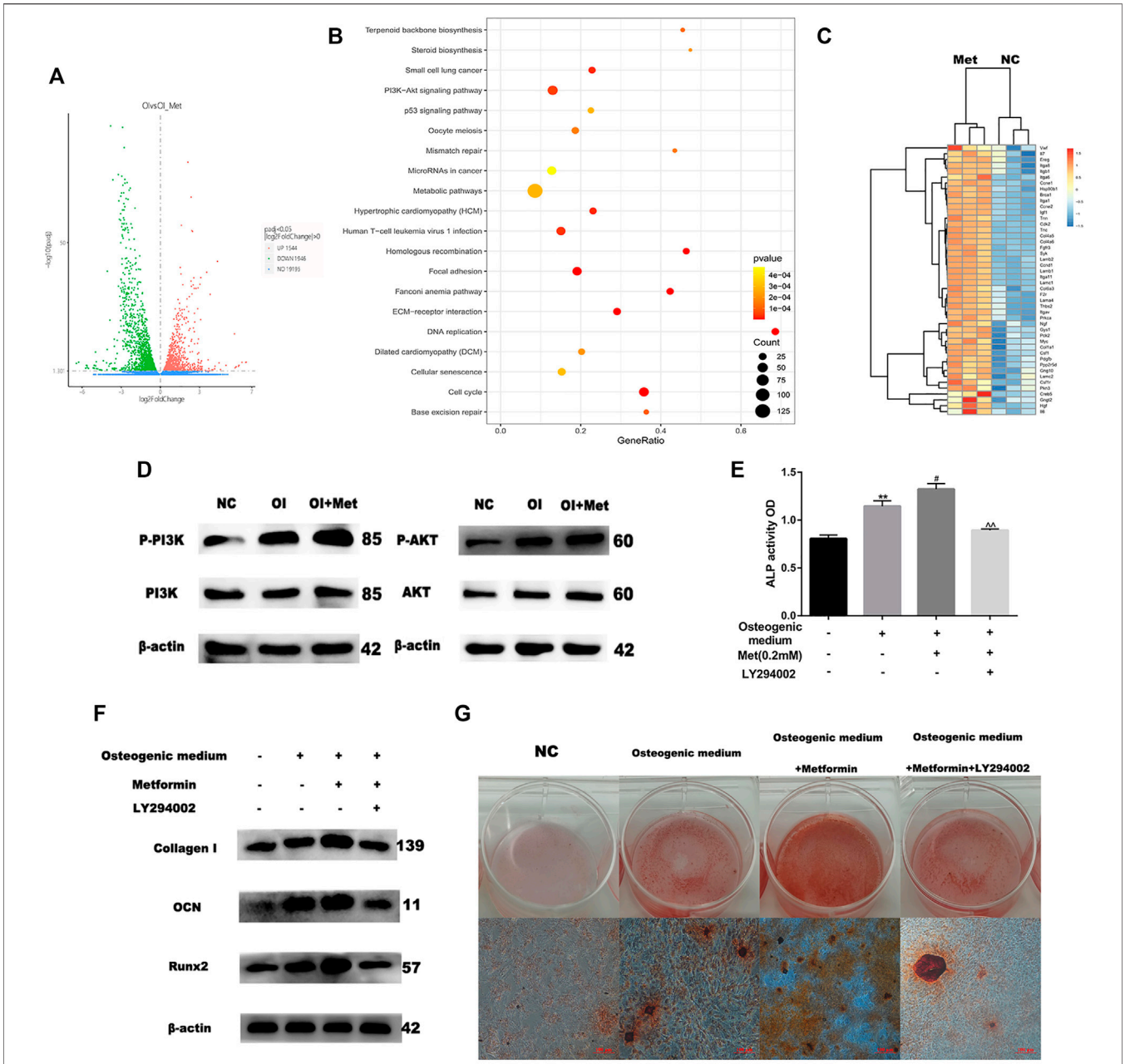

FIGURE 2 | Metformin induces osteogenic differentiation *via* the PI3K/AKT pathway. **(A)** Volcano map of differential genes as osteogenic induction (OI) vs. OI with metformin treatment (OI_Met). **(B)** Kyoto Encyclopedia of Genes and Genomes (KEGG) of up-regulated genes during metformin-induced osteogenic differentiation. **(C)** Heatmap of up-regulated genes involved in PI3K/AKT signaling pathway. **(D)** Protein expression of PI3K-AKT pathway, enhancing effect observed for metformin on PI3K/AKT expression. **(E)** ALP activity was detected to explicit metformin protection of osteogenic differentiation inhibited by H_2O_2 was blocked by LY294002. **(F)** Protein expression of COLL-1, OCN and Runx2 after adding LY294002. **(G)** The activity of osteoblast mineralization decreased with LY294002 treatment detected by using Alizarin red S staining. Experiments were implemented in triplicate. Data are means ± SD, $^{*}p < 0.05$, $^{**}p < 0.01$ compared with control cells and $^{\#}p < 0.05$, $^{\#\#}p < 0.01$ compared with osteogenic induction alone and $^{\hat{}}p < 0.05$, $^{\hat{}\hat{}}p < 0.01$ compared with combined treatment of osteogenic induction and metformin analyzed by using ANOVA.

p-AKT increased in osteogenic medium and metformin promoted it further (**Figure 2D**). To determine the role of PI3K/AKT signaling pathway in osteogenic induction by metformin, we added the PI3K/AKT signaling inhibitor LY294002 to MC3T3-E1 cells and assessed osteogenic indicators. LY294002 can inhibit the enzyme activity of PI3K through competitive inhibition of PI3K. In **Figure 2E**, ALP activity decreased after combined treatment with metformin

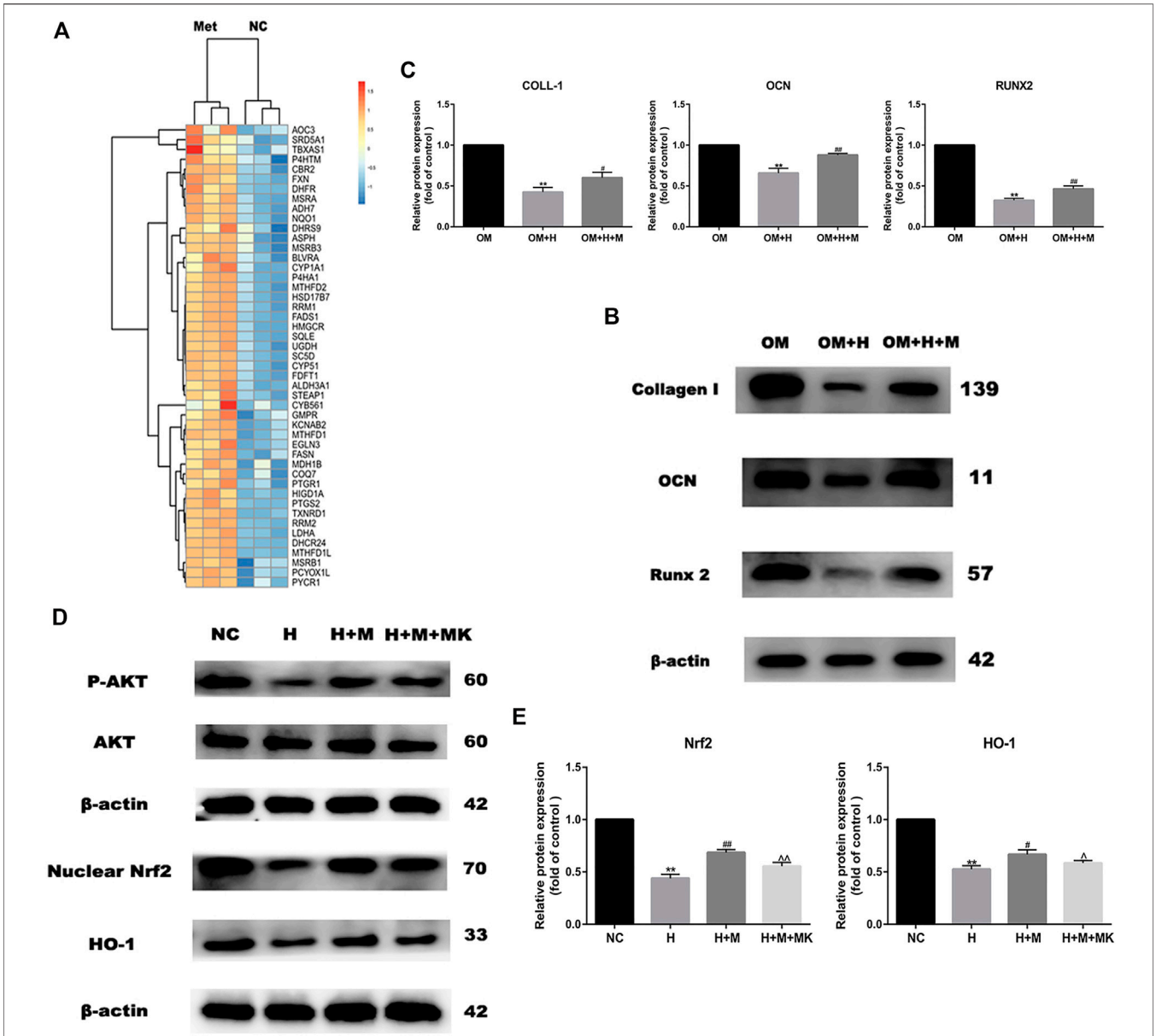

FIGURE 3 | Metformin reserves H_2O_2-induced inhibition of osteogenic differentiation. **(A)** Heatmap of up-regulated genes involved in oxidation-reduction reaction. **(B)** Protein expression of Collagen I, Runx 2 and OCN indicated the protective effect of metformin on H_2O_2 inhibition (OM: osteogenic medium, OM + H: osteogenic medium with H_2O_2, OM + H + M: osteogenic medium mixed with H_2O_2 and MK2206). **(C)** Relative protein expression level of the proteins in **(B)**. **(D)** Protein expression of p-AKT, nuclear Nrf2 and HO-1 after additing AKT inhibitor MK2206. **(E)** Relative protein expression level of the proteins in **(D)**. Experiments were implemented in triplicate. Data are means ± SD, $^{*}p < 0.05$, $^{**}p < 0.01$ compared with control cells and $^{\#}p < 0.05$, $^{\#\#}p < 0.01$ compared with H_2O_2 treatment alone and $^{\Delta}p < 0.05$, $^{\Delta\Delta}p < 0.01$ compared with combined treatment of H_2O_2 and metformin analyzed by using ANOVA.

and LY294002 compared to that with metformin treatment alone. Moreover, the protein levels of Collagen I, OCN and Runx2 decreased after combined treatment with metformin and LY294002 compared with metformin treatment alone (**Figure 2F**). Additionally, we performed Alizarin Red S staining to confirm the effect of the PI3K/AKT signaling pathway on osteoblast formation. The results indicated that LY294002 inhibited mineralization after osteogenic induction (**Figure 2G**).

Metformin Prevents the Oxidative Damage of Osteoblasts Induced by H_2O_2 *via* the AKT/Nrf2/HO-1 Pathway

GO analysis revealed that the genes upregulated expression after metformin treatment were involved in the oxidation-reduction reaction (**Figure 3A**). These genes included many reductase genes such as CBR2, HMGCR, HSD17B7, RRM2, DHCR24, DHFR, and peroxidase gene PTGS2. All of these genes performed a

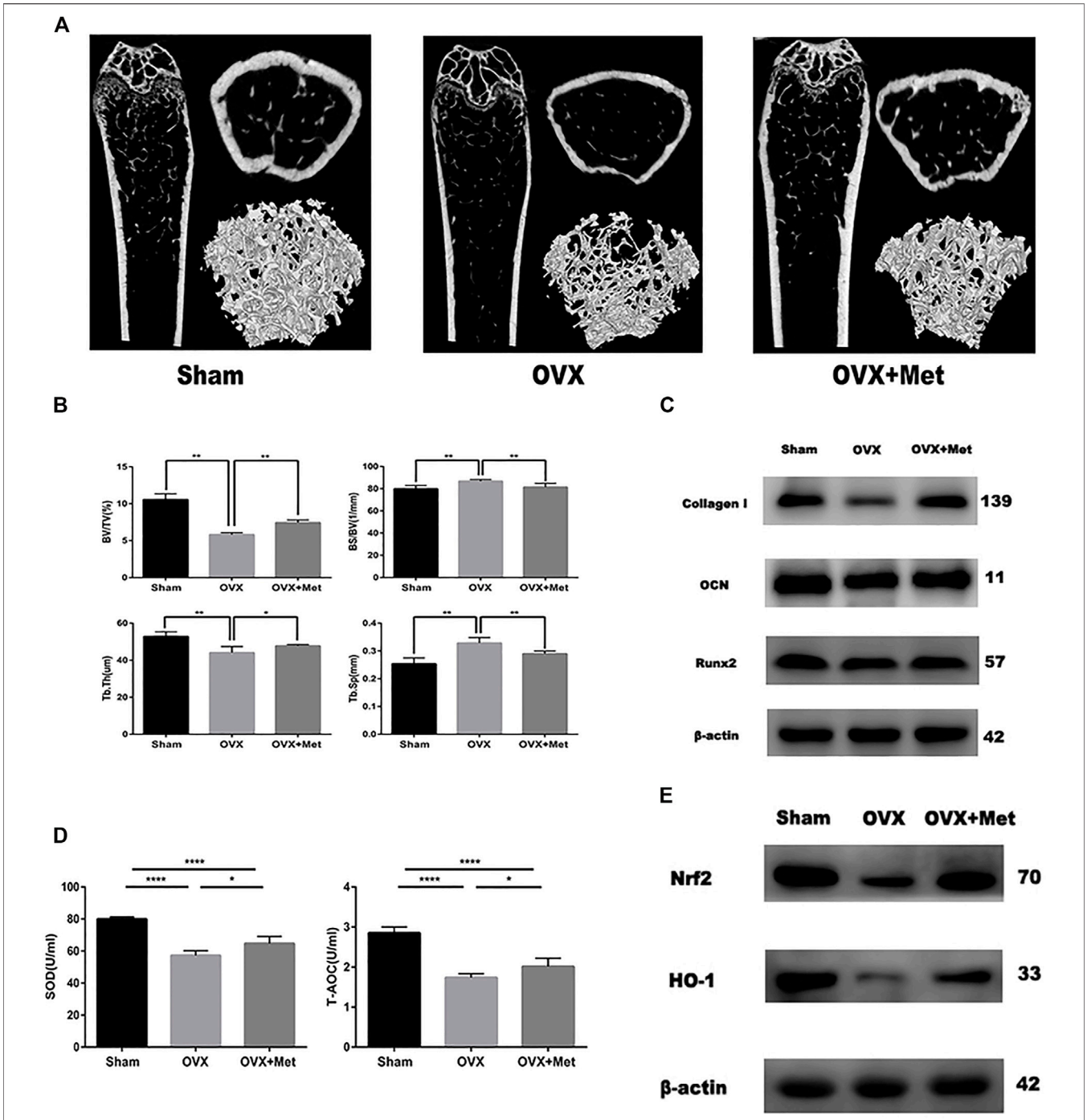

FIGURE 4 | Metformin reserved bone mass loss of OVX mice. **(A)** 2D and 3D reconstruction of the femur micro-CT images. **(B)** Related parameters obtained from image analysis (n = 7 specimens/group). **(C)** Protein level of osteogenic markers Collagen I, Runx2 and OCN in femur samples. **(D)** Serum anti-oxidative level SOD1 and T-AOC in mice (*n* = 5 specimens/group). **(E)** The protein expression of Nrf2 and HO-1 in bone tissue. Data are means ± SD, $^{*}p < 0.05$, $^{**}p < 0.01$, $^{***}p < 0.001$, $^{****}p < 0.0001$ compared with OVX analyzed by using ANOVA.

reductive effect on oxidative substances. In order to detect the protective effect of metformin on osteogenic differentiation in peroxidative status, we added 0.2 mM H_2O_2 into osteogenic medium to stimulate oxidative damage and 0.2 mM metformin to improve. After osteogenic induction and 6 h incubation with H_2O_2 and metformin, we detected the protein expression of Collagen I, OCN and Runx2 (**Figure 3B**). The results indicated the protective effect of metformin (**Figure 3C**). Then, we attempted to explore the mechanism by which metformin protected the oxidative damage of osteoblasts. Our

past studies have proved that metformin can attenuate H_2O_2-induced osteoblast apoptosis *via* the PI3K/AKT pathway (Yang et al., 2021). Nrf2 is an important transcription factor that regulates cellular oxidative stress response. And the Heme Oxygenase-1 (HO-1) is the downstream factor of Nrf2. HO-1 participated in the modulation of mitochondria function and further influenced cell differentiation and apoptosis. We used western blotting to detect the protein level of nuclear Nrf2 and HO-1. Metformin increased the expression of Nrf2 and HO-1 compared with H_2O_2 treatment alone, but which was blocked by adding AKT inhibitor MK2206(**Figures 3D,E**).

Metformin Prevents Bone Mass Loss and Reserves Oxidative Damage in OVX Mice

Finally, we attempted to determine whether metformin could improve bone mass and oxidative level in postmenopausal mice. We performed bilateral ovariectomy on mice to decrease estrogen secretion and fed them a normal diet. Additionally, we fed another set of OVX mice metformin. After 8 weeks, the bone mass of the OVX mice decreased significantly but increased after metformin feeding (**Figure 4A**). The micro-CT data also revealed the therapeutic effect of metformin on postmenopausal osteoporosis. Trabecular thickness (Tb.Th) and percent bone volume (bone volume/tissue volume, BV/TV) decreased in the OVX mice and increased with metformin treatment. Trabecular separation (Tb.Sp) and bone surface/volume ratio (bone surface/bone volume, BS/BV) increased in the OVX mice and metformin preserved these parameters (**Figure 4B**). To detect the osteogenic effect of metformin on postmenopausal mice, we also extracted protein from the mouse femur. As shown in **Figure 4C**, the osteogenic proteins Collagen I, OCN and Runx2 were decreased compared with those in the sham mice, and metformin improved their expression levels. And we also collected the blood of these mice and centrifuged it into serum. The level of superoxide dismutase (SOD) and total antioxidant capacity (T-AOC) were measured by the corresponding kit. And the results indicated metformin reserved the serum level of SOD and T-AOC (**Figure 4D**). We measured the protein expression of Nrf2 and HO-1 to validate the signaling pathway in bone tissue (**Figure 4E**). As mentioned above, metformin could improve bone mass loss by enhancing the osteogenic effects and reserving oxidative damage in the OVX mice.

DISCUSSION

With increased global aging, osteoporosis is a major threat to human health and quality of life, and postmenopausal women have the greatest risk (Chen et al., 2019). The incidence of osteoporotic fractures, which increases the health care burden, is increasing (Jørgensen et al., 2017; Kanis et al., 2021). In recent years, metformin has been found to be a multipotent anti-aging drug with cardiovascular protective and tumor growth inhibitory effects (Bahrambeigi et al., 2019; Elgendy et al., 2019; Deshmukh et al., 2021; Kodali et al., 2021). However, previous studies focused on the hypoglycemic effect of metformin in diabetes-induced osteoporosis but ignored the direct effect on bone metabolism and the molecular mechanism underlying the osteogenic differentiation of metformin. Our study determined the osteogenic effect and optimal concentration of metformin on MC3T3-E1 cell differentiation and the therapeutic effect on postmenopausal osteoporosis. We also performed RNA sequencing to show that the PI3K/AKT signaling pathway and oxidation-reduction reaction were essentially involved in the osteogenic process induced by metformin.

In previous studies, there was no consistent conclusion regarding the pathogenesis of postmenopausal osteoporosis. Our transcriptional data indicated that metformin modulated the expression of genes involved in oxidation-reduction process of osteoblasts. We also believe that oxidation-reduction imbalance is a key factor leading to osteoporosis in postmenopausal women due to the reducibility of estrogen. It has been demonstrated that circulating levels of catalase, superoxide dismutase 2 (SOD 2) and peroxiredoxin 2 (PRX2) are lower in postmenopausal women with osteoporosis than health controls (Azizieh et al., 2019). Mitochondrial dysfunction leads to weakened internal oxidoreductase function, resulting in high levels of free radical, which attacks osteoblasts and induces apoptosis (Zhou et al., 2019). Osteoclasts showed strong differentiation when the inhibitory effect of estrogen was lost (Li et al., 2021). Metformin can improve the oxidative state and protect against oxidative stress damage, which also indicates the therapeutic effect of metformin on osteoporosis (Jia et al., 2021). Therefore, it is essential to determine the mechanism by which metformin acts on the oxidation-reduction process in osteoblasts.

PI3K/AKT signaling is an important pathway involved in the modulation of redox balance. Activation of PI3K/AKT enhances the antioxidant effect (Kim et al., 2021; Wang P et al., 2021). The PI3K/AKT signaling pathway has been demonstrated to have a positive effect on osteoblast differentiation and inhibition of PI3K/AKT signaling suppresses the osteoinduction process (Zhang et al., 2019; Dong et al., 2020). It was reported that multiple drugs promote osteogenic differentiation *via* the PI3K/AKT pathway (Xiong et al., 2020; Liu et al., 2021). In our study, we revealed that metformin promoted osteogenic differentiation of MC3T3-E1 cells by activating the PI3K/AKT pathway. Various osteogenic growth factors and extracellular matrix components can induce the activation of PI3K, including fibroblast growth factor, vascular endothelial growth factor, angiogenic protein I and insulin (Khodabandehloo et al., 2020). These factors activate receptor tyrosine kinases, cause autophosphorylation and induce PI3K/AKT-mediated differentiation. We also demonstrated that the osteogenic effect of metformin was blocked by adding a PI3K/AKT inhibitor. The inhibitor decreased the ratio of OPG/RANKL expression to inhibit osteogenesis (Xu et al., 2021). Additionally, we used H_2O_2 to mimic the oxidative damage of osteoblasts metformin to attenuate it, the anti-apoptosis effect of which has been proven in our previous study (Yang et al., 2021). And in this study, we further explored the downstream mechanism. Nrf2 is an factor involved in the modulation of cellular oxidation-reduction balance (Čipak Gašparović et al., 2021). Nrf2 participates in the expression and maturation of various anti-

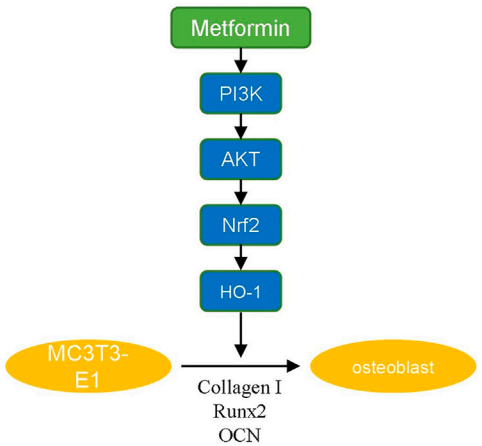

FIGURE 5 | The summarized figure of signaling pathway.

oxidative proteins to maintain the homeostasis of oxidation and reduction (Ying et al., 2018). HO-1 is an essential anti-oxidative factor modulated by Nrf2 (Ma et al., 2021). HO-1 decomposes heme to produce carbon monoxide (CO) that promotes the expression of glutamate-cysteine ligase for GSH transformation (Consoli et al., 2021). As mentioned above, PI3K/AKT/Nrf2/HO-1 pathway is closely related to osteogenic differentiation and anti-oxidative damage of osteoblasts. Our experimental results also indicated protective effect of metformin in postmenopausal osteoporosis *via* this pathway (**Figure 5**).

Due to the complex pathogenesis of osteoporosis, current treatment methods have limited efficacy. According to our experiments, metformin can directly increase the gene expression, protein formation of osteogenic markers and protect H_2O_2-induced oxidative damage. *In vitro*, we further verified that the bone mass of the OVX mice was significantly improved by metformin feeding. As estrogen is a reductive hormone, detecting the role of oxidoreduction in osteoporosis development and the therapeutic effect of metformin in improving the oxidative state in osteoblasts will be further directions for research on postmenopausal osteoporosis.

CONCLUSION

Our study demonstrated that metformin could promote osteogenic differentiation and improve H_2O_2-induced oxidative damage of osteoblasts *via* the PI3K/AKT/Nrf2/HO-1 pathway. Vitro experiments also demonstrated that metformin improved bone mass, enhanced osteogenic protein expression and increased anti-oxidative level in OVX mice. These results provide an important basis for the potential therapeutic effect of metformin in postmenopausal osteoporosis. Along with its effect in controlling blood glucose and reducing lipids, metformin may have applications in the treatment of osteoporosis.

DATA AVAILABILITY STATEMENT

The data presented in the study are deposited in the GEO (NCBI) repository, accession number (GSE198254). https://www.ncbi.nlm.nih.gov/geo/query/acc.cgi?acc=GSE198254/**Supplementary Material**.

ETHICS STATEMENT

The animal study was reviewed and approved by the Animal Ethics Committee of the First Affiliated Hospital of China Medical University (No. 2019014).

AUTHOR CONTRIBUTIONS

KY: Data curation, Formal analysis, Data curation, Methodology, Writing—original draft. FC: Data curation, Methodology, Software, SQ: Conceptualization, Writing—original draft, WJ: Investigation, Methodology, Software, LT: Conceptualization, Software, Validation, Writing—review and editing, YZ: Funding acquisition, Project administration, Resources, Writing—review and editing. All authors read and approved the manuscript.

FUNDING

Our study was supported by National Natural Science Foundation of China (NO. 81472044), Department of Laboratory Animal Science of China Medical University and Construction of Clinical Medical Research Center of Orthopedics in Liaoning Province.

SUPPLEMENTARY MATERIAL

The Supplementary Material for this article can be found online at: https://www.frontiersin.org/articles/10.3389/fphar.2022.829830/full#supplementary-material

REFERENCES

Azizieh, F. Y., Shehab, D., Jarallah, K. A., Gupta, R., and Raghupathy, R. (2019). Circulatory Levels of RANKL, OPG, and Oxidative Stress Markers in Postmenopausal Women with Normal or Low Bone Mineral Density. *Biomark Insights* 14, 1177271919843825. doi:10.1177/1177271919843825

Bahrambeigi, S., Yousefi, B., Rahimi, M., and Shafiei-Irannejad, V. (2019). Metformin; an Old Antidiabetic Drug with New Potentials in Bone Disorders. *Biomed. Pharmacother.* 109, 1593–1601. doi:10.1016/j.biopha.2018.11.032

Buccellato, F. R., D'Anca, M., Fenoglio, C., Scarpini, E., and Galimberti, D. (2021). Role of Oxidative Damage in Alzheimer's Disease and Neurodegeneration: From Pathogenic Mechanisms to Biomarker Discovery. *Antioxidants (Basel)* 10 (9), 1353. doi:10.3390/antiox10091353

Chapurlat, R., Bui, M., Sornay-Rendu, E., Zebaze, R., Delmas, P. D., Liew, D., et al. (2020). Deterioration of Cortical and Trabecular Microstructure Identifies Women with Osteopenia or Normal Bone Mineral Density at Imminent and Long-Term Risk for Fragility Fracture: A Prospective Study. *J. Bone Miner Res.* 35, 833–844. doi:10.1002/jbmr.3924

Chen, D. Y., Li, Y. J., Jiang, R. f., Li, Y. t., Feng, J., and Hu, W. (2021). Effects and Mechanism of lncRNA-27785.1 that Regulates TGF-β1 of Sika Deer on Antler Cell Proliferation. *J. Cel Physiol* 236, 5742–5756. doi:10.1002/jcp.30258

Chen, W. C., Lin, E. Y., and Kang, Y. N. (2019). Efficacy and Safety of Elcatonin in Postmenopausal Women with Osteoporosis: a Systematic Review with Network Meta-Analysis of Randomized Clinical Trials. *Osteoporos. Int.* 30, 1723–1732. doi:10.1007/s00198-019-04997-6

Cho, E., Chen, Z., Ding, M., Seong, J., Lee, S., Min, S. H., et al. (2021). PMSA Prevents Osteoclastogenesis and Estrogen-Dependent Bone Loss in Mice. *Bone* 142, 115707. doi:10.1016/j.bone.2020.115707

Čipak Gašparović, A., Milković, L., Rodrigues, C., Mlinarić, M., and Soveral, G. (2021). Peroxiporins are Induced upon Oxidative Stress Insult and are Associated with Oxidative Stress Resistance in Colon Cancer Cell Lines. *Antioxidants* 10, 1856. doi:10.3390/antiox10111856

Consoli, V., Sorrenti, V., Grosso, S., and Vanella, L. (2021). Heme Oxygenase-1 Signaling and Redox Homeostasis in Physiopathological Conditions. *Biomolecules* 11, 589. doi:10.3390/biom11040589

Cui, Q., Yang, H., Gu, Y., Zong, C., Chen, X., Lin, Y., et al. (2020). RNA Sequencing (RNA-Seq) Analysis of Gene Expression Provides New Insights into Hindlimb Unloading-Induced Skeletal Muscle Atrophy. *Ann. Transl Med.* 8, 1595. doi:10.21037/atm-20-7400

Deshmukh, A., Ghannam, M., Liang, J., Saeed, M., Cunnane, R., Ghanbari, H., et al. (2021). Effect of Metformin on Outcomes of Catheter Ablation for Atrial Fibrillation. *J. Cardiovasc. Electrophysiol.* 32, 1232–1239. doi:10.1111/jce.14954

Dong, J., Xu, X., Zhang, Q., Yuan, Z., and Tan, B. (2020). The PI3K/AKT Pathway Promotes Fracture Healing through its Crosstalk with Wnt/β-Catenin. *Exp. Cel Res* 394, 112137. doi:10.1016/j.yexcr.2020.112137

Elgendy, M., Cirò, M., Hosseini, A., Weiszmann, J., Mazzarella, L., Ferrari, E., et al. (2019). Combination of Hypoglycemia and Metformin Impairs Tumor Metabolic Plasticity and Growth by Modulating the PP2A-GSK3β-MCL-1 Axis. *Cancer cell* 35, 798–815. e795. doi:10.1016/j.ccell.2019.03.007

He, Q., Gu, L., Lin, Q., Ma, Y., Liu, C., Pei, X., et al. (2020). The Immp2l Mutation Causes Ovarian Aging through ROS-Wnt/β-Catenin-Estrogen Pathway: Preventive Effect of Melatonin. *Endocrinology* 161 (9), bqaa119. doi:10.1210/endocr/bqaa119

Hsiao, C. Y., Chen, T. H., Chu, T. H., Ting, Y. N., Tsai, P. J., and Shyu, J. F. (2020). Calcitonin Induces Bone Formation by Increasing Expression of Wnt10b in Osteoclasts in Ovariectomy-Induced Osteoporotic Rats. *Front. Endocrinol. (Lausanne)* 11, 613. doi:10.3389/fendo.2020.00613

Jia, W., Bai, T., Zeng, J., Niu, Z., Fan, D., Xu, X., et al. (2021). Combined Administration of Metformin and Atorvastatin Attenuates Diabetic Cardiomyopathy by Inhibiting Inflammation, Apoptosis, and Oxidative Stress in Type 2 Diabetic Mice. *Front Cel Dev Biol* 9, 634900. doi:10.3389/fcell.2021.634900

Jørgensen, N. R., Schwarz, P., Iversen, H. K., and Vestergaard, P. (2017). P2Y12 Receptor Antagonist, Clopidogrel, Does Not Contribute to Risk of Osteoporotic Fractures in Stroke Patients. *Front. Pharmacol.* 8, 821. doi:10.3389/fphar.2017.00821

Kanis, J. A., Johansson, H., Harvey, N. C., Gudnason, V., Sigurdsson, G., Siggeirsdottir, K., et al. (2021). The Effect on Subsequent Fracture Risk of Age, Sex, and Prior Fracture Site by Recency of Prior Fracture. *Osteoporos. Int.* 32, 1547–1555. doi:10.1007/s00198-020-05803-4

Kashima, S., Inoue, K., and Matsumoto, M. (2021). Low Creatinine Levels in Diabetes Mellitus Among Older Individuals: the Yuport Medical Checkup Center Study. *Sci. Rep.* 11, 15167. doi:10.1038/s41598-021-94441-9

Khodabandehloo, F., Taleahmad, S., Aflatoonian, R., Rajaei, F., Zandieh, Z., Nassiri-Asl, M., et al. (2020). Microarray Analysis Identification of Key Pathways and Interaction Network of Differential Gene Expressions during Osteogenic Differentiation. *Hum. Genomics* 14, 43. doi:10.1186/s40246-020-00293-1

Kim, M.-B., Kang, H., Li, Y., Park, Y.-K., and Lee, J.-Y. (2021). Fucoxanthin Inhibits Lipopolysaccharide-Induced Inflammation and Oxidative Stress by Activating Nuclear Factor E2-Related Factor 2 *via* the Phosphatidylinositol 3-kinase/AKT Pathway in Macrophages. *Eur. J. Nutr.* 60, 3315–3324. doi:10.1007/s00394-021-02509-z

Koborova, O. N., Filimonov, D. A., Zakharov, A. V., Lagunin, A. A., Ivanov, S. M., Kel, A., et al. (2009). In Silico method for Identification of Promising Anticancer Drug Targets. *SAR QSAR Environ. Res.* 20, 755–766. doi:10.1080/10629360903438628

Kodali, M., Attaluri, S., Madhu, L. N., Shuai, B., Upadhya, R., Gonzalez, J. J., et al. (2021). Metformin Treatment in Late Middle Age Improves Cognitive Function with Alleviation of Microglial Activation and Enhancement of Autophagy in the hippocampus. *Aging Cell* 20, e13277. doi:10.1111/acel.13277

Li, Q., Wang, H., Zhang, J., Kong, A. P., Li, G., Lam, T. P., et al. (2021). Deletion of SIRT3 Inhibits Osteoclastogenesis and Alleviates Aging or Estrogen Deficiency-Induced Bone Loss in Female Mice. *Bone* 144, 115827. doi:10.1016/j.bone.2020.115827

Liu, H., Li, X., Lin, J., and Lin, M. (2021). Morroniside Promotes the Osteogenesis by Activating PI3K/Akt/mTOR Signaling. *Biosci. Biotechnol. Biochem.* 85, 332–339. doi:10.1093/bbb/zbaa010

Ma, N., Wei, Z., Hu, J., Gu, W., and Ci, X. (2021). Farrerol Ameliorated Cisplatin-Induced Chronic Kidney Disease through Mitophagy Induction *via* Nrf2/PINK1 Pathway. *Front. Pharmacol.* 12, 768700. doi:10.3389/fphar.2021.768700

Martel, J., Chang, S. H., Wu, C. Y., Peng, H. H., Hwang, T. L., Ko, Y. F., et al. (2021). Recent Advances in the Field of Caloric Restriction Mimetics and Anti-Aging Molecules. *Ageing Res. Rev.* 66, 101240. doi:10.1016/j.arr.2020.101240

Niemi, J., Mittman, E., Landau, W., and Nettleton, D. (2015). Empirical Bayes Analysis of RNA-Seq Data for Detection of Gene Expression Heterosis. *J. Agric. Biol. Environ. Stat.* 20, 614–628. doi:10.1007/s13253-015-0230-5

Ponte, F., Kim, H. N., Iyer, S., Han, L., Almeida, M., and Manolagas, S. C. (2020). Cxcl12 Deletion in Mesenchymal Cells Increases Bone Turnover and Attenuates the Loss of Cortical Bone Caused by Estrogen Deficiency in Mice. *J. Bone Miner Res.* 35, 1441–1451. doi:10.1002/jbmr.4002

Sha, N. N., Zhang, J. L., Poon, C. C., Li, W. X., Li, Y., Wang, Y. F., et al. (2021). Differential Responses of Bone to Angiotensin II and Angiotensin(1-7): Beneficial Effects of ANG(1-7) on Bone with Exposure to High Glucose. *Am. J. Physiol. Endocrinol. Metab.* 320, E55–e70. doi:10.1152/ajpendo.00158.2020

Sharma, S., Nozohouri, S., Vaidya, B., and Abbruscato, T. (2021). Repurposing Metformin to Treat Age-Related Neurodegenerative Disorders and Ischemic Stroke. *Life Sci.* 274, 119343. doi:10.1016/j.lfs.2021.119343

Toriumi, S., Kobayashi, A., and Uesawa, Y. (2020). Comprehensive Study of the Risk Factors for Medication-Related Osteonecrosis of the Jaw Based on the Japanese Adverse Drug Event Report Database. *Pharmaceuticals* 13, 467. doi:10.3390/ph13120467

Tseng, C. H. (2021). Metformin Use Is Associated with a Lower Risk of Osteoporosis/Vertebral Fracture in Taiwanese Patients with Type 2 Diabetes Mellitus. *Eur. J. Endocrinol.* 184, 299–310. doi:10.1530/eje-20-0507

Ukon, Y., Makino, T., Kodama, J., Tsukazaki, H., Tateiwa, D., Yoshikawa, H., et al. (2019). Molecular-Based Treatment Strategies for Osteoporosis: A Literature Review. *Int. J. Mol. Sci.* 20 (10), 2557. doi:10.3390/ijms20102557

Wang, P., Tian, X., Tang, J., Duan, X., Wang, J., Cao, H., et al. (2021). Artemisinin Protects Endothelial Function and Vasodilation from Oxidative Damage *via* Activation of PI3K/Akt/eNOS Pathway. *Exp. Gerontol.* 147, 111270. doi:10.1016/j.exger.2021.111270

Wang, W., Qin, Z., Feng, Z., Wang, X., and Zhang, X. (2013). Identifying Differentially Spliced Genes from Two Groups of RNA-Seq Samples. *Gene* 518, 164–170. doi:10.1016/j.gene.2012.11.045

Wang, Y., Shi, H., Zhang, G., Wu, P., Chen, L., Shen, M., et al. (2021). Transcriptome Analysis of Long Noncoding RNAs and mRNAs in Granulosa Cells of Jinghai Yellow Chickens Illuminated with Red Light. *Front. Genet.* 12, 563623. doi:10.3389/fgene.2021.563623

Xiong, Y., Zhao, B., Zhang, W., Jia, L., Zhang, Y., and Xu, X. (2020). Curcumin Promotes Osteogenic Differentiation of Periodontal Ligament Stem Cells through the PI3K/AKT/Nrf2 Signaling Pathway. *Iran J. Basic Med. Sci.* 23, 954–960. doi:10.22038/ijbms.2020.44070.10351

Xu, A., Yang, Y., Shao, Y., Wu, M., and Sun, Y. (2020). Activation of Cannabinoid Receptor Type 2-induced Osteogenic Differentiation Involves Autophagy Induction and P62-Mediated Nrf2 Deactivation. *Cell Commun Signal* 18, 9. doi:10.1186/s12964-020-0512-6

Xu, L., He, X., Zhou, Y., Yu, K., Yuan, M., Zhang, Q., et al. (2021). Connectivity Map Analysis Identifies Fisetin as a Treatment Compound for Osteoporosis through Activating the PI3K-AKT Signaling Pathway in Mouse Pre-osteoblastic MC3T3-E1 Cells. *Curr. Pharm. Biotechnol.* 22, 2038–2047. doi:10.2174/1389201022666210301141238

Yang, J., Dong, D., Luo, X., Zhou, J., Shang, P., and Zhang, H. (2020). Iron Overload-Induced Osteocyte Apoptosis Stimulates Osteoclast Differentiation through Increasing Osteocytic RANKL Production *In Vitro*. *Calcif Tissue Int.* 107, 499–509. doi:10.1007/s00223-020-00735-x

Yang, K., Pei, L., Zhou, S., Tao, L., and Zhu, Y. (2021). Metformin Attenuates H2O2-Induced Osteoblast Apoptosis by Regulating SIRT3 *via* the PI3K/AKT Pathway. *Exp. Ther. Med.* 22, 1316. doi:10.3892/etm.2021.10751

Ying, Y., Jin, J., Ye, L., Sun, P., Wang, H., and Wang, X. (2018). Phloretin Prevents Diabetic Cardiomyopathy by Dissociating Keap1/Nrf2 Complex and Inhibiting Oxidative Stress. *Front. Endocrinol. (Lausanne)* 9, 774. doi:10.3389/fendo.2018.00774

Zhang, Z., Zhang, X., Zhao, D., Liu, B., Wang, B., Yu, W., et al. (2019). TGF-β1 Promotes the Osteoinduction of Human Osteoblasts *via* the PI3K/AKT/mTOR/S6K1 Signalling Pathway. *Mol. Med. Rep.* 19, 3505–3518. doi:10.3892/mmr.2019.10051

Zhou, L., Poon, C. C.-W., Wong, K.-Y., Cao, S., Dong, X., Zhang, Y., et al. (2021). Icariin Ameliorates Estrogen-Deficiency Induced Bone Loss by Enhancing IGF-I Signaling *via* its Crosstalk with Non-Genomic ERα Signaling. *Phytomedicine* 82, 153413. doi:10.1016/j.phymed.2020.153413

Zhou, R., Ma, Y., Tao, Z., Qiu, S., Gong, Z., Tao, L., et al. (2020). Melatonin Inhibits Glucose-Induced Apoptosis in Osteoblastic Cell Line through PERK-eIF2α-ATF4 Pathway. *Front. Pharmacol.* 11, 602307. doi:10.3389/fphar.2020.602307

Zhou, W., Liu, Y., Shen, J., Yu, B., Bai, J., Lin, J., et al. (2019). Melatonin Increases Bone Mass Around the Prostheses of OVX Rats by Ameliorating Mitochondrial Oxidative Stress *via* the SIRT3/SOD2 Signaling Pathway. *Oxidative Med. Cell Longevity* 2019, 4019619. doi:10.1155/2019/4019619

Conflict of Interest: The authors declare that the research was conducted in the absence of any commercial or financial relationships that could be construed as a potential conflict of interest.

Publisher's Note: All claims expressed in this article are solely those of the authors and do not necessarily represent those of their affiliated organizations, or those of the publisher, the editors and the reviewers. Any product that may be evaluated in this article, or claim that may be made by its manufacturer, is not guaranteed or endorsed by the publisher.

frontiers in Medicine

ORIGINAL RESEARCH
published: 23 March 2022
doi: 10.3389/fmed.2022.832411

DNA Methylation - and Telomere - Based Biological Age Estimation as Markers of Biological Aging in Donors Kidneys

Sofia Pavanello[1†‡], Manuela Campisi[1†‡], Paolo Rigotti[2], Marianna Di Bello[2], Erica Nuzzolese[2], Flavia Neri[2] and Lucrezia Furian[2]*

[1] Occupational Medicine, Department of Cardiac, Thoracic, and Vascular Sciences and Public Health, University Hospital of Padova, Padova, Italy, [2] Kidney and Pancreas Transplantation Unit, Department of Surgery, Oncology and Gastroenterology, University Hospital of Padova, Padova, Italy

OPEN ACCESS

Edited by:
Victoria Bunik,
Lomonosov Moscow State University, Russia

Reviewed by:
Andrey A. Mironov,
Lomonosov Moscow State University, Russia
Waylon James Hastings,
The Pennsylvania State University (PSU), United States
Satoshi Okazaki,
Kobe University, Japan

***Correspondence:**
Sofia Pavanello
sofia.pavanello@unipd.it

†ORCID:
Sofia Pavanello
orcid.org/0000-0002-5229-9900
Manuela Campisi
orcid.org/0000-0002-7372-4136

‡These authors have contributed equally to this work

Specialty section:
This article was submitted to Translational Medicine, a section of the journal Frontiers in Medicine

Received: 09 December 2021
Accepted: 15 February 2022
Published: 23 March 2022

Citation:
Pavanello S, Campisi M, Rigotti P, Bello MD, Nuzzolese E, Neri F and Furian L (2022) DNA Methylation - and Telomere - Based Biological Age Estimation as Markers of Biological Aging in Donors Kidneys. Front. Med. 9:832411. doi: 10.3389/fmed.2022.832411

The biological age of an organ may represent a valuable tool for assessing its quality, especially in the elder. We examined the biological age of the kidneys [right (RK) and left kidney (LK)] and blood leukocytes in the same subject and compared these to assess whether blood mirrors kidney biological aging. Biological age was studied in $n = 36$ donors (median age: 72 years, range: 19–92; male: 42%) by exploring mitotic and non-mitotic pathways, using telomere length (TL) and age-methylation changes (DNAmAge) and its acceleration (AgeAcc). RK and LK DNAmAge are older than blood DNAmAge (RK vs. Blood, $p = 0.0271$ and LK vs. Blood, $p = 0.0245$) and RK and LK AgeAcc present higher score (this mean the AgeAcc is faster) than that of blood leukocytes ($p = 0.0271$ and $p = 0.0245$) in the same donor. TL of RK and LK are instead longer than that of blood ($p = 0.0011$ and $p = 0.0098$) and the increase in Remuzzi-Karpinski score is strongly correlated with kidney TL attrition ($p = 0.0046$). Finally, blood and kidney TL ($p < 0.01$) and DNAmAge ($p < 0.001$) were correlated. These markers can be evaluated in further studies as indicators of biological age of donor organ quality and increase the usage of organs from donors of advanced age therefore offering a potential translational research in kidney transplantation.

Keywords: kidney transplantation, DNA methylation age, telomere length, age acceleration, kidney rejuvenation, biological age

INTRODUCTION

Organ failure represents a dramatic socio-economical burden worldwide which prevalence is likely to increases sharply with population aging. The ideal therapeutic solution is represented by the transplantation of an allogeneic equivalent obtained by a human donor. However, there is a dramatic mismatch between the number of patients in transplantation list and the effective availability of donor's organs (1). Strategies to face this issue have led the transplant scientific community to progressively expand the eligibility criteria for donors to include the elderly (2).

Within the context of kidney transplantation in which organ shortage remains a problem, donor's age is however one of the main factors influencing the decision of accepting the kidneys (1, 2). Kidneys from aged people may have chronic damages, which make them less efficient in the function recovery upon the ischemia and reperfusion injury (3, 4). Furthermore, the assessment of the kidney relies also on the histology (i.e., Remuzzi score), which reflects a morphological feature (5).

Although the chronological age of the donor can influence the quality of the kidney to be transplanted, it may not be a reliable indicator of the rate of physiological breakdown of the body or of the organs, as people do not age at the same rate. Genetic and environmental factors can impact on biological aging, causing different aging trajectories and health outcomes in each person (6–8). In addition, a different rate of aging seems to occur also within the same subject in each system and organ (9). In our previous studies, we demonstrated that the biological age of cardiac tissues procured from deceased donors were consistently younger than their chronological age (10). Therefore, it can be postulated that even the kidney may have a different aging profile. Defining the biological age of kidney may contribute to supporting this process.

The biological age is not that indicated on the identity card but is written on the DNA. Growing indications have shown that telomere length (TL) and age-correlated DNA methylation changes in certain CpG loci (DNAmAge) are early hallmarks of biological aging, and may be primary indicators of cellular dysfunction and in age-related disorders (9, 10). TL, the non-coding DNA sequences that cap chromosomes and shorten at each cell division, measures mitotic or replicative cellular aging (11). DNA methylation age (DNAmAge) is an emerging epigenetic marker of non-mitotic cellular aging (12, 13), assessed through the analysis of methylation at a specific subset of cytosine-guanine dyads (CpG), which showed a strong correlation with the chronological age (14–17). We recently automated the method proposed by Zbieć-Piekarska et al. (16) to increase the efficiency and rapidity, maintaining high prediction accuracy (9, 10). The development of these biomarkers has led to the definition of an "epigenetic clock" theory of aging; the difference between DNAmAge and chronological age defined as "age acceleration" (AgeAcc) (18) is indicative of altered biological functions (13) and elevated risk for morbidity and mortality (19). Findings on TL (20) and DNAmAge (14–16) are quite exclusively based on DNA from blood circulating leukocytes, as they represent an easily available DNA source.

Studies comparing biological age indicators measured in different tissues of the same subject are however in most of cases on TL measures made on cadavers, donors elderly patients, and the measurements seem correlated (21–23). There have been instead few studies investigating correlation of DNAmAge in different tissues (14, 24). Of particular note is the Horvath epigenetic clock that was developed to be applicable across human tissues (14), but correlations were not made between blood and tissues, in the same subject. From a translational perspective, it remains to be clarified whether DNAmAge in lymphocytes mirror that in the different tissues/organs in healthy donors.

Furthermore, the biological age of an organ may then represent a valuable tool for the assessment of its quality, as it could correlate more closely to its functional reserve, and predict the transplantation outcome more accurately than the present evaluation methods.

The aim of our study was:

1) To determine the biological age of the kidneys by measuring the mitotic (TL) and the non-mitotic epigenetic age (DNAmAge) of renal cells collected from kidney samples and to compare it with the Remuzzi score with the purpose of defining a biomarker for organ quality assessment.
2) To compare the DNAmAge of peripheral blood leukocytes and kidneys, in order to establish whether blood may be an accurate indicator of kidney biological age.

MATERIALS AND METHODS

Study Design: Kidney Procurement, Sampling of Donor's Tissue and Blood, and Data Collection

Over a time span of 22 months (from March 2019 to January 2021) renal true-cut biopsies and blood samples were obtained in the same time from 36 deceased kidney donors for whom the procurement was performed by the surgical team of Kidney and Pancreas Transplantation Unit - Department of Surgical, Oncological and Gastroenterological Sciences, University Hospital of Padua. The donors included in the study were those for whom a renal biopsy was deemed clinically indicated either for the assessment of chronic damage (2) or for the presence of acute kidney injury. Donors' Characteristics (median age: 72 years, range: 19–92; male: 42%) are summarized in **Table 1**. Details of the donor's kidney biopsy procedure are reported in the **Supplementary Materials**.

Blood samples (3–4 ml) from the donors were collected in K3EDTA and PAXgene tubes (BD Biosciences, Milano, Italy). The tru-cut biopsies were placed in all protected tissue reagent-RNA Later (Qiagen, Milano, Italy) for DNA/RNA stabilization. All collected samples were then, transferred to our laboratory of Genomic and Environmental Mutagenesis (Department of Cardiac, Thoracic, and Vascular Sciences and Public Health, University-Hospital of Padua) for genetic and epigenetic analyses and stored at −20°C, until analyses were performed. Our Local Ethical Committee, which is named the Ethical Committee for Clinical Trials of the Province of Padova, approved the study (protocol number 2246P) in accordance with principles of the Helsinki Declaration, allowing a waiver from consent. All methods were carried out in accordance with relevant guidelines and regulations.

We collected data on the following donor characteristics: age, gender, smoking, comorbidities, cause of death, blood parameters and renal function. We also recorded the histological Remuzzi-Karpinski score of the kidneys when available for clinical necessity as for the Nord Italian Transplant programm (NITp) algorithm for allocation to single or dual transplantation (2).

DNA Extraction From Blood and Tissue Samples

DNA extraction was performed on all samples of whole blood and renal biopsies using an automated QIAcube

Abbreviations: AgeAcc, Age acceleration; DNAmAge, DNA methylation age; LK, Left Kidney; LTL, Leucocytes telomere length; RK, Right Kidney; TL, Telomere length.

TABLE 1 | Donors' Characteristics.

N	36
Age (y)	72 (19–92)
Gender	
Male (*n*, %)	15 (42%)
Female (*n*, %)	21 (58%)
Smoking	11 (31%)
Comorbidities	
Arterial Hypertension (PAH)	21 (58%)
Diabetes	4 (11%)
Other	4 (11%)
Cause of death	
Ictus	10 (28%)
Cranial trauma	9 (25%)
Subarachnoid hemorrhage (SAH)	14 (39%)
Cardiac arrest	2 (5%)
Other	1 (3%)
Blood parameters	
Leukocytes ($n * 10^9$/L)	12.395 (2.96–32.22)
Renal function	
Creatinine (mg/dL)	0.88 (0.41–1.85)
Histological evaluation of kidneys (Remuzzi Score)	
$0 \leq$ Score ≤ 3	12 (26%)
$4 \leq$ Score ≤ 6	26 (57%)
Score ≥ 7	8 (17%)
TL	
Right kidney	1.18 (0.93–1.63)
Left kidney	1.25 (0.76–1.99)
Blood	1.15 (0.38–2.05)
DNAmAge	
Right kidney	69 (29–80)
Left kidney	66 (23–79)
Blood	65 (13–78)

Data are expressed in median (range) or number (percentage).

System according to the DNAeasy Blood and Tissue kit procedure (Qiagen, Milano, Italy) as previously described (10). Details of DNAmAge analysis are reported in the **Supplementary Materials**.

DNAmAge Analysis

DNAmAge was assessed by analyzing the methylation levels of five selected markers in genomic DNA using bisulfite conversion and Pyrosequencing methodology as previously described (9, 10, 17). Twenty percent of the samples were analyzed in two different days to verify the reproducibility of our results and the coefficient of variation (CV) in replicate pyrosequencing runs was 1.7 %. Details of DNAmAge analysis are reported in the **Supplementary Materials**.

AgeAcc Evaluation

AgeAcc was assessed for both renal tissue and blood leukocytes of each donor. AgeAcc was estimated as the difference between the DNAmAge and the chronological age of the donors.

TL Analysis

TL was measured in genomic DNA by quantitative Real-Time PCR by estimating the ratio of telomere repeat copy number (T) to single nuclear copy gene (S) in experimental DNA samples relative to the T/S ratio of a reference pooled sample as previously reported (25–27). The average of CV for the T/S ratio of samples analyzed over three consecutive days was 9%, which was similar to the original method (28). Details of TL analysis are reported in the **Supplementary Materials**.

Sample Size Estimation

Estimating that a significant correlation would be in the order of r = 0.80, we calculated that the sample to obtain statistical significance (α 0.01) should be $n = 15$ (power 0.9).

Statistical Analysis

Statistical analyses were performed with StatsDirect software. Data are expressed as median, minimum and maximum values unless otherwise specified. Values of TL, DNAmAge and AgeAcc in Kidneys (renal biopsies) and blood, of the same patient, were compared by (two-tailed) paired *T*-test, while comparison between all samples in the two groups was also made using Mann-Whitney U Test. Correlation was evaluated by simple linear regression models (Kendall's rank correlation) in order to provide a measure of the strength of dependence between two variables. Results were considered significant when a p value of < 0.05 was obtained.

RESULTS

Biological Age of Kidneys and Blood Leukocytes Determined by DNAmAge, AgeAcc and TL

In **Figure 1**, DNAmAge of the right (RK) ($n = 27$ paired RK vs blood DNAmAge donors (B), paired *t*-test: median 69 years vs. median 65 years; $p = 0.0271$) and left kidney (LK) ($n = 27$ paired LK vs blood DNAmAge donors (C), paired *t*-test: median 69 years vs. median 65 years; $p = 0.0245$) are significantly older than blood leukocytes DNAmAge. RK and LK DNAmAge are similar (A).

Still in **Figure 1**, AgeAcc of RK and LK present higher score (this mean the AgeAcc is faster) than that of blood leukocytes in the same donor ($n = 27$ RK vs blood AgeAcc donors (E), paired *t*-test: median−5 years vs. median−8 years; $p = 0.0271$, and $n = 27$ LK vs. blood AgeAcc donors (F), paired *t*-test: median−6 years vs. median−7 years; $p = 0.0245$). No difference between RK and LK AgeAcc is observed (D).

Figure 2 shows that TL of RK and LK are significantly longer than that of blood leukocytes in the same donor ($n = 27$ paired *t*-test: RK TL vs. blood donors (B), median 1.18 T/S vs. median 1.15 T/S; $p = 0.0011$; $n = 27$ LK TL vs. blood

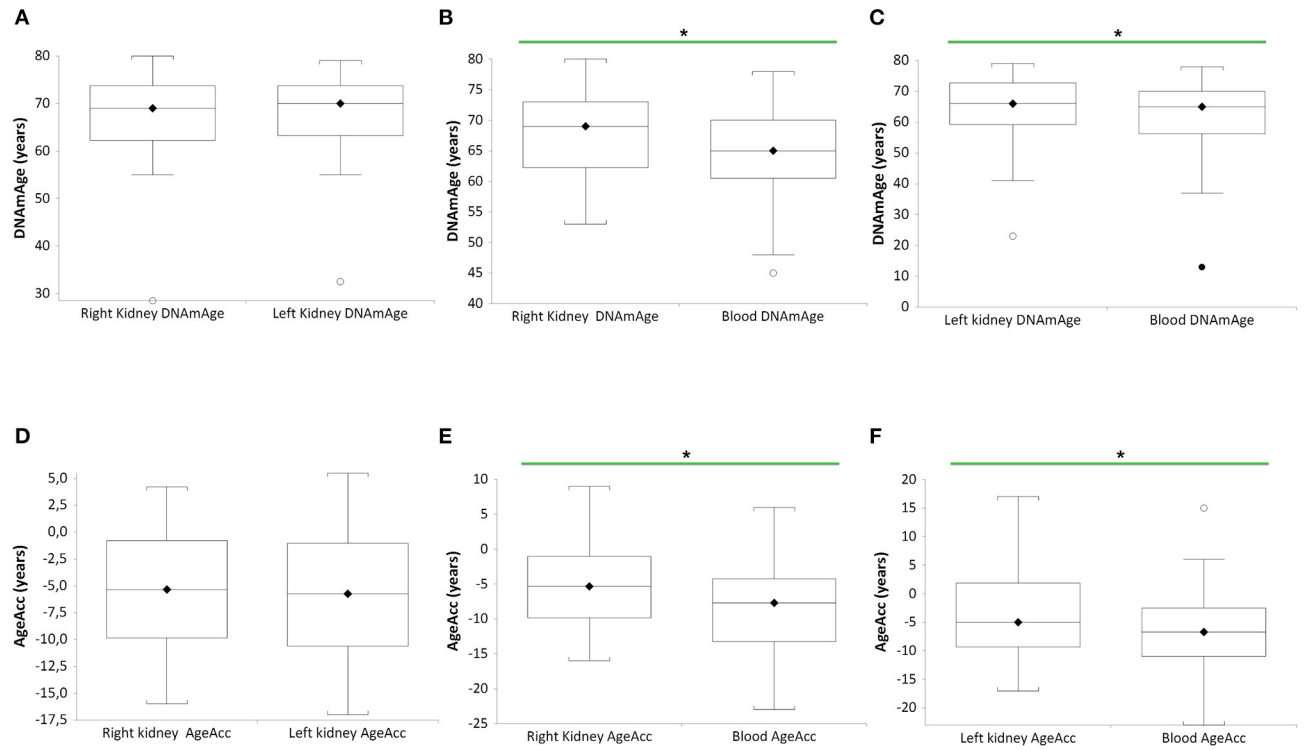

FIGURE 1 | DNAmAge and AgeAcc of both kidneys (right and left) and blood leukocytes in the same donors ($n = 27$). Box plots show levels of DNAmAge in right and left kidneys (RK and LK) **(A)**, in RK and blood **(B)**, and in LK and blood **(C)** of the same donors. In box plots, the boundary of the box closest to the x-axis indicates the 25th percentile, the line within the box marks the mean, and the boundary of the box farthest from the x-axis indicates the 75th percentile. Whiskers (error bars) above and below the box indicate the 95 and 5th percentiles. In **(B)**, the horizontal bar with asterisk indicates the significant comparison between RK DNAmAge and paired blood DNAmAge of the same donor (n = 27) (*Paired *t*-test: median 69 years vs. median 65 years; $p = 0.0271$). In **(C)**, the horizontal bar with asterisk indicates the significant comparison between LK DNAmAge and paired blood DNAmAge of the same donor ($n = 27$) (*Paired *t*-test: median 69 years vs. median 65 years; $p = 0.0245$). Box plots show levels of AgeAcc in right and left kidneys (RK and LK) **(D)**, in RK and blood **(E)**, and in LK and blood **(F)** of the same donors. In box plots, the boundary of the box closest to the x-axis indicates the 25th percentile, the line within the box marks the mean, and the boundary of the box farthest from the x-axis indicates the 75th percentile. Whiskers (error bars) above and below the box indicate the 95 and 5th percentiles. In **(E)**, the horizontal bar with asterisk indicates the significant comparison between RK AgeAcc and paired blood AgeAcc of the same donor ($n = 27$) (*Paired *t*-test: median−5 years vs. median−8 years; $p = 0.0271$). In **(F)**, the horizontal bar with asterisk indicates the significant comparison between LK AgeAcc and paired blood AgeAcc of the same donor ($n = 27$) (*Paired *t*-test: median−6 years vs. median−7 years; $p = 0.0245$).

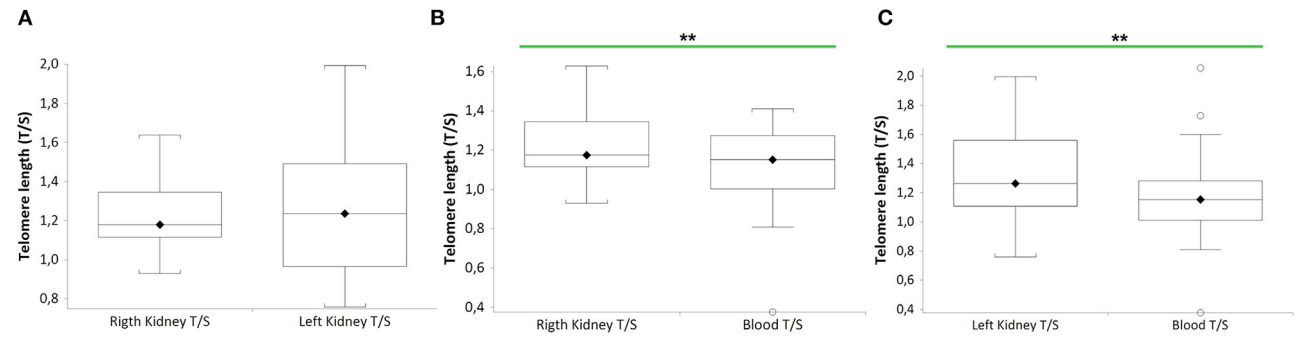

FIGURE 2 | TL of both kidneys (right and left) and blood leukocytes in the same donors ($n = 27$). Box plots show levels of TL in right and left kidneys (RK and LK) **(A)**, in RK and blood **(B)**, and in LK and blood **(C)** of the same donors. In box plots, the boundary of the box closest to the x-axis indicates the 25th percentile, the line within the box marks the mean, and the boundary of the box farthest from the x-axis indicates the 75th percentile. Whiskers (error bars) above and below the box indicate the 95 and 5th percentiles. In **(B)**, the horizontal bar with asterisks indicates the significant comparison between RK TL and paired blood TL of the same donor ($n = 27$) (**Paired *t*-test: median 1.18 T/S vs. median 1.15 T/S; $p = 0.0011$). In **(C)**, the horizontal bar with asterisks indicates the significant comparison between LK TL and paired blood TL of the same donor ($n = 27$) (**Paired *t*-test: median 1.25 T/S vs. median 1.15 T/S; $p = 0.0098$).

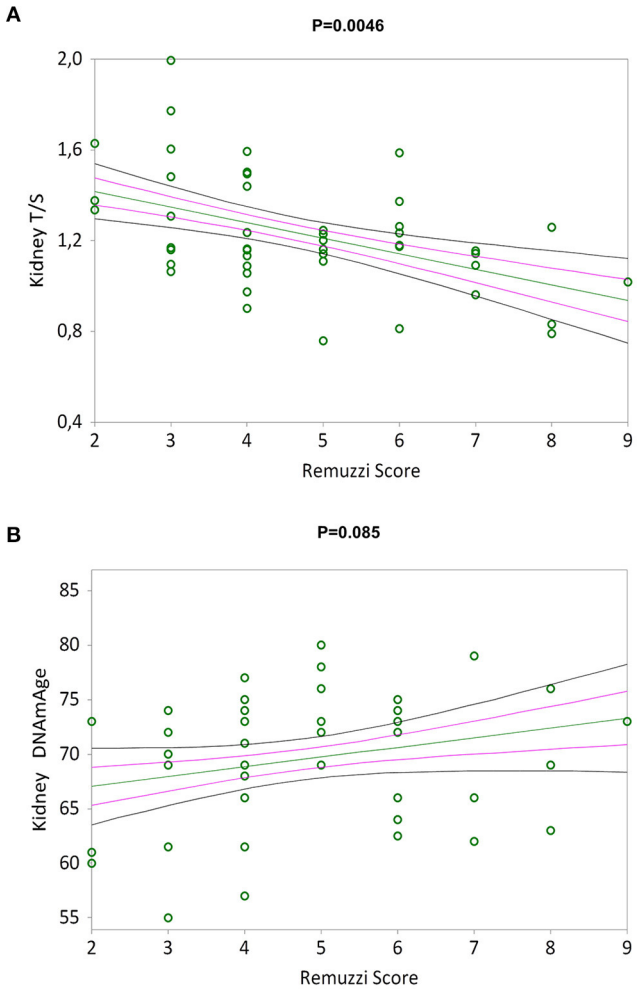

FIGURE 3 | TL and DNAmAge of the kidneys and the Remuzzi-Karpinski score correlations. Non-parametric linear regression plot showing correlations between TL **(A)** and DNAmAge **(B)** of the donors kidneys and the Remuzzi-Karpinski score (Kendall's rank correlation coefficient tau b = −0.310 and Kendall's rank correlation coefficient tau b = 0.192). Mean, Standard Error (SE) and 95% coefficient intervals (CI) are represented as green, pink and black lines, respectively.

donors (C), paired *t*-test: median 1.25 T/S vs. median 1.15 T/S; $p = 0.0098$). No difference between RK and LK TL is observed (A).

Figure 3A shows a negative correlation between the Remuzzi-Karpinski score and kidney TL (Kendall's rank correlation coefficient tau b = −0.310, $p = 0.0046$). Remuzzi-Karpinski score and DNAmAge were instead positive weakly correlated (**Figure 3B**, Kendall's rank correlation coefficient tau b = 0.192, $p = 0.085$). In **Supplementary Table S1**, multiple linear regression analysis of the influence of chronological age, gender, kidneys DNAmAge and TL on Remuzzi-Karpinski score of the donors' kidneys, shows that kidneys TL is the main determinant of the Remuzzi-Karpinski score ($p = 0.0173$), but not age, gender and DNAmAge.

In **Supplementary Table S2** in supplementary material blood leukocytes DNAmAge, AgeAcc and TL are not related to the leukocytes count in donors.

Correlation Between Biological Age (DNAmAge, AgeAcc and TL) and Chronological Age, in RK, LK and Blood Leukocytes

Simple linear regression analyses show that AgeAcc of RK, LK and blood leukocytes are negative correlated with chronological age in **Figures 4A–C** respectively (Kendall's rank correlation coefficient tau b for RK = −0.483, $p = 0.0003$; LK = −0.638, $p < 0.0001$; blood leukocytes = −0.526, $p < 0.0001$).

DNAmAge of RK, LK and blood leukocytes are positive highly correlated with chronological age (Kendall's rank correlation coefficient tau b for RK = 0.546, LK = 0.663 and blood leukocytes = 0.636, $p < 0.0001$ in **Supplementary Figures S1A–C** respectively). Instead, TL of RK, LK and blood leukocytes are negative correlated with chronological age in **Supplementary Figures S1D–F**, respectively (Kendall's rank correlation coefficient tau b for RK = −0.257, $p = 0.0532$; LK = −0.403, $p = 0.0011$; blood leukocytes = −0.277, $p = 0.0224$).

Correlation Between RK, LK and Blood Leukocytes Biological Age (DNAmAge, AgeAcc and TL)

Simple linear regression analyses show that RK and LK DNAmAge correlate with that of blood leukocytes (Kendall's rank correlation coefficient tau b for RK = 0.479, $p = 0.0007$ and LK = 0.540, $p < 0.0001$ in **Figures 5A,B**), as well as RK and LK TL correlate with that of blood leukocytes (Kendall's rank correlation coefficient tau b for RK = 0.396, $p = 0.004$ and LK = 0.432, $p = 0.0007$ in **Figures 5C,D**).

Furthermore, the epigenetic non-mitotic DNAmAge and the mitotic age (TL) of RK, LK and blood leukocytes are negatively associated (Kendall's rank correlation coefficient tau b for: RK = –0.369, $p = 0.0057$; LK = −0.327, $p = 0.0083$; blood leukocytes = −0.346, $p = 0.0046$ in **Supplementary Figures S2A–C** respectively).

Age-adjusted TL of RK, LK and blood (calculated as the residual of a regression of TL onto chronological age) were associated with age-adjusted DNAmAge (i.e., AgeAcc). These positive and significant correlations are reported in **Supplementary Figures S3A–C**, respectively, in **Supplementary Materials** (Kendall's rank correlation coefficient tau b for: RK = 0.476, $p = 0.0004$; LK = 0.632, $p < 0.0001$; blood leukocytes = 0.537, $p < 0.0001$ in **Supplementary Figures S3A–C** respectively).

Determinants of Blood Leukocytes and Kidneys DNAmAge, AgeAcc, and TL

Multiple regression analysis (**Supplementary Table S3** in **Supplementary Material**) of the influence of chronological age (years), gender, leukocytes (10^3/mL), smoking and chronic diseases including arterial hypertension, diabetes and cancer on

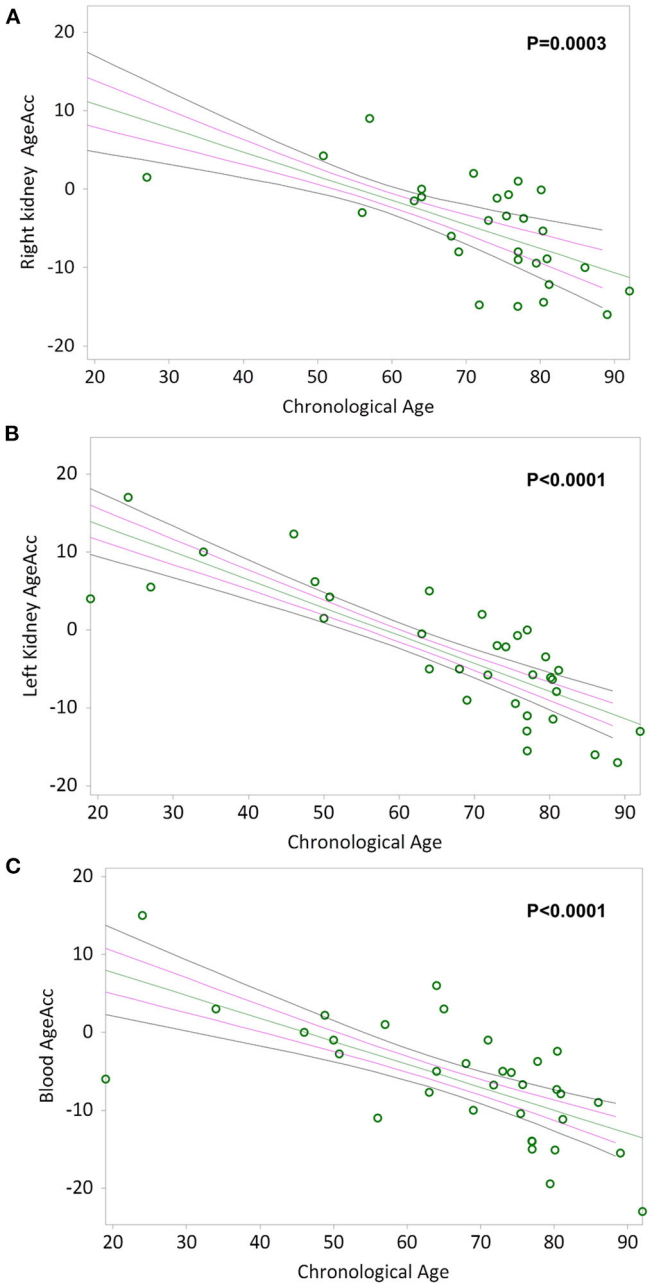

FIGURE 4 | AgeAcc of the right kidney, the left kidney, and blood leukocytes correlation with donors' chronological age. In **(A)** and **(B)**, non-parametric linear regression plots showing the correlation between AgeAcc of RK and LK, and donors chronological age (Kendall's rank correlation coefficient tau b for RK = −0.483 and tau b for LK = −0.638). In **(C)**, non-parametric linear regression plot showing the correlation between AgeAcc of the circulating blood leukocytes (indicated as "blood AgeAcc") and the donors chronological age (Kendall's rank correlation coefficient tau b = −0.526). Mean, Standard Error (SE) and 95% coefficient intervals (CI) are represented as green, pink and black lines, respectively.

blood leukocytes DNAmAge, AgeAcc and TL, shows that the main determinants are chronological age for DNAmAge ($p < 0.0001$) and arterial hypertension for TL ($p = 0.0014$).

Multiple linear regression analysis (**Supplementary Table S4** in **Supplementary Material**) of the influence of creatinine (mg/dL), cancer, Type 2 Diabetes (T2D), arterial hypertension (PAH), smoking, chronological age, suitability of organ for transplantation and gender on kidney DNAmAge, AgeAcc and TL shows that none of the variables considered are related to the DNAmAge, AgeAcc and TL levels. While chronological age is confirmed as determinant of both kidneys DNAmAge ($p < 0.0001$) and kidneys TL ($p = 0.0011$).

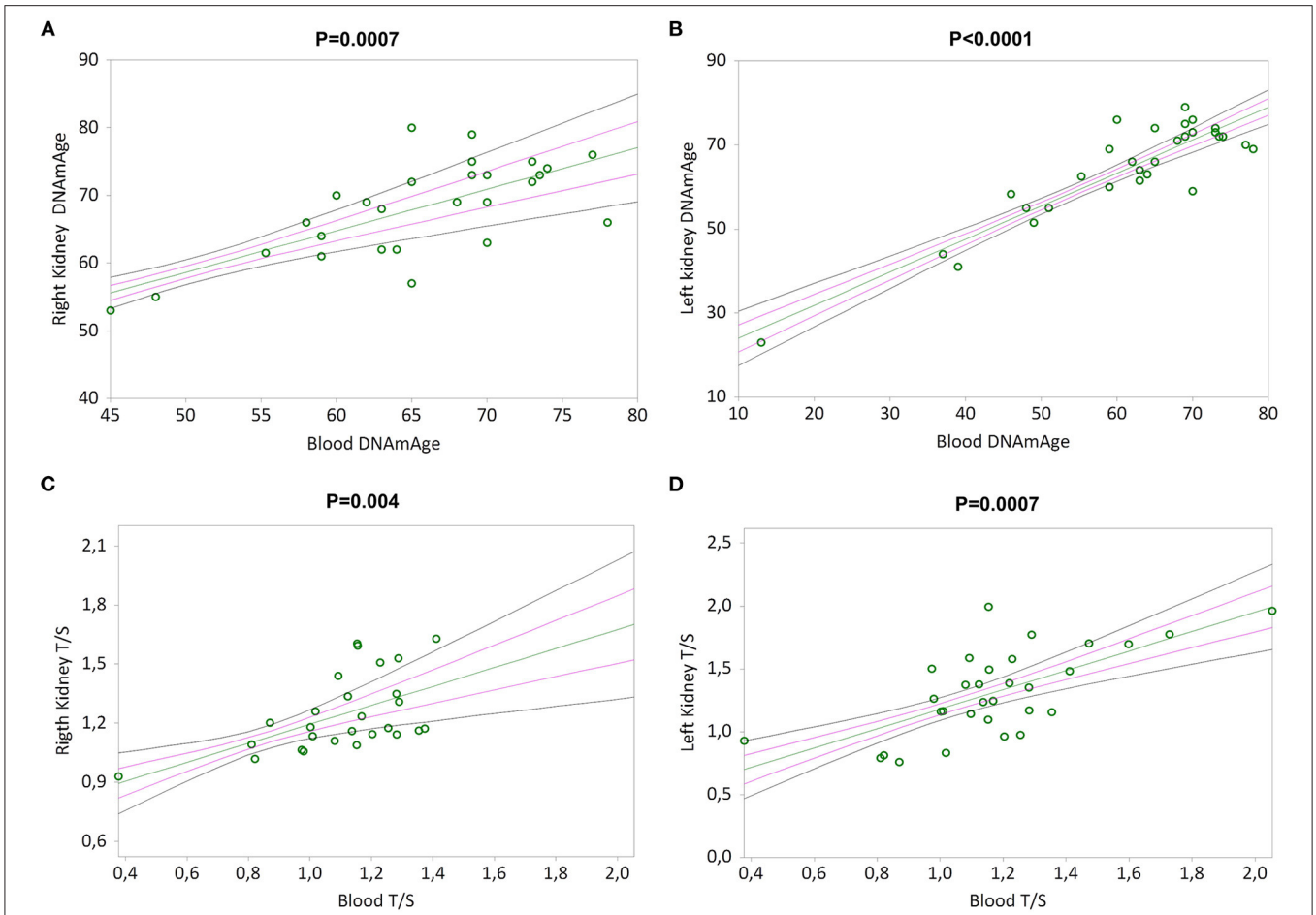

FIGURE 5 | DNAmAge and TL in both kidneys (right and left) correlation with blood leukocytes. In **(A)** and **(B)**, non-parametric linear regression plots showing the correlation between DNAmAge of the right kidney (RK) and the left kidney (LK), and blood DNAmAge (Kendall's rank correlation coefficient tau b for RK = 0.479 and tau b for LK = 0.540). In **(C)** and **(D)**, non-parametric linear regression plots showing the correlation between TL of the right kidney (RK) and the left kidney (LK), and blood TL (Kendall's rank correlation coefficient tau b for RK = 0.396 and tau b for LK = 0.432). Mean, Standard Error (SE) and 95% coefficient intervals (CI) are represented as green, pink and black lines, respectively.

DISCUSSION

In this study, we have determined the biological age of the kidney and of peripheral blood leukocytes of donors, by measuring the non-mitotic epigenetic age (DNAmAge and AgeAcc) and the mitotic age (TL) and correlate it to the Remuzzi-Karpinski score.

The main findings stemming from this work reveal that:

a) The non-mitotic epigenetic age (DNAmAge and AgeAcc) of both kidney tissues (RK and LK) is older than that of blood leukocytes;
b) AgeAcc of both kidney tissues (RK and LK) and blood leukocytes significantly slow down with advancing in chronological age;
c) The mitotic age (TL) of both kidney tissues (RK and LK) is younger than that of blood leukocytes and TL attrition is strongly correlated with the increase in Remuzzi-Karpinski score;
d) DNAmAge, and TL of RK and LK highly correlate with those of blood leukocytes.

DNA methylation is currently the most promising molecular marker for monitoring biological aging and predicting life expectancy (29–31). In humans, DNA methylation changes start early in life, as demonstrated by longitudinal studies of infants' blood (32, 33). Notably, these early epigenetic profiles continue to accumulate changes with the advancement of age, even more so in twins that do not share the same habits and/or environments (34, 35), indicating that aging-associated DNA methylation changes are caused by environmental factors too. In the present study, we demonstrated that epigenetic age (DNAmAge) and AgeAcc of the RK and LK are higher than that of blood leukocytes. This would suggest that the kidney is more susceptible than blood, to epigenetic changes induced by the interaction of advancing age and environmental factors. The aging kidney presents 11.5% of the CpG sites significantly altered (36) in respect to the 0.05–4% of CpG sites reported

for other organs (37, 38). A recent report showed that kidney cells make a negligible contribution in terms of the cellular turnover of the human body compared to blood cells and gut epithelial cells (39). Therefore we cannot exclude that the higher methylation in kidney could be attributable to the fact that kidney cells are differentiated and nonproliferative, which allows for the progressive accumulation of epigenetic changes. The hypermethylation correlates with interstitial fibrosis and glomerulosclerosis after kidney transplantation, as well as to reduced renal function (36). One of the causes proposed for biological aging is the accumulation of background noise at the epigenome level, which disrupts the gene expression patterns, leading to a decrease in tissue function and regenerative capacity. A kidney-specific epigenome-wide study of renal biopsies obtained from donors prior to kidney transplantation (range of age: 16–73 years), demonstrated a causal relationship between DNA hypermethylation and age-associated kidney dysfunction (36). Altered genes included those controlling epithelial cell proliferation, susceptibility to apoptosis, stem cell function, and activation of inflammatory cells. The age-related hypermethylation in kidneys is also associated to loss of DNA hydroxymethylation, suggesting a reduced activity of the ten-eleven traslocation (TET) demethylation enzymes, probably due to increased oxidative stress of the aged kidney, drives these age-related changes. Many key factors that influence DNA methylation, including advanced donor age, alloreactive immune responses, ischemia–reperfusion injury, and fibrosis, have the greatest prognostic impact in kidney transplantation, significantly contributing to allograft survival of transplanted patient (40). Therefore, DNA methylation changes represent an interesting research area in kidney transplantation. Mammalian tissues have recently been shown to retain a record of juvenile epigenetic information, encoded by DNA methylation, which can be accessed by acting on methylation to improve tissue function and promote *in vivo* regeneration. In our previous studies, we demonstrated that intensive relaxing training turns back the epigenetic clock (DNA methylation age, DNAmAge), together with improvement in clinical blood parameters (i.e., stress hormones, inflammatory markers, etc.) and with a clinical regaining of endothelial function, in patients after myocardial infarction, and even more in healthy subjects (17). In the whole this suggests that younger epigenetic information can be recovered and indicators of biological clock may represent an accurate tool to measure the effectiveness of interventions. Given the reversible nature of the epigenetic mechanisms, we hypothesize that a demethylation treatment in a kidney under normothermic reperfusion, by also intervening with DNA methylation inhibitors, which may allow restoring normal cellular functions, could be proposed in order to rejuvenate the kidney.

We found that AgeAcc of both kidney and blood leukocytes significantly decreased with advancing chronological age, while we confirmed that DNAmAge are highly correlated with chronological age as previously reported by Horvath (14) and Hannum et al. (15). The reduction in the aging rate of the epigenetic clock in older donors agrees with the hypothesis proposed by Horvath that the ticking rate of the epigenetic clock slows down in later life (14). Furthermore, the rates of epigenetic AgeAcc, has been associated with symptoms of aging, such as frailty and menopause (41, 42), as well as to several aging-associated pathologies including cancer and neurodegenerative diseases (14, 43, 44). AgeAcc can also predict life expectancy independently of common risk factors (19, 45). Nevertheless, the implications of the biological age determination in the field of kidney transplantation have never been explored before. Our results would suggest that AgeAcc might be the epigenetic clock mirroring the real biological state of the kidney. The reduction in the aging rate (AgeAcc) and therefore the slowing down of biological aging in older donors could have a paramount value on the evaluation and use of organs from these donors.

In this study, we also demonstrated that TL of RK and LK were longer than that of blood leukocytes, suggesting that mitotic age of kidney tissue is younger than blood leukocytes. Our results are consistent with the lower cellular turnover in renal cortex/medulla compared to blood leukocytes (39, 46) and to a drop in telomere shortening 9–29 bp/year in kidney cells compared to 41–84 bp/year in blood leukocytes (46). Furthermore, TL of RK and LK highly correlated with chronological age. In this regard, our results are in line with those reported by Melk and colleagues (47) that explored the relationship between age and TL in surgical samples from 24 human kidneys. They found that TL shortens in an age-dependent manner in the kidney with an average of 29 bp/year. We confirmed the inverse correlation between blood leukocytes TL and chronological age that is well-documented in literature. In a systematic review of such association in adults, an almost identical significant negative correlation of about $R = 0.3$, between mean chronological age and mean LTL, was observed across 124 cross-sectional studies (20).

Furthermore, the rise in DNAmAge and the decline in TL of RK, LK and blood leukocytes were firmly correlated. Studies comparing DNA methylation age and TL in the same sample are few and limited to blood samples (48–52). Our findings are consistent with our previous work on heart donors in which DNAmAge negatively correlated with TL in heart and blood (10), suggesting that DNA methylation and telomeres, even if depending from different mechanisms of the same process (biological aging), they can be associated. Shorter TL is a measure of "mitotic age" also defined as "replicative senescence" (53, 54). Telomeres shorten with every cell division, ticking as a cellular "molecular clock" (55) or a replication "timer." It was shown that telomeres in highly proliferative somatic tissues are shorter than in cells of non- or low rate proliferative tissues (56). On the other hand, the DNAmAge of differentiated cells does not mirror their proliferative history (12), as evidenced in the Horvarth's epigenetic clock, which produces similar DNAmAge estimation within the same individual for highly proliferative tissues (i.e., blood and colon) and less-proliferative ones (i.e., blood and colon) (14).

We also observed a strong correlation between the increase in Remuzzi-Karpinski score and TL attrition. The Remuzzi score is a histological scoring system obtained at pre-implantation biopsy ranging from 0 (no lesions) to 12

score (marked changes in vessels, glomeruli, tubules and connective tissue) (5). An increased Remuzzi score, being related with poor graft outcomes, is currently used for the decision of discarding donor kidneys or transplanting two kidneys with intermediate score (5, 57). Our finding, showing that kidneys with high Remuzzi score present shorter TL, indicates that such damaged organs present more "mitotic clock miles." Considering that TL attrition was also associated with decreased graft survival post-transplant (58), this finding acquires further strategic importance in assessing the quality of the organ.

In order to promptly translating our work into the clinical practice, we also assessed the similarity level of biological ages between kidneys and blood leukocytes in the same donor. We observed a robust correlation between DNAmAge and TL of kidneys (RK and LK) and blood leukocytes, suggesting that the latter could be a surrogate tissue of the kidney status for biological aging studies. To the best of our knowledge, such correlation for DNAmAge has not been investigated before now. Determining the biological age of blood and estimating its correlation with that of the kidneys is of paramount importance to identify and set up a simple and reliable tool for screening potential donors, in particular for accepting the kidneys for transplantation from elderly donors. In a real clinical scenario, at the donor hospital site, blood samples may be easily and quickly acquired and sent to the laboratory for biological age analysis. Further studies are hence needed to optimize the use of blood as a surrogate indicator of kidney's biological age in clinical practice.

Furthermore, the slowing down of biological aging (AgeAcc) in older donors could be a key parameter in the evaluation and use of organs from these donors. For example, we can hypothesize to define a cutoff of AgeAcc, beyond which the donor becomes at risk of graft dysfunction rather than considering the value of the chronological age.

Our study for the first time evaluated the non-mitotic epigenetic age and the mitotic age from kidneys of donors by comparing it with that of their blood leukocytes in healthy donors. This pioneering aspect certainly represents one of the main strengths of our study. Analyzing DNAmAge and TL by using an almost totally automated workflow, which allows us to perform the analyses in a standardized way reducing errors, is another strong point of this study. Furthermore, no significant difference was found in the distribution of RK and LK DNAmAge, and in TL as well. Our study for the first time evaluates the non-mitotic epigenetic age (DNAmAge) and mitotic age (TL) of donor kidneys, and levels were similar for both kidneys. This suggests that, in the future, biological age analysis can be performed either in the RK or LK. Lastly, our results showed that kidneys TL and DNAmAge correlate with those of blood leukocytes, suggesting that blood could be a more easily and quickly acquired surrogate tissue of the kidney for biological aging studies for translating into the clinical practice.

A limitation of our study could be the small number of subjects enrolled and number of samples collected, which was due to the limited available donors on which biopsies can be performed due to clinical reasons. However, samples analyzed are adequate from the statistical point of view. Another limitation could be that renal biopsy, from which we extracted DNA for biological age analysis, contains different cell types. However, up to now, renal biopsy remains the gold standard by which essential diagnostic and prognostic information is obtained in kidney transplantation. Biopsy methodologies have been developed to assess the acceptability of an organ before transplantation and to assess and predict renal allograft performance after implantation (2, 5). In addition, the donor organ biopsy sample provides a valuable baseline against which the results of subsequent biopsies of the renal allograft can be compared (2, 5). Furthermore, the few studies regarding the analyses of telomere and methylation profiles in the kidney were performed on kidney biopsies, as well as our study. However, recent advances in single cell genomics are transforming researchers' ability to characterize single cells (59). Incorporation of these new tools into traditional histopathologic evaluation of renal tissue is needed to improve diagnostic precision and predictive value of the renal biopsy in kidney disease. Therefore, further studies are needed in this field.

Another limitation could be that DNAmAge measure used in this study was composed of only 5 CpG sites while other DNAmAge measures are composed of up to several hundred CpG sites. However, amongst the most robust predictors, we selected the model proposed by Zbieć-Piekarska et al. (16). This method shows that DNAmAge highly correlates ($r = 0.94$) to chronological age with a mean deviations from calendar age (4.5 years) analogous to those from Horvath (14) and Hannum et al. (15) ($r = 0.96$ and $r = 0.91$) with 3.6 and 4.9 years mean considered the reference methods. Zbieć-Piekarska et al. (16) developed the algorithm in a larger sample ($n = 420$) and then they validated it in a smaller one ($n = 300$), covering the entire adult life span. Furthermore, to increase the practicability of these tests, and used the locus-specific technology pyrosequencing which having the potential for multiplexing, makes the technical analysis achievable in few hours and reduce the cost of technical analysis, methods with only few loci were taken into account. Furthermore, we have automated to increase the efficiency and rapidity, maintaining high prediction accuracy (9, 10). Lastly, analyzing DNAmAge by using this process in an almost totally automated workflow, we can perform the analyses in a standardized way reducing errors, and this is a strong point of our study.

In conclusion, main findings stemming from our study are that the epigenetic age of kidney was older than that of the blood leukocytes, but the mitotic age measured by TL of kidney is younger than that of blood leukocytes suggesting that, in view of the low cellular turnover of the kidney cells, they are more susceptible than blood to epigenetic changes, which allows for the progressive accumulation of background noise at the epigenome level. Therefore, given the reversible nature of the epigenetic mechanisms of DNA, in the current era of shortage of organs, methylation changes might represent an interesting research area, which could offer a potential translation into kidney transplantation. Our finding, showing that kidneys with high Remuzzi score present shorter TL, indicates that such marker can be evaluated in further studies as markers of donor organ quality. Our study although deserves future focused investigations on

post-transplant graft performance and durability in relation to the biological age, could contribute to open a novel basic and clinical research platform in the field of all solid organs' transplantation.

DATA AVAILABILITY STATEMENT

The raw data supporting the conclusions of this article will be made available by the authors, without undue reservation.

ETHICS STATEMENT

The studies involving human participants were reviewed and approved by the Ethical Committee for Clinical Trials of the Province of Padova. The patients/participants provided their written informed consent to participate in this study.

AUTHOR CONTRIBUTIONS

SP and MC: conceived and designed the study and provided administrative, technical, or material support (i.e., reporting or organizing data, constructing databases). LF, FN, MB, PR, and EN: provided the samples. MC: performed the samples' analysis. SP and MC: analyzed the data. SP, MC, and FN: wrote the paper. All authors contributed to the article and approved the submitted version.

FUNDING

This study was supported by the funding Grants the L.I.F.E.L.A.B., Consorzio Per La Ricerca Sanitaria-CORIS (Veneto Region).

ACKNOWLEDGMENTS

The authors would like to acknowledge the Department of Surgery, Oncology and Gastroenterology DiSCOG, Bando Pubblicazioni 2021.

SUPPLEMENTARY MATERIAL

The Supplementary Material for this article can be found online at: https://www.frontiersin.org/articles/10.3389/fmed.2022.832411/full#supplementary-material

REFERENCES

1. Hart A, Lentine KL, Smith JM, Miller JM, Skeans MA, Prentice M, et al. OPTN/SRTR 2019 Annual data report: kidney. *Am J Transplant.* (2021) 21 Suppl 2:21–137. doi: 10.1111/ajt.16502
2. Pierobon ES, Sefora PE, Sandrini S, Silvio S, De Fazio N, Nicola DF, et al. Optimizing utilization of kidneys from deceased donors over 60 years: five-year outcomes after implementation of a combined clinical and histological allocation algorithm. *Transpl Int.* (2013) 26:833–41. doi: 10.1111/tri.12135
3. Slegtenhorst BR, Dor FJMF, Elkhal A, Rodriguez H, Yang X, Edtinger K, et al. Mechanisms and consequences of injury and repair in older organ transplants. *Transplantation.* (2014) 97:1091–9. doi: 10.1097/TP.0000000000000072
4. Abdel-Rahman EM, Okusa MD. Effects of aging on renal function and regenerative capacity. *Nephron Clin Pract.* (2014) 127:15–20. doi: 10.1159/000363708
5. Remuzzi G, Grinyò J, Ruggenenti P, Beatini M, Cole EH, Milford EL, et al. Early experience with dual kidney transplantation in adults using expanded donor criteria. Double Kidney Transplant Group (DKG). *J Am Soc Nephrol.* (1999) 10:2591–8. doi: 10.1681/ASN.V10122591
6. Pavanello S, Angelici L, Hoxha M, Cantone L, Campisi M, Tirelli AS, et al. Sterol 27-Hydroxylase polymorphism significantly associates with shorter telomere, higher cardiovascular and type-2 diabetes risk in obese subjects. *Front Endocrinol.* (2018) 9:309. doi: 10.3389/fendo.2018.00309
7. Pavanello S, Carta A, Mastrangelo G, Campisi M, Arici C, Porru S. Relationship between telomere length, genetic traits and environmental/occupational exposures in bladder cancer risk by structural equation modelling. *Int J Environ Res Public Health.* (2018) 15:5. doi: 10.3390/ijerph15010005
8. Pavanello S, Campisi M, Mastrangelo G, Hoxha M, Bollati V. The effects of everyday-life exposure to polycyclic aromatic hydrocarbons on biological age indicators. *Environ Health.* (2020) 19:128. doi: 10.1186/s12940-020-00669-9
9. Campisi M, Liviero F, Maestrelli P, Guarnieri G, Pavanello S. DNA Methylation-based age prediction and telomere length reveal an accelerated aging in induced sputum cells compared to blood leukocytes: a pilot study in COPD patients. *Front Med (Lausanne).* (2021) 8:690312. doi: 10.3389/fmed.2021.690312
10. Pavanello S, Campisi M, Fabozzo A, Cibin G, Tarzia V, Toscano G, et al. The biological age of the heart is consistently younger than chronological age. *Sci Rep.* (2020) 10:10752. doi: 10.1038/s41598-020-67622-1
11. Srinivas N, Rachakonda S, Kumar R. Telomeres and telomere length: a general overview. *Cancers (Basel).* (2020) 12:E558. doi: 10.3390/cancers12030558
12. Lowe D, Horvath S, Raj K. Epigenetic clock analyses of cellular senescence and ageing. *Oncotarget.* (2016) 7:8524–31. doi: 10.18632/oncotarget.7383
13. Horvath S, Raj K. DNA methylation-based biomarkers and the epigenetic clock theory of ageing. *Nat Rev Genet.* (2018) 19:371–84. doi: 10.1038/s41576-018-0004-3
14. Horvath S. DNA methylation age of human tissues and cell types. *Genome Biol.* (2013) 14:R115. doi: 10.1186/gb-2013-14-10-r115
15. Hannum G, Guinney J, Zhao L, Zhang L, Hughes G, Sadda S, et al. Genome-wide methylation profiles reveal quantitative views of human aging rates. *Mol Cell.* (2013) 49:359–67. doi: 10.1016/j.molcel.2012.10.016
16. Zbieć-Piekarska R, Spólnicka M, Kupiec T, Parys-Proszek A, Makowska Z, Pałeczka A, et al. Development of a forensically useful age prediction method based on DNA methylation analysis. *Forensic Sci Int Genet.* (2015) 17:173–9. doi: 10.1016/j.fsigen.2015.05.001
17. Pavanello S, Campisi M, Tona F, Lin CD, Iliceto S. Exploring epigenetic age in response to intensive relaxing training: a pilot study to slow down biological age. *Int J Environ Res Public Health.* (2019) 16:E3074. doi: 10.3390/ijerph16173074
18. Dhingra R, Nwanaji-Enwerem JC, Samet M, Ward-Caviness CK. DNA methylation age—environmental influences, health impacts, and its role in environmental epidemiology. *Curr Envir Health Rpt.* (2018) 5:317–27. doi: 10.1007/s40572-018-0203-2

19. Fransquet PD, Wrigglesworth J, Woods RL, Ernst ME, Ryan J. The epigenetic clock as a predictor of disease and mortality risk: a systematic review and meta-analysis. *Clin Epigenetics.* (2019) 11:62. doi: 10.1186/s13148-019-0656-7
20. Müezzinler A, Zaineddin AK, Brenner H. A systematic review of leukocyte telomere length and age in adults. *Ageing Res Rev.* (2013) 12:509–19. doi: 10.1016/j.arr.2013.01.003
21. Dlouha D, Maluskova J, Kralova Lesna I, Lanska V, Hubacek JA. Comparison of the relative telomere length measured in leukocytes and eleven different human tissues. *Physiol Res.* (2014) 63:S343–350. doi: 10.33549/physiolres.932856
22. Demanelis K, Jasmine F, Chen LS, Chernoff M, Tong L, Delgado D, et al. Determinants of telomere length across human tissues. *Science.* (2020) 369:eaaz6876. doi: 10.1126/science.aaz6876
23. Friedrich U, Griese E, Schwab M, Fritz P, Thon K, Klotz U. Telomere length in different tissues of elderly patients. *Mech Ageing Dev.* (2000) 119:89–99. doi: 10.1016/S0047-6374(00)00173-1
24. Jung SE, Shin KJ, Lee HY. DNA methylation-based age prediction from various tissues and body fluids. *BMB Rep.* (2017) 50:546–53. doi: 10.5483/BMBRep.2017.50.11.175
25. Pavanello S, Stendardo M, Mastrangelo G, Bonci M, Bottazzi B, Campisi M, et al. Inflammatory Long Pentraxin 3 is Associated with Leukocyte Telomere Length in Night-Shift Workers. *Front Immunol.* (2017) 8:516. doi: 10.3389/fimmu.2017.00516
26. Pavanello S, Stendardo M, Mastrangelo G, Casillo V, Nardini M, Mutti A, et al. Higher number of night shifts associates with good perception of work capacity and optimal lung function but correlates with increased oxidative damage and telomere attrition. *Biomed Res Int.* (2019) 2019:e8327629. doi: 10.1155/2019/8327629
27. Pavanello S, Campisi M, Grassi A, Mastrangelo G, Durante E, Veronesi A, et al. Longer Leukocytes Telomere Length Predicts a Significant Survival Advantage in the Elderly TRELONG Cohort, with Short Physical Performance Battery Score and Years of Education as Main Determinants for Telomere Elongation. *J Clin Med.* (2021) 10:3700. doi: 10.3390/jcm10163700
28. Cawthon RM. Telomere length measurement by a novel monochrome multiplex quantitative PCR method. *Nucleic Acids Res.* (2009) 37:e21. doi: 10.1093/nar/gkn1027
29. Bell CG, Lowe R, Adams PD, Baccarelli AA, Beck S, Bell JT, et al. DNA methylation aging clocks: challenges and recommendations. *Genome Biol.* (2019) 20:249. doi: 10.1186/s13059-019-1824-y
30. Levine ME. Assessment of epigenetic clocks as biomarkers of aging in basic and population research. *J Gerontol A Biol Sci Med Sci.* (2020) 75:463–5. doi: 10.1093/gerona/glaa021
31. Salameh Y, Bejaoui Y, El Hajj N. DNA Methylation Biomarkers in Aging and Age-Related Diseases. *Front Genet.* (2020) 11:171. doi: 10.3389/fgene.2020.00171
32. Herbstman JB, Wang S, Perera FP, Lederman SA, Vishnevetsky J, Rundle AG, et al. Predictors and consequences of global DNA methylation in cord blood and at three years. *PLoS ONE.* (2013) 8:e72824. doi: 10.1371/journal.pone.0072824
33. Martino DJ, Tulic MK, Gordon L, Hodder M, Richman TR, Metcalfe J, et al. Evidence for age-related and individual-specific changes in DNA methylation profile of mononuclear cells during early immune development in humans. *Epigenetics.* (2011) 6:1085–94. doi: 10.4161/epi.6.9.16401
34. Fraga MF, Ballestar E, Paz MF, Ropero S, Setien F, Ballestar ML, et al. Epigenetic differences arise during the lifetime of monozygotic twins. *Proc Natl Acad Sci U S A.* (2005) 102:10604–9. doi: 10.1073/pnas.0500398102
35. Tan Q, Heijmans BT, Hjelmborg JVB, Soerensen M, Christensen K, Christiansen L. Epigenetic drift in the aging genome: a ten-year follow-up in an elderly twin cohort. *Int J Epidemiol.* (2016) 45:1146–58. doi: 10.1093/ije/dyw132
36. Heylen L, Thienpont B, Busschaert P, Sprangers B, Kuypers D, Moisse M, et al. Age-related changes in DNA methylation affect renal histology and post-transplant fibrosis. *Kidney Int.* (2019) 96:1195–204. doi: 10.1016/j.kint.2019.06.018
37. Bacos K, Gillberg L, Volkov P, Olsson AH, Hansen T, Pedersen O, et al. Blood-based biomarkers of age-associated epigenetic changes in human islets associate with insulin secretion and diabetes. *Nat Commun.* (2016) 7:11089. doi: 10.1038/ncomms11089
38. Hernandez DG, Nalls MA, Gibbs JR, Arepalli S, van der Brug M, Chong S, et al. Distinct DNA methylation changes highly correlated with chronological age in the human brain. *Hum Mol Genet.* (2011) 20:1164–72. doi: 10.1093/hmg/ddq561
39. Sender R, Milo R. The distribution of cellular turnover in the human body. *Nat Med.* (2021) 27:45–8. doi: 10.1038/s41591-020-01182-9
40. Heylen L, Thienpont B, Naesens M, Lambrechts D, Sprangers B. The Emerging Role of DNA Methylation in Kidney Transplantation: a perspective. *Am J Transplant.* (2016) 16:1070–8. doi: 10.1111/ajt.13585
41. Breitling LP, Saum KU, Perna L, Schöttker B, Holleczek B, Brenner H. Frailty is associated with the epigenetic clock but not with telomere length in a German cohort. *Clin Epigenetics.* (2016) 8:21. doi: 10.1186/s13148-016-0186-5
42. Levine ME, Lu AT, Chen BH, Hernandez DG, Singleton AB, Ferrucci L, et al. Menopause accelerates biological aging. *Proc Natl Acad Sci U S A.* (2016) 113:9327–32. doi: 10.1073/pnas.1604558113
43. Ambatipudi S, Horvath S, Perrier F, Cuenin C, Hernandez-Vargas H, Le Calvez-Kelm F, et al. DNA methylome analysis identifies accelerated epigenetic ageing associated with postmenopausal breast cancer susceptibility. *Eur J Cancer.* (2017) 75:299–307. doi: 10.1016/j.ejca.2017.01.014
44. Levine ME, Lu AT, Bennett DA, Horvath S. Epigenetic age of the pre-frontal cortex is associated with neuritic plaques, amyloid load, and Alzheimer's disease related cognitive functioning. *Aging (Albany NY).* (2015) 7:1198–211. doi: 10.18632/aging.100864
45. Chen BH, Marioni RE, Colicino E, Peters MJ, Ward-Caviness CK, Tsai PC, et al. DNA methylation-based measures of biological age: meta-analysis predicting time to death. *Aging (Albany NY).* (2016) 8:1844–65. doi: 10.18632/aging.101020
46. Takubo K, Izumiyama-Shimomura N, Honma N, Sawabe M, Arai T, Kato M, et al. Telomere lengths are characteristic in each human individual. *Exp Gerontol.* (2002) 37:523–31. doi: 10.1016/S0531-5565(01)00218-2
47. Melk A, Ramassar V, Helms LMH, Moore R, Rayner D, Solez K, et al. Telomere shortening in kidneys with age. *J Am Soc Nephrol.* (2000) 11:444–53. doi: 10.1681/ASN.V113444
48. Weidner CI, Lin Q, Koch CM, Eisele L, Beier F, Ziegler P, et al. Aging of blood can be tracked by DNA methylation changes at just three CpG sites. *Genome Biol.* (2014) 15:R24. doi: 10.1186/gb-2014-15-2-r24
49. Marioni RE, Harris SE, Shah S, McRae AF, von Zglinicki T, Martin-Ruiz C, et al. The epigenetic clock and telomere length are independently associated with chronological age and mortality. *Int J Epidemiol.* (2018) 45:424–32. doi: 10.1093/ije/dyw041
50. Belsky DW, Moffitt TE, Cohen AA, Corcoran DL, Levine ME, Prinz JA, et al. Eleven Telomere, Epigenetic Clock, and Biomarker-Composite Quantifications of Biological Aging: Do They Measure the Same Thing? *Am J Epidemiol.* (2018) 187:1220–30. doi: 10.1093/aje/kwx346
51. Banszerus VL, Vetter VM, Salewsky B, König M, Demuth I. Exploring the Relationship of Relative Telomere Length and the Epigenetic Clock in the LipidCardio Cohort. *Int J Mol Sci.* (2019) 20:E3032. doi: 10.3390/ijms20123032
52. Vetter VM, Meyer A, Karbasiyan M, Steinhagen-Thiessen E, Hopfenmüller W, Demuth I. Epigenetic Clock and Relative Telomere Length Represent Largely Different Aspects of Aging in the Berlin Aging Study II (BASE-II). *J Gerontol A Biol Sci Med Sci.* (2019) 74:27–32. doi: 10.1093/gerona/gly184
53. Harley CB, Futcher AB, Greider CW. Telomeres shorten during ageing of human fibroblasts. *Nature.* (1990) 345:458–60. doi: 10.1038/345458a0
54. Harley CB, Vaziri H, Counter CM, Allsopp RC. The telomere hypothesis of cellular aging. *Exp Gerontol.* (1992) 27:375–82. doi: 10.1016/0531-5565(92)90068-B
55. Bernadotte A, Mikhelson VM, Spivak IM. Markers of cellular senescence. Telomere shortening as a marker of cellular senescence. *Aging.* (2016) 8:3–11. doi: 10.18632/aging.100871
56. Daniali L, Benetos A, Susser E, Kark JD, Labat C, Kimura M, et al. Telomeres shorten at equivalent rates in somatic tissues of adults. *Nat Commun.* (2013) 4:1597. doi: 10.1038/ncomms2602

57. Cecka JM, Cohen B, Rosendale J, Smith M. Could more effective use of kidneys recovered from older deceased donors result in more kidney transplants for older patients? *Transplantation.* (2006) 81:966–70. doi: 10.1097/01.tp.0000216284.81604.d4
58. Koppelstaetter C, Schratzberger G, Perco P, Hofer J, Mark W, Ollinger R, et al. Markers of cellular senescence in zero hour biopsies predict outcome in renal transplantation. *Aging Cell.* (2008) 7:491–7. doi: 10.1111/j.1474-9726.2008.00398.x
59. Malone AF, Wu H, Humphreys BD. Bringing Renal Biopsy Interpretation Into the Molecular Age With Single-Cell RNA Sequencing. *Semin Nephrol.* (2018) 38:31–9. doi: 10.1016/j.semnephrol.2017.09.005

Conflict of Interest: The authors declare that the research was conducted in the absence of any commercial or financial relationships that could be construed as a potential conflict of interest.

frontiers in Medicine

ORIGINAL RESEARCH
published: 23 March 2022
doi: 10.3389/fmed.2022.841887

"The Stakes Are Higher"- Patient and Caregiver Perspectives on Cystic Fibrosis Research and Personalized Medicine

Terese Knoppers[1], Marie Cosquer[1], Julie Hagan[2], Minh Thu Nguyen[1] and Bartha Maria Knoppers[1]*

[1] Centre of Genomics and Policy, McGill University, Montreal, QC, Canada, [2] Department of Sociology, Laval University, Quebec, QC, Canada

Introduction: Making bench to bedside advances in cystic fibrosis (CF) care requires the sustained engagement and trust of people living with CF. However, there is a scarcity of studies exploring their concerns and priorities regarding research and its end products. The aim of this qualitative study was to generate empirical evidence regarding patient and caregiver perspectives on cystic fibrosis research and personalized medicine to foster developments in translational research in Canada.

Methods: A total of 15 focus groups were conducted, engaging 22 adults with CF and 18 caregivers (e.g., parents, siblings and partners) living in Canada. Inductive thematic analysis relied on an iterative process involving themes derived from both participant meaning-making and existing scientific literature. Participant perspectives were considered along intrapersonal, intracommunity, interpersonal, and structural lines.

Results: Overall, participants described a relationship to CF research inextricable from the lived experience of CF as a lifelong progressive and terminal disease and from the goal of advancing medical science. They were enthusiastic and excited about the emergence of CFTR modulators, although they had some knowledge gaps regarding the associated research. They largely spoke to positive experiences with researcher communication but had feedback regarding informed consent processes and the return of study results. Participants also voiced concerns about structural access barriers to research and to its end products. Extensive histories of research participation, a relatively small and intercommunicative CF community, and structural overlap between research and care settings contributed to their perspectives and priorities.

Conclusion: Study findings are valuable for researchers and policy-makers in CF and rare or progressive diseases more broadly. Continuing to solicit and listen to the voices of patients and caregivers is crucial for research ethics and the translation of new therapies in the area of personalized medicine.

Keywords: patient perspectives, caregiver perspectives, cystic fibrosis, personalized medicine, ethics, translation, access, qualitative

OPEN ACCESS

Edited by:
Claudine Habak, Emirates College for Advanced Education, United Arab Emirates

Reviewed by:
Sanja Miodrag Sindjic Antunovic, University of Belgrade, Serbia
Fernando Augusto Lima Marson, São Francisco University, Brazil

****Correspondence:***
Terese Knoppers
theresa.knoppers@mcgill.ca

Specialty section:
This article was submitted to Translational Medicine, a section of the journal Frontiers in Medicine

Received: *22 December 2021*
Accepted: *14 February 2022*
Published: *23 March 2022*

Citation:
Knoppers T, Cosquer M, Hagan J, Nguyen MT and Knoppers BM (2022) "The Stakes Are Higher"- Patient and Caregiver Perspectives on Cystic Fibrosis Research and Personalized Medicine. Front. Med. 9:841887. doi: 10.3389/fmed.2022.841887

INTRODUCTION

> *The reasons for participating [in research] are number one I am a big believer in public science and public information. I really believe that research is crucial in informing medical decisions. But I think that the stakes are higher when you're dealing with a rare disease in which there are fewer patients, and in a disease like this that is progressive, there's also some urgency to figuring out as quickly as possible ways that we can improve bench to bedside protocols and care* (C17).

Cystic fibrosis (CF) is a degenerative multi-system disease caused by pathogenic variants in the cystic fibrosis transmembrane conductance regulator (*CFTR*) gene (1). In Canada, there are approximately 4,300 people living with CF, and CF occurs in an estimated 1 out of 3,600 live births (2). CF causes digestive disorders and progressive lung disease due to recurrent and chronic lung infections, resulting in a shortened lifespan. There are also significant psychosocial and economic impacts for people living with CF, their caregivers, and their families, associated with the intensive ongoing need for medical care and CF's episodic yet progressive symptomology (3).

Advances in diagnosis, therapies, and multi-disciplinary healthcare have greatly improved the quality of life and life expectancy for people with CF over the past decades (3, 4). Treatment focuses on slowing lung function deterioration and addressing digestive system problems. Lung transplants often also become necessary for people with advanced CF. Recently, upstream therapies have been developed to overcome the pathogenic variants that cause CF, improving or even restoring the functioning of the *CFTR* gene (5). These CFTR modulators, which offer treatment to individuals with certain variants, represent a paradigm shift in personalized medicine and disease prognosis for patients with CF (5, 6). The latest to be approved by Health Canada, Trikafta, is particularly ground-breaking in that an estimated 90% of Canadians with CF could benefit from it (7).

Making advances in CF care requires the sustained engagement and trust of people living with CF in research, not least because the population is small (and made smaller due to stratification during research) and patients with CF are already intensively studied. There is a scarcity of studies exploring the relationship of the CF community to research: their perspectives, concerns, and priorities [see (8–10)]. Such a study is particularly appropriate as the field branches into the development of personalized medicine (11). This paradigm shift raises the ethical stakes of research with the CF population because of the cost of the medicines being produced (an estimated $300,000 per person per year) and because the stem cell and genomics research producing this personalized medicine remain widely misunderstood domains (12–15). It is therefore critical and timely that we consider the lived experience of people with CF in research and its translation into personalized medicine (16). We conducted a qualitative study in order to generate empirical evidence regarding patient and caregiver perspectives on the utility and limitations of CF research and personalized medicine in Canada. Findings are valuable for researchers and policy-makers not only in the area of CF but in rare and/or progressive diseases more broadly.

MATERIALS AND METHODS

Recruitment and Study Participants

Given that the number of adults living with CF in Canada is small, we used a convenience sampling strategy to select participants for our study. Our main method of recruitment was through CF Canada and the different local chapters of the organization. We posted our recruitment ads via their Facebook pages as well as their members' email lists. We were also able to recruit through the assistance of several CF clinics across Canada, most notably in Ontario and Quebec. We targeted participants 18 years or older with a CF diagnosis. As most cases of CF are detected very early in life and about 40% of patients with CF are children (2), we decided to seek the opinions and experiences of caregivers (e.g., parents, siblings and partners) in our study to enrich our data. In both cases, we aimed to enroll individuals who had already participated in research and/or contributed to biobanks, databases, or registries in the past, but this was not an exclusion criterion.

Interested participants contacted the Centre of Genomics and Policy via phone and/or email. Those who met the recruitment criteria were sent more information about the study and the study topics as well as the sociodemographic survey and consent form. They were also given an opportunity to ask any initial questions. Focus groups were then organized in sequence of interest by participant type and by language. Recruitment continued until a clear pattern emerged across focus groups and we determined that we had reached data saturation (17).

In total, 22 adults with CF and 18 caregivers participated in our study. Four focus groups took place in French and eleven in English. Participants came from eight Canadian provinces (Alberta, British Columbia, Manitoba, Ontario, New Brunswick, Nova Scotia, Quebec, and Saskatchewan) with half residing in Ontario. Not all participants elected to submit demographic information, so our data is partial. But among our completed socio-demographic surveys most participants were racially White, and a broad range of income levels and educational backgrounds were represented.

Focus Groups

Between March 2019 and March 2021, we conducted fifteen focus groups with patients and caregivers. Six of these focus groups were composed of patients (including an asynchronous online forum held in March 2019) and seven were composed of caregivers of patients with CF. We held two mixed groups to accommodate participants, for example, when an adult patient and their partner wished to participate in the discussion as a couple. In part because of infection control guidelines to prevent person-to-person transmission of pathogens among people with CF (18) and in part because we were adapting to changing research conditions after the onset of COVID-19, our study used a mix of online and in-person, synchronous and asynchronous focus groups. Most focus groups (13/15) were synchronous and online.

Focus groups were led by JH, MC, and MTN, all of whom had previous experience. They began with a discussion of the project and consent form and ended with time for further questions, comments, and debriefing. SA and SF assisted as note-takers. Focus groups explored the perceptions, expectations and priorities of patients and caregivers concerning CF research. Specifically, we asked about their motivation to participate in different studies, their previous research experience, and their communication preferences around research participation. We also discussed their knowledge and perceptions regarding stem cells and genetic-based research to help individualize drug treatments and the value such research may have for patients and their families. Finally, we solicited their opinions about the risks and benefits of contributing to biobanks and the use of cells and tissues, including issues related to confidentiality.

Six adult patients participated in the asynchronous online focus group, which consisted of a seven-day text-based discussion supported by iTracks, a Canadian software company. Participants were given a series of consecutive questions they could answer at their own leisure. A moderator from our team encouraged dialogue by reacting to participant answers and posting new questions and further prompts. Asynchronous focus groups have been used in health research to reach populations with chronic health conditions as the time flexibility of asynchronous discussion can accommodate fatigue and changes in condition (19, 20). The questions used for the asynchronous discussion forum were the same as those used in the focus group script, with minor adaptations. The synchronous focus groups were semi-structured group conversations held via videoconferencing solutions. They consisted of a 1–4 participants, a moderator, and a note-taker, and lasted two hours on average. In two instances, the focus group exceptionally consisted of only one participant due to last minute withdrawal of other participants. Since the focus groups were conducted online, we found that smaller groups were more likely to encourage interactions. Synchronous focus groups were audio recorded and outsourced to a professional transcription service.

Analysis

Two members of the researcher team (JH and SA) analyzed the transcriptions of the focus groups using the qualitative content analysis software NVivo (1.5). Thematic analysis relied on an iterative process engaging themes derived from the existing scientific literature (with themes emerging from the data). First, JH and SA developed content areas that reflected the general topics discussed in the focus groups. Then, they developed themes, sub-themes, and codes from the participants' unit of meaning by coding approximately half of the focus group content. At the end of a process of reflection and discussion, agreed-upon definitions were given to each theme and sub-theme, and a codebook was created. JH then coded the second half of the focus groups. As a final step, TK and MC were able to review the coded data, themes, sub-themes, and definitions and discuss any areas of discrepancy or needed adjustments. TK then devised the conceptual model through which we present and analyze our findings. Supporting quotes were anonymized, cleaned of fillers and dysfluencies and translated to English if relevant (21). We reviewed this report in light of the consolidated criteria for reporting qualitative research (COREQ) (22).

RESULTS

Figure 1 illustrates our conceptual model. We grouped our findings into three themes that together provide a better understanding of patient and caregiver perspectives on cystic fibrosis research and personalized medicine. Our conceptual model was adapted for our research from systems and ecological models in health communication literature (23–25). Our goal was to best represent what participants, who live directly with or alongside this disease, and who contribute to research through their participation in studies, are bringing to the table in terms of their relationship to and priorities for research. In order to do so, we wanted a model that considers not only what researchers are doing and how they can improve in ethical research design and implementation, but participant agency and how research plays out practically in participant's lives, beyond the setting of the research institution. We consider all three dimensions of the conceptual model to raise important questions for researchers and policy makers to consider.

Intrapersonal and Intracommunity Knowledge

Background in Personalized Medicine

Most participants, especially within the adult patient subgroup, were relatively well informed about CFTR modulators, including their genetic aspects: *"I have been very excited to see the new developments that are happening, particularly with treating CF on a more cellular level, rather than just treating the major*

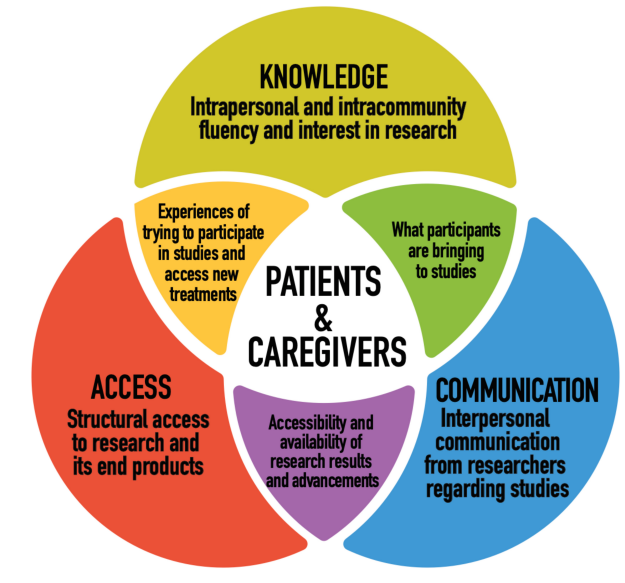

FIGURE 1 | Conceptual model: patient and caregiver perspectives on CF research and personalized medicine.

symptoms!" (P6). They viewed CFTR modulators as heralding a shift in CF care and prognosis: "*I will say that personalized medicine is not only for CF, but just in general is the way of the future. And so, I'm quite hopeful because the Trikafta announcement is the first legit game changer, but it's the first of many, right? Things will only get better*" (C13). Similarly, they anticipated new modulators will be developed that apply to more and more CFTR genotypes:

> *I've heard that there's a lot of new medications, that they're not just stopping at Trikafta and being like, "OK, well, we're done now." It's good to know that there's still ongoing research, especially because Trikafta is great for 90% or 95% of us, but there's still a significant proportion of people who are waiting for their modulator* (P11).

Participants largely felt positively about genetic tests that could assess which medication would be effective, if any - *"It would save us all so much heartache*" (C5)- and voiced hope for personalized medicine to eventually reduce the number of medications they take as well as the side effects they experience. However, opinions were more divided on whether genetic tests should preclude access to existing modulators for people who did not qualify:

> *It can be a factor in making the decision which medication to go with or which treatment. But it's still one factor, there's adherence to it, there's other lifestyle factors, there's medication interactions and then there would be other potential biological interactions that we don't know about and won't know about. So, it doesn't all come down to, it doesn't all fall on what your DNA says; that would certainly be helpful, but it's not the whole [picture]* (P18).

Throughout the focus groups there were some misconceptions and misinformation regarding stem cell research, most commonly confusing the use of pluripotent and adult stem cells in research with stem cell therapy or with the controversial use of embryonic stem cells. While responses evinced room for more patient education regarding stem cell research, ultimately most participants had a solid baseline of knowledge in personalized medicine for CF and kept track of emerging medical technologies, citing their development as a source of hope and excitement.

Interests in Cystic Fibrosis Research

Patients and their caregivers shared a familiarity with and enthusiasm for CF research. Of those who participated in our focus groups, many patients had participated in research projects throughout their lives, often via their relationships with their local CF clinics. They articulated their motivation to participate in research as a means to help medical science advance for the CF community. In other words, to help improve quality of life and prolong lifespan. As one patient expressed: *"I'm of the mindset that if there's anything I can do to help anyone in our generation or next, I'm willing to put myself out there and help out as much as possible*" (P7). A significant number of participants were also involved in CF advocacy efforts and viewed research participation as an extension of this.

Participants also largely expressed trust in the ethical conduct of medical CF research teams in Canada.

> *Whenever I've been asked to participate in research, I've always accepted, especially since the standards of medical research in Canada are very high, with the ethics committees, supervision for research work, so that, you know, I'm basically very confident about the process itself* (P21).

Trust in the reliability of research teams to act in their best interest extended to the emergence of personalized medicine. This is not to say that ethical questions and considerations were not important to participants -for example, some had mixed feelings about pharmaceutical companies: *"I feel like we are giving them a broad empty blank check*" (P15). Rather, they felt that existing research protections to be solid enough that the focus can be on moving research forward: *"To me the consequences and the end stage nature of this disease, we know where this leads, to me that overcomes any security [concerns], even potentially some minor ethical issues that maybe otherwise I would be more sensitive to"* (C17). This priority was evident in the way participants typically responded to questions about privacy and future uses: either as a non-issue or in illustrative ways that drove home their priorities to their researcher audience.

I1: *I'm going to ask you again, are there any hesitations or-*
C7: *No [laughs].*
I1: *-are you still, you know. even if it's identifiable? [. . .] to a certain extent it's still genetic information and the fact that you have a rare disease that can one day be- we can still pinpoint that that sample came from that child; any hesitations there-*
C7: *No.*
C8: *If it's not malicious. Like if it's in the name of research I'm okay with that.*
I2: *The reason we ask that is because there have been ethical debates in the scientific community about that and it's interesting to have the point of view of those most concerned.*
C7: *Yeah, I understand what you were getting at but at the end of the day if it's going to help, I don't care.*

These points are important for researchers because they show a slight disjuncture between research ethics concerns and the primary concerns of the CF community we were interviewing regarding research; we were having two slightly different conversations. As we brought forward research ethics questions, they redirected to and wanted us to understand their interest in CF research advancement as it relates to their lived experience. Within participants' accounts there was strong awareness of both CF as a chronic progressive and ultimately fatal condition and of the role research has played in improving the health and longevity of patients with CF over the past century: *"I mean the grim reality of CF is that it's a fatal disease and research is going to take that word out of our vocabulary – I mean that's the 'F-word' in our house [fatal]"* (C16). Interest in research for participants was thus inextricably entangled in the lived experience of CF, including both personal and intracommunity loss.

> *When you have a disease like CF and you see your future flashing by- you see the [. . .] other CF [patients] around, who eventually fall*

to the fight, and then you see time flashing by-, everything you're able to do yourself to try to make things better. . . You know, if they would have told me, "We're going to take your arm off, then it's going to help the research," I would have said yes (P21).

The degree to which the CF population is researched- *"they're always doing something or other"* (P11)- and their orientation toward research as a vehicle for advancements in the field of CF care has implications for ethical research design and implementation that we will return to in the discussion.

Interpersonal Communication From Researchers

Informed Consent

While the majority of patients with CF and caregivers expressed satisfaction with the way research teams handled the initial stages of their participation, a significant thread throughout the focus groups involved insufficient communication regarding informed consent. While miscommunication most often appeared to result from a combination of researcher and participant factors, in order to obtain informed consent, it is essential that participants fully understand the purpose, nature, or very fact of participation.

One example which indicated that communication was unclear or missing was that during the focus groups, several participants brought up that they had participated in clinical trials involving drugs and did not know afterward whether or not they had taken the placebo. It was not clear for them whether the topic had been covered during the consent process or if they should even have had access to this information. Another example was that some participants referenced times where they only had vague understandings of studies they were contributing to and even whether they were participating. Part of the reason some patients and caregivers had confusion or outstanding questions about their research participation relates back to the volume of studies in which they take part as well as overlap with the physical spaces of their medical care.

C8: *It kind of becomes a routine because yeah- like you see so many people during the day and then-*
C7: *Then half the time you don't even know that you're in the study.*
C8: [Laughs] *And we sign stuff-*
C7: *Yeah you sign stuff and you don't even realize that you're in the study, it's like 'okay sure I'm doing a study now.'*

In terms of participant factors, consent forms were described as long and "a lot of jargon" and this, along with participant interest in research advancement, sometimes impacted the way they interfaced with consent processes: "*It's trying to beat this thing. . . When you go to clinic they hand you a stack of paper, like the research person comes in and says, you know, "Do you consent to us keeping this for CF Canada?" "Sure, I'll sign that one*" (P13). Other participants wished for more time and space to digest information and ask questions: *"I would have asked more questions. And I couldn't because everything was done very quickly. . .I would have liked a heads-up coming into clinic that there was research going on and I would have had the time to think about questions*" (P4). It is important to note, in the context of these accounts of suboptimal consent, that patients and caregivers tended to have limits about which studies they would participate in, such as avoiding ones they considered more invasive or that were not directly tied to CF. Overall, thorough informed consent processes from researchers was viewed as symbolic to respect within the research relationship.

I participated recently in a "trial" (don't know if it qualifies as research) of a new machine to determine my PFTs. Unfortunately, this experience was unpleasant because I wasn't explained what was going on and given instructions or an idea of the tests I was doing. The person was unable to explain to me exactly what was happening, and it took several questions before understanding what was going on. This got me extremely frustrated as I was willing to help but felt mistreated and like another "data" set. This was the most recent experience I had with research; however, generally speaking, I have had good experiences with research. For me it all comes down to the information I'm getting (what are we doing, what is it for, what is expected of me and what will happen next) (P5).

Follow Up After Studies

Once the participation phase of research was over, it was rare that participants were aware of the results of the studies in which they took part: "*Do we ever receive the results of those studies? Basically never. We aren't really included in the follow-up of what the outcomes of the study were*" (C4). There seem to be two main reasons for this. First, there was a lack of follow-up review by research teams with their participants to keep them informed of the progress of the study.

P17: *I've never received any follow up that I can think of.*
P16: *I agree with that.*
P17: *You know when you check that box and you say I want to know what the results are.*
P18: *Yeah, me neither. I was just going to add that same here and we've come across studies that are, you know [that] we must have been in. So. I too wish there was a little more follow up.*

Second, participants did not have the reflex or did not know, when and how to ask for results: *"For any study I've ever been a part of, I've never, ever heard of it"* (P11).

There was a general desire on the part of patients and caregivers to have more follow-up from research teams such as a lay summary of findings or notification of associated publications: *"[...] some sort of follow-up would be nice, I guess. I like knowing things. So, even if the study didn't work out or if it found out the drug was awful or something, I would still be curious to know worst case scenarios just because I find that stuff interesting*" (P15). Many participants reported feeling a sense of pride or satisfaction knowing that their participation may have led to new discoveries. Further, patients form a community where sharing information about updates in ongoing research is important: "[. . .] *it is very much a community that deals with – has to work against the fact that it's smaller, in the grander scope of diseases or trials, as well"* (C11). Finally, the extent to which many patients with CF participate in studies can create a sense of reciprocity with research teams. Studies in which participants invest significant time and energy, in

particular, become a part of their lives, reinforcing a personal interest in the results, not necessarily to know if there was some new important discovery but mainly to have a follow up and conclusion.

I2: *Would you want to know even if they found nothing?*
C7: *Yes.*
C8: *Yeah.*
C7: *Because [this] study took a lot of time and if they found nothing, I would be mad, like that was a lot of time out of my day for a whole year.*
I2: *Because sometimes the results, you know they're, sometimes they're very small.*
C7: *That's fine. I would want to know because it was every day for a full year twice a day to do the study. That's a lot of commitment* [laughs]. *I would want to know what they found even if it's nothing. It was like "well you know there was that". Yeah I would – yeah because we never find out after, like once it's done it's like "well okay, cool"* [laughs].

Some participants allowed that if they had contacted the research team, they would have access to updates. However, they seemed to want the communication of results to be initiated by research teams.

> *I've never received anything. But, like [p10] said, maybe I never followed-up, so maybe that was on me. If I did follow-up, I would have got a response very quickly. But did it come to me without asking, no* (P9).

Patient and caregiver interest in study results tie back into their interests in research in several important ways. The considerable participation in research of many patients with CF- "*sometimes there's been a feeling that you are a research study, like your life is a research study*" (C2)- and the size of the CF community refracted onto their investment in receiving study results. It is not only about knowing results but about sharing that information among the CF community and having the research team follow up with their end of research relationship.

Access to Research and Its End Products

Geographical Inequities

Participants brought up inequities and barriers to research participation based on where they live within Canada. They noted that, in Canada, healthcare is administered on a provincial level and some jurisdictions have more resources and better infrastructure than others: *"The problem is that I have a lack of confidence because the health care system in some provinces has more money than others. So, there are some people that- seriously, I really have a lack of confidence that we're not getting the right care"* (C18). Participants stated further that the facilities with the most cutting-edge research are located in the country's largest urban centers. Those who live more rurally or remotely described relatively limited local medical services and longer wait times for advancements in healthcare as well as long commutes to the nearest CF clinic, experts and/or hospital: *"I live about 5 hours from the nearest adult CF clinic, so getting there and back every 3 months requires a chunk of time, and then if I need to be hospitalized (which is usually twice a year for 2 weeks each time), then I spend the whole time away from family and friends"* (P6). While they would make the commute to access critical medical care, it was sometimes prohibitive in terms of time, energy, and expenses to make such trips for research:

> *I have concerns sometimes in clinical trials about equality of access. I know that there's a lot of clinical trials that I would have liked to have been a part of, but that weren't available in my city, right? [They] were only through bigger centers like in Toronto or Vancouver or whatever. When I lived in [—] which is further north in Ontario, they wanted me to come down for a study in Toronto and they were like just make a trip out of it. It's like are you kidding me? That's a four-hour drive and hotels* (P16).

Some individuals did end up traveling inter-provincially to access research opportunities:

> *We travel to SickKids. They wouldn't be our closest clinic, but we travel to SickKids specifically because research opportunities are really, really important to me. Obviously, gene modulators are like the holy grail of research studies, but just in general I think with rare diseases research studies are just really important and I very much just want [my child] to have the very best opportunities* (C17).

However, even participants who were able to travel to major research centers were sometimes excluded precisely because they did not live locally: "*We weren't always included in the research because we were too far away"* (C18). Increasing access to research opportunities at the provincial level was thus a part of the advocacy work of some interviewees.

Bureaucratic Factors

Patients and caregivers also expressed frustration with several bureaucratic factors that impacted their access to the end products of research. One was the pace of research. Again, this was inseparable from the lived experience of CF: *"The only thing about research for me is I feel there is a lot of red tape, right? Things take years and years and years, and, for some of us, we don't have years and years and years"* (P9). They shared several specific criticisms regarding the research to market access pipeline in Canada. First, some felt that ethics review processes could be simplified and made more efficient: "*To me it's like, knock yourself out, my God you're going through ethics committees and all these different things and all the hoops. I wish you'd just spend the time getting the research started, or getting it done"* (P22). At the federal level, CFTR modulators, Trikafta in particular, were a sore point for many participants, compounding existing frustrations with the current system of drug approval in Canada:

> *If we're talking about Trikafta or most of the modulators, I find it extremely frustrating to see how things are moving much faster in the United States and Europe than here in terms of access. We have finally reached Health Canada, which is studying the issue, but we are far from having it in our pockets. So, it's slow. And it's hard to understand why, because we know that it's approved elsewhere, so it's not a question of its effectiveness. I don't have the impression that we are a priority for the government, and that it is making every effort to ensure that we have access to this drug, which has been shown to change lives* (P19).

Participants further brought up Canada's Special Access Program, which allows practitioners to request compassionate or emergency access to drugs not yet approved for sale for patients whose illness has become life-threatening (26). While patients or caregivers of patients who had qualified shared accounts of substantial improvement in health and quality of life, they understood their situation as exceptional. In general, stratifying access by severity was not popular among participants and some made contrasts to cancer treatment:

> *We would never say to a cancer patient, "We're going to wait until you're at stage 4 before we allow you to have the drug". . . It doesn't make sense to let our lungs get as bad as they can get, when we could be slowing down the progression of the disease and adding decades to a life. So, what are the reasonable costs for that? It doesn't make sense* (P19).

Finally, even for medications that have been approved for sale in Canada, patients and caregivers described long arduous processes advocating and sending documentation between their insurance brokers, medical centers, and drug companies in order to gain access to new treatments: *"If I wasn't vigilant about it on a daily basis, it would not have happened"* (C5). Overall, participants argued that the bench to bedside timeline for crucial and lifesaving treatments evinces problems in research translation on a systemic level:

> *There needs to be a mutually beneficial system for all involved: drug manufacturers, insurance companies and government health care systems. The current system of drug approval and price setting obviously does not work, especially for the more targeted treatments that are coming down the pipeline* (P2).

Accessibility of Information

Living with CF gives patients and their caregivers expertise in understanding their condition, but this does not necessarily translate into the same level of language that medical professionals use in reporting their findings.

> *I would love to know. . .whether there are differences that have been proven to occur depending on the mutation that one has; if other modulators in the pipeline target all types of mutations and other stuff like this. I get discouraged when confronted with medical papers on this because I do feel like I lack knowledge to fully understand, but at the same time, I feel like newspaper articles always say the same thing and don't go as far as I would like* (P5).

In order to learn more about their condition, patients and caregivers often turn to written publications or information online, most often only available in English and aimed at the scientific community: *"I find that the information that is available is very, very scientific and not made for the general population. It seems to be aimed at people who are already familiar with the subject"* (P19). The problem that emerged from the focus group participant responses was thus not so much the amount of information that exists but its accessibility. There is a double challenge for patients with CF and their families of both finding relevant information and being able to understand it.

> *I always wished there was one website that had everything all in one. That would probably be impossible but -that every single researcher worldwide just put everything onto it. It's like a data dump where you could easily access whatever you needed instead of trying to figure out just where to find anything. Because it's so impossible to find anything, I find* (C8).

Difficulty finding plain language scientific information about CF research can easily discourage patients and their families from trying to access important information: "*The motivation to search it out and then read through the scientific jargon is just really not there*" (P7). Further, the fragmentation of information through so many different sources (doctors, researchers, the internet, publications) can also lead to differences in the very nature of the information that is given. This can result in misinformation and delay or even prevent the ability of patients and their families to utilize valuable information coming down the pipeline. At the same time participants acknowledged that the specialized and diffuse nature of research presents limits on lay dissemination by researchers: "*I don't think it's purposeful to hide it. I think it's just that there's not really an accessible way for the general population to be aware of everything that's going on in research*" (C2). Notably, patient advocacy groups (such as CF Canada and groups on social media) were named as very important in regard to the dissemination of accessible and timely CF information.

Financial Inaccessibility

Financial barriers to the end products of research were the most prolific theme under access, particularly regarding CFTR modulators. Respondents described how CF brings added life expenses and limits the ability of many patients and caregivers to work. Individuals with CF are disproportionately in low-income households. They pointed out that the initial costs of these drugs are hugely inaccessible and therefore their access will be dependent on provincial coverage, or, failing that, having private insurance. One participant quipped that in order to have the kind of income necessary to afford Trikafta; *"I would have had to create Trikafta"* (P20). Another person lamented the two-tier system between: *"those who can pay for longer lives and those who cannot"* (P1). CFTR modulators run the risk of exacerbating existing systemic health disparities, not only because of their high price tag, but because they represent the closest thing to a cure:

> *The first time I felt fear about my condition was when the Kalydeco announcement came out. It's a different fear. When you know the cure is there and available, but it's not accessible to you yet. It's like I'm in the ocean, we are all together as a group, there are sharks around, and there are people getting eaten as we go along. It's not the same fear and the same frustration when it's, "Ah, the helicopter is on its way." You know, you say, "Okay, well, let's give it time to get there. That's fine. I'll wait, that's understandable." But if the helicopter is above, and it's waiting to let the rope down because people aren't sure how much it's going to cost, that's extremely frustrating. Once the helicopter is there, it could already be saving people* (P21).

For some, the participation of patients in research leading to the development of these medications compounded a further sense of injustice: *"I've heard from people who participated in the studies for Orkambi, etc., and saw an upward turn in their health, but when the study ended, they didn't qualify for continuing the*

medication after the trial. The only way they could continue this medication that had made a big difference in their health was to pay for it, and the cost was too high to absorb" (P6).

While they had serious financial access concerns about CFTR modulators, participants still wanted research to continue in this area. Most asserted that their development is invaluable: *"if we don't do research than nobody's getting on the drug, period*" (P13). They largely believed these new personalized medicines will eventually become broadly accessible, once patents expire and/or their overall cost effectiveness is demonstrated:

> *I also believe that if more drugs are discovered and are proven to work, and eventually prevent the costs of being sick - including hospital stays, transplants, other medications, etc., and if the criteria are modified to take all of this into consideration, these drugs will eventually be covered. Since I do believe that we can change things in that direction (or very strongly hope so), I think it is crucial that researchers continue to develop these drugs* (P5)

However, this did not preclude calls for systemic change in the timeline and costs of access to medication. As one caregiver put it: *"Right now, our mission is access to medication"* (C9). Participants identified the problem as being: *"a system or global discussion to solve with regards to the pharmaceutical industry*" (P16) and asserted that *"patients, as stakeholders should be a part of that solution"* (P22).

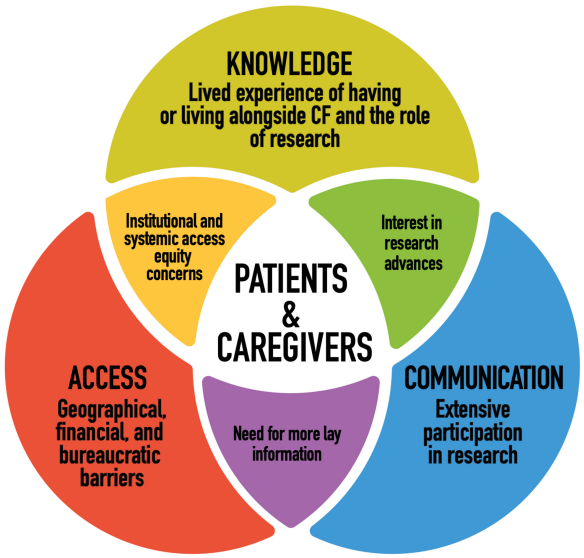

FIGURE 2 | Findings: patient and caregiver perspectives on CF research and personalized medicine.

DISCUSSION

This empirical study considered the perspectives of patients with CF and their caregivers along three dimensions in order to most fully and dynamically represent their relationship to research. Those were: knowledge (intrapersonal and intracommunity fluency and interest in research), communication (interpersonal communication from researchers regarding studies), and access (structural access to research and its end products). **Figure 2** illustrates our main findings.

Participants described a background in and relationship to CF research inextricable from the experience of CF as a lifelong progressive and terminal disease and the goal of advancing medical science. The approach of the CF community to research is thus intertwined with their "fight for life" [p. 356 (27)]. Life not merely as the prevention of death, but life as improved longevity and overall wellbeing. The various ways patients and caregivers articulated their research participation in this study were reminiscent of the findings of Christofides et al. (28) on research participation as a complex helping behavior that simultaneously encompasses prosocial motivations and "a nuanced understanding of the interconnectedness of research and treatment" [p.180 (28)]. Such an interconnected understanding was compounded by the fact that research often takes place in the same settings in which participants receive CF care, that both research participation and care are ongoing aspects of their lifelong medicalization and that progression of their medications and therapies is interwoven with research advancements (27–29). The relationship of participants to CF research thus raises several questions for ethics oversight. On the one hand, some participant accounts venture into therapeutic misconception (i.e., the tendency to misperceive research as treatment). On the other hand, the structural interrelation between research and care for participants as well as their nuanced understandings of the situation echo findings of other studies that question the practicality of binary distinctions between research and care for research ethics including the ideal of a purely altruistic neutral and autonomous research participant (28–32). Overall, the findings of this study highlight the importance of incorporating the lived experience of CF into ethical research design and implementation.

The patients and caregivers we met viewed the emergence of personalized medicine for CF as a major paradigm shift. They were enthusiastic and excited about the emergence of CFTR modulators and emphasized continued research advancement as their primary concern. Focus group discussions about research ethics considerations and personalized medicine brought up two further ethical considerations. The first relates to participants repeated expressed trust in the ethical conduct of Canadian medical researchers. This is a positive finding, especially from those participants who cited decades of research experience. Our findings are also consistent with the results of a recent qualitative research conducted with patients with CF in Europe who show a high degree of trust and a tendency to prioritize research facilitation over other considerations (33). At the same time, participant accounts and illustrative examples de-emphasizing their attention to research ethics (multiple participants only drew the line at the use of research for developing human clones, for example) conversely re-emphasizes the ethical responsibility of researchers to safeguard their rights and wellbeing. This need not be at the expense of the more expedited and accessible ethics process participants asked for but remains an issue of note. Secondly, while participants had a sufficient baseline in the operations regarding CFTR modulators and genomics, their

comments evinced a need for more patient/public education on stem cell research and its convergence with genomics, especially if induced pluripotent stem cells (iPSCs) is to be part of new tests and research (34–36).

Participants spoke to how having good communication with researchers is crucial to their relationship with research. The communication during participation in studies may have an impact on how patients feel or experience their disease later. Poor communication with researchers can lead to mistrust and influence future willingness to participate in research. The accounts of patients and caregivers in this study point to the importance of checking with the participants whether the consent form has been understood and whether all questions have been answered. This includes clearer communication regarding the nature of a given study and what will and will not be communicated about the research in which they are enrolled. Participant anecdotes further suggested that more brevity and plainer language on consent forms would be beneficial. Careful and thorough informed consent is especially important in research settings that overlap with clinical care. Participants also wanted to learn about study results (even if nothing significant or new was discovered) and they wanted this to be initiated by the study researchers. Again, this desire comes in part from a more relational understanding of research: participants volunteering their time and bodies via (often familiar) clinics and then expecting to be kept in the loop about published articles and findings. However, they felt this aspect of researcher communication was lacking. Participant requests for greater communication around results has been a theme in previous studies as well as, interestingly, incidents in which participants did not recall that results had been returned, perhaps due to their form of delivery (9, 37). Finally, while it did not come up in focus groups, it is worth noting that since the basis of studies in personalized medicine depends on the genotypic differences between patients, there is the possibility that these studies will uncover important medically actionable individual information for participants and their families. Researchers should have plans in place to deal with these results should they arise (38). Issues of the return of results and incidental findings are complex, however, as they can further blur the lines between research and clinical care.

The access barriers to research and its end products experienced by participants reaffirm those discussed in the literature and offer several concrete points of reflection for researchers (5, 39, 40). First of all, there are inequities of geographical access in Canada. Patients and caregivers asked to have the opportunity to participate in research interprovincially at Canada's major research centers. The additional time and financial burden for those living more remotely is an argument for travel vouchers or even mobile or multi-site research where possible. Considerations of geographical equity in ethical research design are further important for not compounding the effects of existing disparities in access to CF care and experts in the Canadian context (5). Many participants also argued in favor of more efficient research timelines, including ethics review processes. They believed bureaucratic red tape to be impeding the advancement of research to some degree as well as delaying or obstructing their access to new medications. Participants also had difficulty accessing and understanding much published CF information and wanted researchers to direct more information to lay audiences. Arguably, timely accessible information on CF research is important not only for patient understanding, but for the management of their health. In addition, knowing what is coming down the research pipeline allows patients to better advocate for themselves and the CF community in terms of access to new personalized medicines. The issue of the affordability of the drugs being produced by research also raises several ethical quandaries for researchers, especially given that for many in the CF population, their health condition renders them socioeconomically vulnerable (41). Similar to the lack of effective return of research results, some participants were frustrated with the idea of having helped in the creation of medicines they could not access or afford. It should be noted, however, that the patients and caregivers we spoke with wanted new drugs to continue to be developed regardless because they anticipated they would become accessible eventually. Ultimately, many of the access problems described by participants are systemic and, thus, their resolution would involve the collaboration of multiple stakeholders (policy makers; research and medical institutions; insurance and pharmaceutical companies). Patients with CF and their caregivers explicitly wanted to be part of this process.

Study Limitations

A qualitative approach for this study was chosen to privilege richness of information. Caution should be taken when extrapolating results from our limited sample: a quantitative approach would have provided greater reliability (but less depth). Similarly, as we collected limited demographic data and, in the interest of confidentiality, did not ask about personal health information, our data did not allow for internal comparative analysis according to individual participant factors such as severity or genotype. Considering that participation in the focus groups was on a self-selected basis, we cannot exclude the possibility that our study population is particularly interested in and knowledgeable about CF research. It is possible that there are greater knowledge gaps about CF and advances in care in the general CF population than our study represented. Further, as we recruited through CF Canada, our participants were, for the most part, engaged in the Canadian CF community in a way that is likely not representative of all people in Canada with CF. While participants were heterogeneous in terms of age, income and education, the relative racial homogeneity of our study population may have precluded the discussion of structural racial inequities in personalized medicine and research even as other structural issues came up (5, 42–44). Finally, as we were asking participants to summarize what was often extensive research experience in one sitting, there may have been recall biases in what was shared.

CONCLUSION

The voices of patients with CF and their caregivers are crucial not only in validating or refuting existing concerns in research

ethics but in helping to shape the conversation. The findings of this study contribute perspectives, concerns, and priorities of the CF community to the body of work on research about them. Notably also, as a historically and colloquially childhood disease, perspectives of adults living with CF remain particularly scarce (16). There are themes and considerations that emerged in this study that may be applicable to researchers who work in rare and/or progressive diseases more broadly. Of particular interest are the impacts of having a small intercommunicative community with an extensive familiarity with research, overlapping research and medical care settings, and how profoundly the experience of having or living alongside a chronic degenerative disease influenced how participants interfaced with research. Our conceptual model moored research to its implications and circulation not only within but outside the research setting for participants, providing additional layers of context for issues such as informed consent and the return of results. It also raised broader questions regarding what duty researchers have to make research and its end products accessible, not only specific studies and lay dissemination of advancements in the field, but also in terms of advocacy for equitable access to the medicines research produces. Our conceptual model could be applicable to other research ethics projects interested in engaging with research systemically.

Since our focus groups concluded in March 2021, there have been some substantial developments in Canada. In June 2021, Health Canada granted Trikafta market approval. As of November 2021, every province and territory in Canada had committed to fund Trikafta for eligible people on their public drug plans. These developments are significant gains for the CF community in Canada. The focus of CF Canada has shifted to advocating for improved access (as access qualifications and the relative accessibility of reimbursement systems vary by jurisdiction) as well as for private insurers to provide coverage (45). Issues of research ethics and research translation in personalized medicine will continue to be critical as the landscape of CF care shifts in this direction. This includes the need for the development of multi-media educational tools for patients with CF that are readily available and describe current research developments in lay terms. It will also entail new points of consideration for research and research ethics as more people with CF enter later adulthood. Ultimately, better mutual understanding among researchers, policy-makers, and the CF community is necessary to effective, accessible and relevant research advancement.

DATA AVAILABILITY STATEMENT

The transcripts of focus groups for this study will not be made publicly available. Focus group transcripts cannot be fully anonymized and participants did not provide consent for the sharing of transcripts with parties other than the researchers. The complete codebook will be available upon request. Requests to access the codebook should be directed to TK, theresa.knoppers@mcgill.ca.

ETHICS STATEMENT

This study involving human participants was reviewed and approved by the Research Ethics Board of McGill University's Faculty of Medicine (IRB Study Number A11-B57-18B). Participants provided both written and audio-recorded verbal informed consent.

AUTHOR CONTRIBUTIONS

BMK, MTN, and JH conceived, designed, and obtained the funding for this study. JH obtained ethical approval for the study. MC bottom-lined participant recruitment. JH, MC, and MTN facilitated the focus groups as moderators. JH conducted the qualitative thematic analysis, which was validated by TK and MC. TK created the conceptual model and drafted the manuscript. JH and MC also contributed to writing specific sections of the manuscript. All authors participated in revisions and have read and approved the final draft.

FUNDING

This research was funded by the Government of Canada through Genome Canada, Genome Quebec, and the Ontario Genomics Institute (OGI-148).

ACKNOWLEDGMENTS

We would like to thank all our participants for contributing their time, perspectives, and insights to this project. We also would like to thank three of the CGP's research assistants: Anthea Harvey–Cheetham for helping with participant recruitment, Sina Faraji for helping with focus groups, and Samuel Alarie for helping with focus groups and qualitative analysis.

REFERENCES

1. Ratjen F, Bell SC, Rowe SM, Goss CH, Quittner AL, Bush A. Cystic fibrosis. *Nat Rev Dis Primers.* (2015) 1:15010. doi: 10.1038/nrdp.2015.10
2. Cystic Fibrosis Canada. *The Canadian Cystic Fibrosis Registry 2019 Annual Data Report*. (2020). Available online at: https://www.cysticfibrosis.ca/registry/2019AnnualDataReport.pdf (accessed November 30, 2021).
3. Lopes-Pacheco M. CFTR modulators: the changing face of cystic fibrosis in the era of precision medicine. *Front Pharmacol.* (2020) 10:1662. doi: 10.3389/fphar.2019.01662
4. Bell SC, Mall MA, Gutierrez H, Macek M, Madge S, Davies JC, et al. Future of cystic fibrosis care: a global perspective. *Lancet Respir Med.* (2020) 8:65–124. doi: 10.1016/S2213-2600(19)30337-6
5. Shemie G, Nguyen MT, Wallenburg J, Ratjen F, Knoppers BM. The Equitable implementation of cystic fibrosis personalized medicines in Canada. *J Pers Med.* (2021) 11:382–94. doi: 10.3390/jpm11050382
6. Joshi D, Ehrhardt A, Hong JS, Sorscher EJ. Cystic fibrosis precision therapeutics: emerging considerations. *Pediatr Pulmonol.* (2019) 54:S13–7. doi: 10.1002/ppul.24547

7. Saiman L. Improving outcomes of infections in cystic fibrosis in the era of CFTR modulator therapy. *Pediatr Pulmonol.* (2019) 54:S18–26. doi: 10.1002/ppul.24522
8. Cirilli N, Buzzetti R, Costa S, Magazzu G. 282 patient priorities for research in cystic fibrosis: the IPaCOR experience. *J Cyst Fibros.* (2014) 13:S120. doi: 10.1016/S1569-1993(14)60417-3
9. Christofides E, Stroud K, Tullis DE, O'Doherty KC. Improving dissemination of study results: perspectives of individuals with cystic fibrosis. *Res Ethics.* (2019) 15:1–14. doi: 10.1177/1747016119869847
10. Rowbotham NJ, Smith S, Leighton PA, Rayner OC, Gathercole K, Elliott ZC, et al. The top 10 research priorities in cystic fibrosis developed by a partnership between people with cf and healthcare providers. *Thorax* (2018) 73:388–90. doi: 10.1136/thoraxjnl-2017-210473
11. Budin-Ljøsne I, Harris JR. Patient and interest organizations' views on personalized medicine: a qualitative study. *BMC Med Ethics.* (2016) 17:28. doi: 10.1186/s12910-016-0111-7
12. American Society of Human Genetics (ASHG). *Public Attitudes Toward Genetics & Genomics Research: Literature and Polling Review Report*. (2020). Available online at: https://www.ashg.org/wp-content/uploads/2020/01/2020-Public-Views-Genetics-Literature-Review.pdf (accessed November 30, 2021).
13. Jones AM, Favaro A, St Philip E. *This Drug Can Treat 90 Percent of Cystic Fibrosis Patients, But It's Not Available in Canada. CTV News*. (2020). Available online at: https://www.ctvnews.ca/health/this-drug-can-treat-90-per-cent-of-cystic-fibrosis-patients-but-it-s-not-available-in-canada-1.4991938 (accessed November 30, 2021).
14. Lensch MW. Public perception of stem cell and genomics research. *Genome Med.* (2011) 3:44. doi: 10.1186/gm260
15. Marcon AR, Murdoch B, Caulfield T. Fake news portrayals of stem cells and stem cell research. *Regen Med.* (2017) 12:765–75. doi: 10.2217/rme-2017-0060
16. Varilek BM, Isaacson MJ. The dance of cystic fibrosis: experiences of living with cystic fibrosis as an adult. *J Clin Nurs.* (2020) 29:3553–64. doi: 10.1111/jocn.15397
17. Krueger RA, Casey MA. *Focus Groups: A Practical Guide for Applied Research*. Thousand Oaks, CA: Sage (2000). p. 215.
18. Saiman L, Siegel JD, LiPuma JJ, Brown BF, Bryson EA, Chambers MJ, et al. Infection prevention and control guidelines for cystic fibrosis: 2013 update. *Infect Control Hosp Epidemiol.* (2014) 35:S1–67. doi: 10.1086/676882
19. Cook K, Jack S, Siden H, Thabane L, Browne G. Innovations in research with medically fragile populations: using bulletin board focus groups. *Qual Rep.* (2014) 19:1–12. doi: 10.46743/2160-3715/2014.1000
20. Williams S, Clausen MG, Robertson A, Peacock S, McPherson K. Methodological reflections on the use of asynchronous online focus groups in health research. *Int J Qual Methods.* (2012) 11:368–83. doi: 10.1177/160940691201100405
21. Riessman CK. *Narrative Methods for the Human Sciences*. Thousand Oaks, CA: Sage (2008). p. 251.
22. Tong A, Sainsbury P, Craig J. Consolidated criteria for reporting qualitative research (COREQ): a 32-item checklist for interviews and focus groups. *Int J Quality Health Care.* (2007) 19:349–57. doi: 10.1093/intqhc/mzm042
23. Brofenbrenner U. Toward an experimental ecology of human development. *Am Psychol.* (1977) 32:513–31. doi: 10.1037/0003-066X.32.7.513
24. McLeroy KR, Bibeau D, Steckler A, Glanz K. An ecological perspective on health promotion programs. *Health Educ Q.* (1988) 15:351–77. doi: 10.1177/109019818801500401
25. Sallis JF, Owen N, Fisher EB. Ecological models of health behavior. In: Glanz K, Rimer BL, Viswanath K editors. *Health Behavior and Health Education: Theory, Research, and Practice*. San Francisco, CA: Jossey-Bass (2008). p. 465–86.
26. Government of Canada. *Special Access Program*. (2021). Available online at: https://www.canada.ca/en/health-canada/services/drugs-health-products/special-access/drugs/special-access-programme-drugs.html (accessed November 30, 2021).
27. Jessup M, Parkinson C. "All at sea": the experience of living with cystic fibrosis. *Qual Health Res.* (2010) 20:352–64. doi: 10.1177/1049732309354277
28. Christofides E, Stroud K, Tullis DE, O'Doherty KC. The meanings of helping: an analysis of cystic fibrosis patients' reasons for participating in biomedical research. *J Empir Res Hum Res Ethics.* (2017) 12:180–90. doi: 10.1177/1556264617713098
29. Dobson JA, Christofides E, Solomon M, Waters V, O'Doherty KC. How do young people with cystic fibrosis conceptualize the distinction between research and treatment? A qualitative interview study. *AJOB Empir Bioeth.* (2015) 6:1–11. doi: 10.1080/23294515.2014.997898
30. Hallowell N, Cooke S, Crawford G, Lucassen A, Parker M, Snowdon C. An investigation of patients' motivations for their participation in genetics-related research. *J Med Ethics.* (2010) 36:37–45. doi: 10.1136/jme.2009.029264
31. Kass NE, Faden RR, Goodman SN, Pronovost P, Tunis S, Beauchamp TL. The research treatment distinction: a problematic approach for determining which activities should have ethical oversight. *Hastings Cent Rep.* (2013) 43:S4–15. doi: 10.1002/hast.133
32. Olsen L, DePalma L, Evans JH. Self-interested and altruistic motivations in volunteering for clinical trials: a more complex relationship. *J Empir Res Hum Res Ethics.* (2020) 15:443–51. doi: 10.1177/1556264620914463
33. Lensink MA, Boers SN, Gulmans VA, Jongsma KR, Bredenoord AL. Mini-gut feelings: perspectives of people with cystic fibrosis on the ethics and governance of organoid biobanking. *Per Med.* (2021) 18:241–54. doi: 10.2217/pme-2020-0161
34. Ahmadi S, Bozoky Z, Di Paola M, Xia S, Li C, Wong AP, et al. Phenotypic profiling of CFTR modulators in patient-derived respiratory epithelia. *NPJ Genom Med.* (2017) 2:1–10. doi: 10.1038/s41525-017-0015-6
35. Chen KG, Zhong P, Zheng W, Beekman JM. Pharmacological analysis of CFTR variants of cystic fibrosis using stem cell-derived organoids. *Drug Discov Today.* (2019) 24:2126–38. doi: 10.1016/j.drudis.2019.05.029
36. Eckford PD, McCormack J, Munsie L, He G, Stanojevic S, Pereira SL, et al. The cf canada-sick kids program in individual cf therapy: a resource for the advancement of personalized medicine in CF. *J Cyst Fibros.* (2019) 18:35–43. doi: 10.1016/j.jcf.2018.03.013
37. Richter G, Krawczak M, Lieb W, Wolff L, Schreiber S, Buyx A. Broad consent for health care–embedded biobanking: understanding and reasons to donate in a large patient sample. *Genet Med.* (2018) 20:76–82. doi: 10.1038/gim.2017.82
38. Thorogood A, Dalpé G, Knoppers BM. Return of individual genomic research results: are laws and policies keeping step? *Eur J Hum Genet.* (2019) 27:535–46. doi: 10.1038/s41431-018-0311-3
39. Balfour-Lynn IM. Personalized medicine in cystic fibrosis is unaffordable. *Paediatr Respir Rev.* (2014) 15:2–5. doi: 10.1016/j.prrv.2014.04.003
40. Oates GR, Schechter MS. Socioeconomic status and health outcomes: cystic fibrosis as a model. *Expert Rev Respir Med.* (2016) 10:967–77. doi: 10.1080/17476348.2016.1196140
41. McGarry ME, Williams IIWA, McColley SA. The demographics of adverse outcomes in cystic fibrosis. *Pediatr Pulmonol.* (2019) 54:S74–83. doi: 10.1002/ppul.24434
42. Geneviève LD, Martani A, Shaw D, Elger BS, Wangmo T. Structural racism in precision medicine: leaving no one behind. *BMC Med Ethics.* (2020) 21:17. doi: 10.1186/s12910-020-0457-8
43. McGarry ME, McColley SA. Cystic fibrosis patients of minority race and ethnicity less likely eligible for CFTR modulators based on CFTR genotype. *Pediatr Pulmonol.* (2021) 56:1496–503. doi: 10.1002/ppul.25285
44. Popejoy AB, Fullerton SM. Genomics is failing on diversity. *Nature.* (2016) 538:161–4. doi: 10.1038/538161a
45. Cystic Fibrosis Canada. *News*. (2022). Available online at: https://www.cysticfibrosis.ca/news (accessed February 9, 2022).

Conflict of Interest: The authors declare that the research was conducted in the absence of any commercial or financial relationships that could be construed as a potential conflict of interest.

frontiers | Frontiers in Medicine

ORIGINAL RESEARCH
published: 01 April 2022
doi: 10.3389/fmed.2022.842991

Diagnosis of Myalgic Encephalomyelitis/Chronic Fatigue Syndrome With Partial Least Squares Discriminant Analysis: Relevance of Blood Extracellular Vesicles

*Alba González-Cebrián[1], Eloy Almenar-Pérez[2,3], Jiabao Xu[4], Tong Yu[4], Wei E. Huang[4], Karen Giménez-Orenga[5], Sarah Hutchinson[3], Tiffany Lodge[3], Lubov Nathanson[6,7], Karl J. Morten[3], Alberto Ferrer[1] and Elisa Oltra[2,8]**

[1] Grupo de Ingeniería Estadística Multivariante, Departamento de Estadística e Investigación Operativa Aplicadas y Calidad, Universitat Politècnica de València, Valencia, Spain, [2] Department of Pathology, School of Health Sciences, Universidad Católica de Valencia San Vicente Mártir, Valencia, Spain, [3] Nuffield Department of Women's and Reproductive Health, The Women Centre, University of Oxford, Oxford, United Kingdom, [4] Department of Engineering Science, University of Oxford, Oxford, United Kingdom, [5] Escuela de Doctorado, Universidad Católica de Valencia San Vicente Mártir, Valencia, Spain, [6] Kiran C. Patel College of Osteopathic Medicine, Nova Southeastern University, Fort Lauderdale, FL, United States, [7] Institute for Neuro Immune Medicine, Nova Southeastern University, Fort Lauderdale, FL, United States, [8] Centro de Investigación Traslacional San Alberto Magno, Universidad Católica de Valencia San Vicente Mártir, Valencia, Spain

OPEN ACCESS

Edited by:
Anna Picca,
Catholic University of the Sacred Heart, Italy

Reviewed by:
Brett Lidbury,
Australian National University, Australia
Ludovic Giloteaux,
Cornell University, United States

***Correspondence:**
Elisa Oltra
elisa.oltra@ucv.es
orcid.org/0000-0003-0598-2907

Specialty section:
This article was submitted to Translational Medicine, a section of the journal Frontiers in Medicine

Received: 24 December 2021
Accepted: 21 February 2022
Published: 01 April 2022

Citation:
González-Cebrián A, Almenar-Pérez E, Xu J, Yu T, Huang WE, Giménez-Orenga K, Hutchinson S, Lodge T, Nathanson L, Morten KJ, Ferrer A and Oltra E (2022) Diagnosis of Myalgic Encephalomyelitis/Chronic Fatigue Syndrome With Partial Least Squares Discriminant Analysis: Relevance of Blood Extracellular Vesicles. Front. Med. 9:842991. doi: 10.3389/fmed.2022.842991

Myalgic Encephalomyelitis/Chronic Fatigue Syndrome (ME/CFS), a chronic disease characterized by long-lasting persistent debilitating widespread fatigue and post-exertional malaise, remains diagnosed by clinical criteria. Our group and others have identified differentially expressed miRNA profiles in the blood of patients. However, their diagnostic power individually or in combinations seems limited. A Partial Least Squares-Discriminant Analysis (PLS-DA) model initially based on 817 variables: two demographic, 34 blood analytic, 136 PBMC miRNAs, 639 Extracellular Vesicle (EV) miRNAs, and six EV features, selected an optimal number of five components, and a subset of 32 regressors showing statistically significant discriminant power. The presence of four EV-features (size and *z*-values of EVs prepared with or without proteinase K treatment) among the 32 regressors, suggested that blood vesicles carry relevant disease information. To further explore the features of ME/CFS EVs, we subjected them to Raman micro-spectroscopic analysis, identifying carotenoid peaks as ME/CFS fingerprints, possibly due to erythrocyte deficiencies. Although PLS-DA analysis showed limited capacity of Raman fingerprints for diagnosis (AUC = 0.7067), Raman data served to refine the number of PBMC miRNAs from our previous model still ensuring a perfect classification of subjects (AUC=1). Further investigations to evaluate model performance in extended cohorts of patients, to identify the precise ME/CFS EV components detected by Raman and to reveal their functional significance in the disease are warranted.

Keywords: myalgic encephalomyelitis/chronic fatigue syndrome (ME/CFS), extracellular vesicles (EVs), partial least squares-differential analysis (PLS-DA), Raman spectroscopy, microRNAs, carotenoids, biomarker

INTRODUCTION

Myalgic Encephalomyelitis/Chronic Fatigue Syndrome (ME/CFS) is a highly debilitating disease characterized by unexplained profound fatigue lasting over 6-months (ICD-10 code R53.82 or G93.3 if post-viral) (1), which is exacerbated by physical, mental, or emotional activity, a process known as post-exertional malaise (PEM); lack of restoring sleep, dysautonomia, and frequent additional comorbidities (2). Despite recent intense biomarker research, its diagnosis relies on clinical symptom assessment, after excluding potential underlying health problems that could relate to patient symptoms (3–5).

Historically, pathway biomarkers that have been interrogated in ME/CFS include cytokine profiles, immune cell subpopulations and metabolites, as reviewed by Maes et al. (6). The recognized value of microRNAs as liquid biopsy biomarkers of complex disease (7, 8) led to genome-wide screenings of miRNA profiles in ME/CFS blood fractions by ours and other research groups (9–12). These encouraging findings, however, have so far failed to provide a specific biomarker signature of the disease (6). Extracellular vesicles (EVs) released by most cell types in the organism can be collected from blood potentially reporting information of the entire organism physiology. This was the reason for our previous study to evaluate ME/CFS EVs and their miRNA contents. Although altered levels of overlapping markers were found for some miRNAs from PBMCs and EVs (12), no miRNA has been widely validated as a biomarker of ME/CFS, and all identified so far appear to have limited diagnostic value, individually or when combined.

Rudimentary statistical methods such as two sample tests (i.e., *t*-test or Wilcoxon-Mann Whitney test), followed by multiple comparison corrections [i.e., Bonferroni or False Discovery Rate (13)] for the analysis of "omic" data have several drawbacks. These include low statistical power, lack of interpretability of results, and the omission of complex relationships among variables which could, in principle, be addressed using other statistical approaches such as linear or generalized linear models. However, these methods suffer from other problems when dealing with "omic" data, such as large number of variables and low sample size, which produces overfitting, and the high correlation among variables, which produces multi-collinearity. Those limitations have motivated the development of numerous novel statistical techniques (14).

Prediction methods such as Partial Least Squares (PLS) (15) is one of these novel techniques especially suitable for the analysis of "omic" data due to its ability to deal with more variables than observations, and its good model interpretation capacity (16). Conceived as an alternative to classical regression, PLS, is a statistical multivariate technique that models the latent space of predictors and responses (X and Y subspaces, respectively) finding the subspace which maximizes the covariance between both latent subspaces. PLS-DA (Discriminant Analysis) is a variant of PLS for binary responses (17). The work we are presenting here used PLS-DA approaches to classify individuals in the healthy control (HC) or the case group, but also to determine which variables hold best discriminant power between these two classes of participants.

The study includes three PLS-DA models. The first was applied to over 800 variables obtained from 15 severe ME/CFS female cases and 15 matched HCs from the UK ME/CFS Biobank (UKMEB). Data included subject phenotyping with validated instruments, complete blood analytics, miRNA profiles from peripheral blood mononuclear cells (PBMCs) and from plasma-isolated extracellular vesicles (EVs), plus EV associated features, as previously described (9). The results showed that a combination of 32 variables, including several EV features, best discriminates severe ME/CFS cases from healthy subjects. The value of EV features for the assessment of ME/CFS was further supported by Raman spectroscopic data.

The second PLS-DA model focused on detecting discriminant regions of the Raman spectra. These results were compared with classification based on Raman spectra using three other binary classification techniques: an adaptation of linear discriminant analysis (LDA) (18) to deal with more variables than observations, random forest (RF) (19) and support vector machines (SVM) (20).

Finally, the relevant regions of the discriminatory spectra were included in a third PLS-DA model with the previously mentioned set of 32 variables. Using this approach, ME/CFS EV differences detected by Raman helped to further refine our previous ME/CFS PLS-DA model reducing the number of required miRNAs from PBMCs and further supporting the EV potential biomarker value for the diagnosis of ME/CFS.

To the best of our knowledge, this study is the first to provide a PLS-DA model for the accurate diagnosis of severe ME/CFS based on a discreet combination of variables. In addition, we used for the first time Raman fingerprints of EVs to enhance the ability to discriminate severely affected ME/CFS patients from healthy subjects.

MATERIALS AND METHODS

Samples and Associated Clinical Data

Ethical approval of the study was granted by the Public Health Research Ethics Committee DGSP-CSISP, Valencia (Spain), study number UCV_201701 and by the UCL Biobank Ethical Review Committee-Royal Free London NHS Foundation Trust (B-ERC-RF), study number EC2017.01 before the samples were released by the UKMEB.

Data for the initial PLS-DA analysis corresponded to Nanostring datasets generated during a previous study of our group (12), available from the NCBI Gene Expression Omnibus (GEO) database (Accession Number GSE141770) and the (supplementary material) of the cited article. The samples for the Raman analysis consisted of EV aliquots from the cited study isolated from 0.5 ml of platelet poor plasma from 15 severely ill ME/CFS females and 15 age-population matched healthy females, obtained from dipotassium EDTA blood-collection tubes by UKMEB professionals.

As previously described, patient recruitment and clinical assessment for the UKMEB was mainly performed through the

UK National Health Service (NHS) primary and secondary health care services (9). Compliance with the Canadian Consensus (4), CDC-1994 ("Fukuda") (3) and Institute of Medicine (21) criteria were ensured for patient recruitment (22, 23). Clinical diagnosis was complemented with score differences in the SF-36 questionnaire (24) and the GHQ (General health Questionnaire) (25), the last also assessed by a Likert scale (9, 26).

Participants exclusion criteria were as follows: (i) take antiviral medication or drugs known to alter immune function in the preceding 3 months (ii) had any vaccinations in the preceding 3 months; (iii) had a history of acute and chronic infectious diseases such as hepatitis B and C, tuberculosis, HIV (but not herpes virus or other retrovirus infection); (iv) another chronic disease such as cancer, coronary heart disease, or uncontrolled diabetes; (v) a severe mood disorder; (vi) been pregnant or breastfeeding in the preceding 12 months; or (vii) were morbidly obese (BMI $\geq$ 40).

All methods were performed in accordance with relevant guidelines and regulations. All subjects signed an informed consent before samples could be included in the corresponding sample collection.

Partial Least Squares-Discriminant Analysis (PLS-DA)

In this work we used three PLS-DA models: a first multi-block (27) PLS-DA model (Section PLS-DA Model to Classify ME/CFS Identifies EV Features as Potential Disease Biomarkers), a Raman-based PLS-DA model (Section ME/CFS Classification Model Based on Raman Spectral Fingerprints) and a second multi-block PLS-DA model (Section Refinement of the Initial PLS-DA Model With EV Raman Profiles). It is important to mention that different schemes of calibration and validation were used.

The multi-block PLS-DA models had two goals: to obtain an accurate classifier usable with new individuals and to interpret the set of discriminant features. Given the small sample size of the database, we followed a two-steps procedure. First, we used all observations (i.e., participants) to fit a PLS-DA model obtaining a set of statistically significant discriminant predictors. This way, most observations could be used to fit the PLS-DA model, reducing the uncertainty in the estimation of the parameters of the model, which is a critical aspect for the interpretation goal. Secondly, the dataset was split into calibration and validation subsets. The PLS-DA model was fitted using the relevant predictors of observations from the calibration subset and the model was then used to predict new observations from the validation set. Eight randomly selected individuals were included in the validation subset (four ME/CFS cases and four HCs). For preprocessing, a multi-block approach with block scaling and variable autoscaling was applied. Each block contained a different group of variables with similar features. Five blocks were established: (i) Demographic Variables, (ii) Analytic Variables, (iii) PBMCs' miRNA expression levels, (iv) EVs' miRNA expression levels, and (v) EVs' characteristics (9). The second multi-block PLS-DA model included an additional block with relevant Raman profile features.

For the Raman spectra PLS-DA model, the goal was to determine if an accurate diagnostic tool could be developed solely based on Raman spectra differences. It was crucial to compare all classifiers not only in terms of classification performance, but also in terms of model stability. For this reason, the chosen setup consisted of a three-fold cross-validation scheme. Each fold contained 1/3 of the data, i.e., each fold contained a set of 10 observations (five of each class). In each round, two-folds were used to fit the model and the other fold was used as an external validation set. This way, all observations were used to fit and validate the model, studying the stability on its performance. In this model, the preprocessing consisted of variable centering.

The performance of PLS-DA models was evaluated by the R^2 coefficient (goodness of fit) and the Q^2 coefficient (goodness of prediction). Permutation tests were used to assess the statistical significance of the model using the SIMCA software. A permutation test (28) consists in randomly permuting the values of the response, yielding a randomized data structure. Afterwards, a new PLS-DA model is fitted using the randomized response, obtaining its corresponding R^2 and Q^2 coefficients. The values for the R^2 (and Q^2) coefficients obtained in a series of different permutation testing yields the null distribution of the R^2 (and Q^2) coefficients under the assumption of no discrimination between both classes. Thus, this permutation framework also offers the possibility of calculating p-values associated with testing the hypothesis of model discrimination. Additionally, to evaluate the classification performance of the model, the Receiver Operating Characteristic (ROC) curve was obtained. For each ROC curve, the AUC (Area Under the Curve) was calculated (29).

Beyond its performance, one of the advantages of PLS-DA models is their interpretability. The PLS (b) coefficients coefficients represent the direct relationship between the original predictors' subspace (X) and the response categories (Y). The higher a b coefficient of a variable is (in absolute value), the more discriminant that predictor will be. The sign of the coefficient indicates the type of the relationship between the variable and the class to be predicted (negative or positive relationship). For the parameters and outcomes of the PLS-DA model, statistical significance was assessed by jackknife intervals at a 95% confidence level. These intervals are calculated in a cross-validation scheme implemented by the Aspen ProMV© software used to obtain the PLS-DA model.

Once a PLS-DA model is fitted, it is quite common to follow an iterative depuration procedure variable-wise and observation-wise. On one hand, it is frequent to find that some predictors are not relevant. This can occur when the confidence interval of a b coefficient contains a zero value. In this case, it is possible to perform an initial variable selection, retaining only the relevant predictors to refit the PLS-DA model. For this variable selection the b coefficients and the Variable Importance for the Projection (*VIP*) coefficients, are used. *VIP* coefficients (30) represent the influence of each predictor, accounting its weight in each of the latent variables and the percentage of variability of the Y matrix explained by each latent variable. The threshold value of $\geq$1 for the *VIP* coefficients is a common threshold to identify variables which are potentially important in the model. Thus, predictors having a *VIP* with a confidence interval clearly under the 1 value

and *b* coefficients not statistically significant were removed from the modeling.

In this work, the iterative depuration of predictors also helped to reduce uncertainty of the model estimates by decreasing the number of parameters of the model.

On the other hand, it is also common to perform an iterative model fitting until a PLS-DA model without outliers and relying only in relevant predictors, is obtained. Outliers were studied in terms of the Squared Prediction Error (SPE) and Hotelling's T^2 (31) metrics.

Finally, to confirm and visualize the discriminant properties of the selected variables (i.e., those showing statistical significance in the PLS-DA) a two sample t- test was applied a posteriori to each potential biomarker included in the final multi-block PLS-DA model. These results can be found in the **Supplementary Material**.

Isolation of EVs From Plasma

EVs studied corresponded to aliquots isolated from 0.5 ml aliquots of human plasma supernatants from blood collected in dipotassium EDTA tubes (Becton Dickinson, Franklin Lakes, NJ, USA) (undergoing a single freeze/thaw cycle), upon being centrifuged at 10,000 × g for 10 min, with Total Exosome Isolation Reagent (TEIR) (Invitrogen by Life Technologies, Cat. 4484450), following manufacturer's recommendations, as previously described (12). The isolated EVs were characterized following MISEV (Minimal information for studies of extracellular vesicles) recommendations (32), as described in Almenar-Pérez et al. (12).

Raman Spectroscopy

After dilution of the isolated EVs to a concentration of 5×10^8 EVs/ml in distilled water, 1.5 μL of the suspension was deposited on aluminum Raman slides and exposed to room temperature until the sample was completely dry. Spectra were acquired using an HR Evolution confocal Raman microscope (Horiba Jobin-Yvon, UK, Ltd.) equipped with a 532 nm laser. Laser power was 4.5 mW and a filter of 25%. The acquisition time per spectrum was 3 s at a resolution of 4 μm.

For the analysis of the Raman spectra, all spectra were preprocessed by cosmic ray correction, polyline baseline correction, and area normalization using the entire spectral region, using LabSpec 6 (Horiba Scientific, France). Data analysis, statistics and visualization were carried out using in-house scripts in *R*. Quantification of important biomolecules was performed by integrating the corresponding Raman bands. The quantification results were represented as box plots and sample means of the patients were compared with HCs by using Welch's two sample *t*-test for unequal variance.

Four classification models were trained with a three-fold cross validation setup to classify a spectrum as either severe ME/CFS or HC using an adaptation of linear discriminant analysis (LDA) (18) to deal with more variables than observations, random forest (RF) (19), a support vector machine (SVM) (20), and PLS-DA. For the LDA, RF, and SVM models, the classifier learning app in MATLAB was used, enabling the optimization of model hyperparameters. The AUC was calculated for each model, enabling the comparison of their classification performance.

Pathway and Gene Enrichment Analysis

Analysis of predicted and validated miRNA-mRNA interactions was performed with the freely available software MiRTargetLink 2.0 (https://www.ccb.uni-saarland.de/mirtargetlink2) (33). Gene ontology (GO) enrichment analysis was performed using the miEAA tool incorporated into MiRTargetLink 2.0, targets were retrieved, sorted by adjusted *p*-value, and presented in table format. Selected networks of mRNAs targeted by at least two miRNAs were drawn using Adobe Illustrator software.

RESULTS

As described in a previous study (12), study participants were women with an average age of 46.8 (age range 38–53) for the disease cohort and 45.2 (age range 18–52) years for the matched HC group. Median ages were 48 years and 47 for the ME/CFS and HC group, respectively. Average time from disease onset was 17.5 (range 1.5–30.9) years, with a median value of 18.4 years. Health survey SF-36 and General Health Questionnaire (GHQ) scores, including Likert scale for the GHQ, scores clearly separated ME/CFS and HC groups ($p < 0.05$). Score details can be consulted in the referred work by Almenar-Pérez et al.

PLS-DA Model to Classify ME/CFS Identifies EV Features as Potential Disease Biomarkers

Given the small sample size of the cohort, this first PLS-DA modeling step focused on finding the most statistically significant biomarkers for identifying the severe ME/CFS subjects. All observations (i.e., participants) were used to fit the model in an attempt to reduce as much as possible the uncertainty in the estimation of the model parameters.

ME/CFS Modeling With PLS-DA

ME/CFS PLSA-DA was performed on a collection of data obtained from 30 participants (15 severe ME/CFS females and 15 healthy subjects matched by sex and age (±5 y) of the UKMEB, as previously reported by our group (12) [Nanostring datasets available from the NCBI Gene Expression Omnibus (GEO) database, Accession Number GSE141770]. The complete set of data included 34 blood analyte variables, 775 miRNAs expressed above threshold levels (136 in PBMCs and 639 in EVs), EV concentration, size and *z*-potential of vesicles prepared with and without proteinase K treatments for a total of six EV-associated measures, together with two demographic variables. The 15 variables obtained from the SF-36 questionnaire (24) and the GHQ questionnaire (25), the last also assessed by a Likert scale (26) were not included since a diagnostic based solely on objective measurements was pursued.

The initial model was fitted with three latent variables (obtained by cross-validation) with a cumulative value of 96% for the R^2 coefficient (goodness of fit) and 68% for the Q^2 coefficient (goodness of prediction). After obtaining the PLS-DA model, we checked for potential outliers, removing subjects

with an SPE (i.e., Euclidean distance to the model) overpassing the control limit (an example of outlier can be seen in **Supplementary Figure 1**).

The initial PLS-DA model presented a large number of predictors having a *VIP* with a confidence interval clearly below 1 and non- statistically significant b coefficients (**Supplementary Figure 2**). Thus, after performing an iterative variable selection, as described in Section Materials and Methods, the final model with the most discriminant variables was obtained.

This depurated PLS-DA model with 32 variables (**Figures 1A,B**) had similar cumulative R^2 and Q^2 values (98.71 and 96.31%, respectively), and the optimal number of components based on cross-validation was three (as the initial model). This model was based on a set of N=24 observations, having 12 of each class.

The permutation test illustrated in **Supplementary Figure 3** shows that the R^2 and Q^2 values of the obtained PLS-DA model (points belonging to the 100% correlation between original y and permuted y) are greater than any of those belonging to the permuted datasets. Thus, the statistical significance of the 98.71 and 96.31% values for the R^2 and Q^2, respectively, is accepted, rejecting the hypothesis of having obtained these values by chance (with $p < 0.05$).

Furthermore, the stability and reliability of the final PLS-DA model in terms of its prediction performance can be visualized both in the scores scatterplot (**Figure 1C**) and in the observed vs. prediction plot (**Figure 1E**).

The score scatterplot (**Figure 1C**), showing a clear separation between groups, is directly related with the weighting plot (**Figure 1D**), which shows the correlation structure between the original and the latent variables. Thus, the probability of being a severe ME/CFS individual (orange triangle in the score scatterplot) is positively correlated with the variables at the same side (left) of the weighting plot, which are the same variables with a positive *b* coefficient for the ME/CFS class. This means that those variables tend to have greater values in ME/CFS than in HCs. Analogously, the set of variables placed at the opposite semi plane (right part) of the weighting plot (with negative *b* coefficients for the ME/CFS class), are negatively correlated to the probability of belonging to the ME/CFS class. This means that these variables tend to have lower values in ME/CFS than in HCs. Finally, variables near to the origin (0,0) point are those with coefficients not statistically different from zero (i.e., no statistical differences in both groups of participants).

Finally, the observed vs. prediction results for the participants showed a class prediction with 95% confidence intervals (magenta lines) using just three components, allowing all 12 patient observations to be correctly classified in the ME/CFS group and all 12 observations from healthy subjects in the HC group (**Figure 1E**). The ROC curve of the model shows a perfect classification of the samples (**Figure 1F**), since the AUC for both classes reach a value of 1. This means that the model has a perfect sensitivity and specificity (both equal to 1), i.e., it detects all patients and differentiates all controls as healthy individuals.

Classification Performance of the PLS-DA Model With Calibration and Validation Set

The second modeling approach focused on evaluating the potential of our PLS-DA model as a tool to correctly assign new observations into ME/CFS and HC groups. For this second PLS-DA model, the database was partitioned in a training and validation subsets, as explained in the Section Materials and Methods.

The trained model with three components (the same number as the previous model with all the observations) reaches cumulative values of 99.32% for the goodness of fitting coefficient (R^2) and 88.52% for the goodness of prediction coefficient (Q^2).

The *b* coefficients obtained are almost of the same order, according to their importance, but with wider confidence intervals (**Figures 2A,B**). This is caused by the removal of the validation samples from the training set, decreasing the sample size and leading to an increase in model uncertainty. Once the model is fitted, the observations of the validation set are projected onto the latent subspace, obtaining their correspondent scores and predictions (**Figures 2C,D**). These results support the validity of the model developed in the Section ME/CFS Modeling With PLS-DA for the diagnosis of severe ME/CFS patients. The ROC curve for the validation samples (**Figure 2E**) shows a perfect discrimination (AUC=1) when the PLS-DA model is used to classify new individuals as healthy or those affected by severe ME/CFS. This means that the model maintains the perfect detection of ME/CFS patients (perfect sensitivity) while keeping the perfect discrimination of healthy controls (specificity = 1).

Raman Spectroscopy Analysis Supports Composition Differences in ME/CFS Plasma EVs

Intrigued by the fact that four out of the six physical associated parameters of EVs (EV concentration, size, and *z*-potential obtained with or without proteinase K pretreatment), corresponding to the size and zeta potential of vesicles [as described in Almenar-Pérez et al. (12)] were discriminating features selected by our initial PLS-DA model (**Figures 1A**, **2A**), we decided to further explore the differential nature of ME/CFS EVs by Raman spectroscopy analysis, an approach that has proven to differentiate EVs from various cell sources (34) and has been successfully used to detect ME/CFS specific changes in PBMCs (35).

Raman analysis of the 15 severe ME/CFS cases and 15 HC EVs isolated from aliquots of the plasma used in our earlier study (12), clearly show prominent Raman bands at 1,158 and 1,521 cm^{-1} (**Figure 3A**; **Supplementary Table 2**). These bands are characteristic of carotenoids with the C–C stretching mode (coupled with C–H in-plane bending) contributing to the 1,158-cm^{-1} band and the C = C stretching mode of the conjugated chain in carotenoids contributing to the 1,510-cm^{-1} band (36). Further quantification of results for these two bands are shown in **Figure 3B**, illustrating a significant higher content of carotenoids in ME/CFS patients than in HCs ($p = 0.003$ and $p = 0.005$).

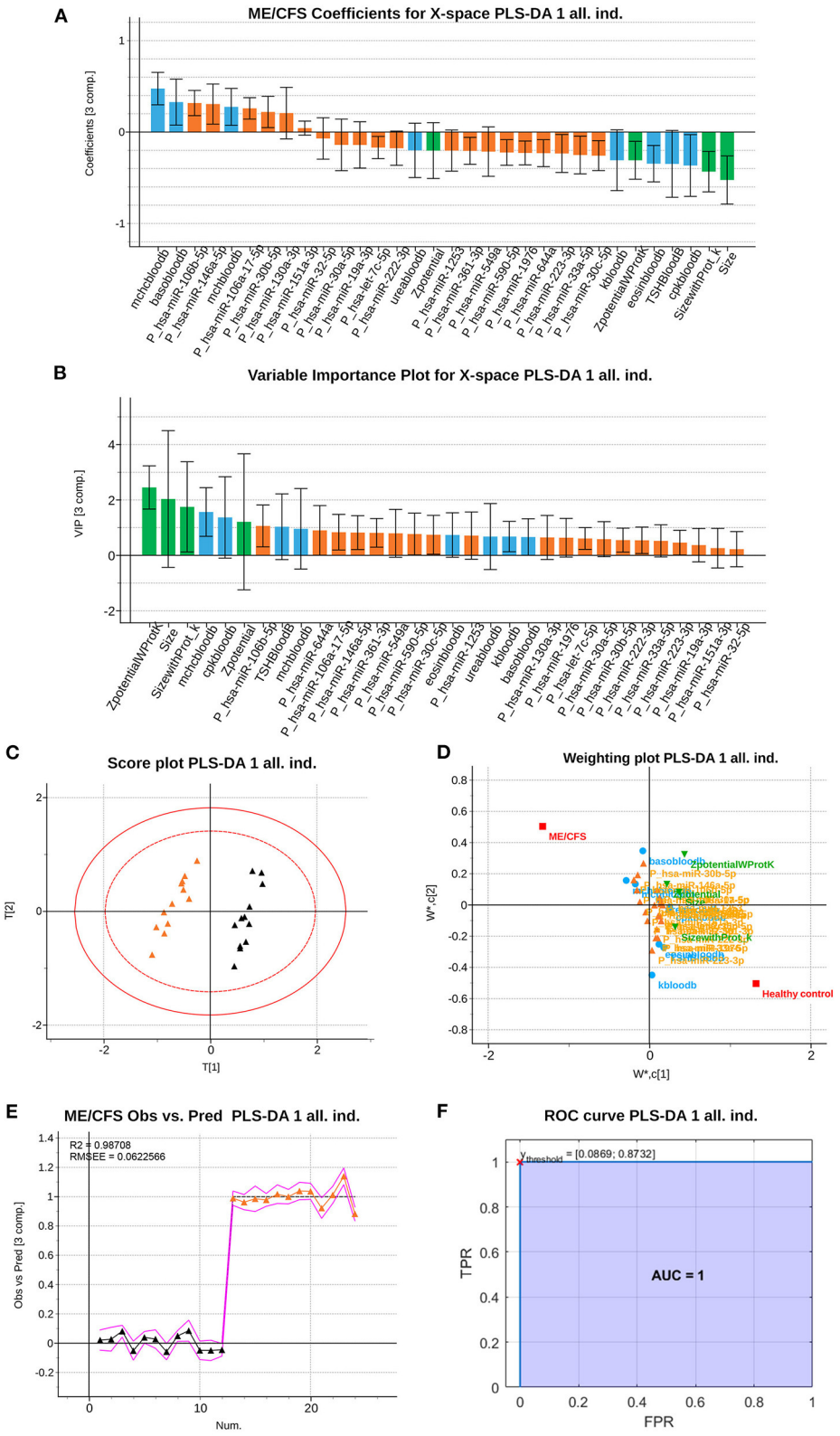

FIGURE 1 | Partial Least Squares (PLS)-Discriminant Analysis (DA) multiblock model based on 32 variables measured from 12 ME/CFS patients and 12 HCs. **(A)** ME/CFS class jackknife *b* coefficients for the X subspace. The color code corresponds to the block each variable belongs to, being those analytical variables (blue), PBMCs' miRNAs (orange) and EVs' characteristics (green). Jackknife confidence Intervals were calculated at a 95% confidence level. **(B)** *VIP* coefficients with

(Continued)

FIGURE 1 | jackknife confidence intervals at 95% of confidence for the X subspace using the calibration dataset. Data set legends can be consulted on **Supplementary Table 1**. The color code is the same as in the rest of the figures. **(C)** Score plot, of the 1st and 2nd components (horizontal and vertical, respectively). **(D)** Weighting plot, of the 1st and 2nd components (horizontal and vertical, respectively). The color code for each variable block is the same as in the rest of the figures. **(E)** Observed vs. Prediction results for participants shows the class prediction with 95% confidence intervals (magenta lines) using three components. The color code is orange for ME/CFS patients, and black markers for Healthy Controls (HCs). RMSEE stands for Root Mean Square Error of Estimation. **(F)** ROC curve for the classification of the observations with the dataset. The red cross locates the optimal performance point (maximum specificity and sensitivity) using the classification threshold between 0.0869 and 0.8732.

ME/CFS Classification Model Based on Raman Spectral Fingerprints

To further investigate the power of Raman spectroscopy to differentiate patients from healthy subjects, we used again PLS-DA as a classifier solely based on the whole Raman spectra. We also compared PLS-DA with a modified version of the LDA, RF, and SVMs to evaluate if there were more suitable techniques to classify individuals using only the Raman spectra as an input.

PLS-DA Model

To evaluate the biomarker value of the observed differential Raman peaks we applied PLS-DA analysis to Raman data. Complete spectra of individuals within each group are represented in **Supplementary Figure 4** (HCs in blue and ME/CFS patients in red). As it can be appreciated, signals were already preprocessed and can be directly used for their further analysis with multivariate statistics techniques. Due to a slight (though not relevant) mismatch in the wavelengths of different records, abscises axes in **Supplementary Figure 4** are representing wavelength bins that contain the signal recorded for wavelengths within each interval.

An PLS-DA model was fitted to determine if the spectra contained information able to discriminate between the groups. The wavelength intervals that carry discriminant information, should appear with significant *b* or *VIP* coefficients. The first PLS-DA model (R^2 of 23.95% and Q^2 of 16.33%) was not able to separate the groups since many variables are non-statistically significant in terms of the *b* and *VIP* coefficients. This can be observed from the high number of jackknife confidence intervals for the VIPs below the $VIP = 1$ threshold (see **Supplementary Figure 5A**), and by the jackknife confidence intervals for the *b* coefficients that contain a zero value (see **Supplementary Figure 5B**).

All non-significant variables according to these parameters were deleted and the model re-estimated. The resulting model selects only one latent variable, slightly increasing its goodness of fit (R^2 of 29.57%) and of prediction (Q^2 of 26.36%). The classification performance of the depurated PLS-DA model (**Figure 4**) is illustrated in the observed vs. predicted values (**Figure 4D**) and in its corresponding ROC curve generated using the 3-fold cross validation scheme (**Figure 4E**). The model reaches an optimal AUC value of 0.7067 setting a threshold of 0.3935 on the predicted response. Despite the poor performance of the model in terms of classification, there might still be statistically significant information which could be useful in discriminating the two groups.

Note that **Figures 4A,B** display the *b* PLS and *VIP* coefficients for the prediction of the ME/CFS class, respectively. Variables with positive *b* coefficients, indicate wavelengths of the spectrum for which the ME/CFS patients show a statistically significant higher signal when compared to the signal of HCs. Relevant variables according to the *b* PLS coefficients highlight the importance of the characteristic peaks on which the previous univariate analysis was focused. In the *b* bar graph, the left window encloses the region close to the 1,158 cm^{-1} peak, while the right window encloses wavelengths close to the 1,521 cm^{-1} peak.

Comparison of PLS-DA Model to Other Classification Models

To further investigate the value of the Raman spectra in differentiating severe ME/CFS patients from HCs, we trained three other binary classification models. We used an adaptation of linear discriminant analysis (LDA) for cases with more variables than observations, a random forest (RF), and a support vector machine (SVM). Some of these techniques (such as RF and SVMs) can model non-linearities which could improve the outcome yielded by the PLS-DA model. The same 3-fold cross validation setup as for the PLS-DA model was used, to make results comparable. All ROC curves with their respective AUCs were obtained, as presented in **Figure 5**. Further information about the comparison between these models can be found on the **Supplementary Methods**.

These results suggest that the Raman spectroscopy data by itself does not hold enough information to accurately discriminate between ME/CFS patients and healthy subjects: to achieve a 100% of true positive rate, classifiers would produce a high rate of false positives. However, AUC values close to 0.7 (**Figure 5**) suggest that EVs might still be representing part of the phenotype of the disease. For this reason, we proposed the last model, combining our initial biomarkers and EV Raman profiles.

Refinement of the Initial PLS-DA Model With EV Raman Profiles

The results of Raman spectrometry analysis show that to be developed as a more comprehensive diagnostic tool the use of further information is required. Therefore, we proceeded to reanalyze our first multi-block PLS-DA model (**Figure 2**) to check if the relevant Raman wavelengths selected by the PLS-DA model on the spectroscopy data (**Figure 4**) could be useful predictors when combined with the previously identified biomarkers.

To study this possibility, we fitted a PLS-DA model using the selected variables from the former PLS-DA model, adding the key differential wavelengths from our PLS-DA analysis of Raman spectroscopy data. It is important to highlight that the

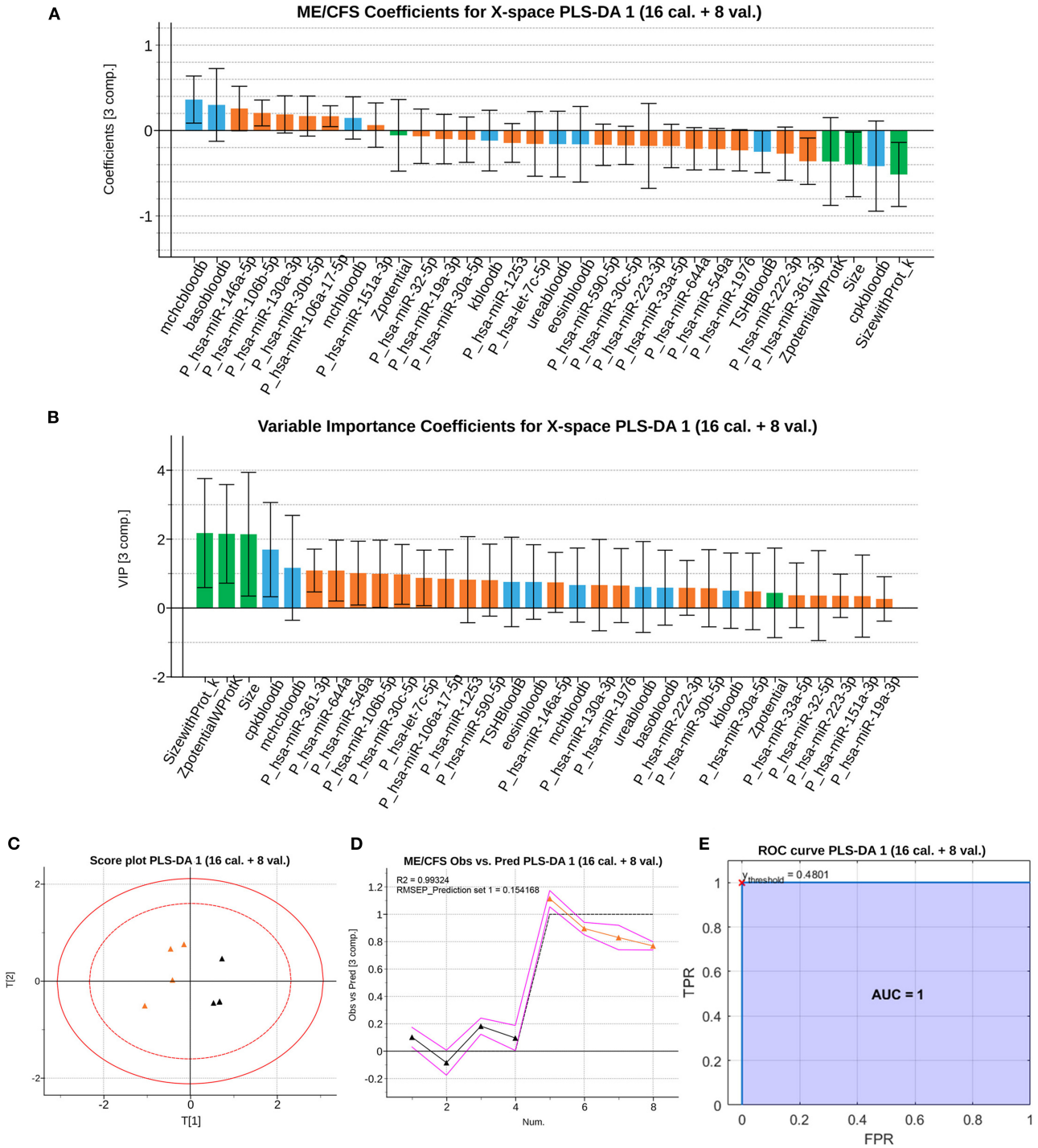

FIGURE 2 | Classification performance of the PLS-DA model with calibration and validation set. **(A)** ME/CFS class *b* jackknife coefficients for the X subspace using the calibration dataset. The color code corresponds the block to which each variable belongs, being those analytical variables (blue), PBMCs' miRNAs (orange) and EVs' characteristics (green). Jackknife confidence intervals were calculated at a 95% confidence level. **(B)** *VIP* coefficients with jackknife confidence intervals at 95% of confidence for the X subspace using the calibration dataset. Data set legends can be consulted on **Supplementary Table 1**. The color code for each variable block is the same as in the rest of the figures. **(C)** Score plot, of the 1st and 2nd components (horizontal and vertical, respectively) for the validation samples. **(D)** Observed vs. Prediction results for the validation samples shows the class prediction with 95% confidence intervals (magenta lines) using three components. The color code is orange for ME/CFS patients, and black markers for Healthy Controls (HCs). RMSEE stands for Root Mean Square Error of Estimation. **(E)** ROC curve for the classification of the validation observations with the trained dataset. The red cross locates the optimal performance point (maximum specificity and sensitivity) using the classification threshold at 0.4801.

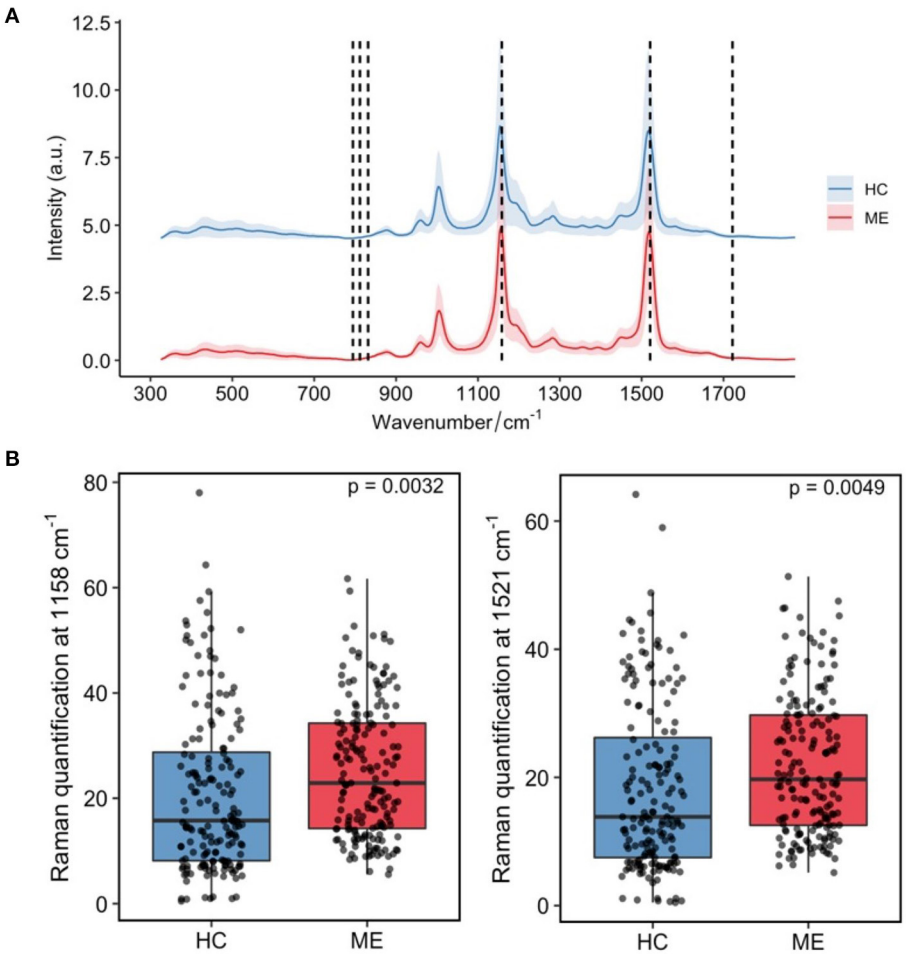

FIGURE 3 | Main differences in plasma derived-EVs Raman spectroscopic profiles from ME/CFS (ME, red, $N = 15$) and matched healthy subjects (HC, blue, $N = 15$). **(A)** Mean profile plot values with indication of chemical nature of peaks with prominent differences. **(B)** Relative quantification of carotenoids by integrating Raman bands at 1,158 cm^{-1} ($p = 0.0032$) (left) and 1,521 cm^{-1} ($p = 0.0049$) (right). The quantification results were represented as box plots and sample mean of the ME/CFS group (ME) compared with the healthy control's (HC) ($N = 15$/group) by using Welch's two sample *t*-test for unequal variance.

adequacy of this approach resides in the fact that the samples used to generate the two models came from the same blood samples. The reason for maintaining the use of PLS-DA, was that according to the previous results, it was a technique yielding one of the best classification performances and the only one enabling the interpretation of the discriminant power of the predictors, establishing a set of statistically significant biomarkers.

An initial PLS-DA model was fitted using all observations to allow for the selection of key discriminating variables and removal of potential outliers. The initial fused model selects an optimal number of nine latent variables (R^2 of 99.37% and Q^2 of 81.15%). This model was depurated observation-wise and variable-wise, as previously described. The *b* coefficients and *VIP* coefficients of the final set of selected variables are shown in **Figures 6A,B**, respectively.

This refined PLS-DA model based on the final set of selected predictors was fitted excluding the observations used for external validation in the first PLS-DA model. The final model obtained presents a similar performance (R^2 of 93.38 and Q^2 of 77.06). **Supplementary Figure 6** shows the result of the permutation test performed on the PLS-DA model fitted with the calibration set, proving the statistical significance of the yielded coefficients.

The observed vs. predicted values for the observations in the calibration set (**Figure 6C**) and in the external validation set, show that classes can be perfectly separated (**Figure 6E**). This is also illustrated by the ROC curves in **Figures 6D,F**, showing that a threshold on the predicted outcome of 0.481 yields a perfect classification with an AUC of 1.

Inspecting the *b* PLS and *VIP* coefficients (**Figures 6A,B**, respectively), although some of the predictors still appear as statistically non-significant, their jackknife confident intervals

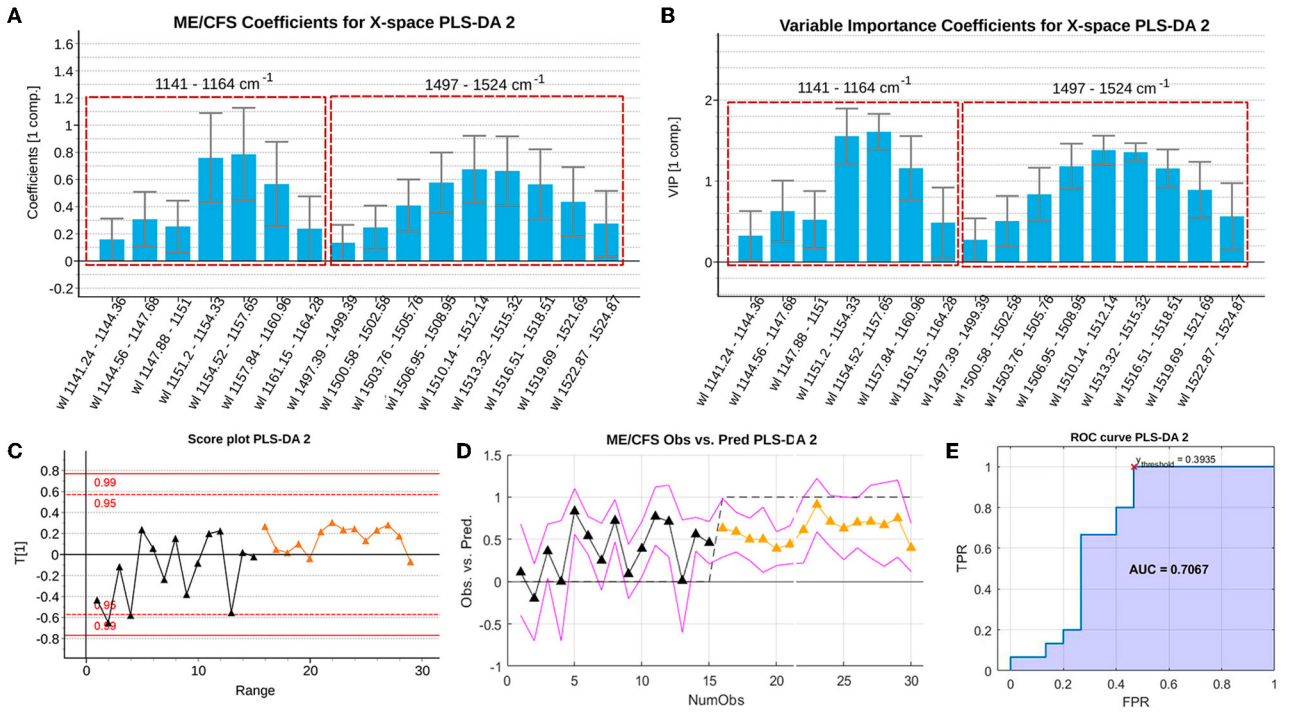

FIGURE 4 | Summary of the *b* PLS coefficients **(A)**, the *VIP* coefficients **(B)**, the scores **(C)**, the observed vs. predicted values (RMSEE stands for Root Mean Square Error of Estimation). **(D)** and ROC curve **(E)** of the depurated PLS-DA model with the Raman spectroscopy data. The red cross locates the optimal performance point (maximum specificity and sensitivity) using the classification threshold at 0.3935. Data set legends can be consulted on **Supplementary Table 1**. Black triangles represent healthy controls, whereas orange triangles represent ME/CFS cases.

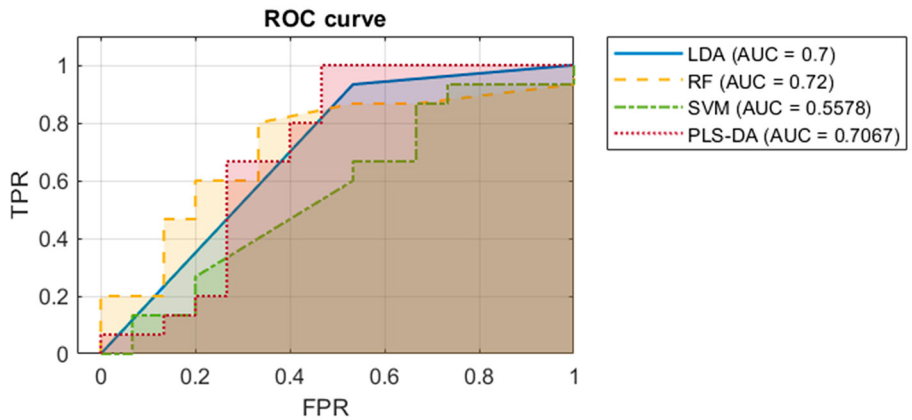

FIGURE 5 | ROC curves with their AUCs of the four models classifying ME/CFS or HC based on their Raman spectra. The ROC curve is plotted with true positive rate against false positive rate.

are almost under or above zero for the *b* coefficients, or almost contain the value $VIP = 1$ for the *VIP* coefficients. This suggests that the width of the confidence intervals might be influenced by the small sample size, which leads to wide jackknife confidence intervals. In conclusion, this final model yields a perfect classification (AUC=1) and has 35 predictors, meaning that some of the most relevant predictors according to the previous PLS-DA model, have been replaced by wavelength intervals of the Raman spectroscopy analysis. Among these relevant wavelengths, both peaks (around 1,158 and 1,521 cm^{-1}) hold important information as potential biomarkers. The majority of eliminated predictors from the previous PLS-DA model, carried information about PBMC miRNAs.

GO pathway analysis of DE miRNAs from PBMCs selected by our refined PLS-DA model (**Figure 6**) show that six out of

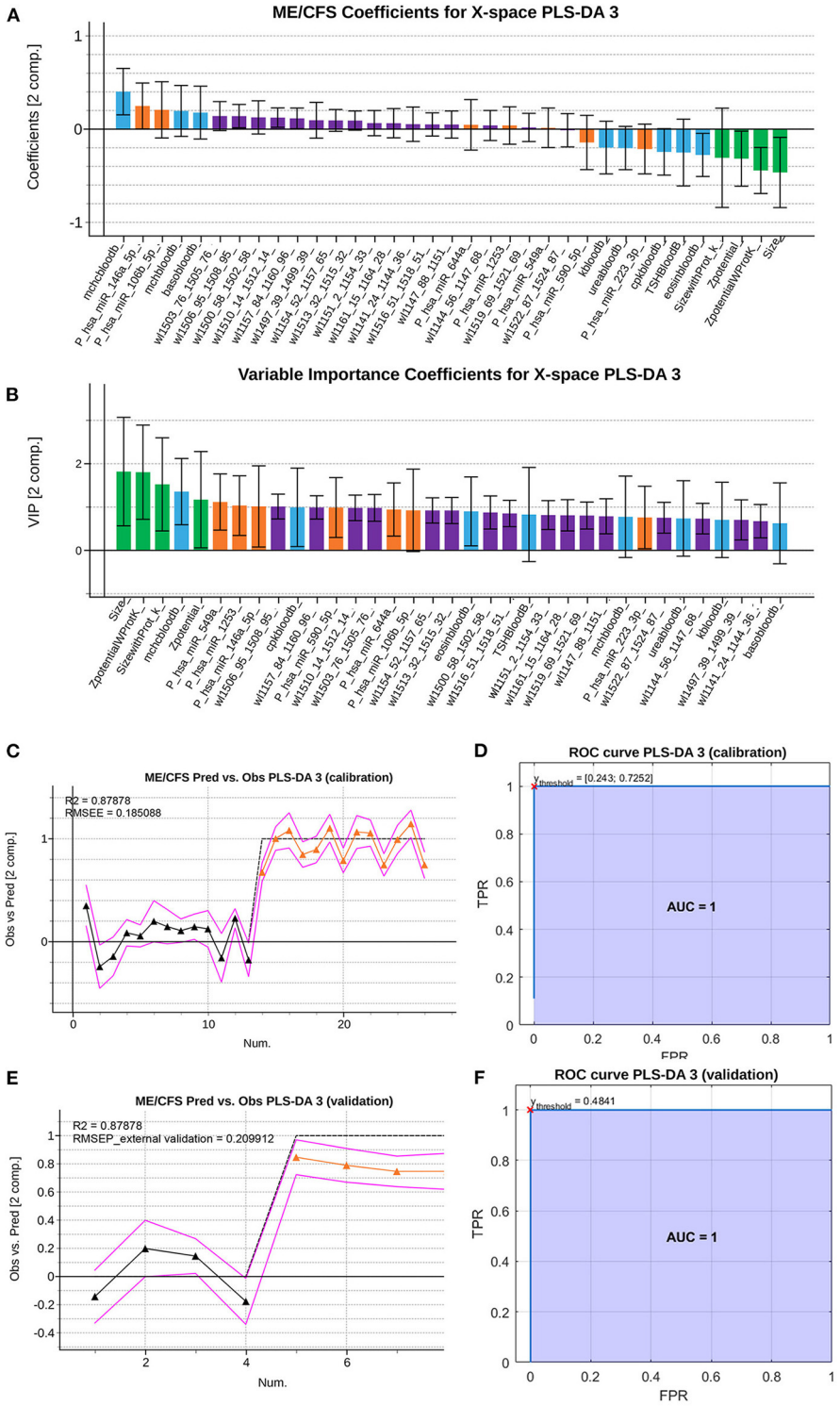

FIGURE 6 | Summary of the *VIP* coefficients **(A)**, *b* PLS coefficients **(B)**, observed vs. predicted values for the training set **(C)**, ROC curve for the training set with red cross indicating the point of optimal performance **(D)** observed vs. predicted values for the validation set (RMSEE stands for Root Mean Square Error of Estimation) **(E)** and ROC curve for the validation set with red cross indicating the point of optimal performance **(F)** of the depurated PLS-DA model with the Raman spectroscopy data. Data set legends can be consulted on **Supplementary Table 1**. Black triangles represent HCs, whereas orange triangles represent ME/CFS patients. Predictor coefficients in **(A,B)** are colored according to their block of information (blue for analytical features, orange for PBMCs miRs features, green for EVs' features and purple for Raman spectra features).

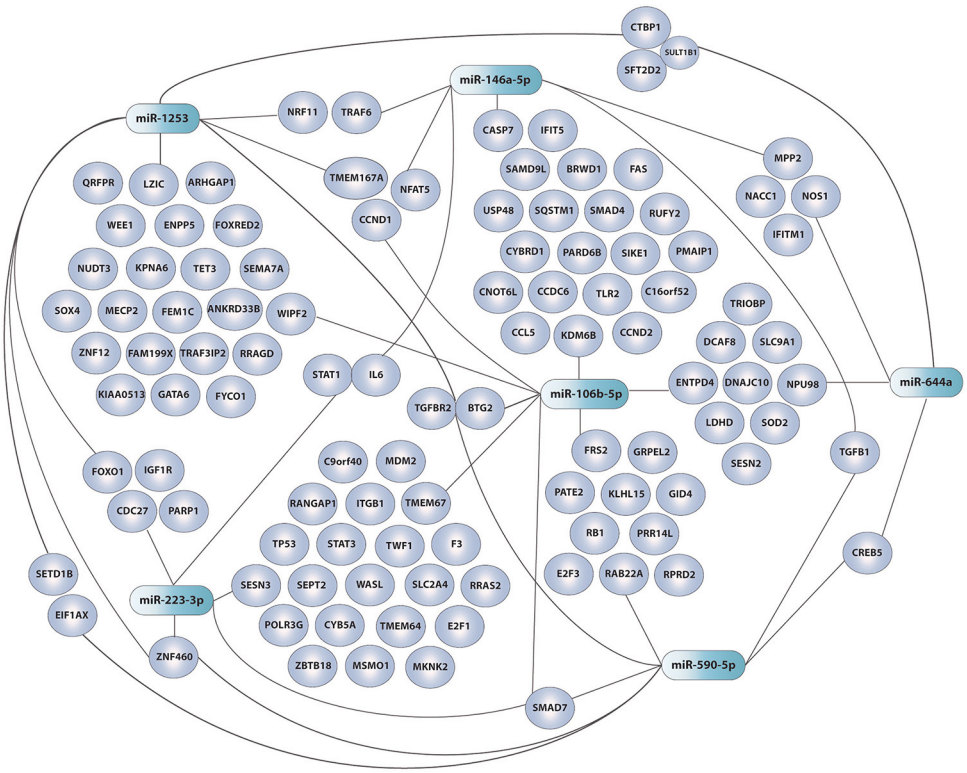

FIGURE 7 | Network of DE miRNAs in ME/CFS PBMCs selected by PLS-DA (shaded green) and their target genes (shaded purple). GO enrichment performed with the miRTargetlink software (33). Adobe Illustrator was the drawing tool used.

seven share common gene targets with top cellular functions belonging to immunity, neuroinflammation, and metabolism (**Supplementary Table 3**; **Figure 7**), all being widely associated with ME/CFS in the literature.

DISCUSSION

Because of the lack of an objective diagnostic laboratory test, the diagnosis of ME/CFS is made by ruling out other conditions. ME/CFS patients may not get a diagnosis in many developed countries while in developing countries ME/CFS is still not considered a "real" illness. The burden on patients and their families is enormous.

In 2015 the Institute of Medicine (IOM) in the US (37) informed that ME/CFS is a medical illness and should not be considered a psychiatric condition. In support of IOM conclusions that ME/CFS has a biological basis numerous studies show neurologic (38), immune (39), and metabolic (40) disturbances in these patients. Still, ME/CFS biomarker validation remains an important challenge with many research groups identifying putative diagnostic markers which could help move forward our understanding of the affected pathways in the disease. Research efforts in ME/CFS remain hampered by low numbers of participants in the cohorts studied with disease heterogeneity also playing a role.

The UK National Institute for Health and Care Excellence (NICE) has recently changed the guidelines to treat ME/CFS patients in the NHS (National Health System) (41). The new guidelines do not include graded exercise as a therapeutic strategy. Recent studies have showed that more than 50% of patients either could not start a GET program or failed to complete it, emphasizing the problems of introducing any exercise support program (42, 43). This highlights the urgent need for not only a diagnostic test but the importance of identifying biological/clinical variables able to select patients who are likely to benefit from a particular treatment program. With rising numbers of Long-Covid patients and the possibility that many end-up developing ME/CFS, having good diagnostic test to help patients manage their condition is more important than ever.

Our previous study by Almenar-Pérez et al., although limited in scope by a low number of participants (N = 30, 15/group) attempted to improve patient homogeneity by restricting the inclusion of participants to only severe female cases. The selection of severe cases was based on the premise that severity concurs with highest differential biomarker levels. Although the scope of the findings may be limited to this patients' group, it remains possible that the mechanisms and, therefore, the detected biomarkers turn up valid to diagnose moderately or mildly affected patients. A design including the study of a large number of variables encompassing PBMC

and EV miRNomes, together with complete blood analytics, thorough patient phenotyping by validated questionnaires, and the study of EV physical features (12) led to the identification of biological differences with limited diagnostic potential at the individual level.

In the current study we combine these variables and add Raman spectroscopic profiling as a new marker of EV function in the same blood samples. By applying PLS-DA analysis to this large set of data: 34 blood analytic variables, 775 different miRNAs being expressed above threshold levels (136 in PBMCs and 639 in EVs), EV concentration, size and z-potential, we identified 32 variables that can effectively differentiate ME/CFS cases from HCs (AUC=1, i.e., sensitivity and specificity = 1) (**Figure 1**). Moreover, a second model using calibration and validation sets further confirms the effective diagnostic power of the selected variables (**Figure 2**), with an AUC still equal to 1 (i.e., sensitivity and specificity are perfect). Strikingly, EV physical features, including EV size and z-potential measures were detected by this model as relevant features for the effective diagnosis of patients indicating a potential important role of EVs in ME/CFS.

Although we and others have consistently found higher counts of EVs in different cohorts of ME/CFS patients (12, 44, 45), even by applying different isolation procedures, EV count in the PLS-DA model was not among the 32 features selected that could discriminate severe ME/CFS patients from healthy subjects. The reasons behind this result are not understood at present. However, the fact that increased EV numbers have been reported for other diseases with an inflammatory component (46, 47) may argue for a restricted disease specificity of this feature.

It is worth mentioning that among the blood analytic group of variables the iterative PLS-DA modeling process selected, blood creatine phosphokinase (CK, labeled as cpkbloodb, please see **Supplementary Table 1** key tab for variable nomenclature used) level was a feature retrieved with and without the inclusion of Raman data (**Figures 1**, **2**, **6**). CK levels being a clinical feature that had been previously reported as a potential biomarker of ME/CFS for showing significant reduced levels in an expanded cohort of patients (48). Highly expressed in muscle, heart, and brain the CK enzyme holds a key role in ATP homeostasis. The low levels found by Nacul et al., possibly reflecting energy dysregulation in these tissues, may be linked to the profound fatigue found in ME/CFS patients with the severe having the lowest levels.

The increased absolute zeta potential values of ME/CFS EVs detected in a previous study by our group (12) suggested differences in the relative abundance of charged groups in their membranes. Modifications of EVs membrane potential has been related to other pathological conditions, including cancer where the change in EV net charge was attributed to a disbalance in the relative abundance of sialic acid (49). Interestingly polysialylation of exosomal membranes has been shown to provide a thermo-protecting effect being able to modulate exosome-plasma membrane interactions and thus their signaling capacity (50). Further evaluation of these modifications present in ME/CFS EVs will be an important component of future studies aimed at determining their functional impacts as proposed in our recent publication (51).

Raman spectroscopy has shown its utility in detecting composition differences in patient's EVs (52, 53) and could be developed as a cost-effective diagnostic method by its ability to identify complex patterns in biological materials. Encouraged by the discriminating potential of this method to unveil composition differences in biological materials, EVs isolated from severe ME/CFS patients which had shown reduced diameter and reduced zeta potential (increased electronegativity) (12), were compared to HC EVs by Raman micro-spectroscopic analysis. The main difference in the EVs Raman spectra between severe ME/CFS patients and HCs related to two carotenoid peaks (**Figure 3**; **Supplementary Figure 4**). Zhang et al., have recently found a shift of a peak at 1,553 cm^{-1} (tryptophan/amide II) to 1,528 cm^{-1} (carotenoid) in trophoblast-derived EVs during late stages of pregnancy (54), time at which circulating EVs counts increase and inflammatory responses vary (55, 56).

In the 1970's Raman spectroscopy was used to study the protein properties of red blood cells (RBC) ghosts (57). RBC ghosts are pale cells which turn up on blood smears, coming from the hemolysis of RBCs, are typically linked to disease. Verma and Wallach identified two Raman peaks in RBC ghosts which were later identified as carotenoids (58, 59). Recent studies have showed RBC deformability was reduced in ME/CFS (60). Thus, it is tempting to speculate that the EV differences we are observing by Raman are due to EVs of RBC origin being generated when the RBC are stressed in the patient's circulation. In support of this hypothesis, it is interesting to observe that increased mean corpuscular hemoglobin (mch) and mean corpuscular hemoglobin concentration (mchc), which have been related to decreased deformability of RBCs (61), were identified by our PLS-DA analysis as variables with high discriminant diagnosis capacity (**Figure 6**; **Supplementary Table 1**). It seems relevant to mention that Fiedor et al., have recently shown that increased beta-carotene concentration in RBC membranes affect cell's shape, sensitivity to osmolysis and alters hemoglobin-oxygen affinity with potential physiologic implications (62).

Regardless of EV composition differences we were interested in exploring if the Raman spectroscopic data was sufficient to efficiently distinguish ME/CFS cases from HCs. Despite its potential discriminatory capacity of ME/CFS body fluid components (**Figures 4**, **5**), in good agreement with the disease "plasma factor" hypothesis reported by Ron Davis' group at Standford University (63), which is also supported by differences in proteins or lipid plasma levels (64, 65), the diagnostic value of Raman data seems limited when compared to our PLS-DA model including analytic variables, PBMC miRNA profiles and EV features (**Figures 1**, **2**).

It needs to be considered that a particular isolation method used to purify EVs from plasma may lead to the purification of EV sets that may differ from another procedure. Despite the high purity attributed to EVs prepared by ultracentrifugation, this procedure is laborious, and

requires both a large volume of fluid and the provision of expensive equipment. A diagnostic method based on EVs requires a much simpler method preferably allowing the analysis of small volumes of fluids without compromising performance. Total Exosome Isolation Reagent (TEIR) was selected from the available kits because according to Helwa et al., it provides higher yields using smaller amounts of plasma when compared to other commercial alternatives or with respect to ultracentrifugation, ultrafiltration, or gel chromatography (66). Moreover, exploratory EV studies using highly purified EV sets (i.e., exosomes) could turn into missing relevant EV subsets, and thus a less restrictive method was preferred.

Unexpectedly our PLS-DA iterative method did not select any of the 639 miRNAs detected above threshold levels in ME/CFS EVs. All miRNAs in our panel of discriminatory measures came from the PBMC's group. Although this may associate with the complexity of ME/CFS, and thus the requirement of features from different compartments for its definition, the possibility that a more selective EV isolation method may render homogenous EV subpopulations with distinctive ME/CFS miRNA profiles cannot be ruled out at present. In support of the first argument, we find that GO pathway analysis of six out of the seven DE miRNAs from PBMCs selected by our PLS-DA model (**Figure 6**) share common gene targets with top cellular functions belonging to immunity, neuroinflammation, and metabolism (**Supplementary Table 3**; **Figure 7**), all being widely associated with ME/CFS in the literature.

In summary, this work describes for the first time an ME/CFS model based on PLS-DA of 32 analytical variables capable of diagnosing the disease with perfect sensitivity and specificity (AUC=1), further confirming the biologic nature of this disease and highlighting the relevance of patient EV features for their diagnosis. An ME/CFS EV Raman spectroscopic fingerprint is also provided, pioneering the potential use of this method for the diagnosis of ME/CFS and for detecting potential RBC defects in severe ME/CFS. Finally, we show that although the diagnostic potential of Raman is limited its simplicity and low amount of sample requirement highlights its potential utility as an early screening tool prior to more comprehensive testing with miRNA's from PBMC's. Moreover, the inclusion of Raman data for the refinement of our previous model, although incapable of increasing the already perfect separation of cases from HCs (AUC=1) (**Figures 1**, **6**), allowed for a significant reduction in the number of PBMC miRNAs from 21 in our initial PLS-DA model (**Figures 1**, **2**) to only 7 in the PLS-DA Raman refined model (**Figure 6**) (**Supplementary Table 1**).

The findings obtained in this study are expected to pave the way for unraveling the subjacent disease mechanisms in which EVs and PBMC miRNAs participate with clear implications for the future diagnosis and treatment of ME/CFS, perhaps embracing other patient groups suffering with chronic fatigue.

DATA AVAILABILITY STATEMENT

The datasets presented in this study are available from the NCBI GEO (Accession number GSE141770) or as **Supplementary Material**.

ETHICS STATEMENT

The studies involving human participants were reviewed and approved by Public Health Research Ethics Committee DGSP-CSISP, Valencia (Spain), study number UCV_201701 and the UCL Biobank Ethical Review Committee-Royal Free London NHS Foundation Trust (B-ERC-RF), study number EC2017.01. The patients/participants provided their written informed consent to participate in this study.

AUTHOR CONTRIBUTIONS

AG-C and AF: data curation, formal analysis, methodology, figure drawing, writing—original draft, review, and editing. EA-P, TY, WH, SH, TL, and LN: formal analysis, investigation, methodology, data curation, and manuscript review. JX: formal analysis, investigation, data curation, methodology, and writing—original draft. KG-O: formal analysis, investigation, data curation, figure drawing, and manuscript review. KM: formal analysis, investigation, data curation, writing—original draft, and manuscript review. EO: conceptualization, main funding acquisition, supervision, formal analysis, investigation, data curation, writing—original draft, and manuscript review. All authors contributed to the article and approved the submitted version.

FUNDING

This study was funded by the Generalitat Valenciana AICO grant number 2020/254 and by a Ramsay Fund MEA (ME Association, UK) grant to EO; by the Research and Development Support Program of the Universitat Politècnica de València (PAID-01-17) to AF; by the Star Exclusivas SL grant to the UCV Gene expression and immunity group. Erasmus staff mobility to KM and EO. SH was supported by a UK Spine Bridge support grant and KG-O by the Generalitat Valenciana ACIF2021/179 grant. Funders were not involved in any of the research stages.

ACKNOWLEDGMENTS

Authors wish to express their gratitude to Dr Katrina Pears (ME Association, UK) for proof-reading the final version of the manuscript.

SUPPLEMENTARY MATERIAL

The Supplementary Material for this article can be found online at: https://www.frontiersin.org/articles/10.3389/fmed.2022.842991/full#supplementary-material

REFERENCES

1. Boerma T, Harrison J, Jakob R, Mathers C, Schmider A, Weber S. Revising the ICD: explaining the WHO approach. *Lancet.* (2016) 388:2476–7. doi: 10.1016/S0140-6736(16)31851-7
2. Clayton EW. Beyond myalgic encephalomyelitis/chronic fatigue syndrome: an IOM report on redefining an illness. *JAMA.* (2015) 313:1101–2. doi: 10.1001/jama.2015.1346
3. Fukuda K, Straus SE, Hickie I, Sharpe MC, Dobbins JG, Komaroff A. The chronic fatigue syndrome: a comprehensive approach to its definition and study. International Chronic Fatigue Syndrome Study Group. *Annals Intern Med.* (1994) 121:953–9. doi: 10.7326/0003-4819-121-12-199412150-00009
4. Carruthers BM, Jain AK, De Meirleir KL, Peterson DL, Klimas NG, Lerner A, et al. Myalgic encephalomyelitis/chronic fatigue syndrome: Clinical working case definition, diagnostic and treatment protocols. *J Chron Fatigue Syndr.* (2003) 11:7–115. doi: 10.1300/J092v11n01_02
5. Carruthers BM, van de Sande MI, De Meirleir KL, Klimas NG, Broderick G, Mitchell T, et al. Myalgic encephalomyelitis: international consensus criteria. *J Intern Med.* (2011) 270:327–38. doi: 10.1111/j.1365-2796.2011.02428.x
6. Maes M, Rodriguez LA, Morris G. Is a diagnostic blood test for chronic fatigue syndrome on the horizon? *Expert Rev Mol Diagn.* (2019) 19:1049–51. doi: 10.1080/14737159.2020.1681976
7. Vishnoi A, Rani S. MiRNA biogenesis and regulation of diseases: an overview. *Methods Mol Biol.* (2017) 1509:1–10. doi: 10.1007/978-1-4939-6524-3_1
8. Slota JA, Booth SA. MicroRNAs in neuroinflammation: implications in disease pathogenesis, biomarker discovery and therapeutic applications. *Non-coding RNA.* (2019) 5:35. doi: 10.3390/ncrna5020035
9. Almenar-Pérez E, Sánchez-Fito T, Ovejero T, Nathanson L, Oltra E. Impact of polypharmacy on candidate biomarker mirnomes for the diagnosis of fibromyalgia and myalgic encephalomyelitis/chronic fatigue syndrome: striking back on treatments. *Pharmaceutics.* (2019) 11:126. doi: 10.3390/pharmaceutics11030126
10. Cheema AK, Sarria L, Bekheit M, Collado F, Almenar-Pérez E, Martín-Martínez E, et al. Unravelling myalgic encephalomyelitis/chronic fatigue syndrome (ME/CFS): Gender-specific changes in the microRNA expression profiling in ME/CFS. *J Cell Mol Med.* (2020) 24:5865–77. doi: 10.1111/jcmm.15260
11. Nepotchatykh E, Elremaly W, Caraus I, Godbout C, Leveau C, Chalder L, et al. Profile of circulating microRNAs in myalgic encephalomyelitis and their relation to symptom severity, and disease pathophysiology. *Sci Rep.* (2020) 10:19620. doi: 10.1038/s41598-020-76438-y
12. Almenar-Pérez E, Sarría L, Nathanson L, Oltra E. Assessing diagnostic value of microRNAs from peripheral blood mononuclear cells and extracellular vesicles in Myalgic Encephalomyelitis/Chronic Fatigue Syndrome. *Sci Rep.* (2020) 10:2064. doi: 10.1038/s41598-020-58506-5
13. Benjamini Y, Hochberg Y. Controlling the false discovery rate – a practical and powerful approach to multiple testing. *J R Statist Soc B.* (1995) 57:289–300. doi: 10.1111/j.2517-6161.1995.tb02031.x
14. Hervás Marín D. *Use of multivariate statistical methods for the analysis of metabolomic data* (Tesis doctoral no publicada). Universitat Politècnica de València, Valencia, Spain (2019). Available online at: https://riunet.upv.es/handle/10251/130847 doi: 10.4995/Thesis/10251/130847
15. Höskuldsson A. PLS regression methods. *J Chemometrics.* (1988) 2:211–28. doi: 10.1002/cem.1180020306
16. Saccenti E, Hoefsloot HCJ, Smilde AK, Westerhuis JA, Hendriks MMWB. Reflections on univariate and multivariate analysis of metabolomics data. *Metabolomics.* (2014) 10:361–74. doi: 10.1007/s11306-013-0598-6
17. Barker M, Rayens W. Partial least squares for discrimination. *J Chemometrics.* (2003) 17:166–73. doi: 10.1002/cem.785
18. Fisher RA. The use of multiple measurements in taxonomic problems. *Ann Eugen.* (1936) 7:179–88. doi: 10.1111/j.1469-1809.1936.tb02137.x
19. Breiman L. Random forests. *Machine Learn.* (2001) 45:5–32. doi: 10.1023/A:1010933404324
20. Cortes C, Vapnik V. Support vector machine. *Mach Learn.* (1995) 20:273–97. doi: 10.1007/BF00994018
21. Institute of Medicine. *Beyond Myalgic Encephalomyelitis/Chronic Fatigue Syndrome: Redefining an Illness.* Washington, DC: The National Academies Press (2015).
22. Lacerda EM, Bowman EW, Cliff JM, Kingdon CC, King EC, Lee JS, et al. The UK ME/CFS Biobank for biomedical research on Myalgic Encephalomyelitis/Chronic Fatigue Syndrome (ME/CFS) and Multiple Sclerosis. *Open J Bioresour.* (2017) 4:4. doi: 10.5334/ojb.28
23. Lacerda EM, Mudie K, Kingdon CC, Butterworth JD, O'Boyle S, Nacul L. The UK ME/CFS biobank: a disease-specific biobank for advancing clinical research into myalgic encephalomyelitis/chronic fatigue syndrome. *Front Neurol.* (2018) 9:1026. doi: 10.3389/fneur.2018.01026
24. McHorney CA, Ware JE Jr, Raczek AE. The MOS 36-item short-form health survey (SF-36): II. Psychometric and clinical tests of validity in measuring physical and mental health constructs. *Med Care.* (1993) 31:247–63. doi: 10.1097/00005650-199303000-00006
25. Jackson C. The general health questionnaire. *Occup Med.* (2006) 57:79. doi: 10.1093/occmed/kql169
26. Likert R. A technique for the measurement of attitudes. *Arch Psychol.* (1932) 140:1–55.
27. Westerhuis JA, Kourti T, Macgregor JF. Analysis of multiblock and hierarchical PCA and PLS models. *J Chemom.* (1998) 12:301–21. doi: 10.1002/(SICI)1099-128X(199809/10)12:5<301::AID-CEM515>3.0.CO;2-S
28. Westerhuis JA, Hoefsloot HCJ, Smit S, Vis DJ, Smilde AK, Van Velzen EJJ, et al. Assessment of PLS-DA cross validation. *Metabolomics.* (2008) 4:81–9. doi: 10.1007/s11306-007-0099-6
29. Fawcett T. An introduction to ROC analysis. *Pattern Recognit Lett.* (2006) 27:861–74. doi: 10.1016/j.patrec.2005.10.010
30. Chong I-G, Jun C-H. Performance of some variable selection methods when multicollinearity is present. *Chemometr Intell Lab Syst.* (2005) 78:103–12. doi: 10.1016/j.chemolab.2004.12.011
31. Hotelling H. The generalization of student's ratio. In: Kotz S, Johnson NL, editors. *Breakthroughs in Statistics*. New York, NY: Springer (1931). p. 360–78. doi: 10.1214/aoms/1177732979
32. Théry C, Witwer KW, Aikawa E, Alcaraz MJ, Anderson JD, Andriantsitohaina R, et al. Minimal information for studies of extracellular vesicles 2018 (MISEV2018): a position statement of the International Society for Extracellular Vesicles and update of the MISEV2014 guidelines. *J Extracell Vesic.* (2018) 7:1535750. doi: 10.1080/20013078.2018.1461450
33. Kern F, Aparicio-Puerta E, Li Y, Fehlmann T, Kehl T, Wagner V, et al. miRTargetLink 2.0-interactive miRNA target gene and target pathway networks. *Nucleic Acids Res.* (2021) 49:W409–16. doi: 10.1093/nar/gkab297
34. Dash M, Palaniyandi K, Ramalingam S, Sahabudeen S, Raja NS. Exosomes isolated from two different cell lines using three different isolation techniques show variation in physical and molecular characteristics. *Biochim Biophys Acta Biomembr.* (2021) 1863:183490. doi: 10.1016/j.bbamem.2020.183490
35. Xu J, Potter M, Tomas C, Elson JL, Morten KJ, Poulton J, et al. A new approach to find biomarkers in chronic fatigue syndrome/myalgic encephalomyelitis (CFS/ME) by single-cell Raman micro-spectroscopy. *Analyst.* (2019) 144:913–20. doi: 10.1039/C8AN01437J
36. Horiue H, Sasaki M, Yoshikawa Y, Toyofuku M, https://www.nature.com/articles/s41598-020-64737-3#auth-Shinsuke-Shigeto S. Raman spectroscopic signatures of carotenoids and polyenes enable label-free visualization of microbial distributions within pink biofilms. *Sci Rep.* (2020) 10:7704. doi: 10.1038/s41598-020-64737-3
37. Institute of Medicine. *Beyond Myalgic Encephalomyelitis/Chronic Fatigue Syndrome: Redefining an Illness.* Washington, DC: National Academies Press (2015).
38. Gandasegui IM, Laka LA, Gargiulo PÁ, Gómez-Esteban JC, Sánchez JL. Myalgic encephalomyelitis/chronic fatigue syndrome: a neurological entity? *Medicina.* (2021) 57:1030. doi: 10.3390/medicina57101030
39. Morris G, Maes M. A neuro-immune model of Myalgic Encephalomyelitis/Chronic fatigue syndrome. *Metab Brain Dis.* (2013) 28:523–40. doi: 10.1007/s11011-012-9324-8
40. Brown AE, Jones DE, Walker M, Newton JL. Abnormalities of AMPK activation and glucose uptake in cultured skeletal muscle cells

from individuals with chronic fatigue syndrome. *PLoS ONE.* (2015) 10:e0122982. doi: 10.1371/journal.pone.0122982
41. National Institute for Health and Care Excellence. *Myalgic Encephalomyelitis (or Encephalopathy)/Chronic Fatigue Syndrome: Diagnosis and Management*. (2021). Available online at: https://www.nice.org.uk/guidance/ng206 (accessed November 28, 2021).
42. Kujawski S, Cossington J, Słomko J, Dawes H, Strong JW, Estevez-Lopez F, et al. Prediction of discontinuation of structured exercise programme in chronic fatigue syndrome patients. *J Clin Med.* (2020) 9:3436. doi: 10.3390/jcm9113436
43. Kujawski S, Cossington J, Słomko J, Zawadka-Kunikowska M, Tafil-Klawe M, Klawe JJ, et al. Relationship between cardiopulmonary, mitochondrial and autonomic nervous system function improvement after an individualised activity programme upon chronic fatigue syndrome patients. *J Clin Med.* (2021) 10:1542. doi: 10.3390/jcm10071542
44. Castro-Marrero J, Serrano-Pertierra E, Oliveira-Rodríguez M, Zaragozá MC, Martínez-Martínez A, Blanco-López M, et al. Circulating extracellular vesicles as potential biomarkers in chronic fatigue syndrome/myalgic encephalomyelitis: an exploratory pilot study. *J Extracell Vesicl.* (2018) 7:1453730. doi: 10.1080/20013078.2018.1453730
45. Giloteaux L, O'Neal A, Castro-Marrero J, Levine SM, Hanson MR. Cytokine profiling of extracellular vesicles isolated from plasma in myalgic encephalomyelitis/chronic fatigue syndrome: a pilot study. *J Transl Med.* (2020) 18:387. doi: 10.1186/s12967-020-02560-0
46. Rajendran L, Honsho M, Zahn TR, Keller P, Geiger KD, Verkade P, et al. Alzheimer's disease beta-amyloid peptides are released in association with exosomes. *Proc Natl Acad Sci USA.* (2006) 103:11172–7. doi: 10.1073/pnas.0603838103
47. Logozzi M, De Milito A, Lugini L, Borghi M, Calabrò L, Spada M, et al. High levels of exosomes expressing CD63 and caveolin-1 in plasma of melanoma patients. *PLoS ONE.* (2009) 4:e5219. doi: 10.1371/journal.pone.0005219
48. Nacul L, de Barros B, Kingdon CC, Cliff JM, Clark TG, Mudie K, et al. Evidence of clinical pathology abnormalities in people with myalgic encephalomyelitis/chronic fatigue syndrome (ME/CFS) from an analytic cross-sectional study. *Diagnostics.* (2019) 9:41. doi: 10.3390/diagnostics9020041
49. Guo Y, Tao J, Li Y, Feng Y, Ju H, Wang Z, et al. Quantitative localized analysis reveals distinct exosomal protein-specific glycosignatures: implications in cancer cell subtyping, exosome biogenesis, and function. *J Am Chem Soc.* (2020) 142:7404–12. doi: 10.1021/jacs.9b12182
50. Sapoń K, Gawrońska I, Janas T, Sikorski AF, Janas T. Exosome-associated polysialic acid modulates membrane potentials, membrane thermotropic properties, and raft-dependent interactions between vesicles. *FEBS Lett.* (2020) 594:1685–97. doi: 10.1002/1873-3468.13785
51. Monzón-Nomdedeu MB, Morten KJ, Oltra E. Induced pluripotent stem cells as suitable sensors for fibromyalgia and myalgic encephalomyelitis/chronic fatigue syndrome. *World J Stem Cells.* (2021) 13:1134–50. doi: 10.4252/wjsc.v13.i8.1134
52. Krafft C, Wilhelm K, Eremin A, Nestel S, von Bubnoff N, Schultze-Seemann W, et al. A specific spectral signature of serum and plasma-derived extracellular vesicles for cancer screening. *Nanomedicine.* (2017) 13:835–41. doi: 10.1016/j.nano.2016.11.016
53. Morasso CF, Sproviero D, Mimmi MC, Giannini M, Gagliardi S, Vanna R, et al. Raman spectroscopy reveals biochemical differences in plasma derived extracellular vesicles from sporadic Amyotrophic Lateral Sclerosis patients. *Nanomedicine.* (2020) 29:102249. doi: 10.1016/j.nano.2020.102249
54. Zhang H, Silva AC, Zhang W, Rutigliano H, Zhou A. Raman Spectroscopy characterization extracellular vesicles from bovine placenta and peripheral blood mononuclear cells. *PLoS ONE.* (2020) 15:e0235214. doi: 10.1371/journal.pone.0235214
55. Holder BS, Tower CL, Jones CJ, Aplin JD, Abrahams VM. Heightened pro-inflammatory effect of preeclamptic placental microvesicles on peripheral blood immune cells in humans. *Biol Reprod.* (2012) 86:103. doi: 10.1095/biolreprod.111.097014
56. Sabapatha A, Gercel-Taylor C, Taylor DD. Specific isolation of placenta-derived exosomes from the circulation of pregnant women and their immunoregulatory consequences. *Am J Reprod Immunol.* (2006) 56:345–55. doi: 10.1111/j.1600-0897.2006.00435.x
57. Bulkin BJ. Raman spectroscopic study of human erythrocyte membranes. *Biochim Biophys Acta.* (1972) 274:649–51. doi: 10.1016/0005-2736(72)90214-3
58. Wallach DF, Verma SP. Raman and resonance-Raman scattering by erythrocyte ghosts. *Biochim Biophys Acta.* (1975) 382:542–51. doi: 10.1016/0005-2736(75)90221-7
59. Verma SP, Wallach DF. Carotenoids as a Raman-active probes of erythrocyte membrane structure. *Biochim Biophys Acta.* (1975) 401:168–76. doi: 10.1016/0005-2736(75)90301-6
60. Saha AK, Schmidt BR, Wilhelmy J, Nguyen V, Abugherir A, Do JK, et al. Red blood cell deformability is diminished in patients with Chronic Fatigue Syndrome. *Clin Hemorheol Microcirc.* (2019) 71:113–6. doi: 10.3233/CH-180469
61. Linderkamp O, Wu PY, Meiselman HJ. Deformability of density separated red blood cells in normal newborn infants and adults. *Pediatr Res.* (1982) 16:964–8. doi: 10.1203/00006450-198211000-00013
62. Fiedor J, Przetocki M, Siniarski A, Gajos G, Spiridis N, Freindl K, et al. β-carotene-induced alterations in haemoglobin affinity to O_2. *Antioxidants.* (2021) 10:451. doi: 10.3390/antiox10030451
63. Esfandyarpour R, Kashi A, Nemat-Gorgani M, Wilhelmy J, Davis RW. A nanoelectronics-blood-based diagnostic biomarker for myalgic encephalomyelitis/chronic fatigue syndrome (ME/CFS). *Proc Natl Acad Sci USA.* (2019) 116:10250–7. doi: 10.1073/pnas.1901274116
64. Germain A, Levine SM, Hanson MR. In-depth analysis of the plasma proteome in ME/CFS exposes disrupted ephrin-eph and immune system signaling. *Proteomes.* (2021) 9:6. doi: 10.3390/proteomes9010006
65. Nkiliza A, Parks M, Cseresznye A, Oberlin S, Evans JE, Darcey T, et al. Sex-specific plasma lipid profiles of ME/CFS patients and their association with pain, fatigue, and cognitive symptoms. *J Transl Med.* (2021) 19:370. doi: 10.1186/s12967-021-03035-6
66. Helwa I, Cai J, Drewry MD, Zimmerman A, Dinkins MB, Khaled ML, et al. A comparative study of serum exosome isolation using differential ultracentrifugation and three commercial reagents. *PLoS ONE.* (2017) 12:e0170628. doi: 10.1371/journal.pone.0170628

Conflict of Interest: The authors declare that the research was conducted in the absence of any commercial or financial relationships that could be construed as a potential conflict of interest.

Publisher's Note: All claims expressed in this article are solely those of the authors and do not necessarily represent those of their affiliated organizations, or those of the publisher, the editors and the reviewers. Any product that may be evaluated in this article, or claim that may be made by its manufacturer, is not guaranteed or endorsed by the publisher.

frontiers | Frontiers in Medicine

MINI REVIEW
published: 04 April 2022
doi: 10.3389/fmed.2022.831096

Circulating Bacterial DNA: A New Paradigm for Cancer Diagnostics

*Tamara Glyn and Rachel Purcell**

Department of Surgery, University of Otago, Christchurch, New Zealand

Cell-free DNA applications for screening, diagnosis and treatment monitoring are increasingly being developed for a range of different cancers. While most of these applications investigate circulating tumor DNA (ctDNA) or methylation profiles of ctDNA, circulating bacterial DNA (cbDNA) has also been detected in plasma and serum samples from cancer patients. Recent publications have the detection of cbDNA in studies of breast, gastric, colorectal, hepatocellular and ovarian cancers. In several cases, distinction between patients and healthy controls was possible, based on cbDNA profiles, in addition to potential prognostic value. A large pan-cancer study demonstrated the feasibility of cbDNA to distinguish between four types of cancer and healthy controls, even in patients with early-stage disease. While improvements in, and standardization of laboratory and bioinformatics analyses are needed, and the clinical relevance of cbDNA yet to be ascertained for each cancer type, cbDNA analysis presents an exciting prospect for future liquid biopsy screening and diagnostics in cancer.

Keywords: cancer, diagnostic test, bacterial DNA, microbiome, liquid biopsy, cell-free DNA

OPEN ACCESS

Edited by:
Bin Yuan,
Anhui Medical University, China

Reviewed by:
Chunlin Ou,
Central South University, China
Tara Patricia Hurst,
Birmingham City University,
United Kingdom

***Correspondence:**
Rachel Purcell
rachel.purcell@otago.ac.nz

Specialty section:
This article was submitted to Translational Medicine, a section of the journal Frontiers in Medicine

Received: *07 December 2021*
Accepted: *18 February 2022*
Published: *04 April 2022*

Citation:
Glyn T and Purcell R (2022) Circulating Bacterial DNA: A New Paradigm for Cancer Diagnostics. Front. Med. 9:831096. doi: 10.3389/fmed.2022.831096

The concept of a liquid biopsy for monitoring cancer progression or treatment response has become increasingly popular, largely due to technical improvements in the ability to measure and analyze small amounts of cell-free (cf) DNA and RNA in plasma, and is in clinical use in some diagnostic centers in the US and Europe. The advantages of a liquid biopsy approach include the minimal invasiveness of a blood test compared to tumor biopsy, and repeatability of testing over time (1). Circulating tumor DNA (ctDNA) containing tumor-specific mutations can be used to predict outcome and monitor response to treatment in several types of solid tumors, including melanoma and lung cancer, with many uses currently in clinical trial. However, a major drawback of current use is that a common cancer mutation must be identified in the primary tumor, and then this mutation must also be detectable in the tiny amount of ctDNA, a veritable "needle in a haystack."

Cell-free DNA acts like a genetic reservoir that carries genetic information from all cells within the body (2), including healthy and diseased cells and microbes (3). Applications of cfDNA sequencing in oncology have been increasingly explored (4, 5), however as of yet, little attention has been paid to the identification and characterization of circulating bacterial DNA (cbDNA) in the oncologic context. To date, identification of microbes in the circulatory system has mainly been applied to infectious disease and sepsis, where sequencing of cfDNA has improved detection of micro-organisms that are difficult to culture, and has augmented traditional culture techniques (6, 7). Emerging research in the field of cfDNA has identified highly divergent cbDNA in a variety of non-communicable diseases, including liver (8), metabolic (9), autoimmune (10), and cardiovascular disease (11, 12). Although the source, route of access and significance of this cbDNA in disease states has yet to be fully elucidated (3), several studies have identified DNA from common gut commensal bacteria in patient plasma samples.

Strong associations between alterations in the gut microbiome (dysbiosis) and numerous non-infectious diseases, including those mentioned previously, have been extensively reported in the literature. The role of the microbiome in cancer is no exception, with well-established links to disease progression and response to therapy in a wide variety of tumor types (13–15). Microbiome-based diagnostic testing and interventions are currently being investigated, and interest in the potential role of cbDNA in cancer has also increased in recent years. While the microbiome includes bacteria, viruses, fungi and archea, the bacterial component is the most well-studied, and this also holds true for studies carried out examining circulating DNA; hence, we focus on cbDNA in this review (**Figure 1**; **Table 1**).

The first reported study of cbDNA in cancer reported its potential as a prognostic indicator in a study of a small number of women with early-onset breast cancer (16). The authors reported that the cbDNA from both patients and healthy controls was predominantly bacterial in origin and limited to a small number of genera. A key finding of this study was that microbial taxa were more diverse in patients compared to controls. A patient with a similar cbDNA profile to that of healthy controls was disease-free after more than 10 years of follow-up. In contrast, patients with more diverse taxa had short disease-free survival, suggesting the potential for cbDNA as a prognostic indicator.

While the aforementioned study used a metagenomics approach to analyse cbDNA in cancer patients, several other studies have looked at the circulating microbiome using an amplicon sequencing method, namely 16S rRNA sequencing, or DNA detection of specific bacterial species of interest using PCR. 16S rRNA is commonly used in microbiome studies to define the bacterial taxonomic composition to the genus level and analyse diversity between samples or environmental conditions. Dong et al. used 16S rRNA sequencing of plasma samples to compare cbDNA from patients with gastric cancer, atypical hyperplasia, chronic gastritis and healthy controls (17). Alpha diversity was significantly lower in gastric cancer patients compared to chronic gastritis patients or healthy controls, and genus-level analysis showed similar profiles between gastric cancer and atypical hyperplasia. Significant correlations were also reported between circulating DNA from specific bacterial genera and clinical indices, such as lymphatic metastases and tumor. A similar approach used 16S rRNA sequencing data from serum samples from patients with hepatocellular cancer, cirrhosis and healthy controls (18). In this study, microbial diversity was also reduced in cancer patients compared to non-cancer patients and controls, with differences in relative abundance of taxa between patients with hepatocellular cancer and controls. A five microbial gene marker model, based on these initial findings, could differentiate cancer patients from controls with >80% accuracy.

Extracellular vesicles (EV) have also been shown to contain microbial DNA arising from the gut microbiome and this phenomena has been exploited to investigate bacterial EV-derived DNA in the circulation of patients with ovarian cancer (19). Comparison of 16S rRNA sequencing data uncovered a significant difference in the abundance of *Acinetobacter* between ovarian cancer patients compared to patients with benign ovarian tumors.

Research into the contribution of the gut microbiome to the development and progression of colorectal cancer (CRC) is an area of intense interest, given the proximity of colorectal tumors to the gut microbiome. Sequencing studies have highlighted the taxonomic differences in the microbiota of CRC patients compared to healthy controls and in tumor tissue compared to matched normal, while functional studies have identified potential mechanisms of action for certain bacterial species, such as *Bacteroides fragilis* and *Fusobacterium nucleatum* in colorectal carcinogenesis. Increased concentrations of cfDNA have been reported to correspond to higher stage in CRC (20), suggesting that tumor DNA is present in the circulation either as part of the haematogenous spread of the primary tumor or due to increased shedding of tumor DNA into the circulatory system from the metastatic site, which is predominantly the liver. Xiao et al. reported the use of metagenomic analysis of plasma samples to investigate the utility of cbDNA as a diagnostic marker in CRC (21). The study compared whole genome sequencing data from plasma samples of CRC and colorectal adenoma patients, and healthy volunteers and found that cbDNA profiles could distinguish between the three patient groups. While the cohorts were small, a classifier model based on 28 species successfully distinguished between the three groups using a separate validation cohort. Two separate studies from a Greek research group have reported the utility of measuring specific bacterial species in the blood, namely *E. coli*, *B. fragilis* and *C. albicans*, for prognostic (22) and predictive (23) purposes. They found that detection of DNA from these microbes using PCR was associated with metastatic disease and shorter survival, whereas the association with circulating tumor cells and response to therapy was less clear.

The most comprehensive pan-cancer study to date was recently published by Poore et al., and described how whole-genome sequencing data from blood and tissue microbiomes can discriminate between 33 different cancer types using data from The Cancer Genome Atlas (TCGA) (24). Using plasma samples from a separate cohort, the authors were also able to distinguish between healthy controls and four types of cancer using cbDNA signatures. A potentially transformational finding from this study was that the cbDNA signatures remained predictive of cancer type, even in Stage I and II cancers, and in cancers lacking any genomic alterations. This is an important point, as current circulating tumor DNA (ctDNA) analysis relies on detecting common genomic alterations that are present in the primary tumor, and implies that cbDNA may be a more sensitive and widely applicable cancer biomarker.

From the currently available literature, there is accumulating evidence that cbDNA may have diagnostic and/or prognostic value in cancer. However, the source of cbDNA in cancer, whether it be from direct shedding into the bloodstream from primary or metastatic tumors, intestinal barrier dysfunction (leaky gut), or other unidentified mechanisms, remains unclear, and future research should address the source and clinical importance of cbDNA in any given cancer type. As with microbiome analysis of other sample types, such as tumor tissue and stool samples, the analytical method (metagenomic, 16S amplicon-based or PCR) will greatly impact the findings and

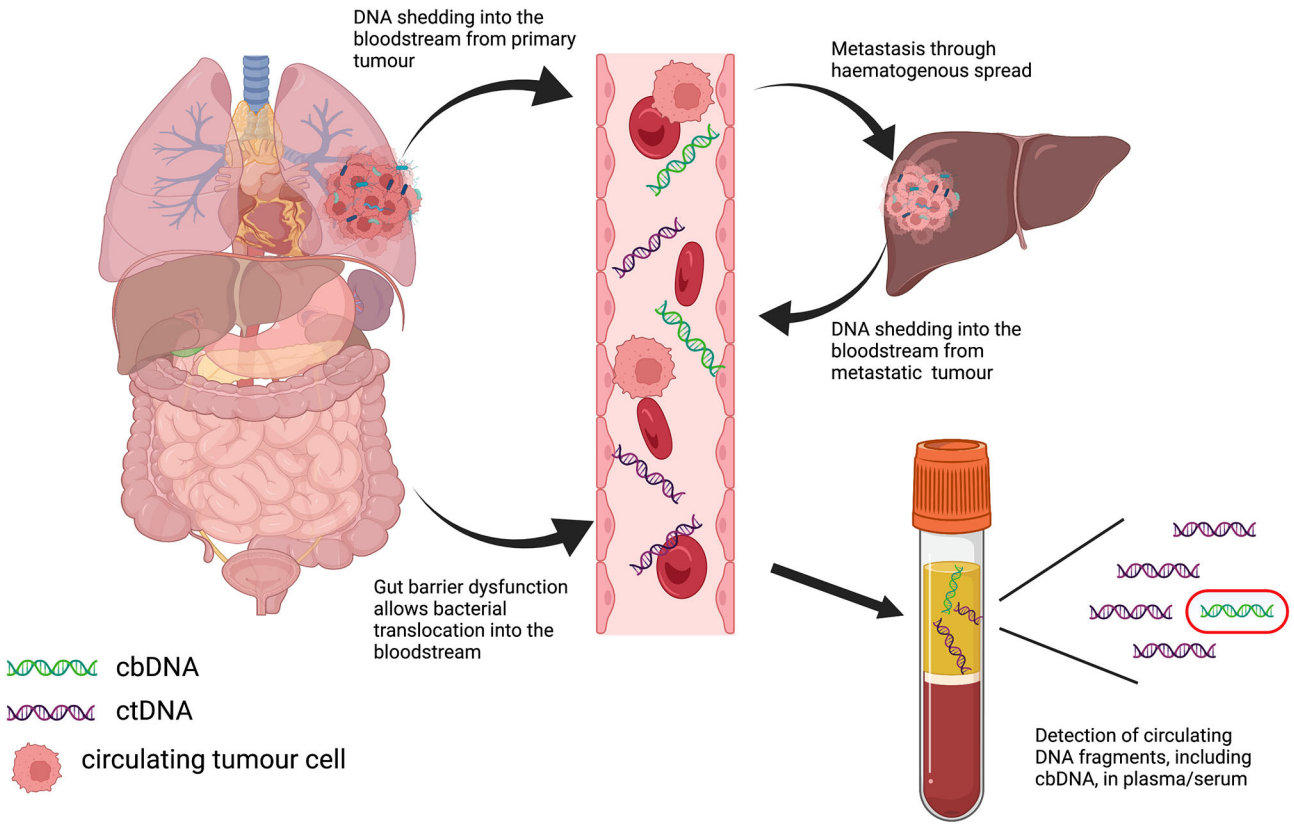

FIGURE 1 | Graphical depiction of potential routes of translocation of bacterial DNA into the bloodstream in cancer, and subsequent detection in plasma samples.

TABLE 1 | Published studies of circulating bacterial DNA in cancer.

Cancer type	Methodology	Main findings	Study
Breast	Metagenomics analysis of plasma DNA	cbDNA identified as a potential prognostic indicator	Huang et al. (16)
Gastric	16S rRNA sequencing of serum samples	Lower alpha diversity in cancer patients compared to controls; specific taxa correlate with clinical indices	Dong et al. (17)
Hepatocellular	16S rRNA sequencing of serum samples	Lower alpha diversity in cancer patients compared to controls; Differentially abundant taxa between cancer and controls; Development of 5-microbial gene marker panel	Cho et al. (18)
Ovarian	Metagenomic analysis of bacterial DNA derived from extra-cellular vesicles from serum samples	Different metagenomic profiles between cancer and controls. Acinetobacter common to cancer samples	Kim et al. (19)
Colorectal	Metagenomics analysis of plasma DNA	Slightly lower diversity in cancer samples; cbDNA mainly from gut-associated species; 28-species model could distinguish cancer from controls.	Xiao et al. (21)
	PCR amplification of specific microbial targets (*16S* gene, *E. coli*, *B. fragilis*, *C. albicans*) from whole blood samples	Higher detection of all fragments, except *E. coli*, in cancer samples; detection of microbial fragments associated with metastasis	Messaritakis et al. (22)
	PCR amplification of specific microbial targets (*16S* gene, *E. coli*, *B. fragilis*, *C. albicans*) from whole blood samples	Association between detection of microbial fragments and circulating tumor cells	Koulouridi et al. (23)
Multiple cancer types	Whole genome sequencing of whole blood samples; metagenomic analysis of plasma samples	Circulating microbial DNA profiles can distinguish between multiple types of cancer, including low-grade tumors; similar discrimination seen in plasma analysis	Poore et al. (24)

make comparisons difficult. Different sequencing platforms and bioinformatics tools will also influence the outcome of cbDNA studies, and benchmarking should be carried out to ascertain the best practice for cbDNA analysis. Consistent with other low-biomass microbiome studies, contamination is also an area of concern, whether physically introduced through analytical reagents and kits, or due to errors and inconsistencies in microbial DNA databases used for identification, and future efforts must include robust controls to mitigate these effects. The development of cbDNA as a diagnostic tool for cancer faces many challenges and is very early in its development, particularly compared to ctDNA, which has already shown to have clinical utility. However, future large-cohort studies with robust sequencing and analytical methodologies may identify potential clinical applications, particularly in the area of screening and early detection for a wide range of malignancies.

AUTHOR CONTRIBUTIONS

Both authors listed have made a substantial, direct, and intellectual contribution to the work and approved it for publication.

REFERENCES

1. De Rubis G, Rajeev Krishnan S, Bebawy M. Liquid biopsies in cancer diagnosis, monitoring, and prognosis. *Trends Pharmacol Sci.* (2019) 40:172–86. doi: 10.1016/j.tips.2019.01.006
2. Qin Z, Ljubimov VA, Zhou C, Tong Y, Liang J. Cell-free circulating tumor DNA in cancer. *Chin J Cancer.* (2016) 35:36. doi: 10.1186/s40880-016-0092-4
3. Kowarsky M, Camunas-Soler J, Kertesz M, De Vlaminck I, Koh W, Pan W, et al. Numerous uncharacterized and highly divergent microbes which colonize humans are revealed by circulating cell-free DNA. *Proc Natl Acad Sci USA.* (2017) 114:9623–8. doi: 10.1073/pnas.1707009114
4. Finotti A, Allegretti M, Gasparello J, Giacomini P, Spandidos DA, Spoto G, et al. Liquid biopsy and PCR-free ultrasensitive detection systems in oncology (Review). *Int J Oncol.* (2018) 53:1395–434. doi: 10.3892/ijo.2018.4516
5. Oellerich M, Schutz E, Beck J, Kanzow P, Plowman PN, Weiss GJ, et al. Using circulating cell-free DNA to monitor personalized cancer therapy. *Crit Rev Clin Lab Sci.* (2017) 54:205–18. doi: 10.1080/10408363.2017.1299683
6. Blauwkamp TA, Thair S, Rosen MJ, Blair L, Lindner MS, Vilfan ID, et al. Analytical and clinical validation of a microbial cell-free DNA sequencing test for infectious disease. *Nat Microbiol.* (2019) 4:663–74. doi: 10.1038/s41564-018-0349-6
7. Grumaz S, Stevens P, Grumaz C, Decker SO, Weigand MA, Hofer ST, et al. Next-generation sequencing diagnostics of bacteremia in septic patients. *Genome Med.* (2016) 8:73. doi: 10.1186/s13073-016-0326-8
8. Lelouvier B, Servant F, Paisse S, Brunet AC, Benyahya S, Serino M, et al. Changes in blood microbiota profiles associated with liver fibrosis in obese patients: a pilot analysis. *Hepatology.* (2016) 64:2015–27. doi: 10.1002/hep.28829
9. Chakaroun RM, Massier L, Heintz-Buschart A, Said N, Fallmann J, Crane A, et al. Circulating bacterial signature is linked to metabolic disease and shifts with metabolic alleviation after bariatric surgery. *Genome Med.* (2021) 13:105. doi: 10.1186/s13073-021-00919-6
10. Ho HE, Radigan L, Bongers G, El-Shamy A, Cunningham-Rundles C. Circulating bioactive bacterial DNA is associated with immune activation and complications in common variable immunodeficiency. *JCI Insight.* (2021) 6:e144777. doi: 10.1172/jci.insight.144777
11. Rajendhran J, Shankar M, Dinakaran V, Rathinavel A, Gunasekaran P. Contrasting circulating microbiome in cardiovascular disease patients and healthy individuals. *Int J Cardiol.* (2013) 168:5118–20. doi: 10.1016/j.ijcard.2013.07.232
12. Szeto CC, Kwan BC, Chow KM, Kwok JS, Lai KB, Cheng PM, et al. Circulating bacterial-derived DNA fragment level is a strong predictor of cardiovascular disease in peritoneal dialysis patients. *PLoS ONE.* (2015) 10:e0125162. doi: 10.1371/journal.pone.0125162
13. Vivarelli S, Salemi R, Candido S, Falzone L, Santagati M, Stefani S, et al. Gut microbiota and cancer: from pathogenesis to therapy. *Cancers.* (2019) 11:38. doi: 10.3390/cancers11010038
14. Fessler J, Matson V, Gajewski TF. Exploring the emerging role of the microbiome in cancer immunotherapy. *J Immunother Cancer.* (2019) 7:108. doi: 10.1186/s40425-019-0574-4
15. Xavier JB, Young VB, Skufca J, Ginty F, Testerman T, Pearson AT, et al. The cancer microbiome: distinguishing direct and indirect effects requires a systemic view. *Trends Cancer.* (2020) 6:192–204. doi: 10.1016/j.trecan.2020.01.004
16. Huang YF, Chen YJ, Fan TC, Chang NC, Chen YJ, Midha MK, et al. Analysis of microbial sequences in plasma cell-free DNA for early-onset breast cancer patients and healthy females. *BMC Med Genomics.* (2018) 11:16. doi: 10.1186/s12920-018-0329-y
17. Dong Z, Chen B, Pan H, Wang D, Liu M, Yang Y, et al. Detection of microbial 16S rRNA gene in the serum of patients with gastric cancer. *Front Oncol.* (2019) 9:608. doi: 10.3389/fonc.2019.00608
18. Cho EJ, Leem S, Kim SA, Yang J, Lee YB, Kim SS, et al. Circulating microbiota-based metagenomic signature for detection of hepatocellular carcinoma. *Sci Rep.* (2019) 9:7536. doi: 10.1038/s41598-019-44012-w
19. Kim SI, Kang N, Leem S, Yang J, Jo H, Lee M, et al. Metagenomic analysis of serum microbe-derived extracellular vesicles and diagnostic models to differentiate ovarian cancer and benign ovarian tumor. *Cancers.* (2020) 12:1309. doi: 10.3390/cancers12051309
20. Reece M, Saluja H, Hollington P, Karapetis CS, Vatandoust S, Young GP, et al. The use of circulating tumor DNA to monitor and predict response to treatment in colorectal cancer. *Front Genet.* (2019) 10:1118. doi: 10.3389/fgene.2019.01118
21. Xiao Q, Lu W, Kong X, Shao YW, Hu Y, Wang A, et al. Alterations of circulating bacterial DNA in colorectal cancer and adenoma: a proof-of-concept study. *Cancer Lett.* (2021) 499:201–8. doi: 10.1016/j.canlet.2020.11.030
22. Messaritakis I, Vogiatzoglou K, Tsantaki K, Ntretaki A, Sfakianaki M, Koulouridi A, et al. The prognostic value of the detection of microbial translocation in the blood of colorectal cancer patients. *Cancers.* (2020) 12:1058. doi: 10.3390/cancers12041058
23. Koulouridi A, Messaritakis I, Theodorakis E, Chondrozoumaki M, Sfakianaki M, Gouvas N, et al. Detection of circulating tumor cells and microbial dna fragments in stage iii colorectal cancer patients under three versus six months of adjuvant treatment. *Cancers.* (2021) 13:3552. doi: 10.3390/cancers13143552
24. Poore GD, Kopylova E, Zhu Q, Carpenter C, Fraraccio S, Wandro S, et al. Microbiome analyses of blood and tissues suggest cancer diagnostic approach. *Nature.* (2020) 579:567–74. doi: 10.1038/s41586-020-2095-1

Conflict of Interest: The authors declare that the research was conducted in the absence of any commercial or financial relationships that could be construed as a potential conflict of interest.

frontiers | Frontiers in Medicine

ORIGINAL RESEARCH
published: 10 May 2022
doi: 10.3389/fmed.2022.828954

Stress and Pain. Predictive (Neuro)Pattern Identification for Chronic Back Pain: A Longitudinal Observational Study

Pia-Maria Wippert[1,2], Laura Puerto Valencia[1] and David Drießlein[3]*

[1] Medical Sociology and Psychobiology, University of Potsdam, Potsdam, Germany, [2] Faculty of Health Sciences, Joint Faculty of the University of Potsdam, Brandenburg Medical School Theodor Fontane, and the Brandenburg University of Technology Cottbus-Senftenberg, Postdam, Germany, [3] Statistical Consulting Unit StaBLab, Ludwig-Maximilians-Universität München, Munich, Germany

Introduction: Low back pain (LBP) leads to considerable impairment of quality of life worldwide and is often accompanied by psychosomatic symptoms.

Objectives: First, to assess the association between stress and chronic low back pain (CLBP) and its simultaneous appearance with fatigue and depression as a symptom triad. Second, to identify the most predictive stress-related pattern set for CLBP for a 1-year diagnosis.

Methods: In a 1-year observational study with four measurement points, a total of 140 volunteers (aged 18–45 years with intermittent pain) were recruited. The primary outcomes were pain [characteristic pain intensity (CPI), subjective pain disability (DISS)], fatigue, and depressive mood. Stress was assessed as chronic stress, perceived stress, effort reward imbalance, life events, and physiological markers [allostatic load index (ALI), hair cortisol concentration (HCC)]. Multiple linear regression models and selection procedures for model shrinkage and variable selection (least absolute shrinkage and selection operator) were applied. Prediction accuracy was calculated by root mean squared error (RMSE) and receiver-operating characteristic curves.

Results: There were 110 participants completed the baseline assessments (28.2 ± 7.5 years, 38.1% female), including HCC, and a further of 46 participants agreed to ALI laboratory measurements. Different stress types were associated with LBP, CLBP, fatigue, and depressive mood and its joint occurrence as a symptom triad at baseline; mainly social-related stress types were of relevance. Work-related stress, such as "excessive demands at work"[b = 0.51 (95%CI -0.23, 1.25), p = 0.18] played a role for upcoming chronic pain disability. "Social overload" [b = 0.45 (95%CI -0.06, 0.96), p = 0.080] and "over-commitment at work" [b = 0.28 (95%CI -0.39, 0.95), p = 0.42] were associated with an upcoming depressive mood within 1-year. Finally, seven psychometric (CPI: RMSE = 12.63; DISS: RMSE = 9.81) and five biomarkers (CPI: RMSE = 12.21; DISS: RMSE = 8.94) could be derived as the most predictive

OPEN ACCESS

Edited by:
Jan Wilke,
Goethe University Frankfurt, Germany

Reviewed by:
Christian Compagnone,
University Hospital of Parma, Italy
Erika Baum,
Self-Employed, Biebertal, Germany

****Correspondence:***
Pia-Maria Wippert
wippert@uni-potsdam.de

Specialty section:
This article was submitted to Translational Medicine, a section of the journal Frontiers in Medicine

Received: *08 December 2021*
Accepted: *11 April 2022*
Published: *10 May 2022*

Citation:
Wippert P-M, Puerto Valencia L and Drießlein D (2022) Stress and Pain. Predictive (Neuro)Pattern Identification for Chronic Back Pain: A Longitudinal Observational Study. Front. Med. 9:828954. doi: 10.3389/fmed.2022.828954

pattern set for a 1-year prediction of CLBP. The biomarker set showed an apparent area under the curve of 0.88 for CPI and 0.99 for DISS.

Conclusion: Stress disrupts allostasis and favors the development of chronic pain, fatigue, and depression and the emergence of a "hypocortisolemic symptom triad," whereby the social-related stressors play a significant role. For translational medicine, a predictive pattern set could be derived which enables to diagnose the individuals at higher risk for the upcoming pain disorders and can be used in practice.

Keywords: allostatic load index, hair cortisol, low back pain, psychosocial moderators, hypocortisolemic symptom triad, stress types

INTRODUCTION

Low back pain (LBP) is the leading cause of disability worldwide. In 2015, approximately 540 million individuals were affected by activity-limiting LBP one time during the year (1). Although the prevalence rates are high, most individuals express no pathological causes and recover quickly, but around 8.5% develop non-specific persistent pain and disability (2). There is evidence that a range of biological, psychological, and social factors contribute to the development of chronic low back pain (CLBP) that accompany impaired function in daily life, reduced social participation, and financial welfare (3).

In particular, stress is discussed as an important risk factor for the development of non-specific CLBP within the yellow flag concept (4). Stress can be both a trigger or/and an amplifier of pain. For example, early life trauma [e.g., pain prone patients (5)] or the accumulation of adverse life events (6) have been described as triggers of pain. In fibromyalgia, stress was an amplifier for pain (7, 8). These two effects may be based on neuroendocrine and psychophysical responses during stress experience, influencing pain perception and pain processing by multiple neuro–functional processes.

During the stress response, neurotransmitters and hormones are released. These processes take place in the so-called stress triangle, which comprises the ergotropic (noradrenergic bundle: Locus coeruleus/sympathetic nervous system, or working system), the glandotropic system (paraventricular nucleus, pituitary gland, adrenal glands, glucocorticoid receptors, or energy supply system), and the trophotropic [raphe nuclei/parasympathetic nervous system, or recovery system (9, 10)]. In this triangle, allostasis and the adaption to stress are organized. During prolonged stress, the glandotropic system habituates, while the ergotropic system remains overactive. This asynchronous change of the involved systems disturbs the body's own tuned protective mechanism of allostasis and leads to an accumulation of physiological imbalances in the long-term, the so called allostatic load (11, 12). One example for such an imbalance regarding the association between stress and pain disorders is the reduced hypothalamus–pituitary–adrenal axis (HPA) activity due to cortisol deficiency (7, 8). This so-called "hypocortisolism symptom triad" comprises the joint occurrence of pain, depression, and fatigue as a result of chronic stress.

The interface between stress and pain is complex because of the various physiological pathways by which pain disorders could be triggered or amplified. First, the messenger substances released during stress exposure [e.g., neurochemical transmitters such as norepinephrine, acetylcholine, dopamine, cytokines, neuropeptides, glutamate, gamma-aminobutyric acid (GABA)] can influence nociception at the peripheral level (recruitment and sensitization) as well as nociceptive processing at the spinal level (signal cascades, afference, and efference) (13). These same transmitters play a further role in the modulation of the descending serotonergic and noradrenergic signals from the brainstem influencing the central reciprocal pain inhibition (14). Additionally, these chemical alterations reduce the amount of nerve growth factor which plays an important role in the differentiation of Aδ or C-fibers, their innervation density and therefore their transmission quality. Second, the stress response is controlled by a synaptic information from the various brain regions, such as the limbic system (including the hippocampus and amygdala) or the brain stem, all involved in the processing of pain stimuli (areas of the pain matrix). Prolonged stress exposure leads to altered connectivity in the pain matrix, to a reduction in cell proliferation and gray matter volume, and to a reorganization of the brain areas of the pain matrix (11, 15). Third, stress-related changes in the metabolic system (e.g., local fat depots, cholesterol in plasma membranes) can influence myelination, peripheral nerve functions (16) and pain transmission (17).

Accordingly, stress is associated with pain and is an important factor in developing chronic pain. However, which types of stress are most relevant and which underlying mechanisms is still not fully assessed. A more differentiated comprehension

Abbreviations: ALI, allostatic load index; AUC, area under the curve; BMI, body mass index; CLBP, chronic low back pain; CPI, chronic pain intensity; CUBP, chronic unspecific back pain; DHEA-S, serum dehydroepiandrosterone sulfate; DISS, pain disability; ECLIA, electrochemical luminescence immunoassay; EDTA, ethylendiaminetetraacetic acid; ECG, electrocardiogram; ELISA, enzyme-linked immunosorbent assay; ERI, effort–reward–imbalance questionnaire; GABA, gamma-aminobutyric acid; GPO–PAP, enzymatic color test; HADS-D, hospital anxiety and depression scale (German version); HbA1c, glycated hemoglobin; HCC, hair cortisol concentration; HDL, high density lipoprotein; HPA, hypothalamus–pituitary–adrenal axis; HOMA, homeostasis model assessment; ICAM-1, intercellular adhesion molecule 1; ILE, inventory of life-changing events; LASSO, least absolute shrinkage and selection operator; LBP, low back pain; LDL, low density lipoprotein; M1 . . . M4, measuring points; *n*, number of participants; n.s., not significant; POMS, profile of mood states, German short version; PSA3, parallel study 3; PSD10, parallel study 10; PSS, perceived stress scale; RMSE, root mean squared error; ROC, receiver-operating characteristic curves; TICS, Trier inventory for chronic stress; VAS, visual analog scale; VE, vital exhaustion; von Korff, chronic pain grade questionnaire; WHR, waist–hip ratio.

of such stress-related mechanisms on musculoskeletal problems and pain (15) would be necessary for the development of more concrete therapeutic treatments and diagnostics (12). Until now, mostly multimodal treatments are generic, and they are not considering specific personal needs. For this reason, a simultaneous assessment of different psychobiological interactions within the stress triangle would be beneficial. It would allow an identification of important predictive stress patterns in the development of chronic pain. In this regard, a predictive pattern set could be the basis for the derivation of a diagnostic tool, as it was done for burnout syndrome (10, 18). Here, a specific Neuropattern (10) diagnostic for burnout symptoms was developed, which is unfortunately still missing with regards to the non-specific pain syndromes (19). Therefore, this study aims to the following factors:

(1) Analyze the associations between different types of stress with non-specific current LBP and its influence on the development of non-specific CLBP as well as on fatigue and depressive mood (as individual outcomes or as symptom triad) within 1 year.

(2) Identify the most important stress types regarding the development of non-specific chronic LBP, fatigue, and depressive mood within 1 year.

(3) Identify the most predictive stress-related (neuro) pattern set regarding the development of non-specific CLBP within 1 year and to test its accuracy for diagnostics.

MATERIALS AND METHODS

Study Design

This observational longitudinal study includes four measurement time points (M1–M4), every 4 months, for a total duration of 1 year. The measurements consisted of hair samples and standardized questionnaires at each time point (M1–M4), as well as blood, urine samples together with clinical and laboratory parameters collected only at baseline (M1) and at the 1 year follow-up (M4) by medical nurses. The study was conducted between August 2013 and June 2015.

Participants

The individuals who were seeking back pain treatment at the Ernst von Bergmann clinic and the outpatient clinic of the University of Potsdam were recruited through announcement at the University Potsdam. In total, 140 subjects with intermittent non-specific LBP between 18 and 45 years of age took part in the study. The participation was not compensated, but the participants received their examination data and an individual stress profile after study completion. Convenience sampling technique was used.

Inclusion criteria were listed as follows: At least one episode ($\geq$4 days) of non-specific LBP in the last 12 months [according to the national treatment guideline NVL (20) and ICD-10: M50-54; LBP appearance defined as a minimum pain intensity score of 20 on a pain 100-point visual analog scale (VAS)], ability to understand the content of the study and to fill in a German questionnaire independently. Exclusion criteria were acute infections, pregnancy, hormonotherapy or the intake of certain types of medication (e.g., antibiotics and glucocorticoids), particular diseases (e.g., cardiovascular, metabolic diseases, thyroid disorders, vascular, malign, lung, liver or autoimmune diseases, hemophilia or psychological disorders, e.g., ICD-10: F70-79), inability to fill in a questionnaire and hair shorter than 2 cm. All participants signed a written informed consent after receiving written and oral information about the study by a study nurse.

The defined criteria on maximal age (individuals aged less than 45 years) was based on epidemiological studies, which indicated that the chronic courses after an acute LBP episode increased abruptly from 40 years of age. Therefore, with a preventive perspective, risk patterns for developing CLBP should be identified earlier (2).

Further, 46 individuals agreed and committed to the protocol of an additional comprehensive medical and laboratory test battery (see **Figure 1**). This protocol included avoiding certain foods (coffee, tea, alcohol, bananas, cheese, nuts, vanilla, and citrus fruits), intensive physical activity (>2 h/day) and medication, as well as collecting one's own urine from 7 p.m. to 7 a.m. (12 h) 1 day before the examination. The fasting blood tests (12 h food abstinence before blood withdrawal) and the medical examination took place between 7 a.m. and 8:00 a.m. at the University of Potsdam outpatient clinic. The blood samples were evaluated both at the outpatient clinic and clinic laboratory of the University of Potsdam, while the hair samples were analyzed in the laboratory of biopsychology of the Technical University of Dresden.

The sample size calculation for the minimal number of subjects required to detect an association between psychometric stress measures and pain disability was based on a medium effect size f^2, as well an α-error probability of 5%, a β-error probability of 20%, suggesting a $n = 85$ [power analysis by G*Power (21)]. The sample size calculation for detecting differences between stress physiological measures [allostatic load index (ALI) scores] within 1 year was based on a medium Cohen's d (0.5) effect size, as well an α-error probability of 5%, a β-error probability of 20%, suggesting a $n = 34$.

Ethics Approval

All clinical investigations, and measures have been conducted according to the principles expressed in the Declaration of Helsinki. The final ethics approval was provided on 6 May 2013 by the major institutional ethics review board of the University of Potsdam, Germany (No. 44/2012).

Assessments

The outcomes non-specific current and chronic LBP, fatigue, and depression were assessed by the standardized questionnaires at each measurement point (M1–M4, **Figure 2**). The exposure or predictor criteria stress was operationalized using both psychometric and physiological/biometric data. Further, sociodemographic and lifestyle factors [alcohol (glasses per week, type of alcohol); tobacco consumption (cigarettes a day, pack years); medication (type, daily dosage); physical activity (frequency per week, duration of unit, intensity according to the

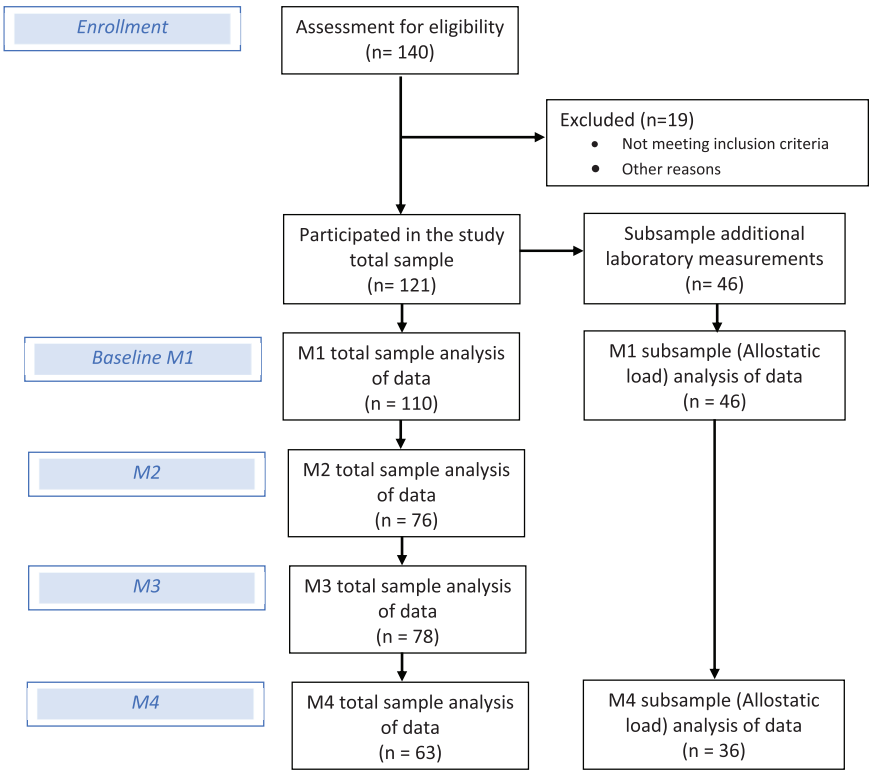

FIGURE 1 | Flow diagram of participants and sample analyzed data.

WHO guidelines (22)); sleep (quality on a 0-10 Likert scale)] were documented for all participants at all time points.

Outcomes

Chronic Pain

Chronic pain was assessed by the German version of the chronic pain grade questionnaire (23) [original English version (24)], which consisted of 7 items; 1 item considered the days of chronic pain and 6 items rated the chronic pain on an 11-point numeric rating scale). The original questionnaire showed a good internal consistency (Cronbach's alpha of 0.91) and good correlations ($p < 0.001$) with the equivalent dimensions of the Short Form 36 Health Survey Questionnaire (convergent validity) cross-sectional (25) and over time in a general practice population in Scotland (26). The translated German version used in our study showed good internal consistency (Cronbach's alpha reported was 0.82), it was significantly correlated with other clinical variables; moderate to high with instruments assessing patient's disability, and weak to moderate but significant with grading and staging chronic pain measurements, all within a population of primary care back pain patients (23). The questionnaire operationalized the severity of pain syndromes on the following two subscales: Characteristic pain intensity (CPI; 0 = "no pain" to 100 = "the worst pain imaginable") and the subjective pain disability (DISS; 0 = "no disability" to 100 = "I was incapable of doing anything") within the past 3 months. Both subscales were defined as the mean of three individual numeric rating scales questions. The high quality of the questionnaire was also confirmed in the context of the International Classification of Functioning, Disability and Health (ICF) (27). Cronbach's alpha in our sample was $\alpha = 0.92$. Current pain intensity (acute pain) was assessed by a horizontally presented 100-mm VAS [0 = "least possible pain" and 100 = "worst possible pain" (28)].

Fatigue

Fatigue was evaluated by the short version of the Maastricht questionnaire vital exhaustion (VE) [9-Item version (29, 30)] and the fatigue subscale from the German short version Profile of Mood States Questionnaire [POMS (31, 32)]. The VE questionnaire included nine questions about disturbed sleep, extreme fatigue, mental and physical irritability, and feelings of hopelessness with four possible answers ("no" = 0; "undetermined" = 1; "yes" = 2). The scale total score ranges from 0 to 18 (scores up to 4 indicate mild-to-moderate exhaustion). Cronbach's alpha in the sample was $\alpha = 0.71$. The POMS fatigue subscale included 7 items to be ranked on a 7-point Likert scale ranging from 1 (= "not at all") to 7 (= "very strong"), so the total score ranged from 0 to 42.

Depressive Mood

Depressive mood was assessed by one scale of the German short version of the POMS (31, 32). The depression subscale comprised 14 mood relevant adjectives that had to be ranked on a 7-point Likert scale ranging from 1 (= "not at all") to 7 (= "very strong").

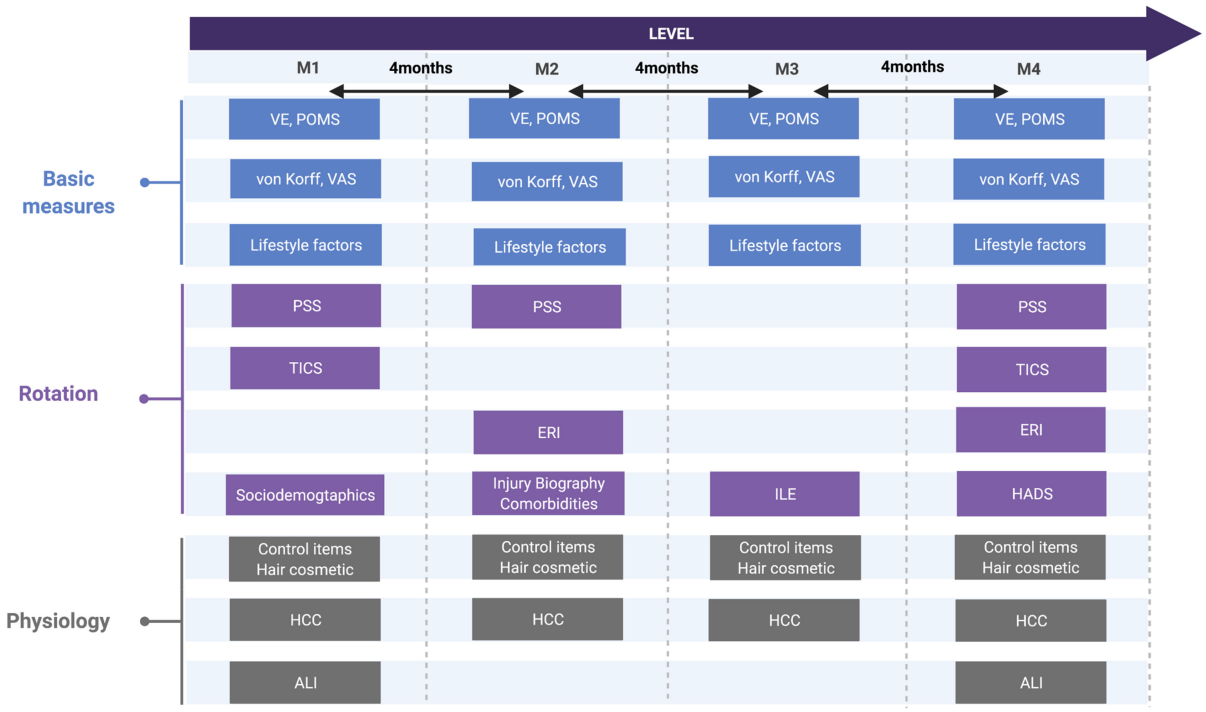

FIGURE 2 | Study design regarding psychometric and biological measures and its rotation. von Korff, CPG, chronic pain grade questionnaire; VAS, visual analog scale; VE, vital exhaustion, TICS: trier inventory of chronic stress; PSS, perceived stress scale; ERI, effort-reward-imbalance; ILE, inventory of life-changing events; POMS, profile of mood status; HADS, hospital anxiety depression scale, sociodemographic and lifestyle factors, hair cosmetic, comorbidities, ALI, allostatic load index; HCC, hair cortisol concentration.

Subjects completing the POMS were asked to reflect on their emotional states over the past week. The internal consistency in this sample was at $\alpha = 0.88$.

Predictor Criteria/Exposure

Stress was defined though psychometric and physiological variables as discussed in the following sub-sections:

Stress Psychometric Tests

The extensive psychometric test battery to measure the different stress types led to the decision to offer questionnaires only in rotation, not at every measurement point as far as feasible in form and content (assessment time frames and stability of attributes). The aim was to record a broader spectrum of stress-related assessments while preserving the motivation of the participants. Long-term prediction should not be limited due to this rotation as assessments at M1 and M4 were complete.

The types of stress were assessed by the following questionnaires: The "Trier Inventory of Chronic Stress" [TICS (33)] with its 57 items (rated on a 5-point Likert scale, from 0 = "never" to 4 = "very often") was used for the assessment of chronic stress in the past 3 months. The items are summed up to nine scales of potential chronic stress domains such as "work overload, social overload, pressure to perform, work discontent, excessive demands at work, lack of social recognition, social tensions, social isolation, and chronic worrying." Cronbach's alpha in the sample was $\alpha = 0.95$.

Perceived stress was assessed by the Perceived Stress Scale (PSS) (34, 35), a questionnaire with 10 items asking about stressful situations during the last 3 months (e.g., "In the past 3 months, how often have you been upset because of something that happened unexpectedly?"). The sum of the answers on a 5-point Likert scale (0 = never to 4 = "very often") gave information about the corresponding stress value ranging from 0 (no perceived stress) to 40 (high perceived stress). Cronbach's alpha was $\alpha = 0.86$.

Stress at work was measured by the effort–reward–imbalance questionnaire (ERI) (36), which consisted of 16 items measuring effort, reward (general reward, esteem, job promotion, and job security),and over-commitment on a 4-point Likert scale (0 = "not true at all" to 3 = "completely true"). Furthermore, an additional scale sets effort and reward into relation. Cronbach's alpha was $\alpha = 0.64$.

The inventory of life-changing events counts for type, number and load of critical life events (ILE) (37), whereby participants rate 40 critical life-events regarding occurrence, frequency, and year of occurrence. For the analysis here, only the scale for the total number of life events was used, for which all critical life-events over lifespan were summed up ranging from 0 to 40.

Stress burden was operationalized by a total stress index which was created by using a median split (score below the median = 0 or above the median = 1) for each stress questionnaire (TICS, PSS,

and ERI). Afterward, the zeros and ones were summed up to an individual stress index. As the total number of life events referred more to a lifespan perspective, the ILE was not sub-summarized in the total stress index, which included mainly tests covering the last months.

Stress Physiological Tests

Regarding the stress burden and the stress-related reactivity of different neurobiological interfaces, mostly analytical techniques and methods less susceptible to daily fluctuations were chosen (38). Also, ALI and hair cortisol concentration (HCC) were not dependent on daily fluctuations and cycle phases and were used in this study. The validity of the methods is well confirmed in different previous studies (39, 40). Within an additional pilot study, HCC and ALI showed a high test-retest reliability of the biomarkers within a 24-h time frame (38).

Allostatic load index represents the physiological load accumulated in the body through prolonged physical or mental stress (11, 12). Current standards suggest an evaluation of 24 indicators on different levels/systems to define total ALI (39). These indicators include the sympathetic nervous system (12-h urinary adrenaline and noradrenaline), parasympathetic nervous system (four heart rate variability indicators measured through electrocardiogram), HPA axis [12-h urinary cortisol and serum dehydroepiandrosterone sulfate (DHEA-S)], immune system [C-reactive protein and fibrinogen in plasma, interleukin-6, E-selectin, and intercellular adhesion molecule 1 (ICAM-1) in serum], cardiovascular system [systolic blood pressure (BPSYS) and diastolic blood pressure (BPDIA), resting heart rate], fat metabolism [body mass index, waist-hip ratio, triglycerides, high density lipoprotein (HDL) cholesterol, and low density lipoprotein (LDL) cholesterol] and sugar metabolism (glycohaemoglobin, fasting glucose and insulin) (41). The biomarkers assessed are discussed as in the following:

(1) Sympathetic nervous biomarkers: Analysis of urinary epinephrine and norepinephrine levels from 12-h overnight urine collections were performed *via* ELISA (norepinephrine RE5926, epinephrine RE59251, both ILB International GmbH Germany).

(2) Parasympathetic nervous biomarkers: Electrocardio graphic (Holter ECG, Schiller MT-101) electrodes were placed in the left lower quadrant on both shoulders. The ECG activity was monitored over an 11-min seated baseline period to assess heart rate variability indicators (SDNN, rMSSD, SDANN, SDNNidx) and resting pulse. The ECG was additionally standardized by breathing rhythm.

(3) The HPA biomarkers: Urine cortisol (μg/day) was measured with ELISA (RE52241, ILB International GmbH Germany). The DHEA-S was measured with ELISA (RE52181, TECAN Hydro Flex, ILB International GmbH Germany).

(4) Immune system biomarkers: Soluble E-selectin (sE-selectin), soluble ICAM-1 as well as interleukin-6 were assessed with enzyme-linked immunosorbent assays (BE59011 for sICAM-1, BE59061 for sE-selectin and BE58061 for IL-6; all from IBL International GmbH, Hamburg Germany). Further, C-reactive protein was measured by an immunoturbidimetry latex test (ABX Pentra 400) and Fibrinogen by traditional turbidimetry according to Claus (Siemens BCS XP).

(5) Cardiovascular biomarkers: Outpatient nurses assessed BPSYS and BPDIA 3 times, each separated by a 30-s rest period. The final blood pressure scores were obtained by averaging the values of the second and third measurements (BOSO BS 90 Blood pressure instrument, BOSCH + SOHN GmbH u. Co., KG, Jungingen, Germany).

(6) Lipid metabolic biomarkers: Triglycerides, HDL cholesterol and LDL cholesterol were assessed *via* enzymatic colorimetric assays (ABBOTT Architect ci8200; Abbott Laboratories, IL, United States). Furthermore, weight (Kern MPS scale; Kern & Sohn GmbH, Balingen, Germany), height (Seca 222 telescopic measuring rod; seca ag, Suisse) and waist/hip circumference (customary measuring tape) were measured, whereby hip circumference was assessed above the umbilicus at the narrowest point between ribs and the iliac crest, the hip circumference at the widest point across the buttocks. Body mass index (BMI) was calculated as weight in kg/(height in m)^2.

(7) Glucose metabolic biomarkers: Glycosylated hemoglobin (HbA1c) was analyzed with HPLC Bio–Rad Variant II (Bio–Rad Laboratories, CA, United States), fasting glucose *via* a hexokinase enzymatic reaction using the Roche Cobas 400 plus (Roche Diagnostics Ltd., Basel, Switzerland), and fasting insulin by an electrochemiluminescence enzyme immunoassay (ECLIA), using Roche Cobas 8000 Modul E620 (Roche Diagnostics Ltd., Basel, Switzerland). Insulin resistance [*via* Homeostasis model assessment index (HOMA)] was calculated using the formula: glucose [mg/dl] × insulin [μU/ml]/405).

The ALI was calculated by classifying each biomarker into quartiles within the sample: subjects with values in the fourth quartile (>75%) were assigned the value 1 (loaded), while the rest were assigned the value 0 (unloaded). Subsequently, ALI was created by summarizing the values for each test person across the 24 biomarkers [ALI-total (39, 40)]. Furthermore, stress burden was represented more differentiated by ALI-sub-scores as discussed in the following: The ALI-I (ALI-primary) represents mediators of the primary stress response and physiological adaptation (first defense line including cortisol, noradrenalin, adrenalin, and DHEA-S). The ALI-II (ALI-secondary) expresses secondary mediators which are involved in the prolonged maladaptation to chronic stress (HbA1c, ratio of total cholesterol to HDL, LDL, BPSYS, BPDIA, and waist–hip ratio (WHR) (40).

Hair cortisol concentration was extracted from two thin hair strands taken from the back of the head below the covering hair (diameter approximately 2 mm; length, 2 cm) and analyzed by ELISA, IBL RE62019 (42). One centimeter of hair corresponds to a 1-month measurement period, so a total of 4 months measurement period was covered retrospectively.

Statistical Analysis

Psychometric tests were prepared in line with test manuals. Physiological data were controlled for outliers and treated along analysis kit recommendations. The total stress burden

was represented by aggregated variables to map a subjective accumulation of stress (total stress index) and a biological accumulation of stress (ALI).

Descriptive and inferential statistics were applied to the data using SPSS (IBM 24.0) and R (43). Regarding the first study objective, the multiple linear regression models for main effects (M1 and M4) were used, whereby these calculations were controlled for age, sex, and the baseline value of the respective variable. For the second study objective, identification of the most predictive stress type concerning the symptom triad (pain, fatigue, and depressive mood), selection procedures for model shrinkage and variable selection [least absolute shrinkage and selection operator (LASSO) (44)] were performed. Considering the third study objective, LASSO was applied on a variable basis for selection of the best predictor set (once for biomarkers, once for psychometric items and then sub-summarized to a psycho and bio-set). Only metric indices were used for the LASSO analysis. Afterward, root mean squared error (RMSE) for prediction accuracy of each set, was calculated for pain intensity and disability. Finally, receiver-operating characteristic curve (ROC) and area under the curve (AUC) were performed to assess the model's ability to discriminate (only applied to the selected biomarker model). The dichotomous reference needed to compute ROC curves classifying low and high risk patients was defined as equal or more than 30% (45) of pain intensity and disability (corresponding to 30 points of the 100 on the von Korff scales). Further, the AUC corrected for optimism using bootstrapping (1,000 iterations) was reported. All LASSO models and RMSE calculations were controlled for lifestyle factors that had a significant effect on the outcomes during previously performed LASSO selections [age, sex, tobacco, alcohol consumption, sleep, sports activity (logarithmic sports variable), monthly income as well as baseline pain/fatigue or depressive mood].

RESULTS

Descriptive

A total of n = 121 participants took part in the longitudinal study, of which n = 110 were included in the analysis at baseline (age mean = 28.2 ± 7.5 years, 38.1% female, BMI mean = 23.4 ± 3.5 and WHR mean = 0.8 ± 0.7). On average, the subjects participated in physical activity (sports) 5.7 ± 5.1 h per week, 23.7% were academic professionals, 28.8% clerical support or sales workers, 10.9% craft and trades workers, 22% of the others included students. 35% reported a monthly net income under €1,250, 22.6% from €1,750–2,249, 17% from €1,250–1,749, and 24.5% over €2,250 (n = 53). The sample shows, on average, low to moderate values for chronic and acute pain complaints; at baseline CPI mean of 26.4 ± 18.3, DISS 12.2 ± 17.4, and current pain VAS 11.1 ± 16.8. Further, participants reported a moderate impairment due to fatigue and symptoms of depressive mood (see **Supplementary Table 1**). Physiological parameters were distributed within normal ranges. Allostatic load index was on average five with a maximum of 11 (possible range: 0–24, see **Supplementary Figure**).

Stress Types and Burden in the Prediction of Pain, Fatigue, and Depressive Mood (Objective 1)

In this objective, the influence of stress types on current and on the development of non-specific back pain, fatigue, and depressive mood in individual appearance or as symptom triad was investigated.

Stress and Back Pain

Cross-sectional results (baseline M1) show that social and work-related stress types such as "Social overload, Social tensions, Excessive demands at work, or Work overload (from TICS), Perceived stress (from PSS)," and total stress index were significantly associated with current LBP pain intensity. Regarding CLBP "Excessive demands at work, Social tensions, and Perceived stress" were significantly associated with CLBP intensity, while "Social tensions, Perceived stress, Over-commitment (from ERI)" and critical life events were associated with CLBP disability. Considering the 1-year prediction of the pain development (M1 to M4 longitudinal), the results differ considerably; CLBP intensity is predicted by Chronic Worrying and current LBP intensity by critical life events and HCC (see **Table 1**).

Stress and Fatigue

Chronic stress (all TICS scales), perceived stress, stress at work (Effort, Over-commitment) and total stress index showed associations to the current fatigue state measured in two different dimensions (VE and POMS, see **Table 1**). Regarding a 1-year prediction, work-related stress types such as "Pressure to perform, Work discontent, Effort, and Over-commitment" as well as physiological stress burden measured by the biomarker index allostatic load (ALI-secondary) had the strongest influence (see **Table 1**).

Stress and Depressive Mood

Cross-sectional results at baseline (M1) indicate that almost all chronic social stress types (TICS and PSS) and stress burden (total stress index) had an influence on the current mood. Moreover, these associations also referred to depressive mood in the future (upcoming 12 months) in the case of some work-related stress types (Over-commitment, Effort), although no biomarker association was found (see **Table 1**).

Stress and Symptom Triad

Including all p-levels ($p < 0.01$ up to $p < 0.05$), significant associations to the appearance of a symptom triad can be shown cross-sectionally for the stress burden (total stress index) and following stress types: "Social overload, Work overload, Excessive demands at work, Social tensions, and Perceived stress." An upcoming symptom triad (longitudinal) is best described by an influence of Over-commitment (see **Table 1** gray area).

TABLE 1 | Main effects: (regression coefficients ß) for the influence of types and burden of stress (psychometric and physiological measures) on the outcome criteria back pain, mood, and fatigue as well as symptom triad (gray marked).

	Back pain						Fatigue				Depressive mood	
	Disability[1]		Intensity[1]		VAS		Fatigue VE[2]		Fatigue[3]		Depression[2]	
	M1	M4	M1	M4	M1	M4	M1	M4	M1	M4	M1	M4
Chronic stress												
Work overload[4]	0.45	−0.09	0.43	−0.13	**0.54***	−0.52	**0.25****	−0.01	**0.48****	0.19	**0.36****	0.26
Social overload[4]	0.62#	0.09	0.52	0.22	**0.81***	−0.22	0.11	0.11	**0.70****	0.50#	**0.57****	0.39
Pressure to perform[4]	−0.06	−0.13	−0.03	−0.05	0.23	−0.21	0.16	0.16	**0.59****	**0.44***	**0.29***	0.32
Work discontent[4]	−0.47	0.42	−0.11	0.57	−0.15	−0.10	**0.18***	**0.28***	0.23	0.06	**0.35***	−0.06
Excessive demands at work[4]	0.74	0.23	**0.93***	0.60	**0.95***	−0.06	**0.40****	−0.14	**0.73****	−0.21	**0.71****	−0.33
Lack of social recognition[4]	0.74	0.18	0.57	1.10#	0.19	0.15	**0.30***	0.06	**1.06****	0.15	**0.99****	−0.54
Social tensions[4]	**1.38***	0.38	**1.08***	0.58	**1.09***	0.68	0.16	0.26	**0.96****	0.04	**0.63****	0.56
Social isolation[4]	−0.26	−0.08	−0.15	0.33	0.20	−0.54	**0.23***	−0.03	0.31	−0.44	**0.63****	−0.60#
Chronic worrying[4]	0.52	1.23#	0.88#	**1.36****	0.81#	1.12	**0.68****	0.19	**0.81****	0.03	**0.91****	0.07
Perceived stress[5]	**0.82****	0.65	**0.80****	0.56#	**0.59***	0.60	**0.37****	0.06	**0.58****	0.07	**0.62****	0.36
Stress at work												
Effort[6]	2.01#	0.97	1.13	1.05	1.70	0.76	**0.50***	0.33	0.85#	**1.53****	0.24	**1.32***
Reward[6]	−0.46	−0.34	−0.20	−0.83	−0.59	0.20	−0.15	−0.04	−0.19	−0.45	−0.28	−0.16
Over-commitment[6]	**1.17***	0.10	0.54	−0.08	0.50	−0.57	**0.37****	0.11	**0.57***	**0.78***	0.18	**0.80***
Critical life events[7]	**0.96***	−0.16	0.59	0.13	0.43	**1.20****	0.05	0.19#	0.25	0.32#	−0.05	0.38#
Stress burden												
Total stress index	0.69	−0.43	0.28	0.12	**1.51***	−1.73	**0.55****	0.38	**1.32****	0.65	**0.72***	0.28
Total allostatic load	0.65	−0.28	1.25	−0.31	0.74	0.76	0.03	0.24	−0.03	0.66#	−0.44	0.03
Primary allostatic load	−0.62	−1.81	0.39	−1.92	1.03	3.02	−0.31	0.42	−1.04	−0.04	−1.14	1.17
Secondary allostatic load	−0.19	1.63	1.59	1.20	0.71	1.70	0.11	0.35	−0.47	**2.05***	−1.20	1.06
HCC	−0.03	−0.12	−0.13	−0.10	0.10	**−0.38***	0.04	−0.01	0.01	0.09	0.04	0.00

*#p < 0.10, *p < 0.05, **p < 0.01, Bold values: p < 0.05, Linear Regression Models; adjusted by age, sex and baseline outcome (M1) in the case of M4. [1]Chronic pain grade questionnaire (DISS, CPI); [2]VE, vitale exhaustion; [3]POMS, profile of moods questionnaire; [4]TICS, trier inventory of chronic stress; [5]PSS, perceived stress scale; [6]ERI, effort-reward-imbalance-questionnaire, [7]ILE, the inventory of life-changing events.*

Inter-correlations regarding different stress types simultaneously within the multiple regression models are shown in **Figure 3**.

Most Important Stress Types for the Development of Pain, Fatigue, and Depressive Mood (Objective 2)

Considering the stricter LASSO model for the 1-year prediction of non-specific CLBP, only "Excessive demands at work (from TICS)" out of all psychometric scales remained predictive for the development of disability (b = 0.51 [95%CI -0.23, 1.25], p = 0.18). No biometric scale could be identified by LASSO models.

For the prediction of fatigue in the upcoming 12 months, no psychometric or biometric scale could be identified by LASSO models.

For the 1-year prediction of depressive mood out of all psychometric scales only "Social overload [b = 0.45 (95%CI -0.06, 0.96), p = 0.080)]and Over-commitment at work [b = 0.28 (95% CI -0.39, 0.95], p = 0.42] remained within the LASSO models." No biometric scale could be identified by LASSO models.

Most Predictive Pattern Set for 1-Year Prediction of Chronic Pain and Its Accuracy (Objective 3)

The LASSO models on item level identified the most predictive (bio)marker set for non-specific CLBP consisting of seven psychometric items (out of 95 items) and five biometric markers (out of 30 markers), see **Figure 4**. Regarding the prediction accuracy for 1 year of these psychometric items, a RMSE = 12.63 for chronic pain intensity and RMSE = 9.81 for the subjective pain disability were found. The biomarker set reached a RMSE of 12.21 for CLBP intensity and a RMSE of 8.94 for CLBP disability, which meant that the prediction for pain disability only differed 8.94 points from the finally observed pain value 12 months later on a 0–100 point from von Korff scale; the prediction error was adjusted for age, gender, tobacco, alcohol, drug use, and physical activity.

Discriminant validity of the biomarker-set (ROC curve) showed an apparent AUC of 0.93 (95%CI: 0.85–1.00) for chronic pain intensity with a corrected AUC of 0.88 (bootstrapping by 728 iterations), the apparent AUC for subjective pain disability

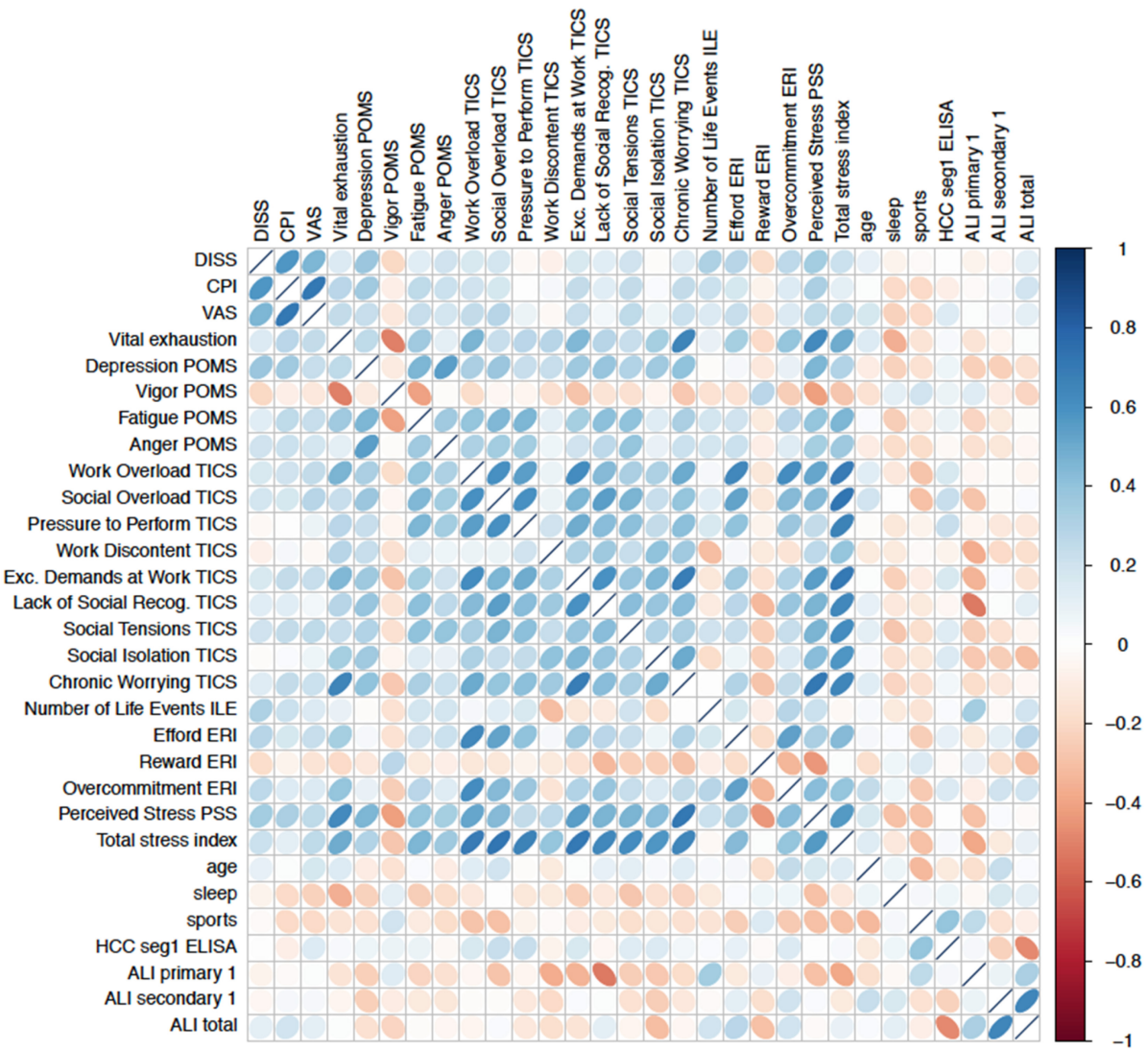

FIGURE 3 | Correlation matrix of baseline measures demonstrate intercorrelations between psychometric stress scales, lifestyle factors (sleep, age, and physical activity) and the outcome criteria. Intercorrelations limit the significance of prediction methods such as linear multiple regressions models in identifying best predictors.

was 1.00 (95%CI: 1.00–1.00) with a corrected AUC of 0.99 (bootstrapping by 950 iterations) (see **Figures 5A,B**) [only in the case of subjective pain disability, our developing sample had very few participants with disability scores higher than 30 ($n = 3$)].

DISCUSSION

Main Findings

First, the associations of stress with current LBP and the development on pain, fatigue, and depressive mood (individually as well as the appearance of a symptom triad) in chronic LBP (1-year after) were cross-sectionally and longitudinally evaluated through regression models. Associations of different types of stress (social, work-related, stress burden and critical life events) with current LBP or CLBP were observed. Furthermore, the same types of stress (excluding critical life events) together were associated with fatigue and mood in LBP (as symptom triad).

However, multiple inter-correlations between the stress types within the regression models were detected, indicating the need of statistical reduction procedures (such as LASSO).

Consequently, to be able to identify the most important stress type influencing the development of non-specific CLBP, fatigue, and depressive mood, a LASSO algorithm was applied. LASSO first results exhibited a reduction of influencing factors within a 1-year prediction; CLBP disability was best predicted by "Excessive demands at work," while depressive mood was predicted by "Social overload" and "Over-commitment at work." For fatigue, none of the stress types was selected.

Beyond and most relevant, to identify the most predictive stress-related (neuro)pattern set regarding the derivation of a diagnosis for the development of non-specific CLBP,

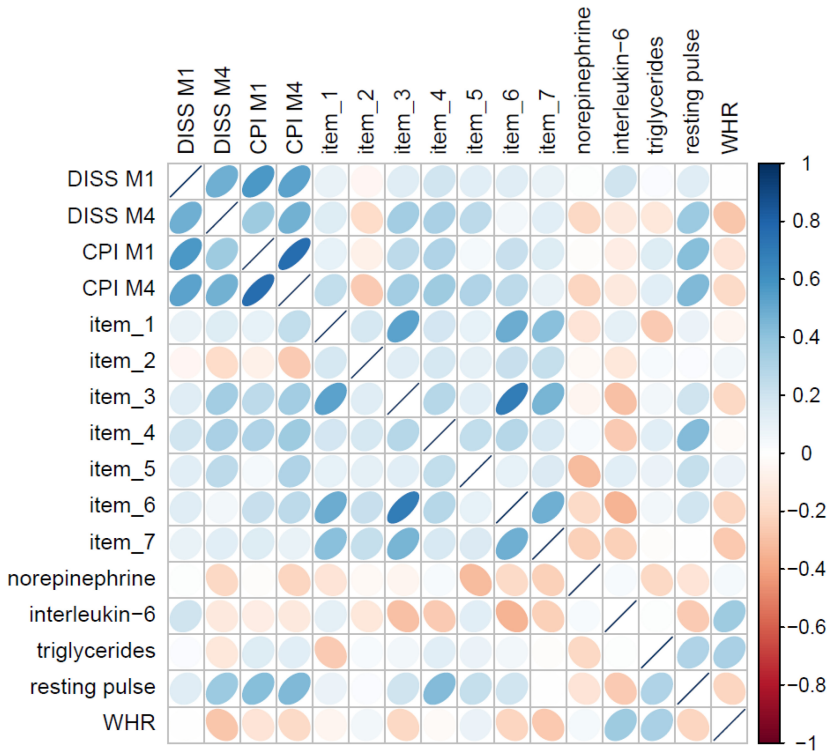

FIGURE 4 | Correlation matrix of the seven psychometric items and five biometric markers from the LASSO models with pain M1 and M4.

LASSO models were further applied. Here, the results offered a psychometric-set based of seven simple questions and a biomarker set of five biomarkers (norepinephrine, interleukin-6, triglycerides, WHR, and resting pulse) with good predictive value.

Comparison With Other Studies, Explanation of Findings

First results, similar to other studies, found that different types of stress (social, work-related, stress-burden, and critical life events) play a significant role in the appearance of current LBP and CLBP (46), fatigue, and depressive mood. Besides, a simultaneous presentation of pain, fatigue, and depressive mood as a symptom triad was observed. This symptom triad might be best explained by the overlapping neuroendocrinological mechanism between stress, pain, mood and fatigue (7, 8) and was in this study associated with almost all stress types at baseline.

A multimodal treatment strategy targeting physical and mental pain complaints—as it is often used in practice—make sense in light of these results. However, considering the influence of stress dimensions on CLBP after 1-year, results were less consistent. For example, on the one hand, the associations of chronic social, perceived or work-related stress and stress burden with current fatigue were observed, but only work-related stress and allostatic load (secondary ALI) seem to be relevant for the 1-year prediction. Similarly, current depressive mood was related to almost all stress types; but only work-related stress seemed to be relevant for the prediction of depressive mood within the upcoming year. Finally, the 12-months prediction of current pain was best described by the number of "critical life events" or "chronic worrying." Therefore, although the data confirmed stress as a trigger (5, 6, 46) or an amplifier of pain (7, 8), methodological questions about prediction accuracy including multiple inter-correlations remained.

Ergo, the issue of a limited prediction quality by regression methods was addressed by applying a LASSO algorithm regarding the development of non-specific CLBP, fatigue, and depressive mood (second objective of this study). Here, all variables (scales) entered the LASSO model at the same time (as competitors), whereby only the strongest predictor remained in the model. In this way, variables were compared with each other while simultaneously controlling for baseline value, age, gender, and lifestyle factors (tobacco, alcohol consumption, sleep, physical activity, and income). Therefore, inter-correlations are prohibited.

Within the regression models, various different work-related stress scales were relevant for the 1-year prediction of fatigue and depression in CLBP, besides one social stress scale and life events for back pain. Otherwise in LASSO models, only two scales from work-related stress and one social stress type were relevant for the prediction of pain and depression in CLBP.

The last results and most important, intended to derive the "best-of" diagnostic set for CLBP (focus solely on pain) showed a psychometric-set based on seven questions and a biomarker set of five, with similar good predictive value. The psychometric

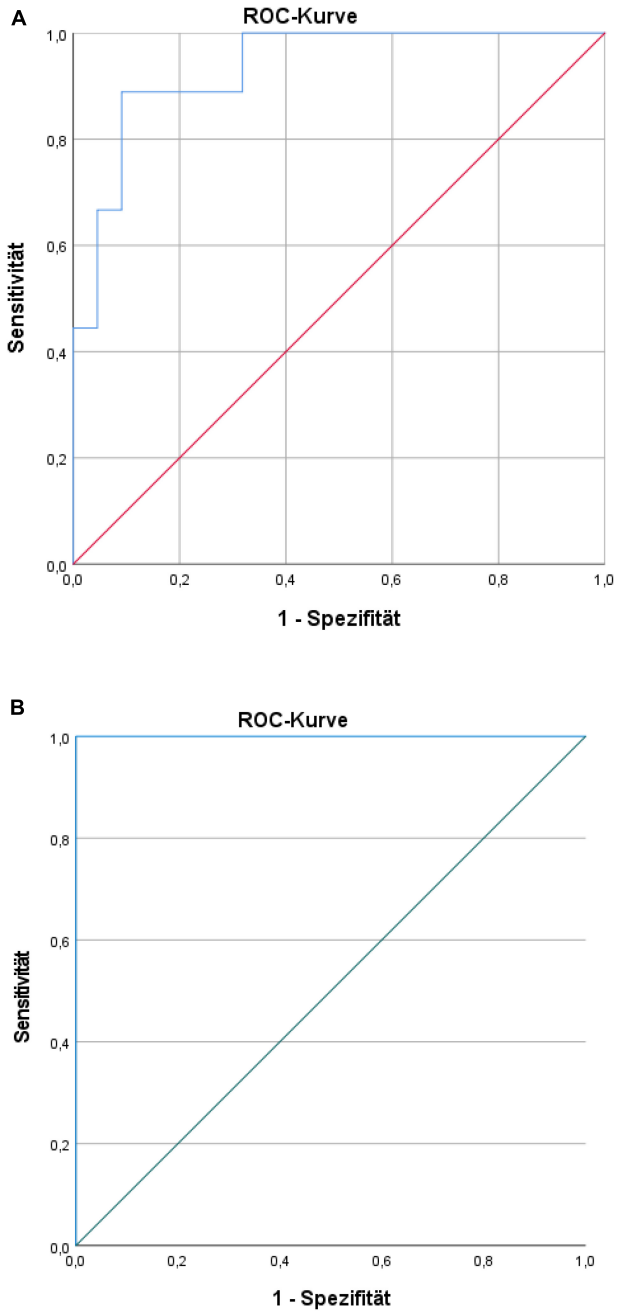

FIGURE 5 | (A) Receiver-operating characteristic (ROC) curve for characteristic pain intensity prediction of the biomarker set. **(B)** ROC curve for pain disability prediction of the biomarker set.

diagnostic set reported a good accuracy in comparison to other psychometric stress screeners within the context of back pain [e.g., RPI-S domain stress with a RSME of 16.72 for CPI and of 16.20 for DISS (47)]. Nevertheless, at the moment there were already diagnostic stress screeners with appropriate sensitivity and specify values and cut-off for treatment personalization (45, 48–51); hence, the focus in this study was on the further development of the biomarker diagnostic set. The RMSE of the biomarker-set of only eight points already indicated a very good diagnostic accuracy with a very accurate clinical prediction sensitivity and specificity for pain intensity as well as disability (AUC 0.93 and 0.99, respectively); however, only few cases reported more than 30 points in the case of pain disability. The five biomarkers included in the set suggested that the prediction model for pain intensity might reside in parameters from the ergotropic system. The over-activity of the ergotropic system was generally associated with high noradrenergic activity, high blood pressure, cardiovascular output, and hypertension (52) as well as a reaction of the glandotropic system corresponding to mobilization of energy stores and metabolic processes. These processes fit to the neurochemical inflammatory mediator noradrenaline and interleukin-6, as well as with the metabolic parameter triglycerides, WHR and resting pulse identified in the study (all together grouped as "bio-set" consisting of the markers norepinephrine, interleukin-6, triglycerides, WHR and resting pulse).

A relation of stress and pain intensity is also conceivable for the reason that noradrenergic neurons have a variety of influences on pain inhibition (14), as well as on fat metabolism and fatty acid concentration (e.g., prostaglandins), which conversely influence the thickness of myelin sheaths and axon length; hence, axonal transport (53). The effect of local storage lipids on peripheral nerves functions is described elsewhere (16). Largely, the results may be best interpreted as meaning that chronic stress can be associated with a habituation of the glandotropic system (with blunted cortisol response, slight hypocortisolism and symptom triad), so that, for example, the prostaglandin synthesis (54) or an over-activation of the ergotropic system could not be sufficiently inhibited (55). Although the results can be understood in such a way and fit to the physiological pathways described in the introduction, many questions remain unanswered and should be investigated in a broader frame (56), for example, in further studies with considerably larger sample size.

Strengths

The overall purpose of this study was to shed light on the question which stress types influence the development of non-specific CLBP. Considering that pain mostly appears in combination with fatigue and depressive symptoms these constructs were likewise included in the study. Further and most relevant, a diagnostic tool for practical use was introduced.

This longitudinal mixed-method study was conducted through a step-by-step methodologic procedure to approach the research questions in a structured way. Difficulties regarding different stress types simultaneously within multiple regression models (intercorrelations, see **Figure 3**) were addressed by specific selection models (e.g., LASSO), which allowed a selection of the most important predictor out of similar dimension within one model and the derivation of a diagnostic pattern set. This procedure highlighted the problems of translating theoretical knowledge into practical application, providing significant hints into understanding how stress influences the development of chronic pain disorders or the pain–fatigue–depression symptom triad and was a strength of this study.

Even though stress is often reported to be associated with pain becoming chronic (57), it becomes distinct in our results that the standard analytic models such as regression models and questionnaires alone might not be appropriate to deeply understand the underlying stress–pain pathways. Furthermore, regarding the stress-associated physiological scenarios on pain discussed at the beginning of this study, our data point out that a plain look at global biometric measures (ALI and HCC) may not be enough for an understanding and giving practical recommendations, even considering that mathematical algorithms were based and used across different biometric indices (58). Pain is represented in a network of biology, driven by genetic, cellular, neuronal, psycho-social or biomechanical triggers (59). For example, motor control exercise improves core stability, spine control, and muscle performance and is an important preventive or therapeutic strategy against CLBP (60, 61). On the other hand, neuromuscular adaption within the sensorimotor system is, for example, influenced by the neurotransmitter concentration. This reciprocal relationship between exercise, pain and stress (49) leads to limitations in the explanation of the pain network constellations (62). Therefore, the results in general may be conflicted or limited by methods or exclusion of important factors (e.g., physical activity/exercising, sleep) (59). Hence, in our LASSO model, physical activity was controlled for. Till today, it is only known that stress has an influence on pain becoming chronic; a remarkable finding from a twin study (63). However, less is known about developmental mechanisms and its detection at early stage for prevention (64). Indeed, our study recruited mostly young individuals to be able to follow them after an acute LBP episode, and so to derive a diagnostic tool with practical relevance.

Limitations

(1) Due to the observational longitudinal design, the study did not include dynamic test procedures which might be better suited to evaluate the HPA-axis and make conclusions about hypo- or hyperactivity.

(2) Restricted sample size of the biomarkers assessments: It was difficult to recruit individuals who were willing to take part in the arduous physiological measurements (e.g., 12-h urine sampling overnight and nutrition protocol).

(3) We did not collect information about menstrual cycle phases of women. Indices such as ALI and HCC were less dependent of these phases, but other biomarkers could be, although there was no hormonal biomarker of relevance.

(4) Relatively small sample size for the applied selection procedure (LASSO), although by its mathematical construction LASSO was able to handle cases where the number of predictors was equal or greater than the sample size. However, the computational test sequences with decision trees (C4.5 algorithm selection) already came to similar results in the preliminary study, corresponding with first literature results from epidemiological data sets (65).

(5) Finally, ROC curves were only calculated in the developmental sample. An external validation of the screening by cross-validation in future studies was needed, and which was essential for the next developmental step.

(6) Development of simplified biomarkers measurements was desired. Practical application remains limited till now.

CONCLUSION

The overall purpose of this study was to shed light on the question of how stress influences non-specific LBP and CLBP. It was shown that different stress types are associated with current LBP and CLBP, fatigue, and depressive mood. Work-related stress (e.g., Over-commitment, Excessive demands at work, and Effort), social stress (Chronic worrying and Social overload), and life events played role in the prediction of upcoming chronic pain complaints and depression in the next 12 months. Most importantly, it was possible to derive a "best-of" marker set for the prediction of a chronic course of LBP, once for psychometric items (7 items) and once for physiological markers (5 biomarkers). For the physiological marker set, additionally, a clinical prediction sensitivity and specificity was calculated with good accuracy. The psychometric items could be best sub-summarized under the broad concept of searching for sense of coherence in daily life, while the biomarker set gave information about possible mechanisms and physiological pathways between stress and pain, and the symptom triad. Finally, a step for step methodological procedure showed that very specific methods were needed to gain knowledge about these associations and their translation in clinical practice for an early screening of persons at risk for pain becoming chronic. One strength of this study was the presentation of the courses of different bio–psycho–social markers over 1 year in combination with lifestyle (such as sleep, physical activity, alcohol, tobacco, and medication) in regard to pain. Opening the possibility of formulating new research questions.

DATA AVAILABILITY STATEMENT

The raw data supporting the conclusions of this article will be made available by the authors, without undue reservation.

ETHICS STATEMENT

The studies involving human participants were reviewed and approved by the Ethic Board University of Potsdam. The patients/participants provided their written informed consent to participate in this study.

AUTHOR CONTRIBUTIONS

P-MW: design, survey, first draft, and study Principal Investigator. DD and LPV: statistical analyses. P-MW, DD, and LPV: critical revision of the manuscript for important intellectual content. All authors contributed to the article and approved the submitted version.

FUNDING

The study was funded by the German Federal Institute of Sport Science on behalf of the Federal Ministry of the Interior of Germany. Realized within MiSpEx – the National Research Network for Medicine in Spine Exercise (Grant No. 080102A/11-14). We further acknowledge the support of the Deutsche Forschungsgemeinschaft and the Open Access Publishing Fund of the University of Potsdam.

ACKNOWLEDGMENTS

We would like to thank Clemens Kirschbaum and Josefine Worseck for their support in the study methods, analysis and its coordination, as well as all involved employees of the Klinikum Ernst v. Bergmann laboratory in Potsdam, the laboratory of the Professorship for Biopsychology in Dresden, of the Professorship for Bioinformatics at the University of Potsdam and of the Institute for Statistics of the Ludwig-Maximilians-University Munich (Küchenhoff). Further, we express our gratitude to Sanne Houtenbos for valuable support in proofreading.

SUPPLEMENTARY MATERIAL

The Supplementary Material for this article can be found online at: https://www.frontiersin.org/articles/10.3389/fmed.2022.828954/full#supplementary-material

REFERENCES

1. Vos T, Allen C, Arora M, Barber R, Bhutta Z, Brown A, et al. Global, regional, and national incidence, prevalence, and years lived with disability for 310 diseases and injuries, 1990–2015: a systematic analysis for the Global Burden of Disease Study 2015. *Lancet.* (2016) 388:1545–602.
2. Henschke N, Kamper SJ, Maher CG. The epidemiology and economic consequences of pain. *Mayo Clin Proc.* (2015) 90:139–47. doi: 10.1016/j.mayocp.2014.09.010
3. Clark S, Horton R. Low back pain: a major global challenge. *Lancet.* (2018) 391:2302. doi: 10.1016/S0140-6736(18)30725-6
4. Nicholas MK, Linton SJ, Watson PJ, Main CJ. Early identification and management of psychological risk factors ("yellow flags") in patients with low back pain: a reappraisal. *Phys Ther.* (2011) 96:1–17. doi: 10.2522/ptj.20100224
5. Egle UT, Egloff N, von Känel R. Stressinduzierte Hyperalgesie (SIH) als Folge von emotionaler Deprivation und psychischer Traumatisierung in der Kindheit. Konsequenzen für die Schmerztherapie. *Der Schmerz.* (2016) 30:526–36. doi: 10.1007/s00482-016-0107-8
6. Wippert PM, Fliesser M, Krause M. Risk and protective factors in the clinical rehabilitation of chronic back pain. *J Pain Res.* (2017) 10:1569–79. doi: 10.2147/JPR.S134976
7. Chaudhuri A, Behan PO. Fatigue in neurological disorders. *Lancet.* (2004) 363:978–88. doi: 10.1016/s0140-6736(04)15794-2
8. Fries E. Hypocortisolemic disorders. In: Hellhammer DH, Hellhammer J editors. *Stress. The Brain-Body Connection. Key Issues in Mental Health*. (Vol. 174), Basel: Karger (2008). p. 60–77. doi: 10.1159/000119047
9. Hellhammer D, Hellhammer J. *Stress: The Brain-body Connection.* Basel: Karger Medical and Scientific Publishers (2008).
10. Hellhammer D, Hero T, Gerhards F, Hellhammer J. Neuropattern: A new translational tool to detect and treat stress pathology I. Strategical consideration. *Stress.* (2012) 15:479–87. doi: 10.3109/10253890.2011.644604
11. McEwen BS. Physiology and neurobiology of stress and adaptation: central role of the brain. *Physiol Rev.* (2007) 87:873–904. doi: 10.1152/physrev.00041.2006
12. Fava GA, McEwen BS, Guidi J, Gostoli S, Offidani E, Sonino N. Clinical characterization of allostatic overload. *Psychoneuroendocrinology.* (2019) 108:94–101. doi: 10.1016/j.psyneuen.2019.05.028
13. Van Houdenhove B, Luyten P. Beyond dualism: the role of life stress in chronic pain. *Pain.* (2005) 113:238–47. doi: 10.1016/j.pain.2004.10.010
14. Baumgärtner U. Nozizeptives System. Nozizeptoren, Fasertypen, spinale Bahnen und Projektionsareale. *Der Schmerz.* (2010) 24:105–13. doi: 10.1007/s00482-010-0904-4
15. McEwen BS, Kalia M. The role of corticosteroids and stress in chronic pain conditions. *Metabolism.* (2010) 59:9–15. doi: 10.1016/j.metabol.2010.07.012
16. Verheijen M, Chrast R, Burrola P, Lemke G. Local regulation of fat metabolism in peripheral nerves. *Genes Dev.* (2003) 17:2450–64. doi: 10.1101/gad.1116203
17. Amsalem M, Poilbout C, Ferracci G, Delmas P, Padilla F. Membrane cholesterol depletion as a trigger of Nav1.9 channel-mediated inflammatory pain. *EMBO J.* (2018) 37:e97349. doi: 10.15252/embj.201797349
18. Hellhammer D, Hellhammer J. *Neuropattern–a Step Towards Neurobehavioral Medicine*. Vol. 174. Basel: Karger (2008).
19. Treede RD, Rief W, Barke A, Aziz Q, Bennett MI, Benoliel R, et al. A classification of chronic pain for ICD-11. *Pain.* (2015) 156:1003–7.
20. Kanowski C, Schorr S, Schaefer C, Menzel C, Prien P, Vader I. *Nationale Versorgungsleitlinie Nicht-spezifischer Rückenschmerz. Leitlinienreport*. Berlin: äzq (2017).
21. Faul F, Erdfelder E, Lang AG, Buchner A. G* Power 3: a flexible statistical power analysis program for the social, behavioral, and biomedical sciences. *Behav Res Methods.* (2007) 39:175–91. doi: 10.3758/bf03193146
22. World Health Organisation [WHO]. *WHO Guidelines on Physical Activity and Sedentary Behaviour*. Geneva: World Health Organisation (2020).
23. Klasen BW, Hallner D, Schaub C, Willburger R, Hasenbring M. Validation and reliability of the German version of the chronic pain grade questionnaire in primary care back pain patients. *Psychosoc Med.* (2004) 1:Doc07–07.
24. Von Korff M, Ormel J, Keefe FJ, Dworkin SF. Grading the severity of chronic pain. *Pain.* (1992) 50:133–49. doi: 10.1016/0304-3959(92)90154-4
25. Smith BH, Penny KI, Purves AM, Munro C, Wilson B, Grimshaw J, et al. The Chronic Pain Grade questionnaire: validation and reliability in postal research. *Pain.* (1997) 71:141–7. doi: 10.1016/s0304-3959(97)03347-2
26. Elliott AM, Smith BH, Smith WC, Chambers WA. Changes in chronic pain severity over time: the Chronic Pain Grade as a valid measure. *Pain.* (2000) 88:303–8. doi: 10.1016/S0304-3959(00)00337-7
27. Dixon D, Pollard B, Johnston M. What does the chronic pain grade questionnaire measure? *Pain.* (2007) 130:249–53. doi: 10.1016/j.pain.2006.12.004
28. Scott J, Huskisson EV. Vertical or horizontal visual analogue scales. *Ann Rheum Dis.* (1979) 38:560. doi: 10.1136/ard.38.6.560
29. Appels A, Hoppener P, Mulder P. A questionnaire to assess premonitory symptoms of myocardial infarction. *Int J Cardiol.* (1987) 17:15–24. doi: 10.1016/0167-5273(87)90029-5
30. von Kaenel R, Frey K, Fischer J. Independent relation of vital exhaustion and inflammation to fibrinolysis in apparently healthy subjects. *Scand Cardiovasc J.* (2004) 38:28–32. doi: 10.1080/14017430310015884
31. Albani C, Blaser G, Geyer M, Schmutzer G, Brähler E, Bailer H, et al. [The German short version of "Profile of Mood States" (POMS): psychometric evaluation in a representative sample]. *Psychother Psychosom Med Psychol.* (2005) 55:324–30.
32. McNair DM. *Manual Profile of Mood States*. San Diego, CA: Educational & Industrial testing service (1971).
33. Schulz P, Schlotz W, Becker P. *Trierer Inventar zum Chronischen Stress (TICS)*. Göttingen: Hofgrefe (2004).
34. Büssing A. *Translation of Cohen's 10 item Perceived Stress Scale (PSS)*. Witten: University of Witten/Herdecke (2011).

35. Cohen S, Williamson G. Perceived stress in probability sample of the United States. In: Spacapan S, Oskamp S editors. *The Social Psychology of Health*. Newbury Park, CA: Sage (1988). p. 31–67.
36. Siegrist J, Starke D, Chandola T, Godin I, Marmot M, Niedhammer I, et al. The measurement of effort-reward imbalance at work: European comparisons. *Soc Sci Med.* (2004) 58:1483–99. doi: 10.1016/S0277-9536(03)00351-4
37. Siegrist J, Geyer S. Inventar lebensverändernder ereignisse. In: Siegrist J, Geyer S editors. *Zusammenstellung Sozialwissenschaftlicher Items und Skalen*. Mannheim: GESIS–Leibniz-Institut für Sozialwissenschaften (1997).
38. Wippert P-M, Honold J, Wang V, Kirschbaum C. Assessment of chronic stress: comparison of hair biomarkers and allostatic load indices. *Psychol Res.* (2014) 4:517–24.
39. Gruenewald TL, Karlamangla AS, Hu P, Stein-Merkin S, Crandall C, Koretz B, et al. History of socioeconomic disadvantage and allostatic load in later life. *Soc Sci Med.* (2012) 74:75–83. doi: 10.1016/j.socscimed.2011.09.037
40. Seeman TE, McEwan BS, Rowe JW, Singer BH. Allostatic load as a marker of cumulative biological risk: MacArthur studies of successful aging. *Proc Natl Acad Sci USA.* (2001) 98:4770–5. doi: 10.1073/pnas.081072698
41. Juster RP, McEwen BS, Lupien SJ. Allostatic load biomarkers of chronic stress and impact on health and cognition. *Neurosci Biobehav Rev.* (2010) 35:2–16. doi: 10.1016/j.neubiorev.2009.10.002
42. Dressendörfer RA, Kirschbaum C, Rohde W, Stahl F, Strasburger CJ. Synthesis of a cortisol-biotin conjugate and evaluation as a tracer in an immunoassay for salivary cortisol measurement. *J Steroid Biochem Mol Biol.* (1992) 43:683–92. doi: 10.1016/0960-0760(92)90294-s
43. R Core Team. *R: A Language and Environment for Statistical Computing*. Vienna: R Foundation for Statistical Computing (2019).
44. Tibshirani R. Regression shrinkage and selection via the lasso. *J R Stat Soc B.* (1996) 58:267–88. doi: 10.1111/j.2517-6161.1996.tb02080.x
45. Karran EL, McAuley JH, Traeger AC, Hillier SL, Grabherr L, Russek LN, et al. Can screening instruments accurately determine poor outcome risk in adults with recent onset low back pain? A systematic review and meta-analysis. *BMC Med.* (2017) 15:13.
46. Puschmann A-K, Drießlein D, Beck H, Arampatzis A, Catalá MM, Schiltenwolf M, et al. Stress and self-efficacy as long-term predictors for chronic low back pain: a prospective longitudinal study. *J Pain Res.* (2020) 13:613–21. doi: 10.2147/JPR.S223893
47. Wippert P-M, Puschmann A-K, Drießlein D, Arampatzis A, Banzer W, Beck H, et al. Development of a risk stratification index and a risk prevention index for chronic low back pain in primary care. focus: yellow flags (MiSpEx network). *Pain Rep.* (2017) 2:e623. doi: 10.1097/PR9.0000000000000623
48. Wippert P-M, Puschmann A-K, Drießlein D, Banzer W, Beck H, Schiltenwolf M, et al. Personalized treatment suggestions: validity and applicability of the risk-prevention-index social in low back pain exercise treatments. *J Clin Med.* (2020) 9:1197. doi: 10.3390/jcm9041197
49. Wippert P-M, Niederer D, Drießlein D, Beck H, Banzer W, Schneider C, et al. Moderators and Mediators of sensorimotor exercise in low back pain: a randomized controlled trial. *Front Psychiatry Psychos Med.* (2021) 12:1034. doi: 10.3389/fpsyt.2021.629474
50. Hill JC, Whitehurst DGT, Lewis M, Bryan S, Dunn KM, Foster NE, et al. Comparison of stratified primary care managment for low back pain with current best practice (STarTBack): a randomised controlled trial. *Lancet.* (2011) 378:1560–71. doi: 10.1016/S0140-6736(11)60937-9
51. Traeger AC, Henschke N, Hubscher M, Williams CM, Kamper SJ, Maher CG, et al. Estimating the risk of chronic pain: development and validation of a prognostic model (pickup) for patients with acute low back pain. *PLoS Med.* (2016) 13:e1002019. doi: 10.1371/journal.pmed.1002019
52. Klingmann PO, Hellhammer DH. Noradrenergic and sympathetic disorders. In: Hellhammer D, Hellhammer J editors. *HStress: the Brain-Body Connection*. Basel: Karger Medical and Scientific Publishers (2008). p. 78–90. doi: 10.1159/000119048
53. Huang K, Ji Y, Huang J, Chen Q. Calculating myelin sheath thickness with watershed algorithm for biological analysis. *J Teknol.* (2015) 78:21–7.
54. Santini G, Patrignani P, Sciulli MG, Seta F, Tacconelli S, Panara MR, et al. The human pharmacology of monocyte cyclooxygenase 2 inhibition by cortisol and synthetic glucocorticoids. *Clin Pharmacol Ther.* (2001) 70:475–83. doi: 10.1067/mcp.2001.119213
55. Schommer NC, Hellhammer DH, Kirschbaum C. Dissociation between reactivity of the hypothalamus-pituitary-adrenal axis and the sympathetic-adrenal-medullary system to repeated psychosocial stress. *Psychosom Med.* (2003) 63:450–60. doi: 10.1097/01.psy.0000035721.12441.17
56. Hendrix J, Nijs J, Ickmans K, Godderis L, Ghosh M, Polli A. The interplay between oxidative stress, exercise, and pain in health and disease: potential role of autonomic regulation and epigenetic mechanisms. *Antioxidants.* (2020) 9:1166. doi: 10.3390/antiox9111166
57. Mickle AM, Garvan C, Service C, Pop R, Marks J, Wu S, et al. Relationships between pain, life stress, sociodemographics, and cortisol: contributions of pain intensity and financial satisfaction. *Chronic Stress.* (2020) 4:2470547020975758. doi: 10.1177/2470547020975758
58. Reckziegel D, Vachon-Presseau E, Petre B, Schnitzer TJ, Baliki MN, Apkarian AV. Deconstructing biomarkers for chronic pain: context- and hypothesis-dependent biomarker types in relation to chronic pain. *Pain.* (2019) 160:S37–48. doi: 10.1097/j.pain.0000000000001529
59. Borsook D, Youssef AM, Simons L, Elman I, Eccleston C. When pain gets stuck: the evolution of pain chronification and treatment resistance. *Pain.* (2018) 159:2421–36. doi: 10.1097/j.pain.0000000000001401
60. Oliveira CB, Franco MR, Maher CG, Tiedemann A, Silva FG, Damato TM, et al. The efficacy of a multimodal physical activity intervention with supervised exercises, health coaching and an activity monitor on physical activity levels of patients with chronic, nonspecific low back pain (Physical Activity for Back Pain (PAyBACK) trial): study protocol for a randomised controlled trial. *Trials.* (2018) 19:1–10. doi: 10.1186/s13063-017-2436-z
61. Saragiotto BT, Maher CG, Yamato TP, Costa LO, Menezes Costa LC, Ostelo RW, et al. Motor control exercise for chronic non-specific low back pain. *Chocrane Datab Syst Rev.* (2016) 8:CD012004.
62. Wippert P-M, Wiebking C. Stress and alterations in the pain matrix: a biopsychosocial perspective on back pain, its prevention and treatment. *Int J Environ Res Public Health.* (2018) 15:785. doi: 10.3390/ijerph15040785
63. Suri P, Boyko EJ, Smith NL, Jarvik JG, Jarvik GP, Williams FMK, et al. Post-traumatic Stress disorder symptoms are associated with incident chronic back pain: a longitudinal twin study of older male veterans. *Spine.* (2019) 44:1220–7. doi: 10.1097/BRS.0000000000003053
64. Palermo TM. Pain prevention and management must begin in childhood: the key role of psychological interventions. *Pain.* (2020) 161:S114–21. doi: 10.1097/j.pain.0000000000001862
65. Slade GD, Sanders AE, By K. Role of allostatic load in sociodemographic patterns of pain prevalence in the US population. *J Pain.* (2012) 13:666–75. doi: 10.1016/j.jpain.2012.04.003

Conflict of Interest: The authors declare that the research was conducted in the absence of any commercial or financial relationships that could be construed as a potential conflict of interest.

frontiers | Frontiers in Medicine

BRIEF RESEARCH REPORT
published: 19 May 2022
doi: 10.3389/fmed.2022.886485

Efficient Assay and Marker Significance of NAD^+ in Human Blood

*Natalia V. Balashova[1,2], Lev G. Zavileyskiy[3], Artem V. Artiukhov[4,5], Leonid A. Shaposhnikov[6], Olga P. Sidorova[7], Vladimir I. Tishkov[6,8], Angela Tramonti[9], Anastasia A. Pometun[6,8] and Victoria I. Bunik[3,4,5]**

[1] Department of Clinical Laboratory Diagnostics, Faculty of Advanced Medicine, M.F. Vladimirsky Moscow Regional Research and Clinical Institute (MONIKI), Moscow, Russia, [2] Department of Dietetics and Clinical Nutritionology, Faculty of Continuing Medical Education, RUDN Medical Institute, Moscow, Russia, [3] Faculty of Bioengineering and Bioinformatics, Lomonosov Moscow State University, Moscow, Russia, [4] Department of Biokinetics, A. N. Belozersky Institute of Physico-Chemical Biology, Lomonosov Moscow State University, Moscow, Russia, [5] Department of Biochemistry, Sechenov University, Moscow, Russia, [6] Department of Chemical Enzymology, Faculty of Chemistry, Lomonosov Moscow State University, Moscow, Russia, [7] Department of Neurology, Faculty of Advanced Medicine, M.F. Vladimirsky Moscow Regional Research and Clinical Institute (MONIKI), Moscow, Russia, [8] Bach Institute of Biochemistry, Federal Research Centre "Fundamentals of Biotechnology" of the Russian Academy of Sciences, Moscow, Russia, [9] Institute of Molecular Biology and Pathology, Italian National Research Council, Department of Biochemical Sciences "A. Rossi Fanelli," Sapienza University of Rome, Rome, Italy

OPEN ACCESS

Edited by:
Matteo Becatti, University of Firenze, Italy

Reviewed by:
Baris Binay, Gebze Technical University, Turkey
Mathias Mericskay, Institut National de la Santé et de la Recherche Médicale (INSERM), France
Mirella L. Meyer-Ficca, Utah State University, United States

***Correspondence:**
Victoria I. Bunik
bunik@belozersky.msu.ru

Specialty section:
This article was submitted to Translational Medicine, a section of the journal Frontiers in Medicine

Received: *28 February 2022*
Accepted: *07 April 2022*
Published: *19 May 2022*

Citation:
Balashova NV, Zavileyskiy LG, Artiukhov AV, Shaposhnikov LA, Sidorova OP, Tishkov VI, Tramonti A, Pometun AA and Bunik VI (2022) Efficient Assay and Marker Significance of NAD^+ in Human Blood. Front. Med. 9:886485. doi: 10.3389/fmed.2022.886485

Oxidized nicotinamide adenine dinucleotide (NAD^+) is a biological molecule of systemic importance. Essential role of NAD^+ in cellular metabolism relies on the substrate action in various redox reactions and cellular signaling. This work introduces an efficient enzymatic assay of NAD^+ content in human blood using recombinant formate dehydrogenase (FDH, EC 1.2.1.2), and demonstrates its diagnostic potential, comparing NAD^+ content in the whole blood of control subjects and patients with cardiac or neurological pathologies. In the control group ($n = 22$, 25–70 years old), our quantification of the blood concentration of NAD^+ (18 μM, minimum 15, max 23) corresponds well to NAD^+ quantifications reported in literature. In patients with demyelinating neurological diseases ($n = 10$, 18–55 years old), the NAD^+ levels significantly ($p < 0.0001$) decrease (to 14 μM, min 13, max 16), compared to the control group. In cardiac patients with the heart failure of stage II and III according to the New York Heart Association (NYHA) functional classification ($n = 24$, 42–83 years old), the blood levels of NAD^+ (13 μM, min 9, max 18) are lower than those in the control subjects ($p < 0.0001$) or neurological patients ($p = 0.1$). A better discrimination of the cardiac and neurological patients is achieved when the ratios of NAD^+ to the blood creatinine levels, mean corpuscular volume or potassium ions are compared. The proposed NAD^+ assay provides an easy and robust tool for clinical analyses of an important metabolic indicator in the human blood.

Keywords: NAD^+ in human blood, formate dehydrogenase, cardiac patient, neurological patient, metabolic markers, Charcot-Marie-Tooth disease

INTRODUCTION

Nicotinamide adenine dinucleotide (NAD, the sum of the oxidised NAD^+ and reduced NADH forms) is a very important biological molecule which is involved in various metabolic and signaling pathways. Undergoing reversible reduction to NADH in many redox reactions, NAD^+ is also involved in signaling of perturbed homeostasis and DNA damage response. The signaling pathways include the NAD^+-degrading reactions catalyzed by protein deacylases sirtuins (1–3), poly(ADP-ribose) polymerases 1 and 2 involved in the DNA damage response (4, 5), and NAD^+ hydrolyzing enzymes CD38 (6)/CD157 (7). These NAD^+-dependent reactions are involved in regulation of circadian rhythms (8), aging (9–11), and immunity (12). Major portion of NAD^+ resides inside the cells, where its concentration may vary from 0.01 to 1 mM, yet some studies also determine significantly lower quantities of NAD^+ in the blood plasma [2–70 nM in humans (10, 13, 14) and 240–290 nM in pigs (15)].

The correlation between the concentrations of NAD^+ in blood/plasma and tissues has been studied in aging (16–18). The reduction in NAD^+ level with age is observed in healthy human brain (19, 20), liver (21), red blood cells (22) and macrophages (23). In plasma, the NAD^+ level is shown to drop from app. 50 nM in young (20–40 years) to app. 10 nM in elderly subjects (60–87 years) (10). Human skin NAD^+ content also sharply declines as people age: from 8.5 ± 1.6 ng/mg protein in newborns to 1.1 ± 0.2 in elders (>51 years) (9). A strong negative correlation is observed between NAD^+ levels in skin and age in both males ($r = -0.706$; $p = 0.001$) and females ($r = -0.537$; $p = 0.01$) (9). The total pool of NAD (both NAD^+ and NADH) in whole blood, however, shows a trend to a negative correlation with age in males that is not observed in females (11). In the population combined from both genders, blood NAD levels in elderly patients (75–101 years old) hospitalized for decompensated heart failure are shown to be lower (20.7 ± 3.6 μM) than those in a healthy population of 151 voluntary donors aged 19 to 68 years (23.4 ± 4.1 μ M) (11).

Changed NAD levels may be associated with cancer (16, 24, 25), obesity and type 2 diabetes (16, 26, 27), various neurological disorders (28–30), intestinal inflammation (31). Many studies point to decreased NAD levels under disturbed nutrient conditions (26). In view of the wide range of pathologies potentially affecting the NAD levels and redox state, the quantitative determination of this metabolite in human blood may be of diagnostic value. Worth noting, a rapid and efficient assay of NAD^+ may be extremely useful to decide on treatments of critically ill patients, as the tissue damage response is associated with the NAD^+ depletion in the poly(ADP-ribose)- polymerase-catalyzed reaction (4, 5). As a basic indicator of the healthy metabolism, NAD^+ level has a potential to be used as a marker of biological age or nutritional state.

Recently, we have published the method of NAD^+ quantitative determination using recombinant formate dehydrogenase (FDH) (32), whose application to the extracts of the rat brain tissue and its mitochondria has demonstrated such advantages of the assay as its high sensitivity and specificity. Compared to the "gold-standard" HPLC- and/or mass-spectrometry-based methods, our FDH assay does not require expensive consumables, neither highly professional supervision. A number of already existing biotechnological applications of FDH (33), also as fusion protein (34–36), enzyme mixture (37, 38) or in whole cell biocatalysis (39), extending from NAD(P)H regeneration to fixing atmospheric CO_2 (40–43), demonstrate the enzyme robustness and utility for the environmentally friendly procedures. In this regard, development of the FDH-based clinical assays has another advantage over the currently employed assays of total NAD pool, using formazan dyes, as the most employed 3-(4,5-dimethylthiazol-2-yl)-2,5-diphenyltetrazolium bromide, known as MTT, is toxic for eucaryotic cells (44, 45). In the present study, we use FDH from *Pseudomonas sp.* that is extremely specific to NAD^+, i.e., does not catalyze the reduction of $NADP^+$, and is characterized by high catalytic efficiency and high thermal stability, compared to FDH from other sources (33, 46, 47). Employing this enzyme and developing the optimized protocol of the extraction of NAD^+ from blood, we demonstrate the diagnostic potential of the assay for medical application by measuring the whole blood NAD^+ in the healthy subjects and patients with neurological and cardiological pathologies.

METHODS

Enrollment of Patients in the Study

The study was approved by the ethics commission of M.F. Vladimirsky Moscow Regional Research and Clinical Institute (MONIKI), decision N 17 of 10. December, 2020. All participants gave informed consent. The neurological patients with demyelinating diseases and cardiological patients with the heart failure of stage II and III according to the New York Heart Association (NYHA) functional classification, were enrolled in the study (**Table 1**) during 1 year. Our choice of the NYHA heart failure stages II and III was based on clinical abundance of these cardiological patients, in contrast to those of stage I, and a lower occurrence in these patients of additional deteriorations associated with the profound pathology of stage IV.

Preparation of Recombinant Formate Dehydrogenase

Recombinant FDH from *Pseudomonas* sp. was produced in *E. coli* as described in (48). The enzyme (1.1 mg/mL, app. 10 U/mg) was stored in 0.1 M sodium phosphate buffer, pH 7.0, containing 10 mM EDTA, at + 4°C.

Preparation of Methanol-Acetic Acid Extracts of Whole Blood

The blood was collected in the morning in a vacutainer tube with heparin (6 ml), aliquoted in 1 ml and frozen at −70°C. The blood levels of NAD^+ did not decay upon the blood storage up to several months. Typically, the samples were accumulated and extracted within 2 months after the blood collection. A modification of the extraction protocol previously elaborated for the rat brain (49) was used. To prepare the extracts, blood samples were thawed on ice, 0.2 ml of each

sample was transferred into a clean microcentrifuge tube and mixed with 1.6 ml of methanol precooled at + 4°C, using the T10 Basic ULTRA-TURRAX disperser (IKA, Staufen, Germany). 0.27 ml of 2% acetic acid was added, followed by 30 min shaking on ice in New Brunswick Excella E24R incubator (Eppendorf, Moscow, Russia) at 180 rpm. The resulting suspension was deproteinized by 20 min centrifugation at 21,500 *g* and 4°C, using Hitachi CT15RE centrifuge (Helicon, Moscow, Russia). The supernatant was transferred into a clean tube and stored at −70°C until analysis, usually performed the day after the extract preparations. Repeated assays of the same blood extracts before and after the storage showed that their NAD^+ content was stable during several months.

NAD^+ Determination Procedure

NAD^+ concentration in the blood extracts was determined enzymatically as described earlier (32), using fluorescence mode of BMG ClarioSTAR Plus plate reader (Helicon, Moscow, Russia). Samples of blood extracts were shaken and 0.01, 0.015 or 0.02 ml aliquots of each sample were added into a 96-well black microplate (Greiner #655076) in duplicates. The mixture of 87% methanol/0.3% acetic acid was added to the aliquots to obtain the total volume of 0.02 ml. The blank contained 0.02 ml of the methanol-acetic acid mixture only. 0.18 ml of 0.6 M sodium formate in 0.1 M sodium phosphate buffer, pH 7.0, was added to all the wells. The background fluorescence (340/475 nm) of the samples was measured during 6 min. After registering the background levels, app. 0.03 U of FDH (app. 3 μg) was added into each well, and the fluorescence change was measured for 20 min. Usually, a plateau in the fluorescence was reached within 10 min, pointing to the completion of the reaction. NAD^+ content in each well was calculated using the calibration curve employing 0.01–0.1 nmol of NAD^+ and 0.03 U of FDH per well. Our comparison to the calibration with added NADH showed that the calibration employing the FDH reaction, better reproduced exact conditions of the NAD^+ fluorescence assay. Simultaneously, the calibration employing the FDH reaction served as an internal control for the linearity and functionality of the enzyme assay in the selected interval of the NAD^+ concentrations. The NAD^+ content in the whole blood was calculated, taking into account the added extract volume and a 10.2-fold dilution of blood upon the extraction procedure.

TABLE 1 | Summary of the studied cohorts where the NAD^+ content in the whole blood is quantified.

Group	Sex	Age, years	Main diagnosis
Healthy controls, Total $n = 22$	45% males ($n = 10$)	25–70	None reported
Neurological patients, Total $n = 10$	40% males ($n = 4$)	18–55	Charcot-marie-tooth neuropathy ($n = 7$)
			Multiple sclerosis ($n = 1$)
			Okinawa neuropathy ($n = 2$)
Cardiological patients, Total $n = 28$	All: 79% males ($n = 22$)	42–83	Heart failure stage NYHA: II – 46% ($n = 13$), III – 54% ($n = 15$)
	Without outliers ($n = 4$, all males): 75% males ($n = 18$), Total $n = 24$	42–83	All outliers are determined in the patients with the heart failure of stage III. Heart failure stage NYHA: II – 54% ($n = 13$), III – 46% ($n = 11$)

The outliers of the determined NAD^+ content in a cohort are identified by the interquartile range rule using 1.5 IQR criterion.

Statistical Analysis

Comparisons between groups were made by one-way ANOVA with Tukey's *post hoc* test or by Mann–Whitney's U test in case of comparisons of two groups (*, **, ***, **** for $p < 0.05$, $p < 0.01$, $p < 0.001$, and $p < 0.0001$, respectively). Outliers were determined using the interquartile range rule (1.5 IQR criterion). Holm-Bonferroni correction was used for multiple testing adjustment. All statistical analysis and data visualization was performed using R Statistical Software (version 4.1.1; R Foundation for Statistical Computing, Vienna, Austria).

RESULTS

In our pilot study, concentrations of NAD^+ in the whole blood are compared in three different cohorts: healthy controls, cardiological patients with the heart failure of the NYHA class II and III, and neurological patients with demyelinating diseases, such as Charcot-Marie-Tooth type, Okinawa type and multiple sclerosis (**Table 1**). All the analyzed neuropathies are characterized by impaired myelination of nerve fibers, either in the central (multiple sclerosis) or peripheral (neuropathies of Charcot-Marie-Tooth and Okinawa types) nervous systems. Analysis of the quantified values of the whole blood NAD^+ within the studied cohorts using the interquartile range rule (1.5 IQR criterion) has revealed four outliers in the group of cardiological patients, all of them determined in the patients with heart failure of the NYHA stage III. All the blood parameters inherent in the studied cohorts are shown as medians, minimum and maximum values in **Supplementary Table 1**, which also presents *p*-values characterizing significance of the group differences.

Independent of the exclusion (**Figure 1**) or inclusion (**Supplementary Table 1**) of the outliers, NAD^+ concentrations in the blood of healthy subjects are significantly higher than those in the cardiological or neurological patients. No gender differences in the NAD^+ levels are detected in our study. Cardiological patients with NYHA stage III show a trend to lower NAD^+ levels, compared to the patients with NYHA stage II ($p = 0.09$, **Supplementary Figure 1**). Taking into account the known decreases in the blood NAD^+ level with age (11) and the different median age of the studied groups (**Supplementary Table 1**), we have verified the finding in the cohorts using their comparison to the controls of similar age. With the studied subjects divided into the age groups of 42–68 years (cardiological

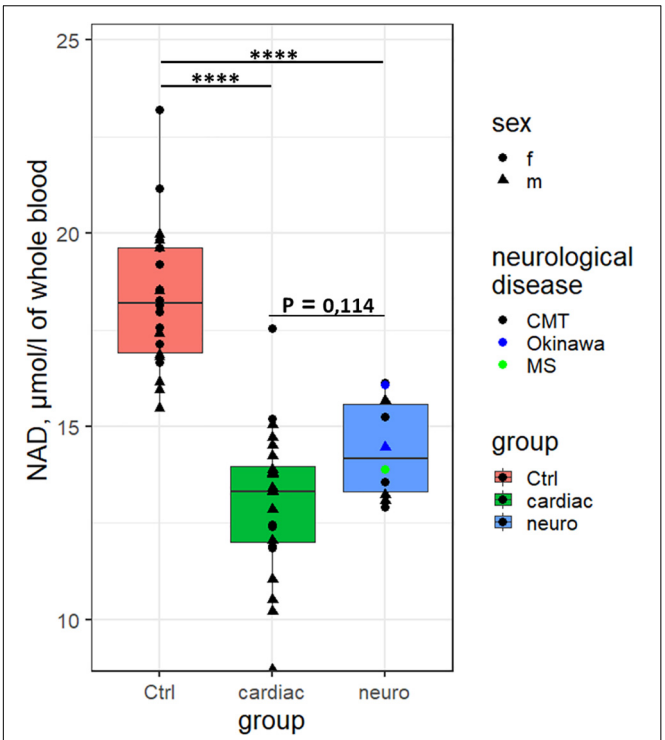

FIGURE 1 | Differences in the concentration of NAD^+ in the whole blood between the control subjects ($n = 22$), the cardiological ($n = 24$, excluding the four outliers) and neurological ($n = 10$) patients. ****$p < 0.0001$.

TABLE 2 | Discriminating power of the ratios of NAD^+ content to other blood parameters.

Ratios	*p*	*p* adj
NAD^+/ Creatinine	0.0008	0.015
NAD^+/ MCV	0.006	0.115
NAD^+/ K^+	0.01	0.18
NAD^+/ MCH	0.01	0.18
NAD^+/ Glucose	0.01	0.18
NAD^+/ Urea	0.03	0.37
NAD^+/ Triglycerides	0.03	0.37
NAD^+/ MCHC	0.03	0.43
NAD^+/ Na^+	0.05	0.52
NAD^+/ Hemoglobin	0.05	0.52
NAD^+/ Hematocryt	0.05	0.52
NAD^+/ Sedimentation rate	0.05	0.52
NAD^+/ Cholesterol_total	0.06	0.52
NAD^+/ Bilirubin_total	0.08	0.52
NAD^+/ RBC	0.19	1
NAD^+/ Asp aminotransferase	0.36	1
NAD^+/ Total_protein	0.40	1
NAD^+/ Lympocytes	0.68	1
NAD^+/ Ala aminotransferase	0.74	1

Statistical significance of the differences in the ratios inherent in the cardiological and neurological patients is analyzed by Mann–Whitney U test (p), followed by the p-values adjusted for the multiple comparison employing the Holm–Bonferroni correction.

patients *vs.* controls of the respective age) and 27–55 years (neurological patients *vs.* controls of respective age), significant differences in the NAD^+ concentrations between the control subjects and cardiological or neurological patients are preserved (**Supplementary Figure 2**).

As the NAD^+ levels alone cannot unambiguously discriminate the cardiological and neurological patients ($p = 0.1$, **Figure 1**), we have attempted to increase the discriminating power of the NAD^+ assay by finding potentially different relationships between the NAD^+ levels and associated blood markers in different pathologies. Correlations of the blood levels of NAD^+ to the available parameters of the clinical and biochemical blood analyses of the studied cohorts indicate that the control correlations are always well separated from those in the patients, while the difference between the cardiological and neurological patients is not so strong (**Supplementary Figure 3** and **Supplementary Table 2**). However, the NAD^+ dependence on Na^+ ions is opposite in the control subjects and neurological patients (**Supplementary Figure 3** and **Supplementary Table 2**), complemented by statistically significant group differences between the median values of Na^+ ions.

Analysis of the ratios of NAD^+ levels to each of the available parameters, inherent in a specific blood sample, reveals that some of the ratios may be used for a better discrimination between the neurological and cardiological patients (**Table 2**). **Figure 2** presents such ratios for the three parameters assayed in the blood along with NAD^+. While one of the parameters (creatinine) is characterized by statistically significant group differences in its median values, the medians of the two other parameters (MCV, mean corpuscular volume, and K^+) do not significantly differ between the groups (**Supplementary Table 1**). It is worth noting in this regard that the ratios presented in **Figure 2** are determined in each patient. Therefore, they manifest the coupled changes better than the overall median values of the parameters. This is exemplified in **Figure 2** by the statistically significant differences between the cardiological and neurological patients in their NAD^+ ratios to creatinine, MCV and K^+ ions. These ratios show a higher statistical significance of the differences between the neurological and cardiological patients, than NAD^+ levels alone (**Figures 1**, **2**). Thus, in addition to the blood levels of NAD^+, taking into account the coupled changes in other parameters may increase the diagnostic power of the NAD^+ assays.

DISCUSSION

The NAD^+ values determined in our study for the healthy volunteers are in good accordance with those of independent studies, where NAD^+ in human blood is measured by mass spectrometry or NMR (**Supplementary Table 3**). Other enzymatic assays of NAD^+ are known to employ lactate dehydrogenase or alcohol dehydrogenase. Unlike our FDH-based assay, these reactions are reversible. The reversibility makes such tests prone to conditional problems when established equilibria interfere with the completion of NAD^+ transformation to NADH. In modern commercial kits, this is overcome by shifting

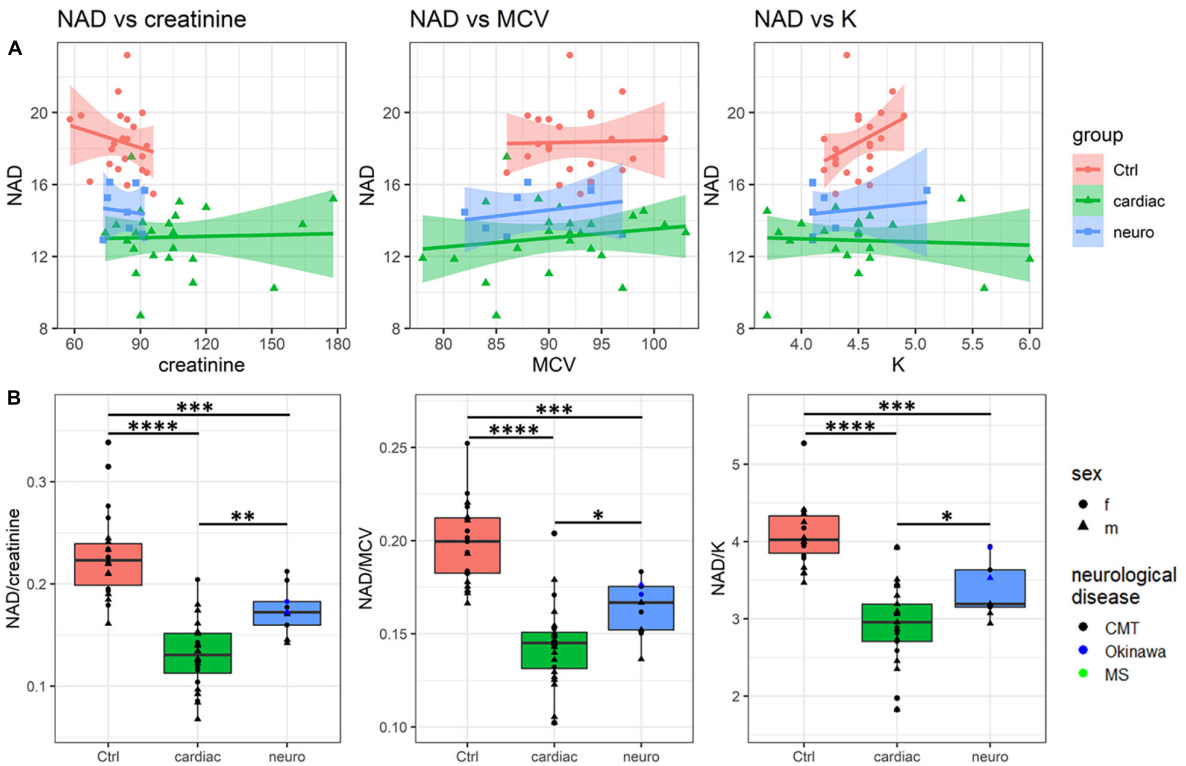

group	min	median	max	age	count
Ctrl	0,161	0,223	0,338	25-70	22
cardiac	0,068	0,131	0,204	42-83	24
neuro	0,142	0,172	0,212	18-55	9

group	min	median	max	age	count
Ctrl	0,166	0,2	0,252	25-70	22
cardiac	0,102	0,145	0,204	42-83	24
neuro	0,136	0,167	0,183	18-55	9

group	min	median	max	age	count
Ctrl	3,467	4,023	5,271	25-70	22
cardiac	1,826	2,955	3,924	42-83	21
neuro	2,941	3,191	3,935	18-55	9

FIGURE 2 | Analysis of discriminating potential of the coupled variations in the NAD^+ concentrations and other parameters of the blood. **(A)** Correlations of the NAD^+ concentrations with the creatinine level, mean corpuscular volume (MCV) and K^+ ions. **(B)** Significance of the differences between the NAD^+ ratios to creatinine, MCV and K^+ ions, determined for each of the studied samples. **(C)** Tabular presentation of the ratios used in panel **(B)**. *$p < 0.05$, **$p < 0.01$, ***$p < 0.001$, ****$p <$ <0.0001.

an equilibrium through coupled reaction(s), usually including the reduction of formazan dyes, such as MTT. However, introduction of each additional coupled reaction makes the test prone to additional artifacts. Moreover, the artifacts are not possible to control when using commercial tests whose components are not disclosed. Furthermore, without additional procedures, the MTT-based tests, employing redox transformation of nicotinamide adenine dinucleotide, do not discriminate between the oxidized (NAD^+) and reduced (NADH) forms of the dinucleotide. In particular, this is characteristic of the enzymatic studies mentioned in **Supplementary Table 3**. Although NADH and the redox ratio of NADH to NAD^+ are important metabolic indicators, additional to NAD^+ alone, the different chemical stability of NADH and NAD^+ poses challenges for simultaneous quantification of both indicators in the same blood extract in clinical settings.

According to some estimates, the blood levels of NADH are 5–10 times lower than those of NAD^+ (50), and thus should not contribute more than 20% to the total NAD pool, comprising both the oxidized and reduced dinucleotide. However, a two-fold variation in the range of the NAD pool, determined by the MTT-employing enzymatic tests (**Supplementary Table 3**), agrees with the notion that such tests are prone to various artifacts (32, 44, 45, 51). More importantly, comparison of the MTT-based tests relies on the arbitrary reaction time rather than the end-point titration, used in our FDH-based assay. In this case, if the sample composition differs, e.g., due to the various prescription drugs in different patients, the drugs may affect the MTT reduction, resulting in an artifactual change of the determined NAD pool. That is, the observed change may be related not to the NAD(H) content, but to the MTT reduction rate. Ascorbic acid, vitamin A, cellular sulfhydryl-containing compounds, such as reduced glutathione and coenzyme A, are known to reduce MTT to formazan (52–55). Varied content of these and other compounds in blood of different patients would thus contribute to the NAD-independent differences in the MTT-reduction. As an example, the MTT-based NADH assay in human erythrocytes shows diurnal oscillations, but they are coupled to changes in the cellular redox metabolism, including the changed expression of a highly abundant thiol-comprising redox enzyme, peroxiredoxin (56). These diurnal changes in the cellular redox metabolism raise questions regarding the nature of the MTT-detected changes,

which do not necessarily reflect the NAD content. In case of the FDH reaction, the inhibitors or activators may also affect the reaction rate. However, in contrast to the MTT-based assay, the assay employing FDH is not dependent on the reaction rate or time, but based on the end-point titration of NADH itself, characterizing the complete transformation of NAD^+ to NADH. Therefore, significant effects of different drugs prescribed to patients on the FDH-based NAD^+ assay are not expected.

Apart from the high resistance to the artifacts discussed above, sensitivity of our fluorometric NAD^+ assay corresponds to the detection limit of 5 pmoles NAD^+ per 50 uL sample, or 100 nM NAD^+, that is better than the detection limit of 400 nM NAD^+, reported by Abcam[1] or Biovision[2] for the MTT-based assays.

It is worth noting that the tissue NAD^+ or total NAD content may be subject to circadian changes, although the oscillation periods do not coincide in different studies (57–59). Probably, this poor coincidence is related to the fact that even in the liver tissue, where the NAD^+ oscillation amplitudes are high, they are mostly within the standard errors of the NAD assays. Nevertheless, to exclude additional source of variations, the blood samples for our analyses are taken in the morning. Using the FDH-based test to detect potential circadian changes in NAD^+ content in human blood may open new perspectives for chronobiological implications in medicine.

Decreased NAD^+ content in demyelinating neuropathies is known from cellular and animal models of the diseases. For instance, rapid NAD^+ drop upon Wallerian (injury-induced) degeneration of axons (29, 60), neurites (61) and in dissected nerves (62) suggests diminished NAD^+ level in Charcot-Marie-Tooth disease and other peripheric neuropathies. Thus, our finding of decreased NAD^+ levels in patients with demyelinating neuropathies is in good accordance with the model studies. Interestingly, the NAD pool is depleted in neurons exposed to toxic prion proteins, or in models of protein misfolding in Alzheimer's and Parkinson's diseases (63). Reduced level of total NAD in the brain tissue is observed in a mouse model of cerebellar ataxia (64), but the depletion does not occur in astrocytes or brain homogenates of scrapie-infected mice (63).

Similarly, decreased content of total NAD in myocardium is shown in mouse models of dilated cardiomyopathy (65) and failing heart (66). These model studies are in good accord with our finding of decreased levels of NAD^+ in the whole human blood of cardiological patients (**Figure 1**). As mentioned in Introduction, the old (75–101 years) patients hospitalized for decompensated heart failure have a lower level of total NAD, compared to the younger (19–68 years) controls (11). In view of the published results on decreased NAD pool in cardiological pathologies, our finding of decreased NAD^+ in the blood of cardiological patients suggests an impairment in NAD biosynthesis rather than increased NADH/NAD^+ ratio in these patients. However, the abovementioned comparison of the MTT-based quantification of total NAD employs the cardiological patients and control subjects of different ages. Hence, further studies are needed to decipher the molecular mechanisms underlying decreases in NAD^+ upon the cardio- and neuropathologies.

Thus, to the best of our knowledge, declines in the blood levels of NAD^+ in the neurological and cardiological patients, shown in our work (**Figure 1** and **Supplementary Figure 2**), have not been demonstrated before, although decreased NAD levels are known in healthy aging (16–18). Our data support this finding, as we also observe a slight decline in the blood NAD^+ content in healthy subjects with age (**Supplementary Figure 3**). For the future studies it is important to note, however, that this and other correlations may be changed in different cohorts, manifesting certain specificity of pathophysiological changes in patients (**Supplementary Figure 3** and **Supplementary Table 2**). Owing to this, the discriminating power of NAD^+ as a clinical indicator of specific pathologies or as a risk factor of their development may be increased by taking into account potential associations of the NAD^+ levels with other clinically relevant parameters (**Figure 2** and **Table 2**). Further studies in these directions may be performed using the FDH-based NAD^+ assay, developed in the current work. Remarkably, the associations between perturbed levels of NAD^+ and creatinine, observed in our study (**Figure 2**), are also known in animals with acute and chronic kidney disease (67) and in patients with pellagra (68).

Supplementation with vitamin B3 (NAD precursor) to subjects under increased risks of neurological, cardiological and other disorders is currently considered as an efficient therapeutic strategy (69). Our easy NAD^+ test may be applied to reveal the best therapies to increase the NAD^+ level for protection from the age-related pathologies.

As a result, the proposed FDH-based assay of NAD^+ in human blood may be useful for a more precise diagnosis of different pathologies and associated risks.

DATA AVAILABILITY STATEMENT

The raw data supporting the conclusions of this article will be made available by the authors, without undue reservation.

ETHICS STATEMENT

The studies involving human participants were reviewed and approved by Independent Ethics Committee of M.F. Vladimirsky Moscow Regional Research and Clinical Institute. The patients/participants provided their written informed consent to participate in this study.

AUTHOR CONTRIBUTIONS

NB and AA performed the NAD^+ measurement and quantification. NB and OS provided the blood samples and medical histories analyses. LS purified the recombinant FDH. VT supervised the FDH production. LZ, AP, and VB analyzed the results. VB and AP wrote the manuscript draft. VB, AA, and AT edited the manuscript. All authors read and agreed on the submitted version of the manuscript.

[1] https://www.abcam.com/nadnadh-assay-kit-colorimetric-ab65348.html

[2] https://www.biovision.com/nad-nadh-quantitation-colorimetric-kit.html

FUNDING

This work was supported by joint grant from Russian Foundation for Basic Research (grant no. 20-54-7804) and National Research Council of Italy (grant CUP B85F20002990005).

SUPPLEMENTARY MATERIAL

The Supplementary Material for this article can be found online at: https://www.frontiersin.org/articles/10.3389/fmed.2022.886485/full#supplementary-material

REFERENCES

1. Moniot S, Weyand M, Steegborn C. Structures, substrates, and regulators of mammalian sirtuins - opportunities and challenges for drug development. *Front Pharmacol.* (2012) 3:16. doi: 10.3389/fphar.2012.00016
2. Imai S, Guarente L. NAD+ and sirtuins in aging and disease. *Trends Cell Biol.* (2014) 24:464–71. doi: 10.1016/j.tcb.2014.04.002
3. Manjula R, Anuja K, Alcain FJ. SIRT1 and SIRT2 activity control in neurodegenerative Diseases. *Front Pharmacol.* (2020) 11:585821. doi: 10.3389/fphar.2020.585821
4. Bai P, Canto C, Brunyanszki A, Huber A, Szanto M, Cen Y, et al. PARP-2 regulates SIRT1 expression and whole-body energy expenditure. *Cell Metab.* (2011) 13:450–60. doi: 10.1016/j.cmet.2011.03.013
5. Bai P, Canto C, Oudart H, Brunyanszki A, Cen Y, Thomas C, et al. PARP-1 inhibition increases mitochondrial metabolism through SIRT1 activation. *Cell Metab.* (2011) 13:461–8. doi: 10.1016/j.cmet.2011.03.004
6. Lee HC. Structure and enzymatic functions of human CD38. *Mol Med.* (2006) 12:317–23. doi: 10.2119/2006âĂŞ00086.Lee
7. Ortolan E, Augeri S, Fissolo G, Musso I, Funaro A. CD157: from immunoregulatory protein to potential therapeutic target. *Immunol Lett.* (2019) 205:59–64. doi: 10.1016/j.imlet.2018.06.007
8. Sahar S, Nin V, Barbosa MT, Chini EN, Sassone-Corsi P. Altered behavioral and metabolic circadian rhythms in mice with disrupted NAD+ oscillation. *Aging.* (2011) 3:794–802. doi: 10.18632/aging.100368
9. Massudi H, Grant R, Braidy N, Guest J, Farnsworth B, Guillemin GJ. Age-associated changes in oxidative stress and NAD+ metabolism in human tissue. *PLoS One.* (2012) 7:e42357. doi: 10.1371/journal.pone.0042357
10. Clement J, Wong M, Poljak A, Sachdev P, Braidy N. The plasma NAD(+) metabolome is dysregulated in "Normal" aging. *Rejuvenation Res.* (2019) 22:121–30. doi: 10.1089/rej.2018.2077
11. Breton M, Costemale-Lacoste JF, Li Z, Lafuente-Lafuente C, Belmin J, Mericskay M. Blood NAD levels are reduced in very old patients hospitalized for heart failure. *Exp Gerontol.* (2020) 139:111051. doi: 10.1016/j.exger.2020.111051
12. Gasparrini M, Sorci L, Raffaelli N. Enzymology of extracellular NAD metabolism. *Cell Mol Life Sci.* (2021) 78:3317–31. doi: 10.1007/s00018-020-03742-1
13. Seyedsadjadi N, Berg J, Bilgin AA, Braidy N, Salonikas C, Grant R. High protein intake is associated with low plasma NAD+ levels in a healthy human cohort. *PLoS One.* (2018) 13:e0201968. doi: 10.1371/journal.pone.0201968
14. Grant R, Berg J, Mestayer R, Braidy N, Bennett J, Broom S, et al. A pilot study investigating changes in the human plasma and urine NAD+ metabolome during a 6 hour intravenous infusion of NAD. *Front Aging Neurosci.* (2019) 11:257. doi: 10.3389/fnagi.2019.00257
15. O'Reilly T, Niven DF. Levels of nicotinamide adenine dinucleotide in extracellular body fluids of pigs may be growth-limiting for *Actinobacillus pleuropneumoniae* and *Haemophilus parasuis*. *Can J Vet Res.* (2003) 67:229–31.
16. Canto C, Menzies KJ, Auwerx J. NAD(+) Metabolism and the control of energy homeostasis: a balancing act between mitochondria and the nucleus. *Cell Metab.* (2015) 22:31–53. doi: 10.1016/j.cmet.2015.05.023
17. McReynolds MR, Chellappa K, Baur JA. Age-related NAD(+) decline. *Exp Gerontol.* (2020) 134:110888. doi: 10.1016/j.exger.2020.110888
18. Peluso A, Damgaard MV, Mori MAS, Treebak JT. Age-dependent decline of NAD(+)-Universal truth or confounded consensus?. *Nutrients.* (2021) 14:101. doi: 10.3390/nu14010101
19. Zhu XH, Lu M, Lee BY, Ugurbil K, Chen W. In vivo NAD assay reveals the intracellular NAD contents and redox state in healthy human brain and their age dependences. *Proc Natl Acad Sci USA.* (2015) 112:2876–81. doi: 10.1073/pnas.1417921112
20. Bagga P, Hariharan H, Wilson NE, Beer JC, Shinohara RT, Elliott MA, et al. Single-Voxel (1) H MR spectroscopy of cerebral nicotinamide adenine dinucleotide (NAD(+)) in humans at 7T using a 32-channel volume coil. *Magn Reson Med.* (2020) 83:806–14. doi: 10.1002/mrm.27971
21. Zhou CC, Yang X, Hua X, Liu J, Fan MB, Li GQ, et al. Hepatic NAD(+) deficiency as a therapeutic target for non-alcoholic fatty liver disease in ageing. *Br J Pharmacol.* (2016) 173:2352–68. doi: 10.1111/bph.13513
22. Chaleckis R, Murakami I, Takada J, Kondoh H, Yanagida M. Individual variability in human blood metabolites identifies age-related differences. *Proc Natl Acad Sci USA.* (2016) 113:4252–9. doi: 10.1073/pnas.1603023113
23. Minhas PS, Liu L, Moon PK, Joshi AU, Dove C, Mhatre S, et al. Macrophage de novo NAD(+) synthesis specifies immune function in aging and inflammation. *Nat Immunol.* (2019) 20:50–63. doi: 10.1038/s41590-018-0255-3
24. Yaku K, Okabe K, Hikosaka K, Nakagawa T. NAD metabolism in cancer therapeutics. *Front Oncol.* (2018) 8:622. doi: 10.3389/fonc.2018.00622
25. Navas LE, Carnero A. NAD(+) metabolism, stemness, the immune response, and cancer. *Signal Transduct Target Ther.* (2021) 6:2. doi: 10.1038/s41392-020-00354-w
26. Okabe K, Yaku K, Tobe K, Nakagawa T. Implications of altered NAD metabolism in metabolic disorders. *J Biomed Sci.* (2019) 26:34. doi: 10.1186/s12929-019-0527-8
27. Fan L, Cacicedo JM, Ido Y. Impaired nicotinamide adenine dinucleotide (NAD(+)) metabolism in diabetes and diabetic tissues: implications for nicotinamide-related compound treatment. *J Diabetes Investig.* (2020) 11:1403–19. doi: 10.1111/jdi.13303
28. Yaku K, Okabe K, Nakagawa T. NAD metabolism: implications in aging and longevity. *Ageing Res Rev.* (2018) 47:1–17. doi: 10.1016/j.arr.2018.05.006
29. Moss KR, Hoke A. Targeting the programmed axon degeneration pathway as a potential therapeutic for charcot-marie-tooth disease. *Brain Res.* (2020) 1727:146539. doi: 10.1016/j.brainres.2019.146539
30. Hikosaka K, Yaku K, Okabe K, Nakagawa T. Implications of NAD metabolism in pathophysiology and therapeutics for neurodegenerative diseases. *Nutr Neurosci.* (2021) 24:371–83. doi: 10.1080/1028415X.2019.1637504
31. Gerner RR, Klepsch V, Macheiner S, Arnhard K, Adolph TE, Grander C, et al. NAD metabolism fuels human and mouse intestinal inflammation. *Gut.* (2018) 67:1813–23. doi: 10.1136/gutjnl-2017-314241
32. Artiukhov AV, Pometun AA, Zubanova SA, Tishkov VI, Bunik VI. Advantages of formate dehydrogenase reaction for efficient NAD(+) quantification in biological samples. *Anal Biochem.* (2020) 603:113797. doi: 10.1016/j.ab.2020.113797
33. Tishkov VI, Popov VO. Protein engineering of formate dehydrogenase. *Biomol Eng.* (2006) 23:89–110. doi: 10.1016/j.bioeng.2006.02.003
34. Gao X, Yang S, Zhao C, Ren Y, Wei D. Artificial multienzyme supramolecular device: highly ordered self-assembly of oligomeric enzymes in vitro and in vivo. *Angew Chem Int Ed Engl.* (2014) 53:14027–30. doi: 10.1002/anie.201405016
35. Jiang W, Fang BS. Construction and evaluation of a novel bifunctional phenylalanine-formate dehydrogenase fusion protein for bienzyme system with cofactor regeneration. *J Ind Microbiol Biotechnol.* (2016) 43:577–84. doi: 10.1007/s10295-016-1738-6
36. Kokorin A, Parshin PD, Bakkes PJ, Pometun AA, Tishkov VI, Urlacher VB. Genetic fusion of P450 BM3 and formate dehydrogenase towards self-sufficient biocatalysts with enhanced activity. *Sci Rep.* (2021) 11:21706. doi: 10.1038/s41598-021-00957-5
37. Seelbach K, Riebel B, Hummel W, Kula MR, Tishkov VI, Egorov AM, et al. A novel, efficient regenerating method of NADPH using a new formate dehydrogenase. *Tetrahedron Lett.* (1996) 37:1377–80. doi: 10.1016/0040-4039(96)00010-x

38. Jiang W, Xu CZ, Jiang SZ, Zhang TD, Wang SZ, Fang BS. Establishing a mathematical equations and improving the production of L-tert-leucine by uniform design and regression analysis. *Appl Biochem Biotechnol.* (2017) 181:1454–64. doi: 10.1007/s12010-016-2295-1
39. Tao R, Jiang Y, Zhu F, Yang S. A one-pot system for production of L-2-aminobutyric acid from L-threonine by L-threonine deaminase and a NADH-regeneration system based on L-leucine dehydrogenase and formate dehydrogenase. *Biotechnol Lett.* (2014) 36:835–41. doi: 10.1007/s10529-013-1424-y
40. Cakar MM, Ruupunen J, Mangas-Sanchez J, Birmingham WR, Yildirim D, Turunen O, et al. Engineered formate dehydrogenase from *Chaetomium thermophilum*, a promising enzymatic solution for biotechnical CO2 fixation. *Biotechnol Lett.* (2020) 42:2251–62. doi: 10.1007/s10529-020-02937-7
41. Alpdagtas S, Turunen O, Valjakka J, Binay B. The challenges of using NAD(+)-dependent formate dehydrogenases for CO2 conversion. *Crit Rev Biotechnol.* (2021). [Online ahead of print]. doi: 10.1080/07388551.2021.1981820
42. Choe MS, Choi S, Kim SY, Back C, Lee D, Lee HS, et al. A hybrid Ru(II)/TiO2 catalyst for steadfast photocatalytic CO2 to CO/formate conversion following a molecular catalytic route. *Inorg Chem.* (2021) 60:10235–48. doi: 10.1021/acs.inorgchem.1c00615
43. Unlu A, Duman-Ozdamar ZE, Caloglu B, Binay B. Enzymes for efficient CO2 conversion. *Protein J.* (2021) 40:489–503. doi: 10.1007/s10930-021-10007-8
44. Riss TL, Moravec RA, Niles AL, Duellman S, Benink HA, Worzella TJ, et al. Cell Viability Assays. In: Markossian S, Grossman A, Brimacombe K, Arkin M, Auld D, Austin CP editors. *Assay Guidance Manual.* Bethesda, MD: Eli Lilly & Company and the National Center for Advancing Translational Sciences (2004).
45. Ghasemi M, Turnbull T, Sebastian S, Kempson I. The MTT assay: utility, limitations, pitfalls, and interpretation in bulk and single-cell analysis. *Int J Mol Sci.* (2021) 22:12827. doi: 10.3390/ijms222312827
46. Pometun AA, Kleymenov SY, Zarubina SA, Kargov IS, Parshin PD, Sadykhov EG, et al. Comparison of thermal stability of new formate dehydrogenases by differential scanning calorimetry. *Mosc Univ Chem Bull.* (2018) 73:80–4. doi: 10.3103/s002713141802013x
47. Tishkov VI, Pometun AA, Stepashkina AV, Fedorchuk VA, Zarubina SA I, Kargov S, et al. Rational design of practically important enzymes. *Mosc Univ Chem Bull.* (2018) 73:1–6. doi: 10.3103/s0027131418020153
48. Alekseeva AA, Fedorchuk VV, Zarubina SA, Sadykhov EG, Matorin AD, Savin SS, et al. The role of ala198 in the stability and coenzyme specificity of bacterial formate dehydrogenases. *Acta Nat.* (2015) 7:60–9. doi: 10.32607/20758251-2015-7-1-60-69
49. Ksenofontov AL, Boyko AI, Mkrtchyan GV, Tashlitsky VN, Timofeeva AV, Graf AV, et al. Analysis of free amino acids in mammalian brain homogenates. *Biochemistry.* (2017) 82:1183–92. doi: 10.1134/s000629791710011x
50. Nagana Gowda GA, Raftery D. Whole blood metabolomics by (1)H NMR spectroscopy provides a new opportunity to evaluate coenzymes and antioxidants. *Anal chem.* (2017) 89:4620–7. doi: 10.1021/acs.analchem.7b00171
51. Aleshin VA, Artiukhov AV, Oppermann H, Kazantsev AV, Lukashev NV, Bunik VI. Mitochondrial impairment may increase cellular NAD(P)H: resazurin oxidoreductase activity, perturbing the NAD(P)H-based viability assays. *Cells.* (2015) 4:427–51. doi: 10.3390/cells4030427
52. Pagliacci MC, Spinozzi F, Migliorati G, Fumi G, Smacchia M, Grignani F, et al. Genistein inhibits tumour cell growth in vitro but enhances mitochondrial reduction of tetrazolium salts: a further pitfall in the use of the MTT assay for evaluating cell growth and survival. *Eur J Cancer.* (1993) 29A:1573–7. doi: 10.1016/0959-8049(93)90297-s
53. Chakrabarti R, Kundu S, Kumar S, Chakrabarti R. Vitamin A as an enzyme that catalyzes the reduction of MTT to formazan by vitamin C. *J Cell Biochem.* (2000) 80:133–8. doi: 10.1002/1097-4644(20010101)80:1<133::aid-jcb120>3.0.co;2-t
54. Bernas T, Dobrucki J. Mitochondrial and nonmitochondrial reduction of MTT: interaction of MTT with TMRE, JC-1, and NAO mitochondrial fluorescent probes. *Cytometry.* (2002) 47:236–42. doi: 10.1002/cyto.10080
55. Ulukaya E, Colakogullari M, Wood EJ. Interference by anti-cancer chemotherapeutic agents in the MTT-tumor chemosensitivity assay. *Chemotherapy.* (2004) 50:43–50. doi: 10.1159/000077285
56. O'Neill JS, Reddy AB. Circadian clocks in human red blood cells. *Nature.* (2011) 469:498–503. doi: 10.1038/nature09702
57. Ramsey KM, Yoshino J, Brace CS, Abrassart D, Kobayashi Y, Marcheva B, et al. Circadian clock feedback cycle through NAMPT-mediated NAD^+ biosynthesis. *Science.* (2009) 324:651–4. doi: 10.1126/science.1171641
58. Peek CB, Affinati AH, Ramsey KM, Kuo HY, Yu W, Sena LA, et al. Circadian clock NAD^+ cycle drives mitochondrial oxidative metabolism in mice. *Science.* (2013) 342:1243417. doi: 10.1126/science.1243417
59. Levine DC, Hong H, Weidemann BJ, Ramsey KM, Affinati AH, Schmidt MS, et al. NAD(+) controls circadian reprogramming through PER2 nuclear translocation to counter aging. *Mol Cell.* (2020) 78:835–849.e7. doi: 10.1016/j.molcel.2020.04.010
60. Wang J, Zhai Q, Chen Y, Lin E, Gu W, McBurney MW, et al. A local mechanism mediates NAD-dependent protection of axon degeneration. *J Cell Biol.* (2005) 170:349–55. doi: 10.1083/jcb.200504028
61. Gerdts J, Brace EJ, Sasaki Y, DiAntonio A, Milbrandt J. SARM1 activation triggers axon degeneration locally via NAD(+) destruction. *Science.* (2015) 348:453–7. doi: 10.1126/science.1258366
62. Gilley J, Orsomando G, Nascimento-Ferreira I, Coleman MP. Absence of SARM1 rescues development and survival of NMNAT2-deficient axons. *Cell Rep.* (2015) 10:1974–81. doi: 10.1016/j.celrep.2015.02.060
63. Zhou M, Ottenberg G, Sferrazza GF, Hubbs C, Fallahi M, Rumbaugh G, et al. Neuronal death induced by misfolded prion protein is due to NAD^+ depletion and can be relieved in vitro and in vivo by NAD^+ replenishment. *Brain.* (2015) 138:992–1008. doi: 10.1093/brain/awv002
64. Fang EF, Scheibye-Knudsen M, Brace LE, Kassahun H, SenGupta T, Nilsen H, et al. Defective mitophagy in XPA via PARP-1 hyperactivation and NAD(+)/SIRT1 reduction. *Cell.* (2014) 157:882–96. doi: 10.1016/j.cell.2014.03.026
65. Diguet N, Trammell SAJ, Tannous C, Deloux R, Piquereau J, Mougenot N, et al. Nicotinamide riboside preserves cardiac function in a mouse model of dilated cardiomyopathy. *Circulation.* (2018) 137:2256–73. doi: 10.1161/circulationaha.116.026099
66. Pillai JB, Isbatan A, Imai S, Gupta MP. Poly(ADP-ribose) polymerase-1-dependent cardiac myocyte cell death during heart failure is mediated by NAD^+ depletion and reduced Sir2alpha deacetylase activity. *J Biol Chem.* (2005) 280:43121–30. doi: 10.1074/jbc.M506162200
67. Faivre A, Katsyuba E, Verissimo T, Lindenmeyer M, Rajaram RD, Naesens M, et al. Differential role of nicotinamide adenine dinucleotide deficiency in acute and chronic kidney disease. *Nephrol Dial Transplant.* (2021) 36:60–8. doi: 10.1093/ndt/gfaa124
68. Creeke PI, Dibari F, Cheung E, van den Briel T, Kyroussis E, Seal AJ. Whole blood NAD and NADP concentrations are not depressed in subjects with clinical pellagra. *J Nutr.* (2007) 137:2013–7. doi: 10.1093/jn/137.9.2013
69. Airhart SE, Shireman LM, Risler LJ, Anderson GD, Nagana Gowda GA, Raftery D, et al. An open-label, non-randomized study of the pharmacokinetics of the nutritional supplement nicotinamide riboside (NR) and its effects on blood NAD^+ levels in healthy volunteers. *PLoS One.* (2017) 12:e0186459. doi: 10.1371/journal.pone.0186459

Conflict of Interest: The authors declare that the research was conducted in the absence of any commercial or financial relationships that could be construed as a potential conflict of interest.

frontiers | Frontiers in Medicine

ORIGINAL RESEARCH
published: 01 June 2022
doi: 10.3389/fmed.2022.896263

Delayed Impact of 2-Oxoadipate Dehydrogenase Inhibition on the Rat Brain Metabolism Is Linked to Protein Glutarylation

*Alexandra I. Boyko[1], Irina S. Karlina[2], Lev G. Zavileyskiy[1], Vasily A. Aleshin[3,4], Artem V. Artiukhov[3,4], Thilo Kaehne[5], Alexander L. Ksenofontov[3], Sergey I. Ryabov[6], Anastasia V. Graf[3,7,8], Angela Tramonti[9] and Victoria I. Bunik[1,3,4]**

[1] Faculty of Bioengineering and Bioinformatics, Lomonosov Moscow State University, Moscow, Russia, [2] N.V. Sklifosovsky Institute of Clinical Medicine, Sechenov First Moscow State Medical University, Moscow, Russia, [3] Belozersky Institute of Physico-Chemical Biology, Lomonosov Moscow State University, Moscow, Russia, [4] Department of Biological Chemistry, Sechenov First Moscow State Medical University, Moscow, Russia, [5] Institute of Experimental Internal Medicine, Otto von Guericke University Magdeburg, Magdeburg, Germany, [6] Russian Cardiology Research and Production Complex, Ministry of Health of the Russian Federation, Moscow, Russia, [7] Faculty of Nano-, Bio-, Informational, Cognitive and Socio-Humanistic Sciences and Technologies, Moscow Institute of Physics and Technology, Moscow, Russia, [8] Faculty of Biology, Lomonosov Moscow State University, Moscow, Russia, [9] Institute of Molecular Biology and Pathology, Council of National Research, Department of Biochemical Sciences "A. Rossi Fanelli", Sapienza University, Rome, Italy

OPEN ACCESS

Edited by:
Matteo Becatti,
University of Firenze, Italy

Reviewed by:
Natalia Nemeria,
Rutgers University, Newark, United States
Bianca Seminotti,
Federal University of Rio Grande do Sul, Brazil
Abhilash P. Appu,
National Institutes of Health (NIH), United States

***Correspondence:**
Victoria I. Bunik
bunik@belozersky.msu.ru

Specialty section:
This article was submitted to Translational Medicine, a section of the journal Frontiers in Medicine

Received: 14 March 2022
Accepted: 28 April 2022
Published: 01 June 2022

Citation:
Boyko AI, Karlina IS, Zavileyskiy LG, Aleshin VA, Artiukhov AV, Kaehne T, Ksenofontov AL, Ryabov SI, Graf AV, Tramonti A and Bunik VI (2022) Delayed Impact of 2-Oxoadipate Dehydrogenase Inhibition on the Rat Brain Metabolism Is Linked to Protein Glutarylation. Front. Med. 9:896263. doi: 10.3389/fmed.2022.896263

Background: The *DHTKD1*-encoded 2-oxoadipate dehydrogenase (OADH) oxidizes 2-oxoadipate—a common intermediate of the lysine and tryptophan catabolism. The mostly low and cell-specific flux through these pathways, and similar activities of OADH and ubiquitously expressed 2-oxoglutarate dehydrogenase (OGDH), agree with often asymptomatic phenotypes of heterozygous mutations in the *DHTKD1* gene. Nevertheless, OADH/*DHTKD1* are linked to impaired insulin sensitivity, cardiovascular disease risks, and Charcot-Marie-Tooth neuropathy. We hypothesize that systemic significance of OADH relies on its generation of glutaryl residues for protein glutarylation. Using pharmacological inhibition of OADH and the animal model of spinal cord injury (SCI), we explore this hypothesis.

Methods: The weight-drop model of SCI, a single intranasal administration of an OADH-directed inhibitor trimethyl adipoyl phosphonate (TMAP), and quantification of the associated metabolic changes in the rat brain employ established methods.

Results: The TMAP-induced metabolic changes in the brain of the control, laminectomized (LE) and SCI rats are long-term and (patho)physiology-dependent. Increased glutarylation of the brain proteins, proportional to OADH expression in the control and LE rats, represents a long-term consequence of the OADH inhibition. The proportionality suggests autoglutarylation of OADH, supported by our mass-spectrometric identification of glutarylated K155 and K818 in recombinant human OADH. In SCI rats, TMAP increases glutarylation of the brain proteins more than OADH expression, inducing a strong perturbation in the brain glutathione metabolism. The redox metabolism is not perturbed by TMAP in LE animals, where the inhibition of OADH

increases expression of deglutarylase sirtuin 5. The results reveal the glutarylation-imposed control of the brain glutathione metabolism. Glutarylation of the ODP2 subunit of pyruvate dehydrogenase complex at K451 is detected in the rat brain, linking the OADH function to the brain glucose oxidation essential for the redox state. Short-term inhibition of OADH by TMAP administration manifests in increased levels of tryptophan and decreased levels of sirtuins 5 and 3 in the brain.

Conclusion: Pharmacological inhibition of OADH affects acylation system of the brain, causing long-term, (patho)physiology-dependent changes in the expression of OADH and sirtuin 5, protein glutarylation and glutathione metabolism. The identified glutarylation of ODP2 subunit of pyruvate dehydrogenase complex provides a molecular mechanism of the OADH association with diabetes.

Keywords: *DHTKD1*, glutathione, glutarylation, 2-oxoadipate dehydrogenase, citrulline, phosphonate analog of 2-oxoadipate, sirtuin 5

INTRODUCTION

DHTKD1-encoded 2-oxoadipate dehydrogenase (OADH, EC 1.2.4.2) is a recently identified member of the family of the thiamine diphosphate (ThDP)-dependent 2-oxo acid dehydrogenases, found in animals and slime mold *Dictyostelium discoideum* (1). Prediction of the catalytic function of the *DHTKD1* protein as OADH (2) has been supported by increased excretion of the OADH substrate, 2-oxoadipate, and its transamination sibling 2-aminoadipate in urine and blood upon human mutations of *DHTKD1* gene (3–5). 2-Oxo- and 2-aminoadipate are intermediates of the metabolic pathways degrading lysine, hydroxylysine, and tryptophan, in which OADH thus takes part.

The *DHTKD1* mutations in humans mostly lack severe phenotypes, but may be associated with muscle weakness and cardiovascular disease risks (3–7). Some *DHTKD1* variants are enriched in patients with eosinophilic esophagitis (8). Other mutations are shown to cause Charcot-Marie-Tooth disease—a hereditary motor sensory neuropathy, characterized by atrophy of the distal parts of limbs (6, 9, 10). According to a recent study, heterozygous *DHTKD1* variants may also contribute to the phenotype of amyotrophic lateral sclerosis (11). In rare cases, 2-oxoadipate accumulation leads to the vitamin B6-responsive epilepsy, supposed to be caused by toxic reactions with vitamin B6, involving a 2-oxoadipate precursor (5, 12). Metabolic corrections in these patients employing a diet with low lysine and high arginine, decrease the epilepsy markers including 2-oxoadipate, improving the neurological symptoms (13, 14).

Several lines of evidence link the *DHTKD1* expression and/or the OADH substrate 2-oxoadipate to glucose homeostasis. The risk of developing cardiometabolic diseases is increased by elevated levels of 2-aminoadipate (15, 16), while the reduced *DHTKD1* expression in adipose tissue correlates to insulin resistance (17). Accordingly, a higher *DHTKD1* expression increases the insulin sensitivity (18). Our previous study on pharmacological inhibition of OADH in cells suggests that the enzyme function may regulate biosynthesis of nicotinamide adenine dinucleotide (NAD) metabolites from tryptophan, the pathway of high homeostatic significance, particularly for glucose metabolism (19).

Thus, OADH regulation may provide an important therapeutic tool to fight systemic pathologies. However, developing such novel therapeutic approaches requires knowledge of molecular mechanisms of the OADH involvement with (patho)physiological events.

A cellular model of the *DHTKD1* gene silencing shows disturbed mitochondrial function and biogenesis, associated with decreased activity of the tricarboxylic (TCA) cycle enzyme 2-oxoglutarate dehydrogenase (OGDH, EC 1.2.4.2), an isoenzyme of OADH (7, 8, 20). These data are in accord with the known inactivation of OGDH by 2-oxoadipate *in vitro* (21). However, *in vivo,* the 2-oxoadipate concentration in brain does not usually exceed 0.01 mM (3, 22), which is 10–20 times lower than that of 2-oxoglutarate. Hence, unlike the observations in cellular models, significant inactivation of OGDH can hardly be expected *in vivo* even when 2-oxoadipate is increased due to the *DHTKD1* mutation (3, 22). Nevertheless, decreased mitochondrial function and increased reactive oxygen species are observed in epithelial cells of patients with allergic inflammation of esophageal epithelium or Charcot-Marie-Tooth disease, where the *DHTKD1* mutations are enriched (8, 20).

In view of the very low concentrations of 2-oxoadipate in most tissues, i.e., small substrate fluxes through OADH, and similar catalytic activities of OADH and the ubiquitously expressed OGDH, we hypothesize that systemic importance of OADH function is linked to the enzyme participation in homeostatic regulation through post-translational modifications of proteins. As a producer of reactive glutaryl residues, either ThDP-bound in the isolated OADH, or CoA-bound in its multienzyme complex (OADHC), OADH may be a part of the

Abbreviations: OADH, 2-oxoadipate dehydrogenase; OADHC, 2-oxoadipate dehydrogenase complex; OADHCem, extramitochondrial activity of OADHC; OGDH, 2-oxoglutarate dehydrogenase; OGDHC, 2-oxoglutarate dehydrogenase complex; PDHC, pyruvate dehydrogenase complex; DLAT, dihydrolipoamide acetyltransferase—PDHC E2 component; SCI, spinal cord injury; LE, laminectomy; TMAP, trimethyl adipoyl phosphonate; ThDP, thiamine diphosphate; GSSG, glutathione disulphide; MS, mass-spectrometry; NO·, nitric oxide.

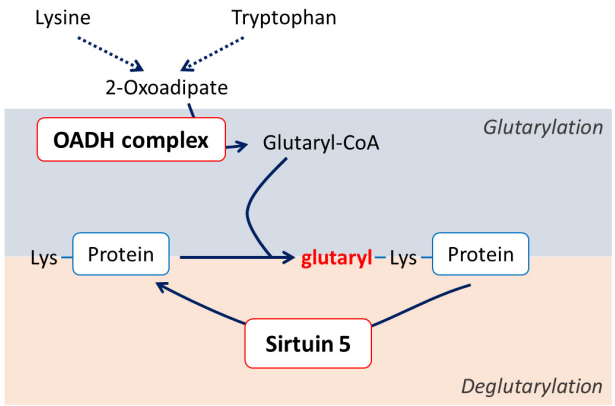

FIGURE 1 | Schematic view of the association between the OADH-catalyzed reaction and protein glutarylation.

system of post-translational protein modification by glutarylation (**Figure 1**). Like other acyl-CoA's, glutaryl-CoA may modify lysine residues of proteins (23). The accompanying change in the lysine residue charge from the positive to negative one may be involved in functional regulation of glutarylated proteins (23, 24). Removal of glutaryl moieties is performed by specific deacylase of the negatively charged acyl groups—NAD^+-dependent deglutarylase/desuccinylase/demalonylase sirtuin 5 (EC 2.3.1.B43). Sirtuin 5 has neuroprotective significance under ischemic conditions in the brain (25). In the model of spinal cord injury (SCI) the protein expression of sirtuin 5 correlates positively with the rehabilitation of animals (26). On the contrary, excessive protein glutarylation upon increased levels of glutaryl-CoA is known to cause neurological disorders (27). Such neurological significance of protein glutarylation implies that the balance of activities of the glutaryl-CoA producer OADH and protein deglutarylase sirtuin 5 may be an important homeostatic determinant in neural tissue.

The goal of our current work is to experimentally test the hypothesis that systemic significance of the function and expression of OADH is related to the enzyme participation in protein glutarylation. Taking into account delayed effects of metabolic alterations in neuropathologies, that may be mediated by post-translational acylation of proteins, mostly studied regarding acetylation of histones (26, 28–33), we characterize long-term changes in protein glutarylation, OADH expression and metabolism, induced by a short-term pharmacological challenge of OADH function in animals of different (patho)physiological states. Our choice of the pathology model for these studies accounts for several considerations. As noted above, the *DHTKD1* mutations are often associated with muscle weakness (4, 5) and Charcot-Marie-Tooth disease (6, 9, 10). It is remarkable in this regard that our search on the *DHTKD1* expression in Gene Expression Omnibus database[1] has revealed that the SCI at T8 vertebra, known to induce muscle atrophy due to impaired muscle innervation, is associated with changed *DHTKD1* expression, both in the injured spinal cord and skeletal muscles (**Supplementary Figure 1**). In the current study we therefore use a rat model of SCI and specific OADH-directed inhibitor adipoyl phosphonate (19, 34) in its membrane-permeable trimethylated form (trimethyl ester of adipoyl phosphonate, TMAP) to investigate (patho)physiological significance of OADH function and its link to glutarylation in neural tissue. Based on previous studies on systemic significance of metabolic changes in cerebral cortex (26, 31, 35–38), we select this brain region to reveal the consequences of the perturbed OADH function for the brain metabolism in healthy and diseased animals. Addressing the goals of current study using this tissue also considers neurological outcome of the *DHTKD1* mutations (3, 6, 9–11) and significant changes in cellular metabolism, including that of the deacylases substrate NAD^+, upon the OADH inhibition in cells where the enzyme expression is low, as also observed in the brain cortex (19).

[1]https://www.ncbi.nlm.nih.gov/geo/

MATERIALS AND METHODS

Materials

All used reagents were of the highest purity grade available. Trimethyl ester of adipoyl phosphonate (TMAP) was synthesized according to (19). EDTA was purchased from Serva (Germany); methanol—from Merck (Germany); Triton-X 100, KH_2PO_4, and NaCl—from Panreac (Spain); glycerol—from MP Biomedicals, LLC (Santa Ana, CA, United States). NAD^+ was obtained from Gerbu (Heidelberg, Germany), oxidized glutathione—from Calbiochem (La Jolla, CA, United States). All other reagents were of the highest purity available and obtained from Sigma-Aldrich (Helicon, Moscow, Russia). Deionized MQ-grade water was used to prepare solutions. The used antibodies are indicated in section "Western-Blotting Quantification of the Protein Levels of OADH, Sirtuin 3, and Sirtuin 5 and of Glutarylated Proteins in Rat Cerebral Cortex."

Animal Husbandry

Manipulations with rats were carried out in accordance with the international recommendations of Good Laboratory Practice (GLP), methodical recommendations for laboratory animal care (Agricultural-Industrial Guidance Document 3.10.07.02-09), European Convention for the Protection of Vertebrate Animals Used for Experimental and Other Scientific Purposes, Strasbourg, 1986 ETS No. 123), as well as Guidelines for accommodation and care of animals, including species-specific provisions for laboratory rodents and rabbits developed by Rus-LASA (No. 33216-2014, 01.07.2016) and internal rules of Russian Cardiology Research and Production Complex. The experimental protocols were approved by Bioethics Committee of Russian Cardiology Research and Production Complex (Protocol No. 3, 23.03.2016) and Bioethics Committee of Lomonosov Moscow State University (protocol number 69-o from 09.06.2016). The study was not pre-registered. The minimum necessary size of the animal sample was estimated by *t*-test using a power of 80% and a level of significance of 0.05.

The study was exploratory, and no exclusion criteria were predetermined. The animals were kept in standard conditions with 12 h light and 12 h dark cycle in individual cages with free access to water and meal.

Spinal Cord Injury Model and Administration of the 2-Oxoadipate Dehydrogenase Inhibitor

The SCI model and postsurgical care were described in details in previous works (26, 33). Severe SCI was performed using the weight-drop method that allows maximal standardization of the injury level (39). The rats were purchased from Nursery of laboratory animals, Institute of Bioorganic Chemistry (Pushchino, Russia). The adult female Sprague–Dawley of 12–13 weeks (weighing 230 ± 20 g) were exposed to laminectomy (LE) or SCI at the T9 vertebra, with their follow-up ended after 8 weeks, i.e., at the corresponding age of 20–21 weeks (weighing 290 ± 20 g in LE group and 265 ± 15 g in SCI group) (**Figure 2B**). Sham-operated animals were subjected to LE without affecting the dura matter. LE was associated with the formation of granuloma, affecting muscles, vessels, and connective tissue at the site of the operation.

Intranasal administration of a water solution of TMAP (at a dose of 0.02 mmol/kg) were performed once in the morning following the operation, i.e., within 15–20 h after the operation. This experimental design imitated potential therapeutic intervention after the neurotrauma. Intranasal application was used as a non-invasive method providing an access to the CNS for different molecules that do not cross the blood-brain barrier (40). Control animals received the corresponding administration of physiological solution (0.9% NaCl). No nasal bleeding was observed. In total, 33 rats were involved in the SCI model study. One rat died during the post-surgical recovery period. The resulting 32 rats were distributed among the experimental groups as shown in **Figures 2A,C**.

Eight weeks after the operations, the rats were decapitated, the brains were excised and transferred on ice. The cerebral hemispheres (called as cerebral cortex further in the text) were separated from other brain parts and frozen in liquid nitrogen 60–90 s after decapitation. The cortices were stored at −70°C before biochemical analyses.

Independent Experiments on Short-Term Effects of Administration of the 2-Oxoadipate Dehydrogenase Inhibitor

Intranasal administration of TMAP was also performed in the study of the short-term consequences of the TMAP treatment (**Figure 2D**), using the male Wistar rats obtained from the Russian Federation State Research Center Institute of Biomedical Problems RAS (IBMP) (265 ± 10 g, 8–10 weeks old). The TMAP administration was as described in section "SCI Model and Administration of the OADH Inhibitor." The rats were sacrificed by decapitation using a guillotine (OpenScience, Russia) 24 h after the administration of the OADH inhibitor. The brain cortices were excised and frozen as described above. No rats died or were excluded during the short-term experiment.

Homogenization and Extraction of Rat Tissues

To assay the enzymatic activities, halves of the cortex tissue were homogenized according to the previously published protocol (41). Homogenization buffer contained 50 mM MOPS pH 7.0, 2.7 mM EDTA, 20% glycerol and the mammalian protease inhibitors cocktail. For metabolic profiling, another half of the brain cortex was extracted with methanol and acetic acid according to the published procedure (33, 42).

Enzymatic Assays

Extramitochondrial activity of multienzyme OADH complex (OADHC), designated as OADHCem in the further text, and activities of enzymes of central carbon metabolism were measured in the brain homogenates as described in (26, 41, 43), using Sunrise microplate reader (Tecan, Grödig, Austria). The multienzyme assay scheme ensured at least three technical replicates for each sample. Activities of enzymes are expressed in μmol of a product generated per min per g of the tissue fresh weight (FW). The enzymatic activities were measured at saturating concentrations of all the substrates and cofactors. The maximal reaction rate of an enzyme or enzymatic complex was thus estimated, corresponding to the functional expression of an enzyme or its multienzyme complex in the tissue homogenate.

Western-Blotting Quantification of the Protein Levels of 2-Oxoadipate Dehydrogenase, Sirtuin 3, and Sirtuin 5 and of Glutarylated Proteins in Rat Cerebral Cortex

The levels of sirtuin 3 (EC 2.3.1.286), sirtuin 5, OADH and protein glutarylation were estimated by western-blotting using primary antibodies from Cell Signaling Technology (Danvers, MA, United States) #8782 and #5490 for sirtuin 5 and sirtuin 3, respectively, Thermo Fisher Scientific (Waltham, MA, United States) #PA5-24208 for OADH and PTM Biolabs (Chicago, IL, United States) #PTM-1151 for glutaryllysine. The primary antibodies for sirtuin 5, sirtuin 3, OADH protein and glutaryllysines were used in 1:1,000, 1:2,000, 1:200 and 1:2,000 dilutions, respectively, with the appropriate secondary anti-rabbit HRP-conjugated antibodies from Cell Signaling Technology, #7074. The relative quantification of chemiluminescence was performed in ChemiDoc Imager (Bio-Rad, Hercules, CA, United States) and Image Lab software version 6.0.1 (Bio-Rad, Hercules, CA, United States). Normalization of the protein levels to the total protein in the corresponding gel lanes was performed using the protein fluorescent quantification with 2,2,2-trichloroethanol, similarly to the published procedure (44). The band intensities from different membranes were compared across all the membranes after the normalization on the levels of the common samples repeated on independent membranes.

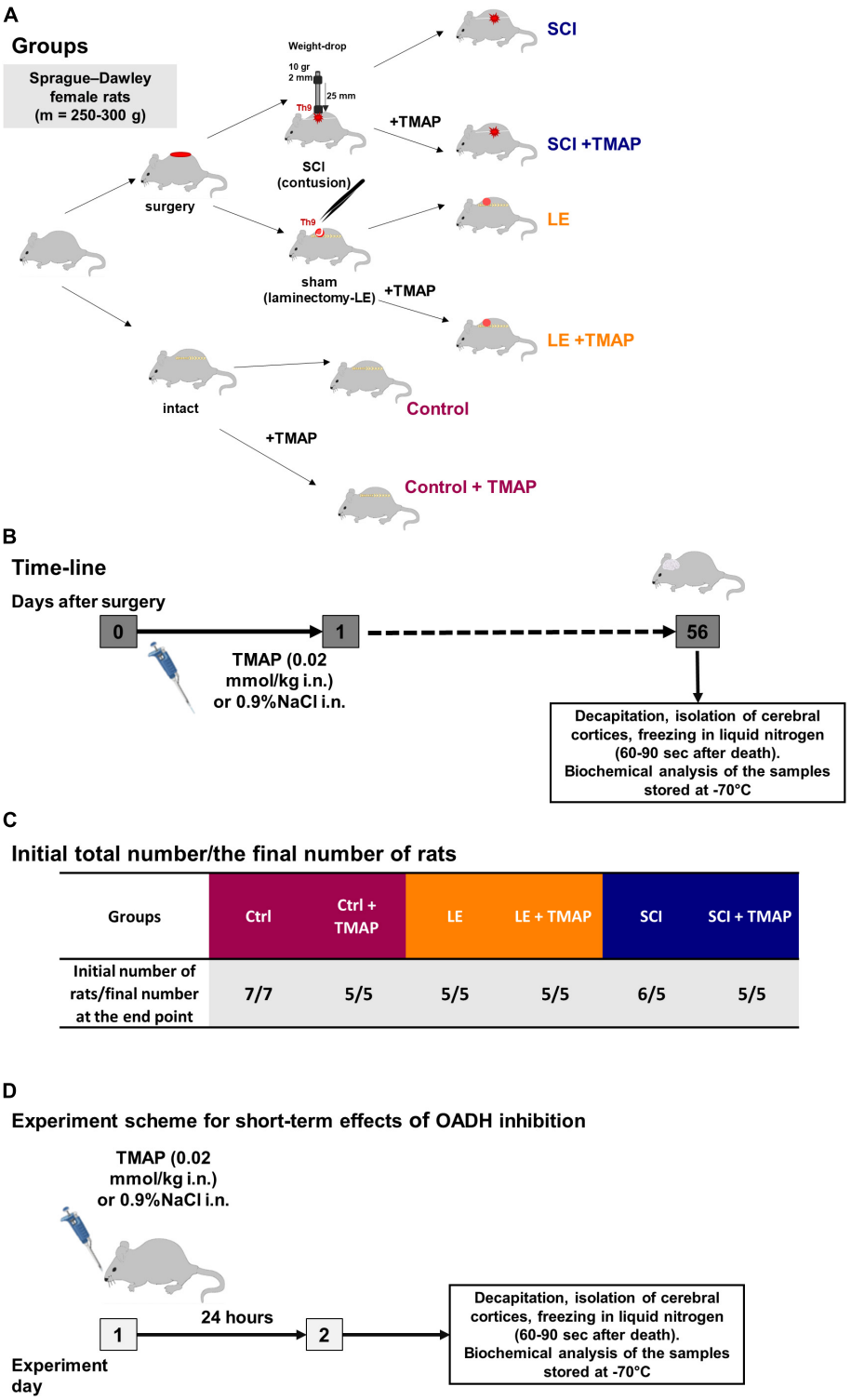

FIGURE 2 | Experimental flow-chart. **(A)** An overview of experimental procedures for each animal group in SCI model. **(B)** Timeline of the procedures in SCI model. **(C)** Distribution of rats across the groups in SCI model with initial and end point number of animals in each group. **(D)** Timeline of the procedures in the study on short-term effects of the OADH-directed inhibitor TMAP. The color code of the experimental groups, given in **(A,C)**, is employed in the following presentation of the results in different figures.

Metabolic Profiling of the Rat Brain Extracts

Amino acids and related compounds were quantified in extracts of cerebral cortices according to (26, 33, 42) using the amino acid analyzer L-8800 (Hitachi Ltd., Japan), employing a gradient of Li-citrate buffers and the ninhydrin reagent (Wako Pure Chemical Industries; P/N 298-69601). Glutathione disulphide (GSSG) was quantified using fluorescence of its product with o-phthalic aldehyde according to the method described in (45) and optimized in (46). Tryptophan levels in the brain extracts were determined as described in (47) with modifications according to (48), using the tryptophan conversion into fluorescent norharman. The fluorescent signal was obtained at λ_{ex}/ λ_{em} of 365/460 nm. NAD^+ levels in the brain extracts were measured as described in (49).

Mass-Spectrometric Detection of Glutarylation

Mass-spectrometric detection of ODP2 (EC 2.3.1.12) glutarylation was carried out in the cerebral cortices of male Wistar rats. The tissue samples were treated according to the previously published protocol (50) and subjected for SDS-PAGE electrophoresis with the concentration of the separating gel of 10% (51). Gel lanes from 25 to 75 kDa were excised, subjected to proteolysis by trypsin, and the resulting peptide fragments were analyzed by LC-MS with detection of modified and unmodified peptides according to the previously published protocol (50). The peptides for quantification of the ODP2 glutarylation level are given in **Table 1**.

Mass-spectrometric detection of OADH glutarylation was performed using the recombinant human OADH expressed in *Pichia pastoris* and purified according to the previously published protocol (1). The major protein band of 100 kDa after SDS-PAGE electrophoresis with the concentration of the separating gel of 10% was analyzed by LC-MS as above.

Statistical Analysis

All data were analyzed using GraphPad Prism 7.0 software (GraphPad Software, Inc., La Jolla, CA, United States) or RStudio[2] and shown as mean ± SEM. For metabolic profiling visualization and correlation analysis *pheatmap* and *ggstatplot* R packages were used, respectively. Changes in specific biochemical parameters are presented as box-and-whisker plots, showing quantiles of each sample distribution. For comparison of more than two groups, two-way analysis of variance (ANOVA) and *post-hoc* Tukey's test were used. The two-tailed *p*-values 0.05 were considered to indicate statistically significant differences, shown in the figures.

[2]https://rstudio.com

TABLE 1 | Characterization of ODP2 peptides.

Peptide	Specification	C13-isotopomeric variants of the precursors		
		monoisotopic	[M+1]	[M+2]
KELNK(+114.03)MLEGK	K451 glutarylated	652.3499++	652.8514++	653.3521++
GLETIASDVVSLASK	normalization peptide	745.409++	745.9105++	746.4119++

The peptides are used for the relative quantification of ODP2 K451 glutarylation by MS in the rat brain cortex. Several precursor variants with monoisotopic mass and the C13-isotopomeric variants ([M+1] and [M+2]) have been detected to increase the quantification accuracy.

RESULTS

Analysis of Overall Metabolic Impact of 2-Oxoadipate Dehydrogenase Inhibition Under Different (Patho)physiological Conditions

To identify the pathways associated with OADH function in the brain, where OADH/*DHTKD1* expression is relatively low (19), the metabolism of the rat cerebral cortex has been challenged by specific OADH inhibitor TMAP in different (patho)physiological states of the rats. Based on an earlier finding of the long-term time-dependent biphasic changes in the *DHTKD1* expression following SCI (**Supplementary Figure 1**), the metabolic changes 8 weeks after a single administration of TMAP have been determined in the female rats of the control, LE and SCI groups (**Figure 3**). The usual levels of the OADH substrate 2-oxoadipate and its transamination sibling 2-aminoadipate are far too low for unambiguous detection of their changes in animal tissues. However, the amino acid metabolism, where OADH takes part, is tightly interconnected. Therefore, the amino acid profiles in the rat cerebral cortex are used as indicators of OADH function. To analyze the associated changes in the functional expression of the enzymes of amino acid metabolism, the activities of such enzymes are included in the metabolic cluster maps. To assay the OADH and OGDH reactions, catalyzed by the enzymes assembled into the multienzyme complexes (OADHC and OGDHC, respectively), the previously elaborated protocol is followed (41). The extramitochondrial activity of OADHC (OADHCem) is assayed before the mitochondrial solubilization that releases the intramitochondrial activities of both the OGDH and OADH complexes. The intramitochondrial activity of OADHC cannot be discriminated from a much higher level of the activity of OGDHC, also catalyzing the reaction with 2-oxoadipate. However, because of its low expression, OADHC does not significantly contribute to the assayed intramitochondrial OGDHC activity. In view of the problems with assaying the intramitochondrial activity of OADH, where major part of the enzyme is supposed to be localized, the expression of the previously identified OADH isoforms of 70 and 130 kDa (1) is determined by western-blotting. Finally, given the possible link between the OADH-dependent production of glutaryl residues and system of post-translational modification of proteins by glutarylation (**Figure 1**), the levels of glutarylated proteins and deglutarylase sirtuin 5 in the brain are also included in the metabolic heatmap. Expression of the major mitochondrial deacetylase sirtuin 3 is

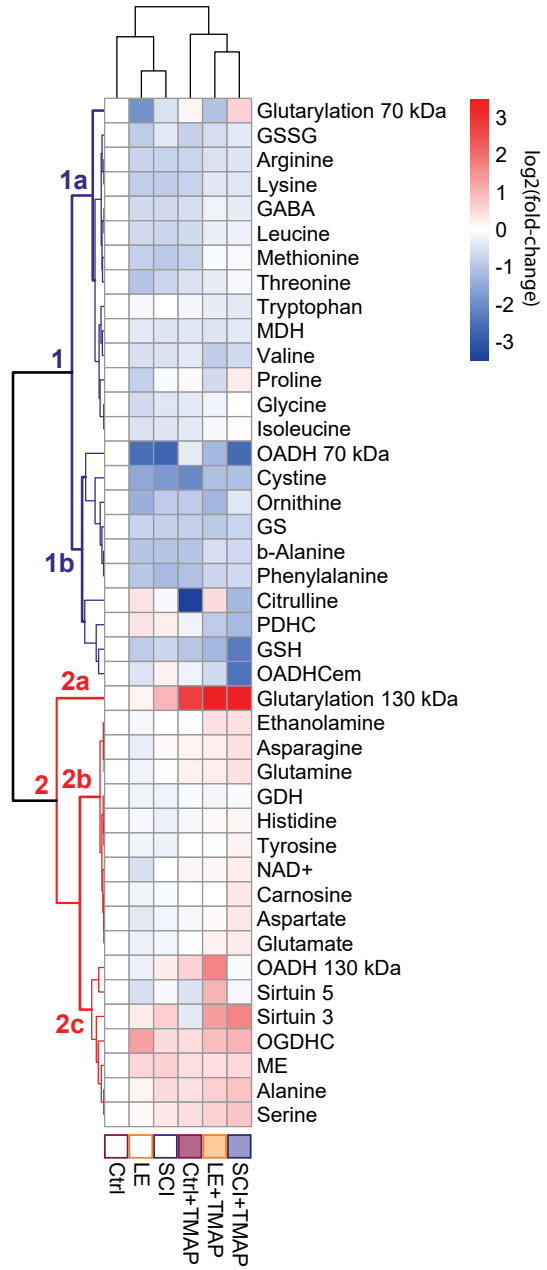

FIGURE 3 | Clusters of metabolic changes induced by the OADH-directed inhibitor TMAP in the cerebral cortices of the control (Ctrl), sham-operated (LE) and SCI rats. Metabolic changes in the cerebral cortex are presented as $\log_2$(fold-change), where a fold-change is a ratio of the mean metabolite level in the treated group to the corresponding mean level in the control group. These normalized values are shown in the heatmap according to the color code of the scale bar. The animal groups are indicated at the bottom of the heatmap and assigned the color code used in all the figures presenting the data on these groups. Metabolites (at the right side of the heatmap) and experimental groups (at the bottom of the heatmap) are clustered using ward.D method from *pheatmap* package in RStudio. The main metabolic clusters are numbered 1 and 2, each having the subclusters designated by the letters. The cluster 1 with decreased levels of metabolites is assigned the blue color, while the cluster 2 with increased levels of metabolites is shown in red. Number of animals in each group: Ctrl, $n = 7$; LE, $n = 5$; SCI, $n = 5$; Ctrl + TMAP, $n = 5$; LE + TMAP, $n = 5$; SCI + TMAP, $n = 5$.

determined in view of its involvement into the regulation of mitochondrial metabolism, particularly the enzymes of the amino acid metabolism (50, 52).

Overall, the changes in 42 biochemical parameters of the brain, quantified 8 weeks after a single TMAP administration to the control, LE or SCI rats, as well as the changes due to LE and SCI, all relative to the control levels, are shown as a heatmap in **Figure 3**. Different sets of biochemical parameters that change in concert, form clusters shown as a tree at the left of the heatmap, while the level of similarity between specific metabolic states is shown in the tree above the heatmap (**Figure 3**). Thus, the clustering procedure reveals certain sets of linked biochemical parameters, as well as specific and common features of the analyzed (patho)physiological states.

The clustering tree of the metabolic states (**Figure 3**, clusters above the heatmap) shows that TMAP administration is the main differentiator between the studied animal groups, as all the groups treated with TMAP are clearly separated from the rats not exposed to TMAP, independently of their (patho)physiological state. The clustering tree of metabolites (**Figure 3**, clusters at the left of the heatmap) points to the two major clusters of the first level, each headed by the glutarylated proteins of 70 and 130 kDa, respectively. Glutarylated proteins of 70 kDa are associated with the cluster 1 combining parameters which mostly decrease after OADH inhibition in different (patho)physiological states, as compared to those in the control rats. This "blue" cluster 1 includes subclusters of the less (above, 1a) and more (below, 1b) strong changes. The stronger changes include the expression of OADH 70 kDa, activity of OADHCem, activity of PDHC and levels of a number of redox metabolites, such as glutathione, its precursor cystine, and citrulline—a marker of NO synthesis from arginine. Glutarylated proteins of 130 kDa (branch 2a at **Figure 3**), representing the key long-term effect of TMAP administration across all the three studied states (control, LE and SCI), are associated with the "red" cluster 2, combining parameters which mostly increase, as compared to those in the control rats. The "red" cluster is further divided into the subclusters of the parameters changing less (above, 2b) and more (below, 2c) across the studied groups in comparison to their levels in the control rat brain. The stronger changes in the subcluster 2c are inherent in the expression of OADH 130 kDa, deglutarylase sirtuin 5, deacetylase sirtuin 3, activities of OGDHC and $NADP^+$-dependent malic enzyme, as well as the levels of the amino acids serine and alanine (**Figure 3**).

Pyruvate Dehydrogenase Complex Glutarylation

It is remarkable that the subcluster 1b within the "blue" cluster 1, which is headed by the glutarylated proteins of 70 kDa, comprises changes in the activity of PDHC, levels of the redox-state-related metabolites, such as glutathione and citrulline, along with changes in expression of OADH 70 kDa and activity of OADHCem (**Figure 3**). While the link of PDHC activity to the brain redox state is well-known, the clustering of these indicators with the expression

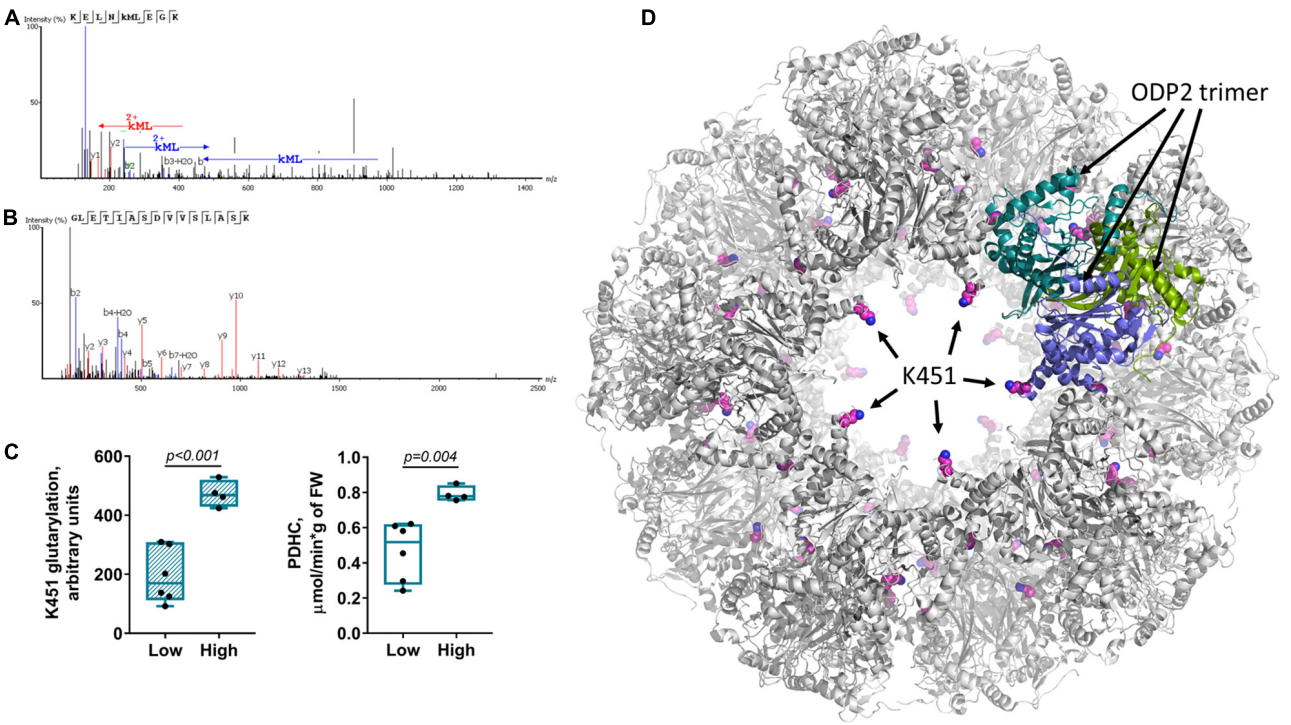

FIGURE 4 | Glutarylation of pyruvate dehydrogenase complex. The glutarylation of lysine K451 of the second component of rat PDHC (ODP2 protein, encoded by *DLAT* gene) is identified in the rat brain by LC-MS. **(A)** The spectra of the peptide with K451 glutarylation. **(B)** The spectra of non-glutarylated peptide, used for normalization. **(C)** Correspondence of K451 glutarylation of ODP2 to PDHC activity: The six animals with the low K451 glutarylation level also have the low PDHC activity, while the four animals with the high glutarylation level have the high PDHC activity. The animal subgroups exhibit significant differences in the parameters, determined by unpaired Mann-Whitney test and shown as *p*-values in the graphs. **(D)** Localization of the glutarylated residue (shown with pink carbon atoms) in the ODP2-formed core of PDHC, according to the structure (PDB: 6CT0) of human protein, whose K466 corresponds to K451 of the rat protein. Subunits of one of the ODP2 trimers, organized by five around the "pore" to the inner cavity of the core, are colored in green, blue and marine. As seen from the structure, K451/K466 residue faces the pore. The residue glutarylation would change electrostatics of the entrance to/exit from the inner cavity of the core.

and activity of OADH suggests the PDHC regulation by glutarylation. In fact, the second enzymatic component of PDHC, dihydrolipoamide acetyltransferase (ODP2, encoded by *DLAT* gene) has the same molecular mass (∼70 kDa) as one of the two major bands of the brain glutarylated proteins (**Supplementary Figure 2**). In view of the known proteolysis of this protein, and potential glutarylation of other PDHC components, we have identified the glutarylated proteins of 25–75 kDa in the homogenates of the rat brain cortex by mass-spectrometric analysis. Glutarylation of the brain ODP2 subunit of PDHC at K451 residue is revealed in this experiment. The corresponding MS/MS spectra of the glutarylated ODP2 peptide are shown in **Figure 4A**.

Quantification of the level of ODP2 glutarylated peptide in a sample of control rats is based on normalization of the glutarylated peptide abundance to ODP2 expression, estimated by simultaneous quantification of the well-defined ODP2 peptide shown in **Figure 4B**. This quantification reveals a high interindividual variability in the levels of glutarylation of ODP2, that interferes with identification of statistically significant differences in this parameter upon comparison of different animal groups. Among the factors potentially affecting the variability, we have assessed its response to such known metabolic regulators of the brain metabolism as vitamins B1 and B6. The animals supplemented with 100 mg per kg of vitamins B1 and B6 as described earlier (43), do not exhibit any shift in the ODP2 glutarylation level, compared to the control animals. In both cases, the two different subgroups of the animals could be seen. Those with the low ODP2 glutarylation level also possess the low PDHC activity, while the animals with the high glutarylation level have high PDHC activity. The differences between these subgroups become statistically significant in the pooled sample of the control and vitamin-supplemented animals (**Figure 4C**). The data suggest regulatory role of K451 glutarylation of ODP2 in PDHC.

Structural analysis reveals that the glutarylated K451, belonging to the catalytic domain of ODP2, extends into the pores of the dodecahedral 60-meric core of mammalian PDHC (**Figure 4D**). As the pores may be important for the CoA entry to the catalytic channel of ODP2 from the inner cavity of the core (53), our analysis favors functional importance of ODP2 glutarylation. As a result, the OADH-dependent glutarylation of PDHC may underlie the common allocation of the PDHC activity, redox-related metabolites, OADH 70 kDa isoform expression and OADHCem activity

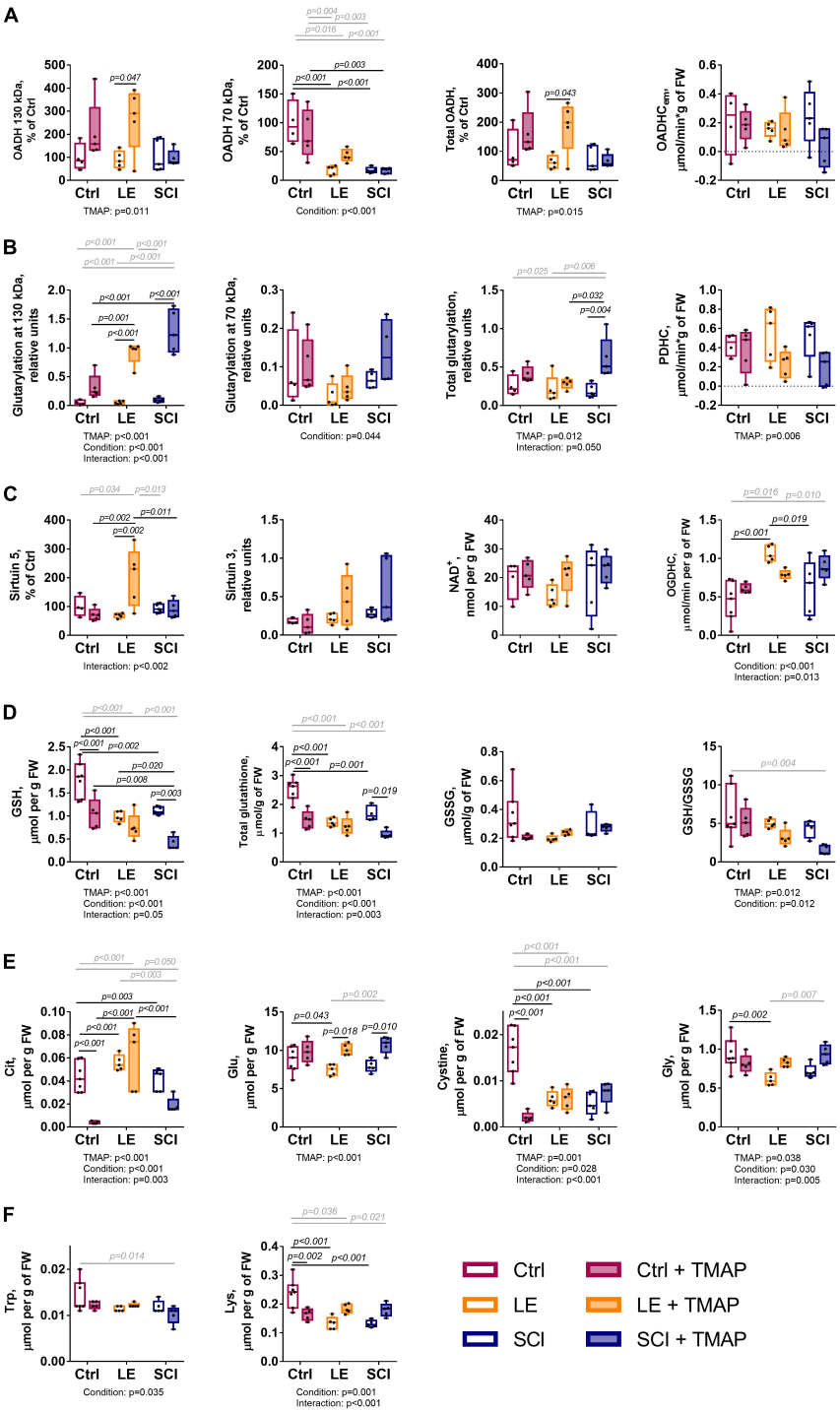

FIGURE 5 | Long-term changes in selected biochemical parameters of the cerebral cortex of the control, LE and SCI rats 8 weeks after a single administration of the OADH-directed inhibitor TMAP. Representative Western blots for relative glutarylation and protein levels are shown in **Supplementary Figures 2–5**. **(A)** Relative expression of the OADH isoforms 130 and 70 kDa, total OADH and enzymatic activity of extramitochondrial OADHC. **(B)** Relative glutarylation of the brain proteins of 130 and 70 kDa, total glutarylated protein and PDHC activity. **(C)** Expression of sirtuin 5, sirtuin 3, level of NAD^+ and enzymatic activity of OGDHC. **(D)** Glutathione redox state homeostasis: levels of reduced glutathione (GSH), total glutathione, oxidized glutathione (GSSG), and the glutathione redox ratio. **(E)** Levels of metabolites involved in glutathione homeostasis: citrulline (Cit), cystine, glutamate (Glu), glycine (Gly). **(F)** Metabolic indicators of the OADH function: tryptophan (Trp) and lysine (Lys). Statistical significance of differences between experimental groups is determined by two-way ANOVA with Tukey's *post-hoc* test. Factor significances and their interaction, estimated by ANOVA, are shown as *p*-values ($p < 0.05$ only) below the graphs. The *p*-values on the graphs show the results of the *post-hoc* test, that are in black or gray for the experimental groups differing by one or two factors, correspondingly.

within the subcluster 1b of the "blue" cluster 1 headed by glutarylated proteins of 70 kDa.

Long-Term Changes in the 2-Oxoadipate Dehydrogenase-Associated Parameters of the Rat Cerebral Cortex

Statistically significant differences between the studied groups have been assessed for selected metabolic parameters (**Figure 5**) from the OADH-comprising subclusters (**Figure 3**). The three indicators of OADH function, i.e., the extramitochondrial activity of OADHCem and the protein expression of the two OADH isoforms, respond differently to the interventions (**Figure 5A**). Expression of 130 kDa isoform of OADH is influenced by the TMAP treatment (p = 0.011 for the TMAP factor), significantly elevated in the TMAP-treated LE animals compared to LE rats without TMAP (p = 0.047). In contrast, 70 kDa isoform of OADH is significantly affected by the (patho)physiological state of animals (p = 0.001 for the condition factor). That is, independent of the TMAP treatment, either LE or SCI animals exhibit a lower level of 70 kDa OADH than is inherent in the control animals (**Figure 5A**). The OADHCem activity does not exhibit significant changes across the studied conditions.

Regarding glutarylation of the brain proteins of 130 kDa, both the TMAP administration and (patho)physiological state are significant and interacting factors, based on the ANOVA analysis provided under the graphs in **Figure 5B**. In contrast, only the animal state significantly affects glutarylation of 70 kDa proteins. Comparison of the studied groups indicates that the TMAP administration significantly increases glutarylation of 130 kDa proteins in both the LE and SCI animals, but not in the control animals. The total glutarylation is increased by TMAP only in SCI animals (**Figure 5B**).

The TMAP effect on the sirtuin 5 expression (**Figure 5C**) reciprocates the TMAP-induced increase in total glutarylation (**Figure 5B**). That is, there is an increase in sirtuin 5 expression by TMAP in LE, but not in SCI animals. In contrast, the total glutarylation increases in SCI animals, but is constant in LE animals. These findings indicate that a long-term effect of the OADH-directed inhibitor on the brain protein glutarylation is tightly linked to the regulation of the sirtuin 5 expression, with the regulation depending on pathophysiological state of the animals.

As shown in **Figure 5D**, the TMAP exposure strongly diminishes the brain glutathione levels in the control and SCI animals, but not in LE animals, where expression of sirtuin 5 is increased. Thus, the TMAP-induced perturbation impairs glutathione homeostasis when the perturbation is not addressed by an increase in the sirtuin 5 expression. However, the mechanisms of the TMAP-induced decreases in the glutathione level in the control and SCI brains are different. This is obvious from the associated changes in the levels of the glutathione precursors—cystine, glutamate, glycine—and the level of the marker of NO· production citrulline (**Figure 5E**). In the control animals, the glutathione decrease is accompanied by the decrease in the cystine level (**Figures 5D** vs. **5E**). Simultaneous decline in the level of citrulline (**Figure 5E**) points to insufficient generation of the cystine transporter activator NO· and diminished cystine transport (54). However, neither cystine, nor citrulline levels are significantly reduced by the TMAP treatment of SCI animals, suggesting another mechanism of the glutathione drop after SCI. Among these mechanisms, OGDHC dysfunction is a factor that may perturb the redox status of the brain glutathione buffer (55). Yet in our experimental settings, the TMAP treatment is not significant for the OGDHC activity, which responds to the (patho)physiological state only (**Figure 5C**, condition significance). From the parameters analyzed, the increased glutarylation in SCI animals coincides with the TMAP-induced decrease in the brain glutathione levels (**Figures 5B** vs. **5D**). The role of glutarylation in the glutathione homeostasis is supported by the fact that in LE animals, neither the glutathione homeostasis nor the glutarylation are perturbed by TMAP, as the inhibitor administration increases the sirtuin 5 expression. The different homeostatic mechanisms maintaining the brain glutathione level in response to the TMAP treatment in different (patho)physiological states, are further supported by the correlation analysis of the three experimental groups comprising the animals with and without TMAP (**Figure 6**). In control animals, cystine and citrulline levels are strongly correlated to each other and to the levels of reduced glutathione, that is in accordance with the $NO^{\cdot}$-dependent cystine supply being limiting for glutathione biosynthesis. In SCI animals, these strong correlations disappear, while the reduced glutathione becomes inversely correlated to the level of its precursor glutamate.

The levels of OADH-related amino acids lysine and tryptophan (**Figure 1**) decrease in the LE and/or SCI animals, compared to the control animals. These decreases depend on the (patho)physiological state of the animals more than on the TMAP administration (**Figure 5F**). The lysine levels show a significant interaction between the animal state and TMAP administration, while the levels of tryptophan decrease significantly in the TMAP-treated SCI animals compared to the control ones (**Figure 5F**).

Concordance Between the 2-Oxoadipate Dehydrogenase Expression and Brain Protein Glutarylation

As revealed by Western-blotting (**Supplementary Figures 2**, **3**), the major glutarylated proteins and OADH isoforms in the brain have the same molecular masses, i.e., 130 and 70 kDa. Together with the known autoacylation reactions in the 2-oxo acid dehydrogenases (53), this finding suggests that the TMAP-induced increases in both the OADH expression (**Figure 5A**) and brain protein glutarylation (**Figure 5B**) manifests autoglutarylation of OADH isoforms, as occurrence of this side reaction is expectedly proportional to the OADH expression. The ratios of the glutarylated proteins to the OADH expression have therefore been calculated for each animal (**Figure 7**). Such analysis shows that the TMAP effects on the brain glutarylation of 130 kDa, 70 kDa and/or total proteins in the control and LE animals disappear when normalized to the OADH expression (**Figure 7**, control and LE rats). In contrast, in the TMAP-treated SCI rats, also the normalized protein glutarylation

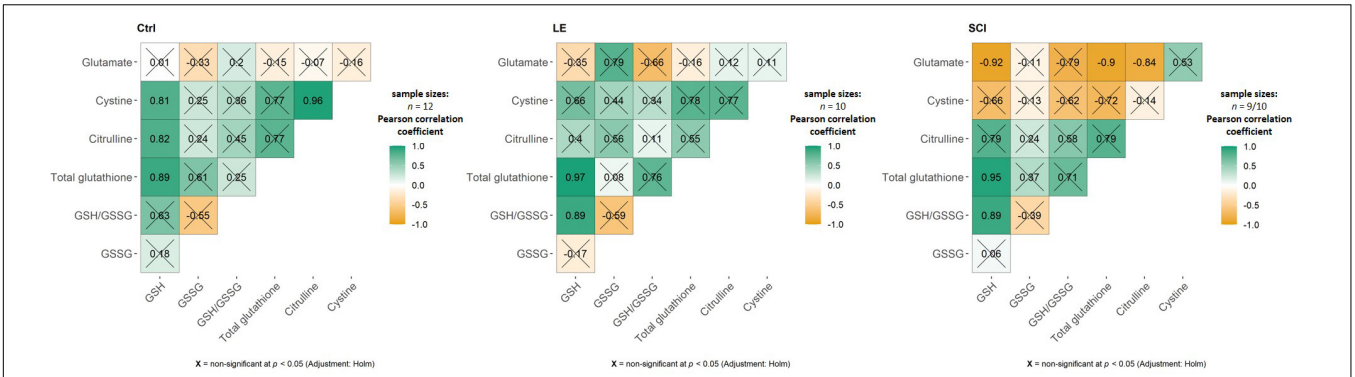

FIGURE 6 | Pearson's correlation matrices between the brain metabolites involved in glutathione biosynthesis. Each of the three shown groups, i.e., the control, LE and SCI rats, include animals with and without administration of the OADH-directed inhibitor TMAP. Sample sizes for the estimated metabolites are indicated in the figure. In SCI, sample with $n = 9$ refers to the GSSG level estimation. Non-significant ($p \geq 0.05$) correlations after Holm-Bonferroni multiple testing adjustment are crossed out. The figure is created using *ggstatsplot* package in Rstudio.

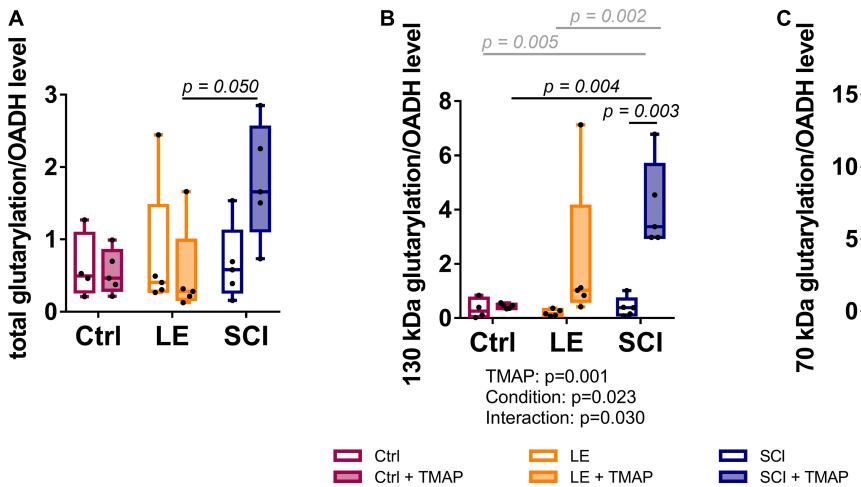

FIGURE 7 | Levels of brain protein glutarylation, normalized to OADH expression, in the rat cerebral cortex of the studied animal groups. Representative Western blots for estimation of relative glutarylation and OADH levels are shown in **Supplementary Figures 2**, **3**, respectively. **(A)** Total protein glutarylation levels normalized to the sum of the expression of the two OADH isoforms. **(B)** Levels of glutarylation of 130 kDa proteins normalized to expression of 130 kDa isoform of OADH. **(C)** Levels of glutarylation of 70 kDa proteins normalized to expression of 70 kDa isoform of OADH. Statistically significant ($p < 0.05$) differences between experimental groups, determined by two-way ANOVA with Tukey's *post-hoc* test, are shown on the graphs. The black and gray colors correspond to the groups differing in one or two factors, respectively. Statistically significant ($p < 0.05$) factors and their interactions, estimated by ANOVA, are shown as *p*-values below the graphs.

exhibits an increase, compared to the non-treated SCI animals (**Figure 7**, SCI rats). The increase is statistically significant regarding glutarylation of 130 kDa proteins (**Figure 7**, SCI in the middle panel). Besides, statistically significant differences in the normalized glutarylation of total proteins and 70 kDa proteins are observed between the TMAP-treated animals after SCI and LE (**Figure 7**, the left and right panels). Thus, only in SCI animals, the normalized glutarylation of brain proteins after the short-term OADH inhibition exceeds the glutarylation proportional to the OADH expression.

In view of the low OADH expression in the brain, the mass-spectrometric identification of the enzyme peptides in the tissue homogenates is below the detection limit. However, glutarylation of OADH is confirmed by our mass-spectrometry analysis of human OADH protein, overexpressed in yeast. In the purified recombinant OADH the peptides with glutarylated OADH residues K155 and K818 are determined (**Figures 8A,B**). Structural analysis shown in **Figure 8C** reveals that the glutarylated residues are located on the protein surface away from the active sites.

Short-Term Changes in Glutarylation System Upon 2-Oxoadipate Dehydrogenase Inhibition

The long-term metabolic consequences of a single TMAP administration cannot be caused by the permanent action of a water-soluble inhibitor during 8 weeks, as such inhibitors are

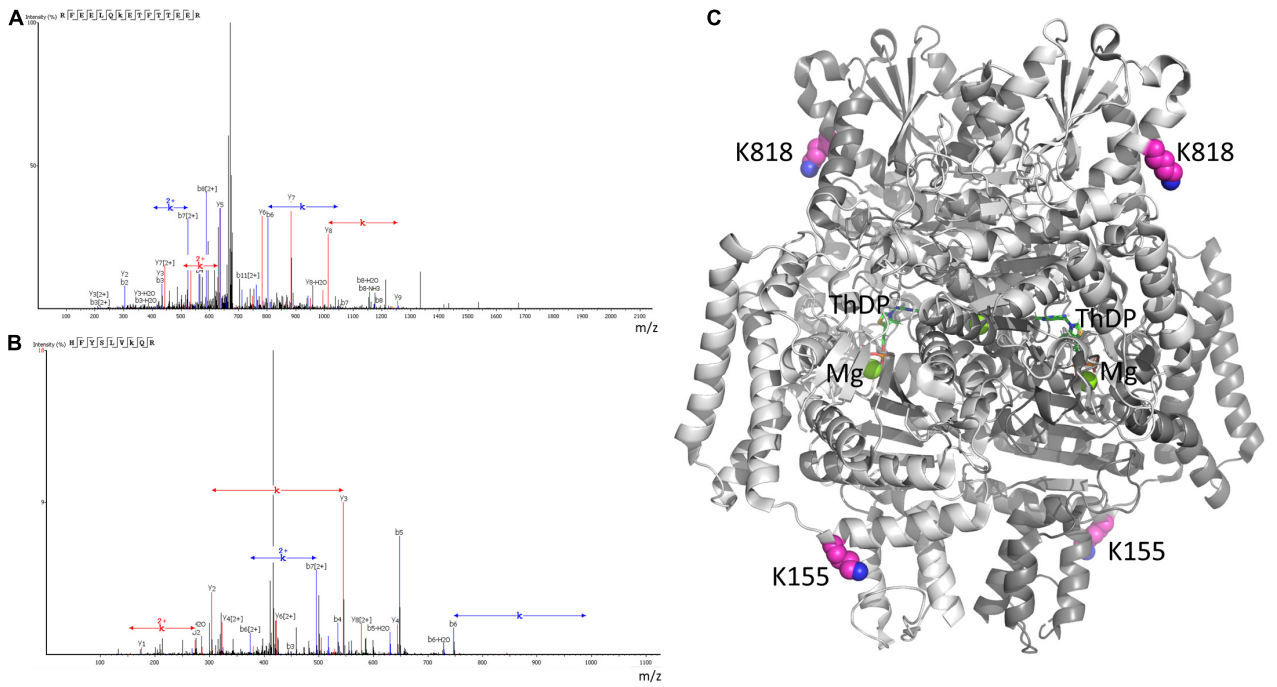

FIGURE 8 | Mass-spectrometric identification of OADH glutarylation. The glutarylation of lysine K155 and K818 is identified by LC-MS in human recombinant OADH expressed in yeast. **(A)** The spectra of the peptide with glutarylated K155, namely RFEELQK(+114.03)ETFTTEER, m/z = 686.3347, retention time (RT) = 96.49; **(B)** the spectra of the peptide with glutarylated K818, namely HFYSLVK(+114.03)QR, m/z = 431.2349, RT = 82.38; **(C)** localization of the identified glutarylated residues (the carbon atoms marked in pink) in the OADH dimer. The available structure of the enzyme dimer crystallized with Mg^{2+}ThDP (PDB: 6SY1) is shown, with the active site regions defined by ThDP and magnesium ions (shown in green).

usually excreted within 24 h. It thus appears that the observed long-term consequences for metabolism (**Figures 3**, **5**) result from the short-term perturbation of the brain glutarylation system by administration of TMAP. To support this assumption, we have assessed the short-term effects of OADH inhibition, estimating key parameters of the brain glutarylation system (**Figure 9**) and metabolism (**Figure 10**) 24 h after the TMAP administration to control animals. Within this time period, prompt responses of the brain metabolism to different challenges including drug administration, are observed, but the time is not enough for metabolic reprogramming (56, 57). Indeed, no significant changes in the brain OADH expression or protein glutarylation are observed in this case (**Figure 9**). However, the TMAP-induced inhibition of the glutaryl-CoA producer OADHC is accompanied by decreased levels of the deglutarylase sirtuin 5 and deacetylase sirtuin 3 (**Figure 9**), linking the OADH function to the brain protein acylation. These short-term changes are not accompanied by metabolic perturbations observed upon the long-term changes in the glutarylation system. Among the metabolites tested in both the long-term and short-term experiments, the only significant short-term effect of TMAP is an increase in tryptophan (**Figure 10**), that is in good accord with the OADH participation in tryptophan degradation. Thus, the short-term consequences of the TMAP administration are an increase in the level of tryptophan manifesting OADH inhibition, and decreased levels of sirtuin 5 and sirtuin 3. The concerted perturbations in the brain acylation system 24 h after the OADH inhibition are thus revealed (**Figure 9**), that may underlie the long-term metabolic rearrangements (**Figure 5**).

DISCUSSION

Post-translational acylation of metabolic proteins and histones through covalent modifications of their lysine residue is an important mechanism contributing to organismal homeostasis and its changes in different pathologies (58–61). The major attention in this regard receives the most abundant modification of lysine residues—acetylation (62–65), whereas significantly less is known about the (patho)physiological role of other types of the acylation (66, 67). In particular, studies of the lysine glutarylation are mostly limited to pathological situations, e.g., when pathogenic mutations in glutaryl-CoA dehydrogenase cause increased levels of the glutarylating agent glutaryl-CoA (27). Our current result on an elevation in protein glutarylation in the animal brain affected by severe SCI, adds to results from independent studies on enhanced abundance of this modification in different pathologies, e.g., in patients with acute myocardial infarction (68), or upon impaired function of deglutarylase sirtuin 5 (69, 70), the enzyme known to be neuroprotective (25, 26).

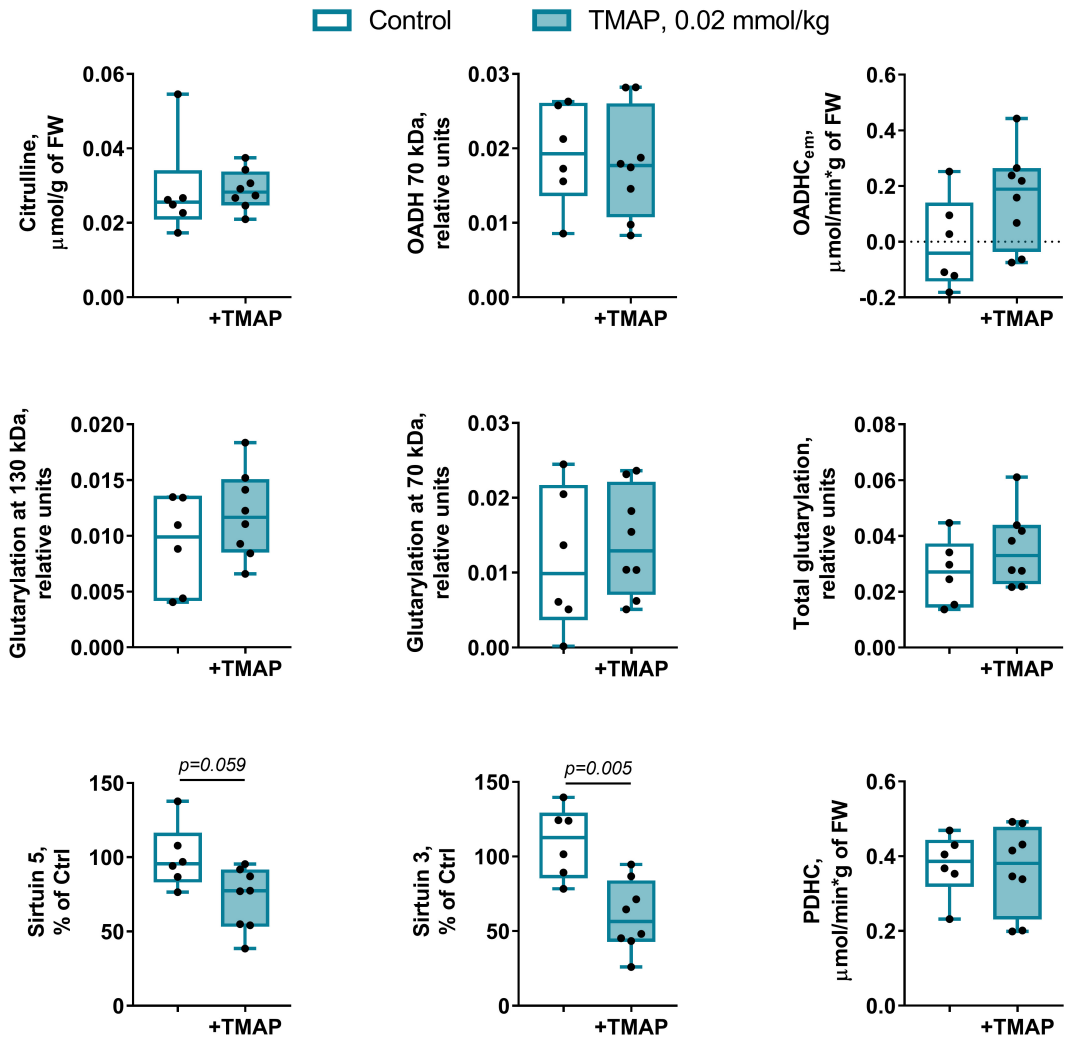

FIGURE 9 | Short-term changes in the protein glutarylation system of the brain cortex 24 h after TMAP administration to the control rats. Representative Western blots for estimation of relative glutarylation and protein levels are shown in **Supplementary Figure 6**. Statistical significance of the differences between experimental groups is determined by unpaired Mann-Whitney test, with p-values < 0.10 shown on the graphs.

In general, tissue level of protein glutarylation depends on the availability of glutaryl-CoA as a source of glutaryl residues, and activity of deglutarylase sirtuin 5. As a producer of glutaryl-CoA, OADH may thus have specific significance for the protein glutarylation. Our results about dependence of the brain protein glutarylation and/or sirtuin 5 expression on administration of the OADH-directed inhibitor TMAP, demonstrate tight connections between the OADH function and glutarylation in the rat brain. The OADH role in regulatory glutarylation is in good accord with the predicted nuclear localization signal of the enzyme (2). In addition to the known mitochondrial localization, the dual localization of the enzyme is also supported by experimental assays of OADH in the extramitochondrial fraction (41). In this regard, the known nuclear localization of the second component of the multienzyme OADH complex (*DLST*-encoded dihydrolipoamide transsuccinylase, EC 2.3.1.61) (71), that is common for the OADH and OGDH complexes, further supports the OADHC role in nuclear production of glutaryl-CoA. Thus, participating in the mitochondrial steps of the lysine and tryptophan catabolism, OADHC may also contribute to glutarylation of proteins, including those in nucleus, e.g., histones. In our samples, glutarylation of the low molecular mass proteins is negligible, compared to the major glutarylated protein bands of 130 and 70 kDa, responding to the TMAP treatment. This is in line with an earlier comparative study of the lysine glutarylation, succinylation, and acetylation detectable by specific antibodies in the brain cortex homogenates: Only the acetylation band is visible in the region of the protein molecular masses below 20 kDa (72). Hence, further studies are required for assessment of the OADH-dependent glutarylation of histones after their enrichment, not compatible with the experimental design of the current work. Nevertheless, nuclear function of OADH in protein glutarylation is in good accordance with our result on the

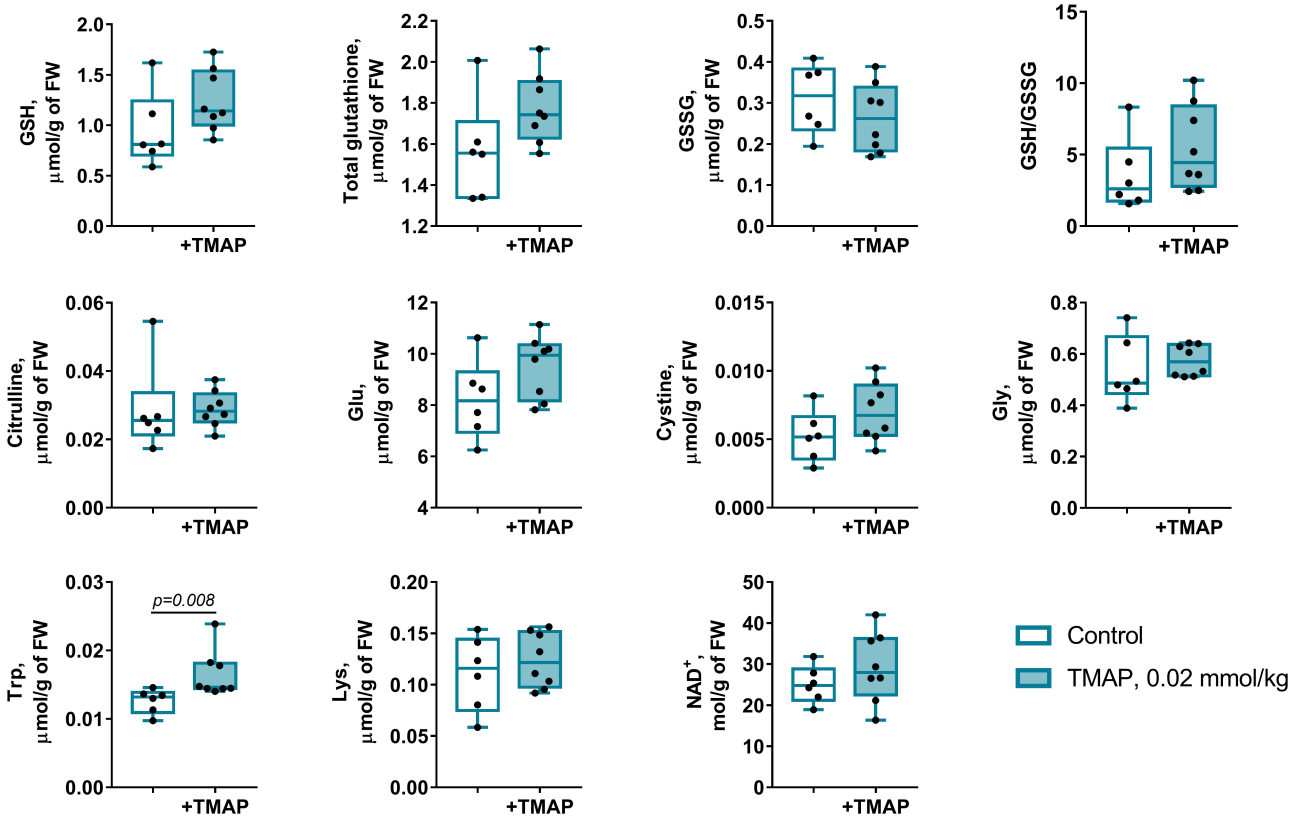

FIGURE 10 | Short-term changes in the redox-state- and OADH-related metabolites in the brain cortex 24 h after a single administration of TMAP. Statistically significant ($p \leq 0.05$) differences between experimental groups are determined by unpaired Mann-Whitney test, with p-values shown on the graphs.

long-term effects of the short-term perturbation of the OADH function by TMAP.

The short-term (24 h after the TMAP administration) inhibition of OADH by TMAP is evident from increased levels of the brain tryptophan (**Figure 10**). This metabolic indicator provides a good measure for the mitochondrial OADH activity that cannot be determined due to its overlap with that of OGDH. In this regard, it is also worth noting that the activity assayed *in vitro* is not equal to the substrate flux through an enzyme *in vivo*, as the flux depends on the *in vivo* concentrations of the enzyme substrates and regulators, which are not equal to those *in vitro*. Hence, the levels of related metabolites are better indicators of the *in vivo* fluxes than the levels of the enzymatic activities *in vitro*, assessing the enzyme functional expression. Simultaneously with the increased tryptophan level (**Figure 10**), the sirtuin 5 expression decreases (**Figure 9**), demonstrating an adaptation in protein deglutarylation to the decreased production of glutaryl-CoA by OADH. Interestingly, also the level of mitochondrial deacetylase sirtuin 3 decreases along with that of sirtuin 5. Apart from confirming the perturbations in the brain acylation system, this finding further links the OADH function to that of PDHC which produces acetylating residues in the form of acetyl-CoA. The lack of other short-term metabolic changes in response to TMAP agrees with the small flux through OADH in the brain, supporting the assumption that the delayed consequences of the TMAP action rely first of all on perturbations in the brain protein acylation.

Thus, the brain metabolic changes 8 weeks after the TMAP administration manifest a new metabolic state that is apparently controlled at epigenetic level by the short-term (patho)physiology-dependent decreases in the OADH function, linked to expression of sirtuin 5 and sirtuin 3. While sirtuin 3 controls mitochondrial metabolism where acetyl-CoA production by PDHC is of immense significance, extramitochondrial OADH may be involved in glutarylation of histones. Certain histones are known to be subject of glutarylation (66, 73)—the type of modification that changes the charge of lysine residues, thus regulating the chromatin state. For example, glutarylation of K91 of H4 histone is associated with higher transcriptional activity (74). Thus, the TMAP-induced changes in the glutarylation system involving the glutaryl-CoA producer OADHC and deglutarylase sirtuin 5, upon the short-term OADH inhibition may lead to the long-term consequences for gene expression due to the glutarylation-dependent chromatin remodeling. Obviously, this mechanism of metabolic regulation should depend on the chromatin state at the time of the TMAP action. This presumption is in good accord with conditional outcomes of the long-term TMAP effects, i.e., their dependence on (patho)physiological state of an organism. Remarkably, the difference between the LE and SCI rat brains

in the reactivity of their glutarylation system to TMAP points to perturbed adaptability of SCI animals to metabolic challenges. After the TMAP treatment, the protein glutarylation does not increase in the brains of LE animals, as these animals are able to up-regulate their sirtuin 5. The upregulation is not possible in SCI animals, as their brain metabolism is significantly perturbed (26). As a result, these animals demonstrate increased glutarylation of the brain proteins in response to TMAP, compared to LE animals (**Figure 7**). A neuroprotective effect of sirtuin 5, observed in previous studies of SCI and other neuropathologies (25, 26), is in good accord with our current data, further supporting importance of the brain protein glutarylation for long-term systemic changes in neuropathologies. Dependence of these systemic changes on OADH inhibition, shown in this work, indicates that biphasic regulation of the OADH expression in spinal cord and skeletal muscles after SCI, known from independent transcriptomics studies (**Supplementary Figure 1**), is involved with the enzyme role in protein glutarylation that is of pathophysiological significance.

TMAP is a membrane-permeable trimethylated derivative of the true inhibitor, adipoyl phosphonate. Inside the cells, TMAP is hydrolyzed to adipoyl phosphonate by the action of intracellular esterases. Specific structural determinants in the active sites of OADH and OGDH are known, that promote preferential binding of AP to OADH, compared to OGDH preferring a shorter phosphonate analog, succinyl phosphonate (34). Our data on the TMAP-induced changes in the protein glutarylation along with the changed expression of OADH and sirtuin 5, are in good accordance with the specific action of TMAP on the brain OADH.

In addition to the TMAP-induced long-term changes in the protein components of the brain glutarylation system, associated with the changes in the level of protein glutarylation, some of the metabolic indicators of the long-term effects agree with independent data. One of the enzymes for which the functional significance of glutarylation is known, is carbamoyl phosphate synthetase 1 (CPS1, molecular mass 165 kDa, EC 6.3.4.16), producing carbamoyl phosphate for citrulline synthesis from ornithine. Glutarylation of CPS1 inhibits its function (23). Hence, the TMAP-induced decrease in citrulline simultaneously with increase in protein glutarylation in SCI vs. LE animals, are in good accordance with increased glutarylation of CPS1 as a molecular mechanism underlying the decreased citrulline level in the TMAP-treated SCI vs. LE animals.

The current study provides further evidence on functional differences between 130 and 70 kDa isoforms of OADH. Changed expression of the full-length 130 kDa isoform is grouped in the cluster 2 including the activity of a key protein of mitochondrial metabolism, OGDHC, and regulators of mitochondrial acylation—sirtuins 3 and 5 (cluster 2c, **Figure 3**). On the other hand, the N-terminal-truncated 70 kDa isoform (1) is clustered with activity of OADHCem (cluster 1b, **Figure 3**). Across all the treated animals groups, metabolic indicators of the two major clusters comprising either 70 (cluster 1) or 130 (cluster 2) kDa isoforms of OADH, undergo opposite changes, as compared to the levels in the control rats. Mostly, the coupled decreases in metabolic indicators occur in the 70-kDa-including cluster 1 (**Figure 3**), while the 130-kDa-including cluster 2 is associated with the increased levels vs. those in the control brains (**Figure 3**). This strong separation of the metabolic clusters associated with the OADH isoforms of 130 and 70 kDa points to the different biological roles of the isoforms.

It is worth noting that the most abundant fractions of glutarylated proteins in the brain cortex homogenates are those of 130 and 70 kDa. These molecular masses accurately match the apparent molecular masses of the previously characterized mammalian isoforms of OADH (26). Remarkably, in homogenates of liver, where the OADH expression is an order of magnitude higher than in the brain (34), the glutarylated proteins of the same molecular masses are stained by anti-glutaryllysine antibodies with a much higher intensity than in the brain homogenates (72). Moreover, the same protein bands are also detected as major glutarylated proteins in the fraction of liver mitochondria (72). After chemical glutarylation of the liver mitochondrial proteins, many additional protein bands become reactive to anti-glutaryl-lysine antibodies.

Autoglutarylation of OADH is supported by the coupled changes in the glutarylation of the brain proteins and expression of OADH isoforms, that is observed in the control and LE animals (**Figure 7**), and mass-spectrometric identification of glutarylation of recombinant human OADH (**Figure 8**). This side reaction of the catalytic process performed by 2-oxo acid dehydrogenases, is well-known from studies of other members of the enzyme family (53). Interestingly, one of the two glutarylated lysine residues of OADH, identified in the current work using eukaryotic expression of human OADH (K818, **Figure 8**), has been detected in the mouse liver enzyme under pathological conditions induced by knockout of glutaryl-CoA dehydrogenase (27).

Under pathological conditions, such as in the brain of SCI animals treated with TMAP, excessive glutarylation of the brain proteins is observed. This is accompanied by the TMAP-induced decline in the levels of the brain glutathione, localized to the same subcluster as PDHC activity. Association of this subcluster with the "blue" cluster 1 comprising glutarylation of 70 kDa proteins and expression of 70 kDa isoform of OADH, suggests that glutarylation of PDHC, the highly regulated system coupling the cytosolic and mitochondrial processes of glucose degradation, may mediate the systemic significance of OADH for insulin sensitivity, observed in independent studies (16–18, 75). The glutarylated residue of the PDHC component ODP2 is outside the enzyme active sites. Nevertheless, the glutarylation may affect the entry of CoA to the complex inner cavity, from where CoA arrives at the ODP2 active site. Thus, the position of the glutarylated ODP2 residue suggests a fine tuning of the PDHC function, probably involving conformational changes of the core, rather than a straightforward effect on the catalysis. One should also take into account that this residue of ODP2 and the neighboring residues are subject to other modifications, such as acetylation and ubiquitination. Hence, the observed effect of the ODP2 glutarylation level on the functional expression of PDHC in the brain homogenates may be due to complex regulation, potentially involving the protein stability. Functional significance of this modification of PDHC requires further studies in view of its potential role in the association between the OADH function and glucose homeostasis.

CONCLUSION

The role of the *DHTKD1*-encoded OADH in the brain protein glutarylation, expression of sirtuins 3 and 5, and homeostasis of glutathione and amino acids is established. Glutarylation of ODP2 component of PDHC is shown, providing a molecular mechanism of the OADH association with systemic pathologies, such as diabetes.

DATA AVAILABILITY STATEMENT

The raw data supporting the conclusions of this article will be made available by the authors, without undue reservation.

ETHICS STATEMENT

The animal study was reviewed and approved by the Bioethics Committee of Russian Cardiology Research and Production Complex and the Bioethics Committee of Lomonosov Moscow State University.

AUTHOR CONTRIBUTIONS

VB: conceptualization, writing—review and editing, supervision, project administration, and funding acquisition. AB, IK, AA, and VA: protein assays. AB and AT: purification of recombinant protein. TK: mass-spectrometry data acquisition. TK, VA, and LZ: analysis of mass-spectrometry data. AK: amino acid profiling. SR and AG: animal experiments. AB, AA, VA, and LZ: validation and formal analysis. VA and LZ: structural analysis. AB: writing—original draft preparation. AB, VA, LZ, and VB: visualization. All authors have read and agreed to the published version of the manuscript.

FUNDING

This study was supported by the Russian Science Foundation (Grant 18-14-00116 to VB).

ACKNOWLEDGMENTS

We thank Prof. N. V. Lukashev and Dr. A. V. Kazantsev (Faculty of Chemistry, Lomonosov Moscow State University) for the synthesis and purification of TMAP.

SUPPLEMENTARY MATERIAL

The Supplementary Material for this article can be found online at: https://www.frontiersin.org/articles/10.3389/fmed.2022.896263/full#supplementary-material

REFERENCES

1. Boyko AI, Artiukhov AV, Kaehne T, di Salvo ML, Bonaccorsi di Patti MC, Contestabile R, et al. Isoforms of the DHTKD1-encoded 2-oxoadipate dehydrogenase, identified in animal tissues, are not observed upon the human DHTKD1 expression in bacterial or yeast systems. *Biochem Biokhimiia.* (2020) 85:920–9. doi: 10.1134/S0006297920080076
2. Bunik VI, Degtyarev D. Structure-function relationships in the 2-oxo acid dehydrogenase family: substrate-specific signatures and functional predictions for the 2-oxoglutarate dehydrogenase-like proteins. *Proteins.* (2008) 71:874–90. doi: 10.1002/prot.21766
3. Danhauser K, Sauer SW, Haack TB, Wieland T, Staufner C, Graf E, et al. DHTKD1 mutations cause 2-aminoadipic and 2-oxoadipic aciduria. *Am J Hum Genet.* (2012) 91:1082–7. doi: 10.1016/j.ajhg.2012.10.006
4. Hagen J, te Brinke H, Wanders RJ, Knegt AC, Oussoren E, Hoogeboom AJ, et al. Genetic basis of alpha-aminoadipic and alpha-ketoadipic aciduria. *J Inherit Metab Dis.* (2015) 38:873–9. doi: 10.1007/s10545-015-9841-9
5. Stiles AR, Venturoni L, Mucci G, Elbalalesy N, Woontner M, Goodman S, et al. New cases of DHTKD1 mutations in patients with 2-ketoadipic aciduria. *JIMD Rep.* (2016) 25:15–9. doi: 10.1007/8904_2015_462
6. Xu WY, Gu MM, Sun LH, Guo WT, Zhu HB, Ma JF, et al. A nonsense mutation in DHTKD1 causes charcot-marie-tooth disease type 2 in a large Chinese pedigree. *Am J Hum Genet.* (2012) 91:1088–94. doi: 10.1016/j.ajhg.2012.09.018
7. Wang C, Calcutt MW, Ferguson JF. Knock-out of DHTKD1 alters mitochondrial respiration and function, and may represent a novel pathway in cardiometabolic disease risk. *Front Endocrinol.* (2021) 12:710698. doi: 10.3389/fendo.2021.710698
8. Sherrill JD, Kc K, Wang X, Wen T, Chamberlin A, Stucke EM, et al. Whole-exome sequencing uncovers oxidoreductases DHTKD1 and OGDHL as linkers between mitochondrial dysfunction and eosinophilic esophagitis. *JCI Insight.* (2018) 3:e99922. doi: 10.1172/jci.insight.99922
9. Luan CJ, Guo W, Chen L, Wei XW, He Y, Chen Y, et al. CMT2Q-causing mutation in the Dhtkd1 gene lead to sensory defects, mitochondrial accumulation and altered metabolism in a knock-in mouse model. *Acta Neuropathol Commun.* (2020) 8:32. doi: 10.1186/s40478-020-00901-0
10. Zhao ZH, Chen ZT, Zhou RL, Wang YZA. Chinese pedigree with a novel mutation in GJB1 gene and a rare variation in DHTKD1 gene for diverse CharcotMarieTooth diseases. *Mol Med Rep.* (2019) 19:4484–90. doi: 10.3892/mmr.2019.10058
11. Osmanovic A, Gogol I, Martens H, Widjaja M, Muller K, Schreiber-Katz O, et al. Heterozygous DHTKD1 variants in two European cohorts of amyotrophic lateral sclerosis patients. *Genes.* (2021) 13:84. doi: 10.3390/genes13010084
12. Tort F, Ugarteburu O, Torres MA, Garcia-Villoria J, Giros M, Ruiz A, et al. Lysine restriction and pyridoxal phosphate administration in a NADK2 patient. *Pediatrics.* (2016) 138:e20154534. doi: 10.1542/peds.2015-4534
13. Yuzyuk T, Thomas A, Viau K, Liu A, De Biase I, Botto LD, et al. Effect of dietary lysine restriction and arginine supplementation in two patients with pyridoxine-dependent epilepsy. *Mol Genet Metab.* (2016) 118:167–72. doi: 10.1016/j.ymgme.2016.04.015
14. Coughlin CR II, van Karnebeek CD, Al-Hertani W, Shuen AY, Jaggumantri S, Jack RM, et al. Triple therapy with pyridoxine, arginine supplementation and dietary lysine restriction in pyridoxine-dependent epilepsy: neurodevelopmental outcome. *Mol Genet Metab.* (2015) 116:35–43. doi: 10.1016/j.ymgme.2015.05.011
15. Wang TJ, Ngo D, Psychogios N, Dejam A, Larson MG, Vasan RS, et al. 2-Aminoadipic acid is a biomarker for diabetes risk. *J Clin Investig.* (2013) 123:4309–17. doi: 10.1172/JCI64801
16. Xu WY, Shen Y, Zhu H, Gao J, Zhang C, Tang L, et al. 2-Aminoadipic acid protects against obesity and diabetes. *J Endocrinol.* (2019) 243:111–23. doi: 10.1530/JOE-19-0157
17. Plubell DL, Fenton AM, Wilmarth PA, Bergstrom P, Zhao Y, Minnier J, et al. GM-CSF driven myeloid cells in adipose tissue link weight gain and insulin

resistance via formation of 2-aminoadipate. *Sci Rep.* (2018) 8:11485. doi: 10.1038/s41598-018-29250-8
18. Timmons JA, Atherton PJ, Larsson O, Sood S, Blokhin IO, Brogan RJ, et al. A coding and non-coding transcriptomic perspective on the genomics of human metabolic disease. *Nucleic Acids Res.* (2018) 46:7772–92. doi: 10.1093/nar/gky570
19. Artiukhov AV, Grabarska A, Gumbarewicz E, Aleshin VA, Kahne T, Obata T, et al. Synthetic analogues of 2-oxo acids discriminate metabolic contribution of the 2-oxoglutarate and 2-oxoadipate dehydrogenases in mammalian cells and tissues. *Sci Rep.* (2020) 10:1886. doi: 10.1038/s41598-020-58701-4
20. Xu W, Zhu H, Gu M, Luo Q, Ding J, Yao Y, et al. DHTKD1 is essential for mitochondrial biogenesis and function maintenance. *FEBS Lett.* (2013) 587:3587–92. doi: 10.1016/j.febslet.2013.08.047
21. Bunik VI, Pavlova OG. Inactivation of alpha-ketoglutarate dehydrogenase during oxidative decarboxylation of alpha-ketoadipic acid. *FEBS Lett.* (1993) 323:166–70. doi: 10.1016/0014-5793(93)81472-c
22. Biagosch C, Ediga RD, Hensler SV, Faerberboeck M, Kuehn R, Wurst W, et al. Elevated glutaric acid levels in Dhtkd1-/Gcdh– double knockout mice challenge our current understanding of lysine metabolism. *Biochim Biophys Acta Mol Basis Dis.* (2017) 1863:2220–8. doi: 10.1016/j.bbadis.2017.05.018
23. Tan M, Peng C, Anderson KA, Chhoy P, Xie Z, Dai L, et al. Lysine glutarylation is a protein posttranslational modification regulated by SIRT5. *Cell Metab.* (2014) 19:605–17. doi: 10.1016/j.cmet.2014.03.014
24. Olp MD, Zhu N, Smith BC. Metabolically derived lysine acylations and neighboring modifications tune the binding of the BET bromodomains to histone H4. *Biochemistry.* (2017) 56:5485–95. doi: 10.1021/acs.biochem.7b00595
25. Morris-Blanco KC, Dave KR, Saul I, Koronowski KB, Stradecki HM, Perez-Pinzon MA. Protein kinase C epsilon promotes cerebral ischemic tolerance via modulation of mitochondrial sirt5. *Sci Rep.* (2016) 6:29790. doi: 10.1038/srep29790
26. Boyko A, Tsepkova P, Aleshin V, Artiukhov A, Mkrtchyan G, Ksenofontov A, et al. Severe spinal cord injury in rats induces chronic changes in the spinal cord and cerebral cortex metabolism, adjusted by thiamine that improves locomotor performance. *Front Mol Neurosci.* (2021) 14:620593. doi: 10.3389/fnmol.2021.620593
27. Schmiesing J, Storch S, Dorfler AC, Schweizer M, Makrypidi-Fraune G, Thelen M, et al. Disease-linked glutarylation impairs function and interactions of mitochondrial proteins and contributes to mitochondrial heterogeneity. *Cell Rep.* (2018) 24:2946–56. doi: 10.1016/j.celrep.2018.08.014
28. Sabari BR, Zhang D, Allis CD, Zhao Y. Metabolic regulation of gene expression through histone acylations. *Nat Rev Mol Cell Biol.* (2017) 18:90–101. doi: 10.1038/nrm.2016.140
29. Chen R, Zhang M, Zhou Y, Guo W, Yi M, Zhang Z, et al. The application of histone deacetylases inhibitors in glioblastoma. *J Exp Clin Cancer Res.* (2020) 39:138. doi: 10.1186/s13046-020-01643-6
30. Patra S, Panigrahi DP, Praharaj PP, Bhol CS, Mahapatra KK, Mishra SR, et al. Dysregulation of histone deacetylases in carcinogenesis and tumor progression: a possible link to apoptosis and autophagy. *Cell Mol Life Sci.* (2019) 76:3263–82. doi: 10.1007/s00018-019-03098-1
31. Graf AV, Maslova MV, Artiukhov AV, Ksenofontov AL, Aleshin VA, Bunik VI. Acute prenatal hypoxia in rats affects physiology and brain metabolism in the offspring. Dependent on sex and gestational age. *Int J Mol Sci.* (2022) 23:2579. doi: 10.3390/ijms23052579
32. Yang G, Yuan Y, Yuan H, Wang J, Yun H, Geng Y, et al. Histone acetyltransferase 1 is a succinyltransferase for histones and non-histones and promotes tumorigenesis. *EMBO Rep.* (2021) 22:e50967. doi: 10.15252/embr.202050967
33. Boyko A, Ksenofontov A, Ryabov S, Baratova L, Graf A, Bunik V. Delayed influence of spinal cord injury on the amino acids of NO metabolism in rat cerebral cortex is attenuated by thiamine. *Front Med.* (2018) 4:249. doi: 10.3389/fmed.2017.00249
34. Artiukhov AV, Kazantsev AV, Lukashev NV, Bellinzoni M, Bunik VI. Selective inhibition of 2-oxoglutarate and 2-oxoadipate dehydrogenases by the phosphonate analogs of their 2-oxo acid substrates. *Front Chem.* (2020) 8:596187. doi: 10.3389/fchem.2020.596187
35. Graf A, Trofimova L, Loshinskaja A, Mkrtchyan G, Strokina A, Lovat M, et al. Up-regulation of 2-oxoglutarate dehydrogenase as a stress response. *Int J Biochem Cell Biol.* (2013) 45:175–89. doi: 10.1016/j.biocel.2012.07.002
36. Jure I, Labombarda F. Spinal cord injury drives chronic brain changes. *Neural Regen Res.* (2017) 12:1044–7. doi: 10.4103/1673-5374.211177
37. Wu J, Zhao Z, Sabirzhanov B, Stoica BA, Kumar A, Luo T, et al. Spinal cord injury causes brain inflammation associated with cognitive and affective changes: role of cell cycle pathways. *J Neurosci.* (2014) 34:10989–1006. doi: 10.1523/JNEUROSCI.5110-13.2014
38. Wu GA, Bogie KM. Effects of conventional and alternating cushion weight-shifting in persons with spinal cord injury. *J Rehabil Res Dev.* (2014) 51:1265–76. doi: 10.1682/JRRD.2014.01.0009
39. Basso DM, Beattie MS, Bresnahan JC. Graded histological and locomotor outcomes after spinal cord contusion using the NYU weight-drop device versus transection. *Exp Neurol.* (1996) 139:244–56. doi: 10.1006/exnr.1996.0098
40. Dhuria SV, Hanson LR, Frey WH II. Intranasal delivery to the central nervous system: mechanisms and experimental considerations. *J Pharm Sci.* (2010) 99:1654–73. doi: 10.1002/jps.21924
41. Tsepkova PM, Artiukhov AV, Boyko AI, Aleshin VA, Mkrtchyan GV, Zvyagintseva MA, et al. Thiamine induces long-term changes in amino acid profiles and activities of 2-oxoglutarate and 2-oxoadipate dehydrogenases in rat brain. *Biochem Biokhimiia.* (2017) 82:723–36. doi: 10.1134/S0006297917060098
42. Ksenofontov AL, Boyko AI, Mkrtchyan GV, Tashlitsky VN, Timofeeva AV, Graf AV, et al. Analysis of Free Amino Acids in Mammalian Brain Extracts. *Biochem Biokhimiia.* (2017) 82:1183–92. doi: 10.1134/S000629791710011X
43. Aleshin VA, Graf AV, Artiukhov AV, Boyko AI, Ksenofontov AL, Maslova MV, et al. Physiological and biochemical markers of the sex-specific sensitivity to epileptogenic factors, delayed consequences of seizures and their response to vitamins B1 and B6 in a rat model. *Pharmaceuticals.* (2021) 14:737. doi: 10.3390/ph14080737
44. Ladner CL, Yang J, Turner RJ, Edwards RA. Visible fluorescent detection of proteins in polyacrylamide gels without staining. *Anal Biochem.* (2004) 326:13–20. doi: 10.1016/j.ab.2003.10.047
45. Hissin PJ, Hilf R. A fluorometric method for determination of oxidized and reduced glutathione in tissues. *Anal Biochem.* (1976) 74:214–26. doi: 10.1016/0003-2697(76)90326-2
46. Senft AP, Dalton TP, Shertzer HG. Determining glutathione and glutathione disulfide using the fluorescence probe o-phthalaldehyde. *Anal Biochem.* (2000) 280:80–6. doi: 10.1006/abio.2000.4498
47. Denckla WD, Dewey HK. The determination of tryptophan in plasma, liver, and urine. *J Lab Clin Med.* (1967) 69:160–9.
48. Bloxam DL, Warren WH. Error in the determination of tryptophan by the method of Denkla and Dewey. A revised procedure. *Anal Biochem.* (1974) 60:621–5. doi: 10.1016/0003-2697(74)90275-9
49. Artiukhov AV, Pometun AA, Zubanova SA, Tishkov VI, Bunik VI. Advantages of formate dehydrogenase reaction for efficient NAD(+) quantification in biological samples. *Anal Biochem.* (2020) 603:113797. doi: 10.1016/j.ab.2020.113797
50. Aleshin VA, Mkrtchyan GV, Kaehne T, Graf AV, Maslova MV, Bunik VI. Diurnal regulation of the function of the rat brain glutamate dehydrogenase by acetylation and its dependence on thiamine administration. *J Neurochem.* (2020) 153:80–102. doi: 10.1111/jnc.14951
51. Laemmli UK. Cleavage of structural proteins during the assembly of the head of bacteriophage T4. *Nature.* (1970) 227:680–5. doi: 10.1038/227680a0
52. Aleshin VA, Artiukhov AV, Kaehne T, Graf AV, Bunik VI. Daytime dependence of the activity of the rat brain pyruvate dehydrogenase corresponds to the mitochondrial sirtuin 3 level and acetylation of brain proteins, all regulated by thiamine administration decreasing phosphorylation of PDHA Ser293. *Int J Mol Sci.* (2021) 22:8006. doi: 10.3390/ijms22158006
53. Bunik V. *Vitamin-Dependent Multienzyme Complexes of 2-Oxo Acid Dehydrogenases: Structure, Function, Regulation and Medical Implications*. Hauppauge, NY: Nova Science Publishers, Inc (2017).
54. Li H, Marshall ZM, Whorton AR. Stimulation of cystine uptake by nitric oxide: regulation of endothelial cell glutathione levels. *Am J Physiol.* (1999) 276:C803–11. doi: 10.1152/ajpcell.1999.276.4.C803

55. Artiukhov AV, Graf AV, Kazantsev AV, Boyko AI, Aleshin VA, Ksenofontov AL, et al. Increasing inhibition of the rat brain 2-oxoglutarate dehydrogenase decreases glutathione redox state, elevating anxiety and perturbing stress adaptation. *Pharmaceuticals.* (2022) 15:82. doi: 10.3390/ph15020182
56. Mkrtchyan GV, Ucal M, Mullebner A, Dumitrescu S, Kames M, Moldzio R, et al. Thiamine preserves mitochondrial function in a rat model of traumatic brain injury, preventing inactivation of the 2-oxoglutarate dehydrogenase complex. *Biochim Biophys Acta Bioenerg.* (2018) 1859:925–31. doi: 10.1016/j.bbabio.2018.05.005
57. Graf A, Trofimova L, Ksenofontov A, Baratova L, Bunik V. Hypoxic adaptation of mitochondrial metabolism in rat cerebellum decreases in pregnancy. *Cells.* (2020) 9:139. doi: 10.3390/cells9010139
58. Ringel AE, Tucker SA, Haigis MC. Chemical and physiological features of mitochondrial acylation. *Mol Cell.* (2018) 72:610–24. doi: 10.1016/j.molcel.2018.10.023
59. Karwi QG, Jorg AR, Lopaschuk GD. Allosteric, transcriptional and post-translational control of mitochondrial energy metabolism. *Biochem J.* (2019) 476:1695–712. doi: 10.1042/BCJ20180617
60. Lutz MI, Milenkovic I, Regelsberger G, Kovacs GG. Distinct patterns of sirtuin expression during progression of Alzheimer's disease. *Neuromol Med.* (2014) 16:405–14. doi: 10.1007/s12017-014-8288-8
61. Simithy J, Sidoli S, Yuan ZF, Coradin M, Bhanu NV, Marchione DM, et al. Characterization of histone acylations links chromatin modifications with metabolism. *Nat Commun.* (2017) 8:1141. doi: 10.1038/s41467-017-01384-9
62. Ohshima K, Oi R, Nojima S, Morii E. Mitochondria govern histone acetylation in colorectal cancer. *J Pathol.* (2022) 256:164–73. doi: 10.1002/path.5818
63. Cohen TJ, Guo JL, Hurtado DE, Kwong LK, Mills IP, Trojanowski JQ, et al. The acetylation of tau inhibits its function and promotes pathological tau aggregation. *Nat Commun.* (2011) 2:252. doi: 10.1038/ncomms1255
64. Rossaert E, Pollari E, Jaspers T, Van Helleputte L, Jarpe M, Van Damme P, et al. Restoration of histone acetylation ameliorates disease and metabolic abnormalities in a FUS mouse model. *Acta Neuropathol Commun.* (2019) 7:107. doi: 10.1186/s40478-019-0750-2
65. Eguchi K, Nakayama K. Prolonged hypoxia decreases nuclear pyruvate dehydrogenase complex and regulates the gene expression. *Biochem Biophys Res Commun.* (2019) 520:128–35. doi: 10.1016/j.bbrc.2019.09.109
66. Zorro Shahidian L, Haas M, Le Gras S, Nitsch S, Mourao A, Geerlof A, et al. Succinylation of H3K122 destabilizes nucleosomes and enhances transcription. *EMBO Rep.* (2021) 22:e51009. doi: 10.15252/embr.202051009
67. Hirschey MD, Zhao Y. Metabolic regulation by lysine malonylation, succinylation, and glutarylation. *Mol Cell Proteom.* (2015) 14:2308–15. doi: 10.1074/mcp.R114.046664
68. Zhou B, Du Y, Xue Y, Miao G, Wei T, Zhang P. Identification of malonylation, succinylation, and glutarylation in serum proteins of acute myocardial infarction patients. *Proteom Clin Appl.* (2020) 14:e1900103. doi: 10.1002/prca.201900103
69. Kumar S, Lombard DB. Functions of the sirtuin deacylase SIRT5 in normal physiology and pathobiology. *Crit Rev Biochem Mol Biol.* (2018) 53:311–34. doi: 10.1080/10409238.2018.1458071
70. Zhang M, Wu J, Sun R, Tao X, Wang X, Kang Q, et al. SIRT5 deficiency suppresses mitochondrial ATP production and promotes AMPK activation in response to energy stress. *PLoS One.* (2019) 14:e0211796. doi: 10.1371/journal.pone.0211796
71. Wang Y, Guo YR, Liu K, Yin Z, Liu R, Xia Y, et al. KAT2A coupled with the alpha-KGDH complex acts as a histone H3 succinyltransferase. *Nature.* (2017) 552:273–7. doi: 10.1038/nature25003
72. Artiukhov AV, Kolesanova EF, Boyko AI, Chashnikova AA, Gnedoy SN, Kaehne T, et al. Preparation of affinity purified antibodies against epsilon-glutaryl-lysine residues in proteins for investigation of glutarylated proteins in animal tissues. *Biomolecules.* (2021) 11:1168. doi: 10.3390/biom1108 1168
73. Matsushima S, Sadoshima J. The role of sirtuins in cardiac disease. *Am J Physiol Heart Circ Physiol.* (2015) 309:H1375–89. doi: 10.1152/ajpheart.00053.2015
74. Bao X, Liu Z, Zhang W, Gladysz K, Fung YME, Tian G, et al. Glutarylation of histone H4 lysine 91 regulates chromatin dynamics. *Mol Cell.* (2019) 76:660–675.e9. doi: 10.1016/j.molcel.2019.08.018
75. Lim J, Liu Z, Apontes P, Feng D, Pessin JE, Sauve AA, et al. Dual mode action of mangiferin in mouse liver under high fat diet. *PLoS One.* (2014) 9:e90137. doi: 10.1371/journal.pone.0090137

Conflict of Interest: The authors declare that the research was conducted in the absence of any commercial or financial relationships that could be construed as a potential conflict of interest.

frontiers | Frontiers in Medicine

TYPE Original Research
PUBLISHED 22 August 2022
DOI 10.3389/fmed.2022.952977

OPEN ACCESS

EDITED BY
Claudine Habak,
Emirates College for Advanced Education, United Arab Emirates

REVIEWED BY
Juandy Jo,
University of Pelita Harapan, Indonesia
Haider Abdul-Lateef Mousa,
University of Basrah, Iraq

*CORRESPONDENCE
Tatyana Strekalova
t.strekalova@maastrichtuniversity.nl

†These authors have contributed equally to this work

SPECIALTY SECTION
This article was submitted to Translational Medicine, a section of the journal Frontiers in Medicine

RECEIVED 25 May 2022
ACCEPTED 15 July 2022
PUBLISHED 22 August 2022

CITATION
Schapovalova O, Gorlova A, de Munter J, Sheveleva E, Eropkin M, Gorbunov N, Sicker M, Umriukhin A, Lyubchyk S, Lesch K-P, Strekalova T and Schroeter CA (2022) Immunomodulatory effects of new phytotherapy on human macrophages and TLR4- and TLR7/8-mediated viral-like inflammation in mice. *Front. Med.* 9:952977. doi: 10.3389/fmed.2022.952977

Immunomodulatory effects of new phytotherapy on human macrophages and TLR4- and TLR7/8-mediated viral-like inflammation in mice

Olesia Schapovalova[1,2†], Anna Gorlova[2,3,4†], Johannes de Munter[2], Elisaveta Sheveleva[3,4], Mikhail Eropkin[5], Nikita Gorbunov[6], Michail Sicker[7], Aleksei Umriukhin[3], Sergiy Lyubchyk[1,8], Klaus-Peter Lesch[2,6], Tatyana Strekalova[2,4,6,9*] and Careen A. Schroeter[10]

[1]Caparica Faculdade de Ciencias e Tecnologia da Universidade Nova de Lisboa, NOVA Lisbon University, Lisbon, Portugal, [2]Department of Psychiatry and Neuropsychology, School for Mental Health and Neuroscience, Maastricht University and Neuroplast BV, Maastricht, Netherlands, [3]Laboratory of Psychiatric Neurobiology, Institute of Molecular Medicine and Department of Normal Physiology, Sechenov First Moscow State Medical University, Moscow, Russia, [4]Laboratory of Cognitive Dysfunctions, Federal Budgetary Institute of General Pathology and Pathophysiology, Moscow, Russia, [5]Department of Etiology and Epidemiology, Smorodintsev Research Institute of Influenza, St. Petersburg State University, Saint Petersburg, Russia, [6]Division of Molecular Psychiatry, Center of Mental Health, University of Würzburg, Würzburg, Germany, [7]Rehabilitation Research Unit of Clinic of Bad Kreuzbach, Bad Kreuzbach, Germany, [8]EIGES Center, Universidade Lusofona, Lisboa, Portugal, [9]Department of Pharmacology, University of Oxford, Oxford, United Kingdom, [10]Preventive and Environmental Medicine, Cologne, Germany

Background: While all efforts have been undertaken to propagate the vaccination and develop remedies against SARS-CoV-2, no satisfactory management of this infection is available yet. Moreover, poor availability of any preventive and treatment measures of SARS-CoV-2 in economically disadvantageous communities aggravates the course of the pandemic. Here, we studied a new immunomodulatory phytotherapy (IP), an extract of blackberry, chamomile, garlic, cloves, and elderberry as a potential low-cost solution for these problems given the reported efficacy of herbal medicine during the previous SARS virus outbreak.

Methods: The key feature of SARS-CoV-2 infection, excessive inflammation, was studied in *in vitro* and *in vivo* assays under the application of the IP. First, changes in tumor-necrosis factor (TNF) and Inteurleukin-1 beta (IL-1β) concentrations were measured in a culture of human macrophages following the lipopolysaccharide (LPS) challenge and treatment with IP or prednisolone. Second, chronically IP-pre-treated CD-1 mice received an agonist of Toll-like receptors (TLR)-7/8 resiquimod and were examined for lung and spleen expression of pro-inflammatory cytokines and blood formula. Finally, chronically IP-pre-treated mice challenged with LPS injection were studied for "sickness" behavior. Additionally, the IP was analyzed using high-potency-liquid chromatography (HPLC)-high-resolution-mass-spectrometry (HRMS).

Results: LPS-induced *in vitro* release of TNF and IL-1β was reduced by both treatments. The IP-treated mice displayed blunted over-expression of SAA-2, ACE-2, CXCL1, and CXCL10 and decreased changes in blood formula in response to an injection with resiquimod. The IP-treated mice injected with LPS showed normalized locomotion, anxiety, and exploration behaviors but not abnormal forced swimming. Isoquercitrin, choline, leucine, chlorogenic acid, and other constituents were identified by HPLC-HRMS and likely underlie the IP immunomodulatory effects.

Conclusions: Herbal IP-therapy decreases inflammation and, partly, "sickness behavior," suggesting its potency to combat SARS-CoV-2 infection first of all via its preventive effects.

KEYWORDS

toll-like receptors, SARS-CoV-2, inflammation, pro-inflammatory cytokines, mice

Introduction

Although the vaccination against SARS-CoV-2 is being implemented worldwide to curb the epidemic, none of the available vaccines provide full protection from the infection, and no specific drug to combat or prevent severe SARS-CoV-2 infection is anticipated (1, 2). As such, the search for alternative approaches to improve this situation has become the focus of much research (3). Excessive inflammation (i.e., the so-called "cytokine storm"), once established as a key pathophysiological feature of SARS-CoV-2 infection (4), became a target of the drug research and development in this area. The anti-inflammatory interventions were shown to be beneficial for both a prevention and treatment of viral infections, including SARS (4–6). These studies have resulted in the implementation of the preventive anti-inflammatory remedies and pathogenetic therapies in SARS-CoV-2 patients, such as hydroxychloroquine, chloroquine, azithromycin, ivermectin, colchicine, thalidomide and glucocorticoids methylprednisolone and dexamethasone, the monoclonal antibody tocilizumab, convalescent plasma interferons, and intravenous immunoglobulin therapy (7–9). However, these types of medicine are often unaffordable in low-income countries (10), which become a natural reservoir of the virus and a prerequisite of the appearance of new mutations (11).

The "cytokine storm" caused by SARS-CoV-2 can result in detrimental effects and even death (12–14). SARS-CoV-2 can activate the pattern recognition receptor (PRR) toll-like receptor (TLR) 4 that triggers the myeloid differentiation primary response (MyD) 88, causing a consequent NF-κB translocation to the nucleus and the upregulation of central and peripheral pro-inflammatory cytokines: tumor-necrosis factor (TNF), interleukin (IL)-1β, and IL-6 that increase the permeability of blood vessels and the migration of immune cells (15, 16). The SARS-CoV-2-induced inflammatory response also involves the IRF7-mediated TLR7/8 induction of type-1 interferon *via* a MyD88-dependent cascade and the upregulation of NFkB *via* the IL-1β receptor-associated kinase 1 (IRAK-1), IRAK-4, and TNF receptor-associated factor 6 (TRAF6) and of the type I interferons (IFNs) (15, 17). The activation of PRR toll-like receptors TLR4 and TLR7/8, *via* a series of molecular cascades, results in the upregulation of central and peripheral cytokines expression (18). It is regulated according to the nature of the pathogen and the TLR signaling pathways activated. Typically, TLR-mediated immune response involves an increase in circulating and central cytokines such as IL-1β, TNF and IL-6, as well as chemokines such as CXCL1, CCL2 and CXCL10 (15, 18, 19) and the induction of "sickness behavior," i.e., reduced activity and exploration, and anxiety-like changes (15, 18–22).

The clinical management of "cytokine storm" is not a trivial challenge. For instance, the use of corticosteroids in SARS patients in 2003 increased mortality (23). Other therapies were not sufficiently effective either (24). At the same time, in the literature, the beneficial effects of herbal medicine combined with traditional medicine in SARS patients were demonstrated (4–6, 25–27), giving hope that therapeutically effective herbal compositions might combat the severe course of SARS-CoV-2. In addition, animal studies suggested possible mechanisms of anti-inflammatory immunomodulatory effects of medicinal herbs that target inflammatory pathways of TLRs-induced mechanisms, e.g., polysaccharides from red seaweed suppressed the expression of TNF, receptor-associated factor-6 in a model of LPS-induced toxicity (26), the use of vanilla extract suppressed free radical production in a mouse model of cancer (28, 29), ginger phenolics decreased lipid peroxidation and oxidative stress in rats (30). Our recent studies with a mouse ultrasound model of "emotional stress" have shown the beneficial action of herbal compositions with anti-inflammatory properties on the oxidative stress markers malondialdehyde and protein carbonyl

and the expression of IL-1β and IL-6 (31, 32). Given important roles of excessive inflammation in the pathophysiology of severe course of SARS-CoV-2 infection, and beneficial effects of preventive and therapeutical application of herbal medicine with viral infections, we sought to study a preventive potential of a novel herbal composition that could be affordable as for instance in the communities with insufficient healthcare systems.

Therefore, we investigated the effects of a new immunomodulatory phytotherapy (IP), an extract of blackberry, chamomile, garlic, cloves, and elderberry (for the IP content, see Supplementary Table 1), that was designed as an anti-inflammatory composition (see Supplementary File) in previously established *in vitro* and *in vivo* models of inflammation (21, 22, 33). These paradigms were adapted from the classic experimental models that are based on the activation of TLRs, which implicate distinct but overlapping pathways (19). In particular, we recently established a model of peripheral inflammation that is induced by resiquimod, an agonist of TLR7/8 (33). In this model, strong up-regulation of IL-1β, TNF, IL-6, and chemokines in lungs, spleen, liver, and brain was decreased by the anti-inflammatory drug nafamostat (33). These recent studies showed that gene over-expression of SAA-2, ACE-2, CXCL1 and CXCL10 in the liver and spleen were effectively reduced by applied anti-inflammatory therapy and thus was investigated in the present work. We also used lipopolysaccharide (LPS), an agonist of TLR4, in an *in vitro* model of macrophage IL-1β and TNF release (19) and in an *in vivo* paradigm of "sickness behavior," measuring inflammation-induced signs of anxiety, hypolocomotion, and suppressed exploration in mice (21, 22, 34, 35). High potency liquid chromatography (HPLC-HRMS) was employed to study the constituents of the IP.

Methods

Study flow

In the *in vitro* study, we studied the release of TNF and IL-1β by LPS-challenged human macrophages that were pre-treated with IP or prednisolone, about 10 samples were used per condition. We next pre-treated CD-1 mice with an IP herbal composition for 2 weeks (36) and intraperitoneally injected them with resiquimod (200 μg). Mice (n = 7–8 in each group) were culled 6 h post-challenge and examined for liver and spleen genes mRNA concentrations of inflammatory markers whose expression was most profoundly altered in our previous study: SAA-2, ACE-2, CXCL1, CXCL10, IL-1β, IL-6, and for blood formula (33) (Figure 1A). Finally, using the same IP dosing conditions, pre-treated CD-1 mice were challenged with a low dose of LPS (0.05 mg/kg) and 6 h post-challenge were investigated for helplessness, locomotion, anxiety-like, and exploratory behaviors in the open field, novel cage, and forced swim models (n = 6–7 in each group, Figure 1B). Separately, high potency liquid chromatography (HPLC)-high resolution-mass-spectrometry (HRMS) was employed to analyze biologically active constituents of the IP. All experiments were approved by the University of Oxford local committees (LERP, ACER) in accordance with the UK Animals (Scientific Procedures) Act 1989 and iCell2 METC Zuyderland Zuid, the Netherlands and MSMU#11-18-2018/2019 and were compliant with ARRIVE guidelines (http://www.nc3rs.org.uk/arrive-guidelines).

Experiments were performed on male 2.5-months-old CD-1 male mice that were purchased by a provider licensed by Charles River (http://www.spf-animals.ru/about/providers/animals). Mice were housed under standard conditions (in plastic cages 27 cm × 22 cm × 15 cm, 22 ± 1°C, 55% humidity, food and water *ad libitum*), reversed 12-h light/dark cycle (lights on at 19:00). All efforts were undertaken to minimize the potential discomfort of the animals.

A study of LPS-induced cytokine release by human macrophages

Human macrophages from healthy volunteers of both sexes were used. The effects of the IP application on the LPS-stimulated release of IL-1β and TNF were determined and compared against potential effects of the IP on non-stimulated macrophages, the effects of a standard anti-inflammatory treatment with prednisolone, and a release of non-treated LPS-challenged macrophages (see Supplementary File). Separate studies that were carried out to rule out potential effects of the IP-alcohol-containing vehicle on these read-outs showed a lack of such effects (Supplementary Figure 1).

Induction of systemic inflammation in mice

The first cohort of mice received an intraperitoneal (i.p.) injection of resiquimod (R848, Enzo Life Sciences, Farmingdale, NY, USA) that was diluted in a DMSO-vehicle (1 mg/mL). Because the administration of DMSO-vehicle alone did not alter the immunological response (37), it was not used in the present study. The second cohort of mice was treated with an i.p. injection of LPS (0.05 mg/kg, *E.coli* 0111:B6, Sigma-Aldrich, Gillingham, UK) dissolved in NaCl (21, 22, 36). The choice of this dose was based on separate control studies showing the "ceiling" behavioral changes in mice injected with the LPS dose of 0.1 mg/kg (see Supplementary Figure 2).

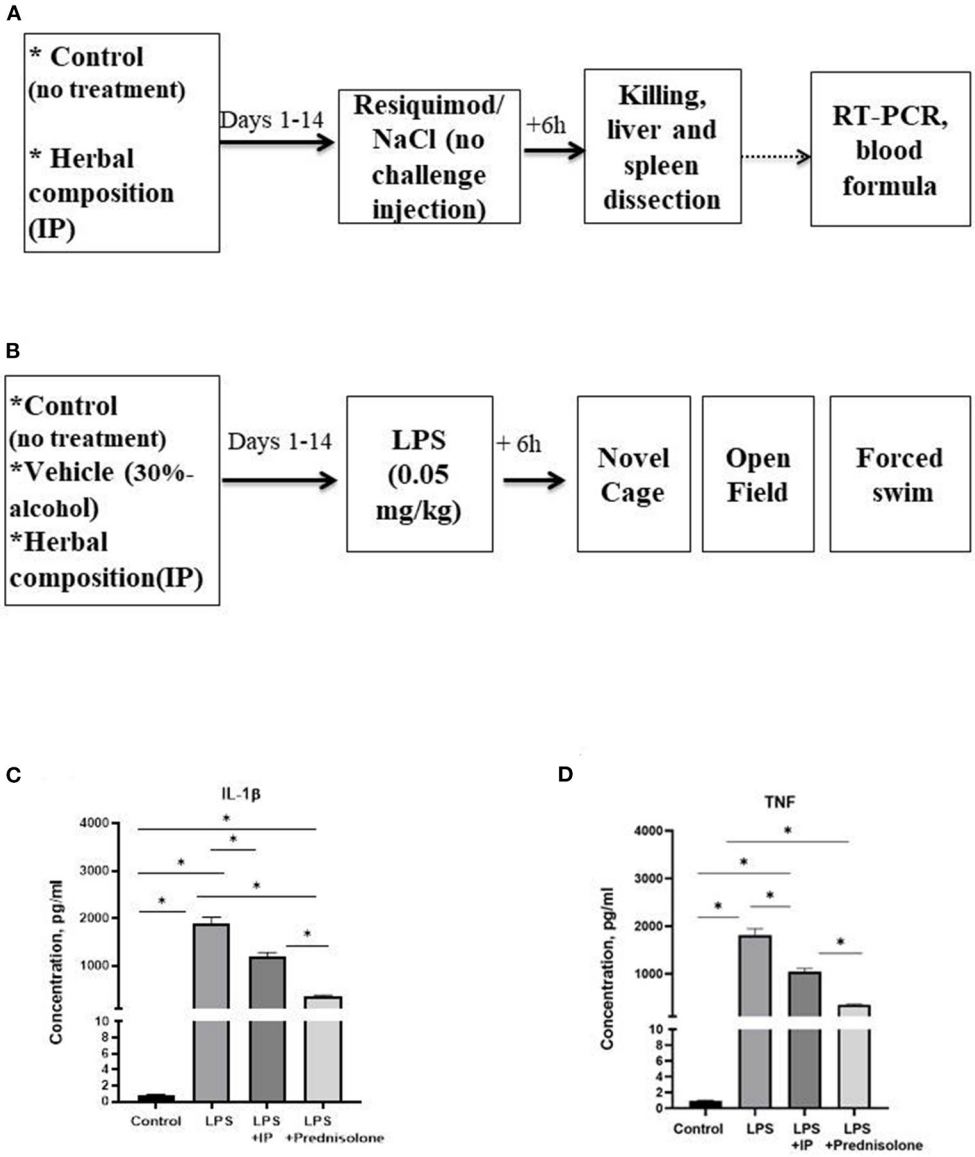

FIGURE 1
Schematic of *in vivo* tests performed and the outcome from the *in vitro* assay. In the *in vivo* experiments, animals were exposed to a daily administration of herbal drops or vehicle during the 14 days. On the day of the experiment, mice received an intraperitoneal injection **(A)** with resiquimod or vehicle and killed 6 h post-challenge, **(B)** with LPS or vehicle and 6 h post-challenge completed the novel cage, open field, and the forced swim test. In the *in vitro* assay, herbal drops or prednisolone was applied in the human macrophage cell culture that was treated with LPS. In comparison with the non-stimulated samples, there was a significant increase in the concentrations of **(C)** IL-1β and **(D)** TNF in all LPS-challenged samples. Significant group differences: *vs. non-challenged samples, (one-way ANOVA and Tukey's test). Data presented as mean ± SEM.

The administration of the IP

The drops of the IP were administered orally (120 μL per day) for each mouse during the morning hours using a pipette (26, 36). A composition of a 30% alcohol IP solution can be found in a Supplementary Table 1.

Behavior

To determine the effect of the IP on the LPS-induced "sickness" behavior, novel cage, open field, and forced swim tests were performed (38), see Supplementary File.

Tissue collection

Mice were anesthetized with isoflurane (21, 22). Blood (200 μL) was then collected by cardiac puncture, transferred into an EDTA-coated tube, and immediately analyzed for blood formula. Animals were then intracardially perfused with cold saline, liver and spleen were collected and snap-frozen.

Blood analysis

Blood was measured in triplicate on the ABX Pentra 60 (Horiba, Northampton, UK). The number of lymphocytes, monocytes, neutrophils, basophils, and eosinophils per μL (cells/μL) and percent of the cells were counted (33).

RNA extraction, CDNA conversion and QPCR

According to the manufacturer's instructions, RNA was extracted from samples of liver and spleen using the Qiagen RNeasy Mini kit, RNA concentration was measured using a NanoDrop, and 1,000 ng of RNA was converted to cDNA with the Applied Biosystems High Capacity cDNA conversion kit. Real-time qPCR was performed with samples in duplicate (25 ng/well) using the SYBR green qPCR master mix (PrimerDesign, Camberley, UK) with the Roche LightCycler 480 (33). Relative expression was determined by the 2-ΔΔCT method, normalized to GAPDH as the housekeeping gene (PrimerDesign, Camberley, UK); for the list of primers, see Supplementary Table 2.

High-potency-liquid chromatography high-resolution-mass-spectrometry

The solution was analyzed using the chromatographic system Agilent 1,290 Infinity II, quadrupole-time streaming high precision mass detector Agilent 6,545 Q-TOF LC/MS, and Zorbax Eclipse Plus C18 RRHD columns (Agilent Technologies, Santa Clara, CA, USA); for details, see Supplementary File.

Statistical analysis

Statistical analyses were performed with the GraphPad Prism 7 software. Data sets were tested for normal distribution; Welch's test and *t-test* were used to perform two group comparisons where appropriate, and one or two-way analysis of variance (ANOVA) was employed for multiple group analysis, with Tukey's *post-hoc* test. Results were considered significant at $p < 0.05$ with 95% confidence intervals. In the study with resiquimod, data were expressed as percent of challenged groups from the respective non-challenged groups that either received the IP or were not treated with the immunomodulatory agent and were compared to a 100%-level. Data are expressed as mean ± standard error of the mean (SEM).

Results

Application of the IP reduces cytokine release from LPS-induced macrophages

The IL-1β and TNF concentrations in the macrophage cell culture were significantly different between the groups ($F = 145.6$ and $F = 94.45$, respectively, both $p < 0.0001$, one-way ANOVA). In the challenged non-treated samples, there were significant increases in these parameters compared to the non-treated group, as well as to the LPS-challenged samples treated with the IP or prednisolone (all $p < 0.0001$, Tukey's test, Figures 1C,D). The IL-1β and TNF levels were significantly higher in both the IP- and prednisolone-treated preparations than in the non-treated samples (IL-1β: $p = 0.0021$ and $p < 0.0001$, respectively, TNF: both $p < 0.0001$), whereas the latter groups had lower IL-1β concentrations compared with the IP-treated group (IL-1β: $p < 0.0001$; TNF: $p = 0.0001$).

Chronic administration of the IP diminishes the resiquimod-induced expression of inflammatory markers in the liver and spleen

All non-normalized to unchallenged values can be found in the Supplementary Tables 3, 4. In the liver, a comparison of the resiquimod-challenged groups showed that the normalized SAA-2mRNA expression in the IP-treated mice was lower than in the non-treated mice ($p < 0.0001$, *Welch's test*, Figure 2A); compared to 100%, both groups had an elevated SAA-2mRNA expression ($p < 0.0001$). Both challenged groups demonstrated an increased normalized SAA-2mRNA expression in the spleen ($p = 0.0137$, vs. 100%, Figure 2A). There was a trend of a lower normalized ACE-2mRNA expression in the IP-treated group than in the resiquimod-challenged non-treated mice ($p = 0.093$, Figure 2B) and a significant decrease in this parameter in the former but not the latter group as compared to 100% ($p = 0.005$ and $p = 0.594$, respectively). No group differences were found in the normalized spleen ACE-2mRNA expression level ($p = 0.874$, Figure 2B). Compared to 100%, no significant difference was observed in any group ($p = 0.877$ and $p = 0.525$, respectively).

The IP-treated group subjected to the resiquimod injection had a significantly decreased normalized liver CXCL1mRNA expression compared with the resiquimod-injected animals ($p = 0.0054$, Figure 2C), while both groups showed a significant

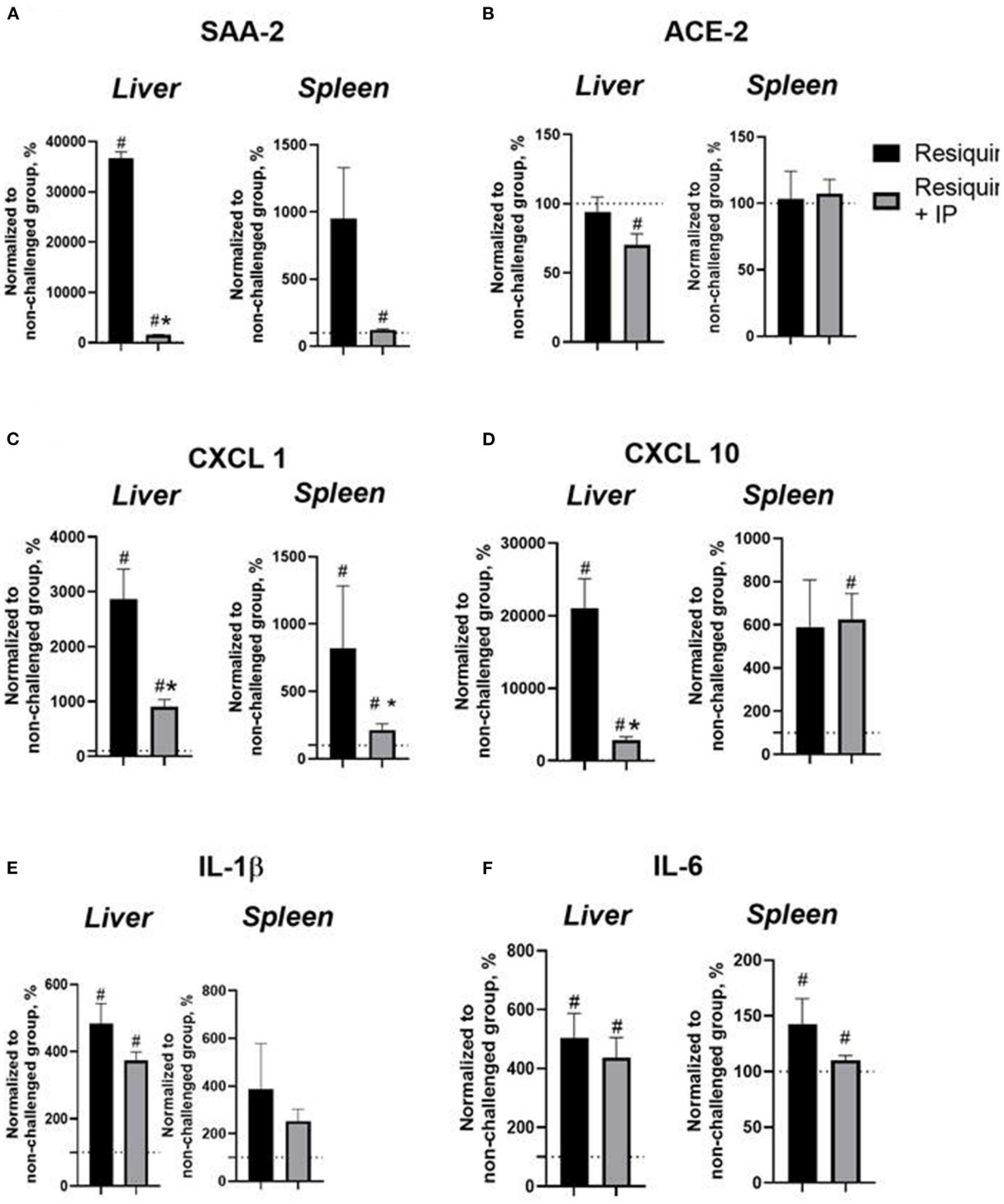

FIGURE 2
Pro-inflammatory resiquimod-induced gene expression changes in the liver and spleen are ameliorated with the herbal IP treatment. **(A)** Resiquimod-challenged groups showed a significant increase in the normalized liver expression of SAA-2mRNA in comparison to a 100%-level. This measure was lower in the liver of IP–treated animals. No such differences were shown for the spleen. **(B)** As compared to a 100%-level, there was a significant decrease in the normalized ACE-2mRNA expression in the liver of the IP-treated group but not in the non-treated resiquimod-challenged mice that was not found for the spleen **(C)** Both resiquimod-challenged groups showed a significant increase in liver CXCL1mRNA normalized concentrations as compared to 100%; the IP-treated group subjected to the resiquimod injection had a significantly decreased normalized liver CXCL1mRNA expression compared with resiquimod-injected animals. In the spleen, compared to 100%, this

(Continued)

FIGURE 2 (Continued)
measure was decreased in the IP-treated resiquimod-challenged group. **(D)** We found a significant increase in the normalized CXCL10mRNA expression in the liver and spleen compared to 100% in both groups, while this measure was lower in the IP-treated group than in resiquimod-challenged mice without treatment; no group difference in this measure was found for the spleen. **(E)** Elevated normalized IL-1βmRNA levels compared to 100% in the liver and spleen were shown for both groups; no other differences were found. **(F)** Normalized mRNA expression of IL-6 was similarly elevated in two groups in the liver and spleen compared to the 100% level. No other differences were found. *vs. 100% level, # vs. the challenged non-treated group (Welch's test and *t*-test, see the text). Data presented as mean ± SEM.

increase in this measure as compared to 100% ($p = 0.0006$ and $p = 0.0001$, respectively). No group differences in the normalized CXCL1mRNA expression in the spleen were found ($p = 0.372$, Figure 2C). However, compared to 100%, the mRNA expression level in the IP-treated resiquimod-challenged group was diminished ($p = 0.034$) with no difference in mice that received the resiquimod alone ($p = 0.137$).

A significant decrease in the normalized CXCL10mRNA expression in the liver was observed for the IP-treated mice with induced inflammation compared with mice treated with resiquimod alone ($p = 0.0016$, Figure 2D). Compared to 100%, the mRNA liver expression of this gene was elevated in both groups ($p = 0.0006$ and $p = 0.0001$, respectively). In the spleen, no group difference in this parameter was found ($p = 0.885$, Figure 2D). Both groups revealed an elevated CXCL10mRNA expression compared to 100% ($p = 0.047$ and $p = 0.002$, respectively).

As for the normalized mRNA concentration of IL-1β in the liver, there was a trend of a decreasing expression level in the IP-treated mice with induced inflammation compared to the resiquimod- challenged group ($p = 0.111$, Figure 2E). Elevated IL-1βmRNA levels compared to 100% were shown for both groups ($p < 0.0001$). No significant group differences were shown in this parameter in the spleen ($p = 0.473$, Figure 2E); IL-1βmRNA expression was elevated compared to 100% in both groups ($p = 0.014$ and $p = 0.0079$, respectively). The normalized mRNA expression of IL-6 was similar in two groups in the liver and spleen ($p = 0.553$ and $p = 0.252$, respectively, Figure 2F) and was elevated compared to 100% in both groups (liver: $p = 0.001$ and $p = 0.0008$; spleen: $p = 0.028$ and $p = 0.037$, respectively).

The effects of the IP on the resiquimod-induced changes in the blood formula

All non-normalized to unchallenged values can be found in the Supplementary Table 5. In the resiquimod-challenged non-treated animals, there was a trend of elevated counts of blood neutrophils, monocytes, and eosinophils compared to a 100%-level (neutrophils: $p = 0.165$, monocytes: $p = 0.151$, eosinophils: $p = 0.066$, *t-test*), while the IP-pre-treated challenged mice showed opposite changes (all $p < 0.0001$, Figures 3A–C). The latter group revealed a significant decrease in all counts compared to the resiquimod-injected animals (neutrophils: $p = 0.038$; monocytes: $p = 0.006$; eosinophils: $p = 0.019$).

Both the non-treated- and IP-treated mice challenged with resiquimod had similar non-significant increases in basophils compared with a 100% level ($p = 0.094$ and $p = 0.099$, respectively, Figure 3D). No differences were found between the challenged groups ($p = 0.655$). The number of lymphocytes did not differ between the resiquimod-treated groups and a 100%-level ($p = 0.564$ and $p = 0.432$, respectively, Figure 3E), nor did it differ between the groups ($p = 0.941$).

Effects of the IP on the LPS-induced "sickness" behavior

In the novel cage test, two-way ANOVA demonstrated a significant LPS effect on the number of exploratory rearings ($F = 103.0$, $p < 0.0001$). There was a significant treatment effect and LPS x treatment interaction ($F = 4.928$, $p = 0.0125$ and $F = 5.093$, $p = 0.011$, respectively). The *post-hoc* test showed that this measure was significantly smaller in the Vehicle LPS group and IP-treated LPS group compared to the corresponding control groups ($p < 0.0001$; $p < 0.0001$ and $p = 0.0053$, respectively, Tukey's test, Figure 4A). The IP-treated group with LPS-induced inflammation had a significantly higher number of rearings compared with the non-treated LPS group and Vehicle LPS group ($p = 0.016$ and $p = 0.048$, respectively, Figure 4A).

Both significant LPS and treatment effects were revealed by two-way ANOVA in the open field test ($F = 125.8$, $p < 0.0001$ and $F = 6.357$, $p = 0.004$, respectively). The number of peripheral rearings was lower in the non-treated LPS group, Vehicle LPS group, and IP-treated LPS group compared to the corresponding control groups ($p < 0.0001$; $p < 0.0001$ and $p = 0.0001$, respectively, Figure 4B). The IP-treated group with LPS-induced inflammation had a significantly higher number of rearings compared with the Vehicle LPS group ($p = 0.028$, Figure 4B).

The two-way ANOVA showed significant LPS and treatment effects in the number of central rearings in the open field test ($F = 37.31$, $p < 0.0001$ and $F = 4.837$, $p = 0.0134$, respectively). This parameter was lower in the non-treated LPS group and Vehicle LPS group compared to the corresponding control groups (both $p = 0.002$, Figure 4C). The number of central rearings in the IP-treated group with LPS induced inflammation

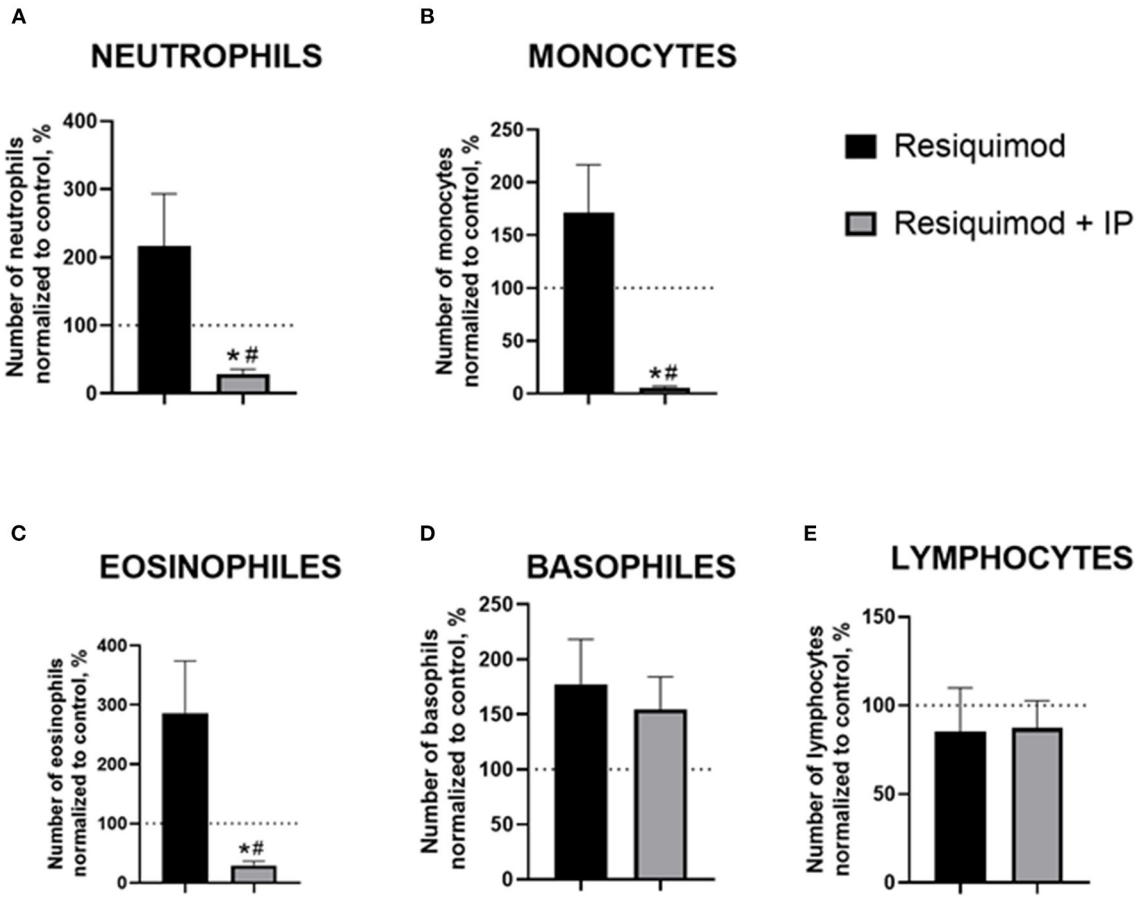

FIGURE 3
Pro-inflammatory effects of resiquimod on blood formula are reduced in mice treated with the herbal IP composition. Normalized counts of **(A)** neutrophils, **(B)** monocytes, **(C)** eosinophils were significantly decreased in IP-treated resiquimod-stimulated mice. **(D)** An increase in basophil counts was similar in the two challenged groups. **(E)** No changes were found in the lymphocyte counts of the resiquimod-injected groups; *vs. 100% level, #vs. the challenged non-treated group (Welch's test and *t*-test, see the text). Data presented as mean ± SEM.

was significantly higher compared to the Vehicle LPS group ($p = 0.028$, Figure 4C).

The two-way ANOVA revealed the LPS effect in the latency of immobility in the forced swim test ($F = 23.84$, $p < 0.0001$). This measure was higher in the control Vehicle group compared to the Vehicle group with LPS-induced inflammation ($p = 0.007$, Figure 4D). The two-way ANOVA showed a significant LPS effect in the total time of immobility in this test ($F = 27.25$, $p < 0.0001$). The total time of immobility was higher in the non-treated LPS group compared to the corresponding control group ($p = 0.002$, Figure 4E). No other significant effects were found.

Thus, chronic IP administration can attenuate some but not all signs of "sickness" behavior caused by the LPS-induced systemic inflammation, whereas the alcohol-containing vehicle does not generate these effects.

HPLC-HRMS

HPLC-HRMS revealed bioactive constituents of the IP: choline, γ-Glutamyl-(S)-allyl-cysteine, N-Fructosyl or glucosyl isoleucine, L-glutamyl–L-phenylalanine (Glu-Phe), chlorogenic acid, phenylalanine, tryptophan, isoleucine, syringin, and isoquercitin (see Supplementary Table 6). The following meta-analysis showed that these components were previously reported to modulate the immune response and inflammation, as well as oxidative and nitrosative stress, and thus, are likely to underlie the reported immunomodulatory properties of the investigated herbal IP (see Supplementary Table 7). The outcome from the meta-analysis study and the main effects of these eleven elements are reviewed in the Supplementary File.

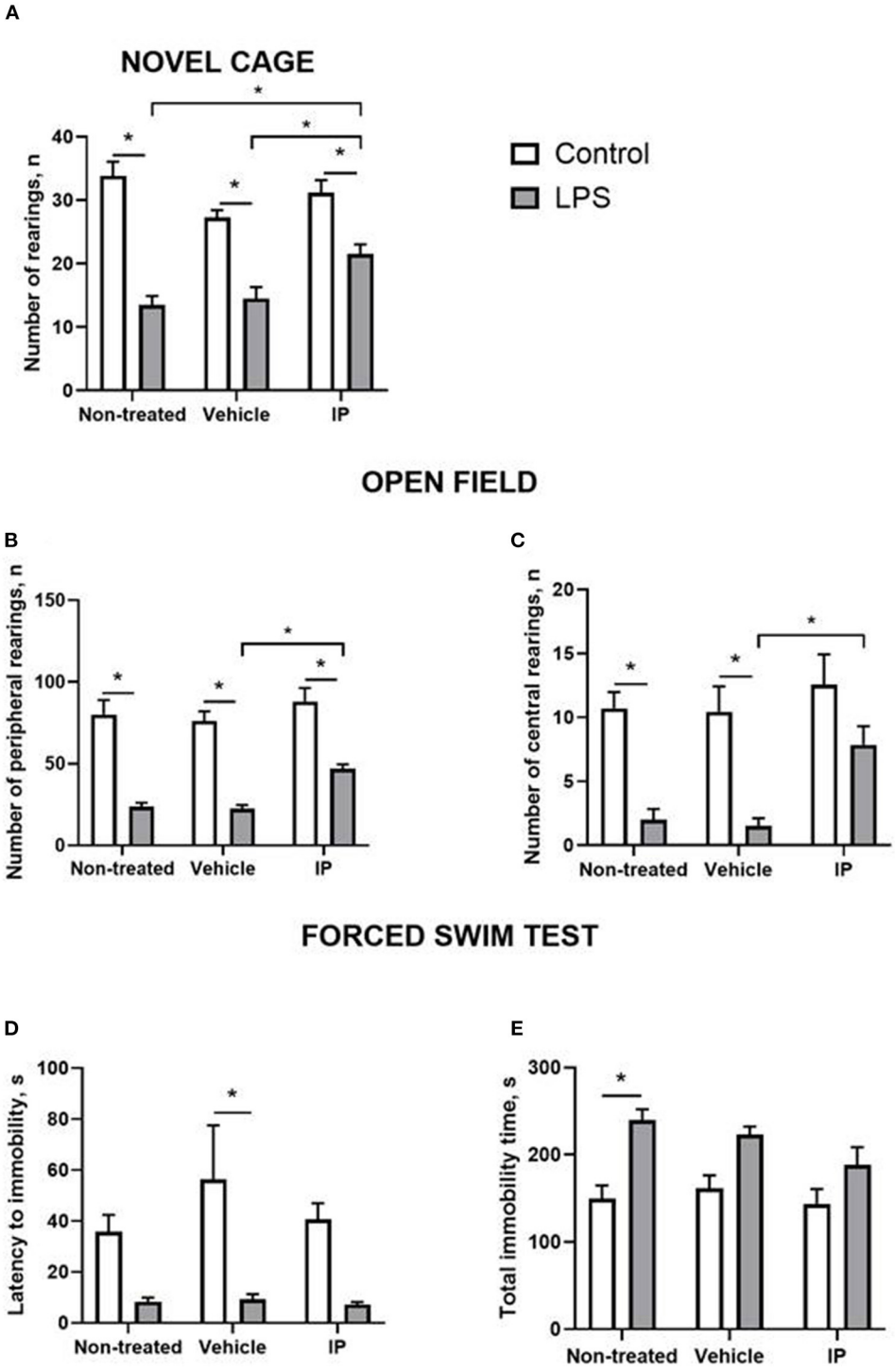

FIGURE 4
LPS induces a sickness behavior phenotype, which is partly normalized by the herbal IP. In comparison to non-treated challenged animals, IP-treated LPS-challenged mice displayed **(A)** a normalized number of exploratory rears, **(B)** a number of peripheral and **(C)** central crossings in the open field (two-way ANOVA and Tukey's test). There were no such differences **(D)** in the latency to float and **(E)** duration of the floating in the forced swim test; *vs. the challenged non-treated group. Data presented as mean ± SEM.

Discussion

Here, we have shown that the administration of the IP herbal composition containing an extract of blackberry, chamomile, garlic, cloves, and elderberry can reduce pro-inflammatory changes that are reminiscent to a "cytokine storm," a key feature of SARS-CoV2 infection. These *in vitro* and *in vivo* effects were demonstrated in the established models of systemic inflammation that are based on triggering of TLR7/8 and TLR4, the key mediators of this pathological condition. While the effects on molecular and behavioral markers of response to inflammatory challenges were suppressed partially, this herbal composition can be efficient in diminishing deleterious manifestations of the "cytokine storm" caused by the SARS-CoV2 virus, at least, in a preventive manner.

The anti-inflammatory effect of the IP was first evaluated by measuring *in vitro* the release of IL-1β and TNF by LPS-challenged macrophages and compared to that of prednisolone. For both cytokines, their release was suppressed by the IP, though the effect of prednisolone was much greater. IL-1β and TNF are inflammatory mediators that have long been associated with the "cytokine storm" caused by SARS-CoV-2 (7, 39, 40). TLRs are strongly expressed in macrophages (41), and it is seems probable that the IP counteracts their activation caused by LPS (42).

The present study revealed the suppressive effect of the IP administration on TLR7/8-mediated inflammation caused by resiquimod. The IP decreased the counts of neutrophils, monocytes, and eosinophils that were elevated by the injection of resiquimod, though the number of basophils was increased regardless of the pre-treatment with the IP. Increases in these blood cell counts in response to the resiquimod administration are considered characteristic signs of excessive immune activation (43–45). A suppression of these responses by the IP administration demonstrates its anti-inflammatory properties, which were shown in this model for the anti-inflammatory treatment with nafamostat (33). These former experiments have validated the applied here model as pharmacologically sensitive to anti-inflammatory interventions. As such, the reported here effects of IP on blood formula can be interpreted to be similar to that of pharmacological anti-inflammatory reference. Previous studies also revealed resiquimod-induced lymphopenia in CD-1 mice, more specifically, a decrease in the counts of circulating lymphocytes recapitulating clinical and experimental observations of acute viral infection (46–48), including after TLR7 stimulation (49) that was also found in SARS-CoV-2 patients (22, 50). In the present study, a decrease in lymphocytes did not reach a level of significance.

The magnitude of the systemic inflammatory response was evaluated by measuring the relative expression of pro-inflammatory genes in the liver and spleen (22, 51, 52). In both organs, the resiquimod challenge induced a significant increase in SAA-2, ACE-2, CXCL1, and CXCL10. These inflammatory mediators were established to accompany viral infection and underlie sickness behavior (40), and were shown to be significantly up-regulated in our previous study with resiquimod (33). TLR7 is strongly expressed in macrophages, and it seems probable that it is the resident tissue macrophages that are responsible for producing these cytokines (42), which would also account for the differential expression levels between the organs, as there is a greater density of macrophages in the liver than the spleen. Here, we were also able to show that the herbal IP had a peripheral anti-inflammatory effect; hepatic SAA-2, CXCL1, and CXCL10 expression induced by resiquimod was significantly ameliorated by the IP treatment, as well as ACE-2, to a lesser extent. As for IL-1β and IL-6, there was just an optical trend for the normalizing effects of the IP. A suppression of these changes in gene expression by the IP administration evidences its anti-inflammatory properties, which were demonstrated in this model for nafamostat (33). Because the SARS-CoV2 virus needs to bind to the host ACE2 receptor *via* its spike protein to infect cells, its suppression by the IP shown in our work let to speculate it can be considered a potential prevention remedy.

In our study, locomotion, anxiety-like, and exploratory behavior in mice were significantly affected by the injection of a low dose of LPS, which is consistent with other inflammatory models such as those employing the classical LPS-CD14-TLR4 challenge (21, 34). Analysis of central crossings in the open field revealed that the LPS-treated animals chose to spend less time in the center of the open field, which suggests that LPS had an anxiogenic effect. Increased anxiety has been reported in LPS models (22, 35) and is associated with the central expression of pro-inflammatory cytokines. In a view of previously reported inter-relation between behavioral and molecular effects of LPS in models of systemic inflammation in mice (21, 22), reported here behavioral effects of the administration of IP can be interpreted as a manifestation of its anti-inflammatory action.

Of note, the behavioral effects of the IP on LPS-challenged mice were partial, as it did not reach a statistical significance in the measures of helplessness during the forced swimming. However, forced swimming in rodents is not often associated with the "sickness" behavior; previous studies with an LPS challenge were unable to demonstrate consistent changes in this test (53). Collectively, for the IP, the behavioral changes observed are indicative of a "sickness" behavior phenotype and were overly reduced by chronic administration.

Importantly, the present study showed that the IP herbal composition has ameliorated the LPS-induced *in vitro* cytokine release and "sickness behavior" that was not altered by alcohol vehicle alone, while alcohol might have subtle anti-inflammatory effects (54, 55). As the inhibition of cytokine signaling in the periphery can attenuate "sickness behaviors" induced by the

injection of IL-1β (56, 57), the suppression of the inflammatory response in liver and spleen in IP-treated animals that is reported here can explain the beneficial behavioral effects of chronic pre-treatment with the employed herbal composition.

Our work has used CD-1 mice as a mouse strain that is highly susceptible to inflammatory challenges in comparison with other mouse lines, as some studies suggest (58). While strain differences were shown to affect the response to a systemic inflammation (58, 59), overly similar molecular and behavioral changes that were reported in C57Bl6 mice, Balb/c and CD-1 mice following pro-inflammatory challenges (58–60) suggest that reported here findings are unlikely to be strain-specific.

Because the pathophysiology of SARS-CoV2 comprises the mechanisms of viral invasion and replication that are SARS-CoV2-specific, as well as excessive, uncontrolled inflammation, which can be a common element of any severe infection, the IP can be regarded as a useful non-specific preventive remedy of this infection. Notably, while the present study was not designed to address the question whether or not, similarly to other herbal medicine, the administration of IP can exert disease-specific therapeutic action (4, 5), its significant effects on highly up-regulated inflammatory markers and expression of ACE-2 mediating the viral binding in the host may suggest such possibility. Further experiments are required to test this hypothesis.

HPLC-HRMS analysis has revealed the main constituents of the IP that likely underlie its beneficial immunomodulatory effects: choline, γ-Glutamyl-(S)-allyl-cysteine, N-Fructosyl or glucosyl isoleucine, L-glutamyl–L-phenylalanine (Glu-Phe), chlorogenic acid, phenylalanine, tryptophan, isoleucine, syringin, and isoquercitin. Choline is a well-established important macronutrient that regulates synaptic plasticity, e.g., *via* several genes, G9a, Prmt1, Ahcy, Dnmt1, Mat2a (61, 62), implicated in neurotrophic processes (63), potentially *via* insulin-like-growth-factor-2 (IGF2) and insulin receptor-mediated mechanisms (64, 65). Of note, the activation of insulin receptor mediated signaling triggers anti-inflammatory cascades (66). Among other activities, γ-Glutamyl-(S)-allyl-cysteine was shown to stabilize radical-scavenging and metal-chelating processes that are important in immune responses and contribute to the immunological regulation of the IP (67). The ability of N-Fructosyl or glucosyl-isoleucine to regulate the mechanisms of stress response has been documented (68). Another IP component, L-glutamyl–L-phenylalanine, was found to diminish liver inflammation *via* reducing lipid accumulation and presumably acting on metabolic processes of the cell (69). Tryptophan, a molecule with the greatest anti-oxidative capacity among amino acids (70) and a precursor of the neurotransmitter serotonin that is known to exert anti-inflammatory action (71), was shown to act *via* calcium-dependent mechanisms of receptor activation (72).

Moreover, the IP contains chlorogenic acid whose anti-inflammatory effects are well-documented in a model of transient forebrain ischemia and associated with a reduction in the levels of pro-inflammatory factors: SOD2, IL-2, TNF and an increase in the expression of anti-inflammatory cytokines: IL-4, IL-13 (73), resulting in anti-oxidative action also *via* the activation of antioxidant enzymes and neuroprotective effects. This spectrum of activities was further demonstrated in rat models of ischemia/re-perfusion of the kidney and liver (74–76). Another IP constituent with documented anti-oxidative stress effects is phenylalanine (77, 78), which was shown to decrease the production of reactive oxygen species (78, 79). Similarly, isoleucine counteracts the mechanisms of oxidative stress, as shown in a model of H_2O_2-stimulated intestinal epithelial cells (80), ameliorates NO-mediated pathways during wound healing (81), and exerts an immunomodulatory action regulating the key molecules of the mammalian innate immunity, β-defensin (82). Finally, isoquercitin is one of the most powerful well-studied natural anti-inflammatory and anti-oxidant agents that acts directly on the scavenging of reactive oxygen/nitrogen species (83), inhibits production of pro-inflammatory cytokines, pro-oxidant enzymes, and prostaglandins (83, 84), and induces antioxidant enzymes (85–87).

Conclusion

Critically, the over-expression of inflammatory markers, blood cell inflammatory response, and "sickness behavior" under conditions of strong pro-inflammatory stimuli were ameliorated by the treatment with the herbal composition IP. Given that the magnitude of these responses was associated with disease severity (39, 87) and anti-inflammatory treatment (88), our findings suggest that the IP preventive treatment may reduce the severity of SARS-CoV2 infection. Since our results were achieved in the absence of viral entry, we propose that the IP may have generally useful anti-inflammatory effects, which may be advantageous in the treatment of various viral infections, including SARS-CoV2. The effect of the new immunomodulatory phytotherapeutic herbal extract is required further evaluation on patients with SARS-CoV-2 infection. Therefore, it is advocated to recommend a future clinical randomized controlled trial study that implement the conventional treatment with herbal extracts. As highlighted previously, the availability of low-cost herbal medicine for economically disadvantageous communities is of particular importance to curb SARS-CoV2 pandemic and enhancing preparedness for future pandemics.

Data availability statement

The raw data supporting the conclusions of this article will be made available by the authors, without undue reservation.

Ethics statement

The animal study was reviewed and approved by University of Oxford Local committees LEPR and ACER, iCell2 METC Zyaderland Zuid, the Netherlands.

Author contributions

CS, TS, SL, and AU conceived the study. JM, SL, TS, and ME designed the experiments. OS, AG, NG, and MS carried out the experiments, data analysis, and performed the literature study. OS, JM, MS, ME, and AG performed the graph preparation and statistical analyses. K-PL, CS, and TS supervised the project. SL, K-PL, TS, and CS got the funding. CS, OS, AG, AU, NG, and TS wrote the initial draft of the manuscript and all other authors listed here revised it. All authors contributed to the article and approved the submitted version.

Funding

This study was supported by Eat2beNice EU framework (2018-2023, to TS and K-PL) and by PhytoAPP EU framework (2021-2025, to OS, SL, and TS). The Eat2beNICE project has received funding from the European Union's Horizon 2020 research and innovation programme under grant agreement No 728018 and the PhytoAPP project has received funding from the the European Union's HORIZON 2020 research and innovation programme under the Marie Sklodowvska-Curie grant agreement 101007642. This publication reflects only the author's views and the European Commission is not liable for any use that may be made of the information contained therein. This publication was supported by the Open Access Publication Fund of the University of Wuerzburg. NG was supported by the German Research Foundation (DFG RTG 2660 under grant No. 433490190).

Acknowledgments

We thank Prof. Daniel C. Anthony, University of Oxford, for valuable conceptual, practical and methodological input and discussions, and Mr. Rene Vendeville, Voorhout, the Netherlands for his input.

Conflict of interest

The authors declare that the research was conducted in the absence of any commercial or financial relationships that could be construed as a potential conflict of interest.

Publisher's note

Supplementary material

The Supplementary Material for this article can be found online at: https://www.frontiersin.org/articles/10.3389/fmed.2022.952977/full#supplementary-material

References

1. Ghosh K, Chattopadyay B, Maity T, Acharya A. A multi-dimensional review on severe acute respiratory syndrome coronavirus-2. *Curr Pharm Biotechnol.* (2022). doi: 10.2174/1389201023666220507003726

2. Ren X, Zhou J, Guo J, Hao C, Zheng M, Zhang R, et al. Reinfection in patients with COVID-19: a systematic review. *Glob Health Res Policy.* (2022) 7:12. doi: 10.1186/s41256-022-00245-3

3. Peters CW, Maguire CA, Hanlon KS. Delivering AAV to the central nervous and sensory systems. *Trends Pharmacol Sci.* (2021) 42:461–74. doi: 10.1016/j.tips.2021.03.004

4. Bekut M, Brkić S, Kladar N, Dragović G, Gavarić N, BožIn B. Potential of selected lamiaceae plants in anti(retro)viral therapy. *Pharmacol Res.* (2018) 133:301–14. doi: 10.1016/j.phrs.2017.12.016

5. Fongnzossie Fedoung E, Biwole AB, Nyangono Biyegue CF, Ngansop Tounkam M, Akono Ntonga P, Nguiamba VP, et al. A review of cameroonian medicinal plants with potentials for the management of the COVID-19 pandemic. *Adv Tradit Med.* (2021) 26:1–26. doi: 10.1007/s13596-021-00567-6

6. Tomazou M, Bourdakou MM, Minadakis G, Zachariou M, Oulas A, Karatzas E, et al. Multi-omics data integration and network-based analysis drives a multiplex drug repurposing approach to a shortlist of candidate drugs against COVID-19. *Brief Bioinform.* (2021) 22:bbab114. doi: 10.1093/bib/bbab114

7. Chen R, Lan Z, Ye J, Pang L, Liu Y, Wu W, et al. Cytokine storm: the primary determinant for the pathophysiological evolution of COVID-19 deterioration. *Front Immunol.* (2021) 12:589095. doi: 10.3389/fimmu.2021.589095

8. Catanzaro M, Fagiani F, Racchi M, Corsini E, Govoni S, Lanni C. Immune response in COVID-19: addressing a pharmacological challenge by targeting pathways triggered by SARS-CoV-2. *Signal Transduct Target Ther.* (2020) 5:84. doi: 10.1038/s41392-020-0191-1

9. Risitano AM, Mastellos DC, Huber-Lang M, Yancopoulou D, Garlanda C, Ciceri F, et al. Complement as a target in COVID-19? *Nat Rev Immunol.* (2020) 20:343–4. doi: 10.1038/s41577-020-0320-7

10. Talisuna A, Iwu C, Okeibunor J, Stephen M, Musa EO, Herring BL, et al. Assessment of COVID-19 pandemic responses in African countries: thematic synthesis of WHO intra-action review reports. *BMJ Open.* (2022) 12:e056896. doi: 10.1136/bmjopen-2021-056896

11. Dol J, Boulos L, Somerville M, Saxinger L, Doroshenko A, Hastings S, et al. Health system impacts of SARS-CoV - 2 variants of concern: a rapid review. *BMC Health Serv Res.* (2022) 22:544. doi: 10.1186/s12913-022-07847-0

12. Tisoncik JR, Korth MJ, Simmons CP, Farrar J, Martin TR, Katze MG. Into the eye of the cytokine storm. *Microbiol Mol Biol Rev.* (2012) 76:16–32. doi: 10.1128/MMBR.05015-11

13. Arango Duque G, Fukuda M, Turco SJ, Stäger S, Descoteaux A. Leishmania promastigotes induce cytokine secretion in macrophages through the degradation of synaptotagmin XI. *J Immunol.* (2014) 193:2363–72. doi: 10.4049/jimmunol.1303043

14. Giamarellos-Bourboulis EJ, Netea MG, Rovina N, Akinosoglou K, Antoniadou A, Antonakos N, et al. Complex immune dysregulation in COVID-19 patients with severe respiratory failure. *Cell Host Microbe.* (2020) 27:992–1000.e3. doi: 10.1016/j.chom.2020.04.009

15. Monguió-Tortajada M, Franquesa M, Sarrias MR, Borràs FE. Low doses of LPS exacerbate the inflammatory response and trigger death on TLR3-primed human monocytes. *Cell Death Dis.* (2018) 9:499. doi: 10.1038/s41419-018-0520-2

16. Van der Made CI, Simons A, Schuurs-Hoeijmakers J, van den Heuvel G, Mantere T, Kersten S, et al. Presence of genetic variants among young men with severe COVID-19. *JAMA.* (2020) 324:663–73. doi: 10.1001/jama.2020.13719

17. Cunningham C, Campion S, Teeling J, Felton L, Perry VH. The sickness behaviour and CNS inflammatory mediator profile induced by systemic challenge of mice with synthetic double-stranded RNA (poly I:C). *Brain Behav Immun.* (2007) 21:490–502. doi: 10.1016/j.bbi.2006.12.007

18. Lu YC, Yeh WC, Ohashi PS. LPS/TLR4 signal transduction pathway. *Cytokine.* (2008) 42:145–51. doi: 10.1016/j.cyto.2008.01.006

19. Kelley KW, Bluthé RM, Dantzer R, Zhou JH, Shen WH, Johnson RW, et al. Cytokine-induced sickness behavior. *Brain Behav Immun.* (2003) (Suppl. 1):S112–8. doi: 10.1016/S0889-1591(02)00077-6

20. Campbell SJ, Anthony DC, Oakley F, Carlsen H, Elsharkawy AM, Blomhoff R, et al. Hepatic nuclear factor kappa B regulates neutrophil recruitment to the injured brain. *J Neuropathol Exp Neurol.* (2008) 67:223–30. doi: 10.1097/NEN.0b013e3181654957

21. Couch FB, Bansbach CE, Driscoll R, Luzwick JW, Glick GG, Bétous R, et al. ATR phosphorylates SMARCAL1 to prevent replication fork collapse. *Genes Dev.* (2013) 27:1610–23. doi: 10.1101/gad.214080.113

22. Couch Y, Trofimov A, Markova N, Nikolenko V, Steinbusch HW, Chekhonin V, et al. Low-dose lipopolysaccharide (LPS) inhibits aggressive and augments depressive behaviours in a chronic mild stress model in mice. *J Neuroinflammation.* (2016) 13:108. doi: 10.1186/s12974-016-0572-0

23. Hui DSC, Zumla A. Severe acute respiratory syndrome: historical, epidemiologic, and clinical features. *Infect Dis Clin North Am.* (2019) 33:869–89. doi: 10.1016/j.idc.2019.07.001

24. Zhou H, Ni WJ, Huang W, Wang Z, Cai M, Sun YC. Advances in pathogenesis, progression, potential targets and targeted therapeutic strategies in SARS-CoV-2-Induced COVID-19. *Front Immunol.* (2022) 13:834942. doi: 10.3389/fimmu.2022.834942

25. Barak V, Kalickman I, Halperin T, Birkenfeld S, Ginsburg I. PADMA-28, a Tibetan herbal preparation is an inhibitor of inflammatory cytokine production. *Eur Cytokine Netw.* (2004) 15:203–9.

26. Adeleye OA, Bamiro OA, Bakre LG, Odeleye FO, Adebowale MN, Okunye OL, et al. Medicinal plants with potential inhibitory bioactive compounds against coronaviruses. *Adv Pharm Bull.* (2022) 12:7–16. doi: 10.34172/apb.2022.003

27. Mahaboob Ali AA, Bugarcic A, Naumovski N, Ghildyal R. Ayurvedic formulations: potential COVID-19 therapeutics? *Phytomed Plus.* (2022) 2:100286. doi: 10.1016/j.phyplu.2022.100286

28. Tai A, Sawano T, Yazama F, Ito H. Evaluation of antioxidant activity of vanillin by using multiple antioxidant assays. *Biochim Biophys Acta.* (2011) 1810:170–7. doi: 10.1016/j.bbagen.2010.11.004

29. Salim S. Oxidative stress and the central nervous system. *J Pharmacol Exp Ther.* (2017) 360:201–5. doi: 10.1124/jpet.116.237503

30. Vipin AV, Raksha Rao K, Nawneet KK, Anu Appaiah KA, Venkateswaran G. Protective effects of phenolics rich extract of ginger against Aflatoxin B1-induced oxidative stress and hepatotoxicity. *Biomed Pharmacother.* (2017) 91:415–24. doi: 10.1016/j.biopha.2017.04.107

31. Costa-Nunes JP, Gorlova A, Pavlov D, Cespuglio R, Gorovaya A, Proshin A, et al. Ultrasound stress compromises the correlates of emotional-like states and brain AMPAR expression in mice: effects of antioxidant and anti-inflammatory herbal treatment. *Stress.* (2020) 23:481–95. doi: 10.1080/10253890.2019.1709435

32. de Munter J, Pavlov D, Gorlova A, Sicker M, Proshin A, Kalueff AV, et al. Increased oxidative stress in the prefrontal cortex as a shared feature of depressive- and PTSD-Like syndromes: effects of a standardized herbal antioxidant. *Front Nutr.* (2021) 8:661455. doi: 10.3389/fnut.2021.661455

33. Yates AG, Weglinski CM, Ying Y, Dunstan IK, Strekalova T, Anthony DC. Nafamostat reduces systemic inflammation in TLR7-mediated virus-like illness. *J Neuroinflammation.* (2022) 19:8. doi: 10.1186/s12974-021-02357-y

34. Domscheit H, Hegeman MA, Carvalho N, Spieth PM. Molecular dynamics of lipopolysaccharide-induced lung injury in rodents. *Front Physiol.* (2020) 11:36. doi: 10.3389/fphys.2020.00036

35. Domínguez-Rivas E, Ávila-Muñoz E, Schwarzacher SW, Zepeda A. Adult hippocampal neurogenesis in the context of lipopolysaccharide-induced neuroinflammation: a molecular, cellular and behavioral review. *Brain Behav Immun.* (2021) 97:286–302. doi: 10.1016/j.bbi.2021.06.014

36. de Munter J, Babaevskaya D, Wolters EC, Pavlov D, Lysikova E, V Kalueff A, et al. Molecular and behavioural abnormalities in the FUS-tg mice mimic frontotemporal lobar degeneration: Effects of old and new anti-inflammatory therapies. *J Cell Mol Med.* (2020) 24:10251–7. doi: 10.1111/jcmm.15628

37. Cui M, Wu J, Wang S, Shu H, Zhang M, Liu K, et al. Characterization and anti-inflammatory effects of sulfated polysaccharide from the red seaweed gelidium pacificum okamura. *Int J Biol Macromol.* (2019) 129:377–85. doi: 10.1016/j.ijbiomac.2019.02.043

38. Strekalova T, Steinbusch HW. Measuring behavior in mice with chronic stress depression paradigm. *Prog Neuropsychopharmacol Biol Psychiatry.* (2010) 34:348–61. doi: 10.1016/j.pnpbp.2009.12.014

39. Henry BM, de Oliveira MHS, Benoit S, Plebani M, Lippi G. Hematologic, biochemical and immune biomarker abnormalities associated with severe illness and mortality in coronavirus disease 2019 (COVID-19): a meta-analysis. *Clin Chem Lab Med.* (2020) 58:1021–8. doi: 10.1515/cclm-2020-0369

40. Chan SY, Probert F, Radford-Smith DE, Hebert JC, Claridge TDW, et al. Post-inflammatory behavioural despair in male mice is associated with reduced cortical glutamate-glutamine ratios, and circulating lipid and energy metabolites. *Sci Rep.* (2020) 10:16857. doi: 10.1038/s41598-020-74008-w

41. Alothaimeen T, Trus E, Basta S, Gee K. Differential TLR7-mediated cytokine expression by R848 in M-CSF- versus GM-CSF-derived macrophages after LCMV infection. *J Gen Virol.* (2021) 102:001541. doi: 10.1099/jgv.0.001541

42. Savignac HM, Couch Y, Stratford M, Bannerman DM, Tzortzis G, et al. Prebiotic administration normalizes lipopolysaccharide (LPS)-induced anxiety and cortical 5-HT2A receptor and IL1-β levels in male mice. *Brain Behav Immun.* (2016) 52:120–31. doi: 10.1016/j.bbi.2015.10.007

43. Maestre-Batlle D, Pena OM, Huff RD, Randhawa A, Carlsten C, Bølling AK. Dibutyl phthalate modulates phenotype of granulocytes in human blood in response to inflammatory stimuli. *Toxicol Lett.* (2018) 296:23–30. doi: 10.1016/j.toxlet.2018.07.046

44. Serrano R, Wesch D, Kabelitz D. Activation of human γδ T Cells: modulation by toll-like receptor 8 ligands and role of monocytes. *Cells.* (2020) 9:713. doi: 10.3390/cells9030713

45. Cassatella MA, Gardiman E, Arruda-Silva F, Bianchetto-Aguilera F, Gasperini S, Bugatti M, et al. Human neutrophils activated by TLR8 agonists, with or without IFNγ, synthesize and release EBI3, but not IL-12, IL-27, IL-35, or IL-39. *J Leukoc Biol.* (2020) 108:1515–26. doi: 10.1002/JLB.3MA0520-054R

46. Damm J, Wiegand F, Harden LM, Gerstberger R, Rummel C, Roth J. Fever, sickness behavior, and expression of inflammatory genes in the hypothalamus after systemic and localized subcutaneous stimulation of rats with the toll-like receptor 7 agonist imiquimod. *Neuroscience.* (2012) 201:166–83. doi: 10.1016/j.neuroscience.2011.11.013

47. Chen T, Wang J, Li C, Zhang W, Zhang L, An L, et al. Nafamostat mesilate attenuates neuronal damage in a rat model of transient focal cerebral ischemia through thrombin inhibition. *Sci Rep.* (2014) 4:5531. doi: 10.1038/srep05531

48. Makris S, Johansson C. R848 or influenza virus can induce potent innate immune responses in the lungs of neonatal mice. *Mucosal Immunol.* (2021) 14:267–76. doi: 10.1038/s41385-020-0314-6

49. Jang S, Rhee JY. Three cases of treatment with nafamostat in elderly patients with COVID-19 pneumonia who need oxygen therapy. *Int J Infect Dis.* (2020) 96:500–2. doi: 10.1016/j.ijid.2020.05.072

50. Li K, Meyerholz DK, Bartlett JA, McCray Jr PB. The TMPRSS2 inhibitor nafamostat reduces SARS-CoV-2 pulmonary infection in mouse models of COVID-19. *mBio.* (2021) 12:e0097021. doi: 10.1128/mBio.00970-21

51. Strekalova T, Markova N, Shevtsova E, Zubareva O, Bakhmet A, Steinbusch HM, et al. Individual differences in behavioural despair predict brain GSK-3beta expression in mice: the power of a modified swim test. *Neural Plast.* (2016) 2016:5098591. doi: 10.1155/2016/5098591

52. Strekalova T, Svirin E, Veniaminova E, Kopeikina E, Veremeyko T, Yung AWY, et al. ASD-like behaviors, a dysregulated inflammatory response and decreased expression of PLP1 characterize mice deficient

for sialyltransferase ST3GAL5. *Brain Behav Immun Health.* (2021) 16:100306. doi: 10.1016/j.bbih.2021.100306

53. Michaelis KA, Norgard MA, Levasseur PR, Olson B, Burfeind KG, Buenafe AC, et al. Persistent toll-like receptor 7 stimulation induces behavioral and molecular innate immune tolerance. *Brain Behav Immun.* (2019) 82:338–53. doi: 10.1016/j.bbi.2019.09.004

54. Stote KS, Tracy RP, Taylor PR, Baer DJ. The effect of moderate alcohol consumption on biomarkers of inflammation and hemostatic factors in postmenopausal women. *Eur J Clin Nutr.* (2016) 70:470–4. doi: 10.1038/ejcn.2015.182

55. Mangnus L, van Steenbergen HW, Nieuwenhuis WP, Reijnierse M, van der Helm-van Mil AHM. Moderate use of alcohol is associated with lower levels of C reactive protein but not with less severe joint inflammation: a cross-sectional study in early RA and healthy volunteers. *RMD Open.* (2018) 4:e000577. doi: 10.1136/rmdopen-2017-000577

56. Careaga M, Taylor SL, Chang C, Chiang A, Ku KM, Berman RF, et al. Variability in PolyIC induced immune response: Implications for preclinical maternal immune activation models. *J Neuroimmunol.* (2018) 323:87–93. doi: 10.1016/j.jneuroim.2018.06.014

57. McGarry N, Murray CL, Garvey S, Wilkinson A, Tortorelli L, Ryan L, et al. Double stranded RNA drives anti-viral innate immune responses, sickness behavior and cognitive dysfunction dependent on dsRNA length, IFNAR1 expression and age. *Brain Behav Immun.* (2021) 95:413–28. doi: 10.1016/j.bbi.2021.04.016

58. Meneses G, Rosetti M, Espinosa A, Florentino A, Bautista M, Díaz G, et al. Recovery from an acute systemic and central LPS-inflammation challenge is affected by mouse sex and genetic background. *PLoS ONE.* (2018) 13:e0201375. doi: 10.1371/journal.pone.0201375

59. Zhao J, Bi W, Xiao S, Lan X, Cheng X, Zhang J, et al. Neuroinflammation induced by lipopolysaccharide causes cognitive impairment in mice. *Sci Rep.* (2019) 9:5790. doi: 10.1038/s41598-019-42286-8

60. Chakraborty A, Yeung S, Pyszczynski NA, Jusko WJ. Pharmacodynamic interactions between recombinant mouse interleukin-10 and prednisolone using a mouse endotoxemia model. *J Pharm Sci.* (2005) 94:590–603. doi: 10.1002/jps.20257

61. Craciunescu CN, Albright CD, Mar MH, Song J, Zeisel SH. Choline availability during embryonic development alters progenitor cell mitosis in developing mouse hippocampus. *J Nutr.* (2003) 133:3614–8. doi: 10.1093/jn/133.11.3614

62. Blusztajn JK, Mellott TJ. Choline nutrition programs brain development via DNA and histone methylation. *Cent Nerv Syst Agents Med Chem.* (2012) 12:82–94. doi: 10.2174/187152412800792706

63. Wong-Goodrich SJ, Mellott TJ, Glenn MJ, Blusztajn JK, Williams CL. Prenatal choline supplementation attenuates neuropathological response to status epilepticus in the adult rat hippocampus. *Neurobiol Dis.* (2008) 30:255–69. doi: 10.1016/j.nbd.2008.01.008

64. Cline BH, Steinbusch HW, Malin D, Revishchin AV, Pavlova GV, Cespuglio R, et al. The neuronal insulin sensitizer dicholine succinate reduces stress-induced depressive traits and memory deficit: possible role of insulin-like growth factor 2. *BMC Neurosci.* (2012) 13:110. doi: 10.1186/1471-2202-13-110

65. Cline BH, Anthony DC, Lysko A, Dolgov O, Anokhin K, Schroeter C, et al. Lasting downregulation of the lipid peroxidation enzymes in the prefrontal cortex of mice susceptible to stress-induced anhedonia. *Behav Brain Res.* (2015) 276:118–29. doi: 10.1016/j.bbr.2014.04.037

66. Pomytkin IA, Cline BH, Anthony DC, Steinbusch HW, Lesch KP, Strekalova T. Endotoxaemia resulting from decreased serotonin tranporter (5-HTT) function: a reciprocal risk factor for depression and insulin resistance? *Behav Brain Res.* (2015) 276:111–7. doi: 10.1016/j.bbr.2014.04.049

67. Tan D, Zhang Y, Chen L, Liu L, Zhang X, Wu Z, et al. Decreased glycation and structural protection properties of γ-glutamyl-S-allyl-cysteine peptide isolated from fresh garlic scales (Allium sativum L.). *Nat Prod Res.* (2015) 29:2219–22. doi: 10.1080/14786419.2014.1003065

68. Strasser R. Plant protein glycosylation. *Glycobiology.* (2016) 26:926–39. doi: 10.1093/glycob/cww023

69. Byun K, Yoo Y, Son M, Lee J, Jeong GB, Park YM, et al. Advanced glycation end-products produced systemically and by macrophages: a common contributor to inflammation and degenerative diseases. *Pharmacol Ther.* (2017) 177:44–55. doi: 10.1016/j.pharmthera.2017.02.030

70. Xu N, Chen G, Liu H. Antioxidative categorization of twenty amino acids based on experimental evaluation. *Molecules.* (2017) 22:2066. doi: 10.3390/molecules22122066

71. Carneiro IBC, Toscano AE, Lacerda DC, da Cunha MSB, de Castro RM, Deiró TCBJ, et al. L-tryptophan administration and increase in cerebral serotonin levels: systematic review. *Eur J Pharmacol.* (2018) 836:129–35. doi: 10.1016/j.ejphar.2018.08.009

72. Kim CJ, Kovacs-Nolan JA, Yang C, Archbold T, Fan MZ, Mine Y. l-Tryptophan exhibits therapeutic function in a porcine model of dextran sodium sulfate (DSS)-induced colitis. *J Nutr Biochem.* (2010) 21:468–75. doi: 10.1016/j.jnutbio.2009.01.019

73. Lee TK, Kang IJ, Kim B, Sim HJ, Kim DW, Ahn JH, et al. Experimental pretreatment with chlorogenic acid prevents transient ischemia-induced cognitive decline and neuronal damage in the hippocampus through anti-oxidative and anti-inflammatory effects. *Molecules.* (2020) 25:3578. doi: 10.3390/molecules25163578

74. Sato Y, Itagaki S, Kurokawa T, Ogura J, Kobayashi M, Hirano T, et al. *In vitro* and *in vivo* antioxidant properties of chlorogenic acid and caffeic acid. *Int J Phar.* (2011) 403:136–8. doi: 10.1016/j.ijpharm.2010.09.035

75. Yun N, Kang JW, Lee SM. Protective effects of chlorogenic acid against ischemia/reperfusion injury in rat liver: molecular evidence of its antioxidant and anti-inflammatory properties. *J Nutr Biochem.* (2012) 23:1249–55. doi: 10.1016/j.jnutbio.2011.06.018

76. Feng Y, Yu YH, Wang ST, Ren J, Camer D, Hua YZ, et al. Chlorogenic acid protects D-galactose-induced liver and kidney injury via antioxidation and anti-inflammation effects in mice. *Pharm Biol.* (2016) 54:1027–34. doi: 10.3109/13880209.2015.1093510

77. Perkowski MC, Warpeha KM. Phenylalanine roles in the seed-to-seedling stage: Not just an amino acid. *Plant Sci.* (2019) 289:110223. doi: 10.1016/j.plantsci.2019.110223

78. Oliva M, Hatan E, Kumar V, Galsurker O, Nisim-Levi A, Ovadia R, et al. Increased phenylalanine levels in plant leaves reduces susceptibility to Botrytis cinerea. *Plant Sci.* (2020) 290:110289. doi: 10.1016/j.plantsci.2019.110289

79. Chen Q, Man C, Li D, Tan H, Xie Y, Huang J. Arogenate dehydratase isoforms differentially regulate anthocyanin biosynthesis in arabidopsis thaliana. *Mol Plant.* (2016) 9:1609–19. doi: 10.1016/j.molp.2016.09.010

80. Katayama S, Ishikawa S, Fan MZ, Mine Y. Oligophosphopeptides derived from egg yolk phosvitin up-regulate gamma-glutamylcysteine synthetase and antioxidant enzymes against oxidative stress in Caco-2 cells. *J Agric Food Chem.* (2007) 55:2829–35. doi: 10.1021/jf0628936

81. Nie C, He T, Zhang W, Zhang G, Ma X. Branched chain amino acids: beyond nutrition metabolism. *Int J Mol Sci.* (2018) 19:954. doi: 10.3390/ijms19040954

82. Mao X, Qi S, Yu B, He J, Yu J, Chen D. Zn(2+) and L-isoleucine induce the expressions of porcine β-defensins in IPEC-J2 cells. *Mol Biol Rep.* (2013) 40:1547–52. doi: 10.1007/s11033-012-2200-0

83. Hammer KD, Hillwig ML, Solco AK, Dixon PM, Delate K, Murphy PA, et al. Inhibition of prostaglandin E(2) production by anti-inflammatory hypericum perforatum extracts and constituents in RAW264.7 mouse macrophage cells. *J Agric Food Chem.* (2007) 55:7323–31. doi: 10.1021/jf0710074

84. Kim AR, Jin Q, Jin HG, Ko HJ, Woo ER. Phenolic compounds with IL-6 inhibitory activity from Aster yomena. *Arch Pharm Res.* (2014) 37:845–51. doi: 10.1007/s12272-013-0236-x

85. Procházková D, Boušová I, Wilhelmová N. Antioxidant and prooxidant properties of flavonoids. *Fitoterapia.* (2011) 82:513–23. doi: 10.1016/j.fitote.2011.01.018

86. Valentová K, Vrba J, Bancírová M, Ulrichová J, Kren V. Isoquercitrin: pharmacology, toxicology, and metabolism. *Food Chem Toxicol.* (2014) 68:267–82. doi: 10.1016/j.fct.2014.03.018

87. Moreno-Eutimio MA, López-Macías C, Pastelin-Palacios R. Bioinformatic analysis and identification of single-stranded RNA sequences recognized by TLR7/8 in the SARS-CoV-2, SARS-CoV, and MERS-CoV genomes. *Microbes Infect.* (2020) 22:226–9. doi: 10.1016/j.micinf.2020.04.009

88. Damsgaard CT, Lauritzen L, Calder PC, Kjaer TM, Frøkiaer H. Whole-blood culture is a valid low-cost method to measure monocytic cytokines - a comparison of cytokine production in cultures of human whole-blood, mononuclear cells and monocytes. *J Immunol Meth.* (2009) 340:95–101. doi: 10.1016/j.jim.2008.10.005

Advantages of publishing in Frontiers

OPEN ACCESS
Articles are free to read for greatest visibility and readership

FAST PUBLICATION
Around 90 days from submission to decision

HIGH QUALITY PEER-REVIEW
Rigorous, collaborative, and constructive peer-review

TRANSPARENT PEER-REVIEW
Editors and reviewers acknowledged by name on published articles

Frontiers
Avenue du Tribunal-Fédéral 34
1005 Lausanne | Switzerland

Visit us: www.frontiersin.org
Contact us: frontiersin.org/about/contact

REPRODUCIBILITY OF RESEARCH
Support open data and methods to enhance research reproducibility

DIGITAL PUBLISHING
Articles designed for optimal readership across devices

FOLLOW US
@frontiersin

IMPACT METRICS
Advanced article metrics track visibility across digital media

EXTENSIVE PROMOTION
Marketing and promotion of impactful research

LOOP RESEARCH NETWORK
Our network increases your article's readership